

N° d'ordre : 42289



THESE

présentée en vue d'obtenir le grade de

DOCTEUR

en :

Spécialité : Optique et Lasers, Physico-Chimie, Atmosphère

par

Diogo Miguel BARROS de OLIVEIRA

Titre de la thèse :

**« Identification of the main sources and geographical origins of
PM₁₀ in the northern part of France »**

Soutenue le 27 Janvier 2017

Jury:

Rapporteur	Willy MAENHAUT	Professeur, Ghent University
Rapporteur	Jean-Luc JAFFREZO	Directeur de Recherche CNRS LGGE
Examinateur	Matthias BEEKMANN	Directeur de Recherche CNRS LISA
Encadrante	Esperanza PERDRIX	Maître-Assistante, Mines Douai
Encadrant	Stéphane SAUVAGE	Maître-Assistant, Mines Douai
Encadrant	Olivier FAVEZ	Ingénieur d'Etude et Recherche, INERIS
Directrice de Thèse	Véronique RIFFAULT	Professeure, Mines Douai

Laboratoire d'accueil :

Département Sciences de l'Atmosphère et Génie de l'Environnement, IMT Lille Douai

Ecole Doctorale SMRE 104 (Lille I, Artois, ULCO, UVHC, Centrale Lille, Mines Douai)

*Para a minha família
Em especial para o meu avô, Victor Oliveira*

ACKNOWLEDGEMENTS

I would like to start by thanking Ecole des Mines de Douai and INERIS for co-funding this thesis and trusting in me to embrace this project. A special thanks to Mines Douai in the form of its Director, Patrice Coddeville and its Research Director, Nadine Locoge for having me during these 3 years.

To the jury committee, Matthias Beekmann, Willy Maenhaut and Jean-Luc Jaffrezo a thank you for accepting to review my work and for your comments and advices on it.

A special thank you to all my supervisors, Véronique Riffault, Olivier Favez, Esperanza Perdrix and Stéphane Sauvage, for being much more than that. To Véronique, for all the knowledge shared, the help and the time provided, but also for being someone to whom I could go to and talk about everything. To Olivier, for his help on my introduction to the subject, advices and guidance during this work and his friendliness and kindness shown since day 1. To Stéphane, for his valuable help on PMF and all its mysteries. Finally, a special thanks to Esperanza, not only for the incredible work support that always showed, for the always interesting scientific discussions we had, but also for being there since the beginning, helping me adjusting to this new reality.

I also have to thank Aude Pascaud, for her help, kindness and patience during these 3 years. To Laurent Alleman, for his knowledge and advices on ICP and EC/OC analysis, uncertainties and PMF. To Bruno, for his help with the EC/OC instrument and always the funny conversations had (even if I was just understanding half).

A big thank you to all my colleagues in the Department SAGE, and special thanks to those that became so much more than that - Thérèse, Malak, Alexandre, Waed, Habib, Berenice, Shouwen, Evi, Antoine, Laura, Roger – this last for his insights on the troubled political situation in Cataluña and “gains” motivation.

To my friends, a group that stuck together since university and was a huge support during these 3 years – no need to name anyone, vocês sabem quem são.

A special and the most important aknowlegment goes to my family, my parents Jorge e Inês, and my brothers Joka, Rico and Kuka, for the constant support and love. And to Sofaki, I'm leaving Douai and Lille complete. We did it.

TABLE OF CONTENTS

Acknowledgements	5
Table of figures	13
List of tables	17
General introduction.....	21
CHAPTER 1 - Bibliography on Composition and sources of tropospheric aerosols	27
1.1 Particulate matter	27
1.1.1 Sources of PM ₁₀	28
1.1.2 PM ₁₀ composition.....	30
1.2 Impacts and Regulation	37
1.2.1 Climate impact of PM	37
1.2.2 Health impact of PM	39
1.2.3 Regulations.....	41
1.3 Source apportionment.....	42
1.3.1 Source apportionment studies worldwide	45
1.3.2 Source apportionment in Northwestern Europe	47
1.4 Geographical location of sources	54
1.5 Objectives of the thesis and scientific strategy.....	56
1.5.1 Objectives of the thesis	56
1.5.2 Scientific strategy	57
CHAPTER 2 - PM ₁₀ chemical speciation: measurements and results	61
2.1 The CARA program	61
2.2 Sampling sites.....	62
2.2.1 Lens (urban site).....	63
2.2.2 Nogent-sur-Oise (urban site).....	65
2.2.3 Rouen (urban site)	66
2.2.4 Revin (remote site)	67

2.2.5	Roubaix (traffic site)	68
2.3	PM ₁₀ characterization methodologies.....	69
2.3.1	Filter sampling.....	69
2.3.2	PM ₁₀ automatic measurement	70
2.3.3	Offline chemical analyses	70
2.3.4	Limits of detection	71
2.3.5	Measurement uncertainties.....	73
2.3.6	Ion balance	79
2.3.7	Mass closure.....	83
2.4	PM ₁₀ chemical composition at each site.....	88
2.4.1	Carbonaceous aerosols	92
2.4.2	Organic species	95
2.4.3	Ions.....	101
2.5	Exceedance episodes	104
2.6	Conclusions of Chapter 2	109
CHAPTER 3 - “Combination of Positive Matrix Factorization and Concentration Field methodologies to investigate the sources and geographical origins of PM ₁₀ chemical species: a French urban site case study” (Publication 1).....		
3.1	Summary of Publication 1	113
3.1.1	Chemical analysis – Methods and results	113
3.1.2	Source apportionment	115
3.1.3	Source location.....	116
Combination of Positive Matrix Factorization and Concentration Field methodologies to investigate the sources and geographical origins of PM ₁₀ chemical species: a French urban site case study		
1	Introduction	119
2	Methodology	120
2.1	Sampling site	120

2.2	Measurements and instrumentation	122
2.3	Data validation.....	123
2.4	Source apportionment using PMF	124
2.5	Geographical allocation	126
2.5.1	NWR.....	127
2.5.2	Concentration Field method	127
3	Results and discussion.....	128
3.1	PM ₁₀ mass and composition	128
3.2	PMF general solution and validation.....	133
3.3	Local factors	136
3.3.1	Traffic factor	136
3.3.2	Biomass burning factor	137
3.3.3	Land biogenic aerosols.....	138
3.4	Regional factors	139
3.4.1	Aged marine aerosols	142
3.4.2	Nitrate-rich aerosols	143
3.4.3	Oxalate-rich aerosols.....	145
3.4.4	Sulfate-rich aerosols.....	146
3.4.5	Marine biogenic aerosols	147
4	Conclusion.....	148
5	Acknowledgments	149
	References	150
	Supplementary material.....	156
3.2	Complement of Publication 1	169
3.2.1	Source apportionment	169
3.2.2	Source location	173

CHAPTER 4 - Multi-site receptor oriented approach for a comprehensive source apportionment of PM in the North of France (Publication 2)	179
4.1 Summary of Publication 2	179
4.1.1 Chemical composition	179
4.1.2 Source apportionment	180
4.1.3 Source location	181
Multi-site receptor-oriented approach for a comprehensive source apportionment of PM ₁₀ in the north of France	183
Introduction	185
Methodology	188
Sites, sampling and chemical analysis	188
Source apportionment using Positive Matrix Factorization (PMF)	190
Geographical location of nearby sources using the Non-parametric Wind Regression (NWR) and distant sources using the Concentration Field (CF) model	191
Results and discussion.....	194
Local factors.....	205
Regional factors.....	207
Natural sources	207
Anthropogenic sources	209
Conclusion.....	213
Acknowledgements	214
References	216
4.2 Complement of Publication 2	231
4.2.1 Meteorological data.....	231
4.2.2 Factors chemical composition	232
4.2.3 Seasonal contribution of factors	235
4.2.4 Contribution during high concentration episodes	239
4.2.5 Local and regional sources. Natural and anthropogenic sources	242

Conclusions and perspectives.....	257
Perspectives.....	260
References	265
Annex 1: Uncertainties and correlations	288
Uncertainties.....	288
Uncertainties and detection limits for the site of Lens.....	288
Uncertainties and detection limits for the site of Nogent-sur-Oise.....	291
Uncertainties and detection limits for the site of Revin.....	293
Uncertainties and detection limits for the site of Rouen.....	295
Uncertainties and detection limits for the site of Roubaix.....	297
Correlations	299
Lens.....	299
Nogent-sur-Oise.....	300
Revin.....	301
Rouen.....	302
Roubaix.....	303
Annex 2: PMF solutions.....	304
Q _{true} /Q _{exp} value for PMF solutions	304
IM and IS values for PMF solutions	305
Bootstrap	306
Lens.....	306
Nogent-sur-Oise.....	307
Revin.....	307
Rouen.....	308
Roubaix.....	308
PMF solution in Lens.....	309
PMF solution Nogent-sur-Oise.....	314

PMF solution Revin	319
PMF solution Rouen.....	324
PMF solution Roubaix	328
Correlation between ionic compounds and factor contributions.....	333
Lens (urban site).....	333
Nogent-sur-Oise (urban site).....	333
Revin (remote site).....	334
Rouen (urban site)	334
Roubaix (traffic site)	335
Annex 3: Concentration fields.....	336
Trajectory cluster analysis:.....	336
Each line represents the mean trajectory of a cluster, numbered from 1 to 5. A different color is given to each line for better visualization. The percentage of the total number of trajectories assigned to each cluster is indicated.	336
Comparison between trajectory density with and without trajectory cut-offs	338
Lens	338
Nogent-sur-Oise	339
Revin	339
Rouen	339
Roubaix	340
Fresh marine aerosols.....	341
Aged marine aerosols	342
Marine biogenic aerosols	343
Nitrate rich aerosols	344
Sulfate rich aerosols	345
Oxalate rich aerosols	346

TABLE OF FIGURES

Figure 1: Principal modes, sources, and particle formation and removal mechanisms shown for an idealized aerosol surface size distribution (Zieger 2011)	29
Figure 2: Bar chart plots summarizing the mass concentration ($\mu\text{g m}^{-3}$) of seven major aerosol components for particles with diameter smaller than $10 \mu\text{m}$, from various rural and urban sites (dots on the central world map) in six continental areas of the world with at least an entire year of data and two marine sites (IPCC, 2013)	31
Figure 3: Relative mass concentration of anhydrosugars in PM per source category (adapted from Pernigotti, Belis, and Spanò, 2016)	34
Figure 4: Radiative forcing components (adapted from IPCC Fourth Assessment Report)	38
Figure 5: Deposition of particles in the respiratory tract as a function of their size, with inset illustrating the proximity of the air spaces (alveoli) to the vasculature (in pink) (source: Elder, Vidyasagar, and DeLouise 2009)	40
Figure 6: Scheme of the different methods for source apportionment (source: Belis et al., 2014).....	43
Figure 7: Synthesis of different approaches for estimating pollution source contributions using receptor models (source: Viana et al., 2008).....	44
Figure 8: Population-weighted averages for relative source contributions to total PM_{10} in urban sites (source: Karagulian et al., 2015)	46
Figure 9: Absolute contribution to total PM_{10} by region and source category (source: Karagulian et al., 2015)	47
Figure 10: Contributions of the identified sources in % to total PM_{10} mass concentration for the full year and according to the seasons (a) and on a monthly basis along with weekdays-to-weekends variations (b) (source: Waked et al., 2014)	50
Figure 11: Average source contribution during the JOAQUIN project	52
Figure 12: Sampling sites involved in the CARA program in 2014	62
Figure 13: Geographical location of the sampling sites of this work.....	63
Figure 14: Geographical location of the sampling site in Lens.....	64
Figure 15: Meteorological data for the site of Lens (temperature and rainfall in the left and windrose in the right)	64
Figure 16: Geographical location of the sampling site of Nogent-sur-Oise	65
Figure 17: Meteorological data for the site of Nogent-sur-Oise (temperature and rainfall in the left and windrose in the right)	66

Figure 18: Geographical location of the sampling site in Rouen	66
Figure 19: Meteorological data for the site of Rouen (temperature and rainfall in the left and windrose in the right)	67
Figure 20: Meteorological data for the site of Revin (temperature and rainfall in the left and windrose in the right)	68
Figure 21: Geographical location of the sampling site of Roubaix.....	69
Figure 22: Meteorological data for the site of Roubaix (temperature and rainfall)	69
Figure 23: High-volume sampler Digitel DA80	70
Figure 24: Scheme of the protocol to obtain uncertainties linked to measurements (source: Ellison et al. 2000)	74
Figure 25: Uncertainties fishbone scheme for ICP measurements (source: Yenisoy-Karakaş 2012).....	75
Figure 26: Uncertainties fishbone scheme for IC measurements (source: Leiva et al., 2012). 76	
Figure 27: Uncertainties fishbone scheme for metal measurements carried out in Mines Douai	77
Figure 28: Balance between anions and cations on each sampling site	79
Figure 29: Correlation between anions and cations on all sampling sites (1:1 ratio)	80
Figure 30: Seasonal variation of the ion balance on each sampling site	81
Figure 31: Difference between anions and cations on each sampling site per season	83
Figure 32: Correlation between PM ₁₀ measurements and mass closure method	85
Figure 33: PM ₁₀ reconstructed mass and unaccounted fraction per season at each sampling site	87
Figure 34: PM ₁₀ average concentration on each site per season	90
Figure 35: Average chemical composition of PM ₁₀ on each sampling site	90
Figure 36: Average chloride per sodium ratio for each site according to their distance to the sea.....	91
Figure 37: EC (top) and OC (bottom) average concentrations on each sampling site, per season	92
Figure 38: Correlation between EC and OC on all sampling sites.....	94
Figure 39: OC/EC ratio at each sampling site per season	95
Figure 40: Average contribution of the organic species measured on each sampling site.....	96
Figure 41: Organic species concentrations on each sampling site, per season	98
Figure 42: Ion contribution to PM ₁₀ mass on each sampling site	101
Figure 43: Ion concentrations on each sampling site, per season	102

Figure 44: Average contributions of the calculated species of NaCl, NaNO ₃ , NH ₄ NO ₃ and (NH ₄) ₂ SO ₄ for each sampling site	104
Figure 45: Seasonal distribution of exceedance episodes on each site	105
Figure 46: Time distribution of exceedance episodes on each sampling site	106
Figure 47: Average chemical composition during exceedance episodes on each sampling site	107
Figure 48: Chemical composition of the samples of March 30, 2013 at all sites, except Nogent-sur-Oise sampled on the 29 th	108
Figure 49: Chemical composition of the samples of March 6, 2013 to all sites	109
Figure 50: Q _{true} /Q _{exp} values for different number of factors in Nogent-sur-Oise.....	172
Figure 51: IM and IS values for different number of factors in Nogent-sur-Oise	172
Figure 52: ZeFir interface for wind (top) and trajectory (bottom) calculations.....	174
Figure 53: Correlations between wood smoke concentrations obtained from levoglucosan and biomass burning contributions calculated from PMF on each sampling site.....	233
Figure 54 & 55: Primary traffic (top) and biomass burning (bottom) average and seasonal contributions in µg m ⁻³	235
Figure 56 & 57: Land biogenic (top) and marine biogenic (bottom) average and seasonal contributions in µg m ⁻³	236
Figure 58 & 59: Fresh marine (top) and aged marine (bottom) average and seasonal contributions in µg m ⁻³	237
Figure 60, 61 & 62: Nitrate rich (top), sulfate rich (middle) and oxalate rich (bottom) average and seasonal contributions in µg m ⁻³	238
Figure 63: Average source contribution during days with PM ₁₀ mass concentration above 50 µg m ⁻³ in Lens, Nogent-sur-Oise, Revin, Rouen and Roubaix	240
Figure 64: Average source contribution during the 6 th of March of 2013 in Lens, Nogent-sur-Oise, Revin, Rouen and Roubaix	241
Figure 65: Average source contribution during the 30 th of March of 2013 in Lens, Nogent-sur-Oise, Revin, Rouen and Roubaix	242
Figure 66: Regional and local (top) and natural and anthropogenic sources (bottom) average contributions on the urban sites (Lens, Nogent-sur-Oise and Rouen)	243
Figure 67: Regional and local (left) and natural and anthropogenic sources (right) average contributions on the traffic site (Roubaix)	244
Figure 68: Regional and local (left) and natural and anthropogenic sources (right) average contributions on the remote site (Revin)	245

Figure 69: Average contribution of the different sources to PM10 mass concentration in Lens in Oliveira et al (left) and Waked et al (right).....	247
Figure 70: Relative contribution of Natural, Anthropogenic and Mixed sources to PM10 mass concentration in 6 sites in the north of France	249
Figure 71: Relative contribution of marine sources to PM10 mass concentration in 6 sites in the north of France	250
Figure 72: Relative contribution of Natural, Anthropogenic and Mixed sources to PM10 mass concentration in 5 European cities	252
Figure 73: Relative contribution of Natural, Anthropogenic and Mixed sources to PM10 mass concentration in 9 sites spread across the north of France and Belgium	253

LIST OF TABLES

Table 1: Main anthropogenic sources of metals in atmospheric particles (source: Riffault et al. 2015).....	37
Table 2: WHO database on local source apportionment studies of particulate matter in air. The studies performed with PMF are highlighted in green (source: WHO)	48
Table 3: Comparison of the meteorological conditions between the winter of 2013 and the winter of 2014	82
Table 4: OM/OC ratio used in each sampling site	84
Table 5: Unaccounted masses for each sampling site	84
Table 6: Number of samples for each sampling site - total and per season	88
Table 7: Validated (checked) species used at each sampling site	89
Table 8: EC and OC average concentrations and standard deviations ($\mu\text{gC m}^{-3}$) at each sampling site, per season	93
Table 9: Between site correlation coefficients for levoglucosan contributions during the studied period from the 5 sites	99
Table 10: Average and seasonal ratios of L/M and L/(M+G) for each sampling site.....	100
Table 11: Number of exceedance episodes on each site, during the sampling period.....	105
Table 12: MeteoFrance stations used for each sampling and their corresponding distance ..	231
Table 13: Contributions to PM ₁₀ mass of wood smoke (calculated from levoglucosan by a factor of 10.7), biomass burning factors (obtained from PMF) and the new calculated factor	232

GENERAL INTRODUCTION

GENERAL INTRODUCTION

Air quality is a major environmental, social and economical issue in this day and age. It is a complex problematic hard to manage and mitigate, and has been proven to be the largest environmental health risk in Europe (WHO, 2016). Although particulate matter (PM), also commonly referred to as ‘aerosols’, is present naturally in the atmosphere, its number greatly increased with the Industrial Revolution in the end of the 19th century due to anthropogenic activities. However, just in 1980 the first legislation concerning PM limit values was put in place in Europe with the Directive 80/779/EEC (Kuklinska, Wolska, and Namiesnik 2015). In order to control and reduce PM emissions it became crucial to understand the nature and sources of these particles in the atmosphere.

PM can then be distinguished by being from natural origin (marine sea salt, biogenic particles, crustal matter from soil erosion, volcanic activity, wild fires, etc.) or anthropogenic origin (industrial activity, processes of fossil fuel combustion, agriculture, traffic, etc.). The nature of the aerosols is directly related with their impact on human health with several studies reporting links between PM chemistry and respiratory and cerebrovascular diseases (Anderson, Thundiyil, and Stolbach 2012), heart disease (Pope III and Dockery 2006) and even carcinogenic potential (Sun et al. 2004; Giakoumi et al. 2009).

Driven by evidence of the ill effects of PM to human health, a limit value of $40 \mu\text{g m}^{-3}$ of PM_{10} as an annual average is now imposed in the European Union by the Air Quality Directive 2008/50/EC. A limit daily average value of $50 \mu\text{g m}^{-3}$ is also imposed and it shouldn't be exceeded more than 35 days in one year. These limits encourage local governments to invest on the knowledge of these particles and their sources in order to reduce its values.

PM can also be characterized as primary or secondary particles. Primary particles are emitted directly to the atmosphere. Secondary particles are formed in the atmosphere from chemical or photochemical reactions and/or physical modification. These secondary particles are associated with precursor gases like sulfur dioxide, NO_x (nitrogen oxide and nitrogen dioxide), ammonia or volatile organic compounds.

The dispersion, transport and deposition of these particles are key parameters to understand the impact of air pollution not only on a local scale but also on regional and global scale. Starting by the latter, deposition of aerosols can occur by dry deposition (gravity effect

(Sehmel 1980)) or by wet deposition (particles may either serve as condensation nuclei for droplet formation or they collide with droplets either within or below clouds (Seinfeld and Pandis 2006). Dispersion and transport are linked with meteorological conditions and particles properties, where the first also depends on emission patterns.

Although PM₁₀ levels have been gradually decreasing over the last 10 years, the constant urban growth of developed and developing countries poses major concerns in terms of the impact of air pollution in citizens. In fact, the exceedance of the daily limit value of PM₁₀ mentioned above was observed in 22 Member States of the EU at one or more stations in the year of 2015. A stricter value of 20 µg m⁻³ is suggested by the World Health Organization (WHO) and this was exceeded at 67% of the stations and in 27 European countries, according to the “Air Quality in Europe” report (EEA, 2016).

In France, where an estimated 42 000 premature deaths per year occur due to air pollution exposure, PM₁₀ is monitored in over 338 stations, most of them inserted in urban environments (~60%), some in close distance to intense traffic activity (~20%) and in rural areas (~7%). Just 4 of these stations exceeded the annual limit value for PM₁₀ levels in 2013 (all in traffic sites), however 12% of all the stations recorded more than 35 days where the average daily value was exceeded, mostly urban and traffic stations. In fact, PM₁₀ levels in France have barely decreased during the last 5 years, and 8 of the 41 largest metropolitan areas (over 250k inhabitants) exceeded PM₁₀ daily limit values (LCSQA, 2016).

The north of France in particular is characterized by short but frequent pollution episodes. In fact, a study from LCSQA identified the Nord-Pas de Calais region as one of the most polluted in France, where about 90% of its population was exposed to more than 35 daily exceedance episodes in the year of 2007. Although the average annual value is below the EU limit (24 µg m⁻³ in 2014) it is still above the one recommended by the WHO, and the number of daily exceedance episodes is concerning (over 35 in 6 urban areas).

To understand and better tackle this issue, information on all these aspects needs to be gathered and measures on the controllable parameters have to be put in place. This requires to assess what are exactly the sources of PM on a given place/region, and to do so several mathematical methods of data treatment are put in place. This work will be based on the ones that are receptor-oriented, meaning that PM is collected at a given sampling site, characterized and this information is used to calculate its probable sources. Based on observations on

chemical speciation, our approach will aim at apportioning and locating source of PM impacting the north of France.

This document will start with a first chapter dedicated to the state of art in order to introduce the main issues and present the objectives and approaches of this work. A second part will present the material and methods used during this work, with a first presentation of the results obtained for the chemical characterization of the samples collected. A third chapter, based on a publication already submitted, aims to present the methodology used on a full source apportionment study on a single sampling site in the north of France. Finally a fourth chapter based on a publication as well, will present the main results of a multi-site approach of the methodology suggested in chapter 3. This manuscript ends with the conclusion where the summary of the main results will be provided and with the suggestion of some perspectives for future improvements.

CHAPTER 1

BIBLIOGRAPHY ON COMPOSITION AND SOURCES OF TROPOSPHERIC AEROSOLS

CHAPTER 1 - BIBLIOGRAPHY ON COMPOSITION AND SOURCES OF TROPOSPHERIC AEROSOLS

1.1 Particulate matter

Particulate matter (PM) is a mixture of solid or liquid particles suspended in air. PM, also commonly referred as “aerosols”, is found in the atmosphere with a multitude of shapes and sizes, originated from wide range of sources which are important characteristics that will determine the lifetime of these particles in the atmosphere. Spanning from a few hours to a few weeks, the lifetime of aerosols (and their link to very specific sources) explains the highly non-uniform distribution of concentrations seen around the globe. In direct relation, the size distribution of PM can range from hundreds of micrometers down to just a few nanometers and it can be used to categorize aerosols by different size modes and relate them with specific sources, chemistry and removal processes. To do so, one can use the aerodynamic diameter of PM as physical property to characterize size modes. Aerodynamic diameter is defined for an irregularly shaped particle in terms of the diameter of an ideal spherical particle of unit density that has an aerodynamic behavior identical to that of the particle in question (Hinds 1982). Based on the equality of their settling velocities, equation 1 gives the relationship between the characteristics of a real particle (effective diameter, particle density, shape coefficient) and its aerodynamic diameter:

$$d_a = d_e \cdot \sqrt{\frac{\rho_p}{\rho_0 \cdot \chi}} \quad (\text{Eq. 1})$$

- d_a aerodynamic diameter of a sphere of unit density (μm)
- d_e effective diameter of the real particle (μm)
- ρ_p real particle density (g cm^{-3})
- ρ_0 unit density (1 g cm^{-3})
- χ shape coefficient of the real particle (χ of a sphere equals to 1)

According to the International Standards Organization (ISO), PM_{10} is defined as particles which pass through a size-selective inlet with a 50 % efficiency cut-off at 10 μm aerodynamic diameter. PM_{10} is therefore a standard size fraction where the median diameter is 10 microns. Similarly with other size fractions, 50% of the PM_x have a diameter greater than x microns (Seinfeld and Pandis 2006).

1.1.1 Sources of PM₁₀

Atmospheric particles can be classified according to their origin. This term can however encompass different meanings, that is to say geographical origin, emitting source or formation process. Before discussing the sources of particles, it is necessary to distinguish between primary and secondary aerosols. Primary aerosols are directly released as particles in the atmosphere. On the other hand, secondary aerosols are formed by gas-to-particle conversion processes from semi-volatile gaseous species or precursor gases through physical or chemical processes.

Concerning sources of particles or their gaseous precursors, two main origins can be distinguished in the atmosphere: natural and anthropogenic sources.

1.1.1.1 Natural sources

The main natural primary aerosols are sea salt particles with contributions that can range from 10% up to 60% (Carslaw et al. 2010), and on average sea spray accounts for half of the natural PM₁₀ (IPCC, 2013) – about 4100 Tg yr⁻¹, which are emitted from the oceans by evaporated sea spray. Mineral dust, originating from arid and semi-arid regions of the world (mainly Saharan and Gobi deserts), is the second important contributor of natural primary particles on average – 2500 Tg yr⁻¹ (IPCC, 2013) and the main contributor in continental regions like South Asia and China. Because mineral desert dust can be transported over thousands of kilometers, it has a global impact. The chemical composition of mineral particles is highly variable and depends on the source region and transport pathways. The main constituents are silicon oxides (SiO₂), carbonates like calcite (CaCO₃) and dolomite (CaMg(CO₃)₂), sulfates, phosphates and iron oxides like hematite (Trochkin et al. 2003). Volcanic dust and biogenic particles (e.g. pollens) are other natural primary particles. All these natural primary particles are mainly found in the coarse mode (i.e. over 2.5 μm) of the aerosol size distribution (see figure 1). Typical natural sources of secondary aerosols are the biosphere and volcanoes that emit sulfur (e.g. in form of dimethyl sulfide, DMS, and sulfur dioxide into the atmosphere) which can be oxidized to sulfate and form sulfuric acid nuclei. These nuclei may then coagulate and grow by water uptake to form small droplets in the accumulation mode. The biosphere can also emit volatile organic compounds (VOCs) that can be oxidized and form new particles, with emissions ranging from 20 up to 380 Tg yr⁻¹ (IPCC, 2013; Kanakidou et al. 2005).

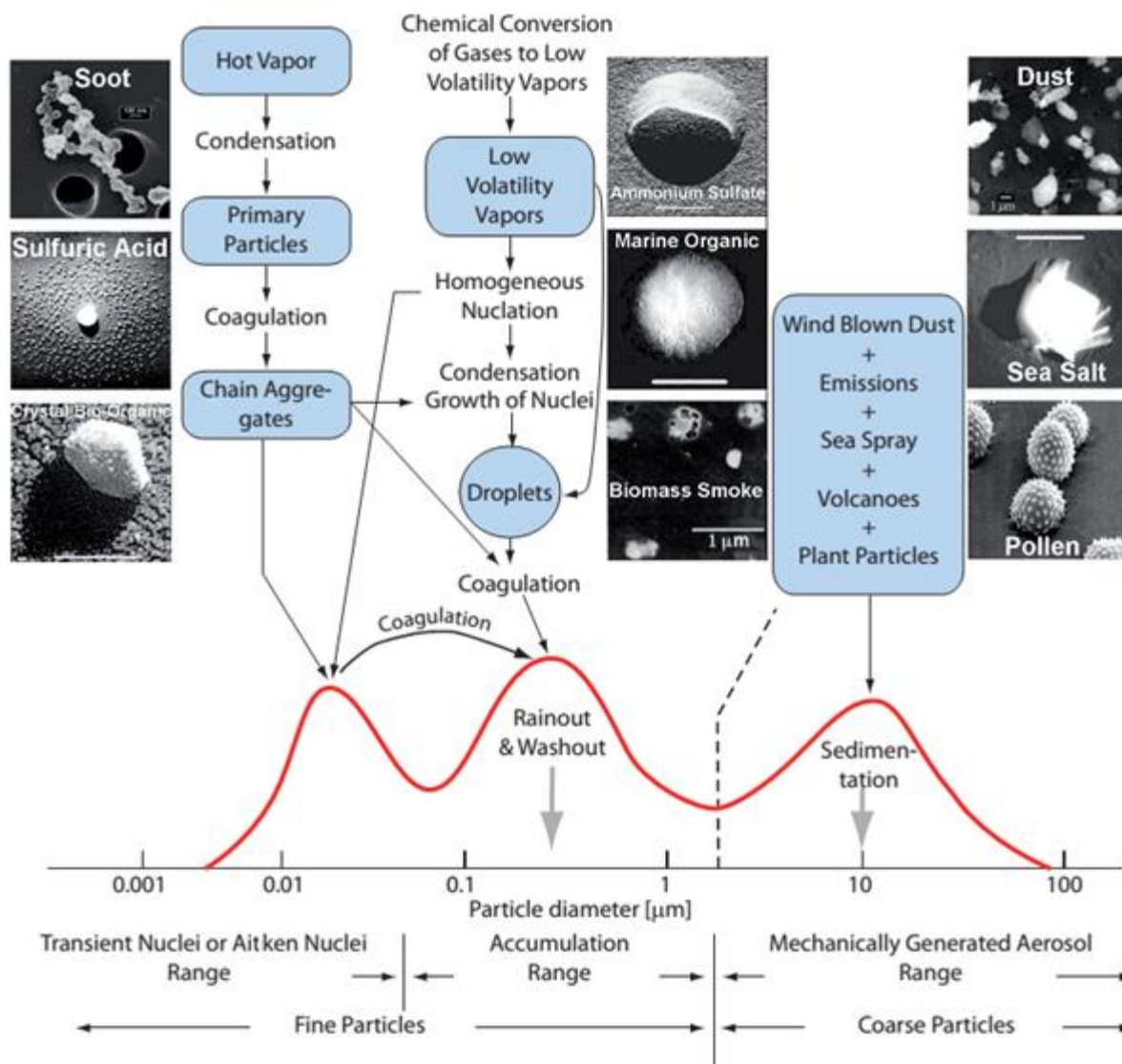


Figure 1: Principal modes, sources, and particle formation and removal mechanisms shown for an idealized aerosol surface size distribution (Zieger 2011)

1.1.1.2 Anthropogenic sources

Anthropogenic emissions of primary particles include black carbon (ranging from 3.6 up to 6 Tg yr⁻¹, averaging 4.8 Tg yr⁻¹ around the globe, according to the IPCC report (2013)) from incomplete combustion and organic matter, which can be the main contributor of anthropogenic emissions in urban areas in the American continent – 20% or more, or around 16% in other regions being the second or third contributor (IPCC, 2013). Dust emissions, although still ill quantified, also have a significant anthropogenic component mainly originating from agricultural and industrial processes and road traffic, with contributions of 20% to 25% of the PM (Ginoux et al. 2012). Secondary aerosol sources of anthropogenic

origin include sulfates from SO₂, nitrates from NO_x and ammonium from ammonia emissions, as well as biomass burning and organics from anthropogenic VOCs. These gases can be emitted, for example, through domestic heating systems based on coal or wood combustion, industrial plants, vehicle emissions and agricultural activities. Although the global emissions are dominated by the natural sources, Seinfeld and Pandis (2006) give an estimate of 3100 Tg yr⁻¹, and more recently IPCC (2013) ranged this emissions from 2920 up to 13000 Tg yr⁻¹, they are mainly related to contributions from the coarse mode, while the emissions from anthropogenic sources (Seinfeld and Pandis, 2006, estimate 450 Tg yr⁻¹) are mainly contributions from the fine mode (with correspondingly higher number concentration). However anthropogenic emissions are mostly seen either in highly populated areas either near them, having a direct effect on inhabitants of these regions.

1.1.2 **PM₁₀ composition**

As mentioned above regarding the main origins of tropospheric aerosols, PM can be classified as primary or secondary aerosols, as previously mentioned. From an analytical point of view, they can also be mentioned as organic or inorganic aerosols. The IPCC report of 2013 on air quality compiled studies where PM was sampled and chemically analyzed, identifying the major components to its mass and their dependence with site typology and region of the world (figure 2).

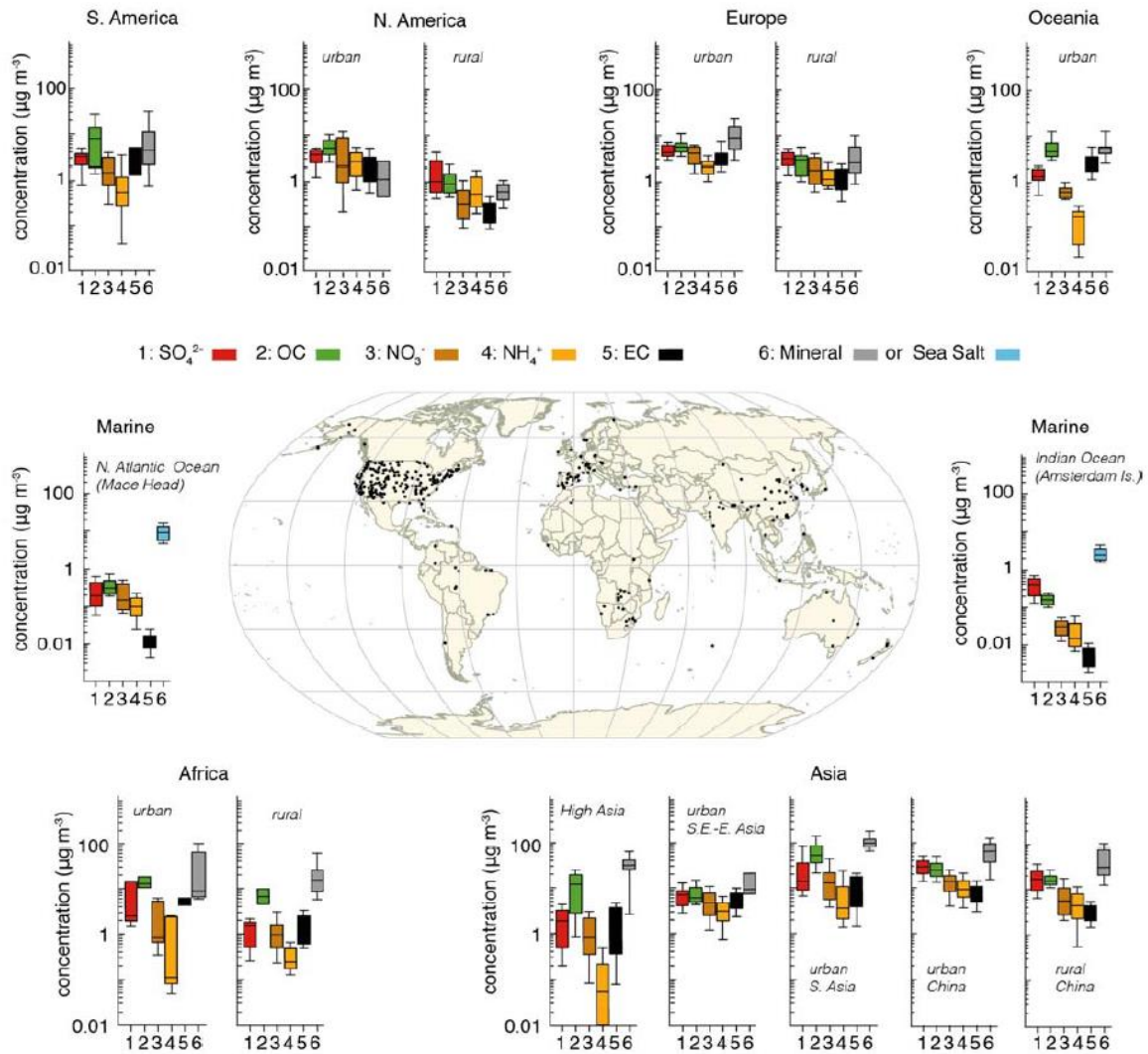


Figure 2: Bar chart plots summarizing the mass concentration ($\mu\text{g m}^{-3}$) of seven major aerosol components for particles with diameter smaller than $10 \mu\text{m}$, from various rural and urban sites (dots on the central world map) in six continental areas of the world with at least an entire year of data and two marine sites (IPCC, 2013)

1.1.2.1 Carbonaceous aerosols

The organic fraction represents a major component of PM, contributing between 20 and 80% of the total mass of PM in urban and industrialized areas (Cheung et al. 2011; Jacobson 2002; Nunes and Pio 1993; Stone et al. 2010). Organic matter (OM) or organic aerosols (OA) can be emitted directly into the atmosphere in the form of particles (POA), or can be formed in the atmosphere due to oxidation reactions of volatile organic compounds (VOCs) followed by gas-particle conversion processes (Seinfeld and Pandis, 2006) forming secondary organic aerosols (SOA). OM mass is not measured directly, but can be estimated by multiplying the measured organic carbon by a determined factor ($\text{OM} = \text{OC} \times \alpha$) to take into account the level

of organic carbon functionalization in the particle (mass of hydrogen and hetero-atoms). This factor has been first estimated by White and Roberts (1977), calculating a ratio of 1.4 for specific organic compounds measured in Los Angeles (USA). Later, Turpin and Lim (2001) concluded that this ratio should be higher than 1.4 and around 1.6 for more urban areas, whereas 1.9–2.3 were suggested for aged aerosols. Unfortunately, there are only a very few experimentally derived conversion factors reported.

The main sources of POA are biomass burning, fossil fuel combustion (industry, domestic, traffic), and wind-driven or traffic-related suspension of soil and road dust, biological materials (plant and animal debris, microorganisms, pollen, spores, etc.), and spray from the sea or other water surfaces with dissolved organic compounds (O'Dowd et al. 2004).

SOA is formed by chemical reaction and gas-to-particle conversion of volatile precursors within the atmosphere. The SOA precursors can be both anthropogenic and biogenic. Current knowledge of precursor emissions and the aerosol formation potential of the individual precursors suggest that SOA formation from biogenic precursors dominates (Andersson-Sköld and Simpson 2001; Mattias Hallquist et al. 2009).

Elemental carbon (EC) is actually a mixture of graphite-like particles and light-absorbing organic matter. Moreover, the surface of EC particles contains numerous adsorption sites that are capable of enhancing catalytic processes (Cao et al. 2004). As the result of its catalytic properties, EC may intervene in some important chemical reactions involving atmospheric sulfur dioxide (SO₂), nitrogen oxides (NO_x), ozone (O₃) and other gaseous compounds (Gundel et al. 1984). On the atmosphere EC is primarily emitted from combustion processes related with anthropogenic activities, such as fossil fuel combustion and biomass burning as house heating method, and naturally also from biomass burning but associated with wild fires. On urban environments, EC is associated with anthropogenic like traffic emissions associated both with exhaust emissions – diesel soot – and non-exhaust emissions – abrasion of tire wearing.

1.1.2.2 Organic tracers

OM contains numerous organic species, including alkanes, alcohols, carboxylic acids, carbonyl compounds, and aromatic compounds, some of which can be used as source, transport, or receptor tracers in conjunction with volatile and inorganic species (B. R. T. Simoneit 1984; B. R. T. Simoneit 1989; Rogge et al. 1996; Schauer et al. 1996). Is then

interesting to understand not only the chemistry associated with PM but also the close connection with between specific species and sources:

- Alkanes (C_nH_{2n+2})

Particulate n-alkanes have been determined in vehicle exhaust (Rogge et al. 1993; Schauer et al. 1999; Schauer et al. 2002), tire abrasion, brake lining dust as well as in road dust (Rogge et al., 1993). They are emitted in natural gas combustion (Rogge et al., 1993), from boilers (Rogge et al. 1997), and are contained in smoke from coal combustion (Oros and Simoneit 2000). The smoke of wood and synthetic logs burning is another source of particulate n-alkanes (Rogge et al. 1998; Schauer et al. 2001; Didyk et al. 2000; Fine, Cass, and Simoneit 2001; Fine, Cass, and Simoneit 2002). A carbon preference index (CPI) has also been commonly used to quantify the relative abundance of odd versus even-numbered carbon chain n-alkanes. It is a key diagnostic parameter in tracking the origin of organic inputs to determine the biogenic and anthropogenic nature of n-alkane sources (Pietrogrande et al. 2010). In particular, anthropogenic emissions from utilization of fossil fuel generate a random distribution of odd vs even terms yielding CPI values close to 1. On the other hand, hydrocarbons originated from terrestrial plant material show a predominance of odd-numbered terms showing $CPI \approx 5-10$ (Cheng et al. 2006; Bi et al. 2005; Cincinelli et al. 2007).

- Anhydrosugars

Anhydrosugars (levoglucosan, mannosan, galactosan) are derived from pyrolysis of cellulose and hemicellulose at high temperatures ($>300^\circ\text{C}$) (B. R. Simoneit et al. 1999). They are better molecular tracers of biomass burning aerosols compared to traditional tracers (e.g. K^+ and BC) because of their single source (figure 3). Levoglucosan presents the higher concentrations. Although it can be degraded in the atmosphere, especially oxidized by OH radicals as reported in some simulation experiments and model studies (M. Hallquist et al. 2009; Hennigan et al. 2010), it is still considered as an ideal tracer for biomass burning due to its relative stability and high emission factors. Levoglucosan has been widely used as a tracer of biomass burning aerosols in many studies in continental and coastal regions (Fraser and Lakshmanan 2000; Xiaolei Zhang, Yang, and Blasiak 2012; Fine, Cass, and Simoneit 2002; Giannoni et al. 2012; T. Zhang et al. 2008; Sang et al. 2011; Křůmal et al. 2010; X. Zhang et al. 2010).

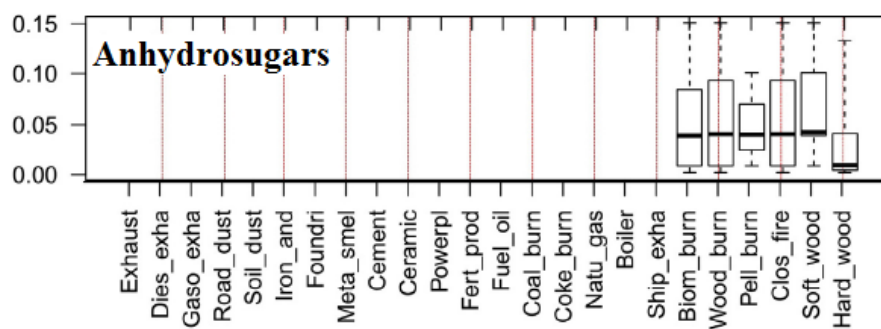


Figure 3: Relative mass concentration of anhydrosugars in PM per source category (adapted from Pernigotti, Belis, and Spanò, 2016)

- Monosaccharides and Polysaccharides

Polysaccharides are complex carbohydrates (sugars), composed of 10 up to several thousand monosaccharides arranged in chains. Monosaccharides like glucose, mannose and galactose are aldohexoses and can form six-membered rings. These compounds are important thermal degradation products of cellulose, and therefore used as tracers for biomass burning activities (Saffari et al. 2013). Also, B. R. Simoneit et al. (2004) suggested that monosaccharides can also be tracers of soil material and associated with microbiota, adding as possible sources other anthropogenic activities like ploughing during agricultural activities (K. E. Yttri et al. 2007). The same study also showed a close relation between the emission of these sugars and ruptured pollen emitted during late spring and early summer, later confirmed by (P. Q. Fu et al. 2012).

- Sugar alcohols

Sugar alcohols are polyols in which the aldose or ketose forms get hydrogenated, keeping the same linear structure as in monosaccharides but with the aldehyde (-CHO) group replaced by an alcohol -CH₂OH group in each unit. Recently, Bauer et al. (2008) suggested that mannitol and arabitol concentrations are correlated with the fungal spore counts in atmospheric PM₁₀. This finding was confirmed by X. Zhang et al. (2010) who measured arabitol and mannitol during April and May 2004 in southern China. These sugar alcohols are common storage substances in fungal spores. Bauer et al. (2008) suggest that using these polyols for spores simplifies sampling, analytical

analysis and evades the need for parallel aerosol collection. Mannitol, although common in fungi, is also a common sugar alcohol in plants; it is particularly abundant in algae and has been detected in at least 70 higher plant families.

- Oxalate

Oxalic acid is the dominant dicarboxylic acid (DCA) in atmospheric PM followed by malonic and succinic acids (Kawamura and Ikushima 1993; Kawamura and Usukura 1993; Yao et al. 2002; Yao, Fang, and Chan 2002), and it constitutes up to 50 - 70% of total atmospheric DCA (Sempéré and Kawamura 1994; Sempéré and Kawamura 1996). Main sources of oxalic acid are thought to be photochemical oxidation of anthropogenic, biogenic and oceanic emissions and/or primary traffic emissions (Kawamura and Kaplan 1987; Kawamura, Kasukabe, and Barrie 1996). Very high concentrations of oxalic acid were detected in biomass burning plumes, suggesting that either oxalic acid is directly emitted or formed in the plume from a biogenic precursor (Jaffrezo, Calas, and Bouchet 1998). Oxalic acid is likely an end-product of the photochemical oxidation reactions and can accumulate in the atmosphere (Chebbi and Carlier 1996; Kawamura and Ikushima 1993). Once formed, it is expected to be very stable and to exist as fine particles. Hence, the major removal mechanism is expected to be wet deposition.

1.1.2.3 Inorganic PM

The inorganic fraction includes mainly the ionic species sulfate (SO_4^{2-}), nitrate (NO_3^-) and ammonium (NH_4^+). Although these species are predominantly from secondary origin, they may also be directly emitted from primary sources such as ship engines (Agrawal et al., 2008) and sea salt (ssSO_4^{2-}). This inorganic water-soluble fraction is generally present in the fine PM fraction as ammonium sulfate ($(\text{NH}_4)_2\text{SO}_4$), and ammonium nitrate (NH_4NO_3), and are formed in the atmosphere from gaseous precursors, such as ammonia (NH_3), nitric acid (HNO_3), and sulfuric acid (H_2SO_4) (Seinfeld and Pandis, 2006). Ammonium nitrate is characterized by its semi-volatility and its presence in the particulate phase depends both on weather conditions and concentrations of its gaseous precursors (NO_x and NH_3).

According to emission inventories, the sources of NH_3 are almost exclusively related to agriculture (livestock, fertilizer use). The major identified sources of ammonia include excreta

from domestic and wild animals, synthetic fertilizers, oceans, biomass burning, crops, human populations and pets, soils, industrial processes and fossil fuels (Bouwman et al. 1997).

HNO₃ is formed in the atmosphere from the oxidation of nitrogen oxides (NO and NO₂), emitted during combustion processes (biomass burning, combustion of fossil fuel) and lightning (S. E. Bauer et al. 2007).

Sulfuric acid is formed from oxidation reactions in the gas or aqueous phases, involving SO₂ emitted directly into the atmosphere by fossil fuels rich in sulfur (oil, coal) and by volcanic activity, or by other sulfur-rich VOCs such as DMS (dimethyl sulfide) emitted by marine sources (Seinfeld and Pandis, 2006).

1.1.2.4 Inorganic tracers

Among the inorganic components of PM, metals are often used as markers of various sources (table 1), which can be found in different size fractions ranging from below 0.01 to 100 µm and larger. Metals such as As, Au, Cd, Co, Cr, Cu, Eu, Fe, Ga, Ni, Mn, Mo, Pb, Se, Sb, V, W, and Zn exist in both the coarse and fine fractions in ambient air. Al, Ca, La, Hf, Mg, Sc, Th, and Ti exist predominantly in the coarse fraction. Metals such as Ba, Cs and Se enrich the fine fraction of PM.

The toxic metals arsenic (As), cadmium (Cd), lead (Pb), mercury (Hg) and nickel (Ni) are mainly emitted as a result of various industrial activities and the combustion of coal. In Europe, their concentrations in ambient air are monitored and regulated (4th Daughter Directive 2004/107/EC). Although the atmospheric concentrations of these metals are generally low, they still contribute to the deposition and build-up of heavy metal contents in soils, sediments and organisms. They bioaccumulate in the environment, causing a long-term poisoning of plants, animals and food chains (EEA, 2016).

Table 1: Main anthropogenic sources of metals in atmospheric particles (source: Riffault et al. 2015)

Sources	Metals
Construction industry (building boards)	Al, Fe, Mn, Si and Ti
Exhaust and non-exhaust emissions (combustion, brake/tire wear, etc)	Ba, Br, Cd, Cr, Cu, Fe, Pb, Sb and Zn
Industrial oil combustion (petrochemistry, refinery and power plants)	La, Ni and V
Energy production	As, Bi, Cd and Hg
Coal combustion	Al, As, Co, Cr, Cu and Se
Metallurgy (steel and non-steel industry)	As, Cu, Fe, Mn, Ni and Pb
Waste incinerators	Cd, Cu, Hg, K, Pb, Sb and Zn

1.2 Impacts and Regulation

The impact of aerosols on the atmosphere is widely acknowledged as one of the most significant and uncertain aspects of climate change projections. The observed global warming trend is considerably less than expected from the increase in greenhouse gases, and much of the difference can be explained by aerosol effects. There is also a growing concern for the impact of aerosols on human health and interest by many sectors such as weather prediction, the green energy industry (regarding their influence on solar energy reaching the ground) and the commercial aircraft industry and military (regarding the impact of PM on visibility and of volcanic ash and dust storms on operations and aircraft).

1.2.1 Climate impact of PM

Aerosols play a significant role in the global energy balance and especially in atmospheric and surface energy balances regionally. A combination of surface direct radiative cooling, atmospheric warming through adiabatic heating, and indirect effects of aerosols on clouds, all contribute to the net aerosol effect. They are represented in modern climate models, yet their magnitudes are highly variable in space and time, and all are highly uncertain.

The term “radiative forcing” has been employed in the IPCC Assessments to denote an externally imposed perturbation in the radiative energy budget of the Earth’s climate system. Such a perturbation can be brought about by secular changes in the concentrations of radiatively active species (e.g., CO₂, aerosols), changes in the solar irradiance incident upon

the planet, or other changes that affect the radiative energy absorbed by the surface (e.g., changes in surface reflection properties). This imbalance in the radiation budget has the potential to lead to changes in climate parameters and thus to result in a new equilibrium state of the climate system.

Anthropogenic aerosols scatter and absorb short-wave and long-wave radiations, thereby perturbing the energy budget of the Earth/atmosphere system and exerting a direct radiative forcing (figure 4).

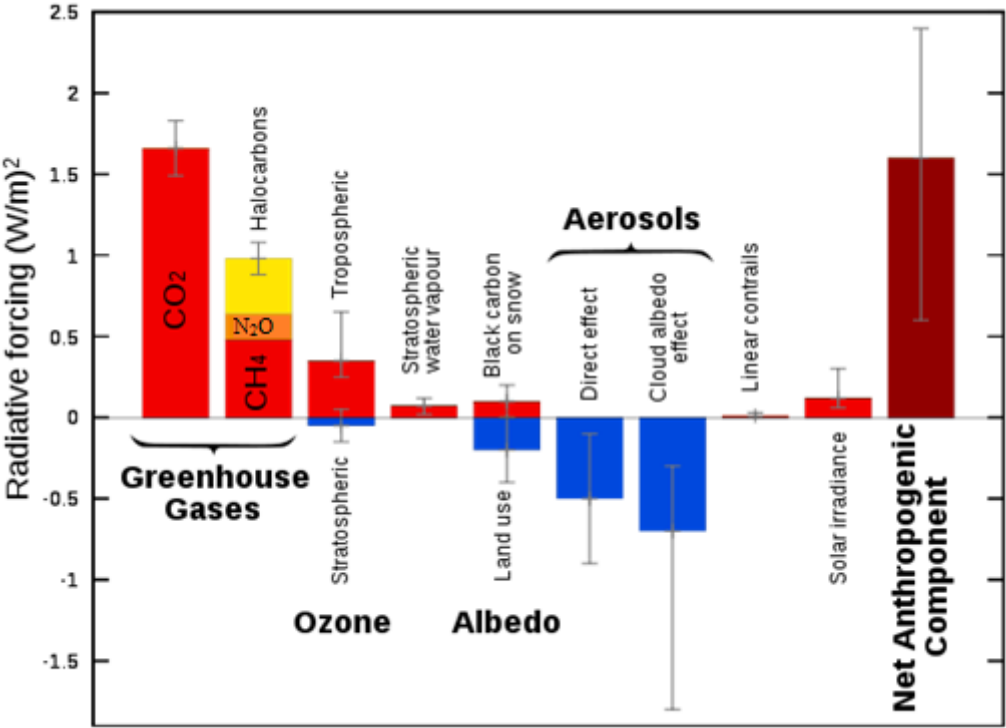


Figure 4: Radiative forcing components (adapted from IPCC Fourth Assessment Report)

Aerosols also serve as cloud condensation and ice nuclei, thereby modifying the microphysics, the radiative properties, and the lifetime of clouds. The aerosol indirect effect is usually split into two effects: the first indirect effect, whereby an increase in aerosols causes an increase in droplet concentration and a decrease in droplet size for fixed liquid water content (Twomey 1974); and the second indirect effect, whereby the reduction in cloud droplet size affects the precipitation efficiency, tending to increase the liquid water content, the cloud lifetime (Albrecht 1989), and the cloud thickness (Pincus and Baker 1994). Finally, it has been also reported a semi-indirect effect of aerosols on the energy budget of the atmosphere linked with the chemical nature of these particles. The presence of light absorbing

compounds (black and/or brown material) leads to an increase of cloud temperature. This increase in cloud temperature then leads to a consequent decrease on the relative humidity of the cloud and increase on the evaporation process of droplets (Lohmann and Feichter 2005).

1.2.2 **Health impact of PM**

PM₁₀ corresponds to the so-called “thoracic convention” (ISO 7708:1995, Clause 6). The 10 micrometer size does not represent a strict boundary between breathable and non-breathable particles, but has been agreed upon for monitoring of airborne PM by most regulatory agencies. Particles larger than about 10 microns are mostly deposited higher up in the respiratory system and removed on the mucociliary escalator and may then be swallowed and subsequently absorbed through the gastro-intestinal tract. Many health effects of PM remain unknown and are estimated by epidemiological studies. These studies have shown a strong correlation between mortality and exposure to PM₁₀ or PM_{2.5}, the mortality being due to bronchial, heart disease or cancer (Analitis et al. 2006; Pope III and Dockery 2006). Indeed, the number of deaths from lung cancer due to exposure to PM_{2.5} represents approximately 11% of total lung cancer (AFSSET, 2005). Furthermore, PM exposure is also associated with the occurrence of diseases such as asthma, chronic bronchitis or chronic obstructive pulmonary disease (COPD) (Sunyer 2001; Liu et al. 2009). Indeed, it appears that a fraction of inhaled particles in the lung persists despite pulmonary clearance mechanisms (Churg et al. 2003). Moreover, the effects of PM are associated with their pulmonary penetrability, PM₁₀ are deposited primarily in the upper alveolar regions while smaller particles penetrate to the airways (figure 5).

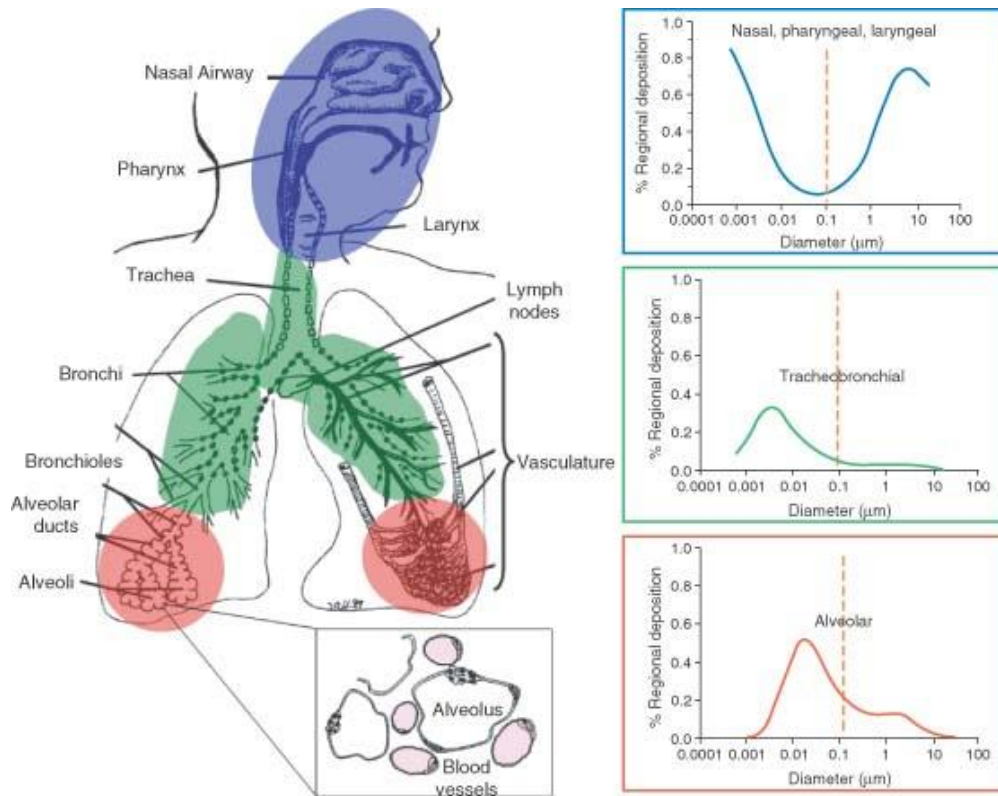


Figure 5: Deposition of particles in the respiratory tract as a function of their size, with inset illustrating the proximity of the air spaces (alveoli) to the vasculature (in pink) (source: Elder, Vidyasagar, and DeLouise 2009)

A recent study (Quan et al. 2010) indicates that $PM_{2.5}$ leads to high plaque deposits in arteries, causing vascular inflammation and atherosclerosis — a hardening of the arteries that reduces elasticity, which can lead to heart attacks and other cardiovascular problems. Nawrot et al. (2011) concluded that traffic exhaust – being responsible of 7.4% of all heart attacks in the general public – is the single most serious preventable cause. Recent studies have shown the influence of PM on short-term morbidity and annual mortality. It was also seen that the toxicity of PM is driven by a complex interaction of size, location, source and season (Lippmann et al. 2013). PM exposure has also shown to have a small but significant adverse effect on cardiovascular, respiratory and cerebrovascular diseases (Anderson, Thundiyil, and Stolbach 2012). The link with specific aerosol sources is also important to understand the ill effects of anthropogenic activities and Kelly and Fussell (2015) suggested that a higher degree of toxicity is associated with traffic-related PM emissions both on fine and ultrafine fractions leading to increased morbidity and mortality from cardiovascular and respiratory conditions.

Penetration of particles is not wholly dependent on their size; shape and chemical composition also play a part. A further complexity that is not entirely documented is how the shape of PM

can affect health. Geometrically angular shapes have more surface area than rounder shapes, which in turn affects the binding capacity of the particles to other possibly more dangerous substances (Nieuwenhuijsen, Gomez-Perales, and Colvile 2007).

Among these dangerous substances, trace elements and aromatic compounds are now considered of paramount importance in the chemistry of the urban atmosphere and for local environmental researches, because of their suspected carcinogenic nature and their abundance in motor vehicle emissions (Monod et al. 2001; Barletta et al. 2005; Sun et al. 2004; Giakoumi et al. 2009). Various trace metals have been investigated regarding their carcinogenic and allergic properties, as e.g. Cd, As, Ni and Pt. For exact risk assessment, it is not sufficient to determine the total concentration of the various trace elements, since their effect on the biological systems strongly depends on their speciation and on the association form with the solid phase to which the element is bound. The bioaccessibility inherent to these metals is also an important characteristic that has to be taken into account. It has been demonstrated that bioaccessibility is completely (but not only) component dependent, ranging from 3.3% for Pb to 92.5% for Zn (Caboche et al. 2011). It has been proven that metal bioaccessibility is also linked with number concentrations and specific surface area and demonstrated that it increased to areas close to emission sources (Mbengue, Alleman, and Flament 2015). In recent decades, it was observed that there has been a growing concern for the potential contribution of ingested dust to metal toxicity in humans (Chirenje, Ma, and Lu 2006; Inyang and Bae 2006). Some trace metals are harmless in low concentrations such as Cu and Zn, but some metals like Pb and Cd are toxic even in extremely low concentrations and are potential cofactors, initiators or promoters in many diseases including cardiovascular diseases and cancer.

1.2.3 **Regulations**

Measurements of particulate matter have been carried out in Europe since many years. During the 80's total suspended particulates were measured, referring to the "Black Smoke OECD" method (Andersen et al. 2007) (Directive 80/779/EC). Studies on health impact assessment of particles have led to the revision of European air quality policy during the 90's. The PM₁₀ and PM_{2.5} fractions of PM, considered as inhalable, were introduced with the publication of Directive 1999/30/EC. In line with the "Clean Air for Europe" strategy of the European Commission to minimize harmful effects of pollution on human health and the environment

and to improve monitoring and assessment of air quality, the measurement of PM₁₀ and PM_{2.5} has been updated by the Air Quality Directive 2008/50/EC. Member States now measure PM_{2.5} concentrations as well on the basis of “common methods and criteria”. The Directive refers to the European Standards EN 12341 (CEN, 1998) and 14907 (Ambient Air Quality, 2005) for the measurement of fine particles in ambient air. Siting criteria are given for sampling locations. Quality objectives are set regarding the accuracy of the measured value and minimum data capture.

A need for quality control and harmonization derives from experience showing that even though common methods and criteria are applied, reported values on PM concentrations may differ considerably. To ensure compliance with the data quality objectives set in the Air Quality Directive, Member States have to establish a quality assurance and control system, as well as a traceability chain in accordance with international guidelines. In addition, institutions designated for QA/QC shall participate in the Community-wide quality assurance programs organized by the Commission.

Currently, under Directive 2008/50/EC, there are 3 different thresholds existing for airborne particles in ambient air:

- PM₁₀ limit value calendar year average 40 µg/m³
- PM₁₀ limit value daily average 50 µg/m³ not to be exceeded more than 35 times a year
- PM_{2.5} target value calendar year average 25 µg/m³

Since 2009 Member States are obliged to evaluate as well an Average Exposure Indicator, a three-year average based upon PM_{2.5} measurements in urban background locations. In fact, a recent study from WHO (2016) estimated that about 80% of people living in urban areas that monitor air pollution are exposed to air quality levels that exceed these limits, with a special impact on low-income cities. Also, the limit values of PM₁₀ recommended by the WHO are still inferior to the ones in practice (20 µg/m³ as an annual average for PM₁₀).

1.3 Source apportionment

Source apportionment (SA) of PM₁₀ aims at identifying and estimating the contributions of the different sources impacting given receptor sites, where data have been recorded (Viana et al. 2008). Its implementation requires the choice of a modeling approach among different

available options. Traditionally source-oriented models were used to estimate contributions, in combination with source emission inventories and the physico-chemical conditions of the atmosphere. The most advanced source-oriented models are deterministic chemistry-transport models (CTMs), which solve both the equations of fluid mechanics for the simulation of pollutant atmospheric transportation and the equations related to the thermodynamics and the kinetics of the atmospheric chemical transformation of pollutants. CTMs are particularly suitable when dealing with reactive species that may be transformed between their emission point and the receptor sites. In addition they are particularly used for running sensitivity analyses to test different strategies of air pollution mitigation and to forecast future trends in atmospheric pollution. Nevertheless, the complex nature of pollutant formation, reactivity and transport, and the uncertainties of estimation and time-variability of emission rates render modeling using CTMs very complex. Therefore, other approaches of SA have been developed, such as the **receptor models** (RMs or receptor-oriented models), based on real observations made at receptor sites, to overcome some of the limitations of CTMs related to the need for an *a priori* exhaustive knowledge of the sources, of the physico-chemical processes occurring in the atmosphere and of the state of the atmosphere (figure 6).

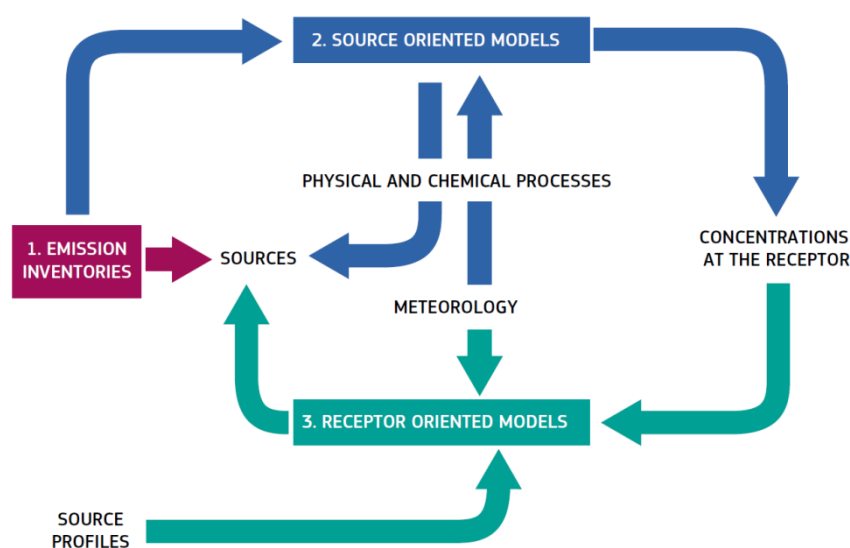


Figure 6: Scheme of the different methods for source apportionment (source: Belis et al., 2014)

Following the definition given by the European Joint Research Centre (JRC), “*Receptor models (RMs) apportion the measured mass of an atmospheric pollutant at a given site to its*

emission sources by solving a mass balance equation” (Belis et al., 2014). The simple mass balance used for identifying and quantifying the sources of ambient air pollutants at a receptor site is independent of the meteorological conditions and emission rates variability but works only on conservative species, *i.e.* on components that do not change their chemical form over time. . Other achievements of RMs are the determination of the chemical signature of sources and the characterization of the mixing process of PM.

Several RMs are being used today towards air quality management. SA techniques use the information on the receptor monitored concentrations and the source emissions to identify the source contributions. Some models that are currently used for receptor modeling are given in figure 7.

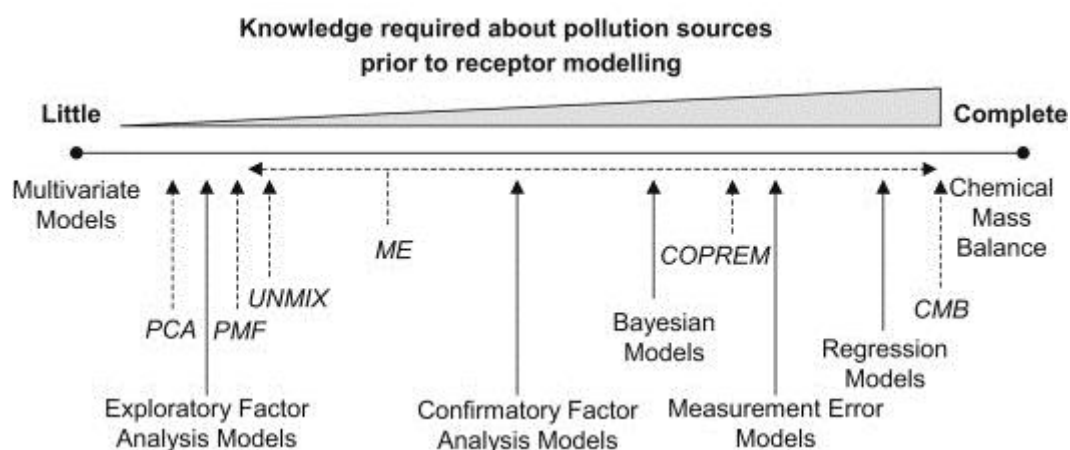


Figure 7: Synthesis of different approaches for estimating pollution source contributions using receptor models (source: Viana et al., 2008)

The fundamental principle of receptor modeling is that mass conservation can be assumed and a mass balance analysis can be used to identify and apportion sources of PM in the atmosphere (Zhao and Hopke 2006). One of the main differences between models is the degree of knowledge required about the pollution sources prior to the application of the mass balance equation. The two main extremes of RMs are, at one end, the chemical mass balance (CMB) model which requires an exhaustive knowledge of all the impacting sources and only one observation, and, on the other end, statistical multivariate models, like the principal component analysis (PCA) which do not require any knowledge on sources but needs a statistically-significant number of measurements of conservative species observed at the receptor site. Although several RMs have been developed and adjusted, all of them present strengths and weaknesses. Many factors like the size of the database, sampling

methodology, time resolution, site selection, uncertainty estimation, among others, may influence the model performance. To overcome the lack of *a priori* information on impacting sources, most RMs will require large datasets, containing multiple observations on several chemical variables that, ideally, should be conservative and specific to given sources. The larger the number of observations, the more likely they might be impacted by the different possible sources. Similarly, the larger the number of chemical variables analyzed, the more likely the different possible sources can be identified through specific associations of tracers.

1.3.1 Source apportionment studies worldwide

Receptor oriented methods have been extensively used for the apportionment of air pollution sources in the last three decades. A study from Karagulian et al. (2015) gathered SA studies covering the period between 1990 and 2014 (year of publication) using the Scopus database and Google search for specific keywords (source apportionment, receptor models, particulate matter (PM), aerosols, PM₁₀, PM_{2.5}). Six categories of main sources of ambient PM, commonly found in SA studies which used RMs and compatible for grouping, have been used for the purpose of this analysis: (1) traffic, (2) industry, (3) domestic fuel burning, (4) natural sources including soil dust (re-suspended), (5) sea salt, and (6) unspecified sources of pollution of human origin. A total of 529 SA studies were collected, with approximately 47 % of these studies carried out just in Europe and 77 % made on an urban receptor site.

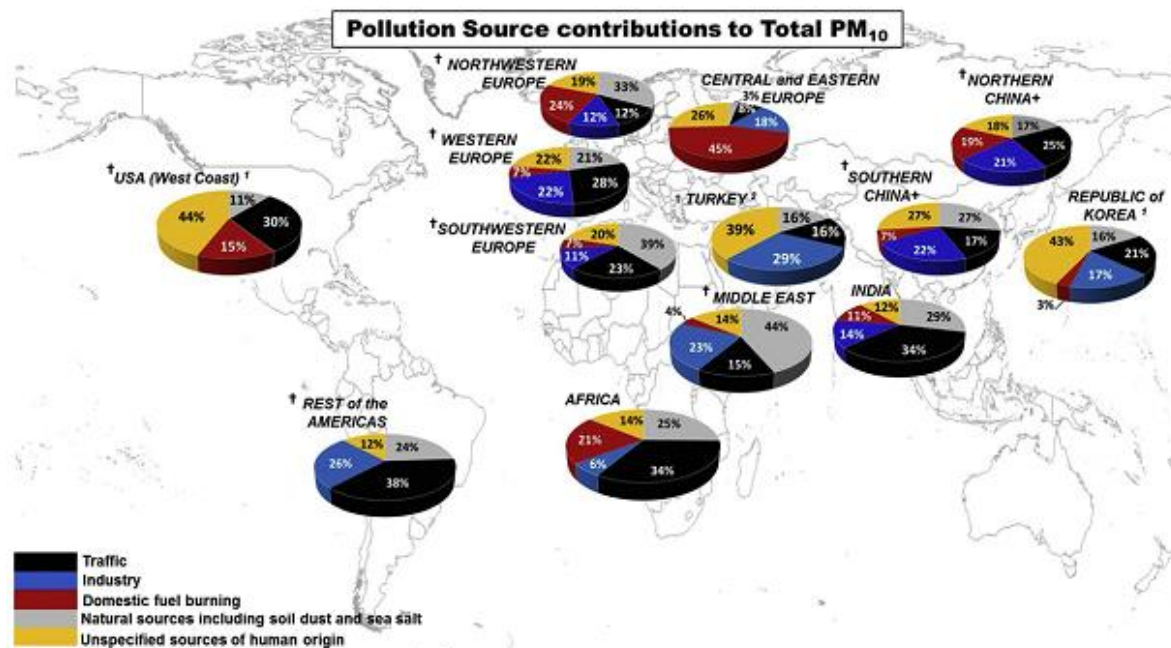


Figure 8: Population-weighted averages for relative source contributions to total PM₁₀ in urban sites (source: Karagulian et al., 2015)

Regarding source contributions across the globe, significant differences can be observed (figure 8). This was expected due to the wide variety of not only PM₁₀ sources but also site typologies, source chemical profiles, emission factors, cultural differences, proximity to specific sources, etc. Traffic appears as one of the main sources to PM₁₀ mass concentration, being the main contributor (on average) in studies carried out in South America, Africa, India, Northern China and Western Europe. Another significant anthropogenic source of PM was industrial emissions, which seem to have special importance in developed and developing countries/regions like South America, the Middle East, Western Europe, China and Korea. Natural sources also appear contributing relevantly in regions like Africa and the Middle East (dust), Northern Europe (sea salt) and Southern Europe (sea salt and dust). In general, unspecified sources of secondary particles showed lower contribution to PM₁₀ rather than PM_{2.5}. This is in line with the evidence that secondary particles occur in the nucleation and accumulation size modes and are therefore assigned to PM_{2.5}. Major contribution of this source to PM₁₀ was found in the USA (44%, based on only one study), Republic of Korea (43%, based only one study), Turkey (39%), and in the Southern China region (27%). In their survey, Karagulian et al. (2015) pointed out some limitations of this kind of approach, regarding unclearly attributed sources. In certain regions the total share of unclearly attributed particles can reach more than 50%, e.g. in North America (Canada) or the Middle East. This

may come from mixtures of primary particles emitted by industrial activities (such as power plants) with particles generated by secondary reactions of precursor gases, attributed to long-range transport emissions that render attribution more difficult. In the Middle East, desert dusts can amount for a large share of fine particles. In addition, there is a lack of information referring to source tracers that is to say to specific chemical compounds that permit identification of unique pollution sources.

1.3.2 Source apportionment in Northwestern Europe

According to the review of PM₁₀ SA studies gathered by Karagulian et al. (2015), it appears that Northwestern Europe presents the lowest average PM₁₀ mass concentration of all the regions considered (figure 9). Its main contributing sources seem to be related with domestic emissions (biomass burning) and natural sources (sea salt), the unspecified anthropogenic sources being at the third place.

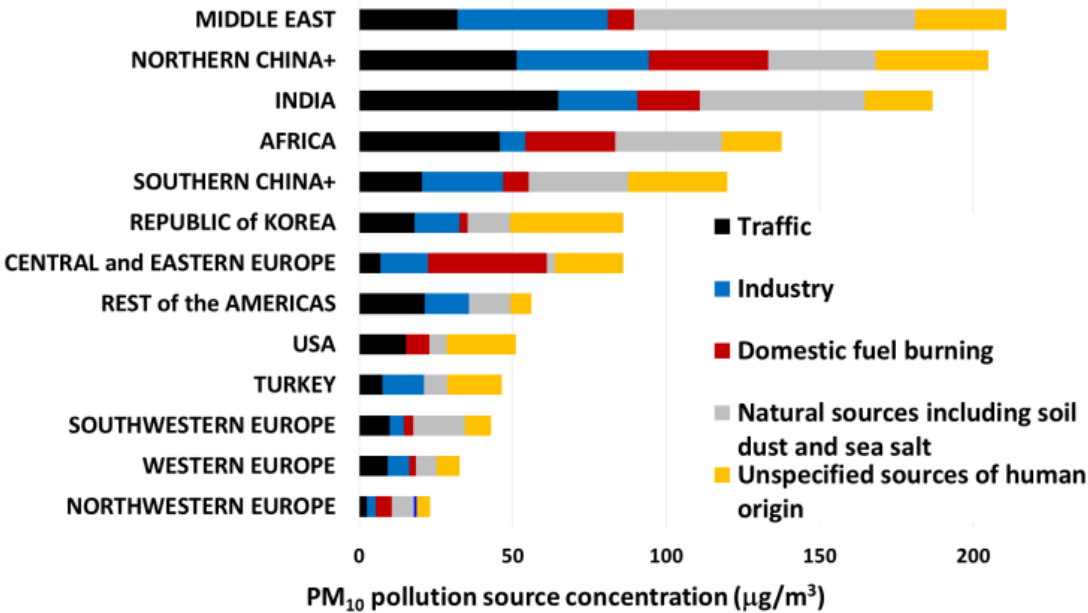


Figure 9: Absolute contribution to total PM₁₀ by region and source category (source: Karagulian et al., 2015)

To better understand the scope of these results it is important to detail some aspects of the different methodologies used in the gathered studies (table 2).

Table 2: WHO database on local source apportionment studies of particulate matter in air. The studies performed with PMF are highlighted in green (source: WHO)

COPREM (Constrained Physical Receptor Model), PMF (Positive Matrix Factorization), PCA (Principal Component Analysis), APEG (Airborne Particles Expert Group receptor model), CMB (chemical mass balance

Site location (Country)	Site typology	Method	Time period	Number of sources	Period	Reference
Copenhagen (Denmark)	urban	COPREM	2002-2003	5	year	Andersen et al. (2007)
Copenhagen (Denmark)	urban	COPREM	2005-2007	5	year	Wählén (2003)
Virolahti (Finland)	rural	PMF	2007-2008	2	year	Vestenius et al. (2011)
County Cork (Ireland)	industrial	PCA	2005-2006	4	year	Byrd, Stack, and Furey (2010)
County Cork (Ireland)	rural	PCA	2005-2007	3	year	
County Cork (Ireland)	urban	PCA	2005-2006	4	year	
County Cork (Ireland)	urban-coastal	PCA	2005	4	spring	
Mace Head (Ireland)	remote-coastal	PMF	1988-1994	2	year	Huang, Arimoto, and A. Rahn (2001)
Lycksele (Sweden)	urban	PMF	2006	3	winter	Krecl et al. (2008)
Stockholm (Sweden)	urban- traffic	PMF	2003-2004	4	year	Furusjö, Sternbeck, and Cousins (2007)
Stockholm (Sweden)	urban- traffic	PMF	2003-2004	4	year	
Belfast (UK)	urban	APEG	2002	4	year	DEFRA (2005)
Birmingham (UK)	urban	APEG	2002	4	year	
Birmingham (UK)	rural	CMB	2007-2008	4	year	Yin et al. (2010)
Birmingham (UK)	urban	CMB	2007-2008	4	year	
Bury (UK)	urban- traffic	APEG	2002	4	year	DEFRA (2005)
Glasgow (UK)	urban	APEG	2002	4	year	
Haringey (UK)	urban- traffic	APEG	2002	4	year	
Harwell (UK)	rural	APEG	2002	4	year	
London Bexley (UK)	urban	APEG	2002	4	year	
London North Kensington (UK)	urban	APEG	2002	4	year	
M25 Staines (UK)	urban	APEG	2002	4	year	
Manchester Piccadilly (UK)	urban	APEG	2002	4	year	
Marylebone Road London (UK)	urban- traffic	APEG	2002	4	year	
Port Talbot (UK)	urban-industrial	PMF	2012	4	spring	
Thurrock (UK)	urban	APEG	2002	4	year	DEFRA (2005)

It appears that the countries used to characterize PM₁₀ pollution in NW Europe were Denmark, Finland, Ireland, Sweden and the United Kingdom, representing only about half of the area and one third of the population, while Belgium, Germany, the Netherlands and France were not taken into account. Table 2 also shows the SA methodology employed; out of the 25 sites where PM₁₀ SA studies were carried out, only 6 used PMF, and only 4 were at least one year long. Interestingly, in these latter studies, the number of sources increases with the density of population, from 2 at remote/rural sites to 4 at urban/traffic ones, as more sources are present and identified, but nevertheless the number of identified sources remains low. It is then important to gather more information concerning PM₁₀ concentrations and sources in NW Europe, through long-term studies and different typologies of sites. Results obtained from recent studies performed in the North of France, UK and Benelux countries are presented hereafter.

A relevant study was coordinated by the regional air quality monitoring network AIRPARIF on the sources of PM_{2.5} in the Paris basin. A latest report issued about impacting sources (AIRPARIF, 2012) was based on 6 sampling sites and emission inventories obtained from the European Monitoring and Evaluation Program (EMEP), identifying 8 possible source groups: energy, industry, residential, crustal, traffic, transported, agriculture and natural sources. The source contribution to PM_{2.5} measured at a traffic site where the importance of local traffic-related emissions, mainly exhaust ones, was visible showed a large contribution of transported particles (nearly 40 %), where secondary inorganic aerosols appear as the main contributors for this fraction.

Using EPA PMF3.0, Bressi et al. (2014) found 7 sources of PM_{2.5} at an urban background site in Paris investigated during 1 year in 2009-2010: ammonium sulfate-rich factor (27% of the PM_{2.5} mass on an annual average basis), ammonium nitrate-rich factor (24%), heavy oil combustion (17%), road traffic (14%), biomass burning (12%), marine aerosols (6%) and metal industry (1%) were identified. In this study, secondary inorganic aerosols appeared as the major yearly contributor of fine aerosols, predominately associated with imported particles.

To the north of Paris (180km), a PMF SA study was held in the French city of Lens, on sampled PM₁₀ at an urban site, between 2011 and 2012 (Waked et al. 2014). A PMF solution of 9 factors was found (figure 10). A clear seasonal pattern of PM₁₀ concentrations was observed, with maximum concentrations in spring ($29 \pm 13 \mu\text{g}/\text{m}^3$) and minimum

concentrations in summer ($14 \pm 13 \mu\text{g}/\text{m}^3$). During the summer season the contribution of primary biogenic emissions, identified through the chemical analysis of specific tracers (polyols), increases and accounts for about 20 % of the total PM_{10} mass concentration at the same time that the secondary nitrate factor decreases due to the thermal instability of ammonium nitrate (figure 10). In winter, the biomass burning source is the major contributor accounting for 25 % of the total PM_{10} mass concentration, related to the use of wood combustion for domestic heating whereas the contribution of primary biogenic emissions are largely decreasing (less sunlight and more rainy days).

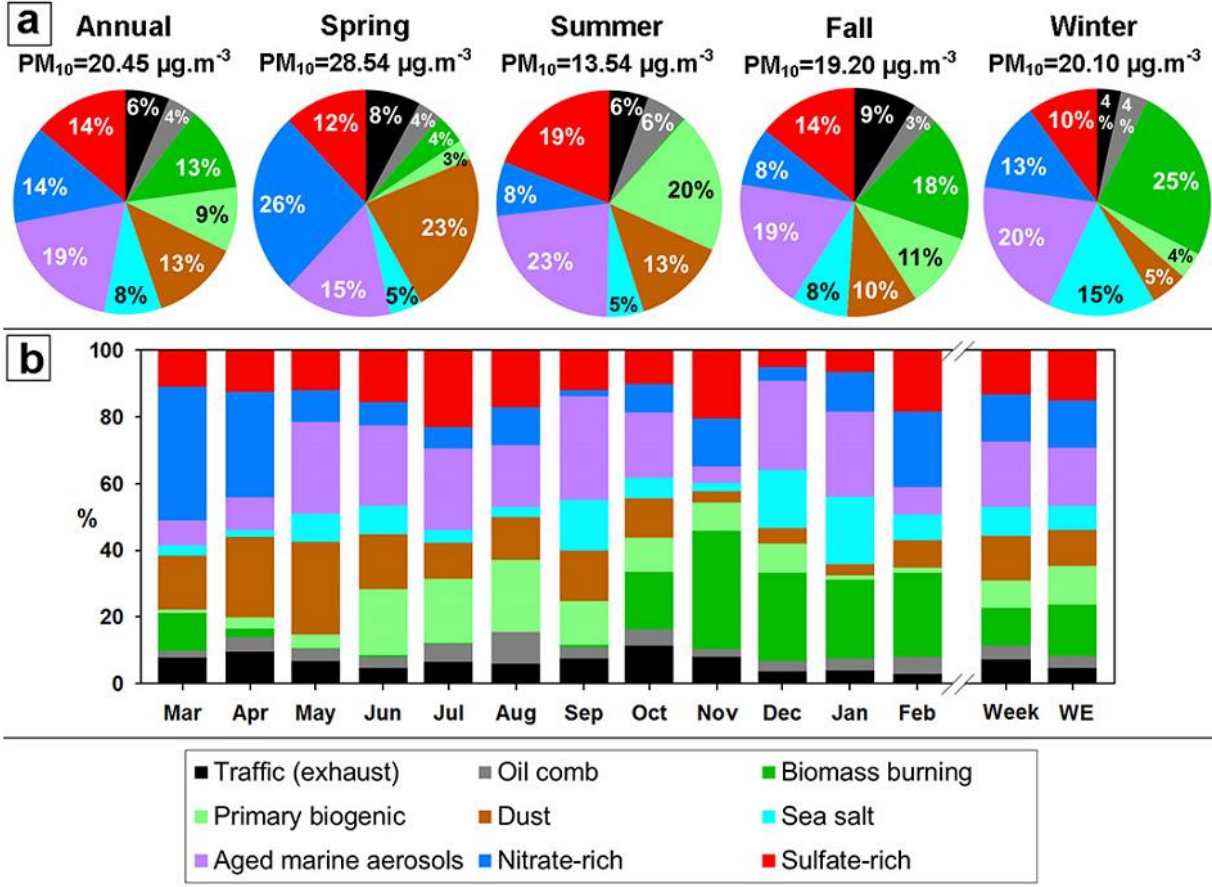


Figure 10: Contributions of the identified sources in % to total PM_{10} mass concentration for the full year and according to the seasons (a) and on a monthly basis along with weekdays-to-weekends variations (b) (source: Waked et al., 2014)

To the northeast of Lens, a study carried out in the region of Flandres (Vercauteren et al. 2011b), collected PM_{10} samples during one year (September 2006 to September 2007) at 6 sampling sites with different typologies. Results identified a large contribution of secondary aerosols for PM_{10} mass, followed by organic matter and crustal matter. The average chemical composition of aerosols showed little variability between the sites, with the main differences

seen mainly in specific tracers with low contribution to PM_{10} . However these differences, affecting mainly crustal matter and elemental carbon, highlight the contribution of local sources and the potential to implement measures to mitigate these values. With data from the same work, the impact of agricultural activities and their contribution to secondary aerosols was also studied (Buekers et al. 2014). With intense agricultural activities, this region comports more than 25000 companies cultivating more than 610000 hectares of land. In fact, Deutsch et al. (2010) attributed a contribution of 54% of agricultural processes to PM_{10} mass in the Flemish region in 2007. Buekers et al. (2014) attributed a large contribution of ammonia to PM_{10} mass concentration derived from this activity sector and its increased impact during favorable meteorological conditions. However, a more recent study (Hendriks et al. 2016) showed that no significant differences in PM concentration would be seen if ammonia emissions were reduced up to 75% during high concentration episodes, and this was attributed to the emission potential of vegetation if concentrations of ammonia in it are high and air concentrations are low due to manure processes.

An important recent study in NW Europe is the JOAQUIN project which aims at improving air quality in the Northwestern European region with partners in Belgium, France, the Netherlands and the United Kingdom. During one year, samples were collected and chemically characterized and a recent report (Staelens et al. 2016) was issued concerning PM_{10} values and sources in the region.

A SA exercise was also performed using the EPA-PMF 5 software. A total of 8 sampling sites located in 5 cities were selected (2 in Amsterdam-NL, 2 in Antwerp-BE, 2 in Leicester-UK, 1 in Lille-FR and 1 in Wijk ann Zee-NL). The authors performed a multi-site PMF analysis, *i.e.* applied the PMF model on all the different sites simultaneously. A total of 13 factors were found: nitrate-rich, sulfate-rich, road dust, aged marine, sea salt, mineral dust, biomass burning, traffic, break wear, metal chemical processing (Cr), residual oil combustion, steel industry (Fe) and metal industry (As, Cd, Pb) (figure 11). Secondary aerosols (nitrate-rich and sulfate-rich) were seen to be the main contributors to total PM_{10} mass concentration (44% on average), where sea spray-related particles and resuspended road dust particles also appeared having significant contributions (16% and 12% respectively). It is also important to point out that contributions generally varied from one site to another; in fact, only secondary aerosols, sea spray and mineral dust showed standard deviations below 50% of the average contribution. Interestingly enough, these are precisely the sources that can be considered to have a regional influence over all the sampling sites.

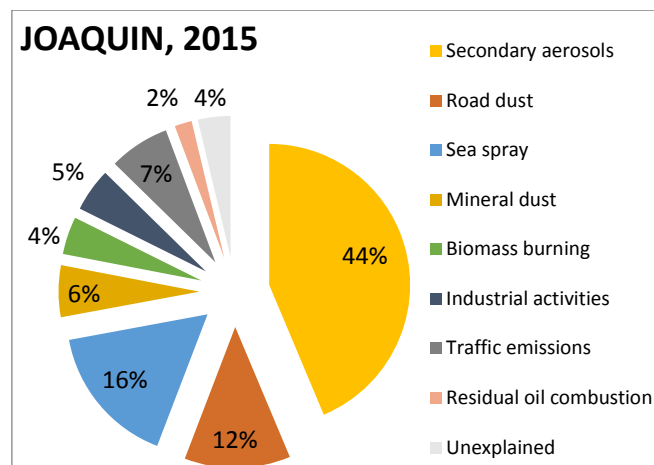


Figure 11: Average source contribution during the JOAQUIN project

In the same region, biomass burning contributions were assessed by sampling PM_{10} and measuring specific markers of this source (levoglucosan, mannosan and galactosan) at 7 sampling sites also with different typologies during one year (February 2010 to February 2011) (Maenhaut et al. 2012). Findings suggested a possible regional influence of biomass burning particles across the region and with a clear seasonal pattern associated with the source, more present during cold periods (mainly winter). These findings were later updated (Maenhaut et al. 2016) by applying PMF to datasets from 4 sampling sites and quantifying the contribution of the biomass burning factor here identified. It was seen that the conversion factor of Levoglucosan to estimate biomass burning OC contributions based on Schmidl et al. (2008) fall short on predicting the impact of this source in PM_{10} mass concentrations and proving the usefulness of receptor oriented models on quantifying a more accurate impact of sources.

A study by Mooibroek et al. (2011) showed the differences of chemical composition of aerosols in the Netherlands. An intensive one-year measurement campaign (from August 2007 to September 2008) was performed at five locations, consisting of three rural background sites, one urban background site and one kerbside site. A seven-factor solution was found. The importance of long-range transport into and across the monitored area was reflected in the small spatial variability. The nitrate-rich secondary aerosol factor also showed a relatively small spatial variability on average. As expected for more local sources, a spatial variability was found for the traffic factor as it reached a 21% contribution in Rotterdam (kerbside site) compared to a 5% contribution in Hellendoorn (rural site) for a 10%

contribution on average. Therefore the main advantage of using various receptor sites in the same SA study lies on the possibility to identify local and long-range sources. For local sources, a big spatial variability is expected, depending on the geographical position of the sampling site and its proximity to specific pollution emitters.

Finally, another transboundary study (Weijers and Schaap 2013) conducted from a combined period of 2 years in 8 sampling sites in Belgium, the Netherlands and Germany showed considerable conformity on the chemical composition of measured PM₁₀. Secondary inorganic aerosols were seen to be the main contributors to PM mass (around 40% on average) on the sampling sites, followed by carbonaceous compounds (around 25%). Sea salt particles were responsible for 5% to 16% of PM, in direct relation with the distance of the sampling site to the coast and the wind speed associated with each daily contribution. In the 3 countries, urban sites constantly reported higher concentrations of PM₁₀ and their main species, with differences being clearer for SIA, mineral dust and EC. An effort to distinguish between natural and anthropogenic sources was made, identifying sea salt as the only 100% natural source. A range of 25% to 50% of OC was associated with natural sources, whereas for the main ions (nitrate, sulfate and ammonium) just 0 to 10% was linked to natural sources. From a source apportionment exercise which allocated each species individually, nitrate was predominantly linked with power generation processes, residential combustion and transport, sulfate with power generation as well, industrial and transport industries and ammonium with agriculture activities. In this study was also suggested that the increment seen for nitrate and sulfate in urban areas could be associated with the reaction nitric acid and sulfuric acid from local sources with sea salt arriving in urban areas – chloride depletion with nitrate and sulfate in coarse mode.

As seen, both regional and local emissions of PM appear to contribute studied sites in this region and, in addition to being submitted to multiple sources with seasonal variations, NW Europe is also frequently impacted by transient long-range transport episodes of anthropogenic pollutants, particularly from Central and Eastern Europe, which episodically increases PM₁₀ concentrations in ambient air above regulated limit values. In the case of the particulate pollution of the Paris megacity, Bessagnet et al. (2005), in their study using a CTM approach of the origins of PM₁₀ pollution episodes in wintertime, found that most of these episodes have a continental origin, and that this outside contribution reaches up to 50% of the PM₁₀ mass, while during non-episode situations the contribution drops down to 20%. Recently, Beekmann et al. (2015) demonstrated that the PM peak levels recorded in Paris

were predominantly from a regional origin (about 70% of fine PM) with mainly secondary aerosols made of sulfate, nitrate and organics of modern origin (from biogenic precursors and wood burning). Similarly in the study led in Lens (Waked et al., 2014), the main sources contributing during exceedance episodes were seen to be essentially secondary aerosol based. Nitrate rich and sulfate rich recorded a combined contribution of 54% for total PM, an increase when compared with the annual average of 29% for these sources.

1.4 Geographical location of sources

Determining the geographic origin of particles on a given sampling site is a complex task that has to take into account several phenomena such as transport, chemical and physical transformation of particles, and deposition. Such an exercise can then allow associating particle chemical characterization with local sources or long-range transport processes. It aims also at guiding public authorities towards more efficiently oriented PM abatement policies. According to Charron et al. (2013), there are essentially two ways of gaining a better understanding of the geographical distribution of aerosol sources impacting a given receptor site: the most frequently used CTMs and alternative statistical RMs which use backtrajectories of air masses.

Several studies have been published on the analysis of air mass backtrajectories to help detecting the long-range transport of pollutant air masses that may have an impact on local PM₁₀ levels (Salvador et al. 2008), to better describe the related tropospheric circulations (Jorba et al. 2004) or to characterize and identify spatial and temporal trends of pollutants (Coury and Dillner 2007). Backtrajectories are provided by suitable dispersion models (Stohl 1998). Usually several trajectories are calculated for each day for backward trajectory periods of 3 or 4 days (Belis et al., 2014). Large numbers of trajectories arriving at a given site can be analyzed in order to determine the origin of the polluted air masses. Several authors performed cluster analyses in order to place trajectories into a relatively small number of groups (Dorling, Davies, and Pierce 1992; Dorling and Davies 1995). Such procedures have been frequently used to interpret the origin and transport of atmospheric pollution (Vardoulakis and Kassomenos 2008; Li et al. 2012).

Based on backtrajectory analysis, source areas of long-range PM₁₀ transport can be identified, such as mineral dust. Escudero et al. (2007) and Cabello et al. (2012) found African origin

dust episodes over Eastern Spain. Karaca and Camci (2010) established that the central part of Northern Africa (Northern Algeria and Libya) is the most significant potential PM₁₀ contributor to Istanbul atmosphere during springtime. Grivas, Chaloulakou, and Kassomenos (2008) traced back some severe dust outbreaks in the air of Athens, Greece, back to the Saharan desert and the Western Mediterranean. Makra et al. (2011) detected an occasional appearance of North African origin dust even over Hungary, the middle latitudes of the temperate belt.

Models based on PM concentrations associated with external information such as backtrajectories are commonly referred to as Hybrid Receptor Models (Han, Holsen, and Hopke 2007) or Trajectory Statistical Methods (TSMs) (Kabashnikov et al. 2011). By dividing the studied area into grid cells where the air mass residence times are calculated, these TSMs aim at apportioning PM levels measured at the receptor site to the trajectory segments, enabling to plot maps where the potential source areas impacting the receptor site are visible. There are several variations of TSMs that have been applied to characterize atmospheric PM (Zhou, Hopke, and Liu 2004), differing in the metrics employed to attribute trajectories to grid cells, and the metrics calculated from the gridded results (Poirot et al. 2001). Among them the most used are: Concentration-Weighted Trajectory (CWT), Concentration Field (CF) (Seibert et al. 1994) and Potential Source Contribution Function (PSCF) (Ashbaugh, Malm, and Sadeh 1985). The CWT and CF methods assign the concentrations observed at the receptor site to corresponding backward trajectories, by calculating for each grid cell the residence time of air masses weighted respectively by the arithmetic (CWT) or the geometric (CF) mean concentration of the pollutant observed at the receptor site. The PSCF method links residence time in upwind areas with high concentrations through a conditional probability field, defined as the ratio of high-concentration endpoints to all data endpoints in each grid cell. Lupu and Maenhaut (2002) made an intercomparison of CF and PSCF and found that they agreed well with each other. Kabashnikov et al. (2011) made an intercomparison of CWT, CF and PSCF based on artificially generated datasets and again found that these three methods were all able to give a first valuable hint on potential source areas.

1.5 Objectives of the thesis and scientific strategy

As identified on this first chapter, PM studies are more and more being put in place to characterize and improve air quality standards worldwide. However, most of these studies show serious practical limitations that compromise the extent of the results obtained. These limitations are common and can be linked with several factors: a non-complete chemical speciation of collected samples, leading to an incomplete knowledge of the potential health and environmental impacts of PM; with the limited regional representation that single sampling sites studies offer, that are often directly impacted by close anthropogenic emissions and therefore neglecting potential regional contributions; single site studies also mean that less data will be available, limiting statistical approaches used for apportioning PM sources.

1.5.1 Objectives of the thesis

European countries are still facing trouble to comply with regulation concerning PM₁₀ limit values in order to improve air quality. Understanding the chemistry associated with these particles allow not only to study their human health effects but also to understand their origin, their sources and their emission profiles. Providing detailed information on possible PM₁₀ sources impacting a certain sampling site, city or region allows policymakers to better tackle this issue with efficient measures. This PhD work is inserted within a large program (CARA program) and focuses on the sources of PM₁₀ impacting the north of France, a region recurrently seen to experience high concentration of pollutants derived from its geographical position, topographical characteristics, densely populated urban areas and intense industrial activities.

This study aims at answering the following questions:

- What is the chemical composition of PM₁₀ particles collected on the 5 sites? How this chemical composition varies with time and from site to site?
- What are the sources contributing to PM₁₀ on each site? How do these sources vary with time and from site to site?
- What is the scale of impact of these sources? What are the local and the regional sources impacting the north of France?
- What is the geographical location of these sources?

Handling a database from a network of 5 different sampling sites, this work expects to improve the knowledge on the main sources of PM₁₀ impacting the north of France. Based on a complete chemical characterization, a representative description of the influence of site typology to PM levels is possible, as well as source apportionment exercises to assess the regional or local nature of collected particles. Furthermore, the geographical location of regional sources can be estimated based on extensive data compiled with trajectory based models.

1.5.2 Scientific strategy

To answer these questions, this work was based on PM₁₀ samples collected at 5 sampling sites every third day during 18 months and analyzed following the same protocol for all sites in order to obtain comparable results. The sites presented different typologies but were all located in the same region (the north of France). The chemical characterization of a large number of chemical compounds allowed a near-to complete knowledge of the chemical composition at each site, which were studied and validated individually, its trends analyzed and characterized. The average and seasonal chemical composition for each site was assessed and compared with previous results when available. Exceedance episodes were also analyzed, characterized and compared between sites. Knowing the chemical composition of PM₁₀, a receptor-oriented statistical method was first applied (PMF) at each sampling site individually to identify the sources and ensure the best mathematical source description. These sources were identified and characterized for all sites, their average and seasonal contribution studied and their importance to high concentration episodes assessed.

The daily contributions of each source at each site were then combined with meteorological information measured at (or nearby) the sampling site like wind speed and wind direction. Local sources, assumed to be associated with lower wind speeds were then linked with possible close emitters in the surroundings. Sources associated with high wind speeds were assumed to have long-distance geographical origins and a potential regional influence. These sources were then compared between sampling sites to assess the extent of possible local inputs to each one and then applied on a trajectory statistical method (CF) together with computed backtrajectories of air masses arriving at each sampling site. Concentration field maps were calculated for each regional source individually and on a multi-site scale to better predict the geographical origins of these long-range transported particles.

CHAPTER 2

PM₁₀ CHEMICAL SPECIATION: MEASUREMENTS AND RESULTS

CHAPTER 2 - PM₁₀ CHEMICAL SPECIATION: MEASUREMENTS AND RESULTS

2.1 The CARA program

The CARA program (chemical characterization of particles) has been created in 2008 to better understand the origins of particulate pollution episodes in France, highlighted by PM₁₀ limit value exceedances in spring 2007. It is managed by the French national reference laboratory (LCSQA), and involves regional air quality monitoring networks (AASQA) as well as research laboratories (LSCE, LGGE, LCME, LCP-IRA, and SAGE). Historically based on the chemical speciation of airborne particles collected on filters at 6 sites, this program now includes offline and online measurements at up to 20 stations (figure 12), with the following objectives:

- Identify the main sources of PM₁₀ in urban environments, to help developing appropriate action plans.
- Optimize the PREV'AIR modelling system (Rouil et al. 2009), through comparison exercises between measurements and model outputs, to allow a better forecast of PM pollution episode.
- Provide technical and scientific support to AASQA in implementing PM chemical speciation campaigns.
- Review methodologies and projects conducted at the national level to better understand the chemical properties of aerosols, their sources and formation mechanisms.
- Report the French expertise within European standardization programs.



Figure 12: Sampling sites involved in the CARA program in 2014

PM₁₀ samplings are performed in "pseudo-continuous" mode, i.e., 4 to 6 days a week, alternately with mandatory PAH monitoring. Only a small fraction of these filters are actually analyzed to investigate selected pollution episodes or to conduct yearly source apportionment studies. More information on this program can be found in LCSQA reports (e.g., Pla, 2016).

The present work is taking advantage of the CARA program, allowing a comprehensive source apportionment study at the 5 sites located in Northern France.

2.2 Sampling sites

Spread across the North of France (figure 13), the chosen sampling sites allow not only a wide coverage of the region, but also to study the influence of different sources at each site and at a regional scale. Indeed, these sites are of different typologies: urban background (3), traffic (1) and remote (1), in order to investigate various emission sources and to observe regional influences of long-distance transformation processes and their interactions with local inputs. In addition, the geographical location of these sites allows for the PM characterization along the predominant wind direction, from south-west to north-east, and along the perpendicular north-west to south-east direction which corresponds to a decreasing maritime influence. All the five sites are characterized by having an oceanic climate, with continental

influences for the site of Revin. The region usually records cold temperatures during winter and mild summers and raining events are frequent as well.

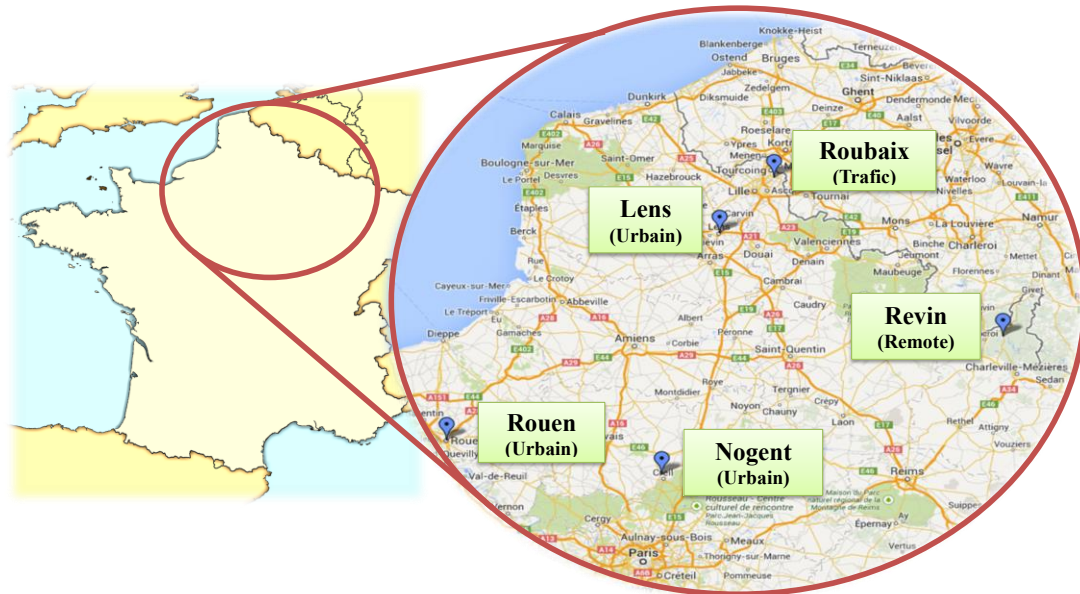


Figure 13: Geographical location of the sampling sites of this work

2.2.1 Lens (urban site)

The city of Lens (32 000 inhab.) is actually part, with the nearby city of Douai, of a larger conurbation of about 500 000 inhabitants located in the former coal mining area of the North of France. It is surrounded by other large populated urban areas, including the conurbations of Lille (~ 1 million inhab.), Béthune (~ 200 000 inhab.) and Valenciennes (~ 350 000 inhab.).

Road transport emissions should be considered, with several busy highways (A1, A21, A26) passing through this North-South transit region. In addition, many petrochemical, metallurgic, and non-metallurgic industrial companies are located in the coastal zone or dispersed in the region. Being a densely-populated area (2705 inhab./km²), it is also influenced by domestic emissions, including residential wood burning (ATMO Nord Pas de Calais, 2009).



Figure 14: Geographical location of the sampling site in Lens

The sampling site used in this study ($50^{\circ} 26' 13''$ N, $2^{\circ} 49' 37''$ E, 47 m above sea level, a.s.l.) corresponds to a monitoring station of ATMO Nord Pas-de-Calais located in the vicinity of a stadium (figure 14).

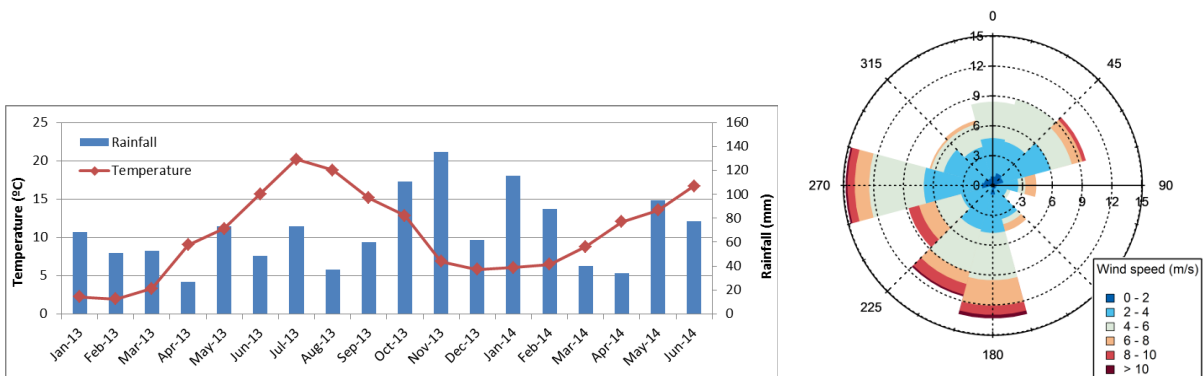


Figure 15: Meteorological data for the site of Lens (temperature and rainfall in the left and windrose in the right)

Lens climate is considered to be oceanic. Due to the distance to the sea (80 km), the oceanic character of its climate is less marked than on the coast. Low temperatures are seen during winter (4°C on average) and mild in summer (18°C). During the sampling period (Jan13 - Jun14) the average registered temperature was 10.4°C , the lowest daily average temperature recorded was -9.2°C and the highest 26.5°C .

Additional information, such as wind direction and wind speed, was gathered from the closest MétéoFrance station, located in Lesquin-Lille, approximately 25 km to the Northeast of the

sampling site. Figure 15 illustrates that higher wind speeds are predominately originated from the West-South quadrant.

2.2.2 Nogent-sur-Oise (urban site)

Nogent-sur-Oise (18 000 inhab.) is located in the south of the department of Oise, 48 km north of Paris megacity (~12 million inhab.), 70 km south of Amiens, 33 km southeast of Beauvais and 37 km northeast of Pontoise. The city is housed in the urban unit of Creil (or Creil basin) comprising about 100 000 inhab. The area included in the triangle between the railway, the Oise river and the busy road RD 1016 is shared between Nogent and Creil (figure 16). Emissions from transport (road, river, railway) and industries (industrial area, river port) have to be considered along with domestic emissions related to the high density of population (2514 inhab./km²).



Figure 16: Geographical location of the sampling site of Nogent-sur-Oise

The sampling site (49° 16' 35.004" N, 2° 28' 55.812" E, 28 m a.s.l.) is a monitoring station of ATMO Picardie, located in a stadium area and near a swimming pool building.

The city of Nogent-sur-Oise has an oceanic climate. Rainfall in Nogent-sur-Oise is important where even in the driest months, shower events are common. The average annual temperature in Nogent-sur-Oise is around 11 °C. There is an average 629 mm of rain per year.

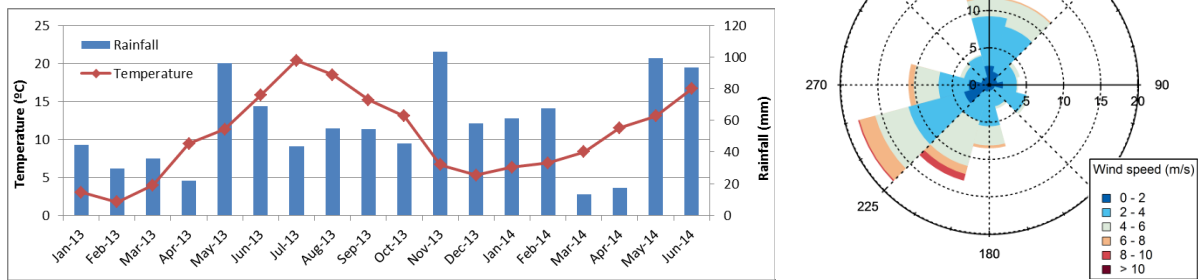


Figure 17: Meteorological data for the site of Nogent-sur-Oise (temperature and rainfall in the left and windrose in the right)

The lowest daily average temperature recorded during the sampling was $-6.9\text{ }^{\circ}\text{C}$ and the highest $26.5\text{ }^{\circ}\text{C}$. The average temperature between Jan13 and Jun14 was $10.4\text{ }^{\circ}\text{C}$. As it is visible in figure 17, once again strong winds are associated with the southwest direction, with an important contribution also of low wind speeds from the north and north-northeast.

2.2.3 Rouen (urban site)

Rouen is a city located in the north-west of France at about 70 km east from the Seine river estuary and its urban area is the 12th biggest in the country. The city is crossed by the Seine river. In 2013 the number of inhabitants was 111 000. The whole urban area accommodates about 650 000 people. The influence of anthropogenic pollutants is expected to be of great importance, namely from traffic, industrial activity (refineries, river port) and biomass burning (the density of population being particularly high with 5180 inhab./km^2).



Figure 18: Geographical location of the sampling site in Rouen

The sampling site used in this study (49°25'41.016" N, 1°3'28.008" E, 9 m a.s.l.), corresponds to the *Petit-Quevilly* station of AIR Normand, located beside a swimming pool and 100 m away from a 4-lane express road (figure 18).

The climate in Rouen is considered oceanic, with rain episodes distributed throughout the year (with more than 130 days in a year with at least 1mm of rain, on average). Winters are mild and summers bearable with the maritime influence of the British Channel sixty kilometers away.

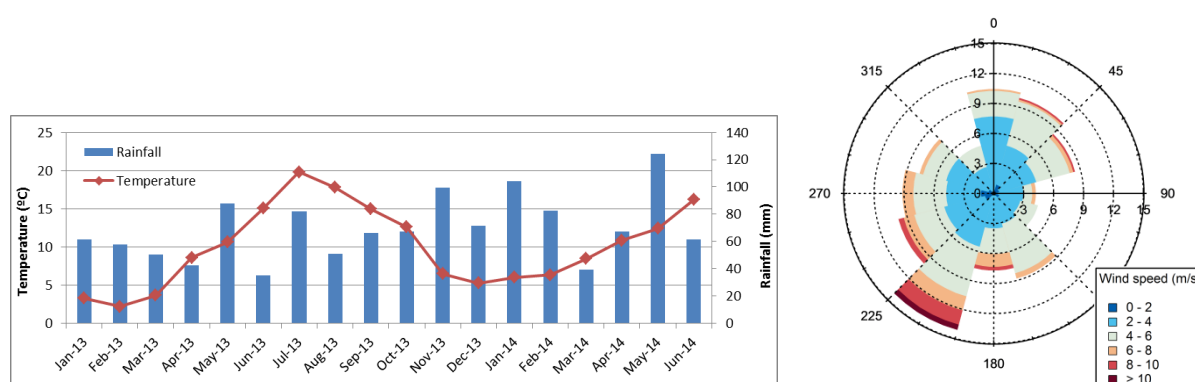


Figure 19: Meteorological data for the site of Rouen (temperature and rainfall in the left and windrose in the right)

The average temperature registered between January 2013 and June 2014 was 10.1 °C and as it can be seen in figure 20 stronger winds origin from southwest.

2.2.4 Revin (remote site)

Located in the Ardennes forest, in a hilly landscape, the site of Revin is part of the European Monitoring and Evaluation Program (EMEP) which is a scientifically based and policy driven program under the Convention on Long-range Transboundary Air Pollution (CLRTAP) aiming for international co-operation to solve transboundary air pollution problems.

Located 3 km outside of the city of Revin that has less than 7000 inhabitants, this site (49° 54' 28.008" N, 4° 37' 48" E, 395 m a.s.l.) is part of the ATMO Champagne-Ardenne air quality monitoring network. As an EMEP station, it is located far away from any potential local anthropogenic sources of particles. The climate in the region is considered oceanic with

continental influence, with relatively cold winters, mild summers and rainfall episodes well distributed throughout the year.

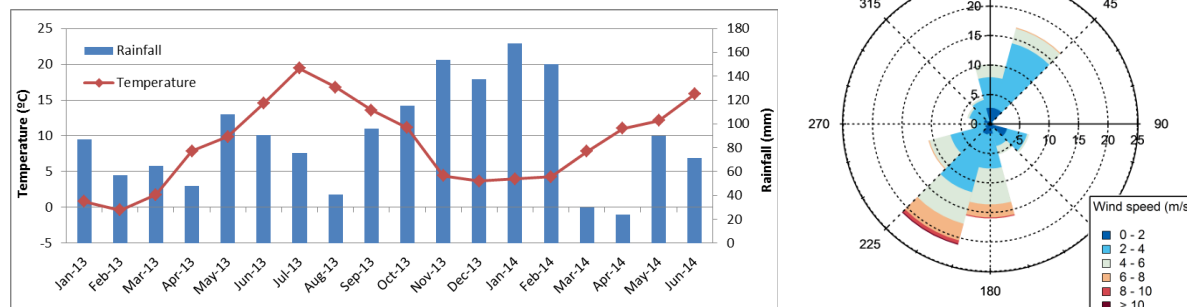


Figure 20: Meteorological data for the site of Revin (temperature and rainfall in the left and windrose in the right)

The average daily temperature during this study was 8.6 °C and, as in the previous sites, strong winds have their origin from Southwest. There is also a significant contribution of low speed winds from Northeast (figure 20).

2.2.5 Roubaix (traffic site)

Roubaix is a French commune in the Nord-Pas-de-Calais region adjoining the border with Belgium. With a population of just under 100 000 inhabitants, Roubaix, the second city of the Nord - Pas de Calais, forms with Lille, Tourcoing, Villeneuve d'Ascq and 81 other cities the Urban Community of Lille Métropole, which has about 1.1 million inhabitants. More broadly, it belongs to a vast conurbation formed with the Belgian cities of Mouscron, Kortrijk, Tournai and Menin, who gave birth in January 2008 to the first European Grouping of Territorial Cooperation, the Lille-Kortrijk-Tournai, with nearly two million inhabitants. The city is characterized by a green-spaces deficit (10 m²/per inhabitant).

The sampling site (50° 42' 24" N, 3° 10' 51" E, 31 m a.s.l.) is located at a few meters from a busy road site, so traffic sources of pollution are expected as well as anthropogenic aerosols coming from the highly populated area (density of 7246 inhab./km²) close by. Also the station is situated alongside the municipal horticultural greenhouses. As Lens, it is part of the ATMO Nord Pas-de-Calais monitoring network.



Figure 21: Geographical location of the sampling site of Roubaix

Due to limitations on the meteorological station situated in Roubaix, only the data from rainfall was collected there; data about wind speed, wind direction and temperature were obtained from the station in Lesquin – Lille, located 12 km to the south-southwest of Roubaix. In consequence, the wind-rose presented in figure 15 is also applicable to Roubaix, whereas the graphic of rainfall and temperature is presented in figure 22.

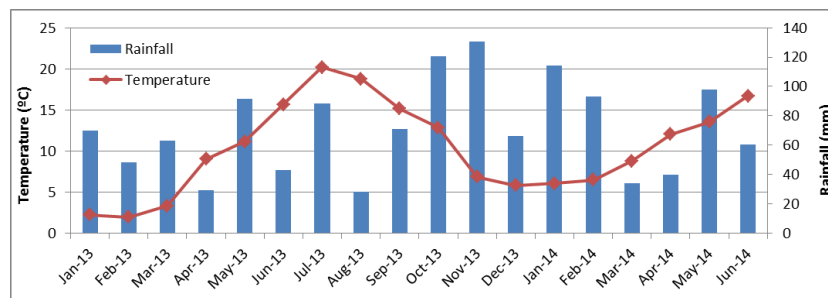


Figure 22: Meteorological data for the site of Roubaix (temperature and rainfall)

2.3 PM_{10} characterization methodologies

2.3.1 Filter sampling

At each site, samples were collected using a sequential High Volume Sampler (HVS, Digital DA80, figure 23) equipped with a PM_{10} sampling head operating at $30 \text{ m}^3/\text{h}$. Particles were sampled on pre-heated 150 mm diameter Pall Tissu Qz filters (100% quartz fiber filters). The samples correspond to a 24 h collection period, from midnight to midnight, except for the

Revin and Nogent-sur-Oise sampling sites where the collection was made from 9 am to 9 pm. Sampling took place between January 2013 and June 2014.



Figure 23: High-volume sampler Digitel DA80

2.3.2 **PM₁₀ automatic measurement**

PM₁₀ data have been obtained and furnished by the regional air quality monitoring networks operating the stations. At Lens, PM₁₀ mass concentrations were measured using a beta gauge (MP101M, Environment S.A.) equipped with a PM₁₀ inlet and smart heater system (so-called RST) allowing for removing water at high ambient relative humidity. At the other 4 sites, PM₁₀ mass concentrations were obtained using Tapered Element Oscillating microbalance (TEOM, Rupprecht & Patashnick) equipped with a Filter Dynamics Measurement System (FDMS, 8500c unit)

Both of the MP101M-RST and TEOM-FDMS systems have been proved to be equivalent to the reference gravimetric measurement method (Fr EN 12341; 2015) required for the monitoring of PM_{2.5} and PM₁₀ in the frame of the 2008/50/EC Directive (LCSQA, 2005 and LCSQA, 2006).

2.3.3 **Offline chemical analyses**

To determine the chemical composition of the samples collected, different techniques were used depending on the type of compound analyzed:

- For trace and major elements, ICP-MS (ELAN 6100 DRC, Perkin Elmer) and ICP-AES (IRIS Intrepid, Thermo-Scientific) were used, respectively (Alleman et al. 2010). Prior to analyses, each sub-samples was acid digested (HNO₃; HF; H₂O₂) with a microwave oven (Milestone ETHOS). Repeated measurements were performed on acid blanks, quality control standard solutions and standard reference material. Analyses were performed by Mines Douai.

- Soluble anions and cations were analyzed by ionic chromatography (IC, Dionex DX-600). Briefly, samples were soaked for one hour in 10 mL of Milli-Q water, and then filtered using 2 µm-porosity Acrodisc filters before analysis. AS/AG 17 and CS/CG 12A columns were used respectively for anions and cations analyses (J. Sciare et al. 2010). Analyses were performed by LSCE (CEA-CNRS-UVSQ).

- Elemental carbon (EC) and organic carbon (OC) were analyzed using the thermo optical transmission (TOT) method on a Sunset Lab analyzer (M. E. Birch and Cary 1996). It was performed according to the National Institute of Occupational Safety and Health (NIOSH) 870 protocol (M. Eileen Birch and Cary 1996). LCSQA (Mines Douai and INERIS) was responsible for these analyses.

- Sugar anhydrides (levoglucosan, mannosan, and galactosan) and sugar alcohols (arabitol, sorbitol and mannitol) were analyzed by HPLC-PAD using a set of Metrohm columns (MetroSep A Supp 15 and Metrosep Carb1) following the procedure previously used by Jean Sciare et al. (2011) These measurements were performed by LSCE (CEA-CNRS-UVSQ).

2.3.4 **Limits of detection**

As an introduction it is important to define an overall detection limit, as it can be associated either with the analytical method, or with the sampling method, as follows (equation 2):

$$LD = LD_a \text{ and/or } LD_{fb} \quad (\text{Eq. 2})$$

This distinction is made due to the fact that not always analytical detection limits (LD_a) were available and field blanks were used to calculate the limits of detection.

The analytical detection limit (LD_a) is directly associated with the analytical method and it defines the limit of detection of this method. In the case of ICP analysis, this limit is obtained

by analyzing a blank acid solution 10 times during the same measurement exercise. By definition, the LD_a is obtained by multiplying the standard deviation of these laboratory blank measurements (σ_b) by a factor 3 (equation 3):

$$LD_a = 3 \times \sigma_b \quad (\text{Eq. 3})$$

The detection limit associated with the sampling method (LD_{fb}) is calculated via the same expression where the blanks are in fact virgin filters that were not submitted to an air flow but that were handled in the exact same way as the rest of the samples, including transportation to the field, handling, storage and analytical procedure (equation 4):

$$LD_{fb} = 3 \times \sigma_{fb} \quad (\text{Eq. 4})$$

where σ_{fb} is the standard deviation of the field blanks.

These measurements are later used to correct and validate all the raw concentrations obtained from the analytical methods. In this study, a protocol was developed where all concentrations were screened and corrected regarding both the analytical and field blanks detection limits:

- All the obtained concentrations from filters, including normal samples and field blanks, go through a process of validation having into account the LD_a , where all the samples below this value are replaced by $LD_a/2$. At this point the lowest value seen at the obtained concentrations will always be $LD_a/2$.
- A second data validation step is added now having into account the field blanks. The LD_{fb} is calculated and used as a parameter to assess the quality of the field blanks recovered. It is also useful to identify possible contaminations on the field blanks by comparing each field blank with the average value of all these filters.
- The final correction of the concentration is made having into account the average concentration of the field blanks: if a sample concentration is superior to at least twice the average concentration of the field blanks then the final concentration will be obtained by subtracting the average concentration of the field blanks (equation 5):

$$\text{If } C_i \geq 2 \times \overline{C_{fb}} \quad \text{then } C = C_i - \overline{C_{fb}} \quad (\text{Eq. 5})$$

where C_i corresponds to a given sample, C_{fb} the average concentration of the field blanks and C the final corrected concentration of sample i .

If a sample concentration is strictly inferior to twice the average concentration of the field blanks then the final concentration will be replaced by $LD_a/2$ (equation 6):

$$\text{If } C_i < 2 \times \overline{C_{fb}} \quad \text{then } C = LD_a/2 \quad (\text{Eq. 6})$$

Here the minimum value of LD_a was chosen (instead of replacing also by LD_{fb}) to avoid obtaining a concentration matrix with minimum values calculated in different ways. By defining the absolute minimum for each variable as LD_a , the methodology is consistent to all species.

2.3.5 Measurement uncertainties

The uncertainty associated with each measurement depends on each step of the analytical process and can, therefore, be linked to the process of sampling, matrix effects, working conditions, analytical uncertainties of the instruments, dilutions, even human error...

One of the classical methods for estimating uncertainty is error propagation. For this method, data uncertainties (i.e. standard deviations of observations) are assumed known. Then the covariance matrix of computed results is obtained by applying the well-known error propagation formula that is based on a linear approximation around the measured values.

Understanding and knowing the nature of the data in question is crucial, and as suggested by the Guide to the expression of Uncertainty in Measurements (ISO, 1993), (that inspired Eurachem to develop the guide EURACHEM/CITAC (Ellison et al. 2000), also explained in the doctoral thesis of Lamaison (2006), one can divide the process of uncertainty calculation in 4 stages (figure 24):

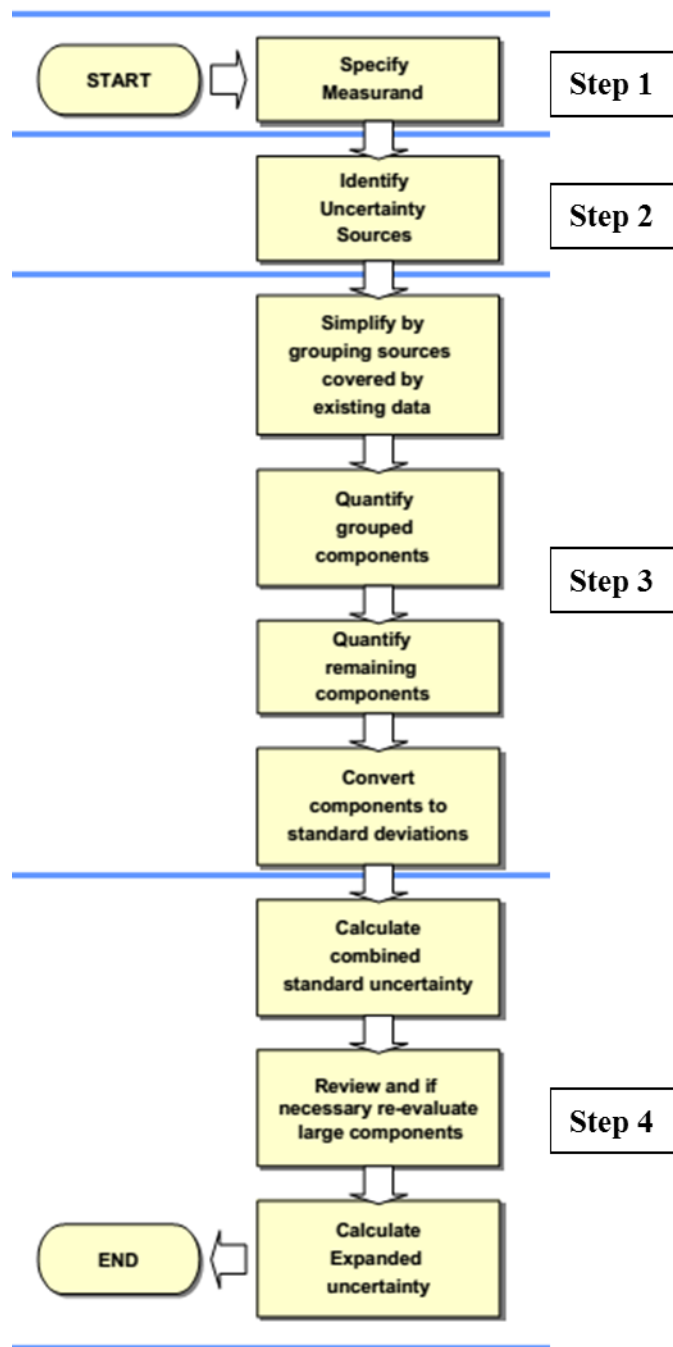


Figure 24: Scheme of the protocol to obtain uncertainties linked to measurements (source: Ellison et al. 2000)

Following the proposed diagram, defining the measurand is to clarify exactly what is being measured and a quantitative expression relating the value of the measurand to the parameters on which it depends. In this case, one is measuring a concentration, defined as the amount of a given component in mass per volume unit ($C = m/V$), specifically in this study is the mass expressed in μg per cubic meter of sampled ambient air ($\mu\text{g}/\text{m}^3$).

The second step points out the importance of identifying uncertainty sources. To do so, one looks at the expression that defines the measurand and identifies all the potential sources of uncertainty associated with each necessary measurement. It should also be said that there may be sources of uncertainty that are not directly related with each measured parameter but can have an impact on the final value (e.g. contamination, human error, etc).

As an example, in the work of Yenisoy-Karakaş (2012) using an ICP-MS analyzer, the estimation of the uncertainty of the concentration obtained was calculated taking into account the main parameters that affected the concentration of the elements, as: mass of sample, calibration curve, final volume of sample digested, dilution factor, recovery and repeatability. All these parameters can be described under a fishbone diagram, as illustrated in Tanase et al. (2015) also for ICP-MS measurements (figure 25):

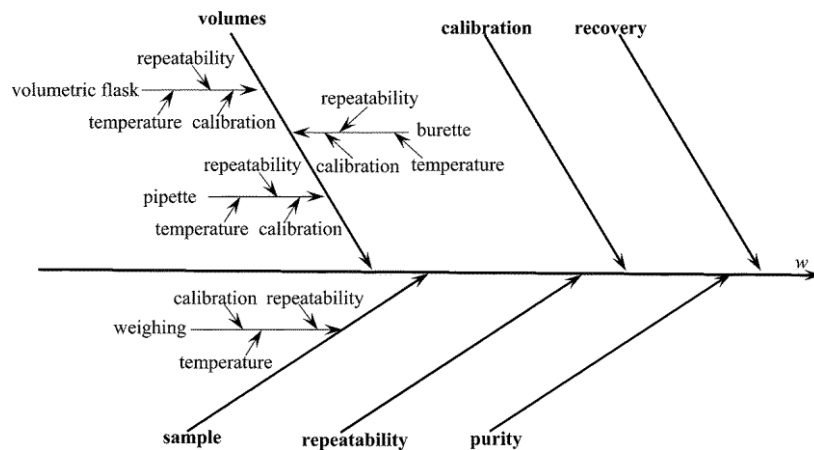


Figure 25: Uncertainties fishbone scheme for ICP measurements (source: Yenisoy-Karakaş 2012)

On another study, carried out by Leiva et al. (2012), a fishbone diagram was also developed for ion chromatography measurements following the same principle: identification of the measurand and understanding of all the steps to reach the final concentration (figure 26):

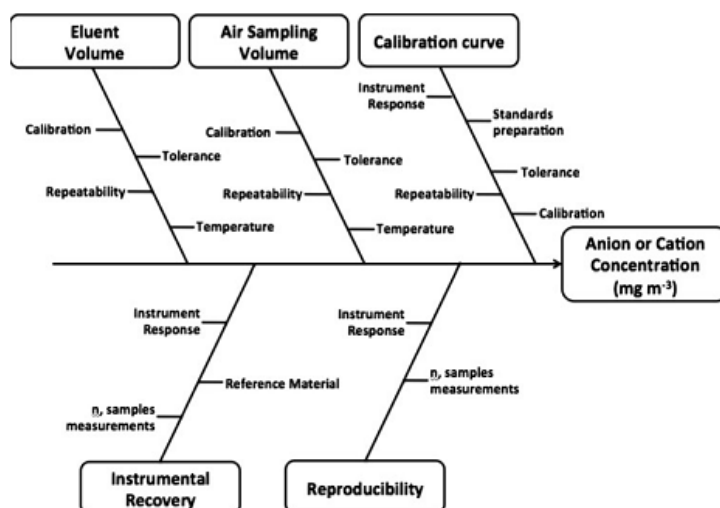


Figure 26: Uncertainties fishbone scheme for IC measurements (source: Leiva et al., 2012)

Once identified all the probable sources of uncertainties to the final concentration, it is time to quantify these uncertainties. This can be done by calculating the uncertainty associated with each individual step of the diagram that later will contribute to the final result.

In the following, the process to calculate the uncertainty associated with elements measurements by ICP-OES and ICP-MS is described, due to the fact that they are the only measurements that were entirely carried out in Mines Douai. For the other used techniques, the detection limits and uncertainties considered in this study are the ones provided by the research laboratories in charge of the analyses.

The following parameters were involved in the calculation of the concentrations of the elements in the samples, following the simplified fishbone diagram of figure 27:

1. Accuracy (A_c)
2. Air sampling volume (V)
3. Repeatability (Rep)
4. Contamination ($Cont$)

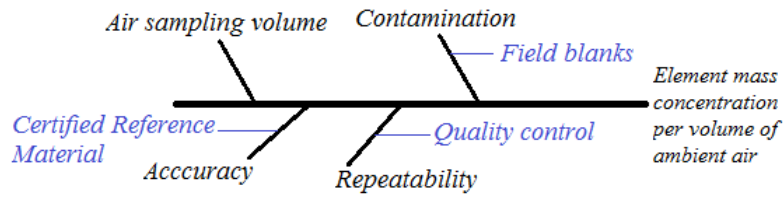


Figure 27: Uncertainties fishbone scheme for metal measurements carried out in Mines Douai

The accuracy of all the measurements is assessed with two standard reference materials, NIST SRM 1648 and NIST SRM CZ120, which are submitted to the same protocol as filtered samples including the acid mineralization step and the whole analytical method (standards preparation, calibration curve, check of the stability of the instrumental response with an internal standard, among other steps). The accuracy of the measurements is calculated with the quantified recovery of each element. Are considered suitable values of recovery the results obtained between 80 % and 120 % of the certified values of the reference material, and if not this species is not included. The uncertainty associated with the accuracy of the method results is given by (equation 7):

$$u_{Ac} = \sqrt{u_{NIST}^2 + \frac{s_{rep}^2}{n_{rep,NIST}}} \quad (\text{Eq. 7})$$

where u_{NIST} is the uncertainty associated with the reference standards, s_{rep}^2 the standard deviation of the NIST analyzed and $n_{rep, NIST}$ the number of repeated NIST analysis.

The sampling volume flow rate in this work was maintained constant at $30 \text{ m}^3 \text{ h}^{-1}$. The uncertainty of the air sampling volume then depends on the time of sampling. Assuming that the uncertainty associated with the time of sampling is neglectable, and considering that the flow has rectangular distribution, a relative uncertainty of 5.6 % is obtained according to the guide EURACHEM/CITAC (2000).

The repeatability and its relative uncertainty can be calculated by using the expression (equation 8):

$$u_{rel}^2(Rep) = \frac{CV(QC)^2}{n_{rep,QC}} \quad (\text{Eq. 8})$$

where $CV(QC)$ is the variability coefficient of the quality control (QC) samples repeated and $n_{rep,QC}$ is the number of QC samples analyzed.

The uncertainty associated with the possible contamination is obtained via the field blank filters measured, by the expression (equation 9):

$$u_{cont}^2 = \left(\frac{\overline{C}_{fb}}{(2 \times 0.1127)} \right)^2 \quad (\text{Eq. 9})$$

where \overline{C}_{fb} is the average concentration of the field blank filters and 0.1127 is the analyzed relative portion of the filter.

Thus the relative uncertainty in a concentration is the combination of the relative uncertainties of each above mentioned parameters. The combined uncertainty (in terms of relative uncertainty) can be calculated by using the equation 10:

$$u_{rel}(C) = \sqrt{u_{rel}(Ac)^2 + u_{rel}(V)^2 + u_{rel}(Rep)^2 + u_{rel}(cont)^2} \quad (\text{Eq. 10})$$

This detailed calculation was possible on the analysis of the elements, however, due to the fact that the other chemical analyses were not performed in Mines Douai, a standard method was used based on the work of Gianini et al. (2012):

$$u_{ij} = \sqrt{DL_j^2 + (CV_j c_{ij})^2 + (a c_{ij})^2} \quad (\text{Eq. 11})$$

where c_{ij} are samples concentrations, DL_j is the detection limit of specie j (calculated as twice the standard deviation of the field blanks), CV_j the coefficient of variation and a a factor to account different sources of uncertainty like the ones mentioned above ($a=0.03$).

In the case of some species an expanded uncertainty was used instead of the CV due to the very low uncertainties associated with low concentrations. This methodology was also applied by Waked et al., 2014 and it takes into account previous studies carried out under the same conditions - 10 % (Lim et al. 2003) for OC, 15 % (Schmid et al. 2001; Cavalli et al. 2010) for EC and 15 % for monosaccharide sugars such as levoglucosan, arabitol and mannitol (Piot et al. 2012; Inuma et al. 2009). The values used for the calculation of the uncertainties are shown in Annex 1.

2.3.6 Ion balance

An ion balance was performed for all sites to assess the nature of the particles collected. This technique calculation is of capital importance because it can give clues about the nature of the unaccounted species. For example, if the account of cations is higher than the anions, this may indicate that the missing species could be carbonates or organic anions. An increase on in the contribution of anions can be associated with pollution episodes driven by secondary particles based on sulfate and nitrate.

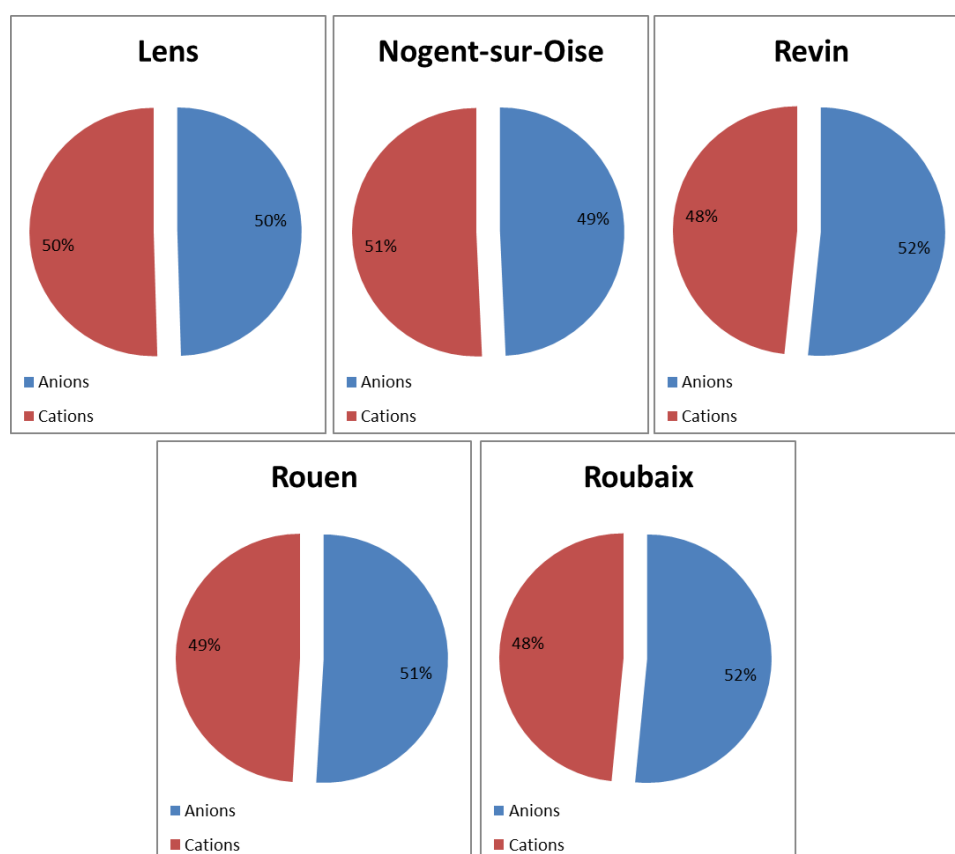


Figure 28: Balance between anions and cations on each sampling site

Figure 28 shows the sum of anions, which comprises water-soluble chloride, nitrate and sulfate and the sum of cations, referring to water-soluble ammonium, sodium, potassium, calcium and magnesium. Quite balanced results were seen on all 5 sites, with distributions always near the 50-50 balance. The general result of a higher contribution of anions (seen on 3 of the 5 sites) can be associated with a significant influence of secondary particles rich in nitrate and sulfate.

Several studies (Ocskay et al. 2006; Koçak, Mihalopoulos, and Kubilay 2007) have shown that the fine fraction of the aerosol ($<2 \mu\text{m}$) is slightly acidic or neutral, while the coarse particles ($2\text{--}10 \mu\text{m}$) are alkaline. The seen results are within the expected range seen in this kind of studies (Brauer et al. 1995). One should however have in mind that species like carbonates were not measured due to limitations in ionic analytical method.

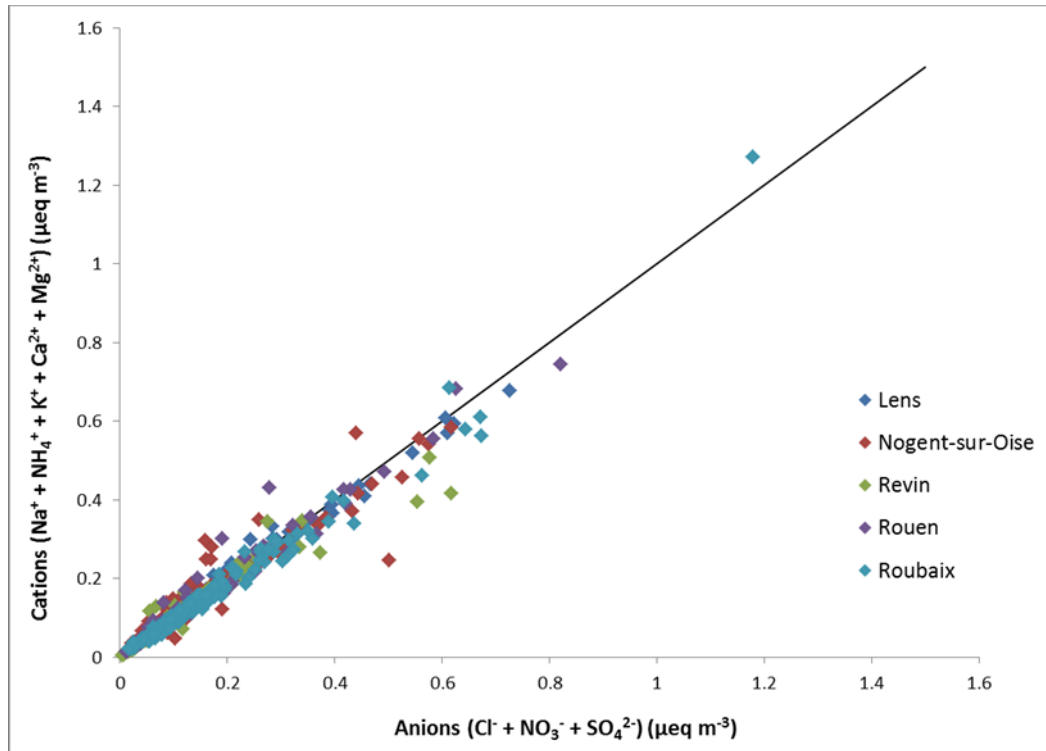


Figure 29: Correlation between anions and cations on all sampling sites (1:1 ratio)

The scatterplot (figure 29) shows the balance between anions and cations for all sites, with the tendency already mentioned of a slightly higher contribution of anions. More significant discrepancies are seen at higher concentrations of ions. To these samples were also associated higher concentrations of PM_{10} mass concentration, leading to believe that the imbalance here identified could be either linked with episodes where the emission of some specific species here measured is more significant, or with the presence of chemical species directly affecting the ion balance.

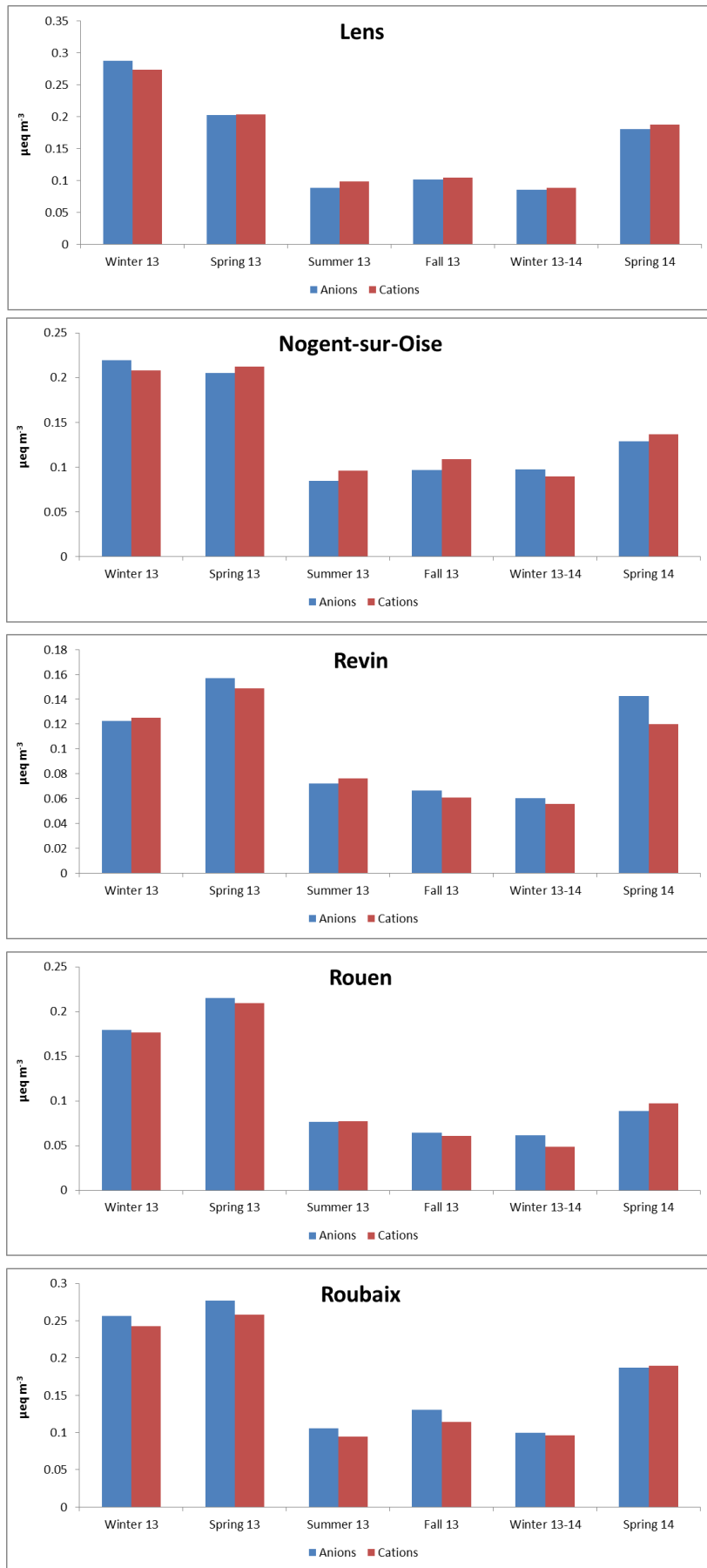


Figure 30: Seasonal variation of the ion balance on each sampling site

A clear seasonality in terms of ion contributions was seen on all five sites (figure 30) with greater concentrations of all ions seen during winter and spring. Also an interesting result is the fact that the winter of 2014 had smaller ion concentrations when compared to the winter of 2013. This can be linked to a multitude of reasons like specific weather conditions, different emission profiles of sources and also the fact that the winter of 2013 in this study is just composed by the months of January and February whereas the winter of 2014 includes the month of December 2013. However, concerning the comparison of wintertime weather conditions, it is noteworthy that on average winter 2014 was warmer, dryer and with a lower average pressure than the winter 2013, all these conditions favoring the partitioning of semivolatile species (like ammonium nitrate) more towards the gaseous phase. In addition, winter 2014 was also more rainy and with higher wind speed, these conditions favoring respectively the wet deposition of water-soluble species and the dispersion of pollutants. Therefore the difference in weather conditions may be a plausible explanation for the lower ions concentrations in winter 2014 compared to winter 2013 (table 3).

Table 3: Comparison of the meteorological conditions between the winter of 2013 and the winter of 2014

	PM ₁₀ ($\mu\text{g m}^{-3}$)	Rainfall (mm)	Mean temperature ($^{\circ}\text{C}$)	Pressure (hPa)	Wind speed (m/s)	RH (%)
Winter 13	28.3	1.8	2.2	1017.0	3.5	89.6
Winter 13-14	18.3	3.1	5.8	1010.8	4.5	86.4

Despite this difference between winter seasons, the difference between anions and cations ($[\text{Anions}] - [\text{Cations}]$) was calculated to try to better assess a possible seasonal trend (figure 31).

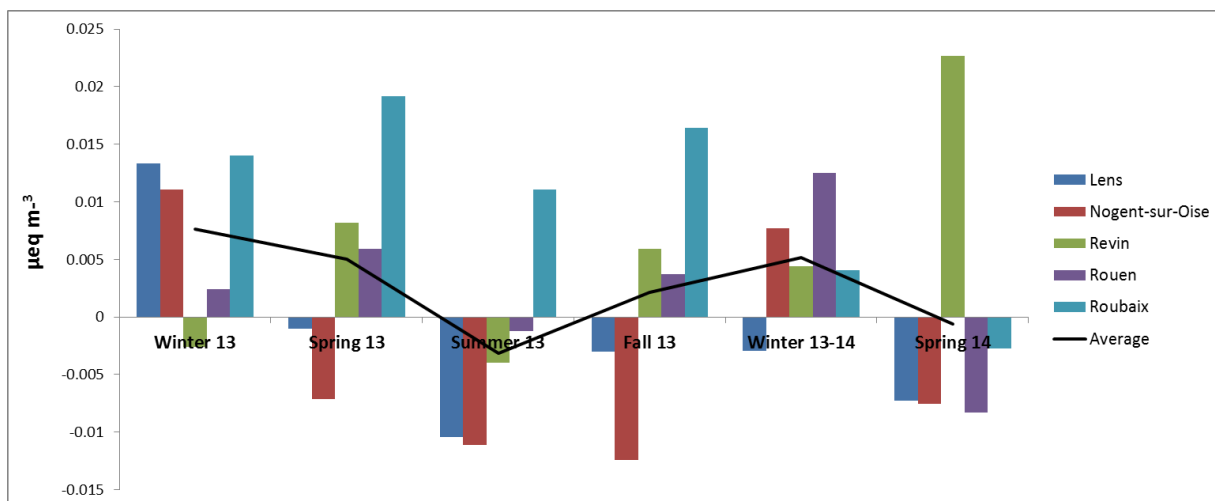


Figure 31: Difference between anions and cations on each sampling site per season

Although there are significant occasional differences between the sites, a possible trend is seen in this study, where the sum of anions seems to be greater than the sum of cations during colder seasons. Again, this can be associated with the previous remarks that summertime conditions (high temperature, low RH) decrease the atmospheric concentrations of particulate semi-volatile species due to more favorable conditions for gases, whereas rainy conditions in fall favor wet deposition of water-soluble species.

2.3.7 Mass closure

In studies where an exhaustive chemical characterization is undertaken, like this one, the chemical mass closure allows to assess the extent of which the PM_{10} mass concentration measured can be explained by the contributions of the measured chemical species (Maenhaut et al. 2002; Putaud et al. 2004; Terzi et al. 2010).

In this work, the PM_{10} reconstructed mass (equation 12) was achieved according to the method described in Waked et al. (2014) and it was chosen due to the similarities between the studies – similar collection period, measured species, typology of sites and geographical location (north of France).

$$PM_{10} = EC + f^* \times OC + 3 \times Na^+ + 10 \times Ca + NO_3^- + nssSO_4^{2-} + NH_4^+ \quad (\text{Eq. 12})$$

where nssSO_4^{2-} represents non-sea salt sulphate, calculated as the difference between total SO_4^{2-} and sea salt sulphate being calculated by multiplying the mass concentration of Na^+ by a factor of 0.252 (following the methodology described by Seinfeld and Pandis, 2006). The OC-to-OM conversion factor (f^*) was estimated based on the work of Turpin and Lim (2001), showing a dependence of this factor according to the expected sources and surroundings (with lower values close to the emission sources and highest ones at remote locations). Therefore, OM:OC ratios chosen in the present ranged from 1.6 (for Roubaix) to 1.9 (for Revin), as summarized in table 4.

Table 4: OM/OC ratio used in each sampling site

	Lens	Nogent-sur-Oise	Revin	Rouen	Roubaix
OM/OC ratio	1.75	1.75	1.9	1.75	1.6

The value of 1.75 was selected for the urban sites because having in consideration previous works in the region, a significant contribution of biomass burning is expected (Waked et al., 2014). The traffic site followed the recommendation of Turpin and Lim (2001) for the value of 1.6, whereas to the remote site, being surrounded by forests was given a ratio of 1.9.

As summarized in table 5, mean unaccounted masses extend from 0% to 20% of the PM_{10} , which is within the expected range reported in previous studies (e.g., Pérez et al. 2016; C. Pio and Alves 2013).

Table 5: Unaccounted masses for each sampling site

Lens	Nogent-sur-Oise	Revin	Rouen	Roubaix
0 %	15 %	10 %	20 %	5 %

Figure 32 allows investigating chemical mass closures in more detail, presenting the scatter plots for the correlations between the measured PM_{10} mass concentration and the reconstructed PM_{10} mass concentration for each site.

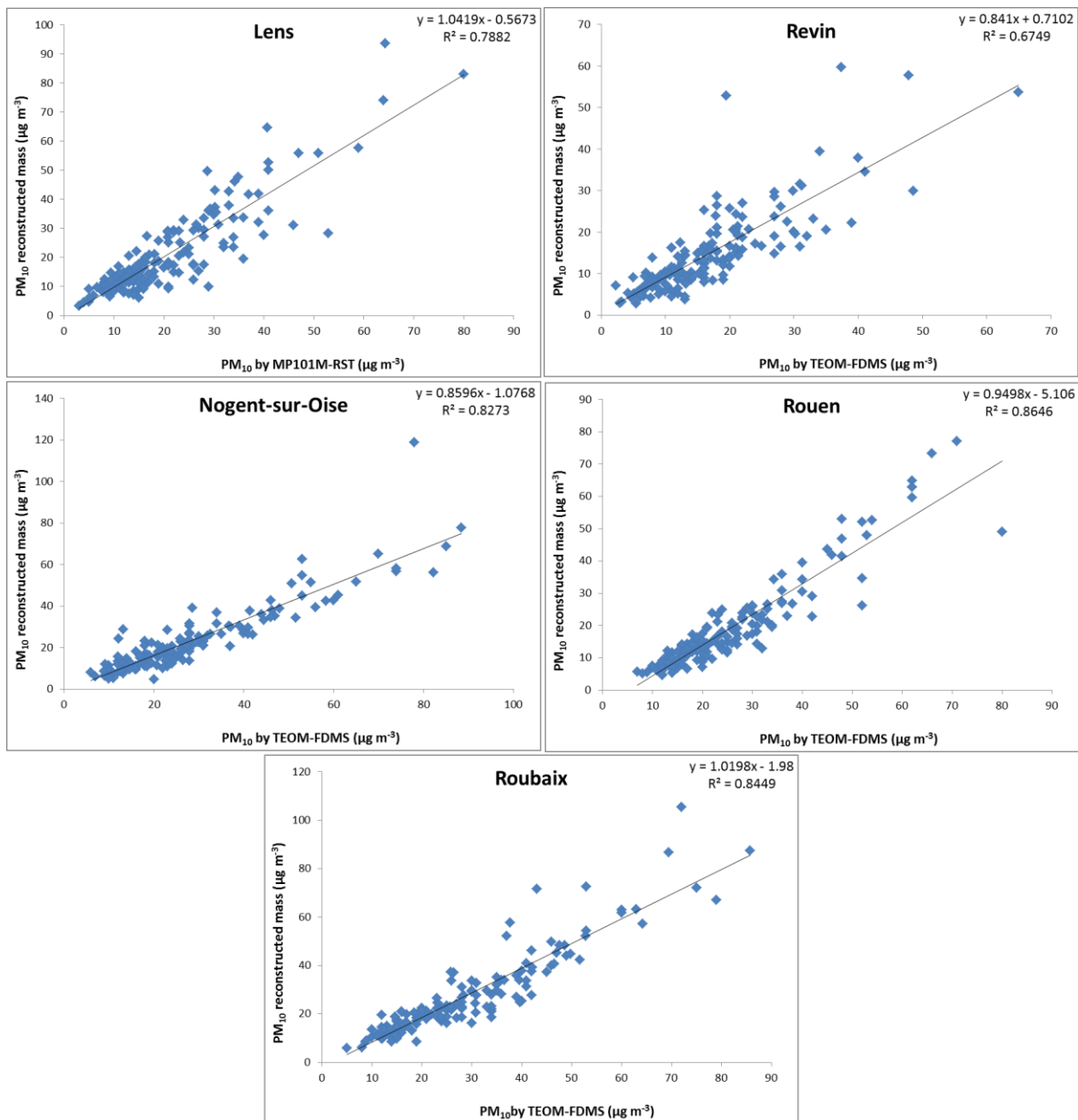


Figure 32: Correlation between PM₁₀ measurements and mass closure method

Better correlations were seen in the traffic site as well as in the urban ones. A larger scattering of points was seen in the remote site of Revin. The differences between the reconstructed mass and measured PM₁₀ mass concentration can be attributed to:

- Uncertainties over the measured total mass (here by TEOM-FDMS or MP101M-RST).
- Uncertainties linked to the estimate of aerosol fractions from specific markers. A typical example here corresponds to the choice of the conversion factor between OC and Organic Matter (OM).

- Uncertainty over the amount of water in the aerosol, not taken into account on the chemical analysis but maybe included in the measurements of total mass.

Figure 33 presents seasonal values of the PM_{10} reconstructed mass and their difference to the ones measured by TEOM-FDMS or MP101M-RST measurements. For each site, differences may be seen from one season to another in the amount of unaccounted PM_{10} mass. The most elevated relative unaccounted masses (reaching up to 40% of the measured PM_{10}) were observed for Rouen in in the summer of 2013 and winter and spring of 2014, in Lens for the summer of 2013 and Nogent-sur-Oise in the winter of 2013. Therefore, no evident common pattern could be identified, neither for a given season nor between sites.

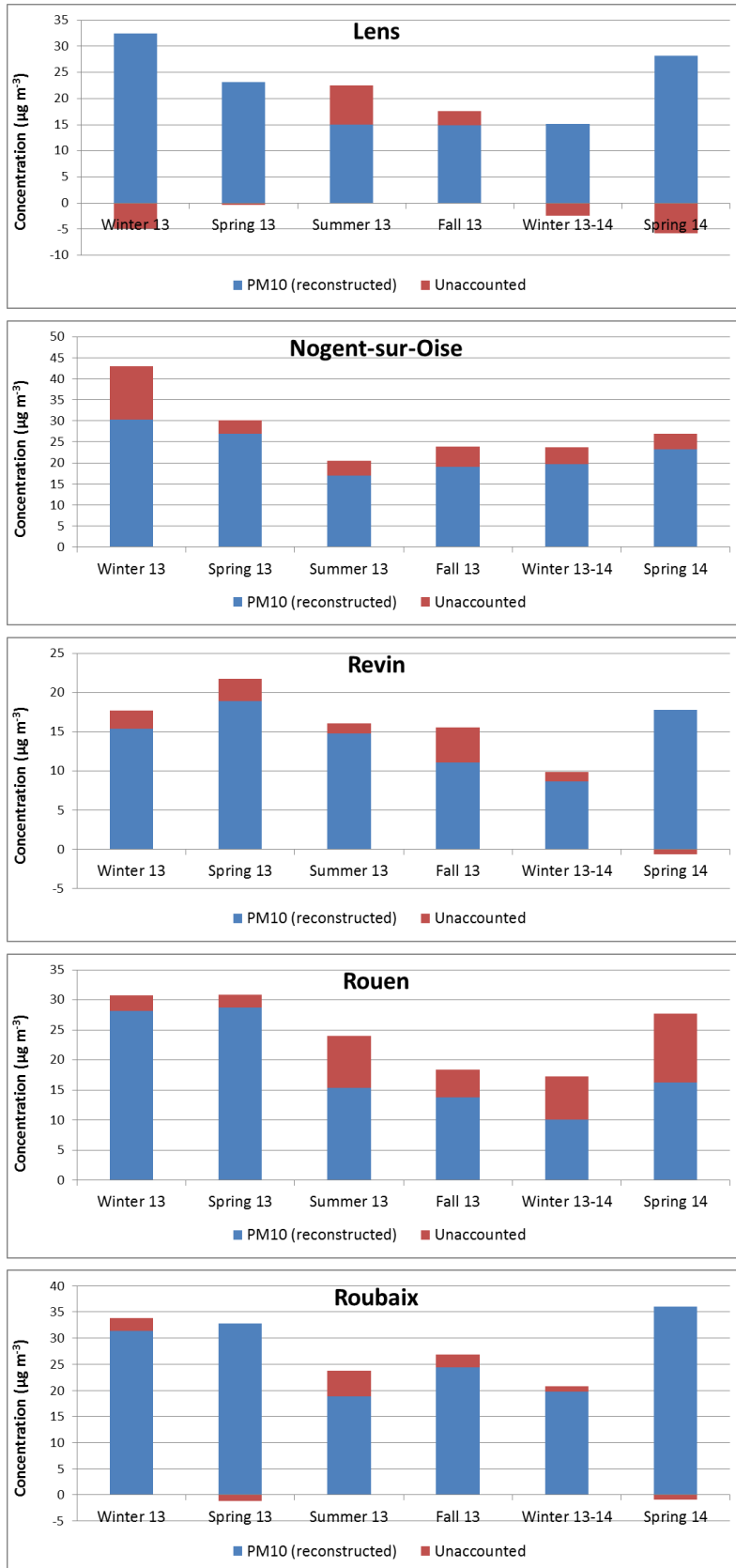


Figure 33: PM₁₀ reconstructed mass and unaccounted fraction per season at each sampling site

2.4 PM₁₀ chemical composition at each site

Once collected and analyzed all the available filters, and after a process of data validation taking into account quality control measurements and blank filters (field and analytical blanks), the final selection of variables per site can be seen in table 7.

Table 6 shows a summary of the samples distribution per site and per season. Due to sampling issues, the total number of available filters was not the same for each sampling site. Moreover, due to the sampling period encompassing 2 winters and 2 springs but only 1 summer and 1 fall, the number of available filters varies from one season to another. This is an important factor to keep in mind, especially when considering the average contribution of species and/or sources throughout the studied period, where a greater weight can be expected for winter and spring-related sources/species.

Table 6: Number of samples for each sampling site - total and per season

	Lens	Nogent-sur-Oise	Revin	Rouen	Roubaix
Total	167	157	168	168	159
Winter	49	45	49	50	41
Spring	59	61	61	61	57
Summer	29	22	28	31	30
Fall	30	28	30	26	31

Table 7: Validated (checked) species used at each sampling site

Species	Lens	Nogent-sur-Oise	Revin	Rouen	Roubaix
PM ₁₀	✓	✓	✓	✓	✓
EC	✓	✓	✓	✓	✓
OC	✓	✓	✓	✓	✓
Cl ⁻	✓	✓	✓	✓	✓
NO ₃ ⁻	✓	✓	✓	✓	✓
SO ₄ ²⁻	✓	✓	✓	✓	✓
Na ⁺	✓	✓	✓	✓	✓
NH ₄ ⁺	✓	✓	✓	✓	✓
K ⁺	✓	✓	✓	✓	✓
Mg ²⁺	✓	✓	✓	✓	✓
MSA	✓	✓	✓	✓	✓
Oxalate	✓	✓	✓	✓	✓
Levogluconan	✓	✓	✓	✓	✓
Polysaccharides	✓	✓	✓	✓	✓
Sugar alcohols	✓	✓	✓	✓	✓
Monosaccharides	✓		✓	✓	✓
Al	✓		✓		✓
Fe	✓	✓	✓	✓	✓
Ca	✓	✓	✓	✓	✓
As	✓	✓	✓	✓	✓
Ba	✓	✓			✓
Cd	✓	✓	✓	✓	✓
Ce	✓		✓	✓	✓
Co	✓	✓	✓	✓	✓
Cs	✓		✓	✓	✓
Cu	✓	✓	✓	✓	✓
La	✓	✓	✓	✓	✓
Mn	✓	✓	✓	✓	✓
Mo	✓	✓	✓	✓	✓
Ni	✓	✓		✓	✓
Pb	✓	✓	✓	✓	✓
Rb	✓	✓	✓	✓	✓
Sb	✓	✓	✓	✓	✓
Se	✓		✓	✓	✓
Sr	✓	✓	✓	✓	✓
Ti	✓		✓		✓
U	✓				✓
V		✓			
Zn	✓	✓	✓	✓	✓

Figure 34 shows the total average mass concentration of PM₁₀ as well as the average concentration per season on each site.

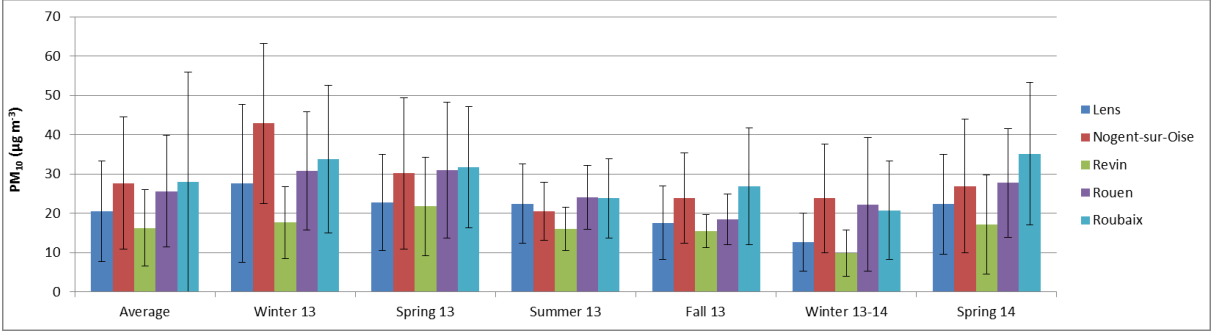


Figure 34: PM₁₀ average concentration on each site per season

The highest average PM₁₀ concentration was recorded in Roubaix, the traffic site, and the lowest was seen in Revin, the remote site. Spring is commonly observed as being the season where the average PM₁₀ is at its highest, with the exception of Nogent-sur-Oise where the winter season recorded the highest average concentration. On the other hand, fall showed to be the season where the average concentration of PM₁₀ was at its minimum in Rouen, Roubaix and Lens. In Nogent-sur-Oise this minimum was seen during summer and in Revin it was seen during winter. This latter result is quite interesting because winter is often a season where high concentrations of particles are seen. This can be explained with the absence of strong anthropogenic sources near the Revin sampling site.

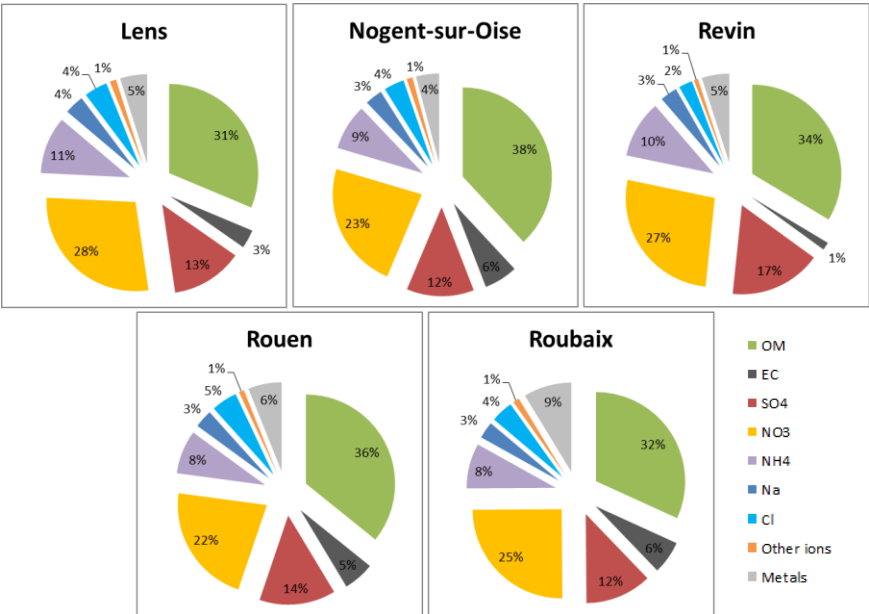


Figure 35: Average chemical composition of PM₁₀ on each sampling site

As observed in figure 35, the chemical characterization of the 5 sites showed the importance of organic matter to the total PM₁₀ mass concentration, being the main contributor on all 5 sites. Nitrate and sulphate also proved to be main components on the sampled particles, nitrate being the second main contributor on all sites and sulphate the third. It is also interesting to point out the contributions of sodium and chloride, which are assumed to have a marine origin, on the different sites according to their distance to the sea (figure 36). The most significant difference is seen in Revin, where the sum of these ions showed a smaller importance to PM₁₀ mass (5 %) when compared with the other sites (7-8 %). This is in accordance with Revin being the sampling site located furthest from the sea. In figure 36, it is observed that the chloride ion to sodium ion molar ratio varies from near 1 at Rouen to 0.5 at Revin. This phenomenon may be attributable to the well-known chloride depletion of NaCl aerosols when mixed with anthropogenic emissions (McInnes et al. 1994), following reactions like the one forming sodium nitrate aerosols:

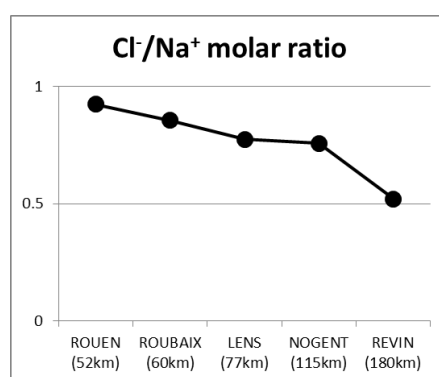
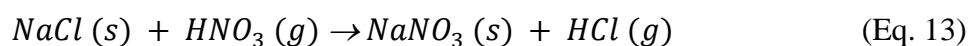


Figure 36: Average chloride per sodium ratio for each site according to their distance to the sea

A comparison was made between the results obtained for the sampling site of Lens and the study carried out by Waked et al. (2014), equally conducted in Lens for filters sampled during 2011-2012. Very similar results were found between the two studies. The present study recorded an average mass concentration of PM₁₀ of $21 \pm 13 \mu\text{g m}^{-3}$, exactly the same values seen in Waked et al. (2014). It should be noted that this study refers to an 18 months sampling period, including 2 full spring seasons and nearly 2 winter seasons, where higher PM concentrations are often found. Indeed, the concentrations observed throughout the seasons

were significantly different between the 2 studies. As an example, during the summer of 2011 the average mass concentration of PM₁₀ measured in Lens was of 13.7 µg m⁻³ but in the summer of 2013 a value of 22.2 µg m⁻³ was seen, corresponding to a 62% increase. As another example, the winter of 2013-2014 was the seasonal period where the present study exhibited the lowest concentrations of PM₁₀ with 12.7 µg m⁻³, that when compared with the value of 19.7 µg m⁻³ recorded during the winter of 2012 represents a decrease of 36%. Despite the seasonal differences seen between the 2 studies, not only the average concentration of PM₁₀ was quite similar, but also its chemical composition. In both studies OM was identified as the main contributor to PM₁₀ mass and the main ions (nitrate, sulfate and ammonium) the following main species.

2.4.1 Carbonaceous aerosols

Organic carbon, when converted to organic matter, is the main contributor to PM₁₀ mass on all sites and elemental carbon has contributions ranging from 1% to PM₁₀ mass (on average) in Revin up to 6% in Nogent-sur-Oise and Roubaix.

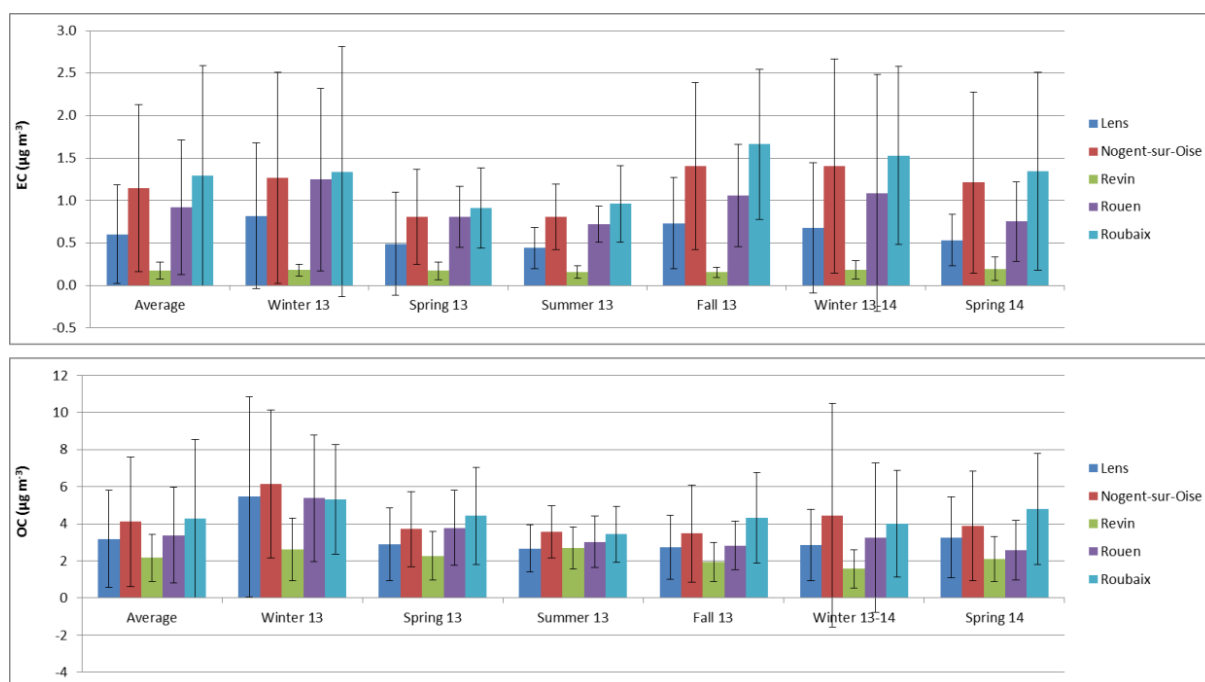


Figure 37: EC (top) and OC (bottom) average concentrations on each sampling site, per season

Table 8: EC and OC average concentrations and standard deviations ($\mu\text{gC m}^{-3}$) at each sampling site, per season

	Lens				Nogent-sur-Oise				Revin				Rouen				Roubaix			
	EC	$\pm 1\sigma$	OC	$\pm 1\sigma$	EC	$\pm 1\sigma$	OC	$\pm 1\sigma$	EC	$\pm 1\sigma$	OC	$\pm 1\sigma$	EC	$\pm 1\sigma$	OC	$\pm 1\sigma$	EC	$\pm 1\sigma$	OC	$\pm 1\sigma$
Average	0.60	0.58	3.19	2.63	1.15	0.98	4.11	3.49	0.17	0.10	2.16	1.27	0.92	0.79	3.37	2.57	1.29	1.29	4.27	4.27
Winter 13	0.82	0.86	5.45	5.38	1.27	1.24	6.15	3.98	0.18	0.07	2.61	1.69	1.25	1.07	5.38	3.40	1.34	1.47	5.32	2.95
Spring 13	0.49	0.61	2.89	1.98	0.81	0.56	3.72	2.02	0.17	0.10	2.27	1.30	0.81	0.36	3.78	2.04	0.91	0.47	4.42	2.62
Summer 13	0.44	0.24	2.67	1.27	0.81	0.39	3.56	1.40	0.16	0.07	2.70	1.13	0.72	0.21	3.02	1.39	0.96	0.45	3.44	1.50
Fall 13	0.73	0.54	2.73	1.74	1.40	0.99	3.48	2.62	0.15	0.06	1.95	1.06	1.06	0.60	2.82	1.30	1.66	0.88	4.33	2.44
Winter 13-14	0.68	0.77	2.84	1.91	1.41	1.26	4.46	6.04	0.18	0.11	1.57	1.03	1.09	1.40	3.25	4.03	1.53	1.05	4.01	2.87
Spring 14	0.53	0.30	3.27	2.17	1.21	1.07	3.88	2.97	0.20	0.14	2.09	1.21	0.75	0.47	2.58	1.59	1.34	1.17	4.79	3.01

The difference in concentration ranges is clearly visible in Revin compared to the other sites, and this was expected due the remoteness of this sampling location (figure 38). This difference is more evident in the case of EC, usually associated more with anthropogenic activities, not found in Revin. Roubaix and Nogent-sur-Oise showed the highest average values both for EC and OC (table 8) indicating that the site of Nogent-sur-Oise, although labelled as an urban site, exhibits similar characteristics to Roubaix, a traffic site. Being EC commonly associated with traffic emissions makes sense to see highest values in Roubaix and leads to the conclusion of a more important traffic influence in Nogent-sur-Oise when compared to the other urban sites (Lens and Rouen). No clear seasonality was observed for both species except for higher levels of OC seen on all sites during the winter 2013.

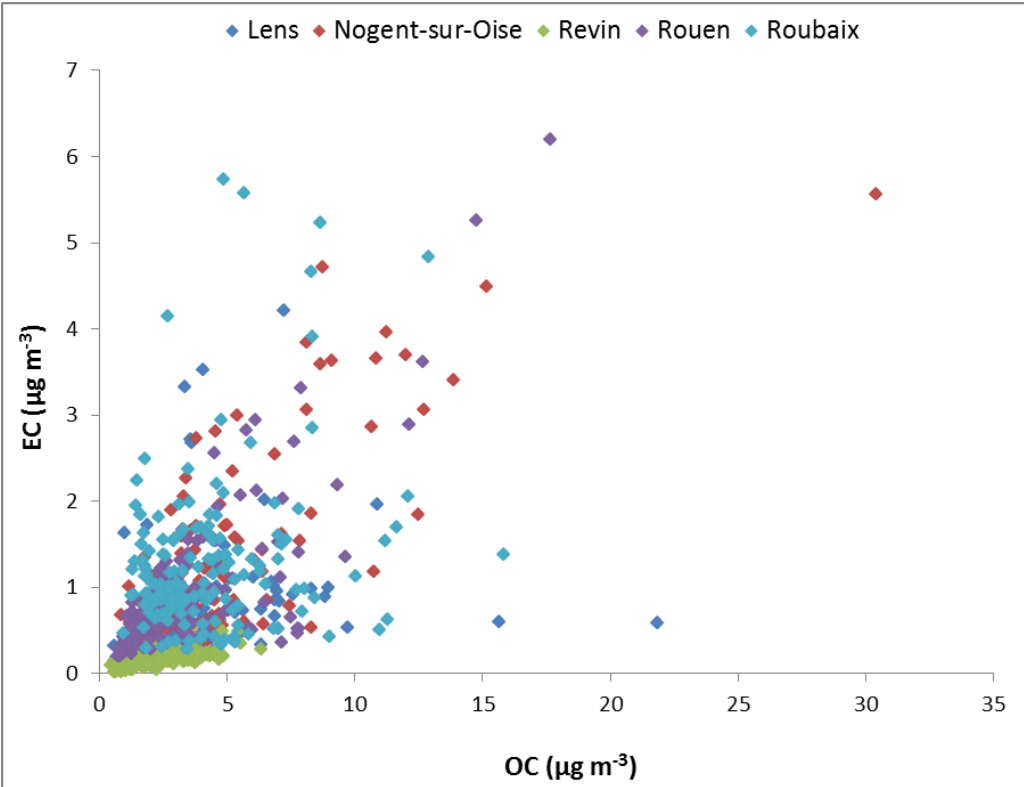


Figure 38: Correlation between EC and OC on all sampling sites

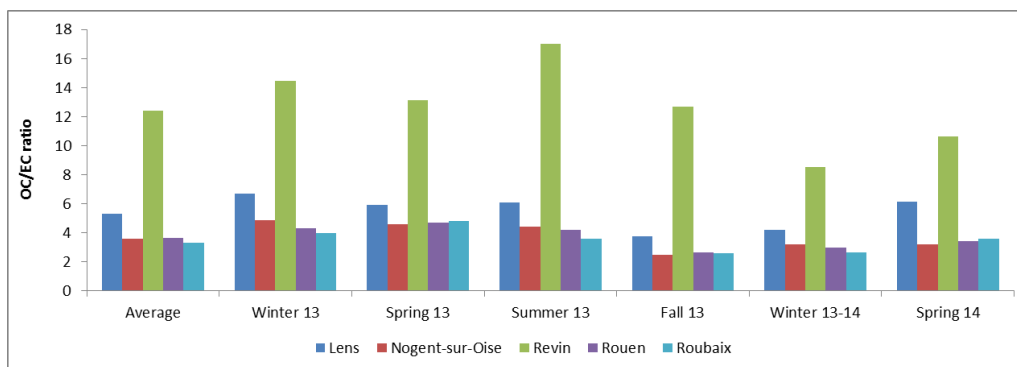


Figure 39: OC/EC ratio at each sampling site per season

Analyzing the ratios between OC and EC clearly demonstrate the completely distinct pattern seen in Revin (figures 38 and 39). This is due to the low contributions of EC in this site indicating the absence of EC sources near Revin. Between the sites located closer to anthropogenic sources, Lens is the one showing a higher OC/EC ratio, and Roubaix, the traffic site, showing the lowest value on average. Again, no clear seasonality was observed, being however interesting to point out the clear difference between the winter of 2013 and the winter of 2013-14.

2.4.2 Organic species

A total of 9 different organic species were measured. Methanesulfonic acid (MSA), oxalate and levoglucosan as main species and then 2 polysaccharides (mannosan and galactosan), 2 polyols (arabitol and mannitol) and 2 monosaccharides (mannose and glucose). Due to very low values of concentration of the last 6 species mentioned, these latter were grouped according to their chemistry. For the site of Nogent-sur-Oise the contributions of monosaccharides were not considered due to the poor data quality of glucose.

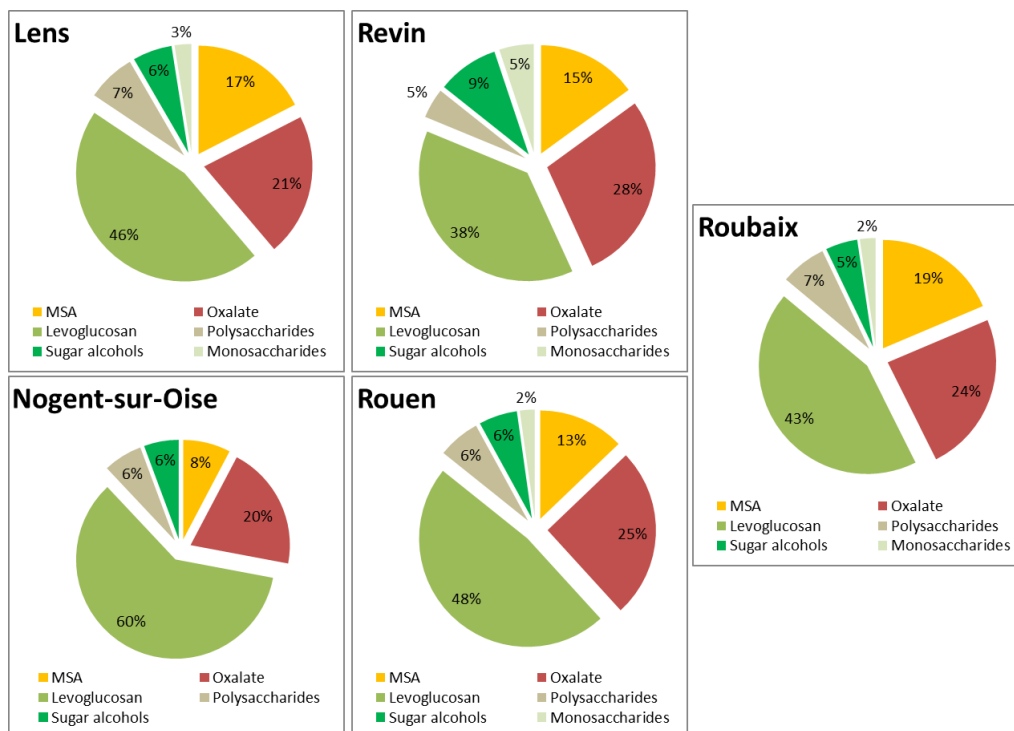


Figure 40: Average contribution of the organic species measured on each sampling site

On all sites levoglucosan was the main contributor among the organic species measured (figure 40). The lowest contribution was seen in Revin, the remote site, and the highest in Nogent-sur-Oise. Levoglucosan is commonly associated with biomass burning activities (B. R. Simoneit et al. 1999) as well as other polysaccharides that are the result of the degradation of cellulose by combustion (Puxbaum et al. 2007), and Nogent-sur-Oise, together with the city of Creil, is known for significant emissions due to house heating practices (ATMO Picardie 2014). Oxalate is found in the atmosphere emitted from both biogenic and anthropogenic primary sources (Kawamura and Kaplan 1987; Kawamura and Ikushima 1993), as well as from oxidation processes of organic precursors in the gaseous and condensed phases (Dabek-Zlotorzynska and McGrath 2000; Chebbi and Carlier 1996; Kawamura, Kasukabe, and Barrie 1996; Myriokefalitakis et al. 2011). MSA (methanesulfonic acid) has been commonly used as a tracer for marine phytoplankton activity (Andreae and Crutzen 1997; Mattias Hallquist et al. 2009; Gaston et al. 2010).

Strong seasonality was seen across the five sites (figure 41). Levoglucosan and polysaccharides showed their highest contributions during both winters in every site supporting the premise of its association with house heating activities. Virtually no contribution is associated with these species during summer on all the sites as well. On the

other hand, MSA exhibited higher contributions during summer and no significant ones during winter also supporting the premise pointed above of it being associated with algae bloom phenomena. Oxalate however showed no clear tendency across the sites or a clear seasonal behavior. Sugar alcohols, commonly associated with biogenic primary emissions, showed an increased contribution during summer and fall on all sites, a result in accordance with the results seen in the work of Waked et al. (2014).

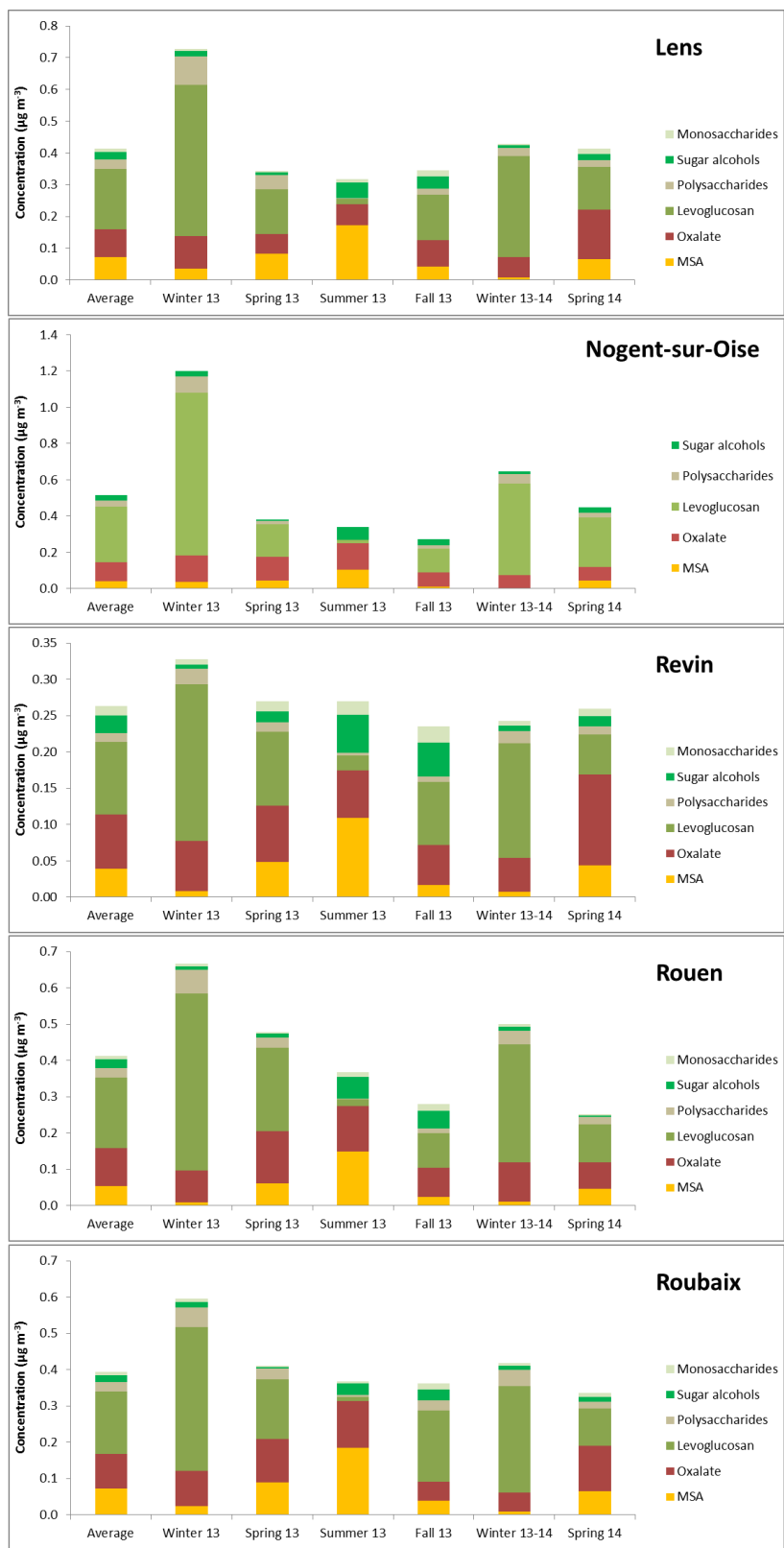


Figure 41: Organic species concentrations on each sampling site, per season

An important characteristic reported in several studies (Schmidl et al. 2008; Maenhaut et al. 2012; Caseiro et al. 2009) is the ratios observed between species, namely the ratios of concentrations of levoglucosan with mannosan and the sum of mannosan and galactosan. These ratios have been associated directly with smoke from wood burning activities and could therefore be used to predict the contribution of these particles to PM₁₀ mass.

Assessing the correlations between levels of levoglucosan observed during the same days in the different sites, one can have an idea if these particles could have a regional influence by showing high correlations.

Table 9: Between site correlation coefficients for levoglucosan contributions during the studied period from the 5 sites

	Lens	Nogent-sur-Oise	Revin	Rouen	Roubaix
Lens	1.00				
Nogent-sur-Oise	0.66	1.00			
Revin	0.73	0.56	1.00		
Rouen	0.50	0.51	0.52	1.00	
Roubaix	0.82	0.59	0.64	0.48	1.00

Table 9 shows that low correlations were seen between the sites, indicating that contributions of levoglucosan are very specific to each sampling site, suggesting rather local sources of this compound. Interestingly, the highest correlation seen was between the site of Lens and Roubaix, the sampling sites that are located closer together, at a distance of 37km of each other.

Studies on the combustion of wood showed that different kinds of wood such as softwoods (like spruce and larch) and hardwoods (like beech or oak) are associated with different ratios of levoglucosan and mannosan in the emitted particles. Several studies have associated lower ratios for softwoods (3.9 – 6.7 in the US; 3.6 – 3.9 in Austria) and higher for hardwoods (13 – 24 in the US; 14 – 15 in Austria) in the US (Fine, Cass, and Simoneit 2004) and in the European country of Austria (Schmidl et al. 2008). The latter also associated a lower ratios of levoglucosan to the sum of mannosan and galactosan to softwoods (1.2 – 2.8) and higher to hardwoods (8.5 – 9.9). Higher concentrations of these compounds were seen during winter, as reported above, so the values during these were the ones used to assess the composition of wood smoke related particles (table 10).

Table 10: Average and seasonal ratios of L/M and L/(M+G) for each sampling site

		L/M	L/(M+G)
Lens	Average	88.1	15.5
	Winter 13	6.8	5.2
	Spring 13	5.6	4.6
	Summer 13	445.8	46.9
	Fall 13	9.0	8.1
	Winter 13-14	18.0	13.9
	Spring 14	14.2	11.0
		L/M	L/(M+G)
Nogent-Sur-Oise	Average	22.1	10.5
	Winter 13	15.5	12.1
	Spring 13	14.2	11.5
	Summer 13	78.8	14.0
	Fall 13	7.9	6.9
	Winter 13-14	14.4	9.9
	Spring 14	13.4	9.6
		L/M	L/(M+G)
Revin	Average	11.9	9.6
	Winter 13	14.0	11.6
	Spring 13	13.3	10.6
	Summer 13	9.2	7.6
	Fall 13	14.6	12.2
	Winter 13-14	13.1	9.9
	Spring 14	7.8	6.3
		L/M	L/(M+G)
Rouen	Average	27.1	9.0
	Winter 13	11.0	7.9
	Spring 13	33.6	11.4
	Summer 13	83.9	13.9
	Fall 13	9.5	7.6
	Winter 13-14	10.6	8.1
	Spring 14	6.5	4.3
		L/M	L/(M+G)
Roubaix	Average	8.1	6.4
	Winter 13	9.5	7.4
	Spring 13	5.8	4.7
	Summer 13	9.2	6.0
	Fall 13	8.3	7.5
	Winter 13-14	9.1	7.5
	Spring 14	7.5	6.0

The north of France is characteristic of a dominance of broad-leafed trees, also known as hardwood according to the French National Institute of Geographic and Forestry Information (Institut National de l'Information Géographique et Forestière – IGN). The results seen for the mentioned ratios show a tendency to be in better accordance with characteristic emissions of these woods. In Chapter 4 of this work, a comparison was made between the predicted contribution of wood smoke particles to PM₁₀ mass and average contributions of the biomass burning factor obtained from the PMF exercise on each site.

2.4.3 Ions

To study the water soluble ions in particles and their contribution is of great importance to any PM based work due to their significant presence in aerosols in general and usefulness on tracing specific natural and anthropogenic sources. In this study 7 main ions were measured (3 anions and 4 cations) identifying, as seen above, sulfate, nitrate and ammonium as 3 of the 4 main contributors in PM₁₀ mass concentration across the 5 sampling sites.

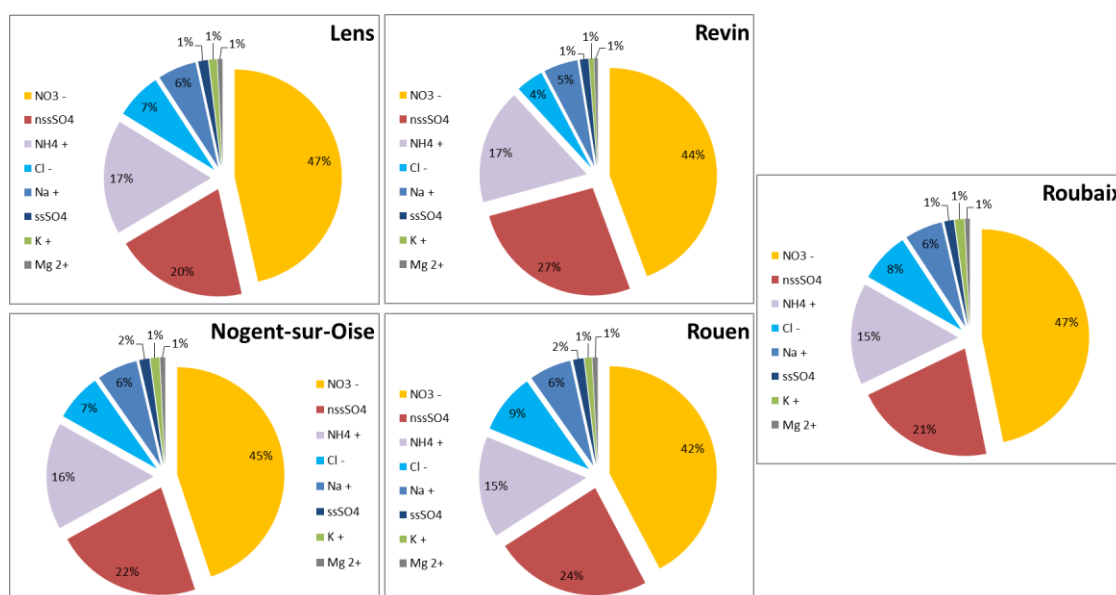


Figure 42: Ion contribution to PM₁₀ mass on each sampling site

No significant differences were found between the sites concerning average contribution of these ions (figure 42). Sulfate, nitrate and ammonium were the main ions on all sites followed by chloride and sodium. The values of chloride and sodium found in Revin were inferior to

the other sites, as explained previously by the bigger distance of this sampling site to the sea. Also in Revin, the proportion of non-sea salt sulfate is higher than in any other site.

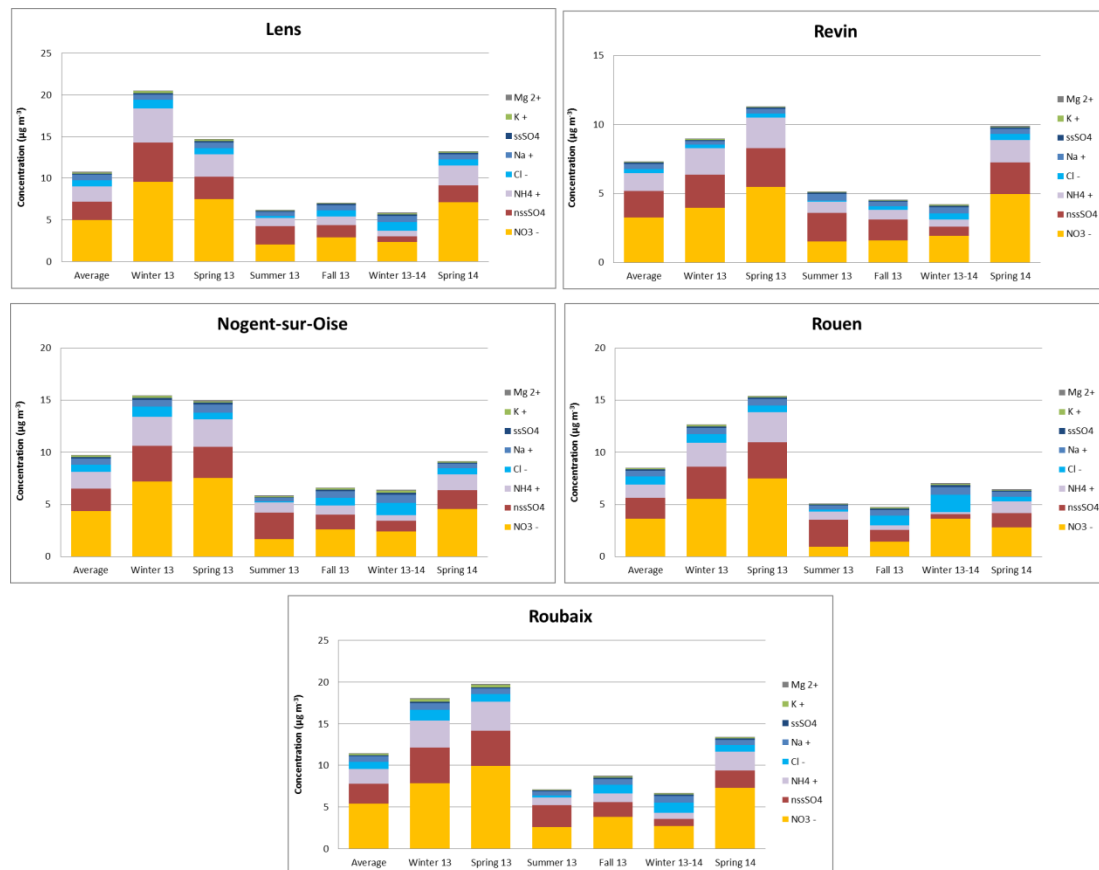


Figure 43: Ion concentrations on each sampling site, per season

Not like EC and OC, the ions showed a strong seasonality on all sites (figure 43). Higher concentrations were seen in winter and spring on all sites, driven by an increase on nitrate, sulfate and ammonium contributions during these seasons. Again the difference between the winter of 2013 and the winter of 2014 is evident in this exercise. Lens showed a significant difference between the winter of 2013 and spring 2013, with a decrease of about 25% of ion average concentrations, something not observed on the other sites. Finally, once more we see Revin with the lowest average contributions when compared with the other sites, but still showing the same seasonal behavior, and similar average contributions in Nogent-sur-Oise and Roubaix.

All these observations contribute to demonstrate that water-soluble ions are mostly related to regional pollution, as all the sites show almost the same composition and the same seasonal variation. However differences are seen between sites regarding the sums of their mass

concentrations (in seasonal average) which may reach up to $20 \mu\text{g}/\text{m}^3$ in Roubaix and Lens (the most northern sites) but only $15 \mu\text{g}/\text{m}^3$ in Nogent-sur-Oise and Rouen (the most southern sites) and $10 \mu\text{g}/\text{m}^3$ in Revin (remote site). This may be due to different local sources that may add their contributions to the regional one, but this may also be related to the impact of a strong emission source area located in the north of the investigated region (i.e. maybe in Belgium and the Netherlands) which could have a decreasing impact along a north-to-south axis.

In order to understand and predict how these ions are found in ambient air a mass closure / ion balance was performed based on the following assumptions and suggested in the work of Alastuey et al. (2005):

- The sodium found in the sampling sites has marine origin and is balanced with chloride
- Ammonium is preferentially associated with sulfate as $(\text{NH}_4)_2\text{SO}_4$ (Seinfeld and Pandis 1998)
- In case of excess of ammonium this is associated with nitrate as NH_4NO_3
- Due to strong presence of nitrate seen during this work this remaining nitrate is associated with excess of sodium and the remaining cations

This method allows to predict the contributions of 4 main compounds: NaCl , NaNO_3 , $(\text{NH}_4)_2\text{SO}_4$, and NH_4NO_3 , where the first and the second are supposed to be associated with marine origins (the first with fresher particles), and the 2 remaining with anthropogenic activities. With this method, all the main species were allocated, with the exception of around 15% of the nitrate. Curiously, this value is then perfectly matched by the sum of the cations that were not used to in the method (i.e. K^+ , Mg^{2+} and Ca^{2+}) The average contribution of these main species can be seen in figure 44.

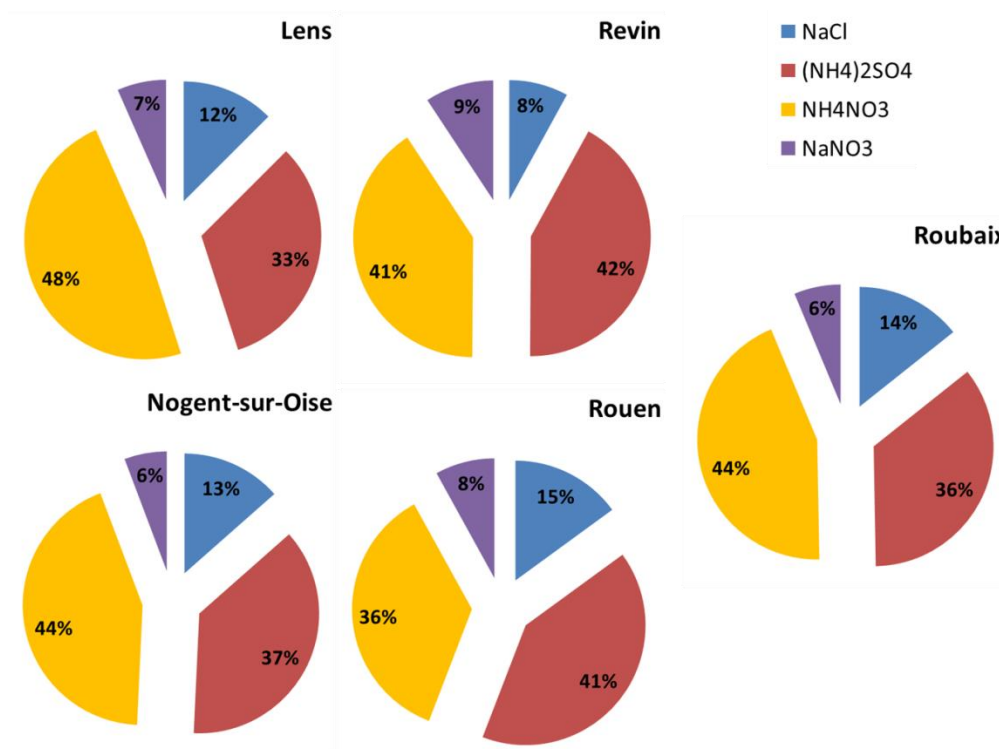


Figure 44: Average contributions of the calculated species of NaCl, NaNO₃, NH₄NO₃ and (NH₄)₂SO₄ for each sampling site

Once again is evident the importance of species related with anthropogenic activities. Is also interesting to point out the lower contribution of sea salt related particles in Revin, the remote site, which at the same showed the largest contribution of more aged marine salts. Revin is also the site located farthest from the coast.

2.5 Exceedance episodes

As reported before and defined by the EU, a limit on PM₁₀ average daily concentration is imposed to all EU countries of 50 µg m⁻³, to not be exceeded more than 35 times in one year. This study collected samples every third day and found the following number of samples with PM₁₀ mass concentration above the mentioned limit during the studied period of 18 months (table 11).

Table 11: Number of exceedance episodes on each site, during the sampling period

	Lens	Nogent-sur-Oise	Revin	Rouen	Roubaix
n° of samples with $PM_{10} > 50 \mu g m^{-3}$	6	18	1	13	13

The sampling site with the larger number of exceedance episodes was unexpectedly Nogent-sur-Oise, which does not present the higher average PM_{10} mass concentration. On the other hand, in Revin just one sample was seen with PM_{10} concentration above $50 \mu g m^{-3}$.

These exceedance episodes also show a clear seasonal dependence, as most were found during spring and winter across the five sites (Figure 45). It is noteworthy also that this study includes two cold periods (winter 13 + spring 13 and winter 13-14 + spring 14) and just one warm period (summer 13 + fall 13) however, and just including the first 4 seasons of this study, most exceedance episodes occur during spring, followed by winter.

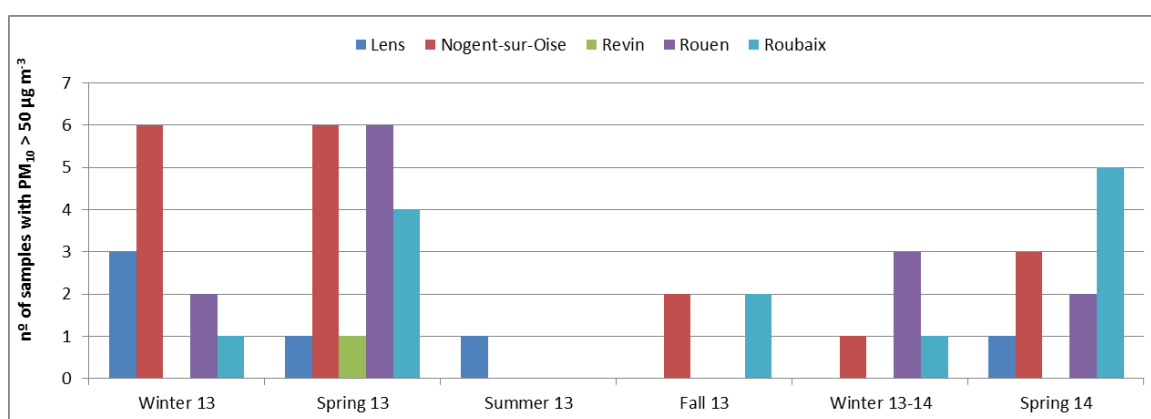


Figure 45: Seasonal distribution of exceedance episodes on each site

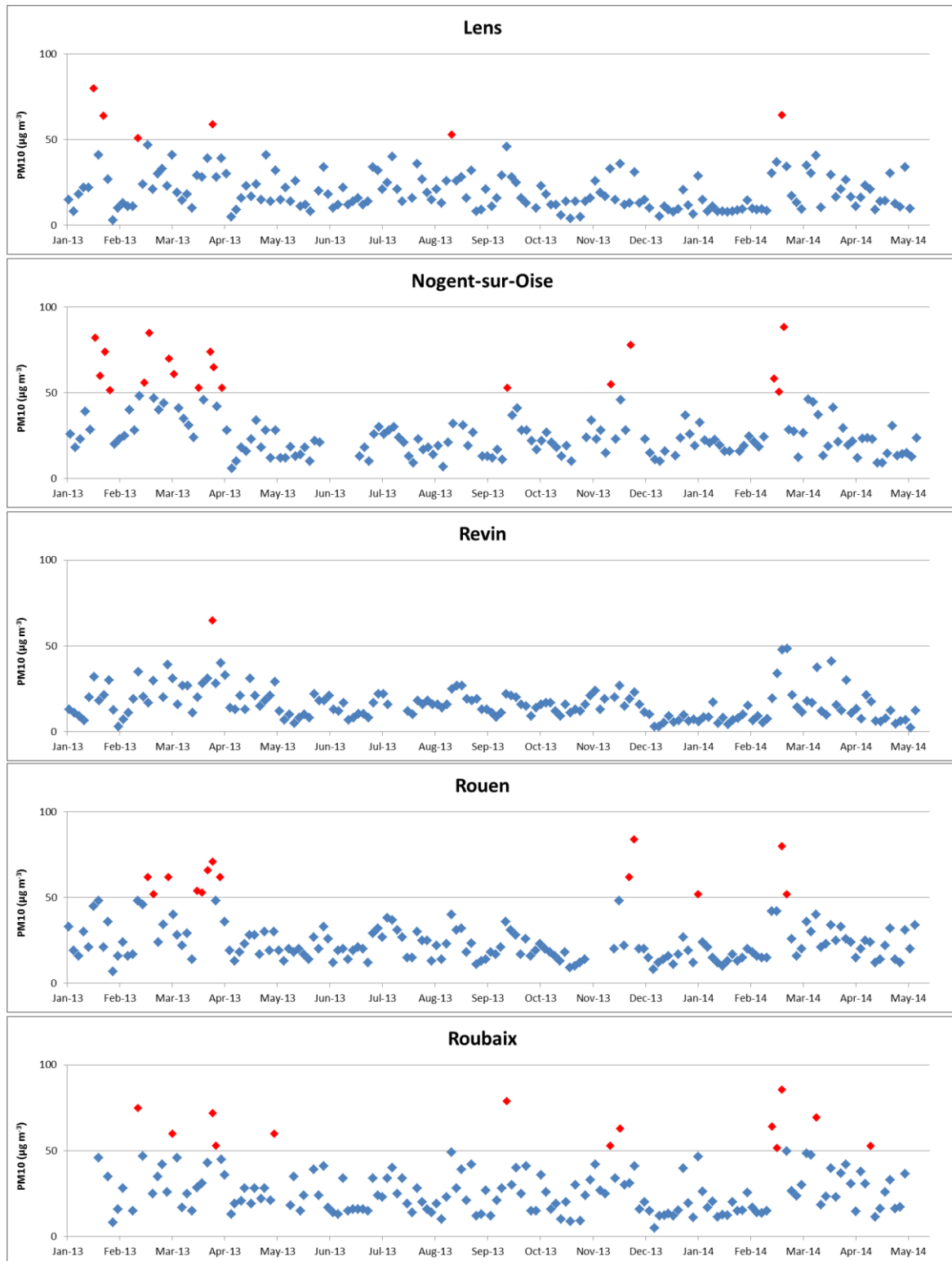


Figure 46: Time distribution of exceedance episodes on each sampling site

It is visible there is some correlation between the 5 sites in terms of exceedance episodes (figure 46). Two periods seem to be evident, one in late March 2013 and the other in late

February 2014. This correlation between sites is an indication and evidence on a possible regional influence of PM₁₀ in the north of France. A chemical speciation during these events shows the importance of the main components like OM and nitrate (figure 47).

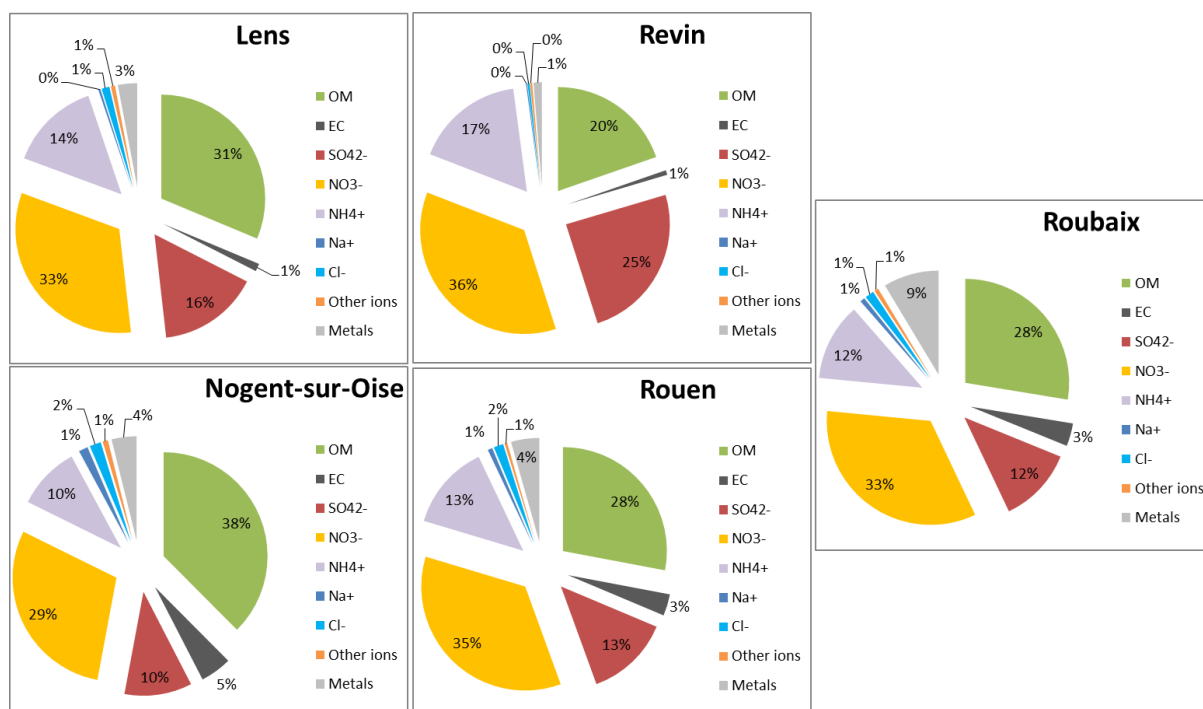


Figure 47: Average chemical composition during exceedance episodes on each sampling site

Across the five sites, once more, the chemical composition during exceedance episodes did not show significant differences from site to site. When compared to the average composition during the studied period one sees the increased importance of the main ions – nitrate, sulfate and ammonium. Nogent-sur-Oise shows a strong contribution of OM as well, followed by Lens, Rouen and Roubaix, all sites with strong anthropogenic influence. The remote site of Revin showed its exceedance episode due to a strong contribution of secondary inorganic aerosols (SIA). To better understand the differences seen across the sites, one can study individual events like the one seen on late March 2013 (figure 48), where all sites recorded PM₁₀ levels above the 50 µg m⁻³ limit (30th of March to all sites, except for Nogent-sur-Oise sampled on the 29th).

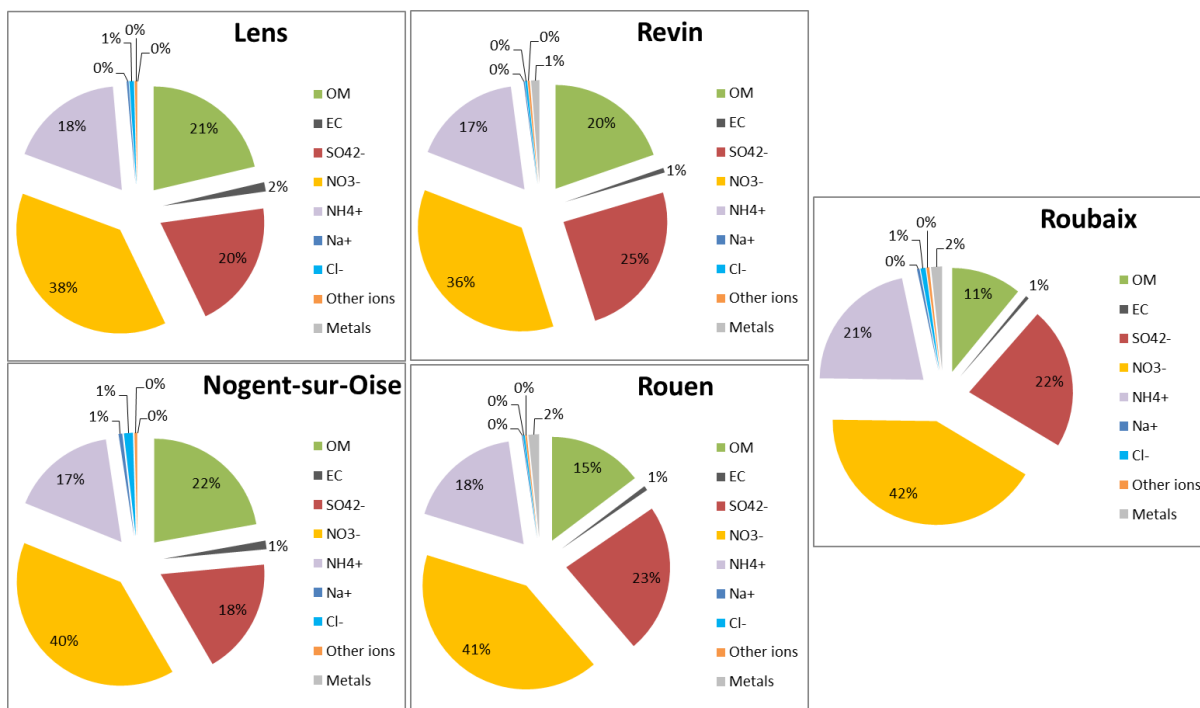


Figure 48: Chemical composition of the samples of March 30, 2013 at all sites, except Nogent-sur-Oise sampled on the 29th

The importance of the main ions is evident, being the main contributors to PM₁₀ mass during this event on all 5 sites. This is evidence of the regional impact of these species and their importance during high concentration episodes.

Other sampled recording high concentration of PM₁₀ was the 6th of March 2013, where the legal limit was exceeded in Nogent-sur-Oise and Roubaix (figure 49).

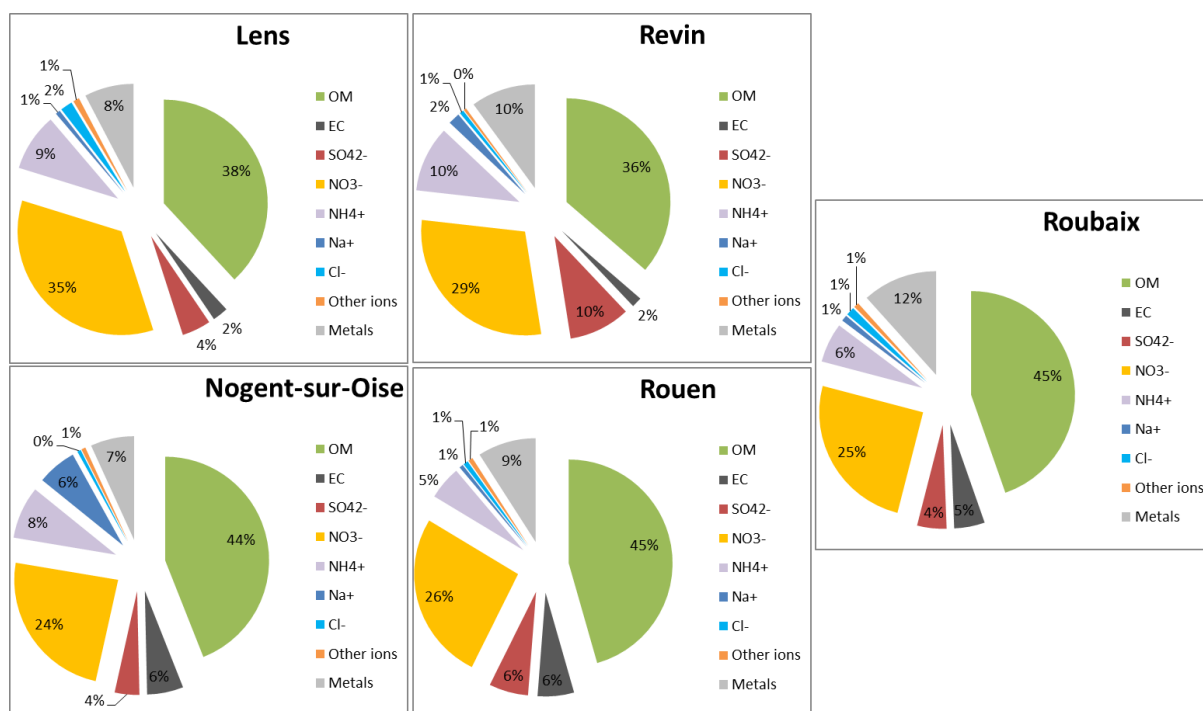


Figure 49: Chemical composition of the samples of March 6, 2013 to all sites

Once again an important fixture of the chemical composition seen for the samples collected on the sites on the same day is the small variability from site to site, however, when comparing the chemical composition of these samples with the ones collected on the last day of March, the stronger influence of OM to the total PM_{10} mass is clear. This is an important indication that different sources are contributing to the high concentrations of PM in the atmosphere, and that a regional influence of the pollutants is expected.

2.6 Conclusions of Chapter 2

Samples collected in 5 sites spread across the north of France were analyzed and validated in this work. These sampling sites were characterized in regards to their typology, surroundings and average meteorological data collected in nearby stations.

The study of the uncertainties associated with the analytical measurements and a methodology of calculation of these uncertainties was defined. The obtained concentrations of measured species were then validated and their ion balance assessed. A good agreement between anions and cations was observed in all sites. PM_{10} mass was also reconstructed and compared to the

mass concentration measured at each sampling site. Unaccounted masses ranged from 0% to 20% on the 5 sites and no particular seasonal dependency was observed.

The traffic site of Roubaix recorded the highest average concentrations of PM_{10} during the studied period and the remote site of Revin the lowest. Interestingly, the average composition of particles was quite similar on all sites, and organic matter was seen to be the main contributor. The major ions showed also significant contributions on all sites.

Strong seasonality was observed on the main contributing ions, driven by higher contributions of nitrate during spring, accounting for approximately 45% on average of the ionic component of PM_{10} . Organic species also demonstrated strong dependency with seasons, namely levoglucosan with higher contributions during winter. No correlation of levoglucosan between sites was found, suggesting an influence of more local sources driven probably by the combustion of hardwood material, as assessed from the ratios of levoglucosan with mannosan and with the sum of mannosan and galactosan.

Finally, a significant number of exceedance episodes was observed in sites with anthropogenic presence. These episodes were observed mainly during spring and winter, and their chemical composition suggests a multitude of factors contributing to them, with some of these samples being driven by secondary inorganic aerosol (nitrate, sulfate and ammonium) and others with organic matter as the main contributor.

This comprehensive chemical characterization of PM_{10} collected in 5 different sampling sites will allow a robust source apportionment exercise on each site and, because the methodologies of analysis and data treatment were kept the same, the results are completely comparable.

CHAPTER 3

***“COMBINATION OF POSITIVE MATRIX
FACTORIZATION AND CONCENTRATION
FIELD METHODOLOGIES TO INVESTIGATE
THE SOURCES AND GEOGRAPHICAL
ORIGINS OF PM_{10} CHEMICAL SPECIES:
A FRENCH URBAN SITE CASE STUDY”***

(Publication 1)

CHAPTER 3 - “COMBINATION OF POSITIVE MATRIX FACTORIZATION AND CONCENTRATION FIELD METHODOLOGIES TO INVESTIGATE THE SOURCES AND GEOGRAPHICAL ORIGINS OF PM₁₀ CHEMICAL SPECIES: A FRENCH URBAN SITE CASE STUDY” (PUBLICATION 1)

This chapter addresses the methodology associated with the source apportionment exercise at an urban sampling site in the north of France, located in Nogent-sur-Oise, and their geographical location. This will be reported as a publication that deals with the chemical characterization of PM₁₀, its seasonality and contributions during exceedance episodes. A distinction is made between local and regional sources and their geographical locations are estimated.

3.1 Summary of Publication 1

This article objective is to uncover the methodology followed to assess a near-to-complete knowledge on a sampling site PM₁₀ concentration masses, its chemical composition and seasonal variability, the main impacting sources of particles and their geographical location. Based on a complete database built with 158 samples collected during 18 months, a total of 36 species were analyzed and quantified. The chemical measurements, including compounds like MSA and oxalate, allowed to perform a PMF analysis and to identify 9 main sources impacting Nogent-sur-Oise. The use of meteorological information like wind speed and wind direction was used to draw NWR plots to help defining local and regional sources. Back-trajectories calculated with HYSPLIT4 permitted the use of the concentration field method to assess the probable location of these regional sources.

3.1.1 Chemical analysis – Methods and results

As mentioned above, a total of 158 samples were collected from the 2nd of January to the 2nd of June. PM₁₀ mass concentration was measured by TEOM-FDMS, ions and organic species were measured by ion chromatography and HPLC-PAD, respectively, EC and OC measured by TOT and metals analyzed by ICP. A total of 5 days did not record PM₁₀ mass

concentration, and these values were replaced by the reconstructed mass following the methodology presented by Waked et al., 2014. Considered as missing values, associated to these reconstructed concentrations a factor of 4 was added to their uncertainty as proposed by Brown et al. (2015). A series of 3 consecutive samples also did not record metal concentrations (29th and 31th of March and 2nd of April of 2013). Here, due to the fact that all the metal concentrations are missing and therefore there is no possibility of reconstructing their concentration, these samples were discarded.

An average mass concentration of PM₁₀ of $27.7 \pm 16.8 \mu\text{g m}^{-3}$ was observed and the main contributing specie to PM₁₀ mass was organic matter, calculated from the concentration of OC multiplied by a factor of 1.75 as proposed by Guinot, Cachier, and Oikonomou (2007) and Favez et al. (2009). OM contributed to 38% of the measured PM₁₀ mass during the sampling period with an average concentration of $7.2 \pm 6.1 \mu\text{g m}^{-3}$. The following main contributors were the major ions: nitrate, sulfate and ammonium contributing 23%, 12% and 8% to PM₁₀ mass, respectively. Finally, EC with an average concentration of $1.2 \pm 1.0 \mu\text{g m}^{-3}$ was the 5th main contributor, followed by the remaining ions and metals.

Strong seasonality was found during the studied period associated with the main contributing species. OM had its highest average concentration during the winter of 2013 (composed just by the months of January and February) of $10.8 \pm 7.0 \mu\text{g m}^{-3}$, and its lowest concentration during the fall of 2013 with $6.1 \pm 4.6 \mu\text{g m}^{-3}$, an decrease 44% in concentration. Nitrate showed even stronger seasonal variability ranging from $7.5 \pm 6.5 \mu\text{g m}^{-3}$ in the spring of 2013, down to $1.7 \pm 1.6 \mu\text{g m}^{-3}$ in the following season, a difference of 77% of the concentration.

An important characteristic was observed related with the winter seasons of the studied period. The average PM₁₀ concentration during the winter of 2013 was the highest recorded ($42.9 \pm 20.4 \mu\text{g m}^{-3}$), however, the winter of 2014 recorded much lower concentrations ($23.8 \pm 13.8 \mu\text{g m}^{-3}$), a difference of 45% between the same seasons one year apart. This difference is mainly attributed to the average concentration of ions, $15.5 \mu\text{g m}^{-3}$ vs $6.4 \mu\text{g m}^{-3}$, a difference of 59% that help to explain the discrepancy between PM₁₀ values.

3.1.2 Source apportionment

A total of 9 factors were identified: traffic, biomass burning, land and marine biogenic, fresh and aged sea salt, oxalate-, sulfate-, and nitrate-rich. Traffic was seen to be the main contributor to PM₁₀ mass (18%) followed by biomass burning (15%), nitrate-rich (14%) and oxalate- and sulfate-rich (13%). Fresh and aged marine aerosols contributed 9% and 8%, respectively, and biogenic particles from land and sea 7% and 3%, respectively.

Traffic, the main contributor, was identified by a significant presence of EC and OC, as well as most of the analyzed metals. The presence of elements such as Cu, Fe, Ba and Zn indicate that this factor is composed not only from exhausted related emissions, but also from non-exhaust related particles originated from brake and tire abrasion. The presence of Ca in its chemical profile suggests also that an important fraction of this factor is composed by crustal matter that can either be transported or resuspended from the traffic activity. This is supported by the presence of nearly 60% of this species was found in this profile and that no crustal matter factor was found. The absence of other crustal matter tracers like Al, Si and Ti may have also contributed to the inability of PMF to account such source. This factor was seen with stronger contributions during spring and fall and lower ones during summer.

The nitrate rich factor, composed mainly by nitrate and ammonium, was an important contributor to PM mass. Its chemical profile suggests that these particles are found in the atmosphere as ammonium nitrate and its strong seasonal variation supports this claim. Higher contributions of nitrate rich particles were seen during winter and especially spring (22%), falling down to just 4% in summer and 8% in fall. The semivolatility of these particles explains the higher contributions during colder months, as well as the seasonality associated with related sources (agricultural activities) that start late winter and spring.

Sulfate rich and oxalate rich particles were also major contributors to PM mass, without however showing the strong seasonality of the previous factor. Contributions of sulfate rich aerosols ranged from 12% in winter to 16% in summer, and oxalate rich from 11% in winter and fall, and 21% in summer. The higher contribution during summer can firstly associated to lower emissions of the remaining factor as well as the increased emission of organic matter and organic compounds, which can be precursors for oxalate.

Finally, a note to the biogenic particles identified in this study thanks to the analysis of specific tracers like sugar alcohols and MSA, both land and marine biogenic factors showed

their highest contributions during summer time. This was expected due to increased solar radiation leading to more intense biological activity.

3.1.3 Source location

To determine the possible geographical location of sources the authors first investigated the NWR associated with each factor. The ones seen to be associated predominately with higher wind speeds were assumed to have distance sources. The local identified factors were traffic, biomass burning and land biogenic. The oxalate rich factor seemed also to have an important local contribution, leading to assume that is an indication of the formation of these particles. On the regional factors of fresh and aged sea salt, nitrate- and sulfate-rich factors the concentration method was used to determine the geographical location of these sources.

From the regional factors identified in this study, a clear distinction was seen between natural and anthropogenic related emissions. Factors like fresh and aged sea salt are originated from the Atlantic Ocean, and the difference between the two seems to be related with the velocity of the back-trajectories. Back-trajectories with higher velocities, originated from the North Atlantic Oscillation, carry “cleaner” particles of sea salt, whereas, air masses with less velocity originated in the Atlantic Ocean carry more aged aerosols. The lower speed of these air masses allows also the input of local anthropogenic emissions in this factor, seen by the presence of metals like Ni and V. Marine biogenic particles are mainly originated from the North Sea, associated with intense algae bloom seen during late spring and beginning of summer in this region.

Anthropogenic related particles, like sulfate and nitrate rich, are originated from continental areas. Central and Eastern Europe were clearly identified as strong sources of these particles. Nitrate-rich particles seem also to be associated with sources located closer to the sampling site, like Belgium and the Netherlands, whereas sulfate rich aerosols seem to have also a possible contribution from ship emissions in the Strait of Gibraltar. Finally, oxalate-rich particles showed a more “scattered” concentration field map which can be linked to the presence of more local sources or local formation of these particles.

**COMBINATION OF POSITIVE MATRIX FACTORIZATION AND CONCENTRATION
FIELD METHODOLOGIES TO INVESTIGATE THE SOURCES AND GEOGRAPHICAL
ORIGINS OF PM₁₀ CHEMICAL SPECIES: A FRENCH URBAN SITE CASE STUDY**

Diogo M. Barros de Oliveira^{1,2,3}, Esperanza Perdrix^{1,3}*, Olivier Favez², Stéphane Sauvage^{1,3},
Laurent Y. Alleman^{1,3}, Benoit Rocq⁴, Véronique Riffault^{1,3}

¹ IMT Lille Douai, Univ. Lille, SAGE, F-59000 Lille, France

² INERIS, F-60550 Verneuil-en-Halatte, France

³ Univ. Lille, F-59000 Lille, France

⁴ Atmo Picardie F-80332 Longueau, France

* Corresponding author: Esperanza Perdrix (esperanza.perdrix@mines-douai.fr)

Abstract

The knowledge of the sources of airborne particulate matter at a given sampling site can provide policymakers with crucial information to implement adequate measures to battle poor air quality in urban areas. A full chemical characterization was performed on samples collected at an urban French site for 18 months. The impacting sources assessment was made using the Positive Matrix Factorization model and showed important contributions of primary and secondary particles on PM₁₀ mass concentration. Traffic and biomass related emissions were seen to be the main causes for primary aerosols production whereas sulfate rich and nitrate rich aerosols, associated with long range transport phenomena, were the main secondary contributors. The use of other statistical tools like the non-parametric wind regression and the Concentration Field method helped confirming not only the local or regional status of the identified sources but also identifying their probable geographical location. Natural sources such as fresh sea salt and marine biogenic were well spotted in the Atlantic Ocean and North Sea, respectively. On the other hand, secondary aerosols origin were clearly found in Central and Eastern Europe and therefore associated with anthropogenic activities.

Keywords

PM₁₀, PM Chemical composition, Receptor-oriented methods, Source apportionment, PMF, Backward trajectories

1 INTRODUCTION

Particulate matter (PM) in ambient air has significant health, economic (World Bank, 2016) and environmental impacts (Kelly and Fussell 2015; Samoli et al. 2008), aggravated during high concentration episodes, which have become an increasing concern for policymakers especially in densely populated areas. Precise information on the particle chemical composition, emission sources, and geographical origin are then required to prepare and implement effective action plans.

Over the last 20 years, different statistical tools have been developed to identify and quantify emission sources of PM based on the knowledge of chemical composition at the sampling site (Paatero and Tapper 1994; Schauer et al. 1996; Ulbrich et al. 2009). Among these tools, generally referred as receptor-oriented models, the Positive Matrix Factorization (PMF) model allows grouping variables in what can be read as factors, or sources, with their corresponding temporal contributions (Waked et al. 2014; Pandolfi et al. 2008; Paw-Armart and Yoshizumi 2013; Maenhaut et al. 2016; Alleman et al. 2010). The identification of sources by PMF highly depends on the data quality provided, for which an exhaustive chemical characterization is recommended, including specific tracers of sources. Common sources such as primary traffic and industrial emissions, sea salt and crustal dust, can generally be quantified using PMF. However the use of new tracers can allow the identification of some less classical sources usually not taken into account, like primary biogenic emissions (Waked et al. 2014; Golly et al. 2015) or secondary marine emissions (Bove et al. 2016).

Together with the identification of sources and their underlying characteristics (factor profiles and temporal contributions), it is also of major interest, in order to implement appropriate and efficient PM reduction policies, to distinguish between local and regional sources and to gain extra knowledge on the geographical location of the latter. This distinction can and should be made according to previous literature studies as well as by interpreting the results obtained with the receptor-oriented model used. The use of external information has proven to be helpful in a number of source apportionment studies (Kim Oanh et al. 2009; Watson et al. 2002; Watson et al. 2008; Belis et al. 2011; Zhao and Hopke 2006). In the present work, meteorological data such as wind speed and direction were used to build pollution roses of local sources while back-trajectories were calculated for the receptor sampling site in order to track regional sources. These back-trajectories were also used for Concentration Field (CF)

analyses. CF is a Trajectory Statistical Methods (TSM) that allows calculating the residence-time averaged concentration measured at the receptor site when back-trajectories pass over of a given area (Seibert et al. 1994). CF outputs can be used to map the probable origins of regional source air masses. Having the information of species concentrations and impacting sources on a given receptor site, one can compute the air mass back-trajectories arriving at this site during the sampled period to assess the origin of air masses to this specific point in space. These models are commonly referred to as Hybrid Receptor Models (Han, Holsen, and Hopke 2007) or Trajectory Statistical Methods (TSMs) (Kabashnikov et al. 2011). There are several variations of TSMs that have been applied to characterize atmospheric PM: Potential Source Contribution Function (PSCF) (Han, Holsen, and Hopke 2007; Abbott et al. 2008; Choi, Choi, and Yi 2011; Xu and Akhtar 2010; X. Fu et al. 2011), Gridded Frequency Distributions (GFD) (Weiss-Penzias, Gustin, and Lyman 2011; Sexauer Gustin, Weiss-Penzias, and Peterson 2012), Concentration Fields Analysis (Rutter et al. 2009) or Concentration-Weighted Trajectory (CWT), and Residence Time Weighted Concentration (RTWC) (Han, Holsen, and Hopke 2007). The main difference between methods has to do with how concentrations are incorporated in the trajectory and the frequencies in each grid cell. The CF allows the identification of the sources and provides computed data which can be used to examine the quantitative relationships between measured concentrations and emissions (A. Charron et al. 1998).

The present study expects to go further by adding – for the first time to the best of our knowledge – the contributions of methanesulfonic acid (MSA), oxalate, sugars, sugar anhydrides, and sugar alcohols to major PM species and trace metals, and evaluate their usefulness as tracers for a source apportionment study at a French urban site. We combined an extensive chemical speciation of PM with both receptor-based and trajectory-based models to identify and localize sources of PM impacting a designated receptor site. This has allowed to geographically allocating not only chemical species but also sources with a regional impact.

2 METHODOLOGY

2.1 Sampling site

For this study, daily PM₁₀ filter samples were collected by ATMO Picardie, the local air quality monitoring network, at an urban site in Nogent-sur-Oise (49°16'35.004'' N,

2°28'55.812" E), and located 70 km north of Paris. This site location allows assessing the regional impact of the Paris megacity, and also verifying the conclusions of previous source apportionment studies showing a strong influence of North-Eastern air masses on urban North-Western European PM₁₀ levels (Sciare et al., 2010; Bressi et al., 2011; Freutel et al., 2013; JOAQUIN, 2015). Nogent-sur-Oise (18,753 inhabitants in 2013) forms with Creil (34,262 inhab. in 2013) and their inner suburbs a continuous urban area with over 100,000 people (around 750 inhab./km²). This area is furthermore, surrounded by important urban agglomerations, mostly Paris in the south (70 km, over 12 million inhab.), Beauvais in the west (40 km, 55k inhab.), Amiens in the north (70 km, 130k inhab.) and Lille in the north-northeast (170 km, 230k inhab.). Various anthropogenic local sources are then expected to significantly influence the sampling site, which is located approximately 200 m away from a busy road (D1016) and 1.5 km away from a busy intersection between the D1016 and D200 (traffic > 15,000 vehicles/day). There is also a railway 160 m to the north of the sampling site, a canal for boating from east to south of the sampling site 1 km away and an industrial area, 2 km to the east (Figure P1.1).



Figure P1. 1: Sampling site map and its surroundings - * Sampling site; ■ Swimming pool; ■ commercial central parking building; / boat canal; | railway; | roadway

The climate in Nogent-sur-Oise is oceanic, with average temperatures of 10.5°C throughout the year, 4.7°C during winter and 17.8°C during summer. Winds come predominantly from the south-west, north and northeast quadrants. Higher wind speeds are more frequently associated with the south-west direction (Figure S.1, S.2 and Table S.1).

2.2 Measurements and instrumentation

Daily PM₁₀ samples were collected (from 9 am to 9 am UTC) on pure quartz fiber filters (Pall Tissuquartz, diameter of 150 mm, pre-baked at 500°C for 2 hours), using a sequential high volume sampler (Digitel DA80) operating at 30 m³/h. Every third day samples were selected to be analyzed, resulting in a total of 158 filters collected from January 2, 2013 to June 2, 2014. PM₁₀ mass concentration was continuously monitored at the same site by the regional air monitoring network (Atmo Picardie) using a TEOM-FDMS instrument (Tapered Element Oscillating Microbalance – Filter Dynamics Measurement System, Thermo-Scientific (Grover et al. 2005)).

The concentrations of a total of 36 different chemical species were measured, including ions, metals, elemental and organic carbon (EC & OC) and organic tracers. A subsample consisting in a 47-mm diameter punch (17.35 cm²) of the initial filter was used for each type of analysis, except for EC/OC (1.5 cm²).

Water-soluble ions were analyzed using ion chromatography (IC, Dionex DX-600) as described in Sciare et al. (2008) and in accordance with the recommendations of the European standardization committee (CEN/TC 264, TR 16269). Before analysis, samples were soaked in 10 mL of Milli-Q water and then filtered in 2 µm-porosity Acrodisc. AS/AG 17 column was used for anions (SO₄²⁻, Cl⁻ and NO₃⁻) and CS/CG 12A column for cations (NH₄⁺, K⁺, Na⁺, Mg²⁺ and Ca²⁺).

For trace and major elements (Al, Ca, Fe, K, As, Ba, Cd, Co, Cu, La, Mn, Mo, Ni, Pb, Rb, Sb, Sr, V), ICP-MS (ELAN 6100 DRC, Perkin Elmer) and ICP-AES (IRIS Intrepid, Thermo-Scientific) were used, respectively (Alleman et al. 2010). Prior to analyses, each sub-sample was acid digested (HNO₃; HF; H₂O₂) at 200°C with a microwave oven (Milestone ETHOS). Repeated measurements were performed on acid blanks, quality control standard solutions and standard reference material (NIST SRM 1648a). Instrumental blanks were used to

validate all the measurements made, and average field blanks were subtracted to obtain the final concentrations.

Elemental carbon (EC) and organic carbon (OC) were analyzed using the thermo-optical transmission (TOT) method on a Sunset Lab analyzer (M. E. Birch and Cary 1996). This analysis was performed according to the NIOSH 870 protocol (Birch and Cary, 1996).

Finally sugars (mannose and glucose), sugar anhydrides (levoglucosan, mannosan and galactosan) and sugar alcohols (arabitol and mannitol) were analyzed by HPLC-PAD using a set of Metrohm columns (MetroSep A Supp 15 and Metrosep Carb1) following a procedure described by (Bressi et al. 2013).

Meteorological data were obtained from the Météo-France station in Creil, located on an airbase 3.5 km from the receptor site. Information such as height and duration of precipitation, average, minimum and maximum temperatures, pressure, wind speed and direction, relative humidity and occurrence of snow events, was retrieved for all sampled days.

2.3 Data validation

All calculated concentrations have taken into account the possibility of contamination by user manipulation and sampling matrix by subtracting the average concentration obtained in field blanks. The ion balance was checked by comparing the sums of cations and anions (Figure S.3 and S4). This procedure allows validating the analyzed ion concentrations (neutralization between cations and anions is expected) and may give clues about the cationic or anionic nature of the unaccounted species if imbalance occurs.

A classical chemical mass closure (CMC) approach was applied in order to assess the global quality of the information obtained and to identify possible outliers. Based on the previous work of Waked et al. (2014) for another urban site in northern France, this CMC was performed as follows:

$$PM_{10} = EC + 1.75 \times OC + 3 \times Na + 10 \times Ca + NO_3^- + nssSO_4^{2-} + NH_4^+ \quad (1)$$

where EC, OC, Na, Ca, NO_3^- , nss (non-sea salt) SO_4^{2-} and NH_4^+ refer to the mass concentrations in $\mu g m^{-3}$ of each component. Sea salt sulfate ($ssSO_4^{2-}$) was calculated by

multiplying the mass concentration of Na by a factor of 0.252, following the methodology described by Seinfeld and Pandis (2006).

Results show a satisfactory agreement between TEOM-FDMS PM₁₀ measurements and the reconstructed mass ($r^2 = 0.88$), allowing to estimate the few missing data of TEOM-FDMS PM₁₀ mass concentrations ($n = 5$) in order to avoid losing a complete sample when all the species were measured except PM₁₀ mass concentration. However, an unknown uncertainty associated with the calculation of PM₁₀ mass concentrations remains, partly due to the value of the conversion factor of OC to OM (assumed constant while there is the possibility of a seasonal influence) and the unaccounted amount of water in the aerosol – leading to an underestimation of the real mass concentration.

- **Uncertainties:** Is important to quantify the uncertainty associated with each measurement, which depends on each step of the analytical process and can, therefore, be linked to the process of sampling, matrix effects, working conditions, analytical uncertainties of the instruments, dilutions, even human error. In this work, the calculation of uncertainties followed the protocol applied by Waked et al (2014) which based the uncertainties of EC/OC, ions and organic species on an expanded uncertainty obtained from intercomparison studies made for each of the analytical methods, and the metal uncertainties obtained from:

$$u_{rel}(C) = \sqrt{u_{rel}^2(Ac) + u_{rel}^2(V) + u_{rel}^2(Rep) + u_{rel}^2(Cont)} \quad (2)$$

where $u^2(Ac)$ is the uncertainty associated with the accuracy of the method by SMR (standard reference materials) measurements, $u^2(V)$ with the sampling volume, $u^2(Rep)$ is the uncertainty associated with the repeatability and $u^2(Cont)$ the contamination.

2.4 Source apportionment using PMF

Receptor site based models can be used to apportion observed concentrations of species into potential sources according to their co-variability. In this study, the Positive Matrix Factorization (PMF) was used as implemented in the EPA PMF 5.0 modelling tool, requiring no prior knowledge on site impacting sources. The database used as input in the PMF software is expressed in a matrix \mathbf{X} with ($n \times m$) dimensions, where n is the number of samples and m the number of chemical species measured, or variables. The goal of the

multivariate source-receptor model is to determine the number of factors p , the chemical profiles of these factors \mathbf{F} ($p \times m$), and the mass contributions \mathbf{G} ($n \times p$) of the factors for each sample, as well as the associated uncertainty estimates. Here, the factors can also be interpreted as sources based on their chemical fingerprint. The model solves the general equation:

$$\mathbf{X} = \mathbf{G} \times \mathbf{F} + \mathbf{E} \quad (3)$$

where \mathbf{E} is the matrix of the residuals (difference between the values measured and the values calculated by the model with regard to the uncertainties). The equation is solved by minimizing the objective function Q through an iterative process:

$$Q = \sum_{i=1}^n \sum_{j=1}^m \left[\frac{x_{ij} - \sum_{k=1}^p g_{ik} f_{kj}}{u_{ij}} \right]^2 \quad (4)$$

where x_{ij} and u_{ij} are the concentration of variable j in the i^{th} observation and its related uncertainty, respectively; g_{ik} and f_{ik} are the mass contribution of source k to the i^{th} sample, and the contribution of variable j to factor k , respectively.

Receptor based models present however some limitations such as the strong dependence on the quality of the database that will be translated into the ability of the model to distinguish (or not) all the sources impacting the sampling site, avoiding mixing emission sources. In addition, the chemical signature of a source is assumed constant throughout time, which can represent a limitation with source signatures that change with time (seasonal influence, chemical aging and gas particle phase partitioning encountered by secondary species which hamper the deconvolution).

The PMF analysis was carried out on the full database of measured chemical species and PM_{10} mass concentrations which were considered as strong or weak variables in the model depending on their uncertainties (table P1.1). Different number of factors (4 to 12) and different combinations of variables were tested to provide the best solution on mathematical robustness and geochemical meaningfulness. Parameters like the scaled residuals, model adjustment to measured concentrations and bootstrap method analyses ensured the robustness of the PMF modeled solution (Tables S.2, S.3 and S.4), while an extensive literature review (Pernigotti, Belis, and Spanò 2016), as well as external meteorological data and back-trajectory information, strengthened the geochemical validation of the source profiles.

From all the measured species, 32 were used in the final PMF solution, including PM₁₀ mass concentration selected as total variable. A small number of constraints (as explained in details in the following sections for each factor) were applied to the PMF modelled solution, based on previous knowledge of the sources signatures.

Table P1. 1: List of variables used in PMF runs and their characterization as "strong" or "weak"

Variable weighting	Variables
Strong	EC, OC, Cl ⁻ , NO ₃ ⁻ , SO ₄ ²⁻ , Na ⁺ , NH ₄ ⁺ , K ⁺ , Mg ²⁺ , MSA, Oxalate, Levoglucosan, Polysaccharides, Sugar alcohols, Ca, As, Cd, Co, Pb, Sb, Sr, V, Zn
Weak	PM ₁₀ (total variable), Fe, Ba, Cu, La, Mn, Mo, Ni, Rb

The solution presented in this work was obtained after performing a constrained run on PMF. Constraint n°1 pulled up the Fe contribution on traffic factor and constraint n°2 set an EC/OC ratio of 2 on the same factor. Both constraints were set with a %dQ parameter equal to 0.5 and the influence on the final solution can be seen in table P1.2.

Table P1. 2: Summary of the applied constraints in PMF run

Traffic	Element	Type	Value	dQ	% dQ
Constraint 1	Fe	Pull up maximally	NA	26.9	0.5
Constraint 2	EC and OC	Expression [EC]/[OC]	2	187.4	0.5
<i>Final solution : dQ = 154.6</i>					

The lower difference seen associated with constraint n°1 is due to the fact that Fe was selected as a weak species and its low concentration leading to an insignificant impact on the final solution. Constraint n°2 resulted on a slight decrease of the average contribution of the traffic to PM₁₀ mass from 19% to 18%, linked with the lower contribution of OC in this factor. The OC “relocated” after the constraint was seen appearing on the land biogenic and biomass burning factors.

2.5 Geographical allocation

The geographical allocation of calculated sources was done using the software ZeFir v3.201 (Petit et al. 2017). Wind sector and wind speed analyses (using NWR see below) allows for

identifying local sources while back-trajectory computation (using CF see below) may help to elucidate the main location of remote primary sources as well as most probable origins of precursors leading to secondary aerosols.

2.5.1 NWR

The non-parametric wind regression allows better representation of general wind direction associated with concentration measurements at a given sampling site by estimating more precisely higher peaks of concentrations and by better distinguishing peaks from nearby directions (Henry, Chang, and Spiegelman 2002). By averaging the observed concentrations of a pollutant based on wind direction (θ) and wind speed (ϑ), the concentration estimate $E(\theta|\vartheta)$ at a wind direction ϑ and wind speed θ is given by:

$$E(\theta|\vartheta) = \frac{\sum_{i=1}^N K_1\left(\frac{\theta-W_i}{\sigma}\right) \cdot K_2\left(\frac{\vartheta-Y_i}{h}\right) \cdot C_i}{\sum_{i=1}^N K_1\left(\frac{\theta-W_i}{\sigma}\right) \cdot K_2\left(\frac{\vartheta-Y_i}{h}\right)} \quad (5)$$

where W_i , Y_i and C_i the wind direction, speed and atmospheric concentrations, respectively, measured at t_i ; σ and h the smoothing factors; and K_1 and K_2 two kernel functions.

Daily contributions of PMF factors were associated with wind speed and wind direction information obtained from the MeteoFrance station situated in the nearby city of Creil with the chosen parameters shown in table P1.3.

Table P1. 3: NWR parameters

Max wind speed	Angle resolution	Radius resolution	Angle smoothing	Radius smoothing
20 m s ⁻¹		0.5	34.7*	6.8*

* Suggested parameters

2.5.2 Concentration Field method

The Concentration Field method (CF) (Seibert et al. 1994) is based on the computation of the residence time-weighted mean of the concentrations logarithm for each grid cell of the domain of trajectory simulations:

$$C_{ij} = \frac{1}{\sum_{l=1}^N \tau_{ijl}} \sum_{l=1}^N \log(c_l) \tau_{ijl} \quad (6)$$

where N is the total number of trajectories, ij the indexes of a grid cell, l the index of a trajectory, c_l the concentration observed at the receptor site on the arrival of a given trajectory l , and τ_{ijl} the residence time of an air mass l on a grid cell ij . A minimum of 10 points per grid cell was imposed to calculate the average concentration in order to ensure the robustness of the results (Charron et al. 2000).

Kinematic back-trajectories were calculated with the Hybrid Single-Particle Lagrangian Integrated Trajectory model (HYSPLIT - developed by the National Oceanic and Atmospheric Administration (NOAA)'s Air Resources Laboratory (ARL) (Stein et al. 2015; Draxler, 1999; Draxler and Hess, 1998; Draxler, and Hess, 1997)) and are based on GDAS (Global Data Assimilation System) where basic information like wind speed, wind direction, temperature and humidity are found on a global scale (source: <ftp://arlftp.arlhq.noaa.gov/pub/archives/gdas1>). A total of 1264 back-trajectories were used with eight 72-hour back-trajectories per sampled day, arriving at an altitude of 500 m above ground level. A 3 day time span and an altitude of 500m were chosen as suggested by (Su et al. 2015).

For each cell of a defined grid, the concentration field method gives the potential contribution to the concentration of a chemical species or to the contribution of a PMF factors. Results are plotted in maps from 84°W and 24°N to 43°E and 78°N, and with grid cells of 0,5° by 0,5°. A Gaussian smoothing factor of 5 was also applied to the results.

3 RESULTS AND DISCUSSION

3.1 PM₁₀ mass and composition

Table P1.4 summarizes the overall and seasonal mass concentrations of the different chemical species determined in this study. A daily average PM₁₀ mass concentration of $27.7 \pm 16.8 \mu\text{g m}^{-3}$ was observed on the sampled days (figure P1.2). This value is representative of the studied period, which showed an annual average PM₁₀ mass concentration of $29 \pm 18 \mu\text{g m}^{-3}$ during 2013 and ranged from 24 to $31 \mu\text{g m}^{-3}$ between 2007 and 2014. Similar or higher values are often observed at urban sites in central Europe or in particular areas known for high concentrations of PM, such as the Po Valley in Italy (Bressi et al. 2016). However, lower annual averages are generally observed at urban background sites

in France, like in Lens (north of France) with $21 \mu\text{g m}^{-3}$ (Waked et al. 2014) and in Toulouse (south of France) with $13 \mu\text{g m}^{-3}$ (Calvo et al. 2008), as well as more generally in Western Europe, like in Vienna, Austria, with $22 \mu\text{g m}^{-3}$ (Astel 2010), Münster, Germany, with $22 \mu\text{g m}^{-3}$ (Gietl and Klemm 2009) and Erfurt, Germany, with $19 \mu\text{g m}^{-3}$ (Yue et al. 2008), or even London with $19 \mu\text{g m}^{-3}$ (DEFRA Report, 2005), among others. This relatively high PM_{10} daily average value is a first indication that the sampling site is commonly subject to high concentrations of airborne particles, as mentioned in recent reports from the local air quality monitoring network, ATMO-Picardie (Atmo Picardie, 2014).

It is also noteworthy that 18 occurrences of the $50 \mu\text{g m}^{-3}$ PM_{10} daily threshold exceedance could be investigated here, with 15 of these exceedances in 2013 and 3 in the first semester of 2014. This number of exceedance days is in accordance with the values observed during the whole campaign, where 42 exceedances were observed in 2013 (which is above the 35 days allowed by the EU directive), and 11 in 2014.

Chemical speciation of the PM collected showed a main contribution of organic matter (OM) to the total mass of aerosols, accounting for 39% on average. Inorganic ions proved to be important contributors to PM_{10} total mass, where nitrate represented 22%, sulfate 12% and ammonium 8%. Elemental carbon was found to be responsible for 6% of the total mass – a contribution also found for the sum of all metals. Unaccounted major species like Al and Si, as well as the water content of particles, can help to explain the 7% of missing PM mass concentration.

Significant seasonality was observed on the main species analyzed. OM showed higher concentrations during winter ($9.8 \mu\text{g m}^{-3}$) compared to other seasons ($6.5 \pm 0.4 \mu\text{g m}^{-3}$). This can be partially explained by a strong influence of biomass burning used for residential heating during cold months (Favez et al. 2009). This is supported by the behavior shown by levoglucosan and potassium during winter, commonly used as biomass burning tracers. However and as mentioned above, concentrations of OM during other seasons are seen to be quite constant, indicating that many sources are present during different periods of the study.

The second main contributor, nitrate, also shows a strong seasonal variation during the sampled period, with concentrations ranging from $6.1 \mu\text{g m}^{-3}$ in spring to $1.7 \mu\text{g m}^{-3}$ in summer. This behavior was expected due to the semivolatility of ammonium nitrate and its dependence on ambient temperature, relative humidity and photochemical episodes. Humid conditions, strong temperature inversion and significant agricultural activities in this region of Europe contribute to a drastic increase of the contribution of nitrate to PM mass at some periods of the year – end of winter and spring (M. Dall'Osto et al. 2009).

Sulfate concentrations present on average higher values during summer, winter and spring (about $2.5 \mu\text{g m}^{-3}$ for these seasons) and minimum average concentration during fall – $1.6 \mu\text{g m}^{-3}$; however, its relative contribution to PM_{10} mass is maximum during summer with 19% – when photochemical processes play an important role on sulfate production (Blando and Turpin 2000).

Ammonium represents the fourth major contributor to PM_{10} mass. Higher concentrations are seen during winter and spring, and lower concentrations during summer and fall. These results are expected as ammonium is partly present under the state of ammonium sulfate and ammonium nitrate, where the latter shows a strong thermal dependence condensing during cold and humid conditions (winter) and evaporating during hot and dry periods (summer). Also, starting from late winter, it is legally allowed to apply ammonia-rich fertilizers in agricultural processes whereas during fall, high water soluble ammonium salts can be washed out by frequent rain episodes.

Finally, EC used as a tracer of combustions processes shows higher concentrations during fall ($1.4 \mu\text{g m}^{-3}$) and lower contributions during summer ($0.8 \mu\text{g m}^{-3}$), which is in accordance to Waked et al. (2014) observations in Lens. Ions used to identify marine sources such as Cl^- and Na^+ show a clear seasonal dependence, with higher concentrations during winter (1.1 and $0.7 \mu\text{g m}^{-3}$, respectively) and lower concentrations during summer (0.1 and $0.3 \mu\text{g m}^{-3}$, respectively).

Looking at the organic species analyzed in this study, levoglucosan proved to be the main organic compound investigated, accounting for 59% of the organic fraction (sum of organic species measured) mass on average, oxalate and MSA were the second and third main contributors with 20% and 8% respectively. A strong seasonality was observed in these species. Levoglucosan exhibited higher concentrations during winter with an average concentration of $0.7 \mu\text{g m}^{-3}$, and lowest values during summer ($0.02 \mu\text{g m}^{-3}$), where most of the values seen during this season being below the detection limit. MSA had highest mean values during summer ($0.1 \mu\text{g m}^{-3}$) and lowest values during fall ($0.01 \mu\text{g m}^{-3}$) which is expected as MSA is commonly linked with phytoplankton activity and summer is known to be a period of algal blooming. Similar behavior was seen for sugar alcohols, which recorded higher concentrations during summer and low contributions during winter, following the expectations once these compounds are linked to primary biogenic emissions as reported in Waked et al. (2014). Oxalate presented a different pattern, showing a rather constant concentration across the different seasons ($0.1 \pm 0.08 \mu\text{g m}^{-3}$).

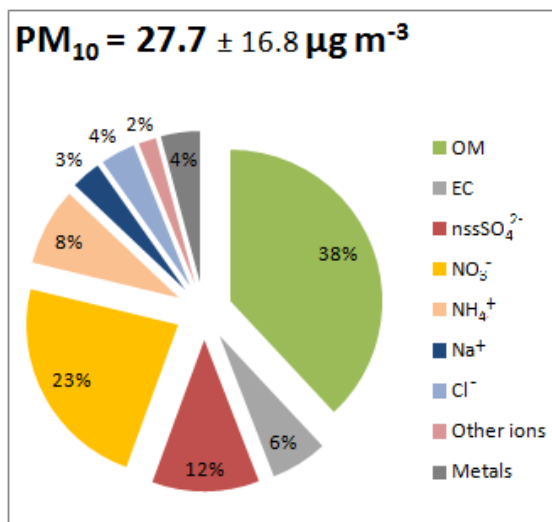


Figure P1. 2: Average chemical composition of PM₁₀ during the sampling period in Nogent-sur-Oise

Table P1. 4: Summary of species average concentrations (in $\mu\text{g m}^{-3}$)

	Average	Winter 13	Spring 13	Summer 13	Fall 13	Winter 13-14	Spring 14
<i>PM₁₀</i>	27.7	42.9	30.2	20.5	23.9	23.8	26.9
EC	1.15	1.27	0.81	0.81	1.40	1.41	1.21
OC	4.11	6.15	3.72	3.56	3.48	4.46	3.88
OM	7.19	10.76	6.51	6.23	6.08	7.80	6.78
<i>Ions</i>	9.77	15.48	14.99	5.87	6.63	6.41	9.18
NO₃⁻	4.38	7.19	7.54	1.65	2.59	2.40	4.57
SO₄²⁻	2.31	3.60	3.17	2.66	1.60	1.22	1.90
NH₄⁺	1.57	2.78	2.69	0.97	0.87	0.56	1.55
Na⁺	0.60	0.65	0.77	0.32	0.61	0.78	0.44
Cl⁻	0.70	1.01	0.63	0.09	0.76	1.18	0.56
<i>Metals</i>	0.79	0.74	0.88	0.74	1.00	0.66	0.69
<i>Organics</i>	0.51	1.20	0.38	0.34	0.27	0.65	0.45
MSA	0.04	0.04	0.04	0.10	0.01	0.00	0.04
Oxalate	0.10	0.14	0.13	0.15	0.08	0.07	0.08
Levogluconan	0.31	0.90	0.18	0.02	0.13	0.50	0.27
Polysaccharides	0.03	0.09	0.02	0.00	0.02	0.06	0.03
Sugar alcohols	0.03	0.03	0.01	0.07	0.03	0.01	0.03

3.2 PMF general solution and validation

PMF analysis indicates a total of 9 different sources: fresh and aged sea salts; marine and land biogenic aerosols; biomass burning; traffic; nitrate-, sulfate- and oxalate-rich sources. These sources were identified based on their chemical profiles with a focus on specific species in each source, known as specific markers. Chemical profiles of most sources are well documented in previous studies and the addition of new tracers, such as MSA and oxalate allowed identifying new sources of aerosols. Figure 2 presents the contribution of each of these sources on average, over the entire period and seasonally. It must be emphasized that with a 24-hour collection period every third day, this study presents a low temporal resolution which may mask sources with relevant daily emission patterns. It is therefore expected that some primary and secondary sources may not be identified or, if identified, may appear within the same factor. Given the sampling and analytical approach of this study, sources with no significant time variation may also cause difficulties to the PMF model; indeed the software algorithm is based on the time behavior of species assuming that similar emission patterns are associated with the same source, thus when two sources present either no significant time variability or almost the same time variability there is a possibility that it cannot distinguish them (Paatero et al. 2002).

Throughout the studied period, primary traffic was the main contributor, with 18% ($4.5 \mu\text{g m}^{-3}$) of the PM_{10} mass concentration. Important contributions were also observed from four other sources: biomass burning (15%; $3.8 \mu\text{g m}^{-3}$), oxalate- (13%; $3.3 \mu\text{g m}^{-3}$), nitrate- (14%; $3.7 \mu\text{g m}^{-3}$) and sulfate-rich (13%; $3.4 \mu\text{g m}^{-3}$) aerosols. Fresh (9%; $2.3 \mu\text{g m}^{-3}$) and aged marine (8%; $2.0 \mu\text{g m}^{-3}$), and land biogenic aerosols (7%; $1.9 \mu\text{g m}^{-3}$) appeared as minor sources. Finally, a last factor was found and identified as marine biogenic (3%; $0.7 \mu\text{g m}^{-3}$). Significant seasonality was observed during the studied period, with higher concentrations of PM_{10} during winter as seen above, enhanced by biomass burning emissions (30%; $9.4 \mu\text{g m}^{-3}$). Spring also recorded high levels of PM_{10} , this time due to nitrate-rich aerosols (22%; $5.5 \mu\text{g m}^{-3}$) and traffic emissions (20%; $5.0 \mu\text{g m}^{-3}$).

A detailed description of each factor and its contributions are presented in the following sections, where traffic, biomass burning and land biogenic aerosols are considered primarily as local sources and all other factors as – at least in part – regional ones.

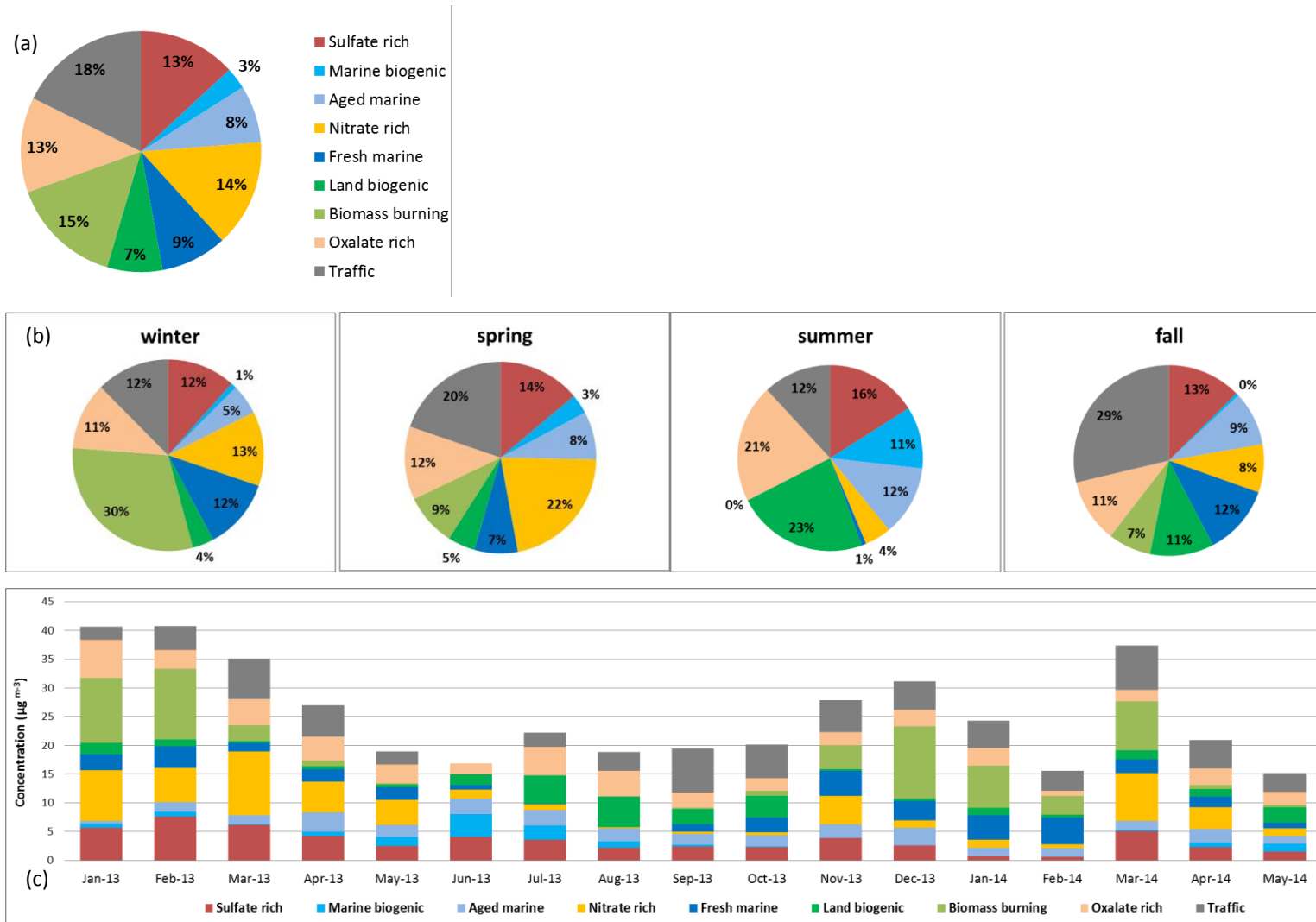
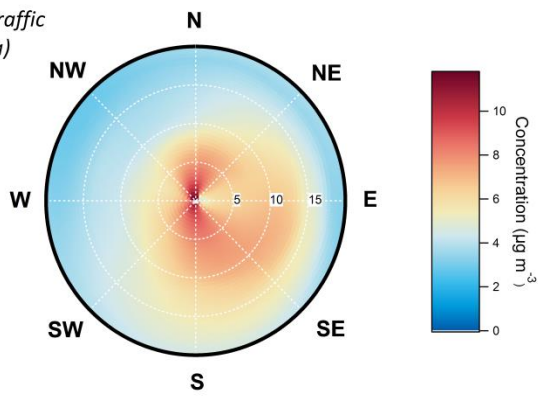
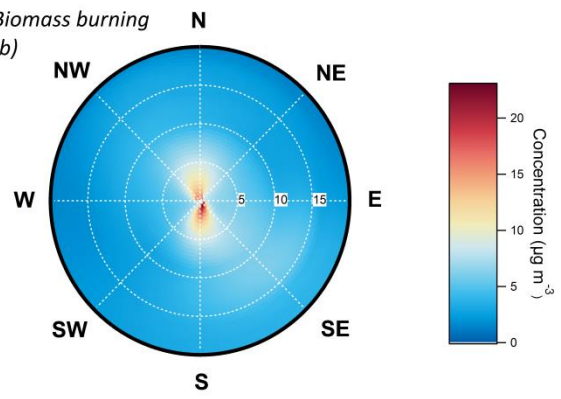


Figure P1. 3: (a) Average, (b) seasonal and (c) monthly contributions of PM10 sources between January 2013 and June 2014 in Nogent-sur-Oise

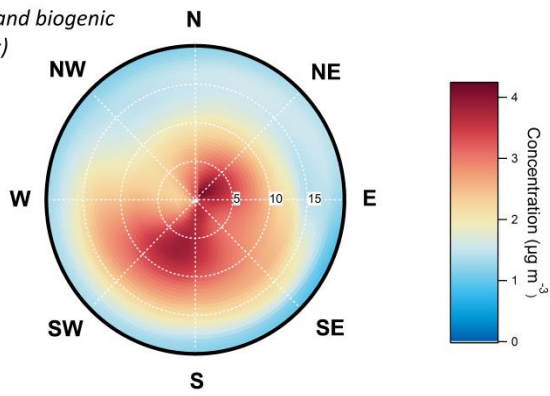
Traffic
(a)



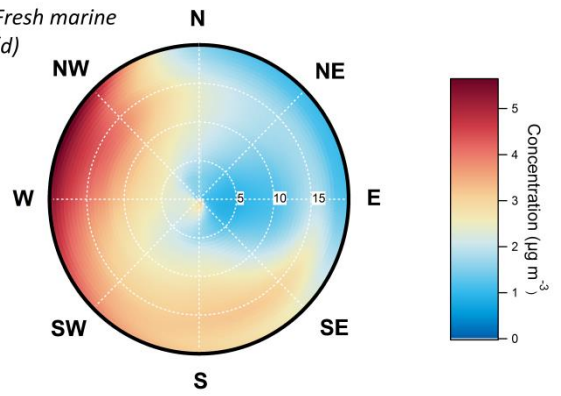
Biomass burning
(b)



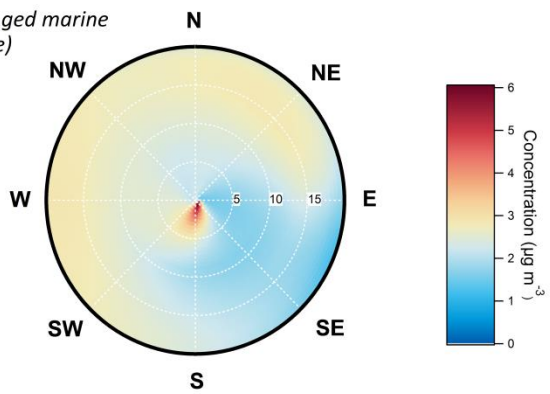
Land biogenic
(c)



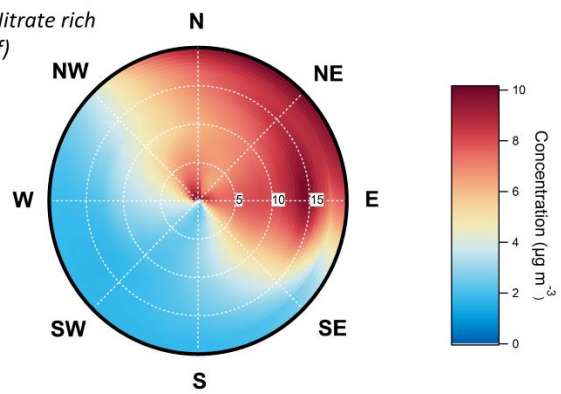
Fresh marine
(d)



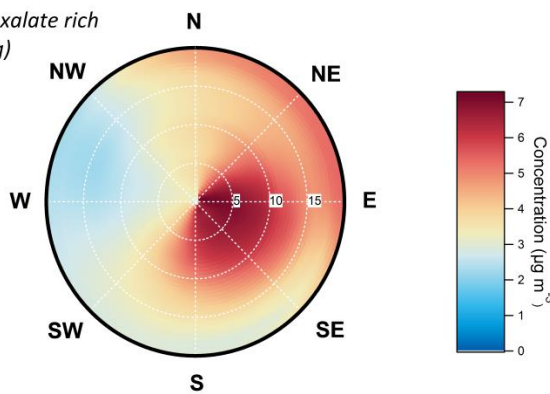
Aged marine
(e)



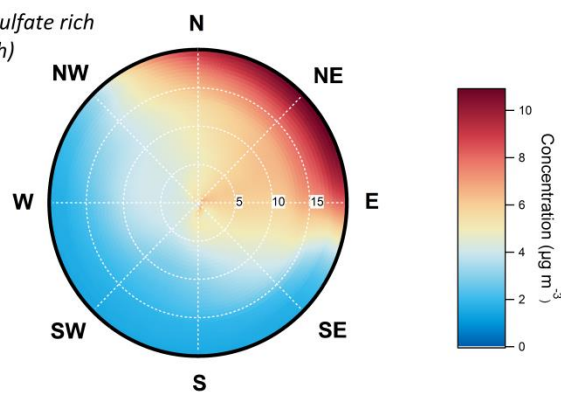
Nitrate rich
(f)



Oxalate rich
(g)



Sulfate rich
(h)



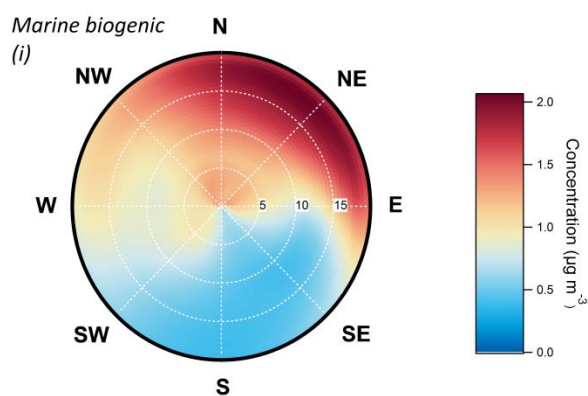


Figure P1. 4: Non parametric wind regression for the impacting sources: (a) Traffic; (b) Biomass burning; (c) Land biogenic; (d) Fresh marine; (e) Aged marine; (f) Nitrate rich; (g) Oxalate rich; (h) Sulfate rich; (i) Marine biogenic

3.3 Local factors

3.3.1 Traffic factor

Identified as the main source of PM in Nogent-sur-Oise during the studied period, the traffic factor accounts for 45% of the EC sampled and for high percentages of most of the metals (Figure S.5). This solution was obtained after slightly constraining the original PMF solution, in which some odd characteristics, one of these being an EC/OC ratio of 0.5, were spotted. This could be explained by the limitations associated with this kind of study, regarding the distribution of contribution of species in factors with no significant time variability. Therefore a mild constraint ($dQ\% = 0.5$) on the EC/OC ratio of 2 as reported in similar studies (C. Pio et al. 2011) – was applied. The results showed no significant change in the final solution, with a slight decrease on the contribution of this factor to the PM total mass from 20% to 18%, related to decreased concentrations of OC.

This factor is also characterized by a strong presence of various metals as pointed before. Besides, calcium was seen in abundance in this factor, which suggests that this factor probably combine exhaust emissions (fuel combustion) with non-exhaust emissions (tires and brakes abrasion) and road resuspension, possibly associated with a crustal source. High contributions of Cu, Ba, Zn and Fe support the assumption of brake abrasion (Johansson, Norman, and Burman 2009), as well as tire abrasion as reported by (Amato et al. 2011). About 59% of the calcium is present in this factor, suggesting a strong contribution of road resuspension and crustal matter to the final chemical profile of the source. The appearance of species linked with crustal matter particles in this factor can be explained by the absence of

common crustal tracers such as Al and Si in addition to a small temporal variability of that source. It should moreover be noted that iron was unexpectedly not observed in this factor, probably due to the fact that it was selected as a weak variable because of its low S/N ratio. To investigate this phenomenon, a second constraint was applied to Fe. Again, a slight constraint was applied, pulling up maximally the contribution of Fe on this factor. An increase in the percentage of Fe in this factor – from 0% to 49% of the total variable – was obtained, with virtually no significant change of the factor contribution, compared to the original solution.

No significant seasonality was observed in this factor, just individual high values associated with meteorological conditions hindering the dispersion of pollutants but also during vacation periods when a higher cars density would be expected in the area near the sampling site including commercial and leisure centers.

Traffic related emissions are often considered as rather local sources; however, as it was described above, this traffic profile may have a non-negligible contribution of crustal matter. From NWR analysis, it is noticeable that higher concentrations of this factor are originating from the south at rather low wind speeds (figure P1.4a), consistent with the presence of a large commercial center with an outdoor 3-story high parking garage 500 meters to the south of the sampling site.

One can also identify contributions coming from the northeast down to south-southwest wind sector, which corresponds to a wide open expanse between the sampling site and the D1016 road that connects the cities of Creil and Nogent-sur-Oise and is used by 50 000 cars per day, on average.

3.3.2 Biomass burning factor

Biomass burning aerosols were found to be the second main contributor to PM₁₀ mass concentrations in Nogent-sur-Oise. This factor is characterized by the large presence of levoglucosan (83.5% of the total levoglucosan mass measured) and related polysaccharides mannosan and galactosan (81.0% of the total mass of the sum of both species) (Figure S.6). The two latter species were summed because their concentrations were quite low and presented a very high correlation factor (0.96). Levoglucosan and other polysaccharides are the result of the degradation of cellulose by combustion (Puxbaum et al. 2007). Other strong

indicators that confirm a biomass burning factor are common species like potassium (25% of its total mass), rubidium (18% of its total mass) and an OC/EC ratio of 4.7, which is in accordance with the values presented in (Fineet al., 2002), characteristic of wood burning emissions.

An average contribution of 15% was found to the PM₁₀ mass throughout the sampling period, which comprised the whole year 2013 and the first 5 months of the year 2014, so the given average includes 2 winters and 2 springs. The average contribution of biomass burning during the year 2013 was nevertheless 14%, so the sampled period proved to be representative. This relative contribution to PM₁₀ mass is in accordance with previous studies carried out in the region where an average contribution of 13% was found during a 1-year study period (Waked et al. 2014), and with other urban areas as described by (Belis et al. 2013) showing an average biomass burning contribution of 12%.

It is important to point out that the contribution of this factor can be underestimated, especially during summer due to the photochemical reactivity of its main tracers (Hennigan et al. 2010). This fact together with the seasonality associated with the source can explain the significant difference seen during winter (average contribution to PM₁₀ of 30%) and summer (0.2%) (Figure S19).

Biomass burning factors are commonly associated with residential heating processes, therefore seen as local sources of aerosols if considering an urban site. Meteorological information was used to construct a graphical representation of the NWR function using ZeFir (figure P1.4b). This points out to a large residential area located north of the sampling site. High concentrations are seen from the east – south quadrant associated with medium wind speeds, and from the north associated with low wind speeds. These directions point out to residential areas, such as Verneuil-en-Halatte in the east and Creil in the south, where suburban individual houses are equipped with fireplaces and chimneys favoring the use of biomass burning as the main source of heating.

3.3.3 Land biogenic aerosols

Primary land biogenic emissions accounted for 7% of the total PM₁₀ mass measured in Nogent-sur-Oise between Jan. 2013 and June 2014, close to the value previously reported for Lens (9%; (Waked et al. 2014)) and within the range of 5 to 50% of total PM estimated by

(Jaenicke 2005). This factor is identified by the presence of sugar alcohols (mannitol, arabitol) and OC in its chemical profile (Figure S.7). Both polyols are reported in the literature as common primary land biogenic emission tracers (Caseiro et al. 2007; Elbert et al. 2007; Jia, Clements, and Fraser 2010; Karl Espen Yttri et al. 2011), especially as markers for fungal spore-related particles (H. Bauer et al. 2008). Indeed, 84% of all the measured polyols contributed to this factor, its mass being mainly driven by OC concentrations (71% of the total factor). A strong seasonality is associated with the average contributions of this factor. In fact, during summertime, primary land biogenic emissions account for 23% of the total PM₁₀ measured, making it the most contributing source, due to intense solar radiation and higher temperatures resulting in an increase in biological activity as has been reported in previous studies (Pashynska et al. 2002; K. E. Yttri et al. 2007; H. Bauer et al. 2008).

The NWR obtained (figure P1.4c) suggests that this factor is associated with local sources, rather than regional ones, pointing south and north-east of the sampling site. The Oise - Pays de France Regional Nature Park is indeed located south and spreads over 60,000 hectares including three forested areas. The north-east hotspot is associated with even lower wind speeds and could be related to the presence of three large football fields next to the sampling site in this exact direction.

3.4 Regional factors

By using the Concentration Field model on PM₁₀ mass (Figure S.14) Central and Eastern Europe appears clearly identified as the source of the highest concentrations seen at the receptor site. This area comprises Germany, the Czech Republic and Poland, three heavy industrialized and densely inhabited countries with continental climate, where fairly cold wintertime conditions may favor particulate and acid gaseous emissions from heating plants (a large part of it being coal combustion plants) and dry and hot summertime conditions may enhance primary emissions from vegetation and soils and subsequent secondary aerosol formation. A second potential source area of high PM₁₀ concentration is located in the western part of the Mediterranean Sea, with two “hotspots”: one in the north of Algeria and another in the south-east of France. Both are situated along a common path of transportation of Saharan dust to Europe. Moreover, in the southeast of France is located one of the most heavily industrialized site of Europe (the Fos-Berre industrial site, near Marseilles).

However, the main sources impacting during high PM₁₀ concentration days are often traffic, biomass burning and nitrate-rich sources, where two of these three sources have been labeled as local ones. Although there is information to extract from the presented map, such as that the main sources of high concentrations of PM₁₀ in Nogent-sur-Oise have continental origin, a further analysis requires a better understand of the chemical composition of these particles and their sources.

All the scales shown on the concentration field maps were set to a maximum value of the 95% percentile of daily contributions. This allows assessing the spatial dispersion of the highest values. A map where the highest concentrations are clearly highlighted in specific hotspots indicates that the back-trajectories associated with these high concentrations have the same pathway, whereas maps with no apparent concentration hotspots indicate that the highest concentrations were associated with back-trajectories with different origins, being then averaged down by lower concentrations.

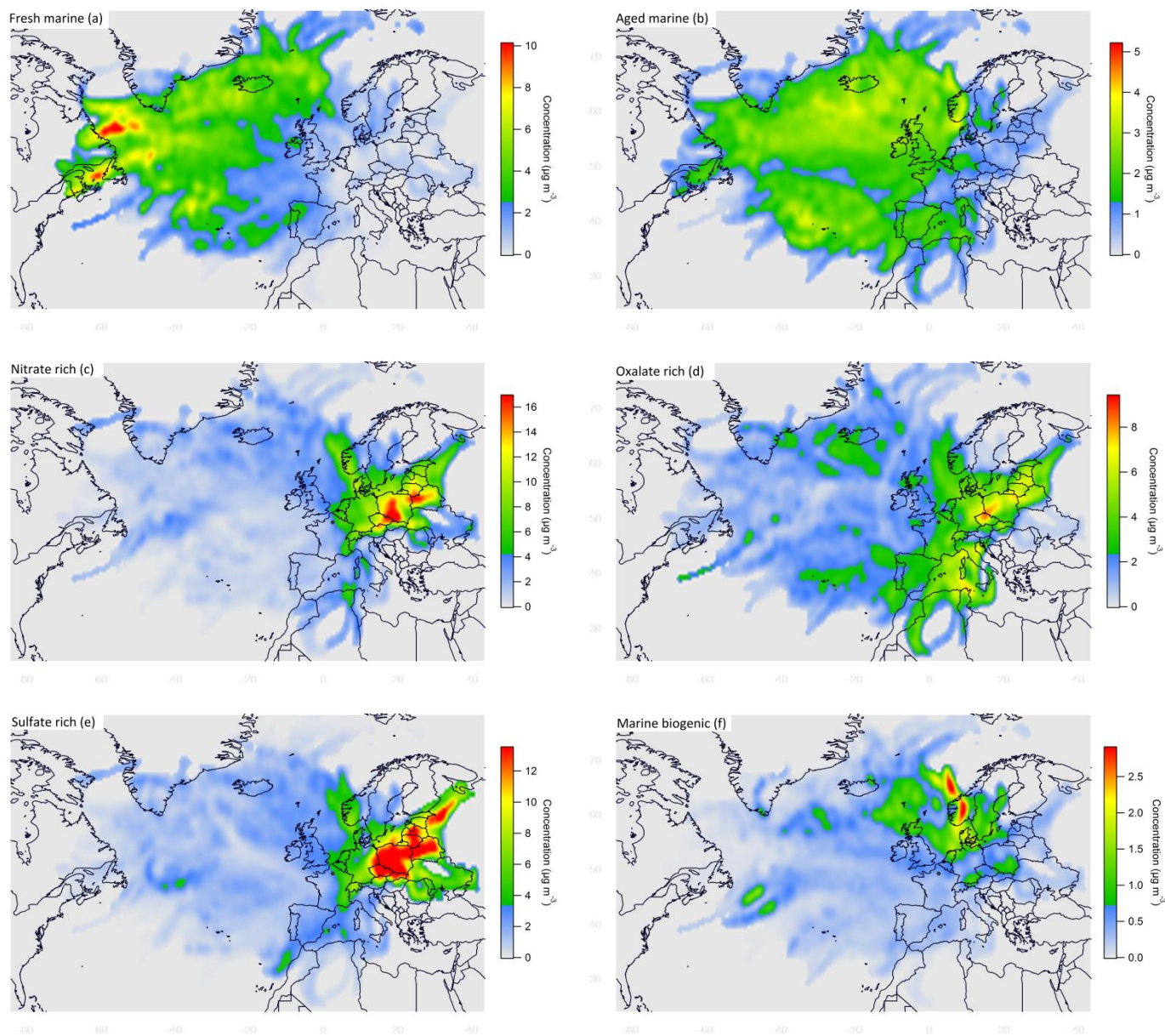


Figure P1. 5: Concentration field maps for the sources: (a) Fresh marine; (b) Aged marine; (c) Nitrate rich; (d) Oxalate rich; (e) Sulfate rich; (f) Marine biogenic

On average, sea salt contributes 9% to the particulate matter collected during the study. This factor is identified by its common tracers: sodium (59% of its mass), chloride (82%) and magnesium (38%). Chloride and sodium have been widely reported in the literature as common sea salt tracers (Pio et al. 1996), together with magnesium in northern European studies (Belis et al. 2013). The Cl/Na and Mg/Na ratios seen in the chemical profile of this factor (Figure S.8) were 1.8 and 0.09, in agreement with previous studies carried out in this region (Waked et al. 2014) and with the reported literature on common sea salt aerosols

(Millero and Lepple 1973; Seinfeld and Pandis 2006). Therefore this factor can be considered as a quite fresh sea salt chemical profile, also given the lack of significant contributions of other metals or ions. In terms of overall contribution to PM_{10} mass, this study shows results similar to the one determined in the city of Lens (8% of total PM_{10}) by (Waked et al. 2014) and close to more continental sites such as in West Germany that recorded between 9% and 10% for regional and urban contributions, respectively (Beuck et al. 2011).

The regional status of this source of aerosols can be assessed using (i) the polar graph of the NWR function (figure P1.4d) that links higher concentrations with the WNW direction and higher wind speeds, which suggests a more distant source, and (ii) the Concentration Field model to the daily contributions of fresh marine aerosols and their associated back-trajectories, to identify more precisely the probable geographical location of their sources (figure P1.5a). A clear influence of long distance sources located in the North-Atlantic Ocean can be observed with highlighted influence in the coast of Canada. This is where high wind speeds are seen due to the North Atlantic Oscillation phenomena, where the low pressure system – cyclone - of Greenland meets the high pressure system of Azores – anti-cyclone – creating a path between the two leading resuspended marine particles (sea spray) to Europe.

3.4.1 Aged marine aerosols

With an average contribution of 8% to the total PM_{10} mass throughout the studied period, this factor (Figure S.9) is also characterized by significant shares of the total sodium (40%) and magnesium (54%) measured as seen in the fresh sea salt factor. However, it contains a negligible amount of chloride, as often reported in several studies (M. Dall'Osto et al. 2013; Beuck et al. 2011) for aged marine aerosols. This attribution is strengthened by the presence of several other compounds in the obtained chemical profile: nitrate (19% of total NO_3^-) and sulfate (12%) suggesting an anthropogenic load in the factor originating from secondary particles; some metals such as iron (30%), strontium (33%) and calcium (26%) can trace crustal matter; and finally other metals like nickel (23%) and vanadium (22%) suggest the influence of heavy oil combustion probably related to coastal industrial activities and shipping emissions. The average contribution to total PM_{10} is in accordance with other continental sampling sites like the one reported in Beuck et al., 2011, and presents lower values than the ones found at more coastal sites like Barcelona (Manuel Dall'Osto et al. 2013).

The polar graph of the NWR function (Figure 3e) does not clearly indicate a possible source direction of these particles, therefore confirming this source is very likely a combination of several secondary ones. However, the Concentration Field map (figure P1.5b) for the entire campaign shows that aged marine aerosols drive the average concentration of PM₁₀ down to a rather low value with influences from both the North Atlantic Ocean and the North Sea, as well as the Mediterranean Sea (and trajectories coming from over Iceland, the UK and Spain).

As mentioned above, both fresh and aged marine aerosols are characterized by the presence of sodium (99% of total variable on both factors) and magnesium (92%) in their chemical profiles. By applying the concentration field map on the factors resulted from the PMF model, it is possible to identify different sources with distinct geographical location that otherwise, would be masked by average distributions (Figure S.15). The concentration field map for Na⁺ highlights even more the fresh marine nature of this element, expected by the stronger presence seen in this factor.

3.4.2 Nitrate-rich aerosols

The nitrate-rich secondary aerosol factor was identified to be the third highest contributor to PM₁₀ mass during the sampling period (14% on average). Having as main tracers nitrate (72% of total NO₃⁻) and ammonium (57% of total NH₄⁺), this is a commonly reported secondary aerosol factor across Europe as shown in (Viana et al. 2008), where the concentrations of NO₃⁻ and NH₄⁺ measured for this factor ($[\text{NO}_3^-]/[\text{NH}_4^+] = 3.5$) are in accordance with the neutralization ratio of ammonium nitrate. It is associated with regional background and long-range transported pollution. An average contribution to total PM₁₀ of 14% is within the range of similar studies carried out in the north of Europe, and in excellent agreement with the results found in Lens for the year 2011-2012 (14% of total PM₁₀).

The nitrate rich factor peaked during spring (22% of total PM₁₀) and was much lower during summer, making up for just 4% of the total PM₁₀ measured. This strong seasonal variability is not only related with the emission profiles of the sources of these aerosols but also with its physicochemical properties. Nitrate-rich aerosols are often linked with agricultural activities (particularly with nitrogen fertilization of soils and soil preparation) so their contribution increases in spring when these activities rise again, especially in the north of France. NO_x emissions from traffic and industrial processes are also commonly reported as sources of these particles. As mentioned above, nitrate-rich aerosols are mainly present in the

atmosphere as ammonium nitrate, which is a semi-volatile compound that has a strong dependence on ambient temperature. During spring, when we commonly see cold nights and mild days, the concentrations of ammonium nitrate tend to increase. However, during summer, even if sources of nitrate or ammonium are present, the temperatures are high enough to volatilize this compound (that goes without mentioning that the analyzed filter samples collected during this period could underestimate the concentrations of these species due to negative sampling artifact, which is a known issue reported repeatedly in the literature (Cheng and Tsai, 1997; Hering and Cass, 1999; Keck and Wittmaack, 2005).

The NWR polar graph obtained from ZeFir (figure P1.4f) indicates that nitrate rich aerosols are associated with high wind speeds coming from continental directions (N to ESE) and also moderate wind speeds from the same direction, which suggests a regional influence that can be assessed by applying the concentration field method both to single species (nitrate and ammonium) and to daily contributions of the nitrate rich factor. The obtained CF map (figure P1.5c) shows a clear influence of long-range transport on the concentration levels for this factor. Several regions are worth mentioning in the map shown: (i) a hotspot above Denmark: although these results have to be approached with caution regarding their statistical representativeness, this region is widely known by its intense agricultural activity and it is interesting that it appears highlighted by the model; (ii) Central Europe: as an averaged concentration in grid cells, hotspots near the limits of the available data have to be considered wisely, but the fact that Poland is strongly identified is an interesting result. This region is known not only for its agricultural activity but also for a strong industrial sector responsible for considerable particulate (and probably NO_x) emissions; (iii) Germany: Recent studies have also pointed out high concentrations of nitrate rich aerosols emitted in Germany (Aksoyoglu, Prévôt, and Baltensperger 2016). These are usually linked with not only agricultural activities but also with an important contribution from combustion of natural gas in turbines, flaring of natural gas and combustion of diesel. These results are supported by the concentration field maps obtained for the single species mentioned above (Figure S18 for nitrate and Figure S19 for ammonium) where the closer contribution of ammonium is seen as well as a possible contribution from northern Italy that is not clear probably due to the presence of the Alps. We are then in the presence of a factor without necessarily the same type of sources of particles but the model seems to be able to identify certain key hotspots always linked with anthropogenic activities.

3.4.3 Oxalate-rich aerosols

The oxalate-rich factor is identified by the presence of most of the oxalate analyzed (80% of the total species). The sources of oxalate in the atmosphere comprise both natural, like biogenic emissions, and anthropogenic primary emissions, like fossil fuel combustion and biomass burning (Kawamura and Kaplan 1987; Kawamura and Ikushima 1993), as well as oxidation processes of organic precursors in the gaseous and condensed phases (Dabek-Zlotorzynska and McGrath 2000; Chebbi and Carlier 1996; Kawamura, Kasukabe, and Barrie 1996; Myriokefalitakis et al. 2011). The presence of 18% of the total sulfate and 20% of the total OC in this factor are also important characteristics to better understand the possible sources of these particles. Interestingly, some iron is also associated to this factor. Iron is a known catalyst of atmospheric sulfur oxidation, from S(IV) to S(VI), particularly in the aqueous phase in clouds where dissolved SO₂ is converted into ionic SO₄²⁻ (Seinfeld and Pandis 2006). Moreover oxalate promotes the aqueous solubility of Fe from poorly soluble mineral phases, like clays, by complexation of Fe with organic matter (Paris and Desboeufs, 2013). In Europe, Fe may originate from topsoil wind erosion, urban soil resuspension, industrial activities (such as metallurgy) and also desert dust storms crossing the Mediterranean Sea. Therefore, one may assume that the aerosols associated with this oxalate-rich factor come mainly from secondary photochemical processes, favored by high temperatures and sunny days (as confirmed by the factor seasonal behavior and its high content of OC), which may include in-cloud aqueous processes catalyzed by iron.

The NWR function (figure P1.4g) showed two distinct directions leading to high concentrations depending on wind speed: (i) low wind speeds associated with the east direction, where a large waste incinerator and an industrial area are located, and (ii) high wind speeds from the north-east, as previously observed for secondary aerosol factors. The interpretation of the CF map (figure P1.5d) is less obvious since part of this factor seems local, therefore a local input of concentrations could be associated with a possibly “clean” back-trajectory. However the results show some similarities with the map obtained for the sulfate-rich factor highlighting once again Central Europe as a possible source for these particles. Additional hotspots were highlighted in the Mediterranean Sea, which is also an area with the highest ozone concentrations, contributing strongly to the oxidation of atmospheric VOCs (Sartelet et al. 2012). Interestingly, these back-trajectories corresponded to specific days where a Saharan dust event reached the northern regions of France.

The pollution rose of this factor showed a double contribution of low and high wind speeds, suggesting that different sources, local and long distance, may be at the origin of these particles. When plotted, the Concentration Field map of the oxalate as a single species (Figure S.16) is very similar to the one seen for the “oxalate rich” factor, as well as the pollution rose. This supports the fact that different sources contribute to the observed concentrations of these oxalate/sulfate rich particles, driving the discussion towards the processes of formation of these particles rather than the geographical location of their sources. However, the sulfate seen in this factor is more probably associated with regional emissions given its pollution rose and the evidence that the main contributions are associated with higher wind speeds. Moreover, the oxalate and OC can be labeled as both local and regional since no evidence was found of a stronger association of these two species with just either high or low wind speeds.

3.4.4 Sulfate-rich aerosols

The sulfate-rich factor was identified by its two main tracers, sulfate (52% of the total SO_4^{2-}) and ammonium (25% of the total NH_4^+). With the nitrate-rich factor, it is one of the two secondary inorganic aerosol factors found in this study and represented by one main species, ammonium sulfate. However, unlike the nitrate-rich factor, no significant time variability was observed. Besides, other metals were also found in this factor, suggesting anthropogenic activities as possible sources of these particles. Compounds such as iron, arsenic, cadmium, molybdenum, nickel, lead and zinc (17%, 22%, 21%, 15%, 13%, 16% and 17% of each total species, respectively) are often linked with industrial activities (Riffault et al. 2015).

The NWR function showed similar results to the nitrate-rich factor (figure P1.4h), with a more clear association with high wind speeds from the continent. However the concentration field map for sulfate-rich aerosols (figure P1.5e) highlights only a large area in Central Europe comprising Poland, the Czech Republic, Byelorussia and the Baltic States, likely pointing out to SO_2 emissions by coal-fired power plants, leading to sulfate formation. As mentioned above, the ammonium associated also with this factor, is mainly emitted in Central Europe with strong contributions seen from Eastern Germany, Czech Republic, Poland and Belarus (Figure S19).

3.4.5 Marine biogenic aerosols

The marine biogenic factor was identified thanks to its main tracer MSA (methanesulfonic acid) which has been commonly used as a tracer for marine phytoplankton activity (Andreae and Crutzen 1997; Mattias Hallquist et al. 2009; Gaston et al. 2010). However, few studies have measured it at continental sites as part of a comprehensive source apportionment study. Most of the measured MSA was found in this factor (81% of the total measured) with the additional presence of its photochemical degradation product, sulfate (12%). Both species are driving the mass contribution of this factor, which is only 3% on average, sulfate contributing as much as 54% of the concentration and MSA 7%. The marine biogenic factor showed also a strong seasonality, reaching higher concentrations during summer (11% of PM₁₀ mass) due to enhanced photosynthetic processes occurring in the marine phytoplankton during sunny days (Chen et al., 2012).

Performing the NWR function for the daily contribution of marine biogenic aerosols (Figure 3i), a strong dependence of higher concentrations to high speed winds from the north-east quadrant can be clearly seen. The obtained CF map (figure P1.5f) evidenced that this source is located in the North Sea, especially near the Netherlands and above Scotland, as well as in the Baltic Sea, which are areas known for intense phytoplankton activity especially during summer time (EEA, 2015). These observations are also supported by NASA satellite observations of average chlorophyll-a concentrations in 2013 and 2014 (Figure S.17), highlighting again the major areas seen on the CF map, together with smaller regions off the coast of Canada and close to Iceland that also seem to be spotted by the CF model.

Sulfate can be found in several factors, most notably the “sulfate rich”, “oxalate rich” and “marine biogenic” factors (52%, 18% and 12% respectively) making up for 82% of the total sulfate measured. The Concentration Field map obtained to the single species of sulfate is presented in Figure S.17. The highlighted region is similar to the one seen in the CF map for the sulfate rich factor. This is an expected result since this factor explains the majority of the measured sulfate, however the sulfate associated marine biogenic emissions is completely masked in this representation due to the lower percentage accounted in it.

4 CONCLUSION

The present study, carried out at an urban site in the city of Nogent-sur-Oise during one year and a half, delivered a total of 158 samples to be analyzed which, after performing the source apportionment model EPA PMF5, identified 9 possible sources for the collected particles. Local emissions of traffic and biomass burning related particles were seen to be the main contributors to PM₁₀ mass concentration (18% and 15% respectively), followed by secondary nitrate, sulfate and oxalate rich aerosols (14%, 13% and 13% respectively). Natural sources like land biogenic (7%) and marine biogenic (3%) were identified in this study, as well as fresh and aged sea salt (9% and 8% respectively), the latter with an important anthropogenic input detected in its chemical profile.

Strong seasonality was also observed on the mentioned sources (except for traffic and sulfate rich). Biomass burning contributions were significantly higher during cold seasons, with an obvious negative correlation with ambient temperature measured at the location, relating it with house heating activities. The nitrate rich factor showed also a clear seasonal pattern with higher contributions during spring. This is related not only with the increase of emission rates of its sources (agricultural activities e.g.) but also with the favorable meteorological conditions to the formation of ammonium nitrate.

Based on wind speed and wind direction information, NWR plots were constructed for each factor having into account its daily contributions. Factors such as fresh and aged sea salt, marine biogenic, nitrate, sulfate and oxalate rich were seen to be associated with high wind speeds, indicating that these particles are rather associated with long-range transport and were labeled as “regional”. Local sources like traffic related emissions, biomass burning and land biogenic particles were associated with lower wind speeds and their geographical origin could be estimated based on the obtained plots and general knowledge of the surrounding area.

The concentration field method, based on 78h back-trajectories computed from HYSPLIT, was then applied to the identified regional factors in order to estimate their geographical origin as well. Associating the obtained back-trajectories with daily contributions of each factor, concentration field maps were obtained, that clearly distinguished natural and anthropogenic sources. Fresh sea salt was seen to be associated with air masses from the northwestern Atlantic Ocean, driven by the North Atlantic Oscillation phenomena, whereas more aged sea salt particles are seen to be originated from all the Atlantic Ocean at closer distances (lower average speed of these air masses). Marine biogenic particles were clearly

associated with the North Sea and supported by satellite imaging of chlorophyll concentrations from NASA. Anthropogenic related factors like sulfate rich and nitrate rich were clearly associated with continental contributions from Central and Eastern Europe. The oxalate rich factor was seen to have a wider range of possible geographic origins than the latter 2 factors, highlighting not only Central and Eastern Europe as possible sources (linked with sulfate contributions) but also the North Sea and the Mediterranean Sea. This is due to the multitude of possible sources of oxalate rich particles. The concentration field maps obtained for the identified maps were also compared with the ones for the main single species measured in this study, making it evident the usefulness of this technique to distinguish different sources of the same species.

A time of 72 hours back-trajectories was chosen to reduce uncertainty associated with the results and also having into account the lifetime of some of the measured species. As a consequence, is possible that more distant sources may have not been identified and still have an impact on the sampling site. It is important to have also in mind that CF maps represent only the probable location of sources seen to impact this specific receptor site. A better picture of regional sources impacting the North of France could be obtained by combining results at several receptor sites.

5 ACKNOWLEDGMENTS

This work was notably funded by the French Ministry of Environment ("Bureau de l'Air du Ministère de l'Ecologie, du Développement durable, et de l'Energie") and included in the CARA air quality monitoring and research project coordinated by the French reference laboratory for air quality monitoring (LCSQA). Technical support for filter sampling was provided by Atmo Nord-Pas-deCalais, Atmo Picardie, Atmo Champagne-Ardenne and Air Normand. Mines Douai participates in the CaPPA project funded by the ANR through the PIA under contract ANR-11-LABX-0005-01, the "Nord Pas de Calais" Regional Council and the European Regional Development Fund (ERDF).The authors gratefully acknowledge the NOAA Air Resources Laboratory (ARL) for the provision of the HYSPLIT transport and dispersion model used in this publication.

REFERENCES

- Abbott, Michael L., Che-Jen Lin, Peter Martian, and Jeffrey J. Einerson. 2008. "Atmospheric Mercury near Salmon Falls Creek Reservoir in Southern Idaho." *Applied Geochemistry, Transport and Fate of Mercury in the Environment*, 23 (3): 438–53. doi:10.1016/j.apgeochem.2007.12.012.
- Aksoyoglu, Sebnem, A. S. H. Prévôt, and U. Baltensperger. 2016. "Contribution of Ship Emissions to the Concentration and Deposition of Pollutants in Europe: Seasonal and Spatial Variation." In *Air Pollution Modeling and Its Application XXIV*, 265–270. Springer. http://link.springer.com/chapter/10.1007/978-3-319-24478-5_43.
- Alleman, Laurent Y., Laure Lamaison, Esperanza Perdrix, Antoine Robache, and Jean-Claude Galloo. 2010. "PM10 Metal Concentrations and Source Identification Using Positive Matrix Factorization and Wind Sectoring in a French Industrial Zone." *Atmospheric Research* 96 (4): 612–25. doi:10.1016/j.atmosres.2010.02.008.
- Amato, F., M. Pandolfi, T. Moreno, M. Furger, J. Pey, A. Alastuey, N. Bukowiecki, A. S. H. Prevot, U. Baltensperger, and X. Querol. 2011. "Sources and Variability of Inhalable Road Dust Particles in Three European Cities." *Atmospheric Environment* 45 (37): 6777–6787.
- Andreae, Meinrat O., and Paul J. Crutzen. 1997. "Atmospheric Aerosols: Biogeochemical Sources and Role in Atmospheric Chemistry." *Science* 276 (5315): 1052–1058.
- Astel, Aleksander M. 2010. "Air Contaminants Modelling by Use of Several Receptor-Oriented Models." *International Journal of Environment and Pollution* 42 (1–3): 32–57. doi:10.1504/IJEP.2010.034225.
- Bauer, Heidi, Elisabeth Schueller, Gert Weinke, Anna Berger, Regina Hitzenberger, Iain L. Marr, and Hans Puxbaum. 2008. "Significant Contributions of Fungal Spores to the Organic Carbon and to the Aerosol Mass Balance of the Urban Atmospheric Aerosol." *Atmospheric Environment* 42 (22): 5542–5549.
- Belis, C. A., J. Cancelinha, M. Duane, V. Forcina, V. Pedroni, R. Passarella, G. Tanet, et al. 2011. "Sources for PM Air Pollution in the Po Plain, Italy: I. Critical Comparison of Methods for Estimating Biomass Burning Contributions to Benzo(a)pyrene." *Atmospheric Environment* 45 (39): 7266–75. doi:10.1016/j.atmosenv.2011.08.061.
- Belis, C. A., F. Karagulian, B. R. Larsen, and P. K. Hopke. 2013. "Critical Review and Meta-Analysis of Ambient Particulate Matter Source Apportionment Using Receptor Models in Europe." *Atmospheric Environment* 69: 94–108.
- Beuck, H., U. Quass, O. Klemm, and T. A. J. Kuhlbusch. 2011. "Assessment of Sea Salt and Mineral Dust Contributions to PM 10 in NW Germany Using Tracer Models and Positive Matrix Factorization." *Atmospheric Environment* 45 (32): 5813–5821.
- Birch, M. E., and R. A. Cary. 1996. "Elemental Carbon-Based Method for Monitoring Occupational Exposures to Particulate Diesel Exhaust." *Aerosol Science and Technology* 25 (3): 221–241.
- Birch, M. Eileen, and Robert A. Cary. 1996. "Elemental Carbon-Based Method for Occupational Monitoring of Particulate Diesel Exhaust: Methodology and Exposure Issues." *Analyst* 121 (9): 1183–1190.
- Blando, James D., and Barbara J. Turpin. 2000. "Secondary Organic Aerosol Formation in Cloud and Fog Droplets: A Literature Evaluation of Plausibility." *Atmospheric Environment* 34 (10): 1623–1632.
- Bove, M. C., P. Broto, G. Calzolari, F. Cassola, F. Cavalli, P. Fermo, J. Hjorth, et al. 2016. "PM10 Source Apportionment Applying PMF and Chemical Tracer Analysis to Ship-Borne Measurements in the Western Mediterranean." *Atmospheric Environment* 125, Part A (January): 140–51. doi:10.1016/j.atmosenv.2015.11.009.
- Bressi, M., F. Cavalli, C. A. Belis, J.-P. Putaud, R. Fröhlich, S. Martins dos Santos, E. Petralia, et al. 2016. "Variations in the Chemical Composition of the Submicron Aerosol and in the Sources of the Organic Fraction at a Regional Background Site of the Po Valley (Italy)." *Atmos. Chem. Phys.* 16 (20): 12875–96. doi:10.5194/acp-16-12875-2016.
- Bressi, M., J. Sciare, V. Ghersi, N. Bonnaire, J. B. Nicolas, J.-E. Petit, S. Moukhtar, A. Rosso, N. Mihalopoulos, and A. Féron. 2013. "A One-Year Comprehensive Chemical Characterisation of Fine Aerosol (PM2.5)

- at Urban, Suburban and Rural Background Sites in the Region of Paris (France).” *Atmos. Chem. Phys.* 13 (15): 7825–44. doi:10.5194/acp-13-7825-2013.
- Calvo, A. I., V. Pont, C. Liousse, B. Dupré, A. Mariscal, C. Zouiten, E. Gardrat, et al. 2008. “Chemical Composition of Urban Aerosols in Toulouse, France during CAPITOUL Experiment.” *Meteorology and Atmospheric Physics* 102 (3–4): 307–23. doi:10.1007/s00703-008-0319-2.
- Caseiro, Alexandre, Iain L. Marr, Magda Claeys, Anne Kasper-Giebl, Hans Puxbaum, and Casimiro A. Pio. 2007. “Determination of Saccharides in Atmospheric Aerosol Using Anion-Exchange High-Performance Liquid Chromatography and Pulsed-Amperometric Detection.” *Journal of Chromatography A* 1171 (1): 37–45.
- Charron, A., H. Plaisance, S. Sauvage, P. Coddeville, J. C. Galloo, and R. Guillermo. 1998. “Intercomparison between Three Receptor-Oriented Models Applied to Acidic Species in Precipitation.” *Science of The Total Environment* 223 (1): 53–63. doi:10.1016/S0048-9697(98)00308-8.
- Charron, Aurélie, Hervé Plaisance, Stéphane Sauvage, Patrice Coddeville, Jean-Claude Galloo, and René Guillermo. 2000. “A Study of the Source–receptor Relationships Influencing the Acidity of Precipitation Collected at a Rural Site in France.” *Atmospheric Environment* 34 (22): 3665–74. doi:10.1016/S1352-2310(00)00096-0.
- Chebbi, A., and P. Carlier. 1996. “Carboxylic Acids in the Troposphere, Occurrence, Sources, and Sinks: A Review.” *Atmospheric Environment* 30 (24): 4233–4249.
- Chen, Bingzhang, Michael R. Landry, Bangqin Huang, and Hongbin Liu. 2012. “Does Warming Enhance the Effect of Microzooplankton Grazing on Marine Phytoplankton in the Ocean?” *Limnology and Oceanography* 57 (2): 519–526.
- Choi, Eunhwa, Kyungho Choi, and Seung-Muk Yi. 2011. “Non-Methane Hydrocarbons in the Atmosphere of a Metropolitan City and a Background Site in South Korea: Sources and Health Risk Potentials.” *Atmospheric Environment, Air Pollution and Health: Bridging the Gap from Sources-to-Health Outcomes*, 45 (40): 7563–73. doi:10.1016/j.atmosenv.2010.11.049.
- Dabek-Zlotorzynska, Ewa, and Marilu McGrath. 2000. “Determination of Low-Molecular-Weight Carboxylic Acids in the Ambient Air and Vehicle Emissions: A Review.” *Fresenius’ Journal of Analytical Chemistry* 367 (6): 507–518.
- Dall’Osto, M., R. M. Harrison, H. Coe, P. I. Williams, and J. D. Allan. 2009. “Real Time Chemical Characterization of Local and Regional Nitrate Aerosols.” *Atmos. Chem. Phys.* 9 (11): 3709–20. doi:10.5194/acp-9-3709-2009.
- Dall’Osto, Manuel, Xavier Querol, Fulvio Amato, Angeliki Karanasiou, F. Lucarelli, S. Nava, G. Calzolari, and M. Chiari. 2013. “Hourly Elemental Concentrations in PM 2.5 Aerosols Sampled Simultaneously at Urban Background and Road Site during SAPUSS–diurnal Variations and PMF Receptor Modelling.” *Atmospheric Chemistry and Physics* 13 (8): 4375–4392.
- Dall’Osto, M., X. Querol, A. Alastuey, C. O’Dowd, R. M. Harrison, J. Wenger, and F. J. Gómez-Moreno. 2013. “On the Spatial Distribution and Evolution of Ultrafine Particles in Barcelona.” *Atmospheric Chemistry and Physics* 13 (2): 741–759.
- DEFRA Report. Summary of the Second Report Produced by the Air Quality Expert Group, Department for the Environment, Food and Rural Affairs, London, 2005.
- Draxler, R.R., 1999: HYSPLIT4 User’s Guide. NOAA Tech. Memo. ERL ARL-230, NOAA Air Resources Laboratory, Silver Spring, MD.
- Draxler, R.R., and G.D. Hess, 1997: Description of the HYSPLIT_4 Modeling System. NOAA Tech. Memo. ERL ARL-224, NOAA Air Resources Laboratory, Silver Spring, MD, 24 Pp.
- Draxler, R.R., and G.D. Hess, 1998: An Overview of the HYSPLIT_4 Modeling System of Trajectories, Dispersion, and Deposition. *Aust. Meteor. Mag.*, 47, 295-308.
- Elbert, W., P. E. Taylor, M. O. Andreae, and U. Pöschl. 2007. “Contribution of Fungi to Primary Biogenic Aerosols in the Atmosphere: Wet and Dry Discharged Spores, Carbohydrates, and Inorganic Ions.” *Atmospheric Chemistry and Physics* 7 (17): 4569–4588.
- Favez, Olivier, Hélène Cachier, Jean Sciare, Roland Sarda-Estève, and Laurent Martinon. 2009. “Evidence for a Significant Contribution of Wood Burning Aerosols to PM2.5 during the Winter Season in Paris, France.” *Atmospheric Environment* 43 (22–23): 3640–44. doi:10.1016/j.atmosenv.2009.04.035.

- Fine, Philip M., Glen R. Cass, and Bernd R. T. Simoneit. 2002. "Organic Compounds in Biomass Smoke from Residential Wood Combustion: Emissions Characterization at a Continental Scale." *Journal of Geophysical Research: Atmospheres* 107 (D21): 8349. doi:10.1029/2001JD000661.
- Fu, Xuewu, Xinbin Feng, Guangle Qiu, Lihai Shang, and Hui Zhang. 2011. "Speciated Atmospheric Mercury and Its Potential Source in Guiyang, China." *Atmospheric Environment* 45 (25): 4205–4212.
- Gaston, Cassandra J., Kerri A. Pratt, Xueying Qin, and Kimberly A. Prather. 2010. "Real-Time Detection and Mixing State of Methanesulfonate in Single Particles at an Inland Urban Location during a Phytoplankton Bloom." *Environmental Science & Technology* 44 (5): 1566–1572.
- Gietl, Johanna K., and Otto Klemm. 2009. "Source Identification of Size-Segregated Aerosol in Münster, Germany, by Factor Analysis." *Aerosol Science and Technology* 43 (8): 828–37. doi:10.1080/02786820902953923.
- Golly, B., G. Brulfert, G. Berlioux, J. -L. Jaffrezo, and J. -L. Besombes. 2015. "Large Chemical Characterisation of PM10 Emitted from Graphite Material Production: Application in Source Apportionment." *Science of The Total Environment* 538: 634–43. doi:10.1016/j.scitotenv.2015.07.115.
- Grover, Brett D., Michael Kleinman, Norman L. Eatough, Delbert J. Eatough, Philip K. Hopke, Russell W. Long, William E. Wilson, Michael B. Meyer, and Jeffrey L. Ambs. 2005. "Measurement of Total PM2.5 Mass (Nonvolatile plus Semivolatile) with the Filter Dynamic Measurement System Tapered Element Oscillating Microbalance Monitor." *Journal of Geophysical Research: Atmospheres* 110 (D7). <http://onlinelibrary.wiley.com/doi/10.1029/2004JD004995/full>.
- Hallquist, Mattias, J. C. Wenger, Urs Baltensperger, Y. Rudich, David Simpson, M. Claeys, J. Dommen, et al. 2009. "The Formation, Properties and Impact of Secondary Organic Aerosol: Current and Emerging Issues." *Atmospheric Chemistry and Physics* 9 (14): 5155–5236.
- Han, Young-Ji, Thomas M. Holsen, and Philip K. Hopke. 2007. "Estimation of Source Locations of Total Gaseous Mercury Measured in New York State Using Trajectory-Based Models." *Atmospheric Environment* 41 (28): 6033–47. doi:10.1016/j.atmosenv.2007.03.027.
- Hennigan, Christopher J., Amy P. Sullivan, Jeffrey L. Collett, and Allen L. Robinson. 2010. "Levoglucosan Stability in Biomass Burning Particles Exposed to Hydroxyl Radicals." *Geophysical Research Letters* 37 (9): L09806. doi:10.1029/2010GL043088.
- Henry, Ronald C., Yu-Shuo Chang, and Clifford H. Spiegelman. 2002. "Locating Nearby Sources of Air Pollution by Nonparametric Regression of Atmospheric Concentrations on Wind Direction." *Atmospheric Environment* 36 (13): 2237–44. doi:10.1016/S1352-2310(02)00164-4.
- Jaenicke, Ruprecht. 2005. "Abundance of Cellular Material and Proteins in the Atmosphere." *Science* 308 (5718): 73–73.
- Jia, Yuling, Andrea L. Clements, and Matthew P. Fraser. 2010. "Saccharide Composition in Atmospheric Particulate Matter in the Southwest US and Estimates of Source Contributions." *Journal of Aerosol Science* 41 (1): 62–73.
- Johansson, Christer, Michael Norman, and Lars Burman. 2009. "Road Traffic Emission Factors for Heavy Metals." *Atmospheric Environment* 43 (31): 4681–4688.
- Kabashnikov, Vitaliy P., Anatoli P. Chaikovskiy, Tom L. Kucsera, and Natalia S. Metelskaya. 2011. "Estimated Accuracy of Three Common Trajectory Statistical Methods." *Atmospheric Environment* 45 (31): 5425–30. doi:10.1016/j.atmosenv.2011.07.006.
- Kawamura, Kimitaka, and Kouichi Ikushima. 1993. "Seasonal Changes in the Distribution of Dicarboxylic Acids in the Urban Atmosphere." *Environmental Science & Technology* 27 (10): 2227–2235.
- Kawamura, Kimitaka, and Isaac R. Kaplan. 1987. "Motor Exhaust Emissions as a Primary Source for Dicarboxylic Acids in Los Angeles Ambient Air." *Environmental Science & Technology* 21 (1): 105–110.
- Kawamura, Kimitaka, Hideki Kasukabe, and Leonard A. Barrie. 1996. "Source and Reaction Pathways of Dicarboxylic Acids, Ketoacids and Dicarbonyls in Arctic Aerosols: One Year of Observations." *Atmospheric Environment* 30 (10): 1709–1722.
- Kelly, Frank J., and Julia C. Fussell. 2015. "Linking Ambient Particulate Matter Pollution Effects with Oxidative Biology and Immune Responses." *Annals of the New York Academy of Sciences* 1340 (1): 84–94. doi:10.1111/nyas.12720.

- Kim Oanh, Nguyen Thi, Prapat Pongkiatkul, Nabin Upadhyay, and Phillip P. Hopke. 2009. "Designing Ambient Particulate Matter Monitoring Program for Source Apportionment Study by Receptor Modeling." *Atmospheric Environment* 43 (21): 3334–44. doi:10.1016/j.atmosenv.2009.04.016.
- Maenhaut, Willy, Reinhilde Vermeylen, Magda Claeys, Jordy Vercauteren, and Edward Roekens. 2016. "Sources of the PM₁₀ Aerosol in Flanders, Belgium, and Re-Assessment of the Contribution from Wood Burning." *The Science of the Total Environment* 562 (August): 550–60. doi:10.1016/j.scitotenv.2016.04.074.
- Millero, Frank J., and Fred K. Lepple. 1973. "The Density and Expansibility of Artificial Seawater Solutions from 0 to 40 C and 0 to 21‰ Chlorinity." *Marine Chemistry* 1 (2): 89–104.
- Myriokefalitakis, S., K. Tsigaridis, N. Mihalopoulos, J. Sciare, A. Nenes, K. Kawamura, A. Segers, and M. Kanakidou. 2011. "In-Cloud Oxalate Formation in the Global Troposphere: A 3-D Modeling Study." *Atmospheric Chemistry and Physics* 11 (12): 5761–5782.
- Paatero, Pentti, Philip K. Hopke, Xin-Hua Song, and Ziad Ramadan. 2002. "Understanding and Controlling Rotations in Factor Analytic Models." *Chemometrics and Intelligent Laboratory Systems* 60 (1): 253–264.
- Paatero, Pentti, and Unto Tapper. 1994. "Positive Matrix Factorization: A Non-Negative Factor Model with Optimal Utilization of Error Estimates of Data Values." *Environmetrics* 5 (2): 111–26. doi:10.1002/env.3170050203.
- Pandolfi, M., M. Viana, M. C. Minguillón, X. Querol, A. Alastuey, F. Amato, I. Celades, A. Escrig, and E. Monfort. 2008. "Receptor Models Application to Multi-Year Ambient PM₁₀ Measurements in an Industrialized Ceramic Area: Comparison of Source Apportionment Results." *Atmospheric Environment* 42 (40): 9007–17. doi:10.1016/j.atmosenv.2008.09.029.
- Paris, R., and K. V. Desboeufs. 2013. "Effect of Atmospheric Organic Complexation on Iron-Bearing Dust Solubility." *Atmospheric Chemistry and Physics* 13: 4895–4905.
- Pashynska, Vlada, Reinhilde Vermeylen, Gyorgy Vas, Willy Maenhaut, and Magda Claeys. 2002. "Development of a Gas Chromatographic/ion Trap Mass Spectrometric Method for the Determination of Levoglucosan and Saccharidic Compounds in Atmospheric Aerosols. Application to Urban Aerosols." *Journal of Mass Spectrometry* 37 (12): 1249–1257.
- Paw-Armart, Ittipol, and Kunio Yoshizumi. 2013. "Size Distributions of Atmospheric Aerosol Compositions in Saitama, Japan." *Open Journal of Air Pollution* 2 (1): 1–6. doi:10.4236/ojap.2013.21001.
- Pernigotti, Denise, Claudio A. Belis, and Luca Spanò. 2016. "SPECIEUROPE: The European Data Base for PM Source Profiles." *Atmospheric Pollution Research* 7 (2): 307–14. doi:10.1016/j.apr.2015.10.007.
- Petit, J. -E., O. Favez, A. Albinet, and F. Canonaco. 2017. "A User-Friendly Tool for Comprehensive Evaluation of the Geographical Origins of Atmospheric Pollution: Wind and Trajectory Analyses." *Environmental Modelling & Software* 88: 183–87. doi:10.1016/j.envsoft.2016.11.022.
- Pio, Casimiro A., Luis M. Castro, Mario A. Cerqueira, Isabel M. Santos, Filipa Belchior, and Maria L. Salgueiro. 1996. "Source Assessment of Particulate Air Pollutants Measured at the Southwest European Coast." *Atmospheric Environment* 30 (19): 3309–3320.
- Pio, Casimiro, Mário Cerqueira, Roy M. Harrison, Teresa Nunes, Fátima Mirante, Célia Alves, César Oliveira, Ana Sanchez de la Campa, Begoña Artíñano, and Manuel Matos. 2011. "OC/EC Ratio Observations in Europe: Re-Thinking the Approach for Apportionment between Primary and Secondary Organic Carbon." *Atmospheric Environment* 45 (34): 6121–32. doi:10.1016/j.atmosenv.2011.08.045.
- Puxbaum, Hans, Alexandre Caseiro, Asunción Sánchez-Ochoa, Anne Kasper-Giebl, Magda Claeys, Andrés Gelencsér, Michel Legrand, Susanne Preunkert, and Casimiro Pio. 2007. "Levoglucosan Levels at Background Sites in Europe for Assessing the Impact of Biomass Combustion on the European Aerosol Background." *Journal of Geophysical Research: Atmospheres* 112 (D23): D23S05. doi:10.1029/2006JD008114.
- Rapport: essai caracterisation PM₁₀ Nogent version Finale. 2016. Accessed October 29. http://www.atmopicardie.com/publications/fichiers/199/Rapport_essai_caracterisation_PM10_Nogent_version_Finale.pdf.
- Riffault, Véronique, Jovanna Arndt, Hélène Marris, Saliou Mbengue, Ari Setyan, Laurent Y. Alleman, Karine Deboudt, et al. 2015. "Fine and Ultrafine Particles in the Vicinity of Industrial Activities: A Review."

- Rutter, A. P., D. C. Snyder, E. A. Stone, J. J. Schauer, R. Gonzalez-Abraham, L. T. Molina, C. Márquez, B. Cárdenas, and B. de Foy. 2009. “In Situ Measurements of Speciated Atmospheric Mercury and the Identification of Source Regions in the Mexico City Metropolitan Area.” *Atmos. Chem. Phys.* 9 (1): 207–20. doi:10.5194/acp-9-207-2009.
- Samoli, Evangelia, Roger Peng, Tim Ramsay, Marina Pipikou, Giota Touloumi, Francesca Dominici, Rick Burnett, et al. 2008. “Acute Effects of Ambient Particulate Matter on Mortality in Europe and North America: Results from the APHENA Study.” *Environmental Health Perspectives* 116 (11): 1480–86. doi:10.1289/ehp.11345.
- Sartelet, Karine N., Florian Couvidat, Christian Seigneur, and Yelva Roustan. 2012. “Impact of Biogenic Emissions on Air Quality over Europe and North America.” *Atmospheric Environment* 53: 131–141.
- Schauer, James J., Wolfgang F. Rogge, Lynn M. Hildemann, Monica A. Mazurek, Glen R. Cass, and Bernd R. T. Simoneit. 1996. “Source Apportionment of Airborne Particulate Matter Using Organic Compounds as Tracers.” *Atmospheric Environment* 30 (22): 3837–55. doi:10.1016/1352-2310(96)00085-4.
- Sciare, J., K. Oikonomou, O. Favez, E. Liakakou, Z. Markaki, H. Cachier, and N. Mihalopoulos. 2008. “Long-Term Measurements of Carbonaceous Aerosols in the Eastern Mediterranean: Evidence of Long-Range Transport of Biomass Burning.” *Atmos. Chem. Phys.* 8 (18): 5551–63. doi:10.5194/acp-8-5551-2008.
- Seibert, P., H. Kromp-Kolb, U. Baltensperger, D. T. Jost, M. Schwikowski, A. Kasper, and H. Puxbaum. 1994. “Trajectory Analysis of Aerosol Measurements at High Alpine Sites.” *Transport and Transformation of Pollutants in the Troposphere*, 689–693.
- Seinfeld, John H., and Spyros N. Pandis. 2006. *Atmospheric Chemistry and Physics*. Hoboken. Vol. 450. NJ: Wiley.
- Sexauer Gustin, M., P. S. Weiss-Penzias, and C. Peterson. 2012. “Investigating Sources of Gaseous Oxidized Mercury in Dry Deposition at Three Sites across Florida, USA.” *Atmos. Chem. Phys.* 12 (19): 9201–19. doi:10.5194/acp-12-9201-2012.
- Stein, A. F., R. R. Draxler, G. D. Rolph, B. J. B. Stunder, M. D. Cohen, and F. Ngan. 2015. “NOAA’s HYSPLIT Atmospheric Transport and Dispersion Modeling System.” *Bulletin of the American Meteorological Society* 96 (12): 2059–77. doi:10.1175/BAMS-D-14-00110.1.
- Su, Lin, Zibing Yuan, Jimmy C. H. Fung, and Alexis K. H. Lau. 2015. “A Comparison of HYSPLIT Backward Trajectories Generated from Two GDAS Datasets.” *Science of The Total Environment* 506–507 (February): 527–37. doi:10.1016/j.scitotenv.2014.11.072.
- Ulbrich, I. M., M. R. Canagaratna, Q. Zhang, D. R. Worsnop, and J. L. Jimenez. 2009. “Interpretation of Organic Components from Positive Matrix Factorization of Aerosol Mass Spectrometric Data.” *Atmos. Chem. Phys.* 9 (9): 2891–2918. doi:10.5194/acp-9-2891-2009.
- Viana, M., T. A. J. Kuhlbusch, X. Querol, A. Alastuey, R. M. Harrison, P. K. Hopke, W. Winiwarter, et al. 2008. “Source Apportionment of Particulate Matter in Europe: A Review of Methods and Results.” *Journal of Aerosol Science* 39 (10): 827–849.
- Waked, A., O. Favez, L. Y. Alleman, C. Piot, J.-E. Petit, T. Delaunay, E. Verlinden, et al. 2014. “Source Apportionment of PM10 in a North-Western Europe Regional Urban Background Site (Lens, France) Using Positive Matrix Factorization and Including Primary Biogenic Emissions.” *Atmos. Chem. Phys.* 14 (7): 3325–46. doi:10.5194/acp-14-3325-2014.
- Watson, John G., L.-W. Antony Chen, Judith C. Chow, Prakash Doraiswamy, and Douglas H. Lowenthal. 2008. “Source Apportionment: Findings from the U.S. Supersites Program.” *Journal of the Air & Waste Management Association* 58 (2): 265–88. doi:10.3155/1047-3289.58.2.265.
- Watson, John G., Tan Zhu, Judith C. Chow, Johann Engelbrecht, Eric M. Fujita, and William E. Wilson. 2002. “Receptor Modeling Application Framework for Particle Source Apportionment.” *Chemosphere* 49 (9): 1093–1136. doi:10.1016/S0045-6535(02)00243-6.
- Weiss-Penzias, Peter S., Mae S. Gustin, and Seth N. Lyman. 2011. “Sources of Gaseous Oxidized Mercury and Mercury Dry Deposition at Two Southeastern US Sites.” *Atmospheric Environment* 45 (27): 4569–4579.

- Xu, X., and U. S. Akhtar. 2010. "Identification of Potential Regional Sources of Atmospheric Total Gaseous Mercury in Windsor, Ontario, Canada Using Hybrid Receptor Modeling." *Atmospheric Chemistry and Physics* 10 (15): 7073–7083.
- Yttri, K. E., W. Aas, A. Bjerke, J. N. Cape, F. Cavalli, D. Ceburnis, C. Dye, et al. 2007. "Elemental and Organic Carbon in PM₁₀: A One Year Measurement Campaign within the European Monitoring and Evaluation Programme EMEP." *Atmospheric Chemistry and Physics* 7 (22): 5711–5725.
- Yttri, Karl Espen, David Simpson, Jacob Klenø Nøjgaard, Kasper Kristensen, Johan Genberg, Kristina Stenström, Erik Swietlicki, et al. 2011. "Source Apportionment of the Summer Time Carbonaceous Aerosol at Nordic Rural Background Sites." *Atmospheric Chemistry and Physics* 11 (24): 13339–13357.
- Yue, Wei, Matthias Stölzel, Josef Cyrus, Mike Pitz, Joachim Heinrich, Wolfgang G. Kreyling, H. -Erich Wichmann, Annette Peters, Sheng Wang, and Philip K. Hopke. 2008. "Source Apportionment of Ambient Fine Particle Size Distribution Using Positive Matrix Factorization in Erfurt, Germany." *Science of The Total Environment* 398 (1–3): 133–44. doi:10.1016/j.scitotenv.2008.02.049.
- Zhao, Weixiang, and Philip K. Hopke. 2006. "Source Identification for Fine Aerosols in Mammoth Cave National Park." *Atmospheric Research* 80 (4): 309–22. doi:10.1016/j.atmosres.2005.10.002.

SUPPLEMENTARY MATERIAL

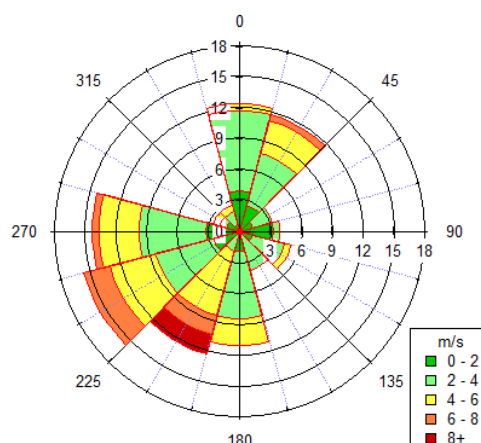


Figure S.1: Wind roses (m s^{-1}) for the sampling site of Nogent-sur-Oise during the period of study

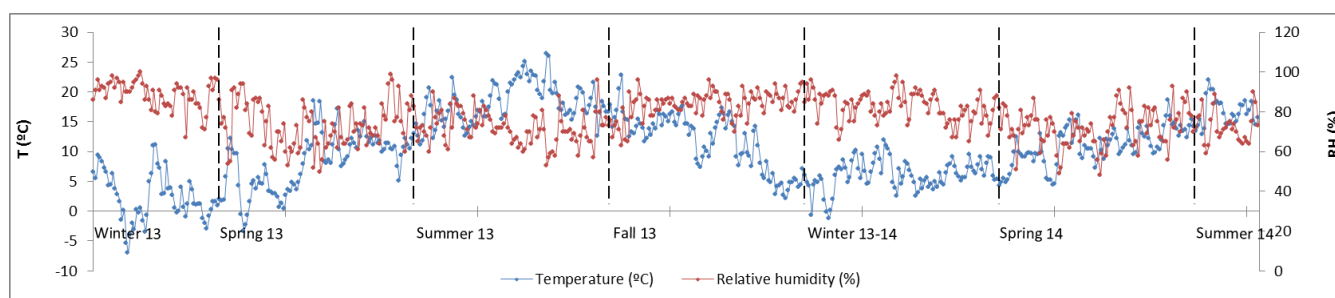


Figure S.2: Time variability of temperature (in $^{\circ}\text{C}$) and relative humidity (in %) in Nogent-sur-Oise during the period of study

Table S.1: Seasonality of the meteorological parameters of rainfall (in mm), rainfall duration (in min day^{-1}), average temperature (in $^{\circ}\text{C}$), pressure (in mbar), wind speed (in m s^{-1}), relative humidity (in %) and number of days in Nogent-sur-Oise

	Rainfall (mm)	Duration (min day^{-1})	Average Temperature ($^{\circ}\text{C}$)	Pressure (mbar)	Wind speed (m/s)	Relative humidity (%)	Days of snow
Winter 13	71	202	2	1016	3.3	89	13
Spring 13	154	124	8	1012	3.5	73	3
Summer 13	168	59	18	1019	2.9	72	0
Fall 13	203	128	12	1016	3.1	84	2
Winter 13-14	187	161	6	1011	4.2	83	0
Spring 14	130	77	11	1016	3.0	72	0
Summer 14	93	57	17	1018	2.8	72	0

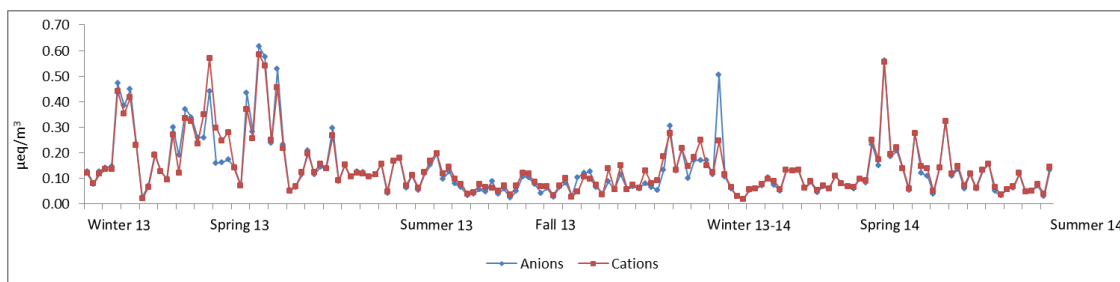


Figure S.3: Time variability of anions and cations in Nogent-sur-Oise

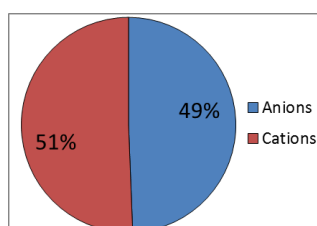


Figure S.4: Ion balance of the samples collected in Nogent-sur-Oise

Table S.2: Scaled residuals beyond 3 standard deviations (dates by species)

Species	Date	Residuals	Species	Date	Residuals
EC	04-10-2013	3.4	Oxalate	24-07-2013	-3.6
	07-10-2013	4.1	Levogluconan	29-01-2013	5.6
	19-10-2013	4.3		09-12-2013	-3.3
	12-01-2014	4.3	Polysaccharides	17-01-2013	3.3
	07-03-2014	3.8		24-03-2013	5.0
	31-03-2014	3.7		25-10-2013	6.1
OC	09-05-2014	-3.1		24-11-2013	3.3
NO ₃ ⁻	16-02-2013	5.9	Ca	06-04-2014	3.5
	09-12-2013	7.9	As	16-03-2014	3.2
SO ₄ ²⁻	08-08-2013	3.8		12-05-2014	3.5
	Na ⁺	17-01-2013		3.5	15-05-2014
20-01-2013		3.2		27-05-2014	3.5
03-03-2013		15.8		30-05-2014	3.4
06-03-2013		17.7	02-06-2014	3.3	
09-03-2013		12.9	Cd	24-05-2014	3.0
12-03-2013		19.3		27-05-2014	3.5
05-09-2013		18.5	Co	06-04-2014	3.1
09-12-2013		-5.1	Pb	23-01-2013	3.2
06-04-2014		3.4		29-01-2013	3.4
NH ₄ ⁺		08-08-2013		-4.8	05-09-2013
	27-11-2013	3.3	27-05-2014	3.5	
K ⁺	08-01-2013	-5.4	Sb	05-01-2013	4.1
	13-02-2013	3.3		01-05-2013	3.3
	16-02-2013	-3.3		30-08-2013	-3.8

	16-05-2013	-3.2		25-09-2013	-3.3	
	19-05-2013	3.6		16-03-2014	3.4	
	08-08-2013	-4.1	Sr	13-05-2013	3.1	
	30-08-2013	3.1		16-05-2013	-4.5	
	01-10-2013	3.2	V	06-04-2014	3.3	
	19-10-2013	3.7		12-03-2013	3.0	
	22-10-2013	3.7		31-05-2013	3.0	
	24-11-2013	3.7		22-10-2013	3.0	
	27-11-2013	3.7		30-12-2013	-3.6	
	03-12-2013	5.1		13-03-2014	-3.5	
	09-12-2013	3.5		19-03-2014	3.1	
	21-12-2013	3.1		06-04-2014	3.4	
	30-12-2013	5.3		15-04-2014	3.1	
	05-02-2014	3.1		24-04-2014	-3.4	
Mg²⁺	17-01-2013	-3.5		Zn	06-05-2014	3.1
	07-05-2013	3.4			12-03-2013	3.4
	15-07-2013	3.5			04-10-2013	3.6
	21-07-2013	3.1			03-11-2013	3.3
	05-09-2013	-3.6	13-11-2013		3.3	
	01-10-2013	-10.4	18-04-2014		3.5	
	13-03-2014	4.0	27-05-2014		3.7	
	06-05-2014	3.3				

Table S.3: Model fitting on observed concentrations

Species	Intercept	Slope	SE	r²
PM₁₀	-0.55	0.97	5.39	0.90
EC	0.11	0.80	0.41	0.79
OC	0.22	0.90	0.84	0.94
Cl⁻	0.01	0.97	0.05	1.00
NO₃⁻	0.10	0.96	0.55	0.99
SO₄²⁻	0.05	0.97	0.12	1.00
Na⁺	0.09	0.77	0.30	0.70
NH₄⁺	-0.03	1.02	0.13	0.99
K⁺	0.03	0.66	0.03	0.87
Mg²⁺	0.00	0.90	0.01	0.97
MSA	0.00	0.93	0.01	0.98
Oxalate	0.00	0.96	0.01	0.96
Levogluconan	-0.02	1.06	0.10	0.97
Polysaccharides	0.00	0.95	0.01	0.99
Sugar alcohols	0.00	0.92	0.00	0.98
Fe	0.07	0.06	0.04	0.14
Ca	0.18	0.37	0.14	0.64
As	0.00	0.29	0.00	0.28
Ba	0.00	0.29	0.00	0.41
Cd	0.00	0.39	0.00	0.60
Co	0.00	0.64	0.00	0.70
Cu	0.01	0.58	0.01	0.64
La	0.00	0.41	0.00	0.47
Mn	0.00	0.39	0.00	0.40
Mo	0.00	0.29	0.00	0.42

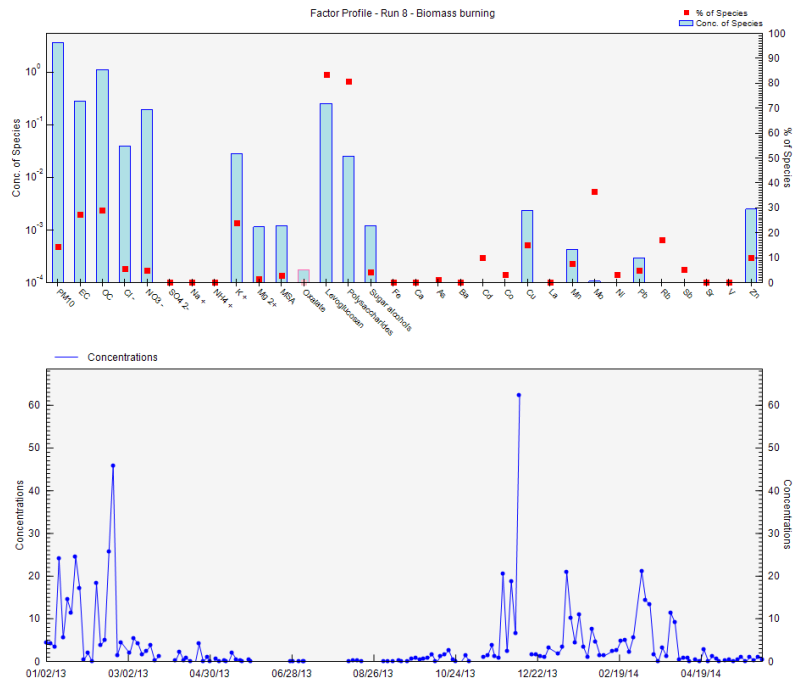


Figure S.6: Chemical and time profile of the biomass burning factor

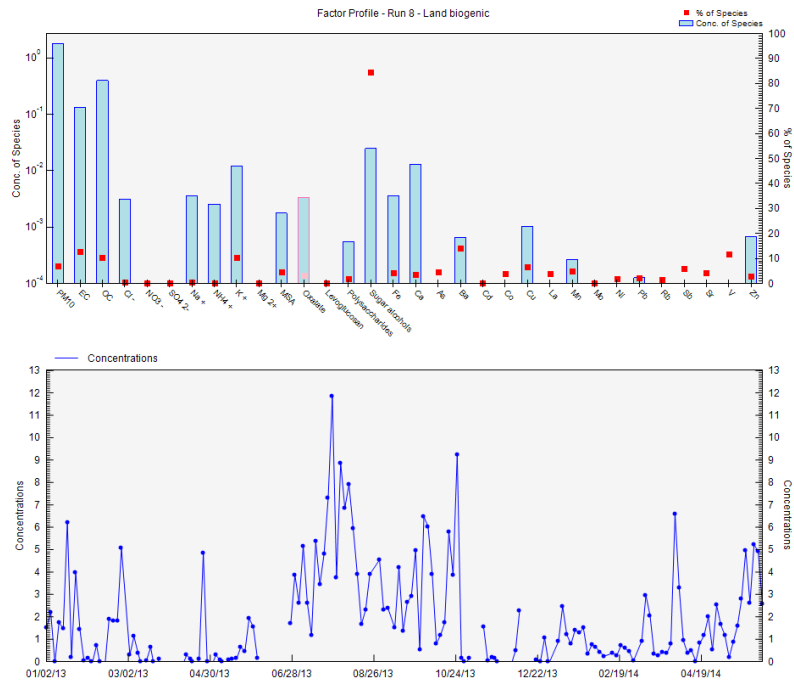


Figure S.7: Chemical and time profile of the land biogenic factor

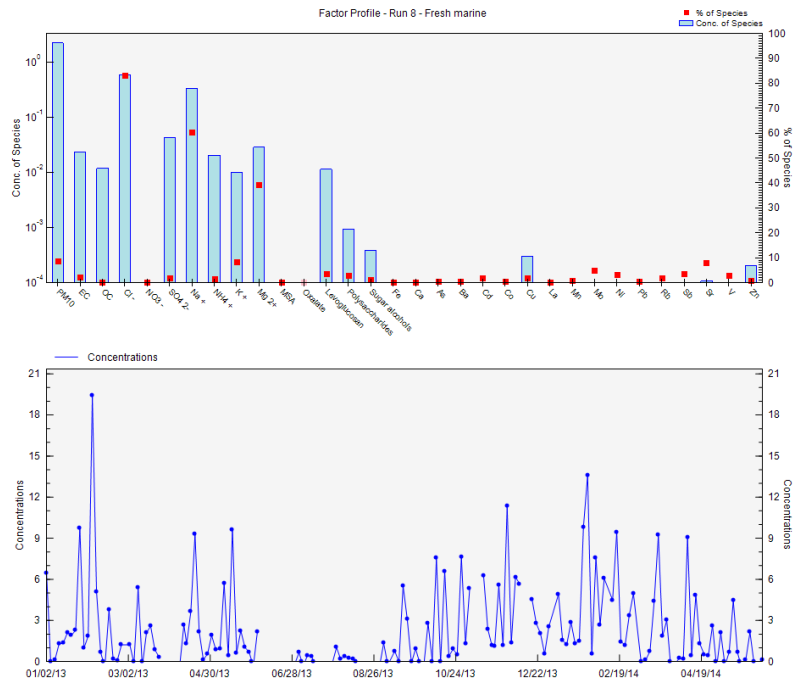


Figure S.8: Chemical and time profile of the fresh marine factor

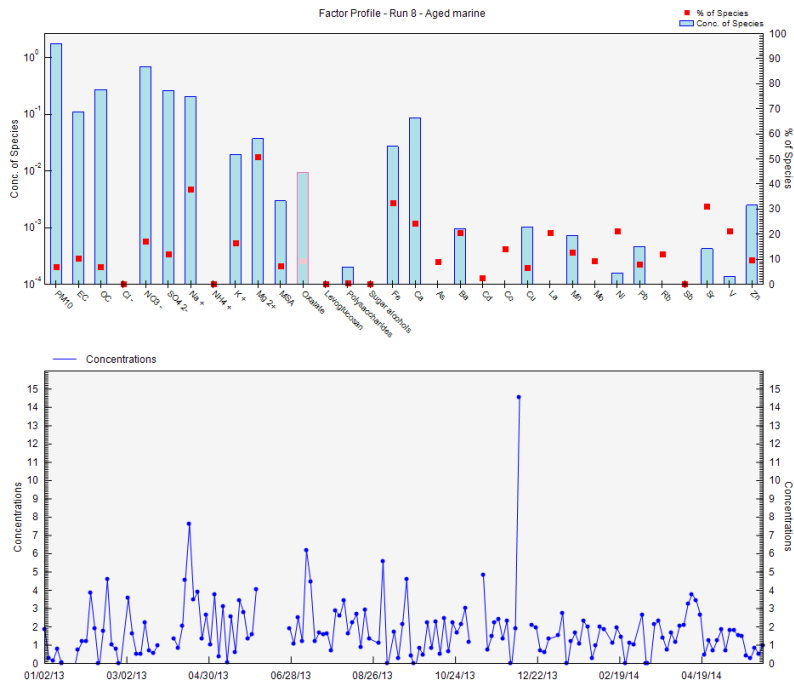


Figure S.9: Chemical and time profile of the aged marine factor

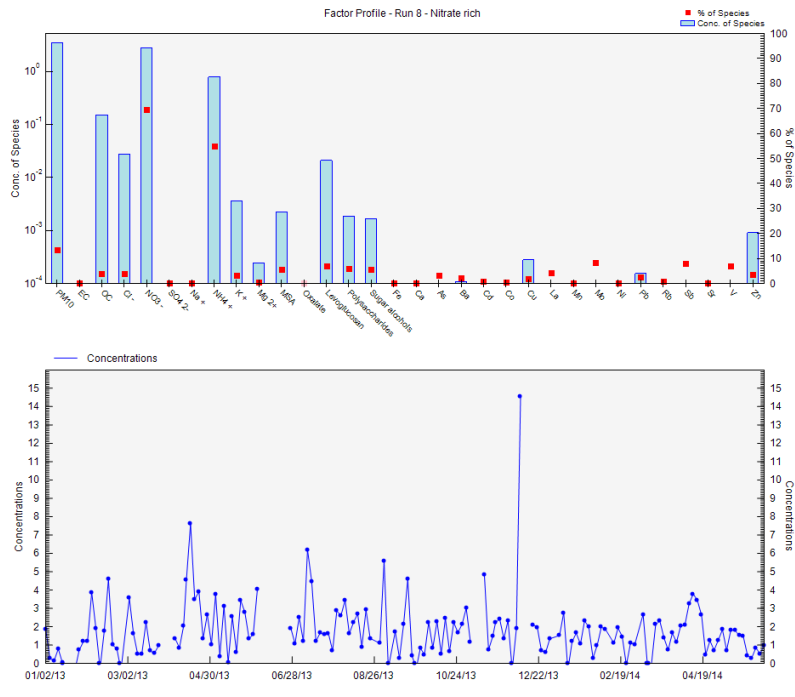


Figure S.10: Chemical and time profile for the nitrate rich factor

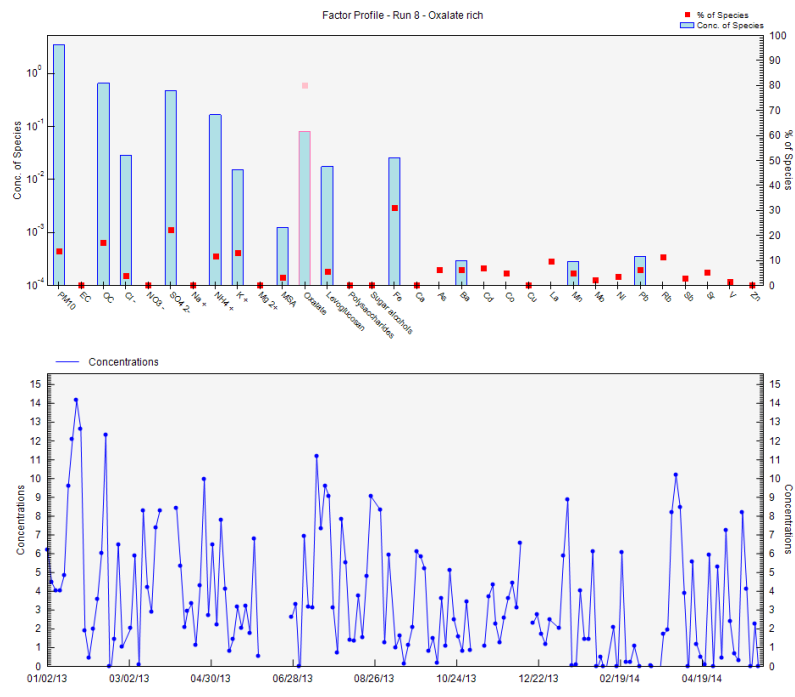


Figure S.11: Chemical and time profile of the oxalate rich factor

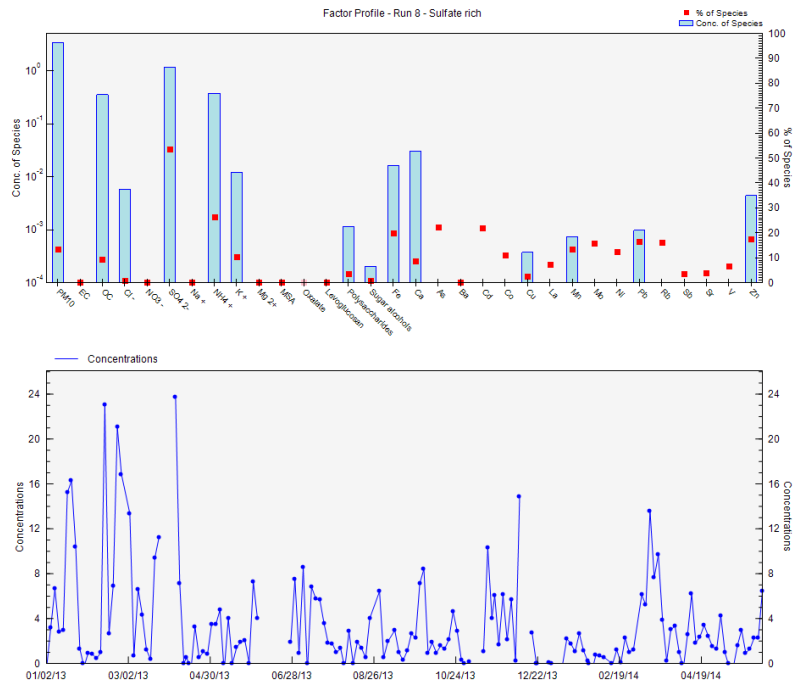


Figure S.12: Chemical and time profile of the sulfate rich factor

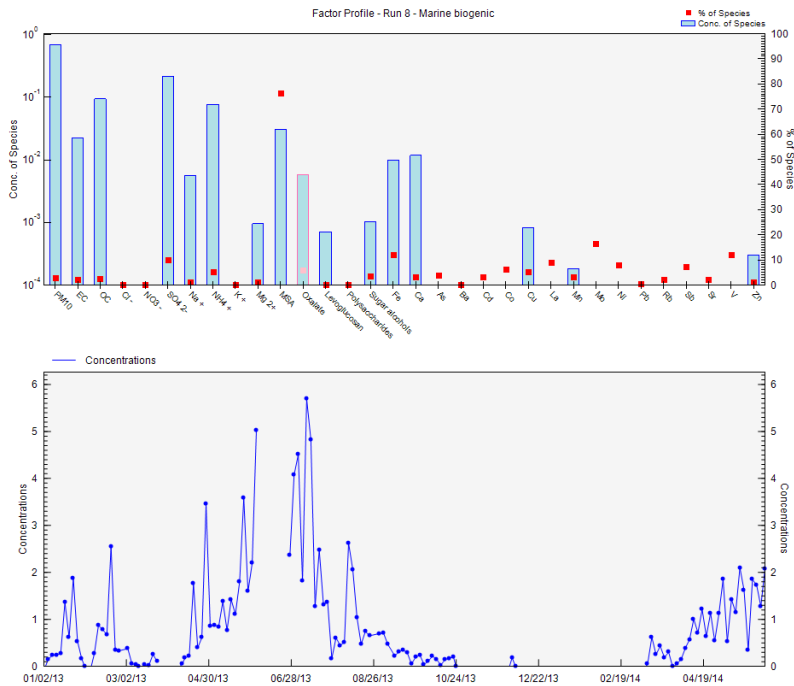


Figure S.13: Chemical and time profile of the marine biogenic factor

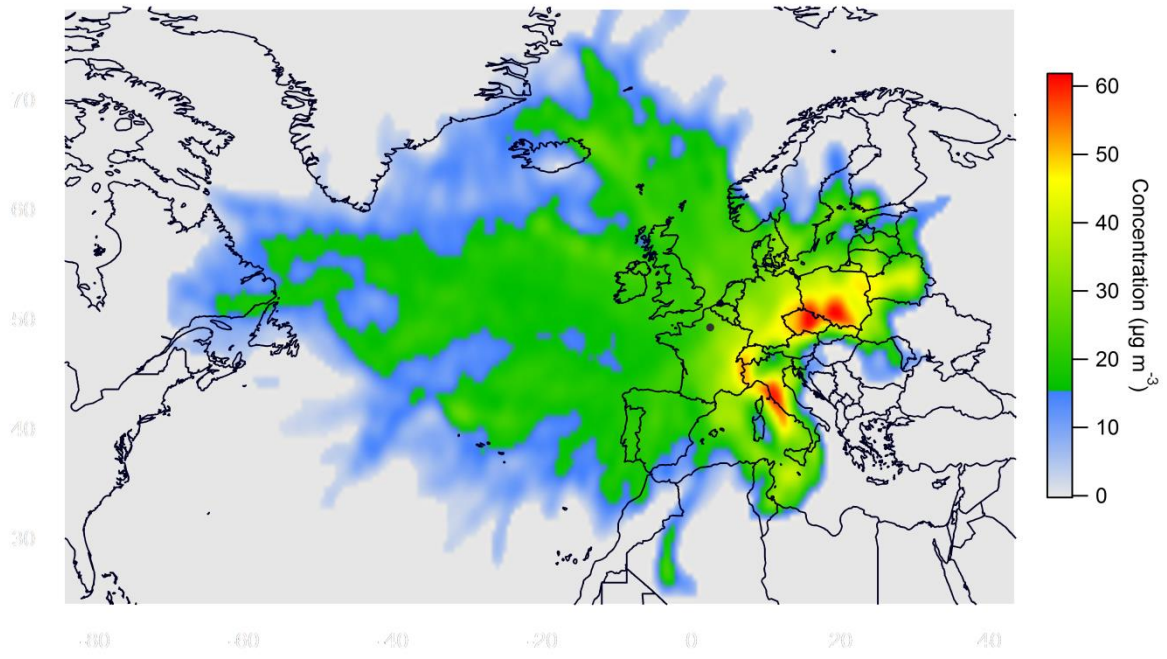


Figure S.14: Concentration field map of PM₁₀ in Nogent-sur-Oise

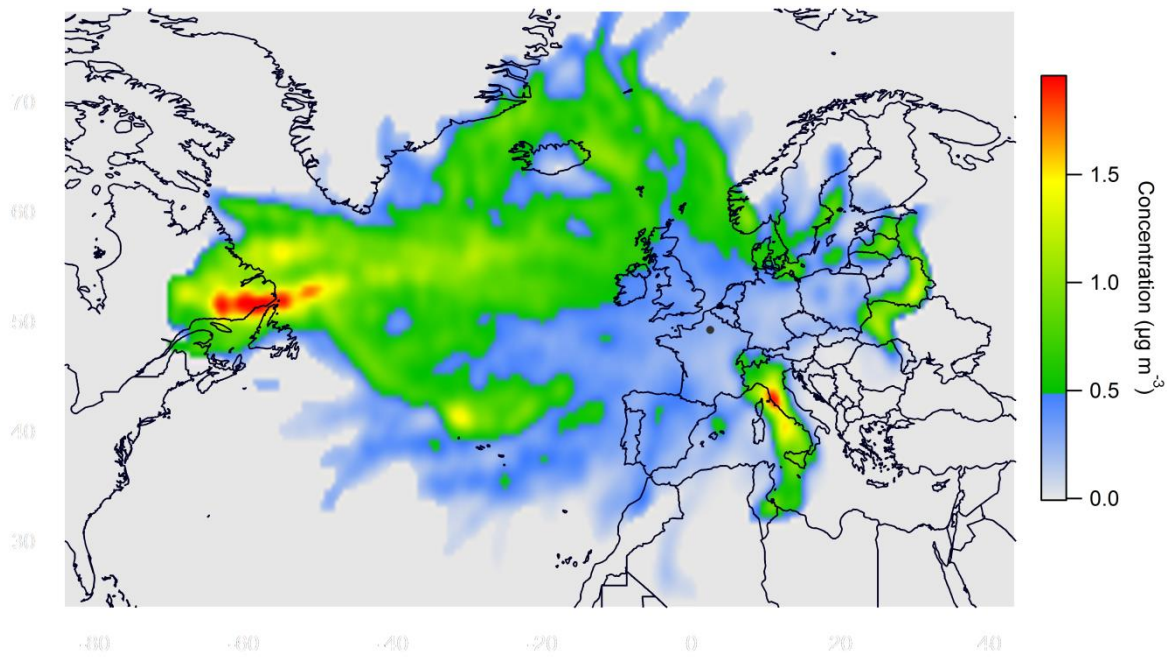


Figure S.15: Concentration field map of sodium in Nogent-sur-Oise

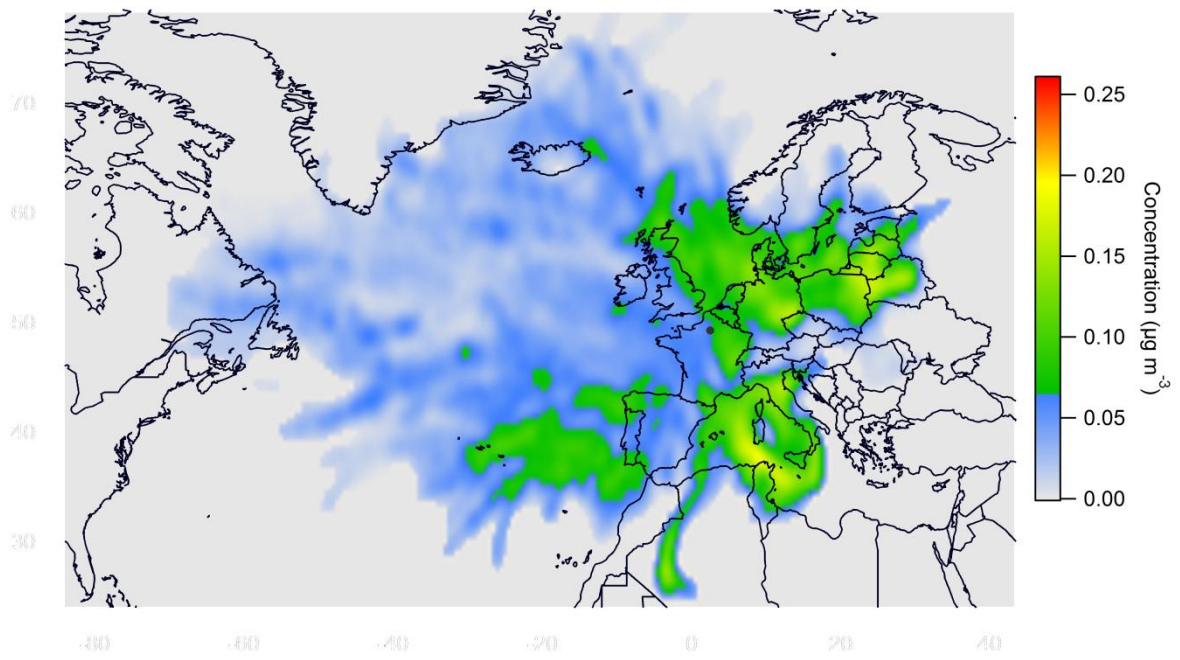


Figure S.16: Concentration field map of oxalate in Nogent-sur-Oise

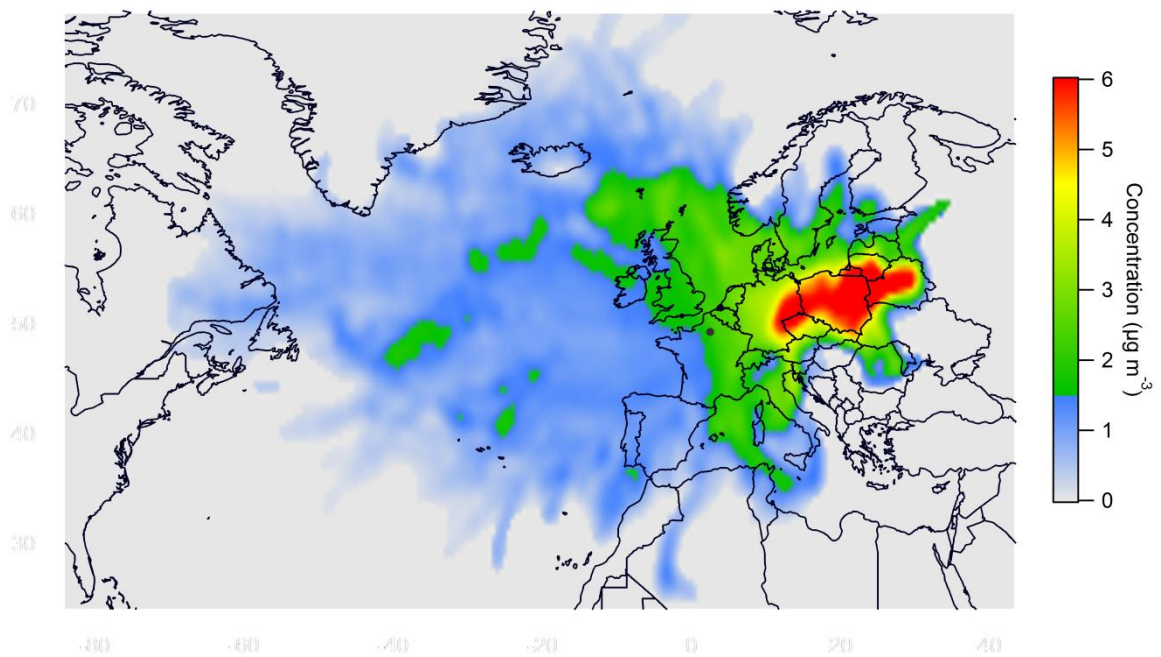


Figure S. 17: Concentration field map of sulfate in Nogent-sur-Oise

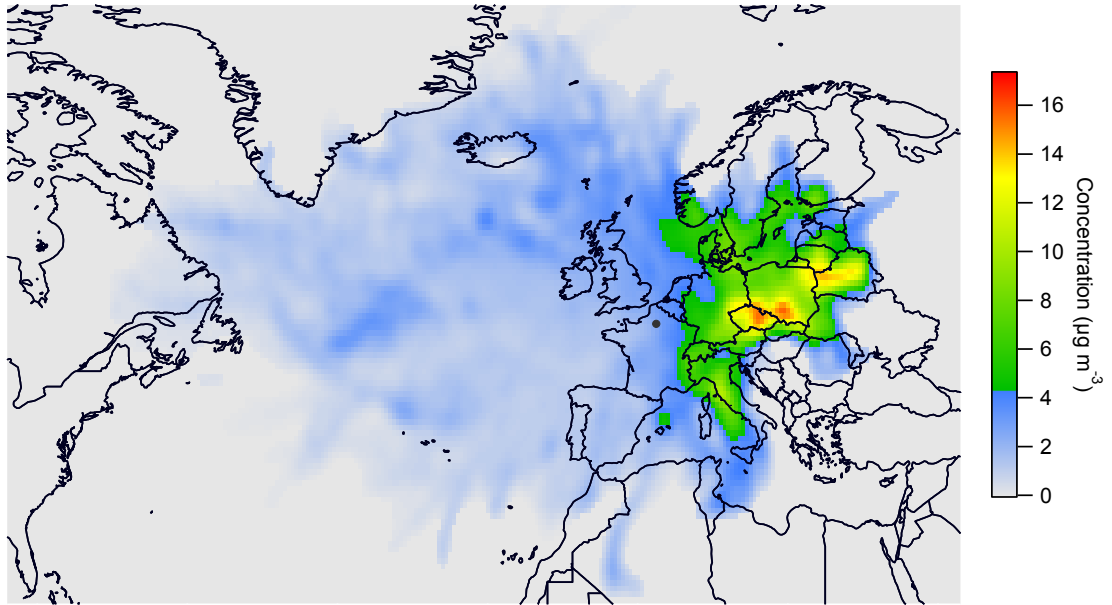


Figure S. 18: Concentration field map of nitrate in Nogent-sur-Oise

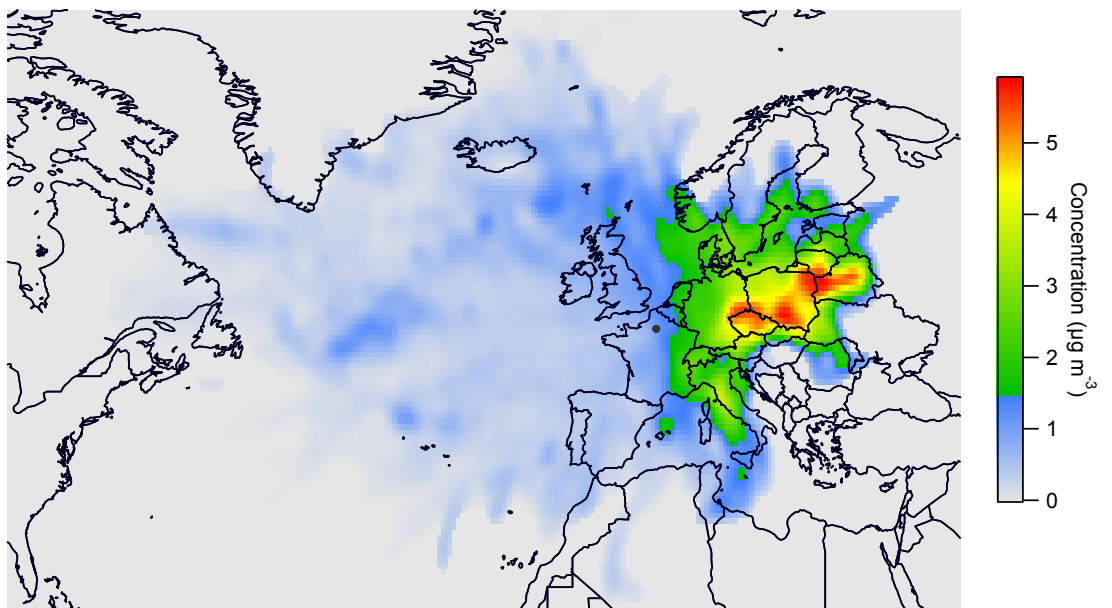


Figure S. 19: Concentration field map of ammonium in Nogent-sur-Oise

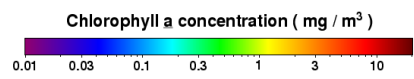
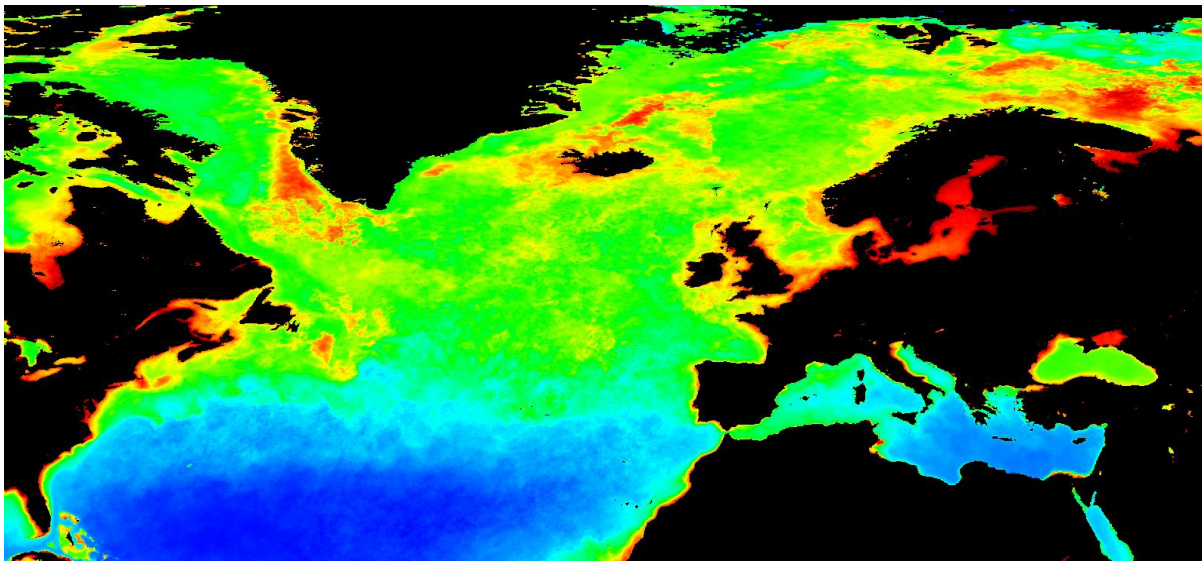
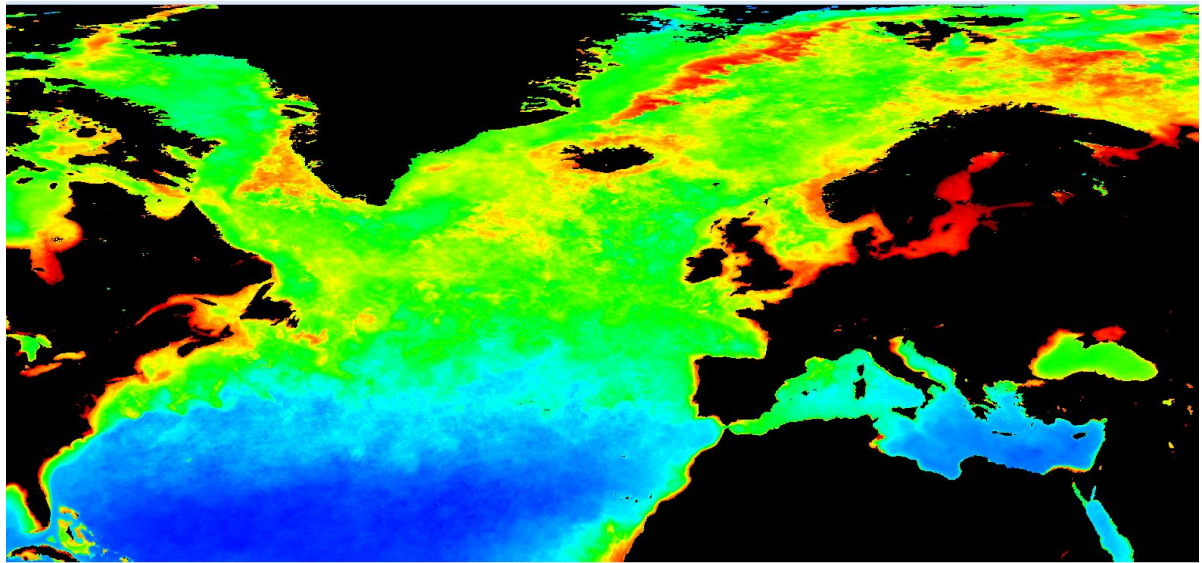


Figure S.20: Chlorophyll-a concentrations (in mg m⁻³) in (top) 2013 and (bottom) 2014 (Source: NASA, 2016)

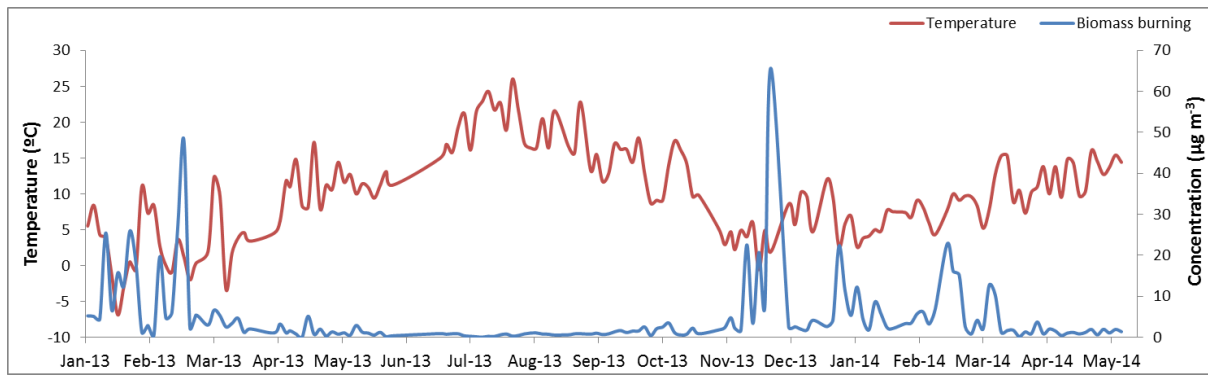


Figure S.21: Time variability of temperature and biomass burning contributions

3.2 Complement of Publication 1

3.2.1 Source apportionment

The PMF model was applied in this study to identify and quantify sources of PM₁₀ in each individual site. This model is based on a factor analysis of the database and uses a least squares algorithm to determine the contributions of factors and their chemical compositions while applying non-negativity constraints in the optimization process.

This work was performed with the EPA PMF version 5.0.12.13261 developed by the Environmental Protection Agency (EPA) in 2013. The optimization of the final solution for each site followed the guidelines suggested in the European Guide on Air Pollution Source Apportionment with Receptor Models, put together by Belis et al, in 2014.

3.2.1.1 Concentration matrix

To perform a PMF analysis one needs to indicate as input 2 main matrixes: a concentration matrix and an uncertainty matrix. The concentration matrix is composed by the contribution of each variable (or species measured) in each sample. The uncertainty matrix has to have the exact same dimensions as the concentration matrix and each cell indicates the uncertainty associated with the correspondent concentration.

To build the concentration matrix one first needs to follow the process mentioned above of data validation for every single concentration to include. This process is of extreme importance because it assures the basic quality of the database. Is important to also have into account the amount of available information for each variable, meaning that an assessment has to be done regarding missing values and number of samples below the DL. In this work was defined a limit of a maximum of 33 % of missing values or 50 % of values below the DL (as suggested by Belis et al., 2014). If a variable presents a large number of either missing values or values below the DL this species was excluded from the input matrix. The larger given for variables with values below de DL was given due to the presence of tracers that are expected to have a strong seasonality, with virtually no sources of these species during certain periods of the year.

Another parameter that allows assessing the quality of the input information is the signal-to-noise ratio. The signal-to-noise ratio (S/N) is defined as the power ratio between a desired signal (S, meaningful information) and the background noise (N, unwanted signal) and in

receptor model analysis this can be interpreted as the relationship between concentrations (x) and uncertainties (s) (Paatero et al. 2002; Paatero and Hopke 2003).

$$\left(\frac{S}{N}\right)_j = \sqrt{\frac{\sum_{i=1}^n (x_{ij} - s_{ij})^2}{\sum_{i=1}^n s_{ij}^2}} \quad (\text{Eq. 14})$$

The signal-to-noise ratio is useful for classifying variables according to the information they supply for the source identification analysis. According to Paatero and Hopke (2003), variables with signal-to-noise ratios below 0.2 (bad) were excluded from the analysis, while variables where the ratio falls between 0.2 and 2.0 are suitable for the analysis but selected as weak variables. The remaining variables with S/N above 2 were selected as strong variables.

Finally, a study of the possible presence of outliers is also important before performing a PMF analyses. An outlier is a value that doesn't follow the normal behavior of similar species. These outliers can be hard to spot and deal with because they can be associated either with a real temporary source of this particular species or can be originated from analytical errors or contamination. In this study no such points were observed. Some strong peaks of some variables were seen but also explainable either by similar behavior of a common tracer or a general increase on all variables and PM₁₀ mass concentration.

PM₁₀ mass concentration was selected as “main variable” for all sites and will be used by the program in the post-processing of results. This total variable should not have a large influence on the solution so it should be given a high uncertainty, therefore, when a species is selected as a total variable, its categorization is automatically set to “weak”.

3.2.1.2 Uncertainty matrix

The uncertainty matrix is particularly critical because every entry is weighted according to its uncertainty. EPA PMF 5.0 accepts two types of uncertainty files: observation-based and equation-based. The observation-based uncertainty file provides an estimate of the uncertainty for each species in a sample. It should have the same dimensions as the concentration file and the first column will still be a date, date time or sample number. The equation-based uncertainty file provides species-specific parameters that EPA PMF 5.0 uses to calculate uncertainties for each sample like the method detection limit and relative uncertainty for each species. This work calculated individual uncertainties to each concentration (observation-based matrix) because the equation-based approach will not capture errors associated with

each specific sample. The methodology followed to calculate the uncertainties was explained above.

Finally, to the values below the detection limit that were replaced by DL/2 its uncertainty was increased by a factor of 5/6 as suggested in the EPA PMF5 user guide and in Belis et al, 2014.

3.2.1.3 Selection of the number of factors

The responsibility of identifying the different factors is purely from the user. This choice is made according to the results obtained on the chemical profile of each factor, the quality of the modelled result when compared to the observations, on the scaled residuals, etc.

To identify the different factors the author of this work used mostly an extensive bibliographic research of studies carried out with the same characteristics, such as: sampling time span, tracers used, typology of sites and global region. This method is highly dependent on the experience that the user has on dealing with similar studies and should obviously be supported by other parameters.

More objective parameters that can help to identify the number of factors of a PMF are related with the residuals of the output solution and can be easily calculated. Examples of these alternatives are the Q/Q_{expected} ratio and the IM & IS values.

The Q_{expected} is equal to the number of non-weak data values in X minus the number of elements in the matrixes of the chemical profiles and factor daily contributions, taken together. For example, in the case of the sampling site of Lens we have a total of 167 samples with 27 strong variables on a 9 factor solution, the Q_{expected} is given by $Q_{\text{exp}} = (167 \times 27) - ((9 \times 167) + (9 \times 27)) = 2763$. For each species, the Q/Q_{exp} for a species is the sum of the squares of the scaled residuals for that species, divided by the overall Q_{expected} divided by the number of strong species. For each sample, the Q/Q_{exp} is the sum of the square of the scaled residuals over all species, divided by the number of species. When examining the overall Q/Q_{exp} and according to Paatero and Tapper, 1993, the increase on the number of factors leads to a decrease on the Q/Q_{exp} value tending to 1 and a good method to estimate the ideal number of factors is when this curve suffers an abrupt change in its tendency, meaning a significant decrease in the residuals and therefore a better overall solution. Again taking as an example the exercise made in Lens, the following Q/Q_{exp} values were obtained:

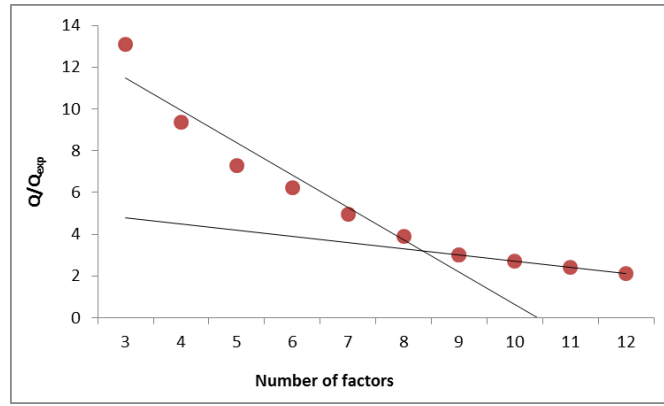


Figure 50: Qtrue/Qexp values for different number of factors in Nogent-sur-Oise

Although there is no evident change in the curve behavior, is seen a difference between the 8 and 9 factor solutions, which may indicate that a 9 factor solution may be the preferred one (figure 50).

Another calculation that can be made using the uncertainty-scaled residuals matrix (r_{ij}) of the obtained solutions to help identifying the optimal number of factors is the calculation of the parameters IM (maximum individual column mean) & IS (maximum individual column standard deviation) and are defined by:

$$IM = \max \left(\frac{1}{n} \sum_{i=1}^n r_{ij} \right) \quad \text{for } j = 1 \dots m \quad (\text{Eq.15})$$

$$IS = \max \left(\sqrt{\frac{1}{n-1} \sum_{i=1}^n (r_{ij} - \bar{r}_j)^2} \right) \quad \text{for } j = 1 \dots m \quad (\text{Eq. 16})$$

In the obtained solutions of Lens the following values were obtained:

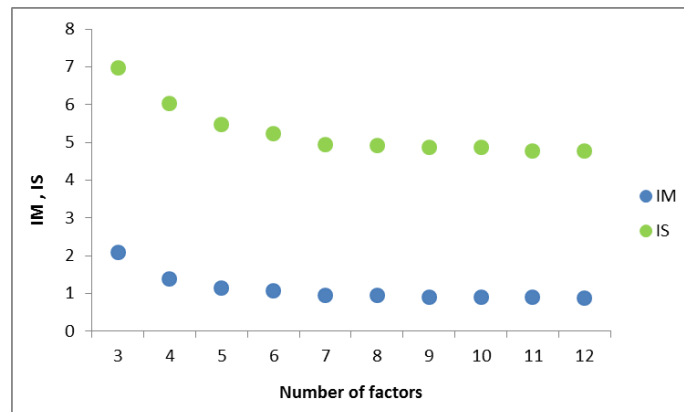


Figure 51: IM and IS values for different number of factors in Nogent-sur-Oise

Again with these parameters one is looking to sudden change on the behavior of both parameters in function of the number of factors, however with this exercise no evident changes are observed, meaning just that a solution with more than 7 factors appears to be a stable one already. This is an important starting point for the author to know what solutions to focus on and the number of factors that need to be identified and given a meaningful label.

To summarize, the Q/Q_{exp} , IM and IS parameters are useful parameters that can be calculated to each PMF solution and give an idea of the ideal number of factors, however once a stable mathematical solution is found, is the authors responsibility to attribute a meaningful source to each factor identified by PMF having into account its chemical profile and time variability supported by bibliographic research.

3.2.2 Source location

All the meteorological parameters used in this work (wind speed, wind direction, pressure, temperature, rainfall, snow episodes and relative humidity) were obtained from https://donneespubliques.meteofrance.fr/?fond=produit&id_produit=111&id_rubrique=37, last consulted on the 11th of October 2016, in this case using the station located in Creil.

To create a concentration field map one needs the backtrajectories of the sampled days. These backtrajectories were obtained using the model Hybrid Single Particle Lagrangian Integrated Trajectory (HYSPPLIT; Draxler and Rolph, 2011). Backtrajectories of 72 hours were calculated for all sites for each day between the 1st of January 2013 and 7th of June 2014 and a total of 8 backtrajectories per day (starting at 00h, 03h, 06h, 09h, 12h, 15h, 18h and 21h) arriving at 500 meters of altitude.

The ZeFir v3.10 software (Igor tool developed by Petit et al. 2017) was used to plot the concentration field maps. This tool requires as input the daily contributions of the pollutant to plot, the associated dates, wind speed and wind direction for each day and the backtrajectories for the period of study (figure 53):

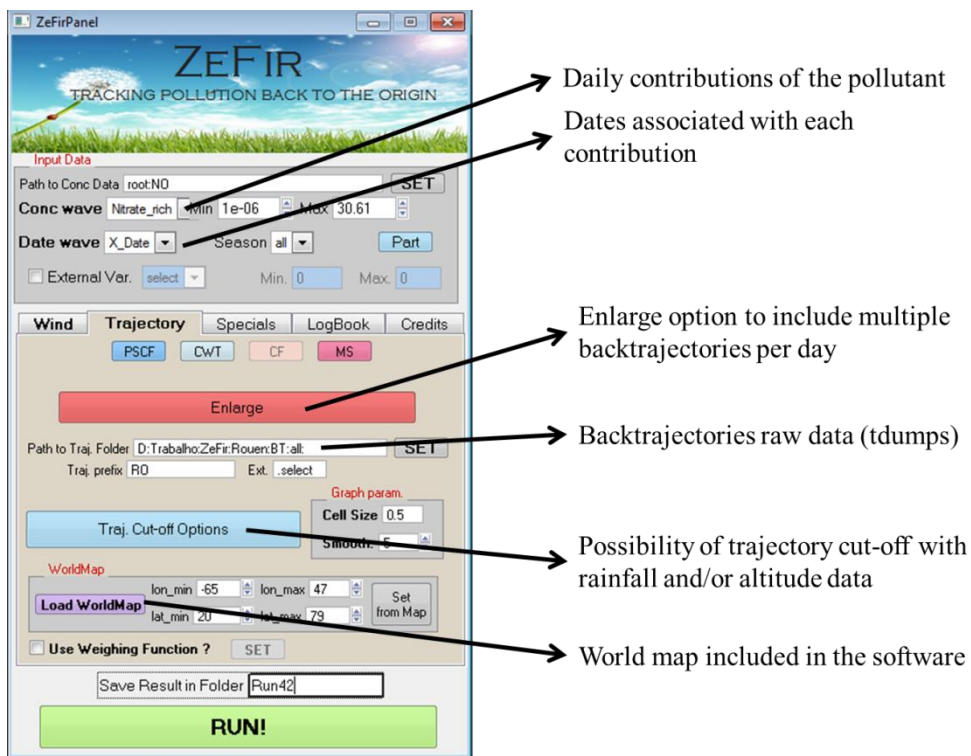
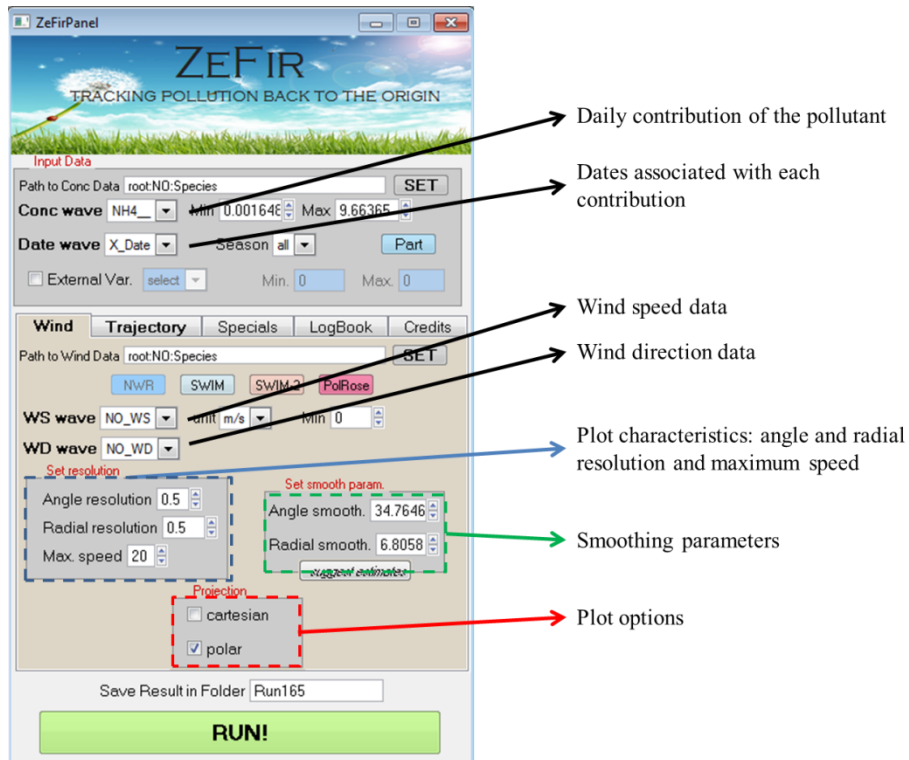


Figure 52: ZEFIR interface for wind (top) and trajectory (bottom) calculations

A powerful solution for more robust results is the multi-site merging of concentration field maps. This allows exploring the bigger picture of source-receptor approaches, by combining several sites all together. This is made very easily within ZeFir. First, where individual calculations for each site need to be performed and saved in specified folders. Then, the user has to fill the “Combine results from Folder” list by the names of all result folders. A final concentration field map is obtained with the probable geographical location of sources. In order to apply the multi-site concentration field method one has first to be assured that the same sources are being associated – regional sources from sampling sites close to each other with insignificant local contributions to the chemical profiles in question. This approach will be addressed in Chapter 4 of this manuscript.

CHAPTER 4

“MULTI-SITE RECEPTOR ORIENTED APPROACH FOR A COMPREHENSIVE SOURCE APPORTIONMENT OF PM₁₀ IN THE NORTH OF FRANCE”

(Publication 2)

CHAPTER 4 - MULTI-SITE RECEPTOR ORIENTED APPROACH FOR A COMPREHENSIVE SOURCE APPORTIONMENT OF PM IN THE NORTH OF FRANCE (PUBLICATION 2)

This Chapter will be based on the 2nd article written during this thesis and addresses the complete chemical analysis done on 5 sites of the north of France, their source apportionment exercise and the geographical location of the identified sources.

4.1 Summary of Publication 2

This publication has as objective to expose a comprehensive study performed on 5 sampling sites spread across the north of France and present what are the main contributors to PM₁₀ mass concentration in terms of chemical composition and source origin impacting the region. To do so, the work is based on samples collected over a period of 18 months on five sampling sites with different typologies (3 urban sites, 1 traffic and 1 remote), to allow a better understanding of the possible sources of PM₁₀, both on a local and regional scale. The total number of samples ranged from 158 in Nogent-sur-Oise up to 169 in Lens, and cover the period from January 2013 to June 2014. A PMF analysis was done on each site individually and the best possible solution was found independently from site to site. The identified sources were then studied regarding their chemical profiles and seasonal behavior and, together with meteorological information of wind speed and wind direction collected at nearby stations, their possible local or regional origin. Regional sources were associated with back-trajectories obtained from HYSPLIT4 for each sampling site and used on the concentration field method it was seen that these regional sources were comparable from site to site, so multi-site concentration fields were calculated as well.

4.1.1 Chemical composition

Higher concentrations of PM₁₀ were seen on the sampling site of Roubaix, the traffic site, (daily average of $28.0 \pm 15.4 \mu\text{g m}^{-3}$) and lower concentrations in the remote site of Revin (daily average of $16.3 \pm 9.7 \mu\text{g m}^{-3}$). Curiously, no major differences were seen from site to site in terms of relative species contribution to PM₁₀ mass, suggesting the existence of similar

impacting sources. Organic matter is the main contributor on all five sites, with average contributions ranging from 38% ($7.2 \pm 6.1 \mu\text{g m}^{-3}$) in Nogent-sur-Oise to 31% ($5.6 \pm 4.6 \mu\text{g m}^{-3}$) in Lens with regard to traffic and urban sites. However, the lowest concentration of organic matter was measured in Revin ($4.1 \pm 2.2 \mu\text{g m}^{-3}$) contributing for 34% of the PM_{10} mass concentration. The major ions (nitrate, sulfate and ammonium) were the following major contributors on all sites as well. Nitrate concentrations ranged from $5.4 \pm 6.3 \mu\text{g m}^{-3}$ in Roubaix (25% of PM_{10}) to $3.3 \pm 4.1 \mu\text{g m}^{-3}$ in Revin (27% of PM_{10}). It is interesting to point out the strong variability of this species, evident by the standard deviation associated with the measured concentrations. Sulfate showed higher contributions in Revin (16%) and lower in Roubaix (11%). Curiously it was in Roubaix where the highest average concentration of sulfate was found ($2.4 \pm 2.7 \mu\text{g m}^{-3}$) and in Revin the lowest ($1.9 \pm 1.8 \mu\text{g m}^{-3}$). Finally, ammonium also showed constant contributions across the sites ranging from 8% in Roubaix, Rouen and Nogent-sur-Oise, to 11% in Lens.

4.1.2 Source apportionment

A source apportionment exercise was performed on the 5 sampling sites following the methodology exposed in Chapter 3 of this work. Different number of factors was found from site to site:

- **Lens (9 factors):** Traffic*, biomass burning, land biogenic, marine biogenic, nitrate rich, sulfate rich, oxalate rich, fresh marine and aged marine
- **Nogent-sur-Oise (9 factors):** Traffic*, biomass burning, land biogenic, marine biogenic, nitrate rich, sulfate rich, oxalate rich, fresh marine and aged marine
- **Revin (10 factors):** Traffic*, crustal, biomass burning, land biogenic, marine biogenic, nitrate rich, sulfate rich, oxalate rich, fresh marine and aged marine
- **Rouen (8 factors):** Traffic*, biomass burning, land biogenic, marine biogenic, nitrate rich, sulfate rich, oxalate rich and fresh marine
- **Roubaix (10 factors):** Traffic, road dust, biomass burning, land biogenic, marine biogenic, nitrate rich, sulfate rich, oxalate rich, fresh marine and aged marine

On all sites, the number of factors identified ranged from 8 (Rouen) to 10 (Revin and Roubaix), and the main differences lied on the ability shown by PMF to identify a crustal

matter factor in Revin, a road dust factor in Roubaix and the absence of an aged marine factor in Rouen.

Concerning the different traffic factors identified, the ones signaled with a ‘*’ were found to have a strong component of various metals in their chemical profile. This indicates that a fraction of the identified factor refers to a contribution of non-exhaust related particles, as shown in Chapter 3. The presence of Ca in factors of the urban sites (Lens, Nogent-sur-Oise and Rouen) indicates also a contribution of crustal/road dust matter. In the sampling site of Revin the traffic factor showed also the presence of metals, however the Ca was found on the crustal matter factor identified in this site, leading to the conclusion that, in this case, the traffic related particles collected are associated with exhaust emissions and break and tire abrasion. In Roubaix, a road dust factor was identified separately from the traffic factor. This factor is composed by a strong contribution of metals as well as some Ca, Fe and Al, however, in this site, the contribution of Ca is not as strong as in Revin, whereas the metals are present in larger significance, leading to believe that this factor, although it may have a crustal influence, is mainly based on road dust resuspension and non-exhaust related particles. The traffic factor identified in this site was mainly composed by EC and OC, with lesser influence of metals, being then associated with exhaust emissions.

Factors labelled the same way were then compared regarding their chemical profile and the observed ratios for the significant tracers. It was assumed that factors known to have regional origins and small discrepancies between sites in terms of their chemical profile would have negligible local inputs, being therefore assumed to be linked with the same source.

4.1.3 **Source location**

The regional factors identified in this study were defined according to their nature: natural or anthropogenic origin. Main natural factors, namely the fresh and aged marine factors and the marine biogenic factor, were seen to be originated in maritime areas. The first two having as source the Atlantic Ocean, where fresh marine aerosols seem to be associated with more distant emissions carried by air masses with higher velocity, and aged marine aerosols were associated with the Atlantic Ocean and North Sea on a more vast area. Marine biogenic aerosols were clearly linked with the North Sea, known for its intense algae blooming during spring and summer seasons.

Anthropogenic related aerosols observed on the 5 sampling sites were associated with continental air masses from Central and Eastern Europe mainly. Both nitrate and sulfate rich factors have these regions highlighted as strong potential sources, with the small particularities already addressed in Chapter 3 and now validated. Nitrate rich particles appear to originate from regions rather close to the sampling sites like the Netherlands and Belgium, whereas sulfate rich particles are rather associated with farther sources, such as Central and Eastern European sources or ship emissions from the Gibraltar Strait caused by the intense maritime traffic seen in this area. Finally, the concentration field maps obtained for the oxalate rich factors on the five sites also highlights remote zones as potential strong source areas of these particles. This is the case for Central and Eastern Europe, as well as regions in the Mediterranean and North Seas. This finding suggests that oxalate-rich particles are probably linked to aged secondary organic aerosols. One may try to deconstruct the CF maps for the oxalate-rich factors into two main influences, assuming that: (i) highlighted areas in Central and Eastern Europe could be mainly related with oxidation of sulfate-containing particles (significantly present in this factor) whereas (ii) the highlighted maritime areas could be linked with sources of organic precursors of oxalate like marine biogenic emissions and maritime traffic (North Sea) or associated with high concentrations of ozone (Mediterranean Sea), an oxidation agent of VOCs.

**MULTI-SITE RECEPTOR-ORIENTED APPROACH FOR A COMPREHENSIVE SOURCE
APPORTIONMENT OF PM₁₀ IN THE NORTH OF FRANCE**

Diogo M. Barros de Oliveira^{1,2,3}, Esperanza Perdrix^{1,3} *, Olivier Favez², Stéphane Sauvage^{1,3},
Laurent Y. Alleman^{1,3}, N. Bonnaire⁴, E. Chrétien⁵, T. Delaunay⁶, S. Lemeur⁷, B. Rocq⁸,
Véronique Riffault^{1,3}

¹ Mines Douai, SAGE, F-59508 Douai, France

² INERIS, F-60550 Verneuil-en-Halatte, France

³ Univ. Lille, F-59000 Lille, France

⁴ LSCE, F-91198 Gif-sur-Yvette, France

⁵ Atmo Champagne-Ardenne, F-51100 Reims, France

⁶ Atmo Nord-Pas de Calais, F-59800 Lille, France

⁷ Air Normand, F-76000 Rouen, France

⁸ Atmo Picardie, F-80332 Longueau, France

* Corresponding author: Esperanza Perdrix (esperanza.perdrix@mines-douai.fr)

Abstract

A PM source apportionment study was carried out using EPA PMF5 on the PM₁₀ chemical composition measured at five different sampling sites (3 urban, 1 traffic and 1 remote) located in the north of France. Between 8 and 10 main sources of PM₁₀ could be identified and quantified at each site. Local sources such as traffic and biomass burning emissions showed to be strong contributors to PM₁₀, with traffic being the main local source at 3 out of the 5 sites. Secondary inorganic aerosols deconvoluted as nitrate-rich and sulfate-rich factors were found as the main regional sources, with combined contributions ranging from 20 % at the remote site (Revin) up to 38 % at one of the urban sites (Lens). A multi-site approach was adopted for the Concentration Field method combining backtrajectories obtained from the HYSPLIT model with daily contributions of the different identified sources. It allowed for a robust estimation of the probable geographical location of each regional source as well as differentiating the origins of natural and anthropogenic particles. Natural sources like fresh sea salt and marine biogenic secondary aerosols were traced back to the far Atlantic Ocean and the North Sea, respectively. Secondary inorganic aerosols, strongly related with anthropogenic activities were found to originate mainly from Central and Eastern Europe in consistency with the European emission inventory from EMEP. Nitrate-rich aerosols were also associated with countries like Belgium and the Netherlands, probably related with intense agricultural activities whereas the Strait of Gibraltar was identified as a source of sulfate-rich aerosols, probably related with the high volume of maritime traffic in this region.

Keywords: PM₁₀, PM chemical composition, source apportionment, PMF, Receptor oriented method, Concentration fields, multi-site approach,

INTRODUCTION

Particulate matter (PM) is a mixture of solid or liquid particles suspended in air. PM, also commonly referred as “aerosols”, impacts the economy, health and environment on a global scale. Many of the effects on human health remain unknown. However, epidemiological studies have revealed a strong correlation between mortality and chronic exposure to high concentrations of PM₁₀ or PM_{2.5}, the mortality being due to bronchial, heart disease or cancer (Analitis et al. 2006; Pope III and Dockery 2006).

An extensive knowledge on the nature of PM sources is then needed to effectively tackle air quality issues, which requires a detailed chemical characterization of PM₁₀. Primary aerosols are directly released as particles in the atmosphere. On the other hand, secondary aerosols are formed by gas-to-particle conversion processes from semi-volatile gaseous species or precursor gases through physical or chemical processes. Concerning sources of particles or their gaseous precursors, two main origins can be distinguished in the atmosphere: natural and anthropogenic sources.

The sources of PM at a given sampling site, based on its chemical characterization and temporal contributions, can be assessed through statistical methods to estimate the probable sources of these aerosols (Watson 1984). Commonly referred to as receptor-based methods, these tools compute temporal contributions into factors, which can be read as sources. The choice of these methods depends on several criteria such as time resolution, database quality, prior knowledge of impacting sources, etc. (Viana et al. 2008). Positive Matrix Factorization (PMF) is a multivariate factor analysis tool that decomposes a matrix of sampled concentrations into two matrices: factor contributions and factor profiles. These factor profiles need to be interpreted and can then be linked with possible sources of PM (Paatero and Tapper 1994; Paatero 1997). PMF results are constrained to provide positive source contributions and the uncertainty weighted difference between the observed and predicted species concentration is minimized (Anttila et al. 1995). The contributions of these sources can then be associated with other parameters like gaseous emissions or meteorological information to better understand and to validate the results obtained.

In France an estimated 42 000 premature deaths per year occur due to air pollution exposure and the region of the north of France is known for often exceeding the daily limit value of 50 µg/m³ on PM₁₀ mass concentration. In 2015 this limit was exceeded more than 35 days in 6 urban areas of the region (LCSQA, 2016), impacting about 90% of its population . Primary

sources of PM₁₀ such as industry, dense urban areas, traffic and agriculture, along with particle long-range transport (enhanced here in a context of rather flat topography), have proven to be the main sources of high concentration episodes in the city of Lens (Waked et al. 2014).

Given the complexity and multitude of possible sources, to estimate their geographical origin can provide crucial knowledge on how to better tackle this issue. Several authors have used backward trajectory analysis to help detecting the long-range transport of pollutant air masses that may have an impact on local PM₁₀ levels (Salvador et al. 2008), to better describe the related tropospheric circulations (Jorba et al. 2004) or to characterize and identify spatial and temporal trends of pollutants (Coury and Dillner 2007). However, single backward trajectories, generally applied to detect source areas of short episodes of extreme PM concentrations impacting given sites (Hongisto and Sofiev 2004), are not suitable for an overall identification of paths and origins of air parcels over a longer period of time. To this latter purpose, rather large numbers of trajectories arriving at a given site have to be analyzed. Several authors performed statistical cluster analyses in order to group trajectories into main pathways (Dorling, Davies, and Pierce 1992; Dorling and Davies 1995). Such procedures have been frequently used to interpret the origin and the transport of atmospheric pollution (Vardoulakis and Kassomenos 2008). However the lack of information on the chemical composition of PM hinders identifying both the nature and the location of emitting sources.

Having therefore available chemical information on species' concentrations and on the contributions of the different sources impacting a given receptor site, one can compute the air mass back-trajectories arriving at this site during the sampled period to assess the geographical origin of given chemical species and sources influencing this specific point in space. These models are commonly referred to as Hybrid Receptor Models (Han, Holsen, and Hopke 2007) or Trajectory Statistical Methods (TSMs) (Kabashnikov et al. 2011). There are several variations of TSMs that have been applied to characterize atmospheric PM: Potential Source Contribution Function (PSCF) (Bessagnet et al. 2005; Han, Holsen, and Hopke 2007; Abbott et al. 2008; Choi, Choi, and Yi 2011; Xu and Akhtar 2010; X. Fu et al. 2011), Gridded Frequency Distributions (GFD) (Weiss-Penzias, Gustin, and Lyman 2011; Sexauer Gustin, Weiss-Penzias, and Peterson 2012), Concentration Field (CF) analyses (Seibert et al. 1994; Rutter et al. 2009), Concentration-Weighted Trajectory (CWT) (Stohl et al. 1995), and Residence Time-Weighted Concentration (RTWC) (Han, Holsen, and Hopke 2007).

The main difference between methods has to do with how concentrations are incorporated in the trajectory and the frequencies in each grid cell. Charron et al. (1998) showed that CF is a suitable methodology to identify potential source areas and provides computed data which could be used to examine their quantitative relationships with the measured concentrations. A previous work from our group has also shown the usefulness of this method to allocate sources impacting an urban site in the north of France (Oliveira et al., submitted).

This work follows the methodology exposed in Oliveira et al. (submitted), extending it to a larger and unique database of five sites with different typologies (3 urban, 1 traffic and 1 remote) spread across the north of France. PM₁₀ samples were collected over an 18-month period and daily contributions of sources were computed from measured species using Positive Matrix Factorization, for a comprehensive source apportionment study at each site taken individually. After identification of the local and regional sources at impacting each site, we combined these results with the CF model to assess the geographical origins of both natural and anthropogenic regional sources.

METHODOLOGY

Sites, sampling and chemical analysis

The chosen sampling sites (figure P2.1 and table P2.1) are of different typologies and spread across the north of France, allowing not only a wide coverage of the region, but also a study of the influence of different or common sources at each site, enabling to assess the impact of local versus regional sources.



Figure P2. 1: Map of the sampling sites. Typologies: remote (green), traffic (grey), urban (orange)

Table P2. 1: Specifications of the five sampling sites

Typology	Location	Coordinates	Population (inhab. in the area)	Reference
Urban	Lens	50°26'12.6"N 2°49'36.7"E	~543,000	Waked et al. (2014)
Urban	Nogent-sur-Oise	49°16'35.0"N 2°28'56.0"E	~117,000	Oliveira et al. (submitted)
Urban	Rouen	49°25'41.4"N 1°03'29.1"E	~650,000	-
Traffic	Roubaix	50°42'23.6"N 3°10'50.5"E	~1.1 million	-
Remote	Revin ^a	49°55'00.0"N 4°38'29.0"E	~8,000	Sicard et al. (2007); Pascaud et al. (2016)

^a part of the French EMEP monitoring network (FR09)

Daily samples of PM₁₀ were collected by filtration using a sequential HVS (Digitel DA80) operating at 30 m³/h. Pre-fired 150 mm diameter Pall TissuQuartz filters were used (100% quartz filters) and samples were selected every three days. All samples correspond to a 24-hour collection period, from midnight to midnight, except for Revin and Nogent-sur-Oise where filters were collected from 9 am to 9 am. PM₁₀ mass concentrations were simultaneously measured using automatic microbalances (TEOM-FDMS, Thermo Scientific) at all sites, except in Lens where a beta gauge (MP101M-RST, Environnement S.A.) was used instead. The dataset used in this study covers the period from January 2013 to June 2014. The analysis of the chemical composition of the PM₁₀ samples was carried out using the same technical protocols for the 5 sites. More information on the chemical analysis can be found in Oliveira et al. (submitted), but a summary is given in table P2.2.

Table P2. 2: Summary of the species measured and methods used

	Method	Reference
Major elements	ICP-AES	Alleman et al. (2010)
Trace elements	ICP-MS	Alleman et al. (2010)
Soluble ions	Ion chromatography	Sciare et al. (2008)
EC/OC	Thermal and optical transmission (TOT)	Birch and Cary (1996)
Monosaccharides, sugar anhydrides and sugar alcohols	HPAEC (IC-PAD)	Iinuma et al. (2009)

To check the consistency of the different chemical results with the total mass of PM₁₀, the PM₁₀ reconstructed mass was calculated according to the method described in Waked et al. (2014). This mass closure method was chosen due to the similarities between the studies – similar measured species, typology of sites, geographical location (north of France) and collection period. A conversion factor of OC to OM is needed and is dependent on the typology of each sampling site. Table 3 shows the conversion factor chosen for each site and the percentage of total PM₁₀ mass not explained by the mass reconstruction method used. These percentages of unexplained mass range from 0 to 20%. The highest percentage was obtained for Rouen, the site closest to the sea, where elevated relative humidity is observed.

In fact, the mass of water adsorbed by the particles is not taken into account in the mass closure calculation.

Table P2. 3: OM/OC ratio and unaccounted masses for each sampling site

	Lens	Nogent-sur-Oise	Revin	Rouen	Roubaix
OM/OC ratio	1.75	1.75	1.9	1.75	1.6
Unaccounted mass	0 %	15 %	10 %	20 %	5 %

The value of 1.75 was selected for the urban sites because, having in consideration a previous study in the region, a significant contribution of biomass burning is expected (Waked et al., 2014). As shown by the null unaccounted mass, this value corresponds perfectly to the case of Lens. However the same value seems slightly underestimated for the two other urban sites (Nogent-sur-Oise and Rouen), as unaccounted masses are higher (respectively 15% and 10%). Noteworthy, the automatic device used in Lens for the PM₁₀ mass determination is different from the ones used in the other sites. The apparently better adequation of the multiplying factor for Lens could therefore be due theoretically to an underestimation of the total PM₁₀ mass concentration. The traffic site followed the recommendation of Turpin and Lim (2001) for the value of 1.6, which gave a good adequacy. Whereas to the remote site, being surrounded by forests, was given a higher ratio of 1.9 to reflect a higher degree of oxidation of OM (due to the likely formation of SOA from biogenic VOCs).

Source apportionment using Positive Matrix Factorization (PMF)

The PMF model was applied in this study to identify and quantify sources of PM₁₀ at each individual site (Paatero and Tapper 1994). This model is based on the mass balance equation and uses a least-square algorithm to solve the matrix equation:

$$x_{ij} = \sum_{k=1}^p g_{ik} \times f_{kj} + e_{ij} \quad [1]$$

where x_{ij} is the measured concentration of the j^{th} species in the i^{th} sample, g_{ik} is the contribution of the k^{th} source to the i^{th} sample and f_{kj} is the concentration of the j^{th} species in

the k^{th} source, e_{ij} is the residual for each sample/species. G and F will then be the matrices of factor contributions and factor chemical profiles, respectively.

Uncertainties were calculated following the procedure described in Oliveira et al. (submitted) and also used by Waked et al. (2014). Expanded uncertainties of 10 % for OC (Lim et al. 2003), 15 % for EC (Schmid et al. 2001; Cavalli et al. 2010) and 15 % for monosaccharide sugars and derivatives such as levoglucosan, mannosan, galactosan, arabitol, and mannitol (Piot et al. 2012; Iinuma et al. 2009) were selected. Metal uncertainties were calculated as in Alleman et al. (2010) and were based on the following expression:

$$u_{rel}(C) = \sqrt{u_{rel}^2(Ac) + u_{rel}^2(V) + u_{rel}^2(Rep) + u_{rel}^2(Cont)} \quad [2]$$

where $u_{rel}(Ac)$ is referred to the relative uncertainty linked with the method's accuracy, $u_{rel}(V)$ with the volume sampled, $u_{rel}(Rep)$ with the repeatability of the analysis and $u_{rel}(Cont)$ with possible contaminations. This detailed calculation was possible for the elements analysed in Mines Douai.

Calculations were performed with the EPA PMF5 (version 5.0.12.13261). The optimization of the final solution for each site followed the guidelines suggested in the European Guide on Air Pollution Source Apportionment with Receptor Models (Belis et al., 2014). Particularly, the optimized PMF solution for each site was sought according to parameters characteristic of each individual solution, particularly the evolution of the Q/Q_{exp} ratio with the number of factors, the bootstrap, f_{peak} and DISP analyses. It is important to mention that all the individual solutions were selected as being the best mathematical fit and chemical description of sources for one site, meaning that a result on a given site did not influence the solution found on the remaining ones. Although EPA PMF5 software enables solving the mass balance equation simultaneously for the 5 sites, a site-by-site individual procedure was preferred because the number of impacting factors is not necessarily the same for the 5 sites.

Geographical location of nearby sources using the Non-parametric Wind Regression (NWR) and distant sources using the Concentration Field (CF) model

NWR is a smoothing algorithm (Eq. 3) allowing a meaningful representation of the relationship between wind (direction and speed) and concentration measurements at a given

sampling site. It determines with accuracy the wind directions related to high concentrations and estimates roughly the distance from the sampling site to the sources (close, or more distant)(Henry, Chang, and Spiegelman 2002). In fact air masses carrying pollutants from far away sources to the sampling site will not follow straight paths, but rather curved ones following synoptic atmospheric conditions. A direction may indeed correspond correctly to a nearby located source but erroneously to a remote one. NWR is therefore recommended to locate nearby sources. We used the NWR procedure of the IGOR package ZeFir v3.201 (Petit et al. 2017). For a given angle (θ) and a given velocity (v), the obtained average concentration is given by:

$$\overline{C(\theta, \vartheta)} = \frac{\sum_i K_1\left(\frac{\theta - wd_i}{\sigma}\right) \cdot K_2\left(\frac{\vartheta - ws_i}{h}\right) \cdot C_i}{\sum_i K_1\left(\frac{\theta - wd_i}{\sigma}\right) \cdot K_2\left(\frac{\vartheta - ws_i}{h}\right)} \quad [3]$$

where K_1 and K_2 are the Kernel smoothing functions for wind direction and wind speed respectively, C_i is the concentration observed in sample i , wd_i and ws_i are respectively the wind direction and speed associated to sample i , and σ and h are the smoothing parameters.

In this work, NWR was applied to locate possible nearby sources related to PMF chemical profiles. Daily contributions of the PMF factors were associated with wind speed and wind direction information obtained from the MétéoFrance nearest stations, with the chosen parameters shown in table P2.4.

Table P2. 4: NWR parameters

Max wind speed	Angle resolution	Radius resolution	Angle smoothing	Radius smoothing
20 m s ⁻¹	0.5°	0.5 m s ⁻¹	35° *	7 m s ⁻¹ *

* Suggested parameters

In a complementary way, the CF method developed by Seibert et al. (1996) was used to estimate the probable geographical location of regional sources, identified across the five sampling sites. CF allows calculating the residence-time averaged concentration C_{ij} measured at the receptor site when air masses backtrajectories pass over a given area, namely a given spatial gridcell (i,j) (Eq. 4). The set of CF output concentrations (C_{ij}) can then be used to map the probable location of air masses.

$$C_{ij} = \frac{1}{\sum_{l=1}^N \tau_{ijl}} \sum_{l=1}^N \log(c_l) \tau_{ijl} \quad [4]$$

where ij are the indices of a grid cell, l the index of a trajectory, N the total number of trajectories, c_l the concentration observed at the receptor site on the arrival of a given trajectory l , and τ_{ijl} the residence time of the air mass trajectory l on a grid cell (i,j) . A minimum of 10 points per grid cell was imposed to calculate the average concentration to ensure the statistical robustness of the final results.

To apply the CF model for locating distant sources, kinematic back-trajectories were calculated with the Hybrid Single-Particle Lagrangian Integrated Trajectory model (HYSPLIT), developed by the National Oceanic and Atmospheric Administration (NOAA)'s Air Resources Laboratory (ARL) (Stein et al. 2015; Draxler 1999; Draxler and Hess 1998; McQueen et al. 1997)), based on GDAS (Global Data Assimilation System) meteorological data (source: <ftp://arlftp.arlhq.noaa.gov/pub/archives/gdas1>). A total of ~6000 back-trajectories were used for the 5 sites with eight 72-hour back-trajectories per sampled day, arriving at an altitude of 500 m above ground level, as suggested by Su et al. (2015). The 72-hour duration was selected in order to satisfactorily represent the transport of PM_{10} at the synoptic scale, avoiding excessive uncertainties in the computed endpoints of the trajectories and also avoiding misrepresentations linked to a higher deposition rate of PM_{10} for longer transport from the farthest source areas. The 500-m final altitude was chosen by taking into account the common range for the height of the planetary boundary layer (PBL), which is highly variable in space and time but can extend from hundred meters to a few kilometers (Stull 1988). In Paris, Dupont et al. (1999) found a range between 0.2 to 2 km in spring. In fact to correctly represent air masses likely to influence surface sampling sites, only backtrajectories staying below the top of the PBL should be considered. The fixed 500-m terminal altitude is a compromise, believed to adequately capture pollutant transport (Hondula et al. 2010), despite of probably being above the PBL during nighttime or at coastal locations where the marine boundary layer extension is lesser.

Using the multi-site option in ZeFir v3.201 (Petit et al. 2017) allows performing the CF model combining all the back trajectories arriving to the 5 sampling sites. Further refinement of the solution can be done by including constraints into the model, such as backtrajectory cut-offs due to rainfall and excessive altitude. The reduction of particles concentration by wash-out is a key process leading to the removal of particulate pollutants in the atmosphere, whose effectiveness depends notably on the intensity of rainfall. Chin et al. (2014) showed that

episodes with light rainfall (< 1 mm/h) only led to a small reduction in PM_{10} concentrations while a significant depletion was observed for more intense precipitation (≥ 1 mm/h). Similarly, Castro et al. (2010) did not observe a reduction in PM_{10} concentrations for very light rainfall (< 0.6 mm/h) while a rapid and significant reduction was observed during intense rainfall (> 3.2 mm/h). Therefore if an air parcel carrying particulate pollution is submitted to a rain event of sufficient intensity, its particulate loading will be significantly reduced. Besides, the altitude of an air mass is a crucial factor to take into account, in order to correctly associate PM concentrations essentially present within the PBL,. Otherwise if backtrajectory endpoints higher than the PBL (i.e. in the free troposphere) are taken into account by the model, there is a risk to incriminate wrongly potential source areas that are unable to effectively impact the air parcels. A 10-year study carried out in Germany between 2000 and 2009 by Von Engeln and Teixeira (2013), at latitudes similar to the north of France, measured the PBL height at noon, i.e. the maximum PBL height . Monthly averages of these maximum values were calculated, with higher altitudes found during warmer months, as expected due to the increased thermal turbulence, and an overall maximum PBL height of about 2km was found. Finally, based on these previous studies, CF constraints based on maximum thresholds of 1 mm/h for precipitation and 2000 m for air mass altitude were defined. Therefore if a given trajectory endpoint is submitted to a rainfall intensity superior than 1mm/h or if the altitude of this endpoint exceeds 2000 m, then the backtrajectory is cut-off so that the whole trajectory segment preceding the impacted endpoint will not be considered in the model. No major difference was found on the final maps, but this constraining increased their robustness by keeping only the most meaningful data.

RESULTS AND DISCUSSION

Previous studies conducted in the north of France, namely in Lens (Waked et al., 2014) and in Nogent-sur-Oise (Oliveira et al., submitted), were used as bibliographic support for the identification of the different factors on the study sites, due to their similarities in terms of time span of the study, analytical and data-treatment methodologies, database and tracers used, typology and geographical location of the sites. Eight to ten factor solutions were identified on the 5 sites: primary traffic, road dust, biomass burning, oxalate-rich, nitrate-rich, sulfate-rich, land biogenic, marine biogenic, fresh marine and aged marine sources. The average contributions of these sources are presented in figure P2.2.

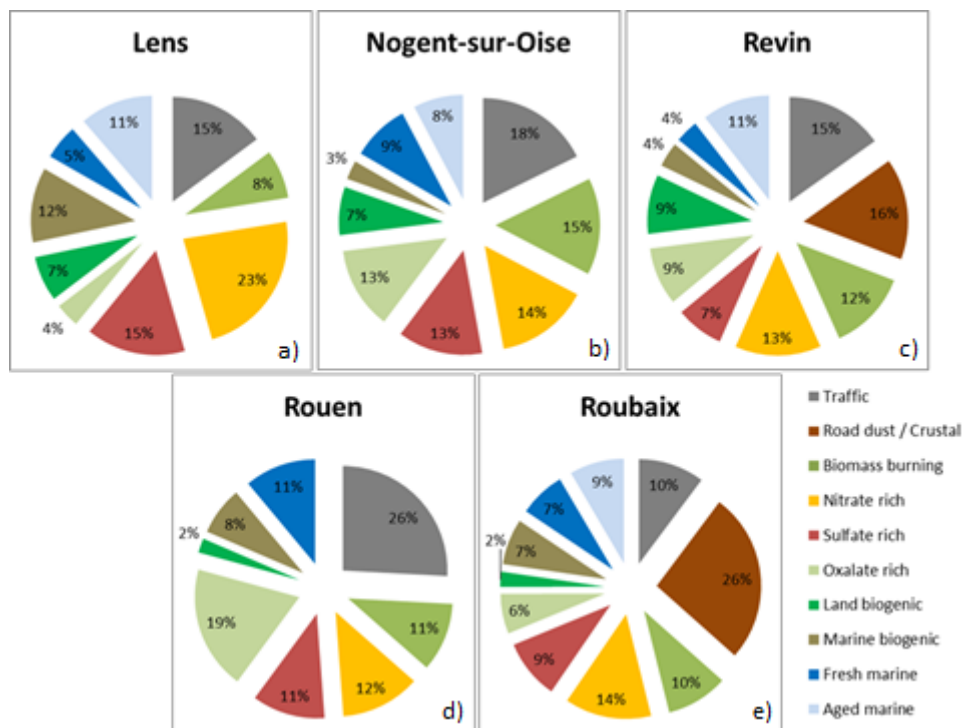


Figure P2. 2: Average contributions of identified factors in a) Lens, b) Nogent-sur-Oise, c) Revin, d) Rouen and e) Roubaix

The chemical profile of the traffic factor varies significantly from site to site (not shown), being mainly constituted by elemental carbon (EC), organic carbon (OC) and metals, with the exception of Roubaix – the traffic site – where a much “cleaner” traffic profile was found with a significant less contribution of crustal metal species. This indicates that the profile identified in Roubaix is less related with road dust resuspension than for the other sites. Contributions of EC and OC for the traffic factor were significant, ranging from 32 % of total EC seen for Revin to 61 % seen for Rouen and from 7 % of the total OC seen in Nogent-sur-Oise up to 32 % in Rouen. Significant contributions of Ca and Al for Nogent-sur-Oise, Lens and Rouen suggest that their respective traffic factors also include a part of resuspended road dust and crustal matter. In the case of Revin (remote site), the large metal contribution seen in the traffic factor is just associated with resuspended road dust since a specific crustal factor composed mainly of Ca and Al was seen in this site. For the sites with large contributions of metals in their traffic factor, these can also be associated with non-exhaust emissions from traffic activity, related with tire and brake abrasion (Johansson, Norman, and Burman 2009; Amato et al. 2011).

A separate road dust / crustal factor was identified just in two of the five studied sampling sites, and with different characteristics between both chemical profiles observed. The

contribution of this factor in Roubaix was of 26 % for total PM₁₀ mass making it the main contributor and 16% in Revin.

In Roubaix the profile appears to include not only a crustal contribution traced by important contributions of Ca, Al and Ti, but also significant contributions of most of other metals analyzed like Fe, Cd, La, Cu or Zn. These are common tracers for break and tire abrasion (Johansson et al., 2009; Amato et al., 2011), also known as non-exhaust traffic emissions.

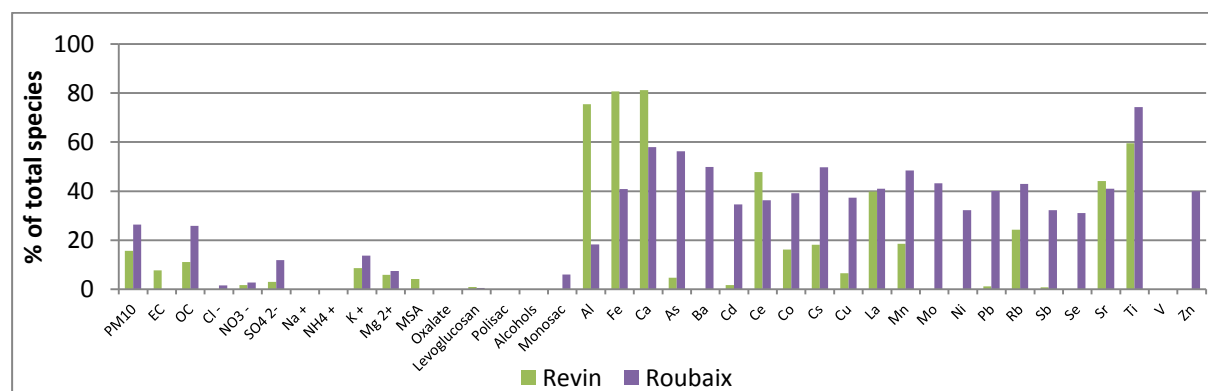


Figure P2.3: Chemical profiles of the factors road dust and crustal matter in Roubaix and Revin, respectively

As seen in figure P2.3, for Revin the factor is characterized by significant contributions of Ca, Fe, Al and Ti but relatively low contributions of other metals when compared to the profile found in Roubaix. The mentioned species are common tracers for crustal matter and, together with the fact that Revin is considered a remote site with less impact from anthropogenic sources such as traffic, the profile identified here is mainly constituted by crustal particles.

Biomass burning was seen on all sites well traced by levoglucosan (83 % to 89 % of total species seen in this factor on the five sites) and the polysaccharides analyzed in this study, mannosan and galactosan (81 % to 83 % of total species seen in this factor across the five sites). The chemical profiles of this factor were found to be quite similar for the 5 sites and with contributions to PM₁₀ mass ranging from 8% in Lens up to 15% in Nogent-sur-Oise.

Sugar alcohols (measured in all sites) and monosaccharides (measured in Lens, Roubaix and Rouen) are tracers for land biogenic particles, which were identified on all sites with the constant presence of the main tracers (83 to 88 % of the total sugar alcohols on each factor across the sites) and also a constant contribution of OC (5 % to 12 % of total species) as expected for biogenic particles. The measured polyols used in this study were mannitol and

arabitol, both reported in the literature as common primary land biogenic emissions tracers (Caseiro et al. 2007; Elbert et al. 2007; Jia, Clements, and Fraser 2010; Karl Espen Yttri et al. 2011), especially as markers for fungal spores related particles (H. Bauer et al. 2008).

The marine biogenic secondary aerosols collected on the 5 sites are traced by measuring MSA. According to current understanding, after being emitted into the marine boundary layer, DMS is oxidized mainly by hydroxyl radicals, resulting in a variety of products such as dimethylsulfoxide (DMSO), dimethylsulfone (DMSO₂), and especially methanesulfonic acid (MSA) and sulphuric acid which can be expected to partition into the particle phase (von Glasow and Crutzen 2003). This factor accommodates 74 % up to 83 % of the total MSA as well as 6 to 15% of the total sulfate, as expected from the chemistry involved.

Fresh marine particles are also a common source seen in SA studies worldwide and are traced by measuring sodium, chloride and magnesium. In this study marine particles were found on all the 5 sites, with different contributions of the main tracers in the chemical profiles. This discrepancy (42 % to 74 % of total sodium, 82 % to 85 % of total chloride, and 38 % to 69 % of total magnesium) found on the % of total species is probably linked to the fact that in Rouen (the site closest to the sea) an aged marine factor was not found, so that Na and Mg just have as main source fresh marine aerosols.

Aged marine factor is characterized by the presence of sodium and magnesium with no chloride at all, as reported in several studies (Beuck et al. 2011; M. Dall'Osto et al. 2009). The chemical profile of this factor in the sites of Lens, Nogent-sur-Oise, Revin and Roubaix was found to be the source of 40 % to 46 % for sodium and 40 % to 54 % for magnesium. Some metals are also seen in the chemical profiles of the aged marine factors identified, suggesting possible anthropogenic inputs in this particles during long-range transport from the sea to the sampling site.

Another main source identified in all 5 sites was the nitrate rich factor, characterized by strong presences of nitrate and ammonium; this is a commonly reported secondary aerosol factor across Europe as shown in Viana et al (2008). With contributions ranging from 12 to 14 % for total PM₁₀ mass in four of the five sites (Nogent-sur-Oise, Revin, Rouen and Roubaix). These results are within the range of similar studies carried out in the north of Europe. In the case of Lens, a higher contribution of this factor was seen, with 23 % of the total PM₁₀. This difference can be explained by looking at the chemical profile of the nitrate rich factor where also sulfate appears (21 % of the total sulfate). This is commonly seen in SA

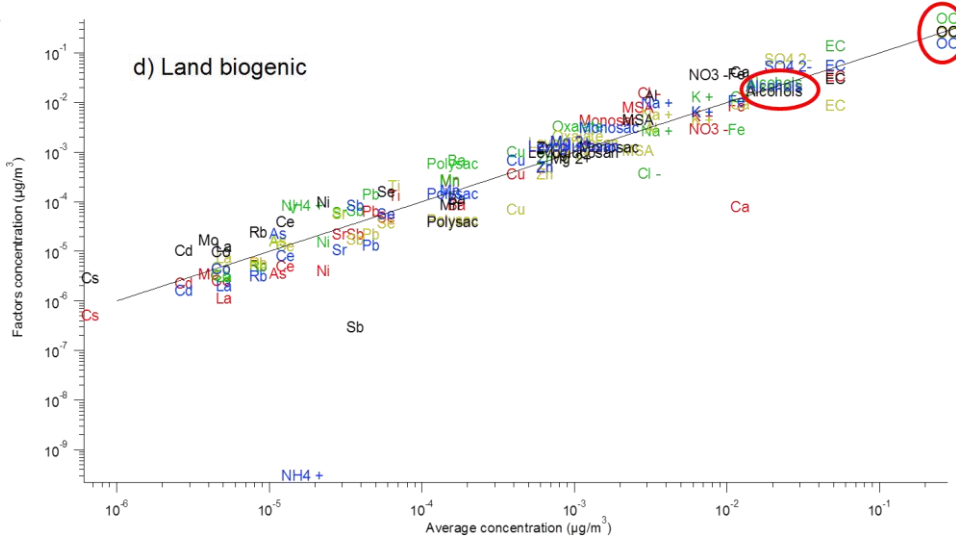
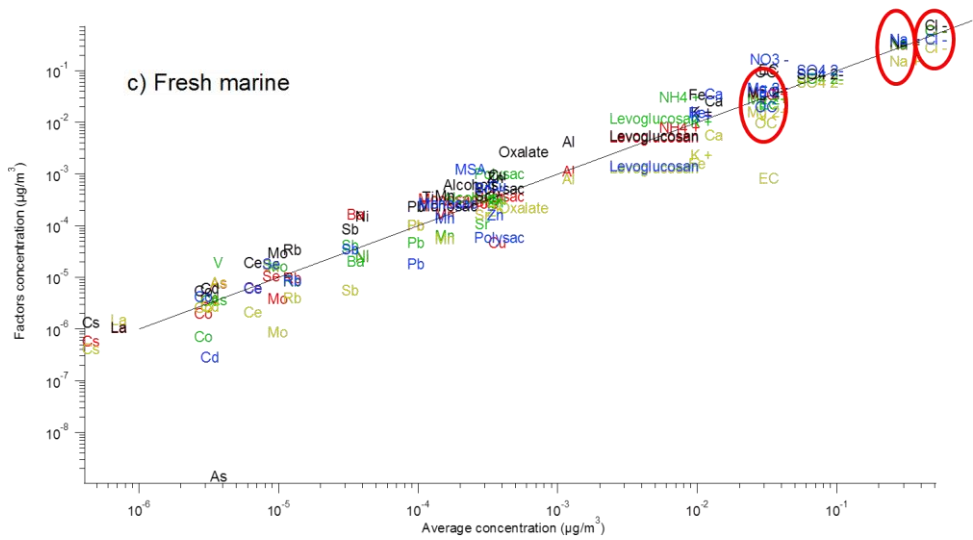
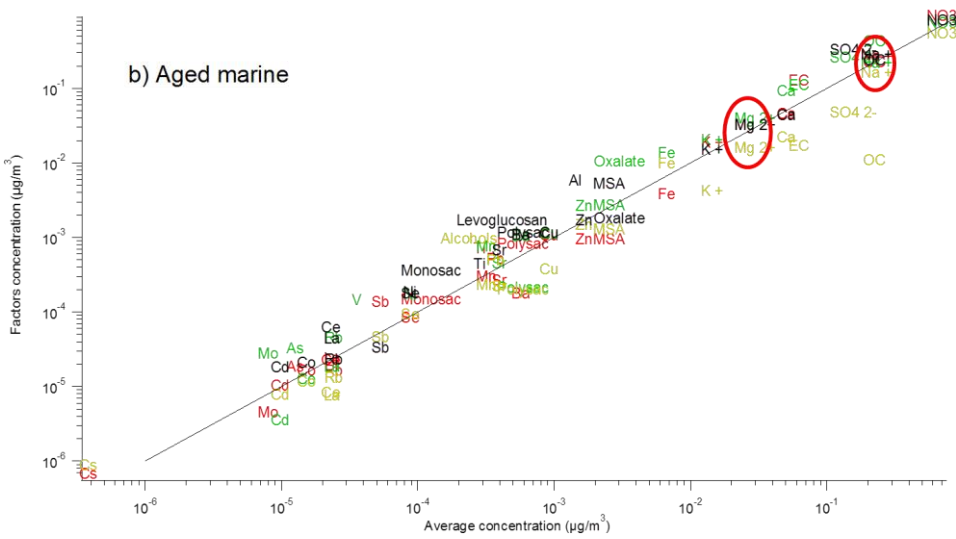
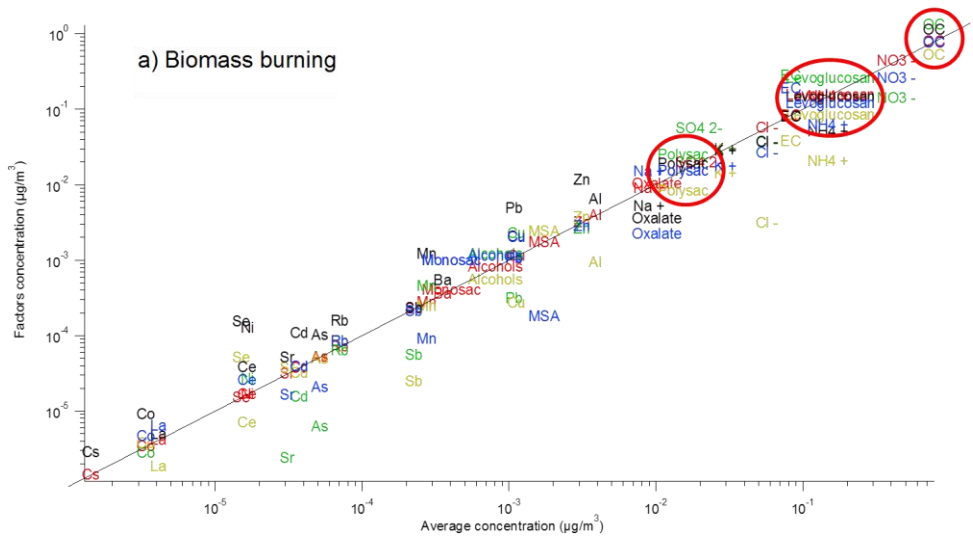
studies, sometimes labeled as a Secondary Inorganic Aerosols (SIA) factor. However, because the ratios seen for nitrate and ammonium are similar to the factors identified in the other sites and also because a sulfate rich factor was found in Lens, the authors of this work made the decision of still labeling this factor as a nitrate rich one.

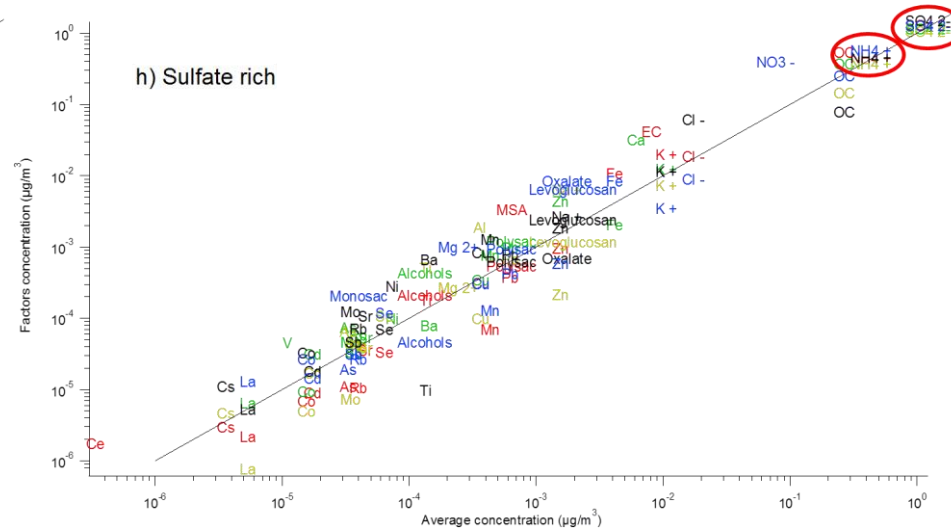
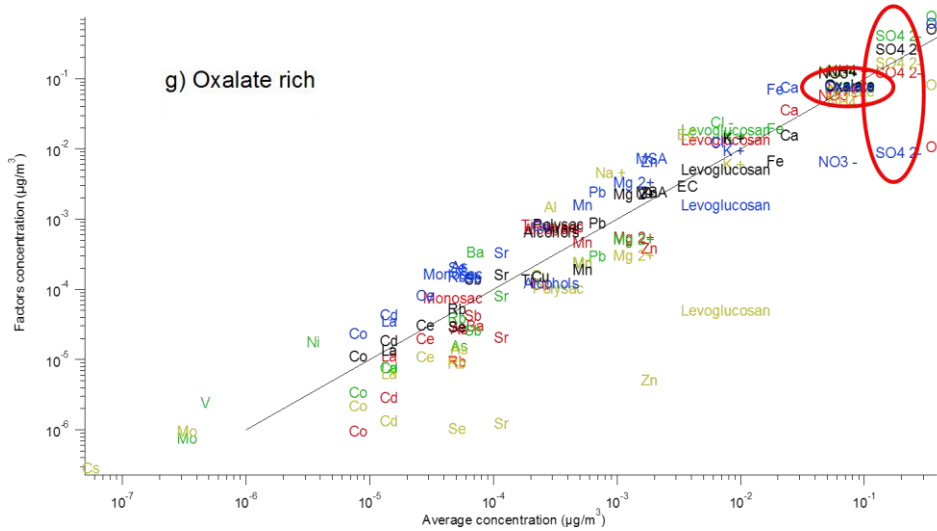
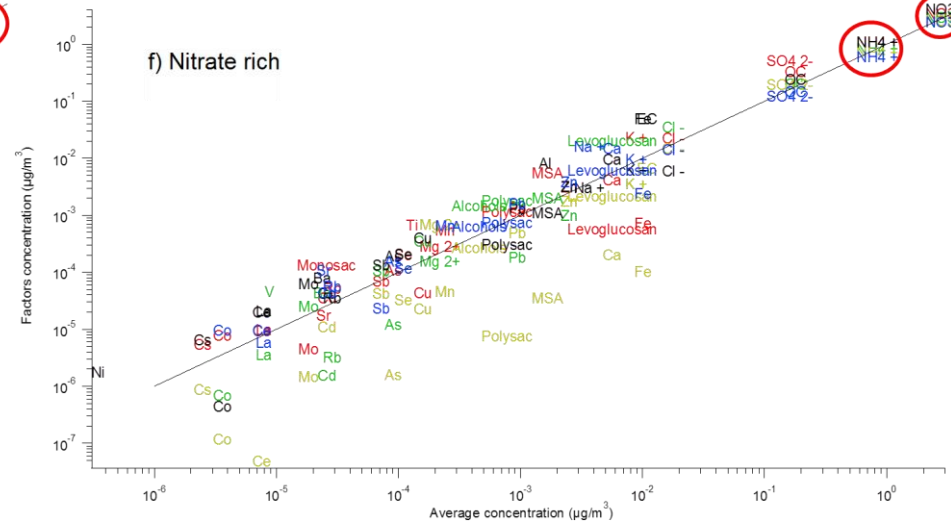
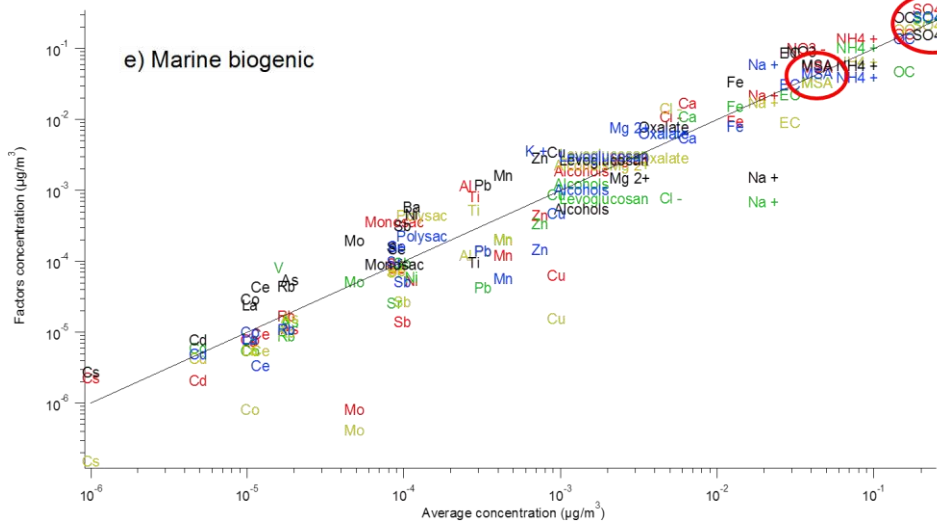
The sulfate rich factor, also a common source of particles found in SA studies, is characterized by a strong presence of sulfate and ammonium (50 % to 57 % of total sulfate found in this factor). The contributions of this factor on the five sites range from 7 % in Revin up to 15 % in Lens. A small presence of nitrate is also seen in the chemical profile for Rouen (12 % of the total nitrate) again showing that these kind of particles are easily accommodated in the same factor. This can happen due to several reasons like same time variability (regional factor) leading PMF to assume a correlation between the species and the same sources of ammonium. Variable contributions of several metals are associated to these chemical profiles for the five sites, emphasizing the anthropogenic typology of this source.

An oxalate rich factor explaining 80 % to 89 % of the oxalate was identified for all the sites. The sources of oxalate in the atmosphere comprise both primary biogenic and primary anthropogenic emissions (Kawamura and Kaplan 1987; Kawamura and Ikushima 1993) and also transformations of organic precursors in the gaseous and condensed phases (Dabek-Zlotorzynska and McGrath 2000; Chebbi and Carlier 1996; Kawamura, Kasukabe, and Barrie 1996; Myriokefalitakis et al. 2011). Together with oxalate, also sulfate is seen in the factors (5 % to 18 % of total sulfate).

Based on other studies and their chemical composition, traffic and biomass burning appear as the main local sources although traffic may exhibit a regional background level, which shows up as significant (15%) for the remote site of Revin. However the particles associated with traffic emissions are characterized by being highly reactive so with more important local influence rather than regional. Biomass burning as also been often characterized as a local source due to the proximity of the sampling sites with direct sources of these particles. Some studies have seen a regional influence of biomass burning as well, when VOCs have been monitored. Nitrate-rich, sulfate-rich, fresh and aged marine and marine biogenic are often characterized as regional sources due to the lack of direct sources near the sampling sites and to their association with high wind speeds. Factors like land biogenic particles and the oxalate-rich factor need further investigation to assess their geographical origin.

One way to study the influence of source location in regards to the sampling site is to study the chemical profiles of the similar factors found across the 5 sites. Figure 3 presents the actual concentration for each species in a given factor versus the one averaged over the five sites.





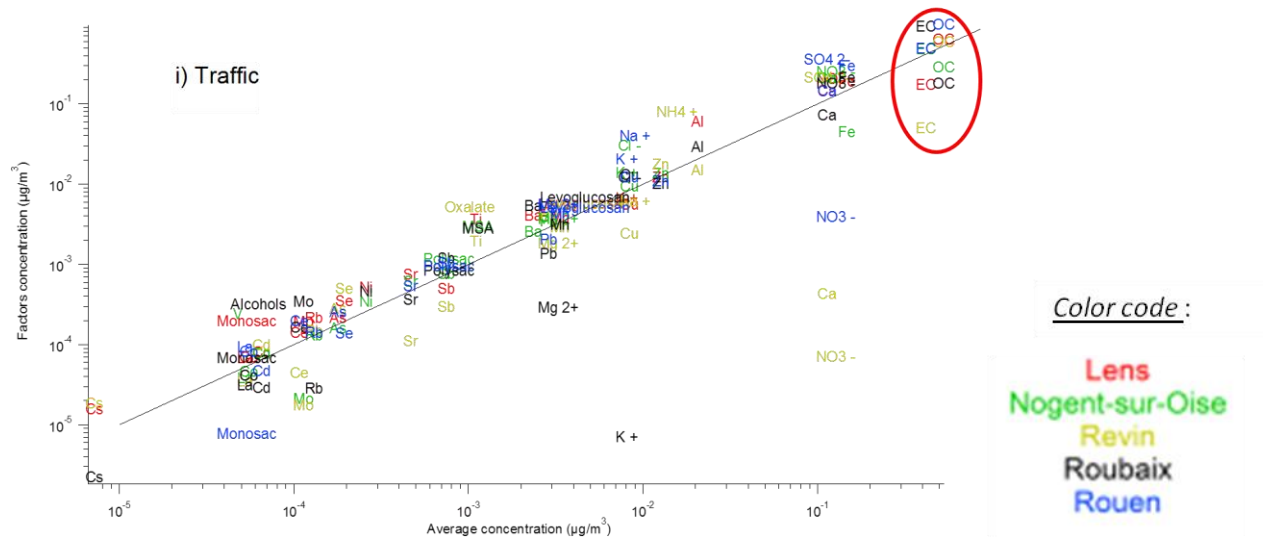


Figure P2. 4: Scatter plots between the averaged and individual concentrations of species at each site for the a) biomass burning, b) aged marine, c) fresh marine, d) land biogenic, e) marine biogenic, f) nitrate-rich, g) oxalate-rich, h) sulfate-rich and i) traffic factors. The solid line corresponds to the 1:1 ratio. The red circles point the main tracers for each factor

The variability seen of the main species and tracers depends on factor to factor. The traffic and oxalate-rich factors appear to be the ones whose chemical composition is less stable from site to site based on its tracers – EC and OC for the former, and oxalate and sulfate for the latter. This is linked to different contributions of the factor from site to site, suggesting a close relationship with possible local sources. Knowing that traffic is dominated by local inputs, seeing the oxalate rich factor showing the same behavior one can assume that an important fraction of the contribution of this source is derived from either local primary sources or specific local formation of secondary particles. Factors like nitrate rich, sulfate rich and fresh marine show a good correlation of the main tracers for each factor on all sites.

To look more into detail on the chemical variability of similar factors, ratios between characteristic species of each chemical profile have been defined (table P2.5). The selected species include at least one non-conservative species with the objective to assess the variability depending on both site typology and source category.

Table P2. 5: Main tracers of each factor used to calculate the ratios

Factor	Biomass burning	Traffic	Nitrate rich	Sulfate rich	Land biogenic	Marine biogenic	Oxalate rich	Aged marine	Fresh marine
Ratio	Lev ^a /OC	EC/OC	NH ₄ ⁺ /NO ₃ ⁻	NH ₄ ⁺ /SO ₄ ²⁻	Alc ^b /OC	MSA/SO ₄ ²⁻	Ox ^c /SO ₄ ²⁻	NO ₃ ⁻ /Na ⁺	Na ⁺ /K ⁺

^a Levoglucosan; ^b Sugar alcohols, ^c Oxalate

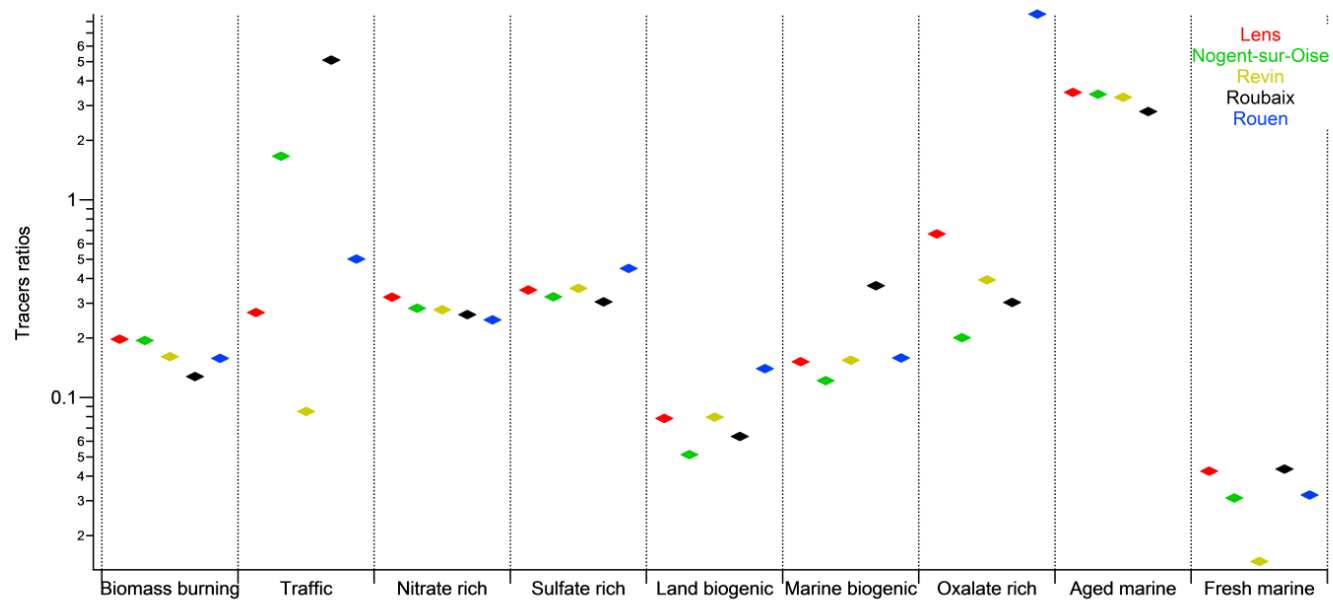


Figure P2. 5: Ratios of selected tracers obtained for each factor for the different sampling sites ($\mu\text{g m}^{-3}$ per $\mu\text{g m}^{-3}$)

As presented in figure P2.5, the highest variability was seen for the traffic and oxalate rich characteristic ratios. The EC/OC ratios obtained are in agreement with the ones found on other urban and traffic sites across Europe (C. Pio et al. 2011) and the higher ratio found in Nogent-sur-Oise when compared to the other urban sites suggest a stronger influence of primary traffic contribution in this site. In the case of the oxalate-rich factor, even if Rouen is not included, a CV of 52 % is seen between the other sites meaning that the chemical profiles of these factors seem to be more dependent on local emission patterns linked with the environment of each site. In the case of biomass burning, a good agreement was seen between the ratios across the five sites and seen to be within range of the ones found in Maenhaut et al. (2016). A study on the pollution roses showed that these contributions were linked to very low wind speeds, low temperatures and no rainfall, indicating that the biomass burning factor seen on all sites is originated mostly by house heating activities at a local scale. Another case worth mentioning is about the marine biogenic ratios, which are in good agreement between sites with the exception of Roubaix. This leads to the assumption that a possible location of strong algal blooming (responsible for marine biogenic aerosols) is the North Sea, situated closer to Roubaix than to any other sites. But this same result could be also explained differently by the presence of an alternate sulfate-emitting sources in Roubaix. Finally, the variability seen for the ratio Na^+/K^+ of the fresh sea salt factor, evident for the site of Revin, can be explained by the distance of this site to the sea. Revin is the sampling site located more inland, resulting therefore on lower concentrations of sodium (in view of the distance to the sea) and higher of potassium (due to a higher influence of the upper continental crust inland) thus having the lowest ratio when compared to the other sites.

Local factors

The primary traffic factor is one of the main contributors to PM_{10} mass concentration and was identified on all sites, including Revin, the remote site. Traffic is often associated with rather local sources however regional transport is possible, as demonstrated in this study. Following the methodology of Oliveira et al., (submitted), NWR allowed to associate wind speed and wind direction with each factor on each site. As illustrated in figure S.2 on all sites traffic is associated with low wind speeds, with the exceptions of Revin and Roubaix. In Revin primary traffic is associated with mild wind speeds suggesting an anthropogenic influence not so far from the sampling site, and the directions highlighted (from the right side of the site – north-east-south) correspond to the location where the road D988 passes by (50 meters away),

which more than 22000 vehicles every day. This fact explains the strong contribution of primary traffic emissions seen in this site, and question the “remoteness” of its characterization. In Roubaix traffic emissions are associated with low and mild wind speeds but here the explanation to this observation is the constant and close presence of a source of primary traffic related particles, meaning that even when weather conditions are favorable for better particle dispersion, a traffic influence is seen in the sampling location – in this case supporting the typology associated with the site. In the site of Lens traffic particles are seen associated with all directions except from southwest, and Lens is surrounded by the highway A21 in the north and east sides, and the highway A221 in the south, supporting the results seen in the NWR plot. In Nogent-sur-Oise, a site already studied in Oliveira et al. (submitted), the direction of particles correspond to the presence of the road D1016 and in Rouen high concentrations were seen from the left side of the sampling site (national road N338) and on the right side, a residential area with several parking lots close by.

The factor biomass burning contribution is logically higher during winter season whatever the site, supporting that these particles originate mainly from house heating. The site with most significant contribution of biomass burning particles to PM_{10} mass was Nogent-sur-Oise, a city where the wood burning is widely used as house heating mean. Lens was the sampling site that recorded the smallest contribution for biomass burning (8 % to total PM_{10} mass) which is smaller than the one reported by Waked et al (2014) for the period between 2011 and 2012 (13 %). NWR plots are clear evidence of the local nature of this factor on all the sites with the exception of Revin (figure S.3). In Revin biomass burning contributions are associated with higher wind speeds from the east-southeast direction. A possible source of these aerosols could be Luxembourg City, located roughly 110 km from the sampling on that same direction. No other big urban agglomerations are found on that direction between these two locations and these observations can be an important evidence of the potential regional influence of these particles.

The land biogenic factor contributions are higher during summer due to more intense solar radiation and higher temperatures resulting in an increase in biological activity as it has been reported in previous studies (Pashynska et al. 2002; K. E. Yttri et al. 2007; H. Bauer et al. 2008). The results from the NWR differ from site to site (Figure S.4). The urban sites of Lens and Rouen show a clear local origin of these particles. In Rouen the direction pointed to the forest of Roumare, located 5km to the west-southwest of the sampling site and in Lens these particles can be associated with emissions from the Jean Moulin stadium, where the sampling

site is located. The results in Nogent-sur-Oise point out to the influence of the Natural Regional Park Oise - Pays de France and the Compiègne Forest. In Revin biogenic particles are associated with speeds from the south-west-east side of the sampling site, pointing to the Regional Natural Park of the Ardennes. Finally, in Roubaix a broader area of possible sources of biogenic particles was found with a southern influence associated with mild wind speeds, possibly linked to the Héron Park which also has a golf court located 8km from the sampling site.

Regional factors

The regional sources identified impacting the north of France were: fresh and aged marine particles, marine biogenic particles, nitrate rich and sulfate rich sources. The oxalate rich factor was also included in this section due to its strong contribution of sulfate to its chemical profile and the regional origin of this species as well as the possible regional influence of oxalate common precursors.

Natural sources

Marine biogenic main contributions are seen during late spring early summer, as expected from known studies on algae bloom events (Udisti et al. 2013; Hopke et al. 1995). Marine biogenic particles found in the north of France seem to have a very well defined geographical origin (figure P2.8c). The concentration field map highlights the North Sea as the main source of these aerosols as seen in Figure 6. Interestingly, Chlorophyll-a concentrations were measured via Moderate Resolution Imaging Spectroradiometer (MODIS) from the Aqua satellite of NASA operating since 2002. Covering the entire surface of the globe in just two days, this satellite identifies the North Sea as a region with high concentrations of chlorophyll during spring and summer. The highlighted area in Sweden can be associated with emissions from the lakes Vanern, Vattern and Malaren, 3 of the biggest lakes found in Europe. This hotspot can also be identified as potential source area for the marine biogenic factor.

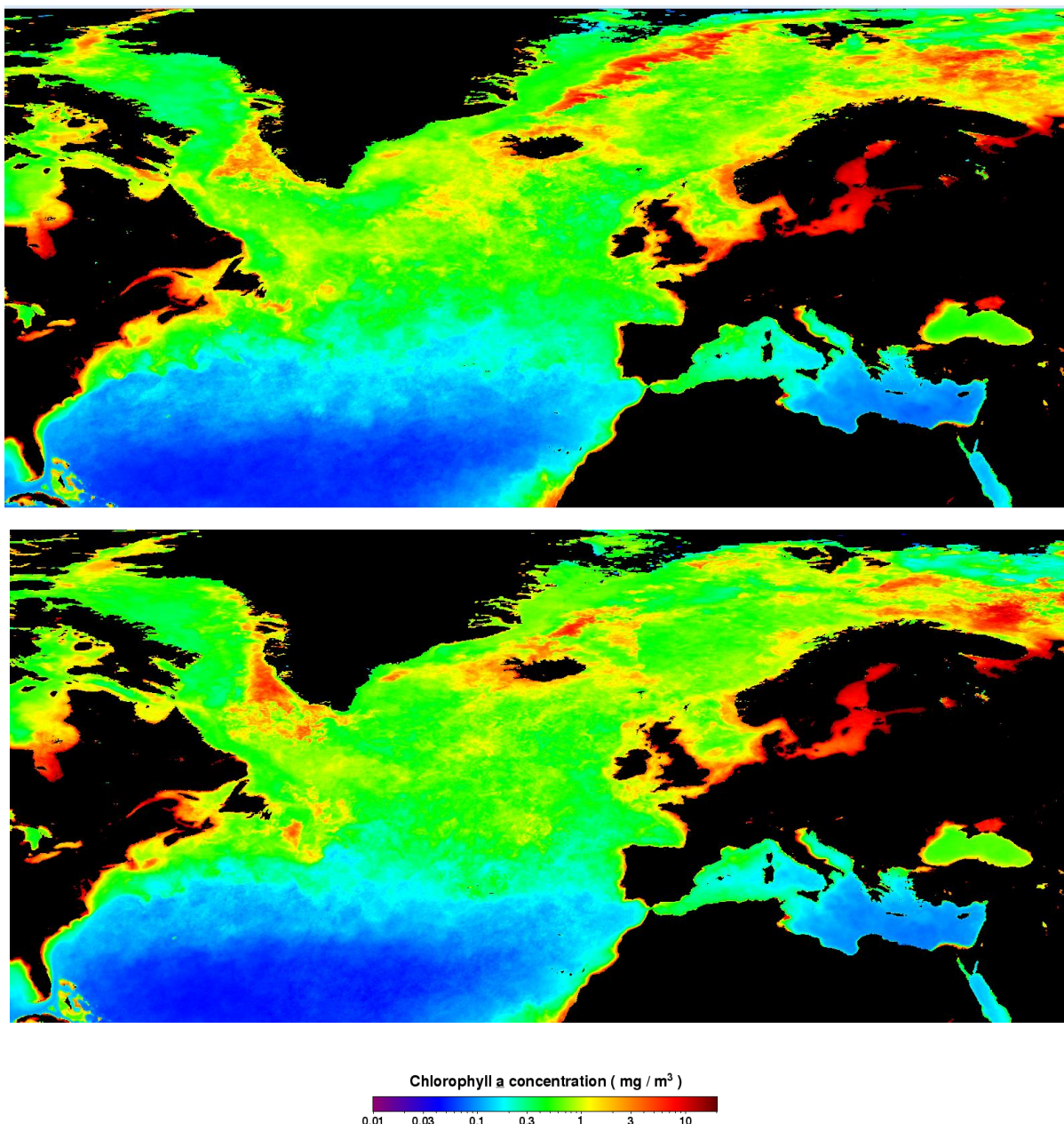


Figure P2. 6: Chlorophyll-a concentrations (in mg m⁻³) in (top) 2013 and (bottom) 2014 (Source: NASA, 2016)

As seen in Figure 6 the North Sea is a potential source of marine biogenic particles, validating the results obtained in this study.

Sea salt aerosols were sampled on all sites, even in the remote site of Revin. The higher percentages of the measured tracers were logically seen in Rouen, the closest site to the sea. Moreover, PMF did not identify an aged marine factor for this site reversely to the others. As seen in figure P2.8a fresh marine particles appear to be originated on the far Atlantic Ocean, associated with high velocity for the back-trajectories. This result is expected and is in

accordance with other studies especially the one of Mann et al. (2012) who computed a model to predict the concentrations of NaCl aerosols in the globe, where was visible the strong presence of sea salt particles on the northern part of the Atlantic Ocean. The long distance transport of these particles is a result of the North Atlantic Oscillation, originated by the different pressures seen in Greenland and Azores, creating a pathway of air masses with high speeds arriving to Europe. This explains the highlighting of the far North Atlantic Ocean, near the coast of Canada.

The aged marine factor was found on 4 of the 5 sampling sites of this study (with Rouen being the exception), and the chemical profiles showed important contributions of species related with anthropogenic emissions. Aged marine aerosols seem to have a much more dispersed area of origin (figure P2.8b) and are associated with different back-trajectories than the fresh sea salt. Areas near the continent are here colored as possible sources and this suggests that the back-trajectories associated with aged marine PM do not have such high velocities as the back-trajectories carrying fresh marine aerosols. This can be an explanation to the presence of anthropogenic related species, since these air masses may have higher residence times over continental areas, being therefore susceptible to be impacted by inputs of more local pollutants.

Anthropogenic sources

Nitrate rich factor is seen more during spring due to favorable meteorological conditions (cold nights, mild days) regarding the thermal instability of ammonium nitrate and to a higher emission intensity of precursors. Indeed fluxes of ammonia are reinforced in spring with agricultural practices and favorable weather conditions (Loubet et al. 2009). Secondary inorganic aerosols showed to be originated from Central and Eastern Europe. Sulfate rich and nitrate rich concentration field maps (figures P2.8d and P2.8e) showed clear anthropogenic origins, highlighting continental areas known as source area for PM precursors. Some differences can be seen between the two maps. Nitrate rich particles seem to have geographical sources more in central Europe (Czech Republic, Slovakia and Poland). Sulfate rich aerosols appear to be associated with more long distanced back-trajectories, highlighting countries further to the East like Belarus, Ukraine, Moldova and Romania. The nitrate rich factor seems to be as well significantly influenced by Belgium, the Netherlands and Denmark. This can be explained by the intense agricultural activities usually associated with these areas

(Vercauteren et al. 2011a; Weijers and Schaap 2013). Studying the emission inventories obtained with the EMEP/MSX-W model version rv4.9 (figure P2.7) for NO_2 , NH_3 and SO_2 , the main gas precursors of ammonium and sulfate particles, respectively, is interesting to observe this phenomena, where emissions of NO_2 are seen to be significant in the Po Valley and in the region of the north of France, Belgium and the Netherlands NH_3 in Germany, Czech Republic and Poland and SO_2 emitted more in eastern Europe, in countries like Ukraine, Romania and southern Poland. Many studies have associated NH_3 emissions with agricultural activities linked with the intense use of fertilizers rich in nitrogen (Kendall, Elliott, and Wankel 2007), whereas SO_2 is commonly emitted from coal combustion (L. Zhang et al. 2007), a common practice in the countries mentioned above (Kryza et al. 2010; Junninen et al. 2009; Lewandowska, Falkowska, and Józwick 2013).

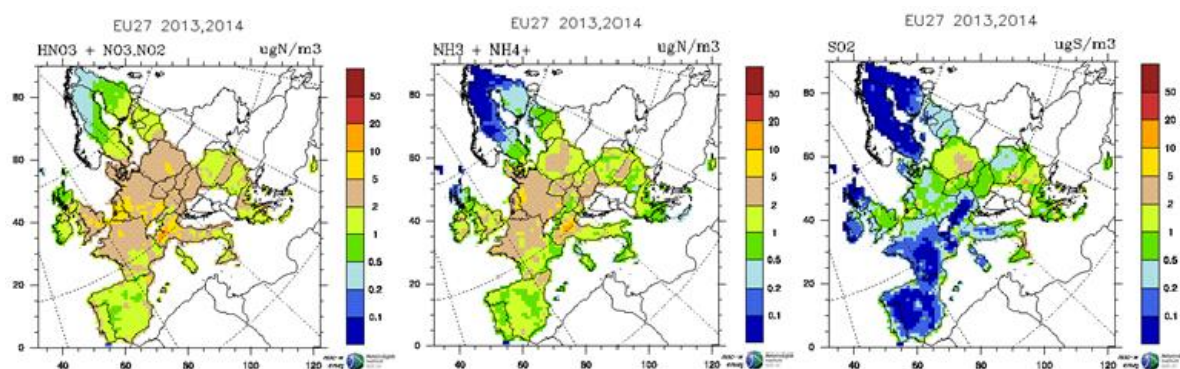


Figure P2. 7: Emission inventories for a) $\text{HNO}_3 + \text{NO}_3$ and NO_2 , b) NH_3 and NH_4^+ , and c) SO_2 (Source: EMEP)

Other interesting difference is the indication of a source of sulfate rich particles from the Gibraltar Strait, not seen in the nitrate rich concentration field map. This strait is well known for intense maritime traffic with strong ship emissions, which can help to explain the obtained result. The British Channel located just next to the studied region is not highlighted in the CF map. This can be due to the limitation associated with CF on spotting emissions sources too near the sampling site(s) used.

An oxalate rich factor was found on every sampling site but regarding the chemical profile of these factors, it is hard to characterize these particles as regional or local since sulfate has probably a regional influence while oxalate can be originated both from local and regional sources. The concentration field map obtained for this factor (Figure 8f) showed interesting results highlighting different regions of the map, however the analysis of these results are associated with the limitation of this method. Central Europe region was seen as a source, and

is probably associated with the contribution of sulfate particles for this factor. Also the Mediterranean Sea is seen as a source of these particles, which is also the European area with the highest ozone concentrations, contributing strongly to the oxidation of atmospheric VOCs (Sartelet et al. 2012). Finally, the North Sea and British Channel appear with important contributions, possibly associated with marine biogenic emissions and/or anthropogenic particles associated with intense ship traffic characteristic of this region.

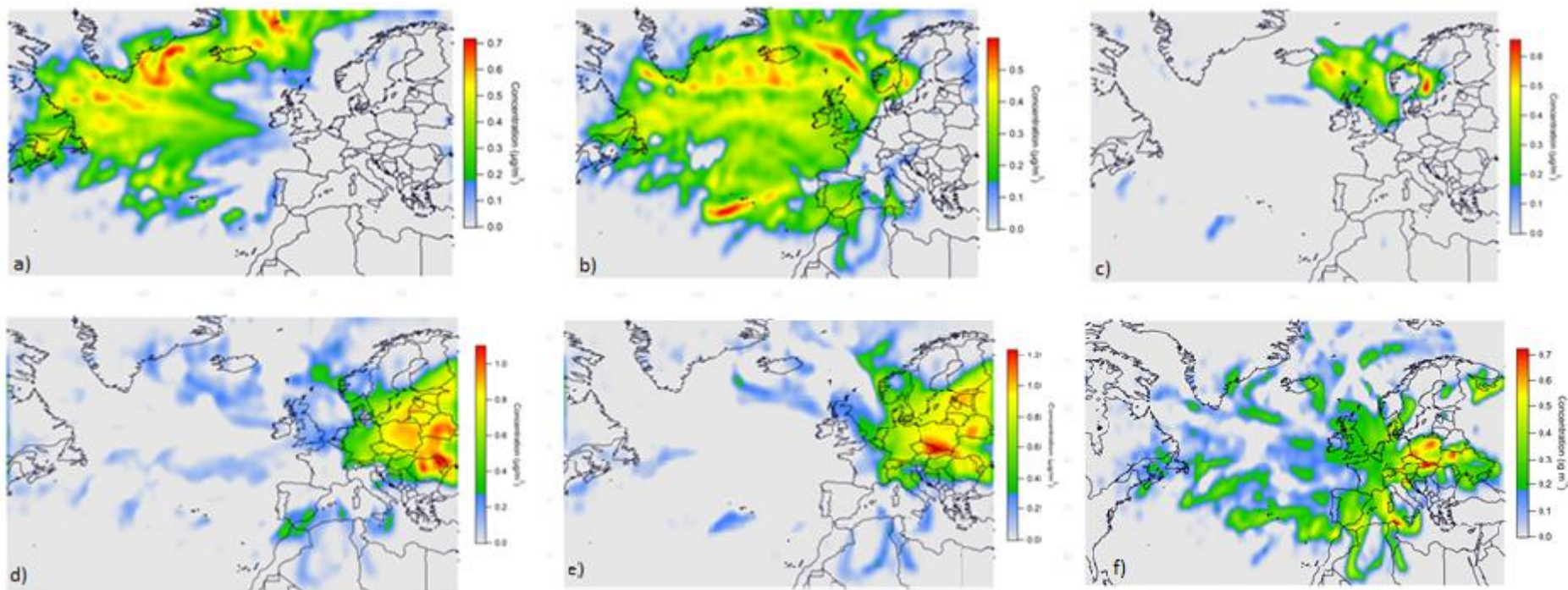


Figure P2. 8: Multi-site concentration field maps obtained for a) fresh sea salt, b) aged marine, c) marine biogenic, d) sulfate rich, e) nitrate rich and f) oxalate rich factor

CONCLUSION

A comprehensive source apportionment study carried out on 5 sites spread across the north of France allowed the identification of an important number of particles sources impacting the region. Thanks to a unique and robust dataset with a wide range of analyzed species on sampling sites with different typologies over a period of more than one year, a near-to-complete chemical characterization of PM₁₀ was obtained. Reconstructed mass by the analyzed species explained more than 80% of PM mass measured in-situ, on average. Organic matter was seen to be main contributor to PM₁₀, followed by the main ions (nitrate, sulfate and ammonium). Interestingly no major differences were seen between the sites in terms of chemical composition.

With an extensive chemical characterization of the PM collected between 8 to 10 different sources were found on each site. The contribution of these sources proved to be dependent on the specific characteristics of each site with significant impact of local sources such as traffic, biomass burning and road dust. An important contribution of more regional sources was also found, where secondary inorganic aerosols proved to play an important role in PM concentrations across the region. The measurement of specific compounds like oxalate and MSA proved to be useful in identifying particles with marine biogenic origin (rich in MSA) and secondary aerosols rich in oxalate and sulfate. By comparing the chemical composition of the factors obtained on each site and combining meteorological information like wind speed and wind direction with daily contributions of the factors on each site, was possible to distinguish between local and regional sources.

The main local sources identified were primary traffic and biomass burning, with contributions varying from site to site according to their typology. These sources were also found in the site of Revin, labeled as a remote site, associated with mild wind speeds. This suggests the potential of these particles to have not only a local impact but also be transported on a regional level. Land biogenic aerosols, traced by sugar alcohols measured, were seen to have an impact on all sites. From site to site, the origin varied in terms of potential localization. In sites like Lens and Rouen these aerosols were associated with very low wind speeds, suggesting a very local source, whereas in the other sites appeared associated with mild wind speeds, pointing to origins a few kilometers away.

The use of the concentration field model allowed to estimate the geographical location of the different regional sources identified, clearly distinguishing the geographical origin of natural

and anthropogenic particles. Natural particles, like fresh and aged sea salt and marine biogenic PM were located in maritime areas. Fresh sea salt appeared associated with high velocity air masses originated from the far North Atlantic Ocean, probably carried by winds originated from the Northern Atlantic Oscillation. Aged sea salt is also originated in the Atlantic Ocean but is associated with air masses with lower velocity. This could explain the presence of particles normally associated with anthropogenic activities seen in the chemical profile of this factor – longer residence time over continental areas. Marine biogenic aerosols were clearly associated with emissions from the North Sea, an area identified by its intense algae bloom phenomena, especially during late spring and summer.

Usually linked with anthropogenic activities, secondary aerosols composed by nitrate rich and sulfate rich particles were clearly spotted in Central and Eastern Europe. Nitrate rich particles also appear to be originating from regions closer to the sampling sites like Belgium and the Netherlands. Czech Republic was also identified as a main source of nitrate rich aerosols, a country the often records high concentrations of these particles in rural areas. The Strait of Gibraltar was seen to be a potential source of sulfate rich particles impacting the north of France, originated from intense maritime traffic seen in this area. This shows the regional impact that intense emissions can have, even at long distances (more than 1700km away from the north of France).

The multi-site approach of CF allowed combining regional sources impacting the north of France and calculating concentration field maps of the probable geographical location of these sources. A multi-site exercise also allowed further refining of its solution by implementing back-trajectories cut-offs on rainfall events and modeled altitude.

Acknowledgements

This work was notably funded by the French Ministry of Environment ("Bureau de l'Air du Ministère de l'Ecologie, du Développement durable, et de l'Energie") and included in the CARA air quality monitoring and research project coordinated by the French reference laboratory for air quality monitoring (LCSQA). Mines Douai participates in the CaPPA project funded by the ANR through the PIA under contract ANR-11-LABX-0005-01, the "Nord Pas de Calais" Regional Council and the European Regional Development Fund

(ERDF). The authors gratefully acknowledge the NOAA Air Resources Laboratory (ARL) for the provision of the HYSPLIT transport and dispersion model used in this publication.

References

- Abbott, Michael L., Che-Jen Lin, Peter Martian, and Jeffrey J. Einerson. 2008. "Atmospheric Mercury near Salmon Falls Creek Reservoir in Southern Idaho." *Applied Geochemistry, Transport and Fate of Mercury in the Environment* 23 (3): 438–53. doi:10.1016/j.apgeochem.2007.12.012.
- Alleman, Laurent Y., Laure Lamaison, Esperanza Perdrix, Antoine Robache, and Jean-Claude Galloo. 2010. "PM10 Metal Concentrations and Source Identification Using Positive Matrix Factorization and Wind Sectoring in a French Industrial Zone." *Atmospheric Research* 96 (4): 612–25. doi:10.1016/j.atmosres.2010.02.008.
- Amato, F., M. Pandolfi, T. Moreno, M. Furger, J. Pey, A. Alastuey, N. Bukowiecki, A. S. H. Prevot, U. Baltensperger, and X. Querol. 2011. "Sources and Variability of Inhalable Road Dust Particles in Three European Cities." *Atmospheric Environment* 45 (37): 6777–6787.
- Analitits, Antonis, Klea Katsouyanni, Konstantina Dimakopoulou, Evangelia Samoli, Aristidis K. Nikoloulopoulos, Yannis Petasakis, Giota Touloumi, et al. 2006. "Short-Term Effects of Ambient Particles on Cardiovascular and Respiratory Mortality." *Epidemiology* 17 (2): 230–233.
- Anttila, Pia, Pentti Paatero, Unto Tapper, and Olli Järvinen. 1995. "Source Identification of Bulk Wet Deposition in Finland by Positive Matrix Factorization." *Atmospheric Environment* 29 (14): 1705–1718.
- Bauer, Heidi, Elisabeth Schueller, Gert Weinke, Anna Berger, Regina Hitzemberger, Iain L. Marr, and Hans Puxbaum. 2008. "Significant Contributions of Fungal Spores to the Organic Carbon and to the Aerosol Mass Balance of the Urban Atmospheric Aerosol." *Atmospheric Environment* 42 (22): 5542–5549.
- Bessagnet, Bertrand, Alma Hodzic, Olivier Blanchard, M. Lattuat, Olivier Le Bihan, H  l  ne Marfaing, and Laurence Rouil. 2005. "Origin of Particulate Matter Pollution Episodes in Wintertime over the Paris Basin." *Atmospheric Environment* 39 (33): 6159–6174.
- Beuck, H., U. Quass, O. Klemm, and T. A. J. Kuhlbusch. 2011. "Assessment of Sea Salt and Mineral Dust Contributions to PM 10 in NW Germany Using Tracer Models and Positive Matrix Factorization." *Atmospheric Environment* 45 (32): 5813–5821.
- "Bilan de La Qualit   de L'air En France En 2015 - Minist  re de l'Environnement, de l'Energie et de La Mer." 2016. Accessed November 20. <http://www.developpement-durable.gouv.fr/Bilan-de-la-Qualite-de-l-air-en,48891.html>.
- Birch, M. E., and R. A. Cary. 1996. "Elemental Carbon-Based Method for Monitoring Occupational Exposures to Particulate Diesel Exhaust." *Aerosol Science and Technology* 25 (3): 221–241.
- Caseiro, Alexandre, Iain L. Marr, Magda Claeys, Anne Kasper-Giebl, Hans Puxbaum, and Casimiro A. Pio. 2007. "Determination of Saccharides in Atmospheric Aerosol Using Anion-Exchange High-Performance Liquid Chromatography and Pulsed-Amperometric Detection." *Journal of Chromatography A* 1171 (1): 37–45.
- Castro, Amaya, Elisabeth Alonso-Blanco, Miguel Gonz  lez-Colino, Ana I. Calvo, Mar  a Fern  ndez-Raga, and Roberto Fraile. 2010. "Aerosol Size Distribution in Precipitation Events in Le  n, Spain." *Atmospheric Research* 96 (2): 421–435.
- Cavalli, Fabrizia, Mar Viana, Karl Espen Yttri, Johan Genberg, and J.-P. Putaud. 2010. "Toward a Standardised Thermal-Optical Protocol for Measuring Atmospheric Organic and Elemental Carbon: The EUSAAR Protocol." *Atmospheric Measurement Techniques* 3 (1): 79–89.
- Charron, A., H. Plaisance, S. Sauvage, P. Coddeville, J. C. Galloo, and R. Guillermo. 1998. "Intercomparison between Three Receptor-Oriented Models Applied to Acidic Species in Precipitation." *Science of The Total Environment* 223 (1): 53–63. doi:10.1016/S0048-9697(98)00308-8.
- Chebbi, A., and P. Carlier. 1996. "Carboxylic Acids in the Troposphere, Occurrence, Sources, and Sinks: A Review." *Atmospheric Environment* 30 (24): 4233–4249.
- Chin, Mian, T. Diehl, Q. Tan, J. M. Prospero, R. A. Kahn, L. A. Remer, H. Yu, et al. 2014. "Multi-Decadal Aerosol Variations from 1980 to 2009: A Perspective from Observations and a Global Model." *Atmospheric Chemistry and Physics* 14 (April): 3657–90. doi:10.5194/acp-14-3657-2014.

- Choi, Eunhwa, Kyungho Choi, and Seung-Muk Yi. 2011. "Non-Methane Hydrocarbons in the Atmosphere of a Metropolitan City and a Background Site in South Korea: Sources and Health Risk Potentials." *Atmospheric Environment, Air Pollution and Health: Bridging the Gap from Sources-to-Health Outcomes*, 45 (40): 7563–73. doi:10.1016/j.atmosenv.2010.11.049.
- Coury, Charity, and Ann M. Dillner. 2007. "Trends and Sources of Particulate Matter in the Superstition Wilderness Using Air Trajectory and Aerosol Cluster Analysis." *Atmospheric Environment* 41 (40): 9309–9323.
- Dabek-Zlotorzynska, Ewa, and Marilu McGrath. 2000. "Determination of Low-Molecular-Weight Carboxylic Acids in the Ambient Air and Vehicle Emissions: A Review." *Fresenius' Journal of Analytical Chemistry* 367 (6): 507–518.
- Dall'Osto, M., R. M. Harrison, H. Coe, P. I. Williams, and J. D. Allan. 2009. "Real Time Chemical Characterization of Local and Regional Nitrate Aerosols." *Atmos. Chem. Phys.* 9 (11): 3709–20. doi:10.5194/acp-9-3709-2009.
- Dorling, S. R., and T. D. Davies. 1995. "Extending Cluster Analysis—synoptic Meteorology Links to Characterise Chemical Climates at Six Northwest European Monitoring Stations." *Atmospheric Environment* 29 (2): 145–167.
- Dorling, S. R., T. D. Davies, and C. E. Pierce. 1992. "Cluster Analysis: A Technique for Estimating the Synoptic Meteorological Controls on Air and Precipitation Chemistry—method and Applications." *Atmospheric Environment. Part A. General Topics* 26 (14): 2575–2581.
- Draxler, Roland R. 1999. "HYSPLIT4 User's Guide." http://www.villasmunta.it/pdf/User_guide.pdf.
- Draxler, Roland R., and G. D. Hess. 1998. "An Overview of the HYSPLIT_4 Modelling System for Trajectories." *Australian Meteorological Magazine* 47 (4): 295–308.
- Elbert, W., P. E. Taylor, M. O. Andreae, and U. Pöschl. 2007. "Contribution of Fungi to Primary Biogenic Aerosols in the Atmosphere: Wet and Dry Discharged Spores, Carbohydrates, and Inorganic Ions." *Atmospheric Chemistry and Physics* 7 (17): 4569–4588.
- Engeln, Axel von, and João Teixeira. 2013. "A Planetary Boundary Layer Height Climatology Derived from ECMWF Reanalysis Data." *Journal of Climate* 26 (17): 6575–6590.
- European Guide on Air Pollution Source Apportionment with Receptor Models. 2014. Publications Office.
- Fu, Xuewu, Xinbin Feng, Guangle Qiu, Lihai Shang, and Hui Zhang. 2011. "Speciated Atmospheric Mercury and Its Potential Source in Guiyang, China." *Atmospheric Environment* 45 (25): 4205–4212.
- Glasow, R. von, and P. J. Crutzen. 2003. "Model Study of Multiphase DMS Oxidation with a Focus on Halogens." *Atmospheric Chemistry & Physics Discussions* 3: 6733–6777.
- Han, Young-Ji, Thomas M. Holsen, and Philip K. Hopke. 2007. "Estimation of Source Locations of Total Gaseous Mercury Measured in New York State Using Trajectory-Based Models." *Atmospheric Environment* 41 (28): 6033–47. doi:10.1016/j.atmosenv.2007.03.027.
- Henry, Ronald C., Yu-Shuo Chang, and Clifford H. Spiegelman. 2002. "Locating Nearby Sources of Air Pollution by Nonparametric Regression of Atmospheric Concentrations on Wind Direction." *Atmospheric Environment* 36 (13): 2237–44. doi:10.1016/S1352-2310(02)00164-4.
- Hongisto, Marke, and Mikhail Sofiev. 2004. "Long-Range Transport of Dust to the Baltic Sea Region." *International Journal of Environment and Pollution* 22 (1–2): 72–86.
- Hopke, P. K., L. A. Barrie, S.-M. Li, M.-D. Cheng, C. Li, and Y. Xie. 1995. "Possible Sources and Preferred Pathways for Biogenic and Non-Sea-Salt Sulfur for the High Arctic." *Journal of Geophysical Research: Atmospheres* 100 (D8): 16595–16603.
- Iinuma, Yoshiteru, Guenter Engling, Hans Puxbaum, and Hartmut Herrmann. 2009. "A Highly Resolved Anion-Exchange Chromatographic Method for Determination of Saccharidic Tracers for Biomass Combustion and Primary Bio-Particles in Atmospheric Aerosol." *Atmospheric Environment* 43 (6): 1367–1371.
- Jia, Yuling, Andrea L. Clements, and Matthew P. Fraser. 2010. "Saccharide Composition in Atmospheric Particulate Matter in the Southwest US and Estimates of Source Contributions." *Journal of Aerosol Science* 41 (1): 62–73.

- Johansson, Christer, Michael Norman, and Lars Burman. 2009. "Road Traffic Emission Factors for Heavy Metals." *Atmospheric Environment* 43 (31): 4681–4688.
- Jorba, Oriol, Carlos Pérez, Francesc Rocadenbosch, and JoséM Baldasano. 2004. "Cluster Analysis of 4-Day Back Trajectories Arriving in the Barcelona Area, Spain, from 1997 to 2002." *Journal of Applied Meteorology* 43 (6): 887–901.
- Junninen, Heikki, Jacob Mønster, Maria Rey, Jose Cancelinha, Kevin Douglas, Matthew Duane, Victorio Forcina, et al. 2009. "Quantifying the Impact of Residential Heating on the Urban Air Quality in a Typical European Coal Combustion Region." *Environmental Science & Technology* 43 (20): 7964–70. doi:10.1021/es8032082.
- Kabashnikov, Vitaliy P., Anatoli P. Chaikovskiy, Tom L. Kucsera, and Natalia S. Metelskaya. 2011. "Estimated Accuracy of Three Common Trajectory Statistical Methods." *Atmospheric Environment* 45 (31): 5425–30. doi:10.1016/j.atmosenv.2011.07.006.
- Kawamura, Kimitaka, and Kouichi Ikushima. 1993. "Seasonal Changes in the Distribution of Dicarboxylic Acids in the Urban Atmosphere." *Environmental Science & Technology* 27 (10): 2227–2235.
- Kawamura, Kimitaka, and Isaac R. Kaplan. 1987. "Motor Exhaust Emissions as a Primary Source for Dicarboxylic Acids in Los Angeles Ambient Air." *Environmental Science & Technology* 21 (1): 105–110.
- Kawamura, Kimitaka, Hideki Kasukabe, and Leonard A. Barrie. 1996. "Source and Reaction Pathways of Dicarboxylic Acids, Ketoacids and Dicarbonyls in Arctic Aerosols: One Year of Observations." *Atmospheric Environment* 30 (10): 1709–1722.
- Kendall, Carol, Emily M. Elliott, and SCOTT D. Wankel. 2007. "Tracing Anthropogenic Inputs of Nitrogen to Ecosystems." *Stable Isotopes in Ecology and Environmental Science* 2: 375–449.
- Kryza, Maciej, Małgorzata Werner, Marek Błaś, Anthony J. Dore, and Mieczysław Sobik. 2010. "The Effect of Emission from Coal Combustion in Nonindustrial Sources on Deposition of Sulfur and Oxidized Nitrogen in Poland." *Journal of the Air & Waste Management Association* 60 (7): 856–866.
- Lewandowska, Anita, Lucyna Falkowska, and Joanna Józwiak. 2013. "Factors Determining the Fluctuation of Fluoride Concentrations in PM10 Aerosols in the Urbanized Coastal Area of the Baltic Sea (Gdynia, Poland)." *Environmental Science and Pollution Research* 20 (9): 6109–6118.
- Lim, Ho-Jin, Barbara J. Turpin, Eric Edgerton, Susanne V. Hering, George Allen, Hal Maring, and Paul Solomon. 2003. "Semicontinuous Aerosol Carbon Measurements: Comparison of Atlanta Supersite Measurements." *Journal of Geophysical Research: Atmospheres* 108 (D7): 8419. doi:10.1029/2001JD001214.
- Loubet, B., C. Milford, A. Hensen, U. Daemmgen, J.-W. Erismann, P. Cellier, and M. A. Sutton. 2009. "Advection of NH₃ over a Pasture Field and Its Effect on Gradient Flux Measurements." *Biogeosciences* 6 (7): 1295–1309. doi:10.5194/bg-6-1295-2009.
- Maenhaut, Willy, Reinhilde Vermeulen, Magda Claeys, Jordy Vercauteren, and Edward Roekens. 2016. "Sources of the PM10 Aerosol in Flanders, Belgium, and Re-Assessment of the Contribution from Wood Burning." *The Science of the Total Environment* 562 (August): 550–60. doi:10.1016/j.scitotenv.2016.04.074.
- Mann, G. W., K. S. Carslaw, D. A. Ridley, D. V. Spracklen, K. J. Pringle, Joonas Merikanto, Hanelle Korhonen, et al. 2012. "Intercomparison of Modal and Sectional Aerosol Microphysics Representations within the Same 3-D Global Chemical Transport Model." *Atmospheric Chemistry and Physics* 12 (10): 4449–4476.
- McQueen, J. T., R. R. Draxler, B. J. B. Stunder, and G. D. Rolph. 1997. "Applications of the Regional Atmospheric Modeling System(RAMS) at the NOAA Air Resources Laboratory." National Oceanic and Atmospheric Administration.
- Myriokefalitakis, S., K. Tsigaridis, N. Mihalopoulos, J. Sciare, A. Nenes, K. Kawamura, A. Segers, and M. Kanakidou. 2011. "In-Cloud Oxalate Formation in the Global Troposphere: A 3-D Modeling Study." *Atmospheric Chemistry and Physics* 11 (12): 5761–5782.
- Paatero, Pentti. 1997. "Least Squares Formulation of Robust Non-Negative Factor Analysis." *Chemometrics and Intelligent Laboratory Systems* 37 (1): 23–35.

- Paatero, Pentti, and Unto Tapper. 1994. "Positive Matrix Factorization: A Non-Negative Factor Model with Optimal Utilization of Error Estimates of Data Values." *Environmetrics* 5 (2): 111–26. doi:10.1002/env.3170050203.
- Pascaud, A., S. Sauvage, P. Coddeville, M. Nicolas, L. Croisé, A. Mezdour, and A. Probst. 2016. "Contrasted Spatial and Long-Term Trends in Precipitation Chemistry and Deposition Fluxes at Rural Stations in France." *Atmospheric Environment, Acid Rain and its Environmental Effects: Recent Scientific Advances Papers from the Ninth International Conference on Acid Deposition*, 146: 28–43. doi:10.1016/j.atmosenv.2016.05.019.
- Pashynska, Vlada, Reinhilde Vermeulen, Gyorgy Vas, Willy Maenhaut, and Magda Claeys. 2002. "Development of a Gas Chromatographic/ion Trap Mass Spectrometric Method for the Determination of Levoglucosan and Saccharidic Compounds in Atmospheric Aerosols. Application to Urban Aerosols." *Journal of Mass Spectrometry* 37 (12): 1249–1257.
- Petit, J. -E., O. Favez, A. Albinet, and F. Canonaco. 2017. "A User-Friendly Tool for Comprehensive Evaluation of the Geographical Origins of Atmospheric Pollution: Wind and Trajectory Analyses." *Environmental Modelling & Software* 88: 183–87. doi:10.1016/j.envsoft.2016.11.022.
- Piot, Christine, Jean-Luc Jaffrezo, Julie Cozic, Nicolas Pissot, Imad El Haddad, Nicolas Marchand, and Jean-Luc Besombes. 2012. "Quantification of Levoglucosan and Its Isomers by High Performance Liquid Chromatography-Electrospray Ionization Tandem Mass Spectrometry and Its Application to Atmospheric and Soil Samples." *Atmospheric Measurement Techniques* 5: 141–148.
- Pope III, C. Arden, and Douglas W. Dockery. 2006. "Health Effects of Fine Particulate Air Pollution: Lines That Connect." *Journal of the Air & Waste Management Association* 56 (6): 709–742.
- Rutter, A. P., D. C. Snyder, E. A. Stone, J. J. Schauer, R. Gonzalez-Abraham, L. T. Molina, C. Márquez, B. Cárdenas, and B. de Foy. 2009. "In Situ Measurements of Speciated Atmospheric Mercury and the Identification of Source Regions in the Mexico City Metropolitan Area." *Atmos. Chem. Phys.* 9 (1): 207–20. doi:10.5194/acp-9-207-2009.
- Salvador, Pedro, Begoña Artíñano, Xavier Querol, and Andres Alastuey. 2008. "A Combined Analysis of Backward Trajectories and Aerosol Chemistry to Characterise Long-Range Transport Episodes of Particulate Matter: The Madrid Air Basin, a Case Study." *Science of the Total Environment* 390 (2): 495–506.
- Sartelet, Karine N., Florian Couvidat, Christian Seigneur, and Yelva Roustan. 2012. "Impact of Biogenic Emissions on Air Quality over Europe and North America." *Atmospheric Environment* 53: 131–141.
- Schmid, Heidrun, Lothar Laskus, Hans Jürgen Abraham, Urs Baltensperger, Vincent Lavanchy, Mirko Bizjak, Peter Burba, et al. 2001. "Results of the 'carbon Conference' International Aerosol Carbon Round Robin Test Stage I." *Atmospheric Environment* 35 (12): 2111–2121.
- Sciare, J., K. Oikonomou, O. Favez, E. Liakakou, Z. Markaki, H. Cachier, and N. Mihalopoulos. 2008. "Long-Term Measurements of Carbonaceous Aerosols in the Eastern Mediterranean: Evidence of Long-Range Transport of Biomass Burning." *Atmos. Chem. Phys.* 8 (18): 5551–63. doi:10.5194/acp-8-5551-2008.
- Seibert, P., H. Kromp-Kolb, U. Baltensperger, D. T. Jost, M. Schwikowski, A. Kasper, and H. Puxbaum. 1994. "Trajectory Analysis of Aerosol Measurements at High Alpine Sites." *Transport and Transformation of Pollutants in the Troposphere*, 689–693.
- Sexauer Gustin, M., P. S. Weiss-Penzias, and C. Peterson. 2012. "Investigating Sources of Gaseous Oxidized Mercury in Dry Deposition at Three Sites across Florida, USA." *Atmos. Chem. Phys.* 12 (19): 9201–19. doi:10.5194/acp-12-9201-2012.
- Sicard, Pierre, Patrice Coddeville, Stéphane Sauvage, and Jean-Claude Galloo. 2007. "Trends in Chemical Composition of Wet-Only Precipitation at Rural French Monitoring Stations over the 1990–2003 Period." *Water, Air, & Soil Pollution: Focus* 7 (1–3): 49–58.
- Stein, A. F., R. R. Draxler, G. D. Rolph, B. J. B. Stunder, M. D. Cohen, and F. Ngan. 2015. "NOAA's HYSPLIT Atmospheric Transport and Dispersion Modeling System." *Bulletin of the American Meteorological Society* 96 (12): 2059–77. doi:10.1175/BAMS-D-14-00110.1.
- Stohl, Andreas, Gerhard Wotawa, Petra Seibert, and Helga Kromp-Kolb. 1995. "Interpolation Errors in Wind Fields as a Function of Spatial and Temporal Resolution and Their Impact on Different Types of Kinematic Trajectories." *Journal of Applied Meteorology* 34 (10): 2149–2165.

- Stull, Roland B. 1988. *An Introduction to Boundary Layer Meteorology*. Softcover reprint of the original 1st ed. 1988 edition. Dordrecht: Springer.
- Su, Lin, Zibing Yuan, Jimmy C. H. Fung, and Alexis K. H. Lau. 2015. "A Comparison of HYSPLIT Backward Trajectories Generated from Two GDAS Datasets." *Science of The Total Environment* 506–507 (February): 527–37. doi:10.1016/j.scitotenv.2014.11.072.
- Turpin, Barbara J., and Ho-Jin Lim. 2001. "Species Contributions to PM_{2.5} Mass Concentrations: Revisiting Common Assumptions for Estimating Organic Mass." *Aerosol Science and Technology* 35 (1): 602–10. doi:10.1080/02786820152051454.
- Udisti, Roberto, Francesco Rugi, Silvia Becagli, Ezio Bolzacchini, Giulia Calzolari, Massimo Chiari, Daniele Frosini, et al. 2013. "Spatial Distribution of Biogenic Sulphur Compounds in the Arctic Aerosol Collected during the ARES 2011 and 2012 Oceania Ship Cruises." In *EGU General Assembly Conference Abstracts*, 15:10400. <http://adsabs.harvard.edu/abs/2013EGUGA..1510400U>.
- Vardoulakis, Sotiris, and Pavlos Kassomenos. 2008. "Sources and Factors Affecting PM₁₀ Levels in Two European Cities: Implications for Local Air Quality Management." *Atmospheric Environment* 42 (17): 3949–3963.
- Vercauteren, Jordy, Christina Mattheussen, Eric Wauters, Edward Roekens, René van Grieken, Agnieszka Krata, Yaroslava Makarovska, Willy Maenhaut, Xuguang Chi, and Benny Geypens. 2011. "Chemkar PM₁₀: An Extensive Look at the Local Differences in Chemical Composition of PM₁₀ in Flanders, Belgium." *Atmospheric Environment* 45 (1): 108–116.
- Viana, M., T. A. J. Kuhlbusch, X. Querol, A. Alastuey, R. M. Harrison, P. K. Hopke, W. Winiwarter, et al. 2008. "Source Apportionment of Particulate Matter in Europe: A Review of Methods and Results." *Journal of Aerosol Science* 39 (10): 827–849.
- Waked, A., O. Favez, L. Y. Alleman, C. Piot, J.-E. Petit, T. Delaunay, E. Verlinden, et al. 2014. "Source Apportionment of PM₁₀ in a North-Western Europe Regional Urban Background Site (Lens, France) Using Positive Matrix Factorization and Including Primary Biogenic Emissions." *Atmos. Chem. Phys.* 14 (7): 3325–46. doi:10.5194/acp-14-3325-2014.
- Watson, John G. 1984. "Overview of Receptor Model Principles." *Journal of the Air Pollution Control Association* 34 (6): 619–23. doi:10.1080/00022470.1984.10465780.
- Weijers, Ernie, and Martijn Schaap. 2013. "Anthropogenic and Natural Constituents in PM₁₀ at Urban and Rural Sites in North-Western Europe: Concentrations, Chemical Composition and Sources." In *Urban Air Quality in Europe*, 239–258. Springer. http://link.springer.com/chapter/10.1007/698_2012_207.
- Weiss-Penzias, Peter S., Mae S. Gustin, and Seth N. Lyman. 2011. "Sources of Gaseous Oxidized Mercury and Mercury Dry Deposition at Two Southeastern US Sites." *Atmospheric Environment* 45 (27): 4569–4579.
- Xu, X., and U. S. Akhtar. 2010. "Identification of Potential Regional Sources of Atmospheric Total Gaseous Mercury in Windsor, Ontario, Canada Using Hybrid Receptor Modeling." *Atmospheric Chemistry and Physics* 10 (15): 7073–7083.
- Yttri, K. E., W. Aas, A. Bjerke, J. N. Cape, F. Cavalli, D. Ceburnis, C. Dye, et al. 2007. "Elemental and Organic Carbon in PM₁₀: A One Year Measurement Campaign within the European Monitoring and Evaluation Programme EMEP." *Atmospheric Chemistry and Physics* 7 (22): 5711–5725.
- Yttri, Karl Espen, David Simpson, Jacob Klenø Nøjgaard, Kasper Kristensen, Johan Genberg, Kristina Stenström, Erik Swietlicki, et al. 2011. "Source Apportionment of the Summer Time Carbonaceous Aerosol at Nordic Rural Background Sites." *Atmospheric Chemistry and Physics* 11 (24): 13339–13357.
- Zhang, Lian, Qunying Wang, Atsushi Sato, Yoshihiko Ninomiya, and Toru Yamashita. 2007. "Interactions among Inherent Minerals during Coal Combustion and Their Impacts on the Emission of PM₁₀. 2. Emission of Submicrometer-Sized Particles." *Energy & Fuels* 21 (2): 766–777

SUPPLEMENTARY MATERIAL TO:

Multi-site receptor oriented approach for a comprehensive source apportionment of PM in the North of France

Diogo M. Barros de Oliveira^{1,2,3}, Esperanza Perdrix^{1,3} *, Olivier Favez², Stéphane Sauvage^{1,3}, Laurent Y. Alleman^{1,3}, N. Bonnaire⁴, E. Chrétien⁵, T. Delaunay⁶, S. Lemeur⁷, B. Rocq⁸, Véronique Riffault^{1,3}

¹ Mines Douai, SAGE, F-59508 Douai, France

² INERIS, F-60550 Verneuil-en-Halatte, France

³ Univ. Lille, F-59000 Lille, France

⁴ LSCE, F-91198 Gif-sur-Yvette, France

⁵ Atmo Champagne-Ardenne, F-51100 Reims, France

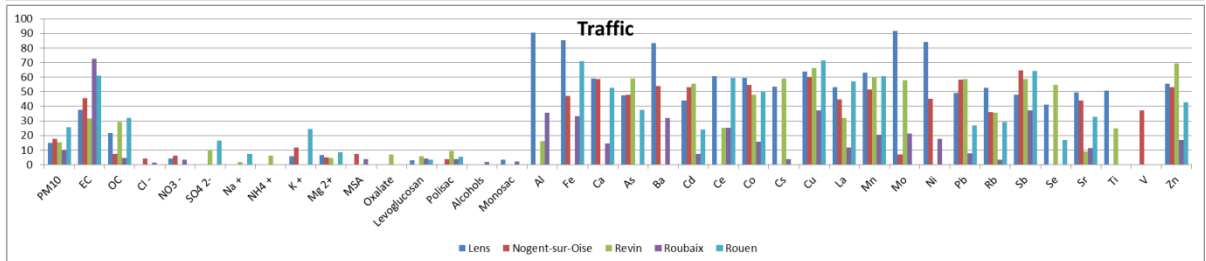
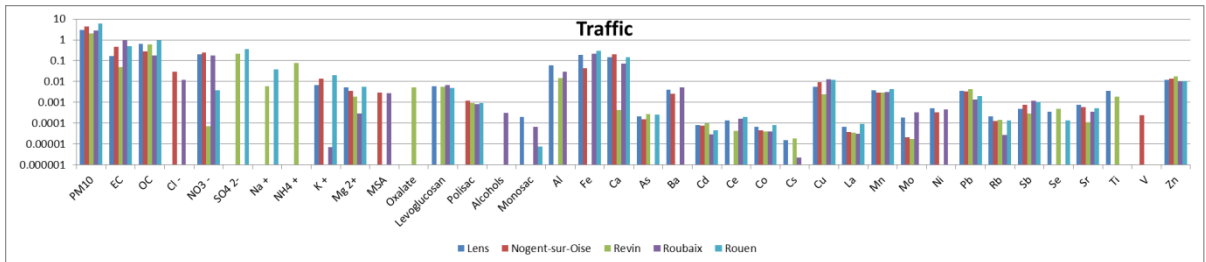
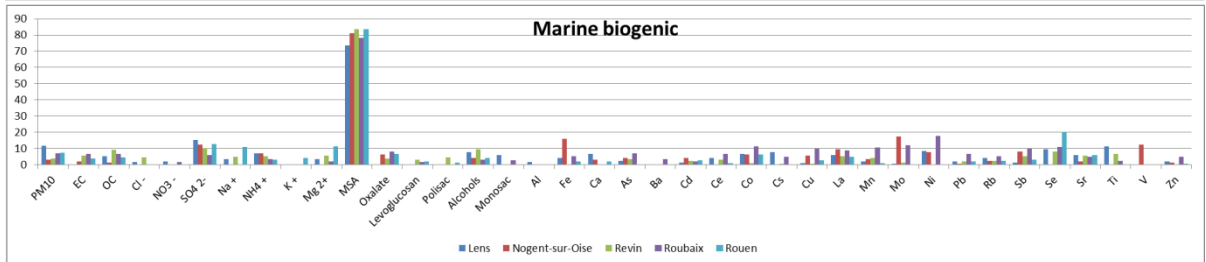
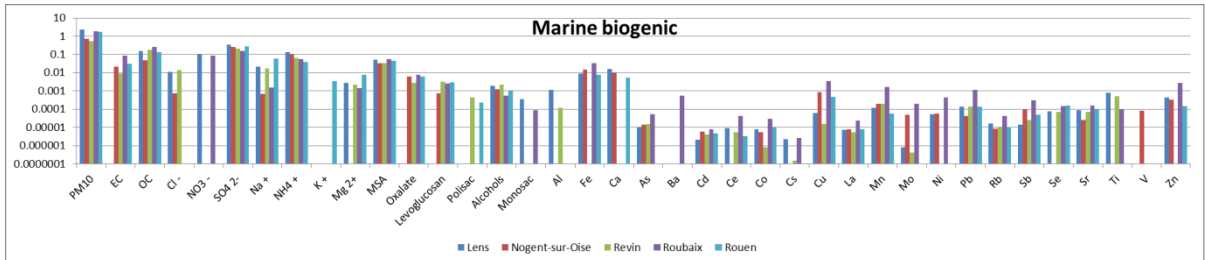
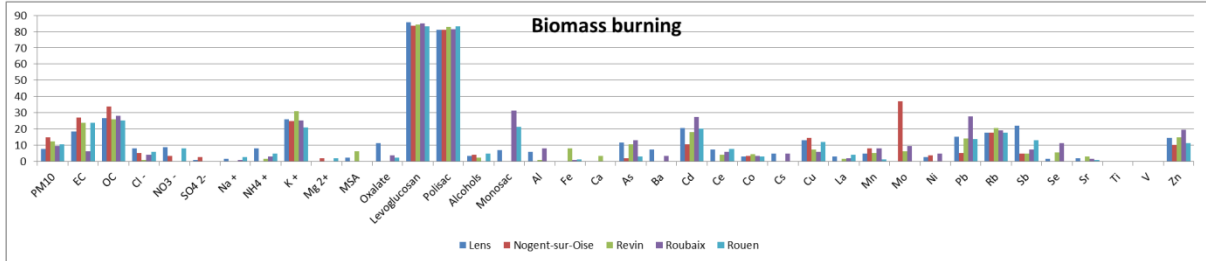
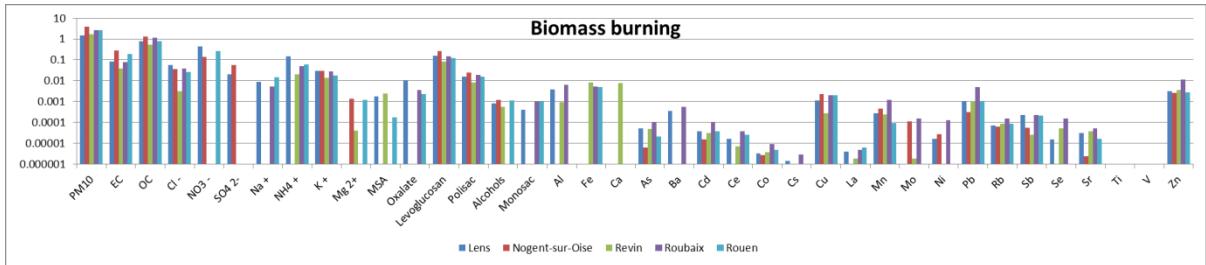
⁶ Atmo Nord-Pas de Calais, F-59800 Lille, France

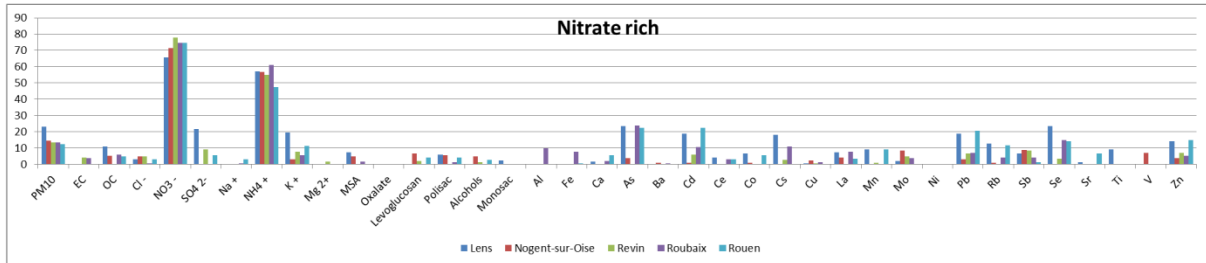
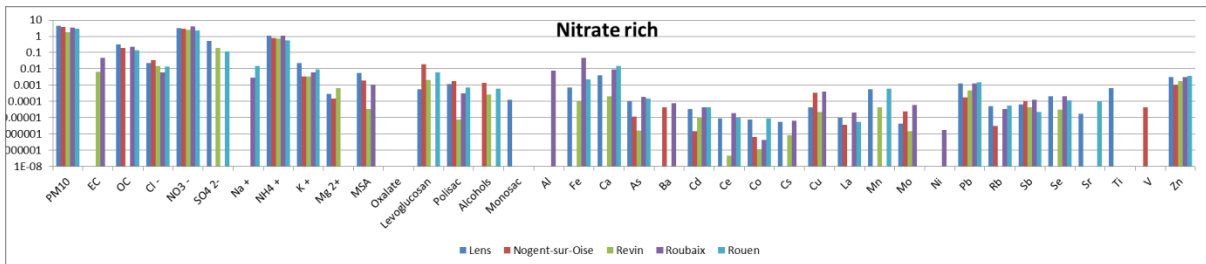
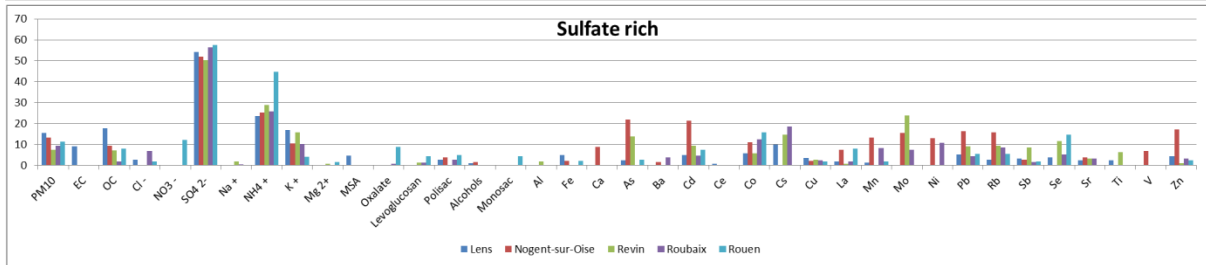
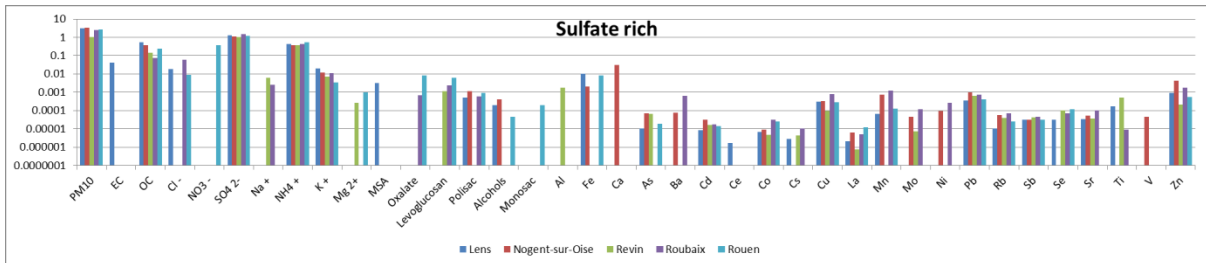
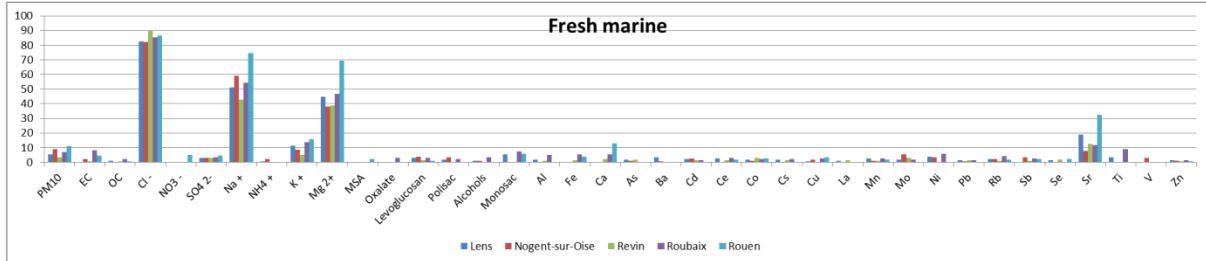
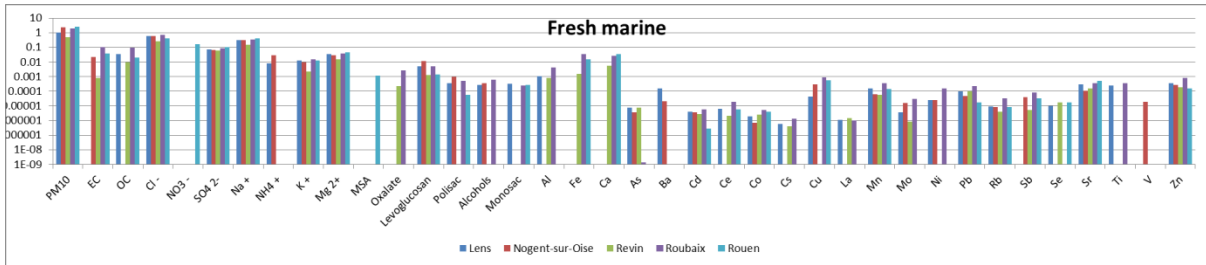
⁷ Air Normand, F-76000 Rouen, France

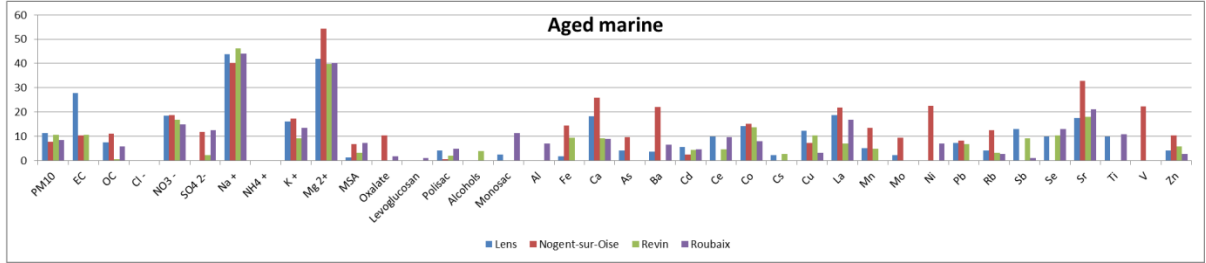
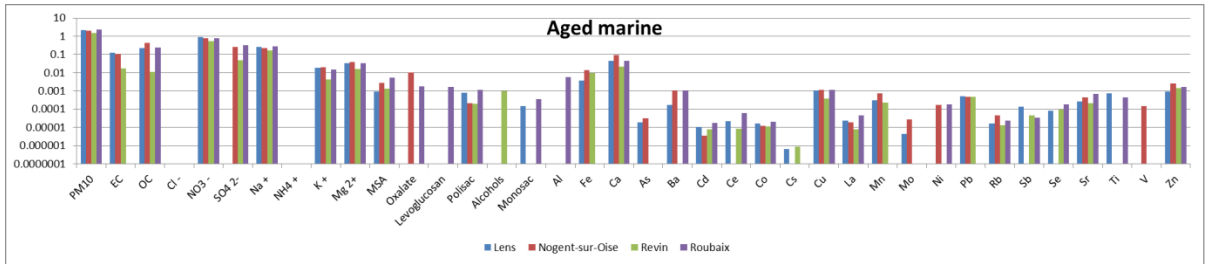
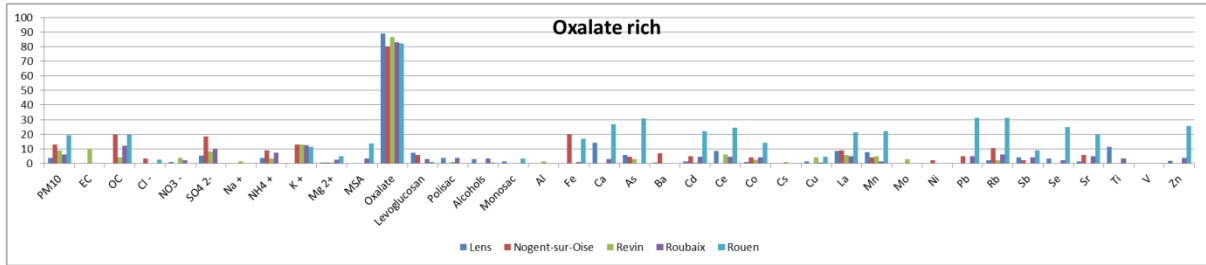
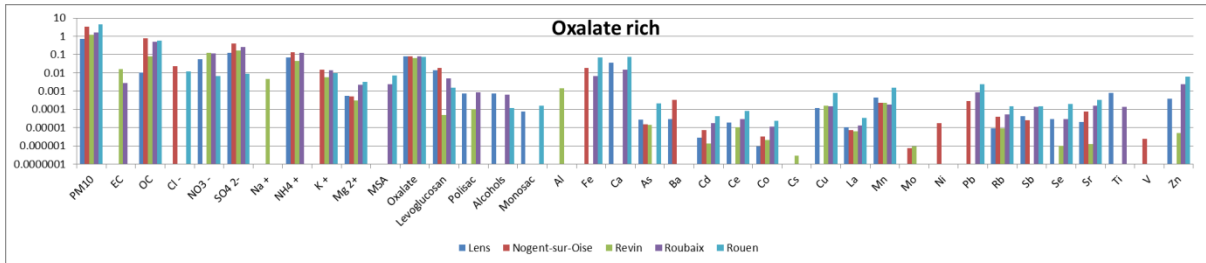
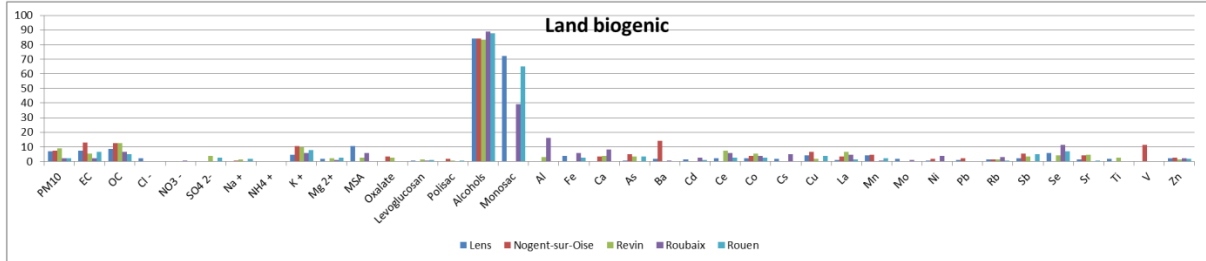
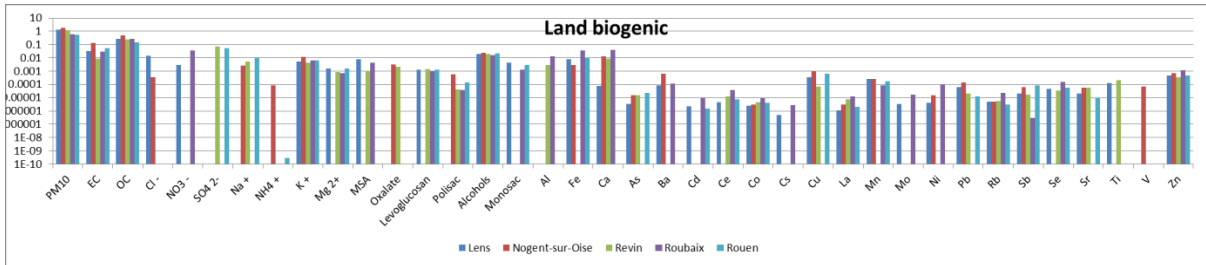
⁸ Atmo Picardie, F-80332 Longueau, France

Table S. 5: Variables characterization as PMF input

	Strong	Weak	Bad
Lens	EC, OC, Cl ⁻ , NO ₃ ⁻ , SO ₄ ²⁻ , Na ⁺ , NH ₄ ⁺ , K ⁺ , Mg ²⁺ , MSA, Oxalate, Levoglucosan, Sugar alcohols, Ca, As, Ba, Cd, Co, Cu, La, Mn, Pb, Sb, Se, Sr, Ti, Zn	PM ₁₀ , Polysaccharides, Monosaccharides, Al, Fe, Ce, Cs, Mo, Ni, Rb	U
Nogent-sur-Oise	EC, OC, Cl ⁻ , NO ₃ ⁻ , SO ₄ ²⁻ , Na ⁺ , NH ₄ ⁺ , K ⁺ , Mg ²⁺ , MSA, Oxalate, Levoglucosan, Polysaccharides, Sugar alcohols, Ca, As, Cd, Co, Pb, Sb, Sr, V, Zn	PM ₁₀ , Monosaccharides, Fe, Ba, Cu, La, Mn, Mo, Ni, Rb	-
Revin	EC, OC, Cl ⁻ , NO ₃ ⁻ , SO ₄ ²⁻ , Na ⁺ , NH ₄ ⁺ , K ⁺ , Mg ²⁺ , MSA, Oxalate, Levoglucosan, Polysaccharides, Sugar alcohols, Ca, As, Cd, Ce, Co, Cu, La, Mn, Pb, Rb, Sb, Se, Sr, Ti, Zn	PM ₁₀ , Al, Fe, Cs, Mo	Monosaccharides
Rouen	EC, OC, Cl ⁻ , NO ₃ ⁻ , SO ₄ ²⁻ , Na ⁺ , NH ₄ ⁺ , K ⁺ , Mg ²⁺ , MSA, Oxalate, Levoglucosan, Sugar alcohols, Ca, As, Cd, Ce, Co, Cu, La, Mn, Pb, Rb, Sb, Se, Sr, Zn	PM ₁₀ , Polysaccharides, Monosaccharides, Fe	U
Roubaix	EC, OC, Cl ⁻ , NO ₃ ⁻ , SO ₄ ²⁻ , Na ⁺ , NH ₄ ⁺ , K ⁺ , Mg ²⁺ , MSA, Oxalate, Levoglucosan, Sugar alcohols, Ca, As, Ba, Cd, Ce, Co, Cu, La, Mn, Ni, Pb, Rb, Sb, Se, Sr, Zn	PM ₁₀ , Polysaccharides, Monosaccharides, Al, Fe, Cs, Mo, Ti	U







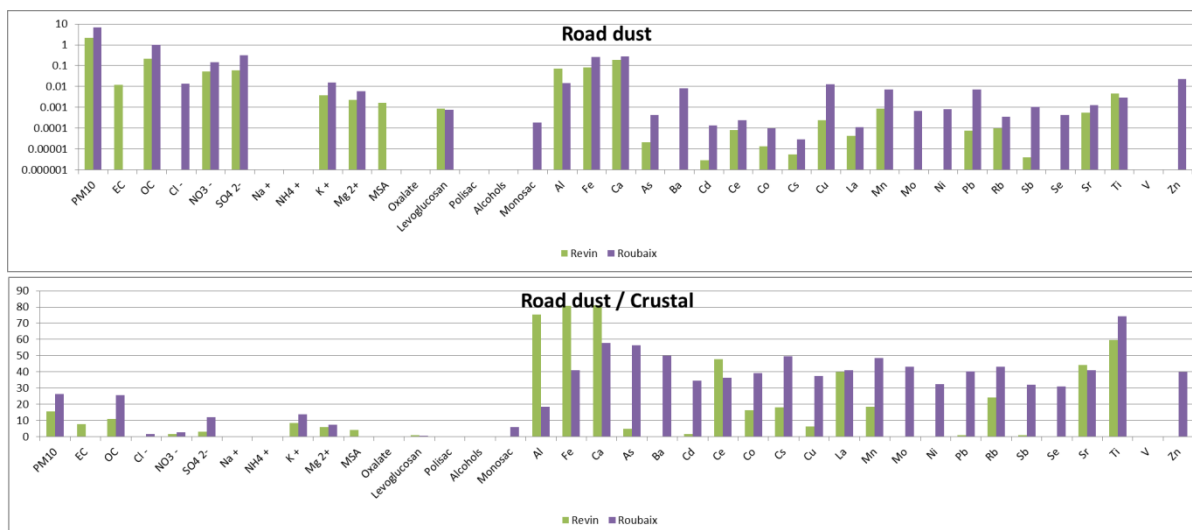


Figure S. 22: Chemical profiles of all the factors found in Lens (dark blue), Nogent-sur-Oise (red), Revin (green), Roubaix (purple) and Rouen (light blue). (top) Concentrations of species in the factor (in $\mu\text{g m}^{-3}$); (bottom) Relative contributions (in %) of species

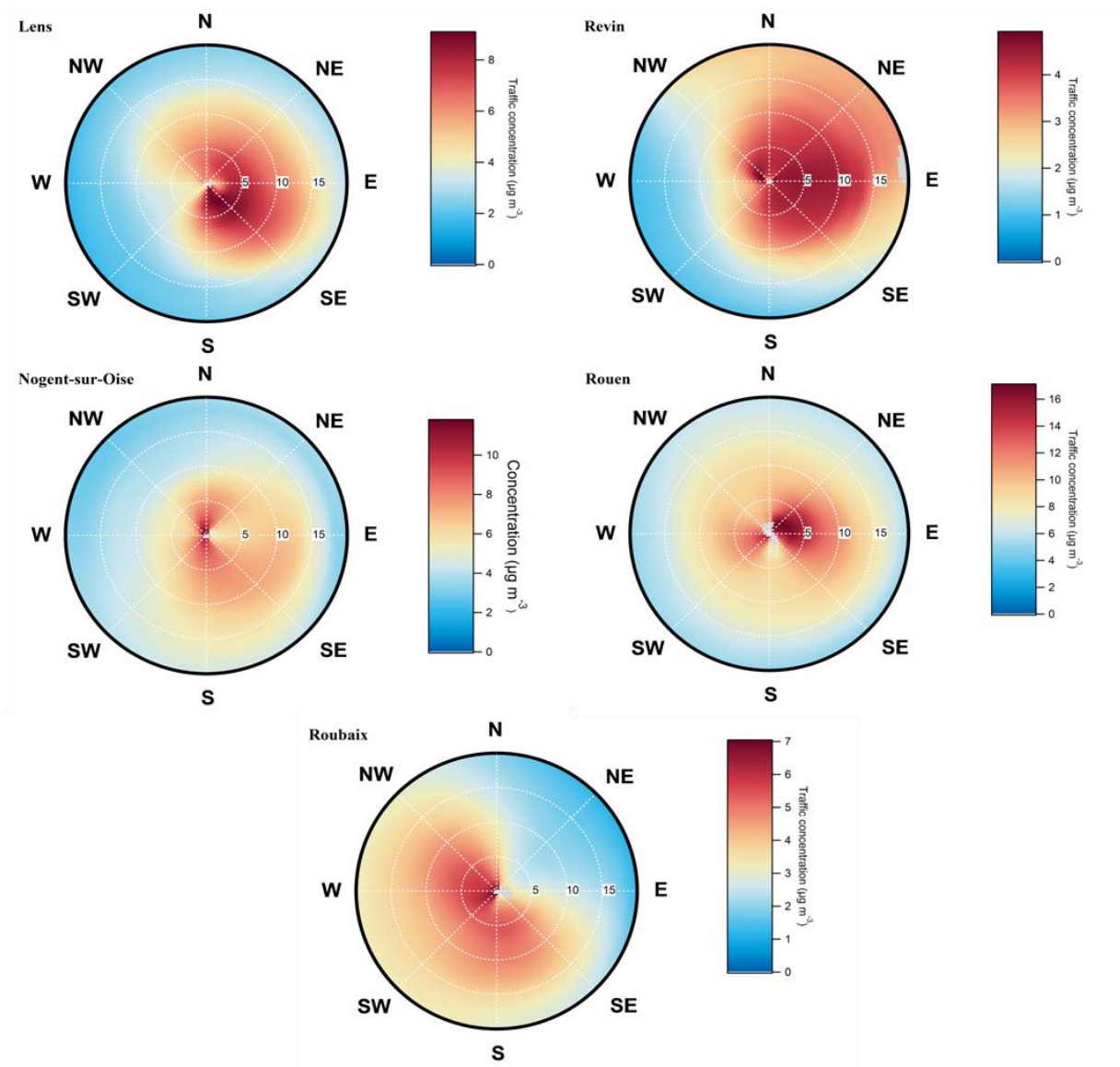


Figure S. 23: NWR plots for primary traffic in Lens, Nogent-sur-Oise, Revin, Rouen and Roubaix

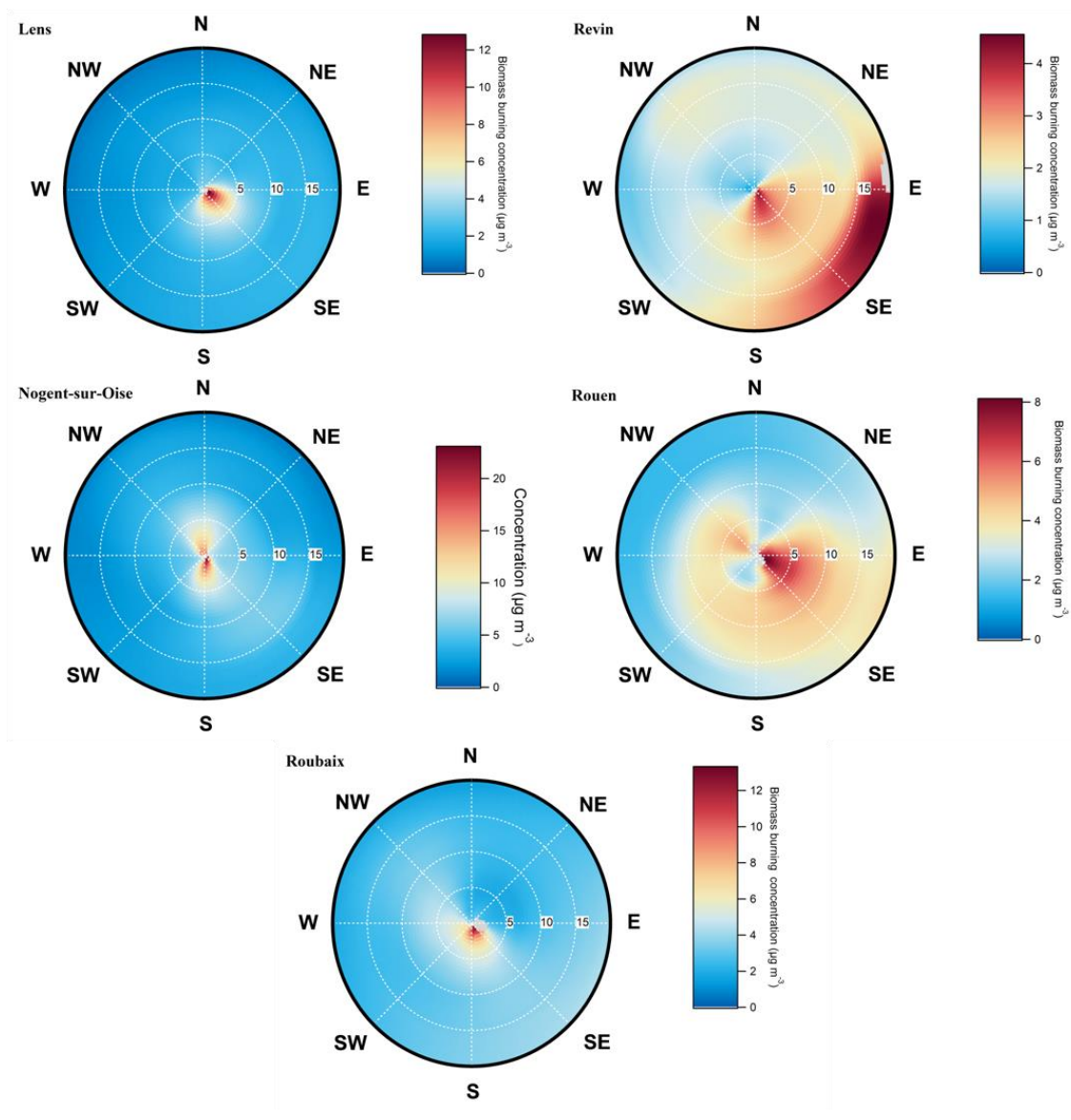


Figure S. 24: NWR plots for biomass burning in Lens, Nogent-sur-Oise, Revin, Rouen and Roubaix

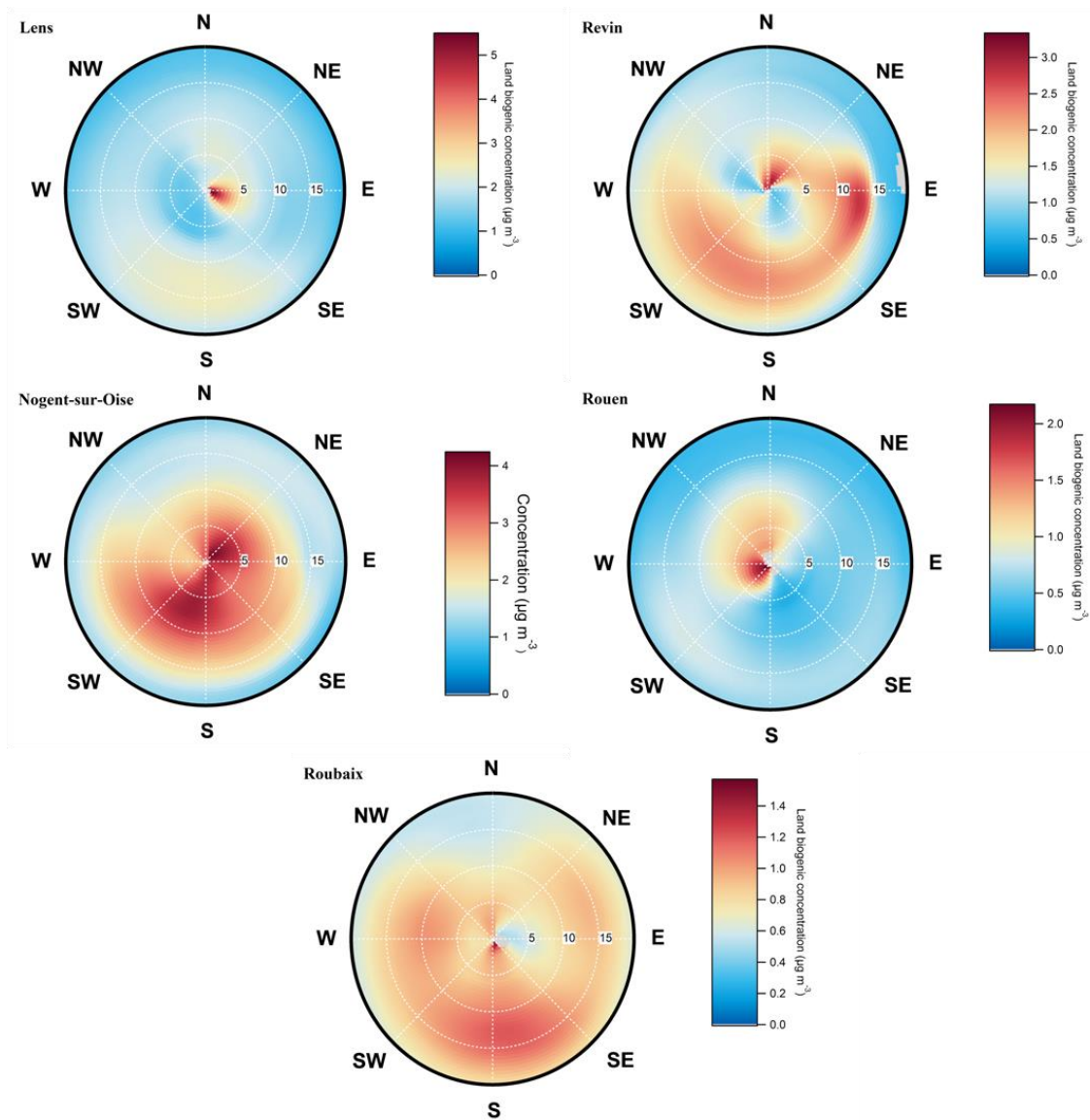


Figure S. 25: NWR plots for land biogenic in Lens, Nogent-sur-Oise, Revin, Rouen and Roubaix

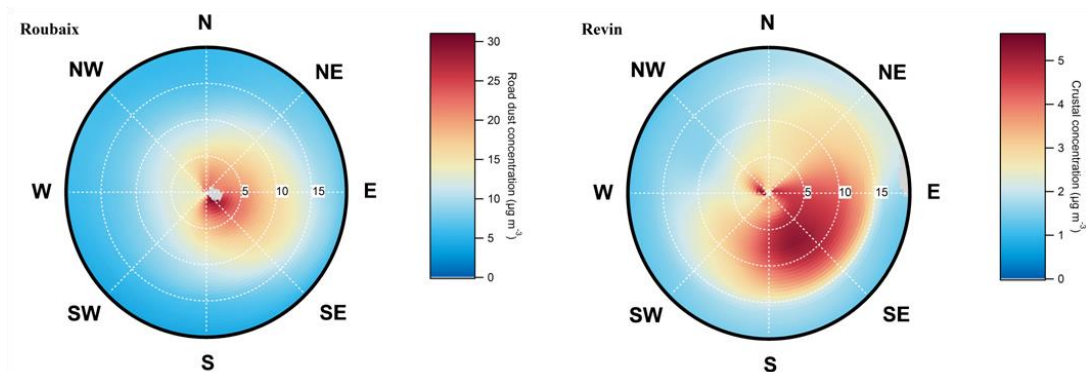


Figure S. 26: NWR for road dust in Roubaix and crustal matter in Revin

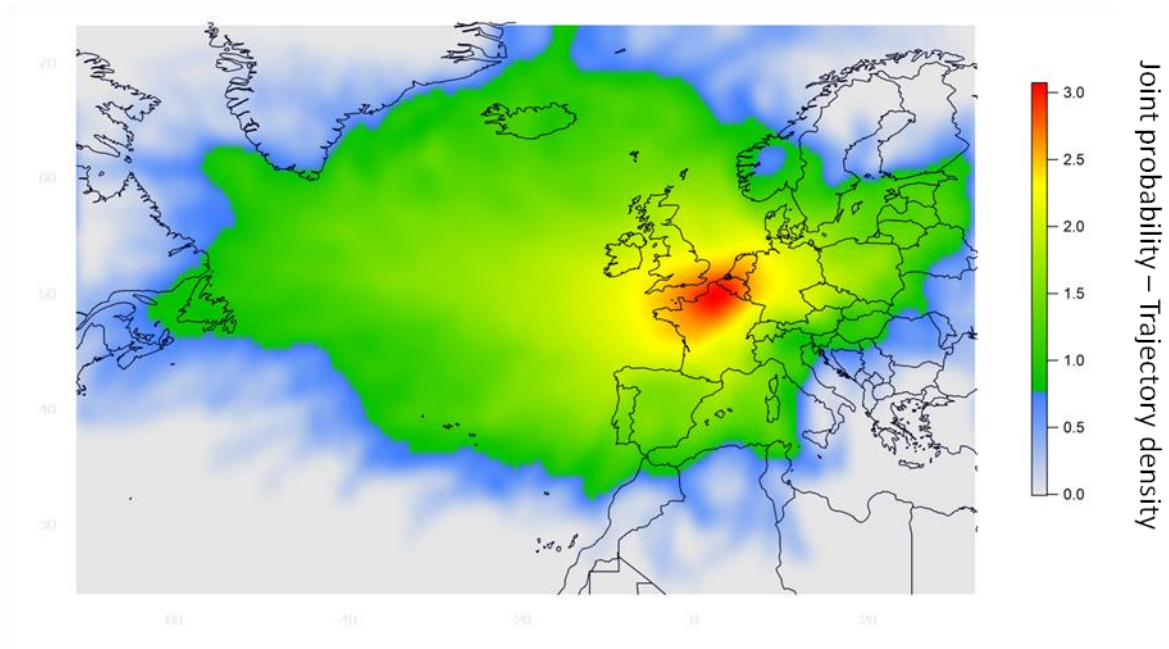


Figure S. 27: Trajectory density for the multi-site Concentration Field method

4.2 Complement of Publication 2

4.2.1 Meteorological data

Regarding local sources meteorological data (wind speed and wind direction) was used to build the pollution roses. Daily averages of wind speed and wind direction were obtained from different meteorological stations of MétéoFrance. Due to the fact that not all the sampling sites had a meteorological station near the sampling apparatus or the needed parameters, close by stations were used instead. Table 12 indicates location and distance of the meteorological stations used for each sampling site:

Table 12: MétéoFrance stations used for each sampling and their corresponding distance

Sampling site	MétéoFrance station	Distance to sampling site (km)
Lens	Lesquin – Lille	26
Nogent-sur-Oise	Creil	3.5
Revin	Rocroi	8
Rouen	Rouen	8.5
Roubaix	Lesquin - Lille	13

The biggest distance seen between a sampling site and the meteorological station used is the case of Lens, where the MétéoFrance station located in Lille, 26 km to the northeast of the sampling site, had to be used. The author understands that there is an associated uncertainty linked to this distance, however it is important to mention that the topography of the terrain in the region is characterized by being very flat. Actually, the highest elevation of land between Lens and Lille is of about 30 to 40 meters. This leads to very similar meteorological conditions in the both cities, minimizing the error associated with the distance between the two.

A cluster study on the backtrajectories arriving to each sampling site was also conducted, showing the predominance of maritime air masses reach the region. On all sites, contributions from continental areas were also identified. These cluster studies are shown in Annex 3, and roughly about 1000 backtrajectories were used in the calculation.

4.2.2 Factors chemical composition

Due to the difficulty of finding uniformed source apportionment factor profiles with the relevant similarities of this work, to understand the chemical composition of the factors obtained several exercises were made related to the species found on each factor. All the chemical and time profiles of these factors are shown in Annex 2.

Starting with the biomass burning factor, the chemical profiles obtained for the 5 sites showed good agreement between them and a local nature associated with low wind speeds on 4 of the 5 sites. Predominance on wood burning activities for house heating purposes was then assumed. Several studies have tried to estimate the contributions of biomass burning to PM₁₀ mass having into account measured concentrations of levoglucosan (Caseiro et al. 2009; Schmidl et al. 2008; Maenhaut et al. 2012; Maenhaut et al. 2016). On these studies, that had similar characteristics to the one here conducted, a factor of 10.7 was used to convert levoglucosan levels to the PM₁₀ mass associated with wood smoke. These values were compared to the ones obtained for the biomass burning factors on each site.

Table 13: Contributions to PM₁₀ mass of wood smoke (calculated from levoglucosan by a factor of 10.7), biomass burning factors (obtained from PMF) and the new calculated factor

		Wood smoke (% of PM ₁₀)	Biomass burning (% of PM ₁₀)	→ (factor)
Lens	Average	11	8	8
	Winter 13	16	14	9
	Winter 13-14	26	18	7
Nogent-sur-Oise	Average	9	15	17
	Winter 13	20	27	14
	Winter 13-14	18	29	17
Revin	Average	8	13	18
	Winter 13	14	26	20
	Winter 13-14	18	29	17
Rouen	Average	8	11	14
	Winter 13	22	21	10
	Winter 13-14	12	23	20
Roubaix	Average	7	10	15
	Winter 13	14	20	16
	Winter 13-14	16	20	14

Results (table 13) show that the contribution of wood smoke to PM₁₀ was underestimated in 4 of the 5 sites, being Lens the only exception. A new factor was calculated that would explain

the contribution of PM₁₀ based on levoglucosan concentrations. A slight overestimation of wood smoke is obtained in Lens when compared to the PMF solution obtained, whereas in the other sites higher contributions of this factor were found, suggesting a greater importance of other species present in the chemical profiles.

When comparing the daily contributions obtained from both methods the following scatterplot is obtained:

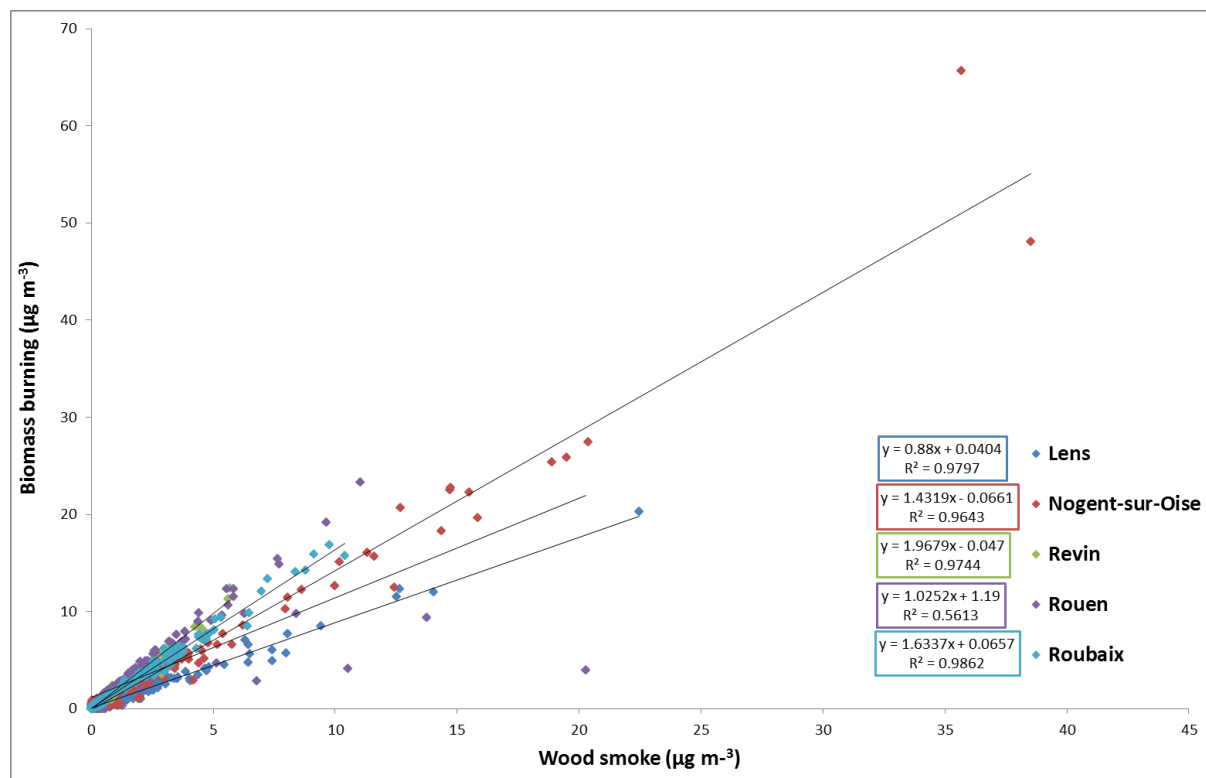


Figure 53: Correlations between wood smoke concentrations obtained from levoglucosan and biomass burning contributions calculated from PMF on each sampling site

Good correlations were seen for 4 of the 5 sites (figure 53), here Rouen being the exception. This was found to be linked with just 4 to 5 points identified in February 2013, where higher concentrations of levoglucosan were recorded, without however being followed by other important biomass burning compounds like OC and K⁺. Once these points are not considered, the correlation obtained between both methods increases to R²=0.97 instead of R²=0.56, much more in accordance with the other sampling sites. With this, one must consider the possibility of a possible analytical error associated these samples and show the ability of PMF to overcome this fact. One should also consider the possibility of the presence of a specific isolated source contributing to levoglucosan emissions during these days, with

PMF not being able to identify it. In both cases, the reduced number of samples in question explains the results seen.

This results allow to conclude that although the method is able to reproduce wood smoke emission tendencies, values to estimate its actual contribution to PM₁₀ mass are suspected to be higher than 10.7.

Based on the mass closure / ion balance performed to the main ions contributing to PM₁₀ and exposed on point 2.4.2 of this manuscript, the main species derived were NaCl, NaNO₃, (NH₄)₂SO₄, and NH₄NO₃. Since several factors with important contributions of ions were found on all sites, is then interesting to verify if these species were found under the same formulation by PMF. Daily contributions of fresh sea salt were compared with concentrations of calculated NaCl, nitrate rich contributions were compared with NH₄NO₃, sulfate rich aerosols with concentrations of (NH₄)₂SO₄ and aged marine contributions with NaNO₃. These results are presented in Annex 2 and is visible a good agreement between the obtained factors and the calculated salts, with the lowest R² seen in Nogent-sur-Oise for the aged marine correlation. Aged marine factors shown weaker correlation with the calculated salt NaNO₃, which was expected since to calculate contributions of this salt, assumptions were already made on preferable state of both sodium and nitrate. Also, species with nitrate are often unstable and depend highly on meteorological conditions, so lower concentrations with this salt are not strange. Also, for aged marine aerosols, factor contributions were always around 2 times higher than the concentrations of NaNO₃, suggesting the presence of other species with significant importance to the mass of these particles. Correlations between the fresh marine factors and contributions of NaCl on each site were seen to be always very good, with R² values above 0.94. In Roubaix, Revin and Lens the slope of the correlation was seen to be near the unit, indicating that the contribution of the factor is well explained by concentrations of NaCl, however in Nogent-sur-Oise and Rouen, factor contributions were seen to be 2.5 times than NaCl concentrations, again suggesting that this salt is not the only contributor to fresh marine particles collected in these sites. Even in the case of Rouen, where an aged marine factor was not identified, the sum of NaCl and NaNO₃ still underestimates this factor contribution. Finally, for secondary inorganic aerosols, good correlations were also found between the factors and the calculated concentrations of this species (R² above 0.82). The slopes of these correlations were also found to be near the unit, with a slight tendency to overestimate factor contributions based on components concentrations. This suggests than not

all the sulfate and nitrate rich particles are as $(\text{NH}_4)_2\text{SO}_4$, and NH_4NO_3 , respectively, and that other species are also found associated with these aerosols.

4.2.3 Seasonal contribution of factors

From the obtained solutions of PMF on each site, the seasonal contributions were calculated for the different sources. These sources were divided first in local and regional influence, and also characterized as being from natural and anthropogenic processes.

From the local sources identified in this study, traffic and biomass burning are associated with anthropogenic activities

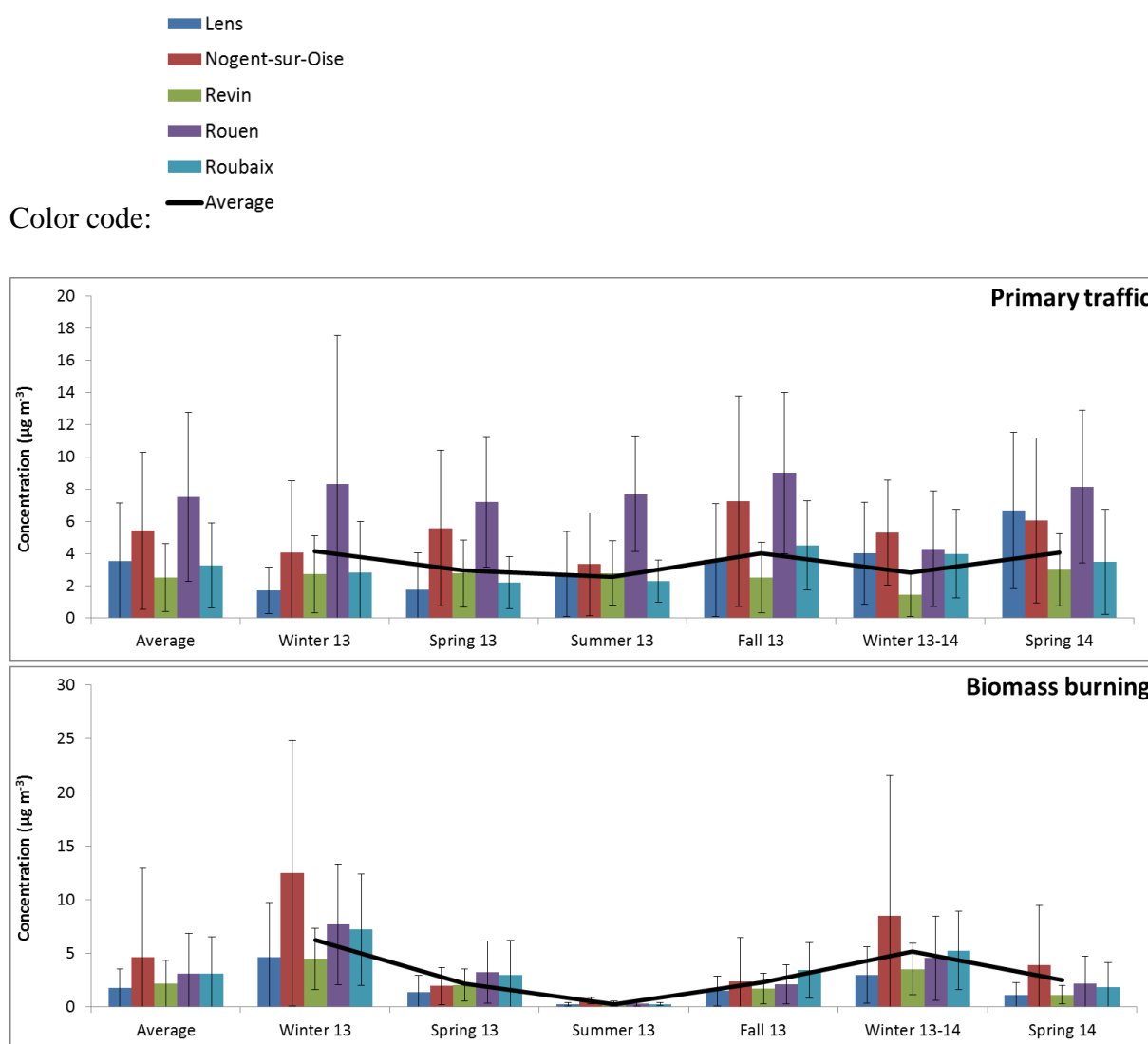


Figure 54 & 55: Primary traffic (top) and biomass burning (bottom) average and seasonal contributions in $\mu\text{g m}^{-3}$

From primary traffic (figure 54), highest concentrations were seen Roubaix, the traffic site of this study. Nogent-sur-Oise also showed important contributions of this source to PM₁₀ concentration. No particular seasonality was seen associated with traffic related particles. Biomass burning (figure 55), in this study associated with house heating combustion showed in Nogent-sur-Oise its higher concentrations. A clear seasonality is associated with these emissions, with an increase during winter on all sites, as expected. Higher contributions were seen also in Revin, the remote site, during this season, proving the potential regional impact of these emissions.

Biogenic particles were identified in this study in all sites. Biogenic particles with land origin were traced by sugar alcohols and were seen to have either a local impact, or a relatively small regional impact (in some sites associated with mild wind speeds). On the other hand, biogenic with maritime origin, traced by MSA, have a regional impact and are originated in the North Sea.

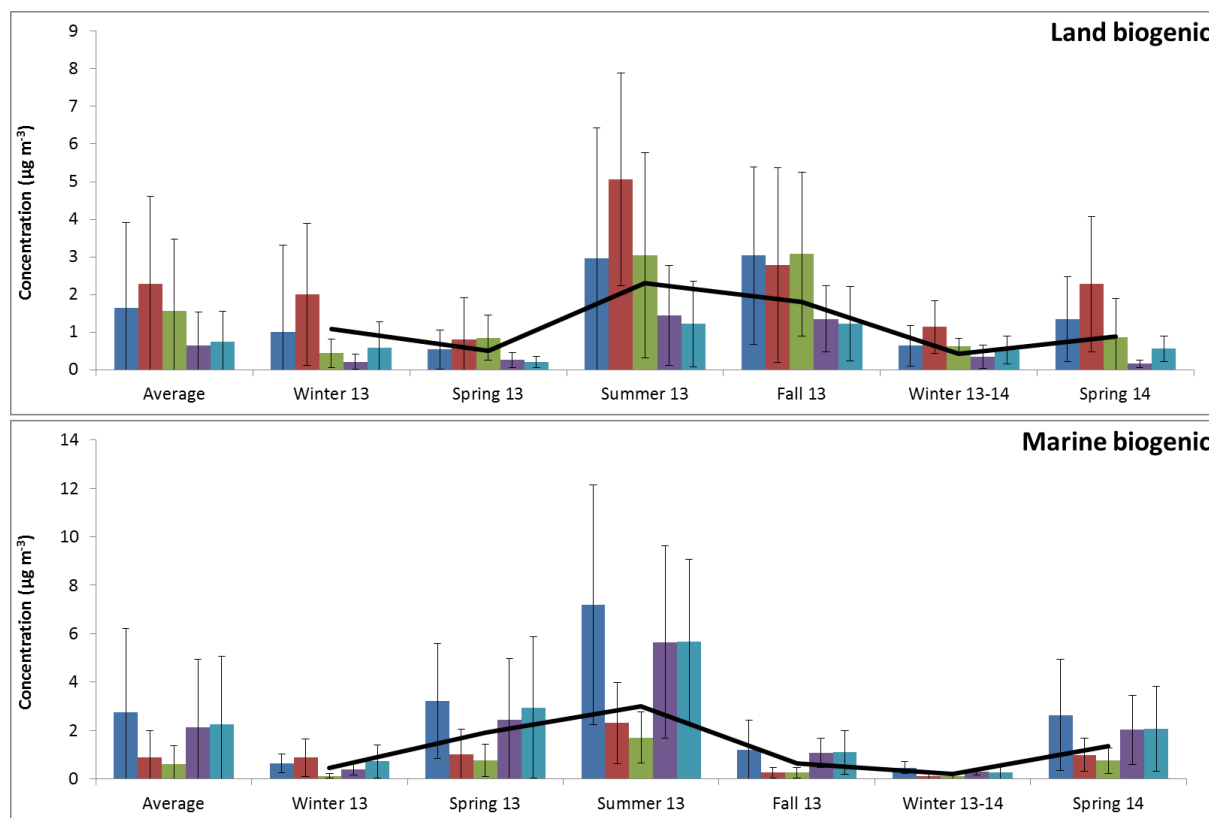


Figure 56 & 57: Land biogenic (top) and marine biogenic (bottom) average and seasonal contributions in µg m⁻³

Clear seasonality was seen associated with both types of aerosols, with higher contributions during summer. Land biogenic particles (figure 56) recorded higher concentrations during

summer and fall on all sites, result also seen in other studies (H. Bauer et al. 2008; Winiwarter et al. 2009; Burshtein, Lang-Yona, and Rudich 2011; Kourtchev et al. 2009), and marine biogenic (figure 57) during spring and summer, also an expected result according to (Bove et al. 2016; Healy et al. 2015; Bougiatioti et al. 2013). A reference to the fact that lower concentrations were seen in the sampling sites of Nogent-sur-Oise and Revin, both sites the ones located farthest from the coast.

Identified as natural regional sources, fresh and aged sea salts were seen in all sites in this study with the exception of the site of Rouen, where an aged sea salt was not identified. This was attributed to the fact that Rouen is the site located closest to the coast.

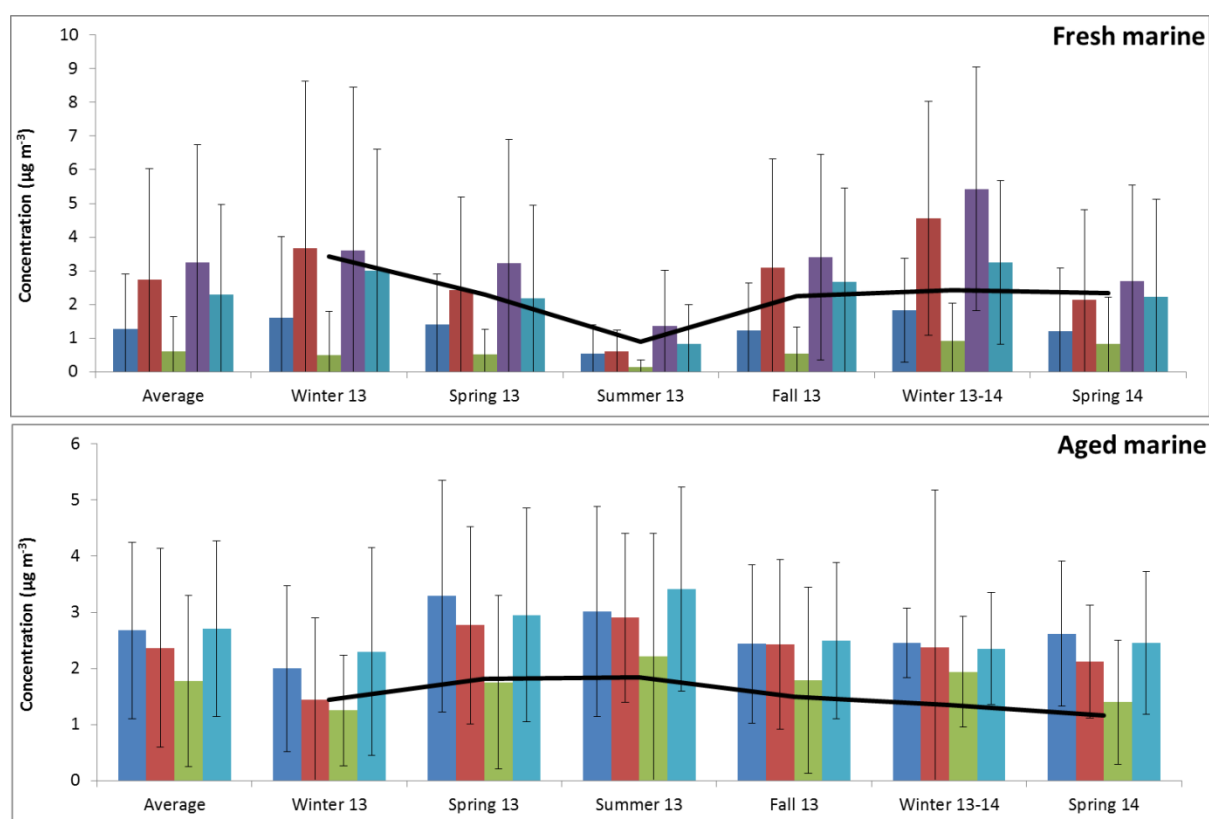


Figure 58 & 59: Fresh marine (top) and aged marine (bottom) average and seasonal contributions in $\mu\text{g m}^{-3}$

A seasonal pattern was observed to fresh sea salt particles (figure 58), with lower contributions during summer, remaining rather constant throughout the rest of the year for all sites. This can be associate with the fact that in summer, storms in the Atlantic Ocean are rarer (Manders et al., 2009). On the other hand, aged sea salt did not show any particular seasonal trend (figure 59). This is an indication that not only the regional origin of these particles is not the same as fresh sea salt (Publication 2), but also the processes of formation

and emission of these particles have to be different. For both sources of aerosols, the sampling less impacted is Revin, the site farthest from sea water.

On all the sites, secondary aerosols were found under the form of nitrate rich, sulfate rich and oxalate rich particles.

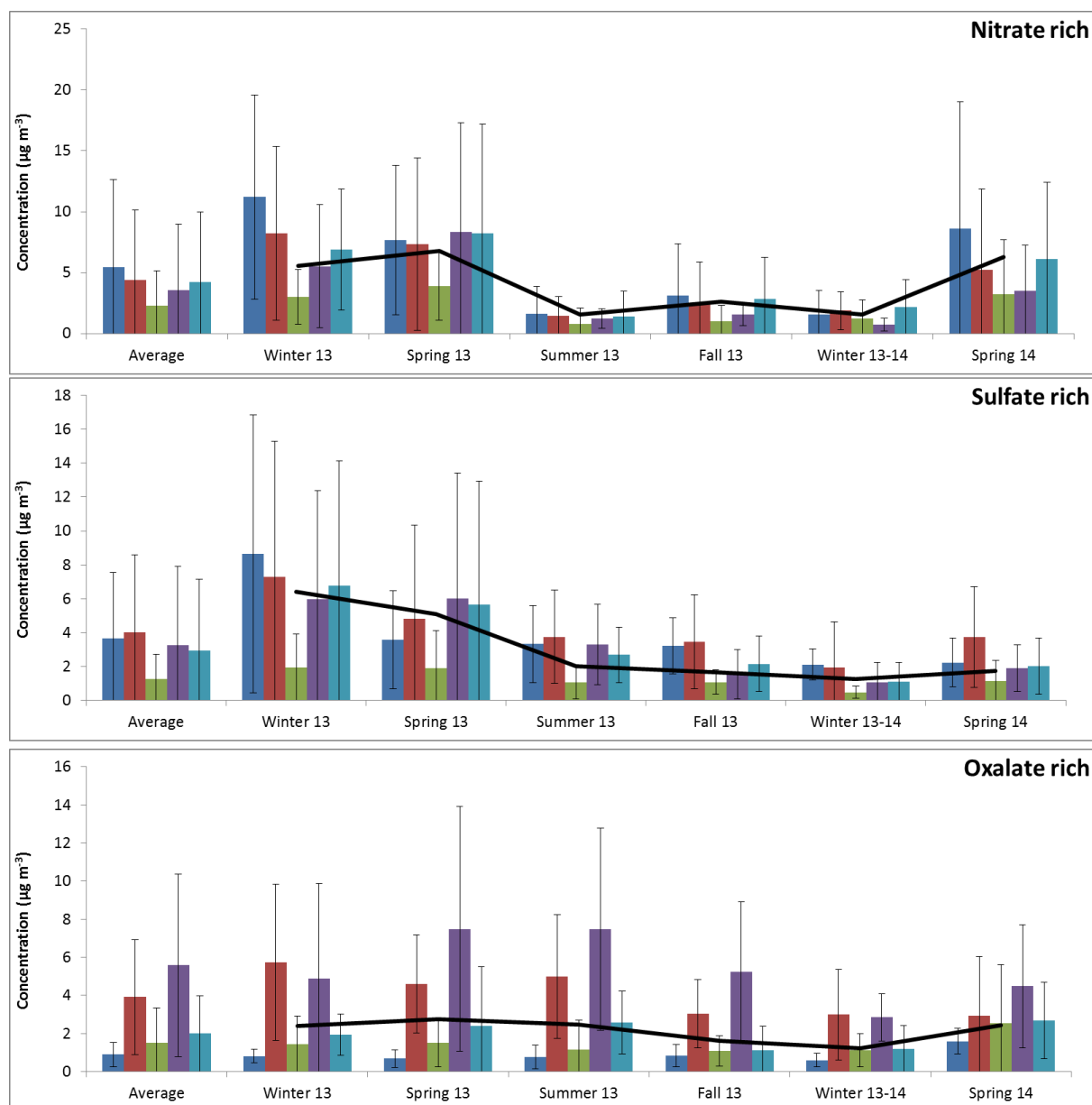


Figure 60, 61 & 62: Nitrate rich (top), sulfate rich (middle) and oxalate rich (bottom) average and seasonal contributions in $\mu\text{g m}^{-3}$

The secondary inorganic aerosols found in this showed similar seasonal trends. Higher concentrations were recorded during spring for nitrate rich particles, and winter for sulfate rich particles. It is visible that the winter of 2013 and the winter of 2013-2014 were quite

different regarding contributions of these sources. It was already showed the meteorological differences seen between these two seasons, which help to explain the discrepancy seen from one year to the other. Other factor that may have influenciated these levels is linked with the studied period. In 2013 samples were collected from January, not accounting therefore the month of December like for the winter of 2013-2014. It also known that nitrate rich particles are associated with agricultural activities which tend to start late winter / early spring, being a possible reason for the seasonal discrepancy seen for the nitrate rich factor. However, for sulfate rich particles the seasons of 2013 recorded considerable higher concentrations than in 2014, and here the only explanation resides in the meteorological conditions seen in each case. The oxalate rich factor did not show any particular seasonal trend during the studied period, leading to the hypothesis already exposed that these particles are a result of a multitude of precursor species with different emission patterns.

4.2.4 Contribution during high concentration episodes

The source apportionment exercise carried out in the 5 sampling sites allows also assessing what are the impacting sources during high concentration episodes but averaging the daily contributions of the factors. This study has to be made with care because high concentration episodes can be associated with a multitude of parameters that are not always easy to identify. Another source of uncertainty concerning these results is the different number of these episodes from site to site. As mentioned before in this work, for example the site of Revin just recorded one day with PM₁₀ concentrations above the legal limit of 50 µg m⁻³. Also, with the study of the chemical composition of PM₁₀ during these episodes it was seen a variability on the average composition as well as differences on the chemical composition on specific episodes.

Figure 63 shows the average contributions of sources during days with PM₁₀ concentrations above 50 µg m⁻³.

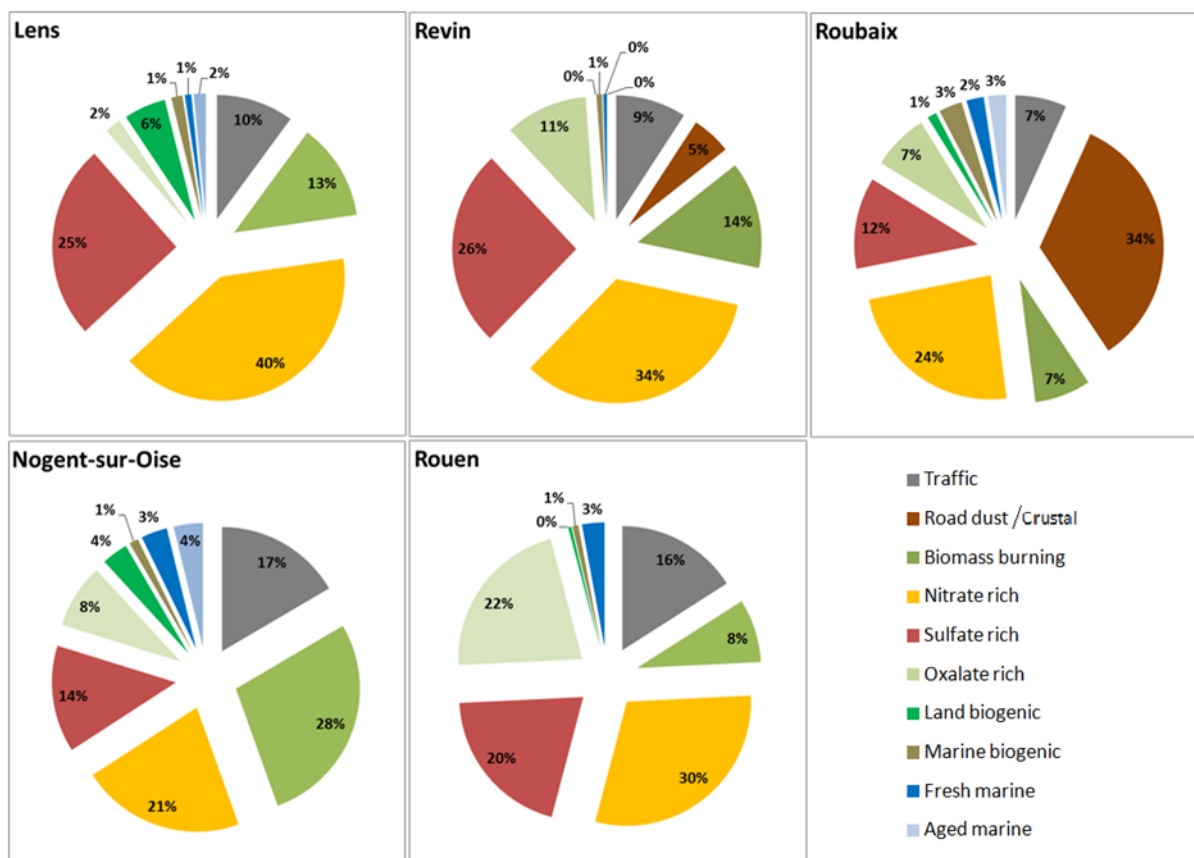


Figure 63: Average source contribution during days with PM_{10} mass concentration above $50 \mu g m^{-3}$ in Lens, Nogent-sur-Oise, Revin, Rouen and Roubaix

Source contributions vary from site to site. The sites of Revin, Rouen and Lens showed important contributions of secondary aerosols. In Revin and Lens, nitrate rich and sulfate rich contributed 60% and 65%, respectively to PM_{10} concentrations. Also in both sites biomass burn as an important contribution during these events being followed by oxalate rich particles in Revin and primary traffic in Lens. In Rouen, also oxalate rich and primary traffic were major sources for high PM_{10} , with less impact of biomass burning. Nogent-sur-Oise recorded the largest contribution of biomass burning of all sites during high concentration episodes supporting the observations of intensive use of this mean to house heating proposes. Nitrate and primary traffic were the following main contributors, followed by sulfate rich and oxalate rich particles. Finally in the site of Roubaix high concentrations were seen linked with high concentrations of road dust which in this site was found associated with traffic. Also nitrate rich particles have a significant contribution during these events.

As mentioned, is interesting also to differentiate source contributions in specific days. Two days were selected during chemical characterization – 6th and 30th of March 2013.

During the 6th of March 2013 the main contributing can be seen in figure 64:

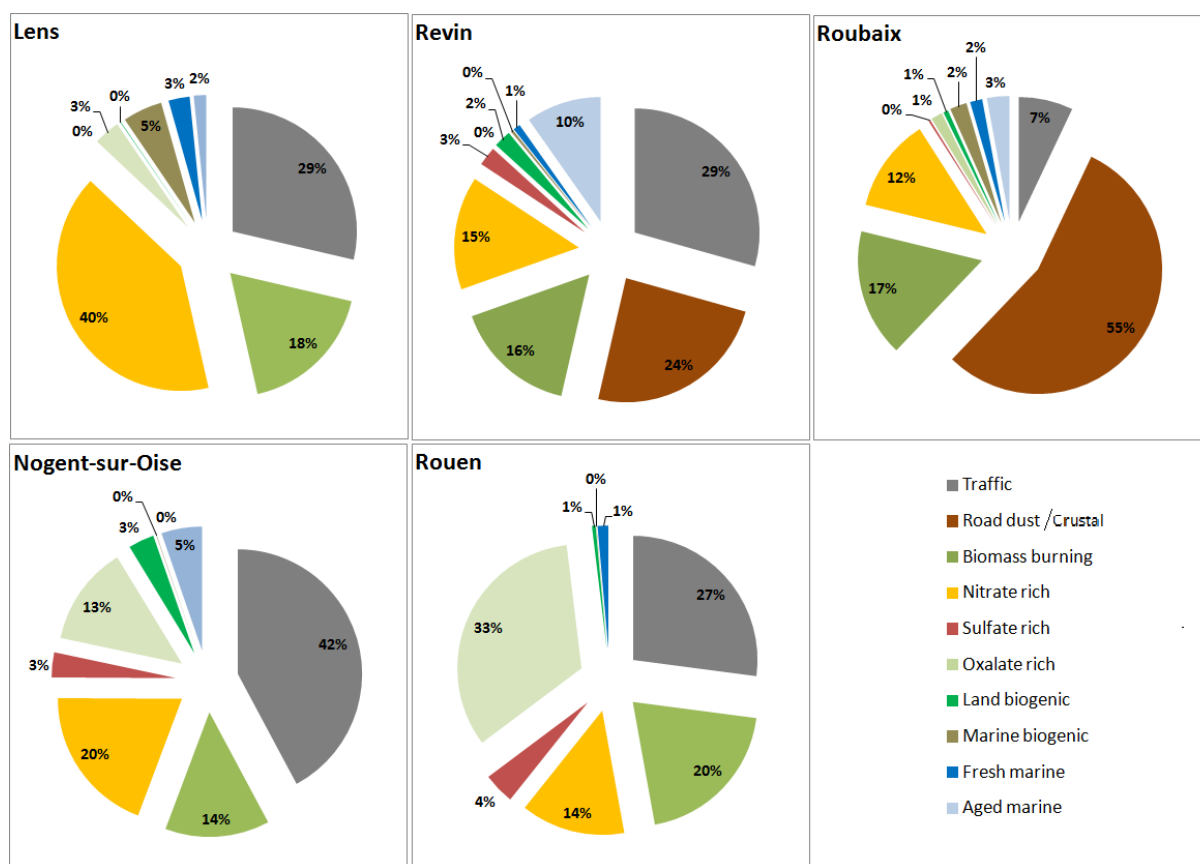


Figure 64: Average source contribution during the 6th of March of 2013 in Lens, Nogent-sur-Oise, Revin, Rouen and Roubaix

During this day, on all sites was seen an important contribution of more local sources to PM_{10} concentration. In Nogent-sur-Oise a significant contribution of nitrate rich particles was observed. Curiously no contribution of sulfate rich particles was observed so there is the possibility that this nitrate rich particles were formed from local emissions of nitrate precursors. On the other sites, strong contributions of traffic related emissions were observed, ranging from 42% to 27% in Rouen. Rouen also recorded high concentrations of biomass burning and oxalate rich particles. In Roubaix road dust emissions were the main source during this day with more than 55% contribution to PM_{10} . Primary exhaust traffic emissions did not show a strong increase, suggesting that this episode is motivated from favorable meteorological conditions in the sites, with low temperatures and low wind speeds.

Another selected sample was the 30th of March 2013 (figure 65).

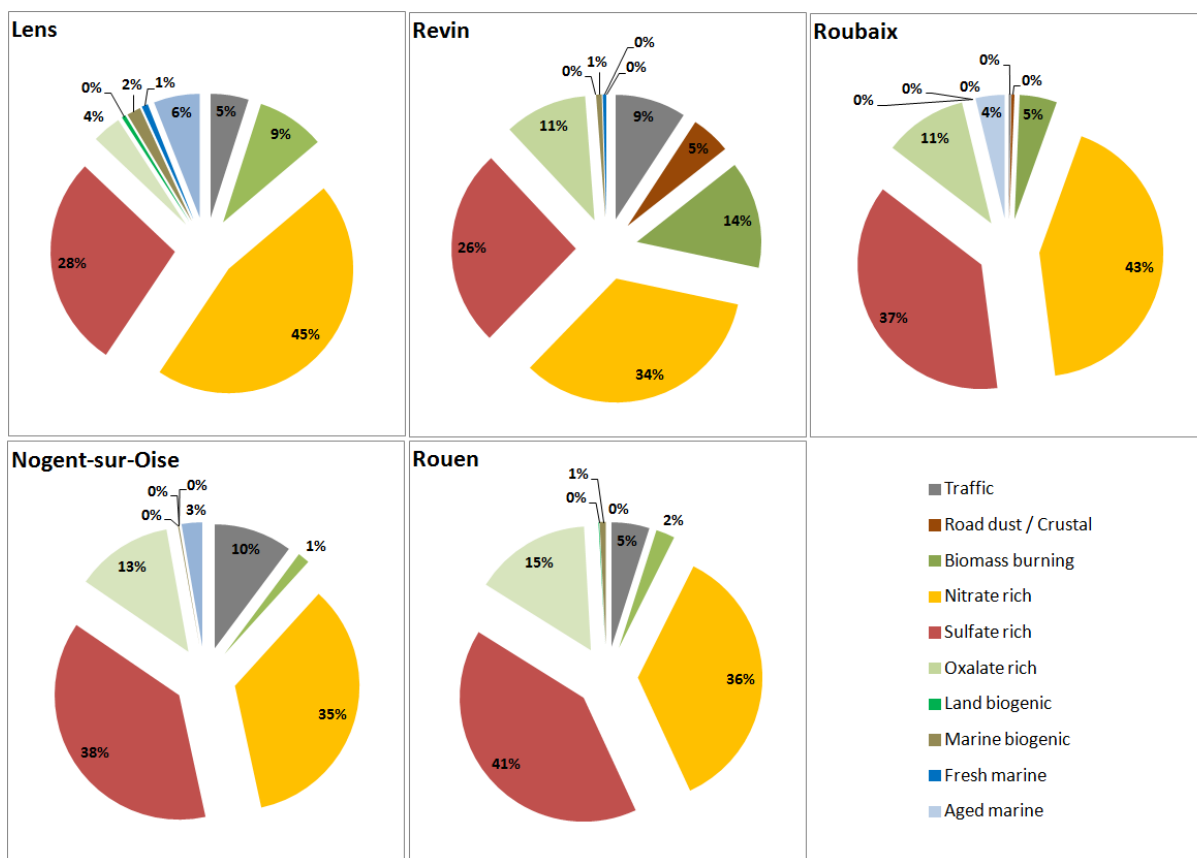


Figure 65: Average source contribution during the 30th of March of 2013 in Lens, Nogent-sur-Oise, Revin, Rouen and Roubaix

This day has clear distinct influence of sources to the high concentrations of PM₁₀ observed. On all sites, a large contribution of secondary inorganic aerosols was observed ranging from contributions of 60% in Revin, up to 80% in Roubaix. This is an important indication that high concentrations of PM₁₀ can occur in the region being driven either by local sources either by long-range aerosols.

4.2.5 Local and regional sources. Natural and anthropogenic sources

The sources seen on each were characterized as local and regional, according to literature, tracers ratios and NWR plots on each site. The origin of particles was directly linked with the typology of each site. These sources were also characterized by the nature of the emitting sources as natural and anthropogenic. Here a couple of these sources have to be dealt with care:

- The aged marine aerosols identified in this study, although the natural origin of sea salts, important contributions of metals was seen in all sites. Metal concentrations are overall low when compared with the ions, so this factor can be characterized as a natural one but an anthropogenic input cannot be ignored
- Oxalate rich particles were seen to be formed from a multitude of precursors with different origins. An anthropogenic fraction is associated first with the sulfate present in the chemical profile of this factor, and also with the emission of VOC's from combustion processes. Also a natural component of this factor can be associated with the natural origin of organic matter precursor to oxalate. Linked to this, one can also see a possible local and regional origin of oxalate rich particles, evident in the NWR plots obtained. However, from the strong contribution of sulfate, this factor can be labelled as from regional and anthropogenic origin, having in mind that there will be a fraction impossible to quantify of local and natural influences

With these, the origin of particles was assessed for urban sites (figure 66):

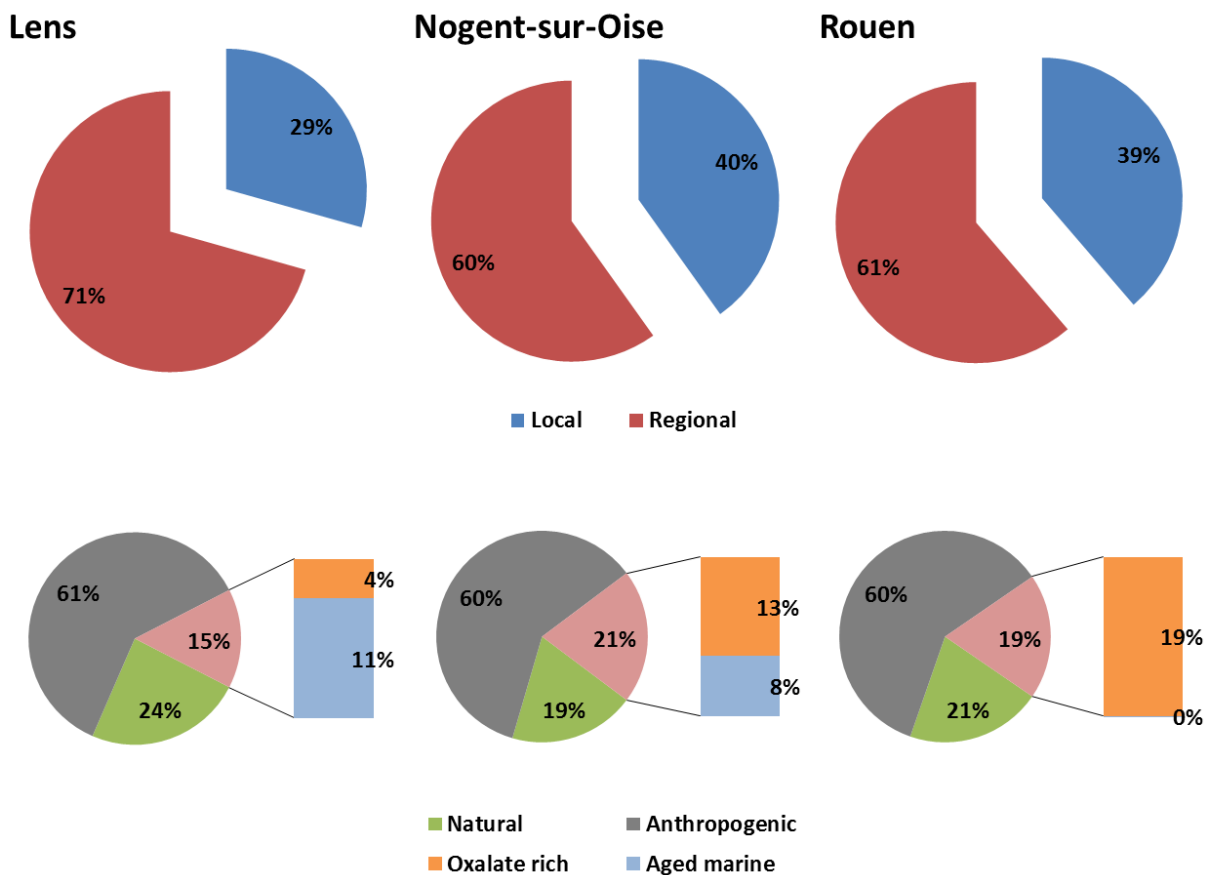


Figure 66: Regional and local (top) and natural and anthropogenic sources (bottom) average contributions on the urban sites (Lens, Nogent-sur-Oise and Rouen)

Recalling results already presented, PM₁₀ mass concentration levels were higher in Nogent-sur-Oise with $27.7 \pm 16.8 \mu\text{g m}^{-3}$. This site was also the one see higher contribution of local sources (40%) driven by primary traffic and biomass burning particles. Rouen, which recorded a PM₁₀ concentration close to Nogent-sur-Oise ($25.6 \pm 14.2 \mu\text{g m}^{-3}$) also showed similar distribution of local and anthropogenic sources contribution (39% of local and 61% of regional sources). In Rouen however, traffic was the main contributor of the local sources. Finally Lens had more significant contributions of regional sources when compared with the other urban sites due to significant lower traffic emissions and higher contribution of secondary aerosols.

Regarding the nature of the sources of aerosols, anthropogenic sources were: nitrate and sulfate rich, primary traffic, road dust and biomass burning; and natural sources were: fresh sea salt and land and biogenic particles. The oxalate rich and aged marine factors were considered as “mixed” factors, with the first with a more anthropogenic influence and the latest with more natural influence.

It is interesting to see that on the 3 sites the anthropogenic contributions are very similar (between 60% and 61%). Oxalate rich particles appear with a bigger influence in Rouen and lower in Lens and aged marine aerosols were not seen Rouen, but showed an important contribution in Lens.

For the sampling site of Roubaix, the traffic site, the same exercise was carried out.

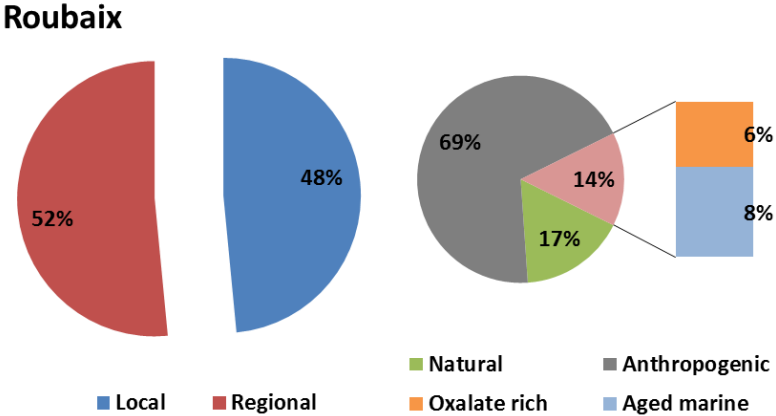


Figure 67: Regional and local (left) and natural and anthropogenic sources (right) average contributions on the traffic site (Roubaix)

Here, a stronger influence of local sources is clear, when compared to the urban sites, accounting for 48% of PM_{10} (figure 67). This is an expected result given the proximity of the site to primary traffic emissions and the high contribution of road dust particles already shown in this work. Consequently, also a higher fraction of PM_{10} is then associated with anthropogenic activities when compared to the other sites, and lower impact of natural sources, an expected result as well. This site was one where higher average concentrations of PM_{10} were seen throughout the study ($28.0 \pm 15.4 \mu\text{g m}^{-3}$).

Finally, for the remote site of Revin different considerations were done.

Revin

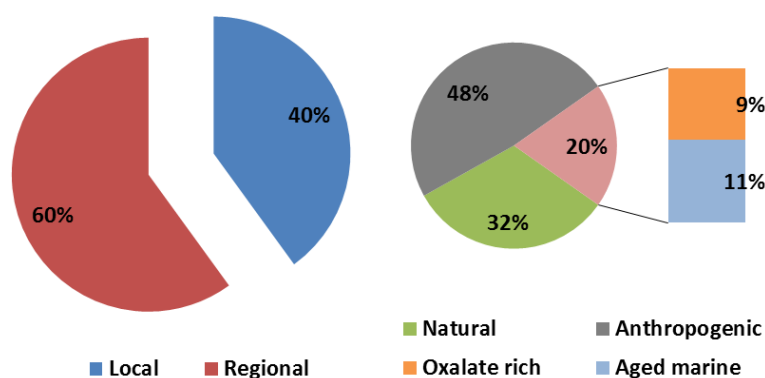


Figure 68: Regional and local (left) and natural and anthropogenic sources (right) average contributions on the remote site (Revin)

For this site, and based on the obtained plots of NWR associated with the different sources, the local sources impacting this site were seen to be primary traffic, crustal matter and land biogenic particles. It is important to point that these sources were not seen to be associated with very low wind speeds, but rather with mild wind speeds, suggesting that although the geographical location of the emission sources of these particles is not located very close to the sampling site, one can assume that they are located in vicinity. This is an interesting discussion regarding the definition of local and regional sources, and how it related with the distance between sampling site and source location.

Was seen that in Revin 40% of the sources contributing to PM_{10} mass had local origin, a result similar to the one obtained for the urban sites (figure 68). Again, here it should be pointed out that for example primary traffic in urban areas was associated with very low wind speeds, whereas in Revin with mild wind speeds. A contribution of crustal matter with the same characteristics was also identified in Revin but not on the urban sites. The results

concerning the nature of sources impacting this site are more consistent with expectations, with larger contribution of natural sources when compared with the other sites.

As complementary information, all the concentration fields obtained for single regional factors, as well as the influence of applying trajectories cut-offs on trajectory density for each sampling site, are shown in Annex 3.

From these results, one can see the importance of transported particles to levels of PM_{10} not only on urban areas but also in a traffic site, where local emissions are expected to be in higher number. From the nature of the sources of aerosols, it was seen that anthropogenic emissions are the main sources of PM_{10} , suggesting that there is a large room for air quality improvement with measures that can benefit the population not only on a local scale, but on a regional scale as well.

4.2.5.1 Study comparison

As mentioned in a previous section of this manuscript, several other studies were already carried out in the region. Given the punctual differences observed according to the methodology adopted in each case, a comparison study has to be carried out with care.

The following methodologies differ in important aspects such dates and sampling periods, measured species, analytical methodology, statistical approach and results interpretation. All these are important factors that can result in divergences between the studies.

The author chose 4 different works that can be directly compared with this project, ranging from local scale comparison to regional source apportionment studies.

4.2.5.2 Lens (Waked et al., 2014)

In this work, the source of ambient particulate matter (PM_{10}) collected over a one-year period at an urban background site in Lens (France) was determined and investigated using a positive matrix factorization receptor model (US EPA PMF v3.0). In addition, a potential source contribution function (PSCF) was performed by means of the Hybrid Single-Particle Lagrangian Integrated Trajectory (Hysplit) v4.9 model to assess prevailing geographical origins of the identified sources. A selective iteration process was followed for the qualification of the more robust and meaningful PMF solution. Components measured and

used in the PMF included inorganic and organic species: soluble ionic species, trace elements, elemental carbon (EC), sugar alcohols, sugar anhydride, and organic carbon (OC).

This work can be directly compared with the results found for the sampling site of Lens presented in this manuscript.

The average PM10 concentration measured in both studies was found to be the same (20.5 $\mu\text{g}\cdot\text{m}^{-3}$) showing that PM10 levels did not change significantly in the city of Lens. When a source apportionment study is made, the number of sources identified was the same however, the identified sources differed between both studies. In Waked et al., a heavy oil combustion source of PM10 was identified, being characterized by the significant presence of Ni and V in its chemical profile. This source was not seen in this work, that found, on the other hand, a marine biogenic source (characterized by MSA) and an oxalate rich source of PM10. The final number was factors found in both studies was the same because in Waked et al, a split between the traffic and the crustal factor was possible.

Interestingly, the relative contributions of the different sources did not show significant disparities between both studies :

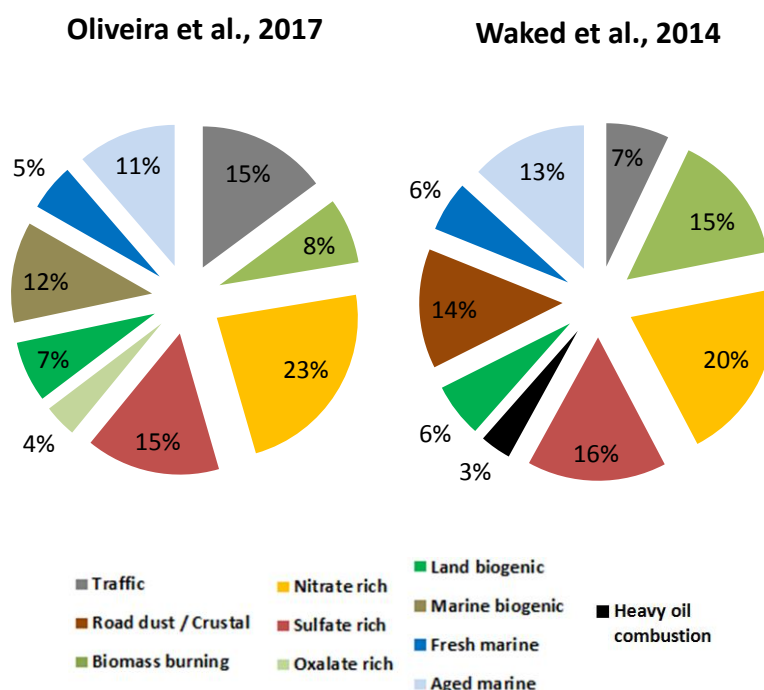


Figure 69: Average contribution of the different sources to PM10 mass concentration in Lens in Oliveira et al (left) and Waked et al (right)

As pointed above, some differences are seen on the sources identified, as well as in the relative contributions of the common ones. Interestingly, the relative contribution of more

local primary emissions (traffic and biomass burning) exhibited very similar average concentrations on both studies (4.5 $\mu\text{g}\cdot\text{m}^{-3}$ in Waken et al, and 4.4 $\mu\text{g}\cdot\text{m}^{-3}$ in Oliveira et al.), representing about 23% of PM10 total mass concentration. Secondary sources such as nitrate rich and sulfate rich factors were identified in both studies, however, due to the fact that the present study also measured oxalate, a oxalate rich factor was found in Lens in this work. The relative contribution of these secondary sources was 8.3 $\mu\text{g}\cdot\text{m}^{-3}$ (42% of total PM10) in the present study, whereas Waked et al, measured an average concentration of 7.4 $\mu\text{g}\cdot\text{m}^{-3}$ (36% of total PM10).

4.2.5.3 Cap Gris-Nez (Thesis of Chloe Roche)

On the shoreline, particulate atmospheric background levels are sometimes elevated, although relatively far from the main sources of particulate matter, road traffic and industry. While many studies have been conducted on industrial-port emissions, there is a lack of knowledge about the impact of emissions from the marine sector, whether natural (marine) or anthropogenic (Maritime traffic). In this work, two measurement campaigns were conducted: in 2013 at Cap Gris-Nez and in the first quarter of 2014, simultaneously with Cap Gris-Nez and the port of Calais. The concentration of PM10 was monitored and the chemical composition (metals, water-soluble ions, EC, OC, organic tracers) was determined. At the site of Cap Gris-Nez in 2013, the evolution of PM10 levels is similar to that observed in the regions, reflecting the fluctuation of the atmospheric background.

The comparison of the results obtained in this study is crucial to understand the influence of marine aerosols on land sites. Given the proximity to the coast, the similarities on the methodology followed and the equivalent sampling period, one can assess the gradual impact of particles with marine origins.

In Cap Gris-Nez, a total of 10 different factors were identified using PMF: Marine, aged marine, crustal, secondary nitrates, secondary sulfates, biomass burning, road traffic, heavy fuel combustion, primary biogenic emissions and a factor rich in metals.

Has seen, similar factors were found in both studies, with equivalent chemical profiles. One can therefore group the identified sources in such a manner that facilitates the nature of the different contributions. As applied previously, one can characterize a source as being from natural, anthropogenic or mixed origins. Using the same principal to both studies, and based

on the chemical profiles of each factor, a relative contribution of sources by their nature can be assessed:

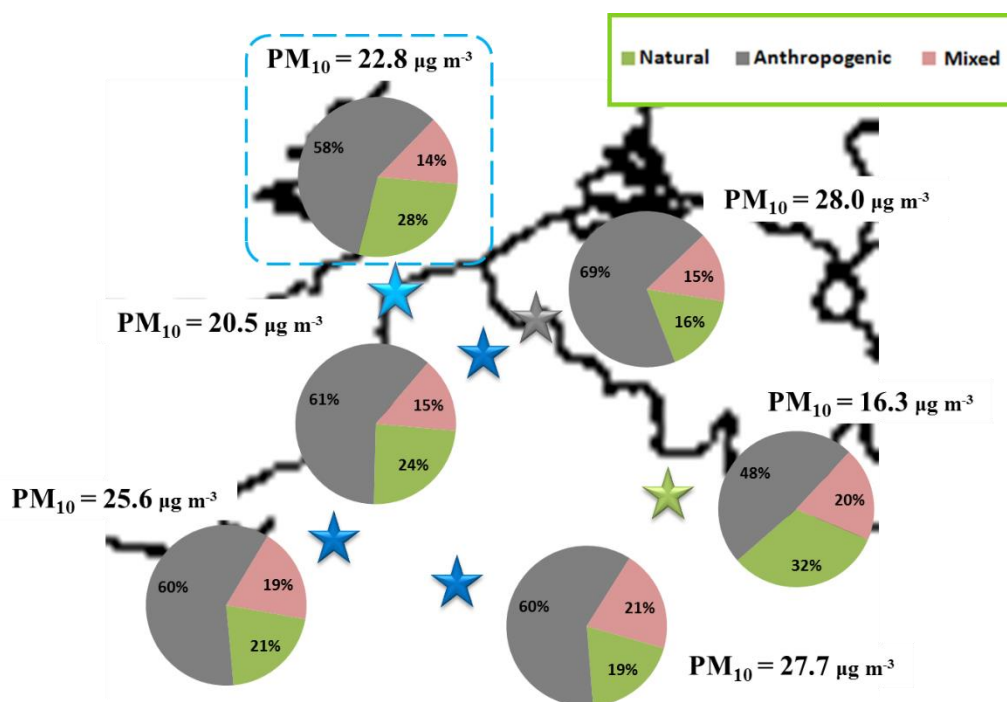


Figure 70: Relative contribution of Natural, Anthropogenic and Mixed sources to PM₁₀ mass concentration in 6 sites in the north of France

As seen in FIG70, the relative contribution of natural and anthropogenic sources in Cap Gris-Nez is in accordance with the results found on the samplings sites of this work. Anthropogenic originated particles are the main driver of PM₁₀ mass concentration. Natural sources of PM appear to have a bigger importance in this site, especially when compared with more urban sites like Lens, Nogent-sur-Oise, Rouen and Roubaix. This result is expected as marine salts have higher contribution on a coastal site such as Cap Gris-Nez.

However, marine contribution can also accommodate some anthropogenic originated particles, mainly on the aged marine factor, where in both works the chemical profile obtained for this factor showed important contributions of heavy metals. It is then interesting to study the influence of marine particles alone and their contribution to PM₁₀ mass concentrations. To do so, both marine and aged marine sources were combined, as well as the marine biogenic factor found in the present study.

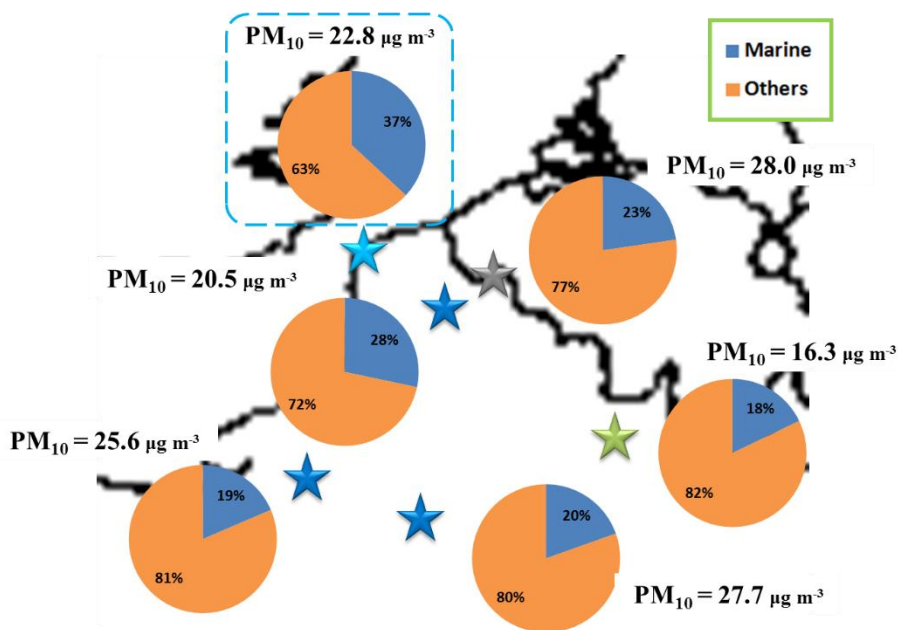


Figure 71: Relative contribution of marine sources to PM10 mass concentration in 6 sites in the north of France

The graphical representation clearly shows the importance of marine particles on PM10 mass concentration on the coastal site of Cap Gris-Nez, where the highest relative contribution was found among all sites (37 %). Notably, sampling sites located closer to the coast line such as Rouen, Lens and Roubaix showed marine influences ranging from 28% to 19%, whereas sampling sites located more inland recorded marine contributions of around 19%, mainly driven by aged marine particles.

The comparison between both studies allows to understand and quantify the contribution of particles with maritime origins and assess their influence both in coastal and in inland sites. However, some important considerations have to be made. First, this comparison between sites is just possible due to the similarities on methodologies followed by both studies, once again highlighting the value of common approaches to similar studies. Second, careful considerations associated with space dimension are essential. This comparison is possible due to the geographical characteristics of the region (flat terrain) and proximity between sites. Finally, backtrajectory study is crucial to understand the representativeness of the results obtained. Often, inland sites show significant variability in air masses trajectories, here, however, results shown very good agreement between all sites, possibly linked with the particular geographic characteristics of these region.

4.2.5.4 JOAQUIN Project

The JOAQUIN Project consists in a 14-month measurement campaign of the composition of particle matter (PM₁₀) at five monitoring sites and a mobile station (trailer) in NW Europe. The study was carried out as part of the Joint Air Quality Initiative and has as general objective the study to establish a link between the composition of PM₁₀ and air pollution sources and to relate the PM₁₀ composition to toxicological effects.

From April 2013 to May 2014, aerosol samples were collected at fixed sites in Amsterdam, Antwerp, Wijk-aan-Zee, Lille and Leicester. The receptor-oriented model EPA-PMF 5.0.14 was used to carry out a source apportionment using the pooled data of the five sites.

During the common sampling period at the five sites (1 June 2013 to 31 May 2014), the mean ambient PM₁₀ concentration was highest at the site in Wijk aan Zee (annual mean of 25.0 µg.m⁻³) and Antwerp (24.5 µg.m⁻³), intermediate in Lille (22.4 µg.m⁻³) and Amsterdam (20.3 µg.m⁻³) and lowest in Leicester (16.0 µg.m⁻³). These results are in accordance to the ones found on the present work in the north of France.

A source apportionment study was made with a joint database, composed from the contributions found on all sites. This methodology differs from the one applied on this work due to the understanding of the author that a joint database may be forcing common factors with the same chemical to all, giving place to the possibility of local influences end up hidden on an averaged chemical signature. However, this methodology increases significantly the number of samples used in the PMF, awarding the final solution with greater statistical robustness.

The PMF analysis resulted in a solution with 13 factor profiles, which could be aggregated to eight groups: secondary aerosol; furnace slacks, road wear and construction; sea spray; mineral dust; biomass burning; industrial activities; traffic emissions and brake wear; and residual oil combustion.

Following the methodology applied in site intercomparisons, sources were also grouped as being from natural, anthropogenic and mixed origins, based on their chemical profiles.

Results show a greater contribution of anthropogenic sources to PM₁₀ levels on the sites of the JOAQUIN Project. This can be related to the nature (densely populated urban areas) of these sampling sites and the lack of biogenic markers from the analytical characterization.

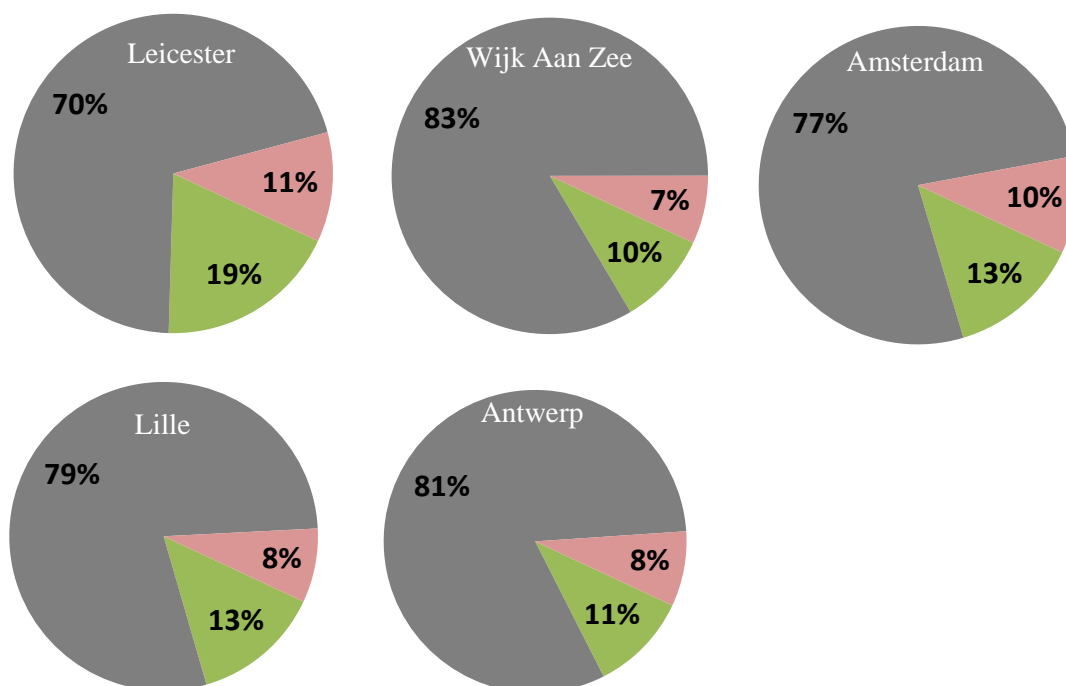


Figure 72: Relative contribution of Natural, Anthropogenic and Mixed sources to PM10 mass concentration in 5 European cities

The observed contributions of anthropogenic sources far exceeded the natural sources, ranging from 70% in the city of Leicester, up to 83% in Wijk Aan Zee, an industrial site in the north of the Netherlands. As in the present study, most of PM10 mass is associated with secondary particles and explained by nitrate-rich (27-37%) and sulphate-rich (9-13%) secondary aerosol. The second-most important source profiles were related to sea spray and aged sea spray (11-21%).

Concerning the followed methodology, it would be interesting to study the results found on both studies when using a combined database PMF run or a single site source apportionment study. Comparisons could be done both between projects as well as between methodologies.

4.2.5.5 Maenhaut et al., 2016

From 30 June 2011 to 2 July 2012 PM10 aerosol samples were simultaneously taken every 4th day at four urban background sites in Flanders, Belgium. The sites were in Antwerpen, Gent, Brugge, and Oostende. The PM10 mass concentration was determined by weighing; organic and elemental carbon (OC and EC) were measured by thermal-optical analysis, the wood burning tracers levoglucosan, mannosan and galactosan were determined by gas chromatography/mass spectrometry, 8 water-soluble ions were measured by ion

chromatography, and 15 elements were determined by a combination of inductively coupled plasma atomic emission spectrometry and mass spectrometry. The multi-species dataset was subjected to receptor modeling by PMF. The 10 retained factors (with their overall average percentage contributions to the experimental PM10 mass) were wood burning (9.5%), secondary nitrate (24%), secondary sulfate (12.6%), sea salt (10.0%), aged sea salt (19.2%), crustal matter (9.7%), non-ferrous metals (1.81%), traffic (10.3%), non-exhaust traffic (0.52%), and heavy oil burning (3.0%).

These factors, according to their chemical composition, were referred in terms of their origin as natural, anthropogenic or mixed. The results obtained show a very good agreement with the ones obtained for the north of France.

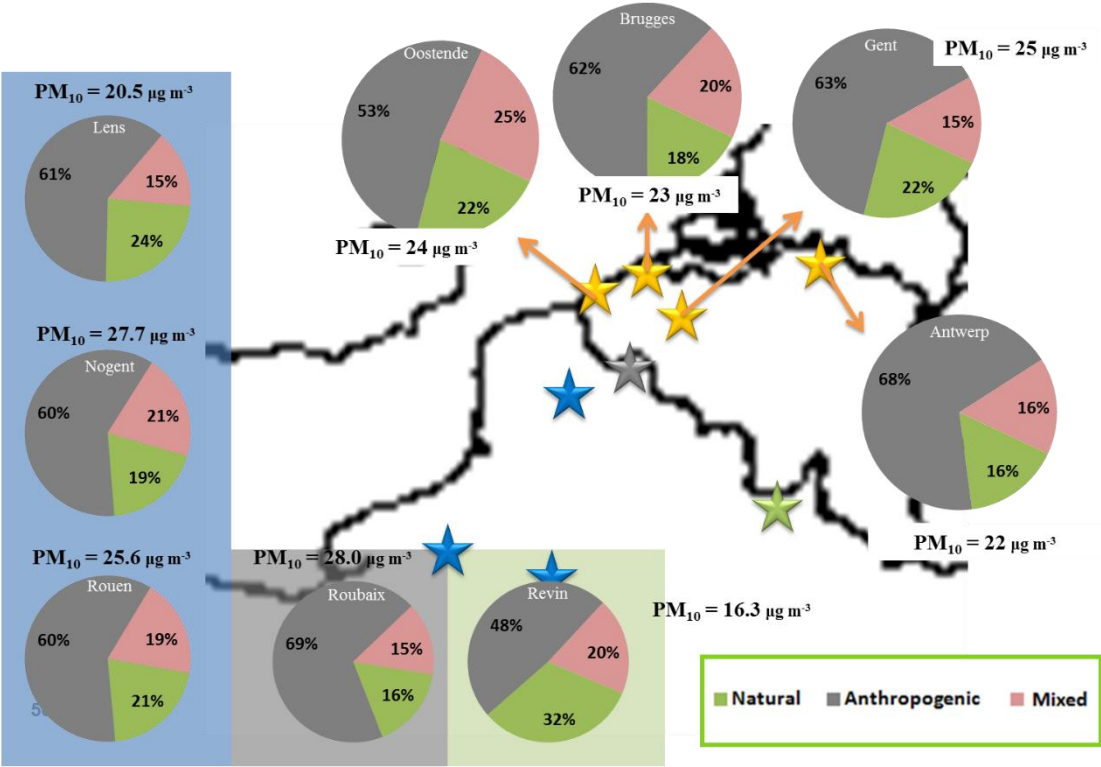


Figure 73: Relative contribution of Natural, Anthropogenic and Mixed sources to PM10 mass concentration in 9 sites spread across the north of France and Belgium

The similarities found in both studies can be explained by the proximity of the sampling sites involved. Despite the proximity and the similar cultural influences of the sites, also the geographical characteristics of the surrounding terrain contribute to the often uniform weather conditions seen in the sampling sites. Backtrajectories from all sites show very good correlation, leading to similar influence of more regional sources.

The intercomparison of these two studies highlights the clear transboundary impact of air pollution and the necessity of international collaboration to understand and assess the scale of PM footprint on a regional level.

CONCLUSIONS AND PERSPECTIVES

CONCLUSIONS AND PERSPECTIVES

The objective of this work was to apportion sources of PM impacting the north of France and distinguish between regional and local influences. By means of a full chemical characterization of samples collected in 5 sampling sites spread across the region and the study of the origins of these particles: their sources, chemical profiles, seasonal variations and geographical location, in this section of the manuscript the main conclusions of this work will be presented.

On a first phase, PM₁₀ mass concentration was measured and samples collected in the 5 sites were chemically analyzed. A first approach to the raw data obtained involved the validation of the concentrations measured. Tests such as mass closure and ion balance were applied. By reconstructing PM₁₀ mass based on the chemical species quantified, different results were shown from site to site, with no apparent correlation to their typology. A possible seasonal trend was observed with higher unaccounted masses occurring during summer and fall (warmer months) however a few exceptions to this trend were seen, not allowing to fully assuming a link between both facts. The ion balance was studied on all sites, accounting the concentrations of anions and cations measured throughout this work. On all sites the balance was seen around the 1:1 ratio, with a small excess of anions on the sites of Revin, Rouen and Roubaix and the opposite in Nogent-sur-Oise. Again no apparent correlation was found to the typology of each site. An apparent seasonal trend was seen, showing colder seasons often with an excess of anions, and the opposite in warmer seasons. This is probably related with the volatility associated with some of these species as well as emissions patterns of their sources (agricultural activities predominantly during late winter and spring). Concerning the average chemical composition of PM₁₀ collected, minor differences were seen on all sites. Organic matter was found to be main contributor to PM₁₀ mass concentration on all sites. The major ions (nitrate, sulfate and ammonium) appeared as the next major contributors on the same order on all sites. Highest average concentrations of these species were found in the traffic site of Roubaix and the lowest in the remote site of Revin, showing here a clear dependence between site typology and PM concentration. The same seasonal pattern was found on all the sites for PM₁₀ mass concentration and for the main species. Other parameter clearly related with site typology was the number of exceedance episodes (PM₁₀ > 50 µg m⁻³). Bigger differences were seen on the chemical composition of PM₁₀ during these episodes; however, different numbers of episodes were registered from site to site, changing therefore

the statistical representativeness. The sampling site of Revin just recorded one exceedance episode, here secondary particles were the main contributors (78%). On the other sites, the contribution of these species was lower but still very significant (63% in Lens, 49% in Nogent-sur-Oise, 61% in Rouen and 57% in Roubaix). The lower contribution in the site of Nogent-sur-Oise was associated with a higher importance of OM and levoglucosan leading to the assumption of an important contribution of biomass burning during these episodes. In Roubaix the slight lower importance of secondary particles was due to a larger contribution of metals, linking exceedance episodes in this sampling site with traffic related emissions as well. This exercise puts in evidence the crucial importance of secondary aerosols in the air quality of the north of France, which are commonly associated with long range transport processes, having therefore a regional impact.

The source apportionment study carried out on the 5 sites identified between 8 and 10 possible sources of PM₁₀. The use of specific tracers like MSA and oxalate allowed indentifying marine biogenic and oxalate rich particles, respectively, impacting the north of France. The measurement of sugar alcohols was also important to quantify the impact of land biogenic particles. As suspected from the chemical characterization, secondary aerosols are major sources of PM₁₀, as well as traffic related particles. In Lens, an urban site, the main contributors to PM₁₀ mass were nitrate rich particles, under the form of ammonium nitrate, followed by sulfate rich and traffic related emissions. An important fraction of marine biogenic particles was also found in this site. In Nogent-sur-Oise a multitude of sources contribute to PM₁₀ concentrations, all with predominant anthropogenic origin, such as traffic related, biomass burning, nitrate rich, sulfate rich and oxalate rich particles. In Rouen, an urban site as well, the main impacting source is traffic related emissions – which include exhaust and non-exhaust emissions and a crustal fraction that is not quantifiable. Oxalate rich particles were also identified as a major source in this site. Roubaix, the traffic site, was the only site where a source of just exhaust emissions was identified separately from non-exhaust emissions. The latter appeared associated with crustal matter on a road dust factor, composed mainly by non-exhaust traffic related particles. Finally the remote site of Revin was the only to identify a natural crustal matter factor. An important fraction of traffic related particles was also found in this site leading to question its “remoteness”.

The use of methods in order to predict factor contributions based solely on mass apportionment and chemical balances of single species proved to be useful to simulate time behaviors and seasonal trends but proved flawed when trying to quantify these contributions.

All the identified sources on each site were associated with wind speed and wind direction information collected at nearby meteorological stations. NWR plots allowed categorizing each factor as local or regional. All sites showed similar results in this characterization, and local sources were identified to be biomass burning and traffic. Land biogenic particles were associated with mild wind speeds whereas oxalate rich particles showed often to have different directions of their sources being associated with low, mild and high wind speeds. The direction associated with high concentrations during high wind speeds was always found to be the northeast, assumed to be the sulfate contribution to these particles. This oxalate rich factor can't then be labelled as local or regional. The regional factors identified in this study were either marine related (fresh and aged sea salt and marine biogenic) or secondary particles from anthropogenic activities (sulfate and nitrate rich).

Daily contributions of the regional factors were then associated with back-trajectories calculated for each sampling site and concentration field maps were plotted. Given the fact that all the regional sources identified were well correlated in terms of chemical profiles and given the proximity of the sampling sites, it was assumed that the geographical location of each regional source impacting the sites would be the same. This was supported with well-defined multi-site concentration field maps, highlighting the probable geographical location of these sources. Natural sources like fresh and aged sea salt were seen originating from the Atlantic Ocean. Fresh sea salt is originated in the far west side of the Atlantic Ocean, being associated with high velocity air masses created by the North Atlantic Oscillation. Marine biogenic particles are originated from the North Sea, linked with intense algae bloom reported in this area occurring during late spring and summer. Anthropogenic sources of secondary particles have continental origin, especially from Central and Eastern Europe. Nitrate rich particles seem also to be linked with emissions from Belgium and the Netherlands, probably linked with intense agricultural activities abundant in this region of Europe. Sulfate rich particles were also linked with emissions from the Strait of Gibraltar, an area of intense maritime traffic.

With this work one can conclude that air quality in the north of France remains an important issue to be tackled with, not only because of the high concentrations often seen, but also due to the complexity of sources contributing to these events. Although in densely populated urban areas local sources like traffic emissions and biomass burning are important sources of PM that can be prevented by new policies, an important fraction of PM was seen associated with secondary aerosols with a regional impact. These are transboundary particles that in

order to reduce their levels in the atmosphere, measures have to be taken on an international level.

Finally, this work allowed the characterization of PM_{10} in 5 sites representative of the north of France, to understand its composition and seasonal variation and to identify the main sources of these particles. Secondary aerosols have an important overall impact in the air quality of this region, as well as local sources in urban and traffic areas.

Perspectives

The study of air pollution, PM in particular, has always room for improvement and efforts should be made to deepen our knowledge on how to mitigate this issue.

- From an organizational point of view, efforts should be made not only to increase the monitoring of these pollutants but also to make available and better share the information already existent. Countries can and should work closer together on how to approach this problem and address it on a transboundary level.
- Just in recent years the scientific community is moving towards an uniformization of the analytical and mathematical protocols to approach this kind of studies. This brings many advantages but the most important is that it allows performing comparative analysis between studies even if they are carried out by different users, labs and associations – facilitating the first point exposed in this paragraph.
- Improvements can be made on the collection and assessment of PM_{10} mass, especially on accounting water content and prevent volatilization of some compounds.
- The use of specific tracers proved to be very important in this work and can be an important tool to develop further in order to identify specific sources of aerosols

It was clear during this project that information about pollutants and their impacts has been made publically available just in recent years. This leads to an overall underestimation of the adverse effects that air pollution, with PM in particular, have on our day-to-day life. Local governments, driven either by strict regulation or preferably by general concern, must provide the necessary bases for the scientific community to study these issues. The scientific community has as well to open and provide their findings in order to effective political measures be put in place on a regional (and ideally international) level.

During this work, I participated in the Forum for Air quality Modeling (FAIRMODE) project. FAIRMODE was launched in 2007 as a joint response initiative of the European Environment Agency (EEA) and the European Commission Joint Research Centre (JRC). The forum is currently chaired by the Joint Research Centre. Its aim is to bring together air quality modelers and users in order to promote and support the harmonized use of models by EU Member States, with emphasis on model application under the European Air Quality directives. Using the same database, more than 70 working groups applied source apportionment exercises and all data was collected and analyzed in order not only to investigate the different results obtained, but also to study the different methodologies followed and their influence on the final results. This is an important first step on trying to harmonizing the different approaches that similar studies can have. This will allow not only improving information quality but also a possible intercomparison between studies that followed the same methodology.

A level of uncertainty is attached to the results that this study exposes. These uncertainties are not only linked with the methodology followed but also with the analytical limitations associated with the protocols and instruments used. Scientific investigation to reduce these uncertainties will not only help the user on a practical way but also will provide more trustworthy and accurate information.

Finally, from an analytical point of view, the use of specific chemical species proved to be a valuable asset by helping to identify sources of particles normally not allocated in this kind of studies. When considering the plan to put in place similar studies, it is important to collect as much information as possible, without neglecting species that may have small contributions but may provide valuable information on specific pollution sources.

REFERENCES

REFERENCES

- Abbott, Michael L., Che-Jen Lin, Peter Martian, and Jeffrey J. Einerson. 2008. "Atmospheric Mercury near Salmon Falls Creek Reservoir in Southern Idaho." *Applied Geochemistry*, Transport and Fate of Mercury in the Environment, 23 (3): 438–53. doi:10.1016/j.apgeochem.2007.12.012.
- "Air Quality in Europe — 2015 Report — European Environment Agency." 2016. Publication. Accessed November 24. <http://www.eea.europa.eu/publications/air-quality-in-europe-2015>.
- Aksoyoglu, Sebnem, A. S. H. Prévôt, and U. Baltensperger. 2016. "Contribution of Ship Emissions to the Concentration and Deposition of Pollutants in Europe: Seasonal and Spatial Variation." In *Air Pollution Modeling and Its Application XXIV*, 265–270. Springer. http://link.springer.com/chapter/10.1007/978-3-319-24478-5_43.
- Alastuey, Andrés, Xavier Querol, Sonia Castillo, Miguel Escudero, Anna Avila, Emilio Cuevas, Carlos Torres, et al. 2005. "Characterisation of TSP and PM_{2.5} at Izaña and Sta. Cruz de Tenerife (Canary Islands, Spain) during a Saharan Dust Episode (July 2002)." *Atmospheric Environment* 39 (26): 4715–4728.
- Albrecht, Bruce A. 1989. "Aerosols, Cloud Microphysics, and Fractional Cloudiness." *Science* 245 (4923): 1227–1230.
- Alleman, Laurent Y., Laure Lamaison, Esperanza Perdrix, Antoine Robache, and Jean-Claude Galloo. 2010. "PM₁₀ Metal Concentrations and Source Identification Using Positive Matrix Factorization and Wind Sectoring in a French Industrial Zone." *Atmospheric Research* 96 (4): 612–25. doi:10.1016/j.atmosres.2010.02.008.
- Amato, F., M. Pandolfi, T. Moreno, M. Furger, J. Pey, A. Alastuey, N. Bukowiecki, A. S. H. Prevot, U. Baltensperger, and X. Querol. 2011. "Sources and Variability of Inhalable Road Dust Particles in Three European Cities." *Atmospheric Environment* 45 (37): 6777–6787.
- Analitis, Antonis, Klea Katsouyanni, Konstantina Dimakopoulou, Evangelia Samoli, Aristidis K. Nikoloulopoulos, Yannis Petasakis, Giota Touloumi, et al. 2006. "Short-Term Effects of Ambient Particles on Cardiovascular and Respiratory Mortality." *Epidemiology* 17 (2): 230–233.
- Andersen, Zorana J., Peter Wahlin, Ole Raaschou-Nielsen, Thomas Scheike, and Steffen Loft. 2007. "Ambient Particle Source Apportionment and Daily Hospital Admissions among Children and Elderly in Copenhagen." *Journal of Exposure Science & Environmental Epidemiology* 17 (7): 625–36. doi:10.1038/sj.jes.7500546.
- Anderson, Jonathan O., Josef G. Thundiyil, and Andrew Stolbach. 2012. "Clearing the Air: A Review of the Effects of Particulate Matter Air Pollution on Human Health." *Journal of Medical Toxicology* 8 (2): 166–75. doi:10.1007/s13181-011-0203-1.
- Andersson-Sköld, Yvonne, and David Simpson. 2001. "Secondary Organic Aerosol Formation in Northern Europe: A Model Study." *Journal of Geophysical Research: Atmospheres* 106 (D7): 7357–74. doi:10.1029/2000JD900656.
- Andreae, Meinrat O., and Paul J. Crutzen. 1997. "Atmospheric Aerosols: Biogeochemical Sources and Role in Atmospheric Chemistry." *Science* 276 (5315): 1052–1058.
- Anttila, Pia, Pentti Paatero, Unto Tapper, and Olli Järvinen. 1995. "Source Identification of Bulk Wet Deposition in Finland by Positive Matrix Factorization." *Atmospheric Environment* 29 (14): 1705–1718.
- Ashbaugh, Lowell L., William C. Malm, and Willy Z. Sadeh. 1985. "A Residence Time Probability Analysis of Sulfur Concentrations at Grand Canyon National Park." *Atmospheric Environment (1967)* 19 (8): 1263–1270.

- Astel, Aleksander M. 2010. "Air Contaminants Modelling by Use of Several Receptor-Oriented Models." *International Journal of Environment and Pollution* 42 (1–3): 32–57. doi:10.1504/IJEP.2010.034225.
- ATMO Picardie. 2014. "Caractérisation Des PM10 Sur Les Sites de Nogent Sur Oise et de Creil Au Cours de L'année 2013." Edited by Benoit Rocq.
- Barletta, Barbara, Simone Meinardi, F. Sherwood Rowland, Chuen-Yu Chan, Xinming Wang, Shichun Zou, Lo Yin Chan, and Donald R. Blake. 2005. "Volatile Organic Compounds in 43 Chinese Cities." *Atmospheric Environment* 39 (32): 5979–5990.
- Bauer, Heidi, Elisabeth Schueller, Gert Weinke, Anna Berger, Regina Hitzenberger, Iain L. Marr, and Hans Puxbaum. 2008. "Significant Contributions of Fungal Spores to the Organic Carbon and to the Aerosol Mass Balance of the Urban Atmospheric Aerosol." *Atmospheric Environment* 42 (22): 5542–5549.
- Bauer, S. E., D. Koch, N. Unger, S. M. Metzger, D. T. Shindell, and D. G. Streets. 2007. "Nitrate Aerosols Today and in 2030: A Global Simulation Including Aerosols and Tropospheric Ozone." *Atmospheric Chemistry and Physics* 7 (19): 5043–5059.
- Beekmann, Matthias, André SH Prévôt, Frank Drewnick, Jean Sciare, Spyros N. Pandis, Hugo AC Denier Van Der Gon, Monica Crippa, et al. 2015. "In Situ, Satellite Measurement and Model Evidence on the Dominant Regional Contribution to Fine Particulate Matter Levels in the Paris Megacity." *Atmospheric Chemistry and Physics* 15 (16): 9577–9591.
- Belis, C. A., J. Cancelinha, M. Duane, V. Forcina, V. Pedroni, R. Passarella, G. Tanet, et al. 2011. "Sources for PM Air Pollution in the Po Plain, Italy: I. Critical Comparison of Methods for Estimating Biomass Burning Contributions to Benzo(a)pyrene." *Atmospheric Environment* 45 (39): 7266–75. doi:10.1016/j.atmosenv.2011.08.061.
- Belis, C. A., F. Karagulian, B. R. Larsen, and P. K. Hopke. 2013. "Critical Review and Meta-Analysis of Ambient Particulate Matter Source Apportionment Using Receptor Models in Europe." *Atmospheric Environment* 69: 94–108.
- Belis Claudio A., Larsen Bo R., Amato Fulvio, El Haddad Imad, Favez Olivier, Roy Harrison M., Hopke Philip K., Nava Silvia, Paatero Pentti, Prévôt André, Quass Ulrich, Vecchi Roberta, Viana Mar. 2014. European Guide on air pollution source apportionment with Receptor Models. Reference report EUR 26080 – Joint Research Centre – Institute for Environment and Sustainability, 88 pp. doi:10.2788/9307
- Bessagnet, Bertrand, Alma Hodzic, Olivier Blanchard, M. Lattuati, Olivier Le Bihan, Héléne Marfaing, and Laurence Rouil. 2005. "Origin of Particulate Matter Pollution Episodes in Wintertime over the Paris Basin." *Atmospheric Environment* 39 (33): 6159–6174.
- Beuck, H., U. Quass, O. Klemm, and T. A. J. Kuhlbusch. 2011. "Assessment of Sea Salt and Mineral Dust Contributions to PM 10 in NW Germany Using Tracer Models and Positive Matrix Factorization." *Atmospheric Environment* 45 (32): 5813–5821.
- Bi, Xinhui, Guoying Sheng, Ping'an Peng, Yingjun Chen, and Jiamo Fu. 2005. "Size Distribution of N-Alkanes and Polycyclic Aromatic Hydrocarbons (PAHs) in Urban and Rural Atmospheres of Guangzhou, China." *Atmospheric Environment* 39 (3): 477–87. doi:10.1016/j.atmosenv.2004.09.052.
- "Bilan de La Qualité de L'air En France En 2015 - Ministère de l'Environnement, de l'Energie et de La Mer." 2016. Accessed November 20. <http://www.developpement-durable.gouv.fr/Bilan-de-la-Qualite-de-l-air-en,48891.html>.
- Birch, M. E., and R. A. Cary. 1996. "Elemental Carbon-Based Method for Monitoring Occupational Exposures to Particulate Diesel Exhaust." *Aerosol Science and Technology* 25 (3): 221–241.

- Birch, M. Eileen, and Robert A. Cary. 1996. "Elemental Carbon-Based Method for Occupational Monitoring of Particulate Diesel Exhaust: Methodology and Exposure Issues." *Analyst* 121 (9): 1183–1190.
- Blando, James D., and Barbara J. Turpin. 2000. "Secondary Organic Aerosol Formation in Cloud and Fog Droplets: A Literature Evaluation of Plausibility." *Atmospheric Environment* 34 (10): 1623–1632.
- Bougiatioti, A., P. Zampas, E. Koulouri, M. Antoniou, C. Theodosi, G. Kouvarakis, S. Saarikoski, T. Mäkelä, R. Hillamo, and N. Mihalopoulos. 2013. "Organic, Elemental and Water-Soluble Organic Carbon in Size Segregated Aerosols, in the Marine Boundary Layer of the Eastern Mediterranean." *Atmospheric Environment* 64 (January): 251–62. doi:10.1016/j.atmosenv.2012.09.071.
- Bouwman, A. F., D. S. Lee, W. A. H. Asman, F. J. Dentener, K. W. van der Hoek, and J. G. J. Olivier. 1997. "A Global High-Resolution Emission Inventory for Ammonia." *Global Biogeochemical Cycles* 11: 561–587.
- Bove, M. C., P. Brotto, G. Calzolari, F. Cassola, F. Cavalli, P. Fermo, J. Hjorth, et al. 2016. "PM10 Source Apportionment Applying PMF and Chemical Tracer Analysis to Ship-Borne Measurements in the Western Mediterranean." *Atmospheric Environment* 125, Part A (January): 140–51. doi:10.1016/j.atmosenv.2015.11.009.
- Brauer, Michael, Thomas S. Dumyahn, John D. Spengler, Kersten Gutschmidt, Joachim Heinrich, and H.-Erich Wichmann. 1995. "Measurement of Acidic Aerosol Species in Eastern Europe: Implications for Air Pollution Epidemiology." *Environmental Health Perspectives* 103 (5): 482.
- Bressi, M., F. Cavalli, C. A. Belis, J.-P. Putaud, R. Fröhlich, S. Martins dos Santos, E. Petralia, et al. 2016. "Variations in the Chemical Composition of the Submicron Aerosol and in the Sources of the Organic Fraction at a Regional Background Site of the Po Valley (Italy)." *Atmos. Chem. Phys.* 16 (20): 12875–96. doi:10.5194/acp-16-12875-2016.
- Bressi, M., J. Sciare, V. Ghersi, N. Bonnaire, J. B. Nicolas, J.-E. Petit, S. Moukhtar, A. Rosso, N. Mihalopoulos, and A. Féron. 2013. "A One-Year Comprehensive Chemical Characterisation of Fine Aerosol (PM_{2.5}) at Urban, Suburban and Rural Background Sites in the Region of Paris (France)." *Atmos. Chem. Phys.* 13 (15): 7825–44. doi:10.5194/acp-13-7825-2013.
- Bressi, M., J. Sciare, V. Ghersi, N. Mihalopoulos, J.-E. Petit, J. B. Nicolas, S. Moukhtar, et al. 2014. "Sources and Geographical Origins of Fine Aerosols in Paris (France)." *Atmos. Chem. Phys.* 14 (16): 8813–39. doi:10.5194/acp-14-8813-2014.
- Brown, Steven G., Shelly Eberly, Pentti Paatero, and Gary A. Norris. 2015. "Methods for Estimating Uncertainty in PMF Solutions: Examples with Ambient Air and Water Quality Data and Guidance on Reporting PMF Results." *Science of The Total Environment* 518–519: 626–35. doi:10.1016/j.scitotenv.2015.01.022.
- Buekers, Jurgen, Felix Deutsch, Nele Veldeman, Stijn Janssen, and Luc Int Panis. 2014. "Fine Atmospheric Particles from Agricultural Practices in Flanders: From Emissions to Health Effects and Limit Values." *Outlook on Agriculture* 43 (1): 39–44. doi:10.5367/oa.2014.0153.
- Burshtein, N., N. Lang-Yona, and Y. Rudich. 2011. "Ergosterol, Arabitol and Mannitol as Tracers for Biogenic Aerosols in the Eastern Mediterranean." *Atmos. Chem. Phys.* 11 (2): 829–39. doi:10.5194/acp-11-829-2011.
- Byrd, Tony, Mary Stack, and Ambrose Furey. 2010. "The Assessment of the Presence and Main Constituents of Particulate Matter Ten Microns (PM₁₀) in Irish, Rural and Urban Air." *Atmospheric Environment* 44 (1): 75–87. doi:10.1016/j.atmosenv.2009.09.037.

- Cabello, M., J. A. G. Orza, M. A. Barrero, E. Gordo, A. Berasaluce, L. Cantón, C. Dueñas, M. C. Fernández, and M. Pérez. 2012. "Spatial and Temporal Variation of the Impact of an Extreme Saharan Dust Event." *Journal of Geophysical Research (Atmospheres)* 117 (D16): 11204.
- Caboche, Julien, Esperanza Perdrix, Bruno Malet, and Laurent Y. Alleman. 2011. "Development of an in Vitro Method to Estimate Lung Bioaccessibility of Metals from Atmospheric Particles" 13 (3): 621–30. doi:10.1039/C0EM00439A.
- Calvo, A. I., V. Pont, C. Lioussé, B. Dupré, A. Mariscal, C. Zouiten, E. Gardrat, et al. 2008. "Chemical Composition of Urban Aerosols in Toulouse, France during CAPITOUL Experiment." *Meteorology and Atmospheric Physics* 102 (3–4): 307–23. doi:10.1007/s00703-008-0319-2.
- Cao, J. J., S. C. Lee, K. F. Ho, S. C. Zou, Kochy Fung, Y. Li, John G. Watson, and Judith C. Chow. 2004. "Spatial and Seasonal Variations of Atmospheric Organic Carbon and Elemental Carbon in Pearl River Delta Region, China." *Atmospheric Environment* 38 (27): 4447–4456.
- Carslaw, K. S., O. Boucher, D. V. Spracklen, G. W. Mann, J. G. L. Rae, S. Woodward, and M. Kulmala. 2010. "A Review of Natural Aerosol Interactions and Feedbacks within the Earth System." *Atmos. Chem. Phys.* 10 (4): 1701–37. doi:10.5194/acp-10-1701-2010.
- Caseiro, Alexandre, Heidi Bauer, Christoph Schmidl, Casimiro A. Pio, and Hans Puxbaum. 2009. "Wood Burning Impact on PM10 in Three Austrian Regions." *Atmospheric Environment* 43 (13): 2186–95. doi:10.1016/j.atmosenv.2009.01.012.
- Caseiro, Alexandre, Iain L. Marr, Magda Claeys, Anne Kasper-Giebl, Hans Puxbaum, and Casimiro A. Pio. 2007. "Determination of Saccharides in Atmospheric Aerosol Using Anion-Exchange High-Performance Liquid Chromatography and Pulsed-Amperometric Detection." *Journal of Chromatography A* 1171 (1): 37–45.
- Castro, Amaya, Elisabeth Alonso-Blanco, Miguel González-Colino, Ana I. Calvo, María Fernández-Raga, and Roberto Fraile. 2010. "Aerosol Size Distribution in Precipitation Events in León, Spain." *Atmospheric Research* 96 (2): 421–435.
- Cavalli, Fabrizia, Mar Viana, Karl Espen Yttri, Johan Genberg, and J.-P. Putaud. 2010. "Toward a Standardised Thermal-Optical Protocol for Measuring Atmospheric Organic and Elemental Carbon: The EUSAAR Protocol." *Atmospheric Measurement Techniques* 3 (1): 79–89.
- "CEN, 1998 CEN, 1998. Air Quality—determination of the PM10 Fraction of Suspended Particulate Matter—reference Method and Field Test Procedure to Demonstrate Reference Equivalence of Measurement Methods. European Standard EN 12341." n.d.
- Charron, A., C. Degrendele, B. Laongsri, and R. M. Harrison. 2013. "Receptor Modelling of Secondary and Carbonaceous Particulate Matter at a Southern UK Site." *Atmos. Chem. Phys.* 13: 1879–1894.
- Charron, A., H. Plaisance, S. Sauvage, P. Coddeville, J. C. Galloo, and R. Guillermo. 1998. "Intercomparison between Three Receptor-Oriented Models Applied to Acidic Species in Precipitation." *Science of The Total Environment* 223 (1): 53–63. doi:10.1016/S0048-9697(98)00308-8.
- Charron, Aurélie, Hervé Plaisance, Stéphane Sauvage, Patrice Coddeville, Jean-Claude Galloo, and René Guillermo. 2000. "A Study of the Source–receptor Relationships Influencing the Acidity of Precipitation Collected at a Rural Site in France." *Atmospheric Environment* 34 (22): 3665–74. doi:10.1016/S1352-2310(00)00096-0.
- Cebbi, A., and P. Carlier. 1996. "Carboxylic Acids in the Troposphere, Occurrence, Sources, and Sinks: A Review." *Atmospheric Environment* 30 (24): 4233–4249.

- Chen, Bingzhang, Michael R. Landry, Bangqin Huang, and Hongbin Liu. 2012. "Does Warming Enhance the Effect of Microzooplankton Grazing on Marine Phytoplankton in the Ocean?" *Limnology and Oceanography* 57 (2): 519–526.
- Cheng, Yu, Shao-Meng Li, Amy Leithead, and Jeffrey R. Brook. 2006. "Spatial and Diurnal Distributions of N-Alkanes and N-Alkan-2-Ones on PM_{2.5} Aerosols in the Lower Fraser Valley, Canada." *Atmospheric Environment*, The Pacific 2001 Air Quality Study II, 40 (15): 2706–20. doi:10.1016/j.atmosenv.2005.11.066.
- Cheung, Kalam, Nancy Daher, Winnie Kam, Martin M. Shafer, Zhi Ning, James J. Schauer, and Constantinos Sioutas. 2011. "Spatial and Temporal Variation of Chemical Composition and Mass Closure of Ambient Coarse Particulate Matter (PM_{10-2.5}) in the Los Angeles Area." *Atmospheric Environment* 45 (16): 2651–62. doi:10.1016/j.atmosenv.2011.02.066.
- Chin, Mian, T. Diehl, Q. Tan, J. M. Prospero, R. A. Kahn, L. A. Remer, H. Yu, et al. 2014. "Multi-Decadal Aerosol Variations from 1980 to 2009: A Perspective from Observations and a Global Model." *Atmospheric Chemistry and Physics* 14 (April): 3657–90. doi:10.5194/acp-14-3657-2014.
- Chirenje, Tait, Lena Q. Ma, and Liping Lu. 2006. "Retention of Cd, Cu, Pb and Zn by Wood Ash, Lime and Fume Dust." *Water, Air, & Soil Pollution* 171 (1–4): 301–314.
- Choi, Eunhwa, Kyungho Choi, and Seung-Muk Yi. 2011. "Non-Methane Hydrocarbons in the Atmosphere of a Metropolitan City and a Background Site in South Korea: Sources and Health Risk Potentials." *Atmospheric Environment, Air Pollution and Health: Bridging the Gap from Sources-to-Health Outcomes*, 45 (40): 7563–73. doi:10.1016/j.atmosenv.2010.11.049.
- Churg, Andrew, Michael Brauer, Maria del Carmen Avila-Casado, Teresa I. Fortoul, and Joanne L. Wright. 2003. "Chronic Exposure to High Levels of Particulate Air Pollution and Small Airway Remodeling." *Environmental Health Perspectives* 111 (5): 714.
- Cincinelli, Alessandra, Massimo Del Bubba, Tania Martellini, Andrea Gambaro, and Luciano Lepri. 2007. "Gas-Particle Concentration and Distribution of N-Alkanes and Polycyclic Aromatic Hydrocarbons in the Atmosphere of Prato (Italy)." *Chemosphere* 68 (3): 472–78. doi:10.1016/j.chemosphere.2006.12.089.
- Coury, Charity, and Ann M. Dillner. 2007. "Trends and Sources of Particulate Matter in the Superstition Wilderness Using Air Trajectory and Aerosol Cluster Analysis." *Atmospheric Environment* 41 (40): 9309–9323.
- Dabek-Zlotorzynska, Ewa, and Marilu McGrath. 2000. "Determination of Low-Molecular-Weight Carboxylic Acids in the Ambient Air and Vehicle Emissions: A Review." *Fresenius' Journal of Analytical Chemistry* 367 (6): 507–518.
- Dall'Osto, M., R. M. Harrison, H. Coe, P. I. Williams, and J. D. Allan. 2009. "Real Time Chemical Characterization of Local and Regional Nitrate Aerosols." *Atmos. Chem. Phys.* 9 (11): 3709–20. doi:10.5194/acp-9-3709-2009.
- Dall'Osto, Manuel, Xavier Querol, Fulvio Amato, Angeliki Karanasiou, F. Lucarelli, S. Nava, G. Calzolari, and M. Chiari. 2013. "Hourly Elemental Concentrations in PM_{2.5} Aerosols Sampled Simultaneously at Urban Background and Road Site during SAPUSS—diurnal Variations and PMF Receptor Modelling." *Atmospheric Chemistry and Physics* 13 (8): 4375–4392.
- Dall'Osto, M., X. Querol, A. Alastuey, C. O'Dowd, R. M. Harrison, J. Wenger, and F. J. Gómez-Moreno. 2013. "On the Spatial Distribution and Evolution of Ultrafine Particles in Barcelona." *Atmospheric Chemistry and Physics* 13 (2): 741–759.
- "DEFRA Report. Summary of the Second Report Produced by the Air Quality Expert Group, Department for the Environment, Food and Rural Affairs, London, 2005." n.d.

- Deutsch, F., J. Vankerkom, B. Veldeman, W. Peelaerts, F. Fierens, C. Vanpoucke, E. Trimpeneers, L. Vancraeynest, M. Bossuyt, and H. Buysse. 2010. “Verklarende Factoren Voor Evolutes in Luchtkwaliteit.” *Studie Uitgevoerd in Opdracht van Vlaamse Milieumaatschappij (VMM). VITO, Mol, Belgium.*
- Didyk, Borys M., Bernd RT Simoneit, L. Alvaro Pezoa, M. Luis Riveros, and A. Anselmo Flores. 2000. “Urban Aerosol Particles of Santiago, Chile:: Organic Content and Molecular Characterization.” *Atmospheric Environment* 34 (8): 1167–1179.
- Dorling, S. R., and T. D. Davies. 1995. “Extending Cluster Analysis—synoptic Meteorology Links to Characterise Chemical Climates at Six Northwest European Monitoring Stations.” *Atmospheric Environment* 29 (2): 145–167.
- Dorling, S. R., T. D. Davies, and C. E. Pierce. 1992. “Cluster Analysis: A Technique for Estimating the Synoptic Meteorological Controls on Air and Precipitation Chemistry—method and Applications.” *Atmospheric Environment. Part A. General Topics* 26 (14): 2575–2581.
- Draxler, Roland R. 1999. “HYSPLIT4 User’s Guide.” http://www.villasmunta.it/pdf/User_guide.pdf.
- Draxler, Roland R., and G. D. Hess. 1998. “An Overview of the HYSPLIT_4 Modelling System for Trajectories.” *Australian Meteorological Magazine* 47 (4): 295–308.
- “Draxler, R.R., 1999: HYSPLIT4 User’s Guide. NOAA Tech. Memo. ERL ARL-230, NOAA Air Resources Laboratory, Silver Spring, MD.” n.d.
- “Draxler, R.R., and G.D. Hess, 1997: Description of the HYSPLIT_4 Modeling System. NOAA Tech. Memo. ERL ARL-224, NOAA Air Resources Laboratory, Silver Spring, MD, 24 Pp.” n.d.
- “Draxler, R.R., and G.D. Hess, 1998: An Overview of the HYSPLIT_4 Modeling System of Trajectories, Dispersion, and Deposition. Aust. Meteor. Mag., 47, 295-308.” n.d.
- Dupont, E., L. Menut, B. Carissimo, J. Pelon, and P. Flamant. 1999. “Comparison between the Atmospheric Boundary Layer in Paris and Its Rural Suburbs during the ECLAP Experiment.” *Atmospheric Environment* 33 (6): 979–994.
- Elbert, W., P. E. Taylor, M. O. Andreae, and U. Pöschl. 2007. “Contribution of Fungi to Primary Biogenic Aerosols in the Atmosphere: Wet and Dry Discharged Spores, Carbohydrates, and Inorganic Ions.” *Atmospheric Chemistry and Physics* 7 (17): 4569–4588.
- Elder, Alison, Sadasivan Vidyasagar, and Lisa DeLouise. 2009. “Physicochemical Factors That Affect Metal and Metal Oxide Nanoparticle Passage across Epithelial Barriers.” *Wiley Interdisciplinary Reviews. Nanomedicine and Nanobiotechnology* 1 (4): 434–50. doi:10.1002/wnan.44.
- Ellison, S. R., M. Rosslein, A. Williams, M. Berglund, W. Haesselbarth, K. Hedegaard, R. Karls, et al. 2000. *Eurachem/CITAC Guide CG4. Quantifying Measurement Uncertainty in Analytical Measurement.* https://www.researchgate.net/publication/236884859_EurachemCITAC_Guide_CG4_Quantifying_Measurement_Uncertainty_in_Analytical_Measurement.
- “EN 14907:2005, Ambient Air Quality – Standard Gravimetric Measurement Method for the Determination of the PM2.5 Mass Fraction of Suspended Particulate Matter, 2005.” n.d.
- Engeln, Axel von, and João Teixeira. 2013. “A Planetary Boundary Layer Height Climatology Derived from ECMWF Reanalysis Data.” *Journal of Climate* 26 (17): 6575–6590.
- Escudero, M., X. Querol, J. Pey, A. Alastuey, N. Pérez, F. Ferreira, S. Alonso, S. Rodríguez, and E. Cuevas. 2007. “A Methodology for the Quantification of the Net African Dust

- Load in Air Quality Monitoring Networks.” *Atmospheric Environment* 41 (26): 5516–5524.
- European Guide on Air Pollution Source Apportionment with Receptor Models. 2014. Publications Office.
- Favez, Olivier, Hélène Cachier, Jean Sciare, Roland Sarda-Estève, and Laurent Martinon. 2009. “Evidence for a Significant Contribution of Wood Burning Aerosols to PM_{2.5} during the Winter Season in Paris, France.” *Atmospheric Environment* 43 (22–23): 3640–44. doi:10.1016/j.atmosenv.2009.04.035.
- Fine, Philip M., Glen R. Cass, and Bernd R. T. Simoneit. 2002. “Organic Compounds in Biomass Smoke from Residential Wood Combustion: Emissions Characterization at a Continental Scale.” *Journal of Geophysical Research: Atmospheres* 107 (D21): 8349. doi:10.1029/2001JD000661.
- Fine, Philip M., Glen R. Cass, and Bernd RT Simoneit. 2001. “Chemical Characterization of Fine Particle Emissions from Fireplace Combustion of Woods Grown in the Northeastern United States.” *Environmental Science & Technology* 35 (13): 2665–2675.
- . 2004. “Chemical Characterization of Fine Particle Emissions from the Wood Stove Combustion of Prevalent United States Tree Species.” *Environmental Engineering Science* 21 (6): 705–721.
- Fraser, Matthew P., and Kalyan Lakshmanan. 2000. “Using Levoglucosan as a Molecular Marker for the Long-Range Transport of Biomass Combustion Aerosols.” *Environmental Science & Technology* 34 (21): 4560–4564.
- Fu, P. Q., K. Kawamura, J. Chen, J. Li, Y. L. Sun, Y. Liu, E. Tachibana, et al. 2012. “Diurnal Variations of Organic Molecular Tracers and Stable Carbon Isotopic Composition in Atmospheric Aerosols over Mt. Tai in the North China Plain: An Influence of Biomass Burning.” *Atmos. Chem. Phys.* 12 (18): 8359–75. doi:10.5194/acp-12-8359-2012.
- Fu, Xuewu, Xinbin Feng, Guangle Qiu, Lihai Shang, and Hui Zhang. 2011. “Speciated Atmospheric Mercury and Its Potential Source in Guiyang, China.” *Atmospheric Environment* 45 (25): 4205–4212.
- Furusjö, Erik, John Sternbeck, and Anna Palm Cousins. 2007. “PM₁₀ Source Characterization at Urban and Highway Roadside Locations.” *Science of The Total Environment* 387 (1–3): 206–19. doi:10.1016/j.scitotenv.2007.07.021.
- G, Manuel A. Leiva, Ma Consuelo Araya, Ana Maria Alvarado, and Rodrigo J. Seguel. 2012. “Uncertainty Estimation of Anions and Cations Measured by Ion Chromatography in Fine Urban Ambient Particles (PM_{2.5}).” *Accreditation and Quality Assurance* 17 (1): 53–63. doi:10.1007/s00769-011-0844-4.
- Gaston, Cassandra J., Kerri A. Pratt, Xueying Qin, and Kimberly A. Prather. 2010. “Real-Time Detection and Mixing State of Methanesulfonate in Single Particles at an Inland Urban Location during a Phytoplankton Bloom.” *Environmental Science & Technology* 44 (5): 1566–1572.
- Giakoumi, A., T. H. Maggos, J. Michopoulos, C. Helmis, and C. H. Vasilakos. 2009. “PM_{2.5} and Volatile Organic Compounds (VOCs) in Ambient Air: A Focus on the Effect of Meteorology.” *Environmental Monitoring and Assessment* 152 (1–4): 83–95.
- Gianini, M. F. D., A. Fischer, R. Gehrig, A. Ulrich, A. Wichser, C. Piot, J.-L. Besombes, and C. Hueglin. 2012. “Comparative Source Apportionment of PM₁₀ in Switzerland for 2008/2009 and 1998/1999 by Positive Matrix Factorisation.” *Atmospheric Environment* 54: 149–158.
- Giannoni, Martina, Tania Martellini, Massimo Del Bubba, Andrea Gambaro, Roberta Zangrando, Massimo Chiari, Luciano Lepri, and Alessandra Cincinelli. 2012. “The

- Use of Levoglucosan for Tracing Biomass Burning in PM 2.5 Samples in Tuscany (Italy)." *Environmental Pollution* 167: 7–15.
- Gietl, Johanna K., and Otto Klemm. 2009. "Source Identification of Size-Segregated Aerosol in Münster, Germany, by Factor Analysis." *Aerosol Science and Technology* 43 (8): 828–37. doi:10.1080/02786820902953923.
- Ginoux, Paul, Joseph M. Prospero, Thomas E. Gill, N. Christina Hsu, and Ming Zhao. 2012. "Global-Scale Attribution of Anthropogenic and Natural Dust Sources and Their Emission Rates Based on MODIS Deep Blue Aerosol Products." *Reviews of Geophysics* 50 (3): RG3005. doi:10.1029/2012RG000388.
- Glasow, R. von, and P. J. Crutzen. 2003. "Model Study of Multiphase DMS Oxidation with a Focus on Halogens." *Atmospheric Chemistry & Physics Discussions* 3: 6733–6777.
- Golly, B., G. Brulfert, G. Berlioux, J. -L. Jaffrezo, and J. -L. Besombes. 2015. "Large Chemical Characterisation of PM10 Emitted from Graphite Material Production: Application in Source Apportionment." *Science of The Total Environment* 538: 634–43. doi:10.1016/j.scitotenv.2015.07.115.
- Grivas, G., A. Chaloulakou, and P. Kassomenos. 2008. "An Overview of the PM 10 Pollution Problem, in the Metropolitan Area of Athens, Greece. Assessment of Controlling Factors and Potential Impact of Long Range Transport." *Science of the Total Environment* 389 (1): 165–177.
- Grover, Brett D., Michael Kleinman, Norman L. Eatough, Delbert J. Eatough, Philip K. Hopke, Russell W. Long, William E. Wilson, Michael B. Meyer, and Jeffrey L. Ambs. 2005. "Measurement of Total PM2. 5 Mass (Nonvolatile plus Semivolatile) with the Filter Dynamic Measurement System Tapered Element Oscillating Microbalance Monitor." *Journal of Geophysical Research: Atmospheres* 110 (D7). <http://onlinelibrary.wiley.com/doi/10.1029/2004JD004995/full>.
- Guinot, B., H. Cachier, and K. Oikonomou. 2007. "Geochemical Perspectives from a New Aerosol Chemical Mass Closure." *Atmos. Chem. Phys.* 7 (6): 1657–70. doi:10.5194/acp-7-1657-2007.
- Gundel, L. A., R. L. Dod, H. Rosen, and T. Novakov. 1984. "The Relationship between Optical Attenuation and Black Carbon Concentration for Ambient and Source Particles." *Science of the Total Environment* 36: 197–202.
- Hallquist, Mattias, J. C. Wenger, Urs Baltensperger, Y. Rudich, David Simpson, M. Claeys, J. Dommen, et al. 2009. "The Formation, Properties and Impact of Secondary Organic Aerosol: Current and Emerging Issues." *Atmospheric Chemistry and Physics* 9 (14): 5155–5236.
- Hallquist, M., J. C. Wenger, U. Baltensperger, Y. Rudich, D. Simpson, M. Claeys, J. Dommen, et al. 2009. "The Formation, Properties and Impact of Secondary Organic Aerosol: Current and Emerging Issues." *Atmos. Chem. Phys.* 9 (14): 5155–5236. doi:10.5194/acp-9-5155-2009.
- Han, Young-Ji, Thomas M. Holsen, and Philip K. Hopke. 2007. "Estimation of Source Locations of Total Gaseous Mercury Measured in New York State Using Trajectory-Based Models." *Atmospheric Environment* 41 (28): 6033–47. doi:10.1016/j.atmosenv.2007.03.027.
- Healy, Robert M., Greg J. Evans, Michael Murphy, Berko Sierau, Jovanna Arndt, Eoin McGillicuddy, Ian P. O'Connor, John R. Sodeau, and John C. Wenger. 2015. "Single-Particle Speciation of Alkylamines in Ambient Aerosol at Five European Sites." *Analytical and Bioanalytical Chemistry* 407 (20): 5899–5909. doi:10.1007/s00216-014-8092-1.
- Hendriks, C., R. Kranenburg, J. J. P. Kuenen, B. Van den Bril, V. Verguts, and M. Schaap. 2016. "Ammonia Emission Time Profiles Based on Manure Transport Data Improve

- Ammonia Modelling across North Western Europe.” *Atmospheric Environment* 131: 83–96. doi:10.1016/j.atmosenv.2016.01.043.
- Hennigan, Christopher J., Amy P. Sullivan, Jeffrey L. Collett, and Allen L. Robinson. 2010. “Levoglucosan Stability in Biomass Burning Particles Exposed to Hydroxyl Radicals.” *Geophysical Research Letters* 37 (9): L09806. doi:10.1029/2010GL043088.
- Henry, Ronald C., Yu-Shuo Chang, and Clifford H. Spiegelman. 2002. “Locating Nearby Sources of Air Pollution by Nonparametric Regression of Atmospheric Concentrations on Wind Direction.” *Atmospheric Environment* 36 (13): 2237–44. doi:10.1016/S1352-2310(02)00164-4.
- Hinds, W. C. 1982. *Aerosol Technology: Properties, Behavior, and Measurement of Airborne Particles*. <http://adsabs.harvard.edu/abs/1982wi...bookQ...H>.
- Hondula, David M., Luke Sitka, Robert E. Davis, David B. Knight, Stephen D. Gawtry, Michael L. Deaton, Temple R. Lee, Caroline P. Normile, and Philip J. Stenger. 2010. “A Back-Trajectory and Air Mass Climatology for the Northern Shenandoah Valley, USA.” *International Journal of Climatology* 30 (4): 569–581.
- Hongisto, Marke, and Mikhail Sofiev. 2004. “Long-Range Transport of Dust to the Baltic Sea Region.” *International Journal of Environment and Pollution* 22 (1–2): 72–86.
- Hopke, P. K., L. A. Barrie, S.-M. Li, M.-D. Cheng, C. Li, and Y. Xie. 1995. “Possible Sources and Preferred Pathways for Biogenic and Non-Sea-Salt Sulfur for the High Arctic.” *Journal of Geophysical Research: Atmospheres* 100 (D8): 16595–16603.
- Huang, Sulou, Richard Arimoto, and Kenneth A. Rahn. 2001. “Sources and Source Variations for Aerosol at Mace Head, Ireland.” *Atmospheric Environment* 35 (8): 1421–37. doi:10.1016/S1352-2310(00)00368-X.
- Iinuma, Yoshiteru, Guenter Engling, Hans Puxbaum, and Hartmut Herrmann. 2009. “A Highly Resolved Anion-Exchange Chromatographic Method for Determination of Saccharidic Tracers for Biomass Combustion and Primary Bio-Particles in Atmospheric Aerosol.” *Atmospheric Environment* 43 (6): 1367–1371.
- Inyang, Hilary I., and Sunyoung Bae. 2006. “Impacts of Dust on Environmental Systems and Human Health.” *Journal of Hazardous Materials* 132 (1): v–vi. doi:10.1016/j.jhazmat.2005.11.082.
- “IPCC, 2013: Climate Change 2013: The Physical Science Basis. Contribution of Working Group I to the Fifth Assessment Report of the Intergovernmental Panel on Climate Change [Stocker, T.F., D. Qin, G. - K. Plattner, M. Tignor, S.K. Allen, J. Bosc Hung, A. Nauels, Y. Xia, V. Bex and P.M. Midgley (Eds.)]. Cambridge University Press, Cambridge, United Kingdom and New York, NY, USA, 1535 Pp , doi:10.1017/CBO9781107415324.” n.d.
- Jacobson, Mark Z. 2002. “Control of Fossil-Fuel Particulate Black Carbon and Organic Matter, Possibly the Most Effective Method of Slowing Global Warming.” *Journal of Geophysical Research: Atmospheres* 107 (D19): 4410. doi:10.1029/2001JD001376.
- Jaenicke, Ruprecht. 2005. “Abundance of Cellular Material and Proteins in the Atmosphere.” *Science* 308 (5718): 73–73.
- Jaffrezo, J. L., N. Calas, and M. Bouchet. 1998. “Carboxylic Acids Measurements with Ionic Chromatography.” *Atmospheric Environment* 32 (14): 2705–2708.
- Jia, Yuling, Andrea L. Clements, and Matthew P. Fraser. 2010. “Saccharide Composition in Atmospheric Particulate Matter in the Southwest US and Estimates of Source Contributions.” *Journal of Aerosol Science* 41 (1): 62–73.
- Johansson, Christer, Michael Norman, and Lars Burman. 2009. “Road Traffic Emission Factors for Heavy Metals.” *Atmospheric Environment* 43 (31): 4681–4688.

- Jorba, Oriol, Carlos Pérez, Francesc Rocadenbosch, and JoséM Baldasano. 2004. "Cluster Analysis of 4-Day Back Trajectories Arriving in the Barcelona Area, Spain, from 1997 to 2002." *Journal of Applied Meteorology* 43 (6): 887–901.
- Junninen, Heikki, Jacob Mønster, Maria Rey, Jose Cancelinha, Kevin Douglas, Matthew Duane, Vittorio Forcina, et al. 2009. "Quantifying the Impact of Residential Heating on the Urban Air Quality in a Typical European Coal Combustion Region." *Environmental Science & Technology* 43 (20): 7964–70. doi:10.1021/es8032082.
- Kabashnikov, Vitaliy P., Anatoli P. Chaikovsky, Tom L. Kucsera, and Natalia S. Metelskaya. 2011. "Estimated Accuracy of Three Common Trajectory Statistical Methods." *Atmospheric Environment* 45 (31): 5425–30. doi:10.1016/j.atmosenv.2011.07.006.
- Kanakidou, M., J. H. Seinfeld, S. N. Pandis, I. Barnes, F. J. Dentener, M. C. Facchini, R. Van Dingenen, et al. 2005. "Organic Aerosol and Global Climate Modelling: A Review." *Atmos. Chem. Phys.* 5 (4): 1053–1123. doi:10.5194/acp-5-1053-2005.
- Karaca, Ferhat, and Fatih Camci. 2010. "Distant Source Contributions to PM 10 Profile Evaluated by SOM Based Cluster Analysis of Air Mass Trajectory Sets." *Atmospheric Environment* 44 (7): 892–899.
- Karagulian, Federico, Claudio A. Belis, Carlos Francisco C. Dora, Annette M. Prüss-Ustün, Sophie Bonjour, Heather Adair-Rohani, and Markus Amann. 2015. "Contributions to Cities' Ambient Particulate Matter (PM): A Systematic Review of Local Source Contributions at Global Level." *Atmospheric Environment* 120: 475–483.
- Kawamura, Kimitaka, and Kouichi Ikushima. 1993. "Seasonal Changes in the Distribution of Dicarboxylic Acids in the Urban Atmosphere." *Environmental Science & Technology* 27 (10): 2227–2235.
- Kawamura, Kimitaka, and Isaac R. Kaplan. 1987. "Motor Exhaust Emissions as a Primary Source for Dicarboxylic Acids in Los Angeles Ambient Air." *Environmental Science & Technology* 21 (1): 105–110.
- Kawamura, Kimitaka, Hideki Kasukabe, and Leonard A. Barrie. 1996. "Source and Reaction Pathways of Dicarboxylic Acids, Ketoacids and Dicarbonyls in Arctic Aerosols: One Year of Observations." *Atmospheric Environment* 30 (10): 1709–1722.
- Kawamura, Kimitaka, and Kouichi Usukura. 1993. "Distributions of Low Molecular Weight Dicarboxylic Acids in the North Pacific Aerosol Samples." *Journal of Oceanography* 49 (3): 271–283.
- Kelly, Frank J., and Julia C. Fussell. 2015. "Linking Ambient Particulate Matter Pollution Effects with Oxidative Biology and Immune Responses." *Annals of the New York Academy of Sciences* 1340 (1): 84–94. doi:10.1111/nyas.12720.
- Kendall, Carol, Emily M. Elliott, and SCOTT D. Wankel. 2007. "Tracing Anthropogenic Inputs of Nitrogen to Ecosystems." *Stable Isotopes in Ecology and Environmental Science* 2: 375–449.
- Kettle A. J., M. O. Andreae, D. Amouroux, T. W. Andreae, T. S. Bates, H. Berresheim, H. Bingemer, R. Boniforti, M. A. J. Curran, G. R. DiTullio, G. Helas, G. B. Jones, M. D. Keller, R. P. Kiene, C. Leck, M. Lévassieur, G. Malin, M. Maspero, P. Matrai, A. R. McTaggart, N. Mihalopoulos, B. C. Nguyen, A. Novo, J. P. Putaud, S. Rapsomanikis, G. Roberts, G. Schebeske, S. Sharma, R. Simó, R. Staubes, S. Turner, G. Uher. A global database of sea surface dimethylsulfide (DMS) measurements and a procedure to predict sea surface DMS as a function of latitude, longitude, and month, *Global Biogeochem. Cycles*, 13(2), 399–444, doi:[10.1029/1999GB900004](https://doi.org/10.1029/1999GB900004)
- Kim Oanh, Nguyen Thi, Prapat Pongkiatkul, Nabin Upadhyay, and Phillip P. Hopke. 2009. "Designing Ambient Particulate Matter Monitoring Program for Source Apportionment Study by Receptor Modeling." *Atmospheric Environment* 43 (21): 3334–44. doi:10.1016/j.atmosenv.2009.04.016.

- Koçak, Mustafa, Nikos Mihalopoulos, and Nilgün Kubilay. 2007. "Chemical Composition of the Fine and Coarse Fraction of Aerosols in the Northeastern Mediterranean." *Atmospheric Environment* 41 (34): 7351–68. doi:10.1016/j.atmosenv.2007.05.011.
- Kourtchev, Ivan, Lucian Copolovici, Magda Claeys, and Willy Maenhaut. 2009. "Characterization of Atmospheric Aerosols at a Forested Site in Central Europe." *Environmental Science & Technology* 43 (13): 4665–71. doi:10.1021/es803055w.
- Krecl, P., E. Hedberg Larsson, J. Ström, and C. Johansson. 2008. "Contribution of Residential Wood Combustion and Other Sources to Hourly Winter Aerosol in Northern Sweden Determined by Positive Matrix Factorization." *Atmos. Chem. Phys.* 8 (13): 3639–53. doi:10.5194/acp-8-3639-2008.
- Křůmal, K., P. Mikuška, M. Vojtěšek, and Z. Večeřa. 2010. "Seasonal Variations of Monosaccharide Anhydrides in PM₁ and PM_{2.5} Aerosol in Urban Areas." *Atmospheric Environment* 44 (39): 5148–5155.
- Kryza, Maciej, Małgorzata Werner, Marek Błaś, Anthony J. Dore, and Mieczysław Sobik. 2010. "The Effect of Emission from Coal Combustion in Nonindustrial Sources on Deposition of Sulfur and Oxidized Nitrogen in Poland." *Journal of the Air & Waste Management Association* 60 (7): 856–866.
- Kuklinska, Karolina, Lidia Wolska, and Jacek Namiesnik. 2015. "Air Quality Policy in the U.S. and the EU – a Review." *Atmospheric Pollution Research* 6 (1): 129–37. doi:10.5094/APR.2015.015.
- "La Qualité de L'air En Île-de-France En 2012 - Bilan-2012.pdf." 2016. Accessed November 15. http://www.airparif.asso.fr/_pdf/publications/bilan-2012.pdf.
- Lamaison, Laure. 2006. *Caractérisation Des Particules Atmosphériques et Identification de Leurs Sources Dans Une Atmosphère Urbaine Sous Influence Industrielle*. Lille 1. <http://www.theses.fr/2006LIL10071>.
- Lewandowska, Anita, Lucyna Falkowska, and Joanna Józwik. 2013. "Factors Determining the Fluctuation of Fluoride Concentrations in PM₁₀ Aerosols in the Urbanized Coastal Area of the Baltic Sea (Gdynia, Poland)." *Environmental Science and Pollution Research* 20 (9): 6109–6118.
- Li, Mengmeng, Xin Huang, Lei Zhu, Jianfeng Li, Yu Song, Xuhui Cai, and Shaodong Xie. 2012. "Analysis of the Transport Pathways and Potential Sources of PM₁₀ in Shanghai Based on Three Methods." *Science of the Total Environment* 414: 525–534.
- Lim, Ho-Jin, Barbara J. Turpin, Eric Edgerton, Susanne V. Hering, George Allen, Hal Maring, and Paul Solomon. 2003. "Semicontinuous Aerosol Carbon Measurements: Comparison of Atlanta Supersite Measurements." *Journal of Geophysical Research: Atmospheres* 108 (D7): 8419. doi:10.1029/2001JD001214.
- Lippmann, Morton, Lung-Chi Chen, Terry Gordon, Kazuhiko Ito, and George D. Thurston. 2013. "National Particle Component Toxicity (NPACT) Initiative: Integrated Epidemiologic and Toxicologic Studies of the Health Effects of Particulate Matter Components." *Research Report (Health Effects Institute)*, no. 177(October): 5–13.
- Liu, Ling, Raymond Poon, Li Chen, Anna-Maria Frescura, Paolo Montuschi, Giovanni Ciabattini, Amanda Wheeler, and Robert Dales. 2009. "Acute Effects of Air Pollution on Pulmonary Function, Airway Inflammation, and Oxidative Stress in Asthmatic Children." *Environmental Health Perspectives* 117 (4): 668.
- Lohmann, U., and J. Feichter. 2005. "Global Indirect Aerosol Effects: A Review." *Atmospheric Chemistry and Physics* 5 (3): 715–37.
- Loubet, B., C. Milford, A. Hensen, U. Daemmgen, J.-W. Erismann, P. Cellier, and M. A. Sutton. 2009. "Advection of NH₃ over a Pasture Field and Its Effect on Gradient Flux Measurements." *Biogeosciences* 6 (7): 1295–1309. doi:10.5194/bg-6-1295-2009.

- Lupu, Alexandru, and Willy Maenhaut. 2002. "Application and Comparison of Two Statistical Trajectory Techniques for Identification of Source Regions of Atmospheric Aerosol Species." *Atmospheric Environment* 36 (36): 5607–5618.
- Maenhaut, Willy, Jan Cafmeyer, Sergei Dubtsov, and Xuguang Chi. 2002. "Detailed Mass Size Distributions of Elements and Species, and Aerosol Chemical Mass Closure during Fall 1999 at Gent, Belgium." *Nuclear Instruments and Methods in Physics Research Section B: Beam Interactions with Materials and Atoms* 189 (1–4): 238–42. doi:10.1016/S0168-583X(01)01049-7.
- Maenhaut, Willy, Reinhilde Vermeulen, Magda Claeys, Jordy Vercauteren, Christina Matheussen, and Edward Roekens. 2012. "Assessment of the Contribution from Wood Burning to the PM10 Aerosol in Flanders, Belgium." *Science of The Total Environment* 437 (October): 226–36. doi:10.1016/j.scitotenv.2012.08.015.
- Maenhaut, Willy, Reinhilde Vermeulen, Magda Claeys, Jordy Vercauteren, and Edward Roekens. 2016. "Sources of the PM10 Aerosol in Flanders, Belgium, and Re-Assessment of the Contribution from Wood Burning." *The Science of the Total Environment* 562 (August): 550–60. doi:10.1016/j.scitotenv.2016.04.074.
- Makra, László, István Matyasovszky, Zoltán Guba, Kostas Karatzas, and Pia Anttila. 2011. "Monitoring the Long-Range Transport Effects on Urban PM10 Levels Using 3D Clusters of Backward Trajectories." *Atmospheric Environment* 45 (16): 2630–2641.
- "Manders, A.M.M., Schaap, M., Jozwicka, M., Van Arkel, F., Weijers, E.P., and Matthijsen, J.: The Contribution of Sea Salt to PM10 and PM2.5 in the Netherlands, Netherlands Environmental Assessment Agency, 2009." n.d.
- Mann, G. W., K. S. Carslaw, D. A. Ridley, D. V. Spracklen, K. J. Pringle, Joonas Merikanto, Hannelle Korhonen, et al. 2012. "Intercomparison of Modal and Sectional Aerosol Microphysics Representations within the Same 3-D Global Chemical Transport Model." *Atmospheric Chemistry and Physics* 12 (10): 4449–4476.
- Mbengue, Saliou, Laurent Y. Alleman, and Pascal Flament. 2015. "Bioaccessibility of Trace Elements in Fine and Ultrafine Atmospheric Particles in an Industrial Environment." *Environmental Geochemistry and Health* 37 (5): 875–89. doi:10.1007/s10653-015-9756-2.
- McInnes, L. M., D. S. Covert, P. K. Quinn, and M. S. Germani. 1994. "Measurements of Chloride Depletion and Sulfur Enrichment in Individual Sea-Salt Particles Collected from the Remote Marine Boundary Layer." *Journal of Geophysical Research: Atmospheres* 99 (D4): 8257–68. doi:10.1029/93JD03453.
- McQueen, J. T., R. R. Draxler, B. J. B. Stunder, and G. D. Rolph. 1997. "Applications of the Regional Atmospheric Modeling System(RAMS) at the NOAA Air Resources Laboratory." National Oceanic and Atmospheric Administration.
- Millero, Frank J., and Fred K. Lepple. 1973. "The Density and Expansibility of Artificial Seawater Solutions from 0 to 40 C and 0 to 21‰ Chlorinity." *Marine Chemistry* 1 (2): 89–104.
- Monod, Anne, Barkley C. Sive, Pasquale Avino, Tai Chen, Donald R. Blake, and F. Sherwood Rowland. 2001. "Monoaromatic Compounds in Ambient Air of Various Cities: A Focus on Correlations between the Xylenes and Ethylbenzene." *Atmospheric Environment* 35 (1): 135–149.
- Mooibroek, D., M. Schaap, E. P. Weijers, and R. Hoogerbrugge. 2011. "Source Apportionment and Spatial Variability of PM2.5 Using Measurements at Five Sites in the Netherlands." *Atmospheric Environment* 45 (25): 4180–91. doi:10.1016/j.atmosenv.2011.05.017.
- Myriokefalitakis, S., K. Tsigaridis, N. Mihalopoulos, J. Sciare, A. Nenes, K. Kawamura, A. Segers, and M. Kanakidou. 2011. "In-Cloud Oxalate Formation in the Global

- Troposphere: A 3-D Modeling Study.” *Atmospheric Chemistry and Physics* 11 (12): 5761–5782.
- “NASA Goddard Space Flight Center, Ocean Ecology Laboratory, Ocean Biology Processing Group. VIIRS Chlorophyll Data; 2014 Reprocessing. NASA OB.DAAC, Greenbelt, MD, USA. Doi: 10.5067/NPP/VIIRS/L3M/CHL/2014. Accessed on 10/21/2016.” n.d.
- Nawrot, T. S., R. Vos, L. Jacobs, S. E. Verleden, S. Wauters, V. Mertens, C. Dooms, et al. 2011. “The Impact of Traffic Air Pollution on Bronchiolitis Obliterans Syndrome and Mortality after Lung Transplantation.” *Thorax* 66 (9): 748–754.
- Nieuwenhuijsen, M. J., J. E. Gomez-Perales, and R. N. Colvile. 2007. “Levels of Particulate Air Pollution, Its Elemental Composition, Determinants and Health Effects in Metro Systems.” *Atmospheric Environment* 41 (37): 7995–8006.
- Nunes, Teresa V., and Casimiro A. Pio. 1993. “Carbonaceous Aerosols in Industrial and Coastal Atmospheres.” *Atmospheric Environment. Part A. General Topics* 27 (8): 1339–46. doi:10.1016/0960-1686(93)90259-2.
- Ocskay, Rita, Imre Salma, Wan Wang, and Willy Maenhaut. 2006. “Characterization and Diurnal Variation of Size-Resolved Inorganic Water-Soluble Ions at a Rural Background Site.” *Journal of Environmental Monitoring: JEM* 8 (2): 300–306. doi:10.1039/b513915e.
- O’Dowd, Colin D., Maria Cristina Facchini, Fabrizia Cavalli, Darius Ceburnis, Mihaela Mircea, Stefano Decesari, Sandro Fuzzi, Young Jun Yoon, and Jean-Philippe Putaud. 2004. “Biogenically Driven Organic Contribution to Marine Aerosol.” *Nature* 431 (7009): 676–80. doi:10.1038/nature02959.
- Oros, D. R., and B. R. T. Simoneit. 2000. “Identification and Emission Rates of Molecular Tracers in Coal Smoke Particulate Matter.” *Fuel* 79 (5): 515–536.
- Paatero, Pentti. 1997. “Least Squares Formulation of Robust Non-Negative Factor Analysis.” *Chemometrics and Intelligent Laboratory Systems* 37 (1): 23–35.
- Paatero, Pentti, and Philip K. Hopke. 2003. “Discarding or Downweighting High-Noise Variables in Factor Analytic Models.” *Analytica Chimica Acta* 490 (1): 277–289.
- Paatero, Pentti, Philip K. Hopke, Xin-Hua Song, and Ziad Ramadan. 2002. “Understanding and Controlling Rotations in Factor Analytic Models.” *Chemometrics and Intelligent Laboratory Systems* 60 (1): 253–264.
- Paatero, Pentti, and Unto Tapper. 1994. “Positive Matrix Factorization: A Non-Negative Factor Model with Optimal Utilization of Error Estimates of Data Values.” *Environmetrics* 5 (2): 111–26. doi:10.1002/env.3170050203.
- Pandolfi, M., M. Viana, M. C. Minguillón, X. Querol, A. Alastuey, F. Amato, I. Celades, A. Escrig, and E. Monfort. 2008. “Receptor Models Application to Multi-Year Ambient PM10 Measurements in an Industrialized Ceramic Area: Comparison of Source Apportionment Results.” *Atmospheric Environment* 42 (40): 9007–17. doi:10.1016/j.atmosenv.2008.09.029.
- Paris, R., and K. V. Desboeufs. 2013. “Effect of Atmospheric Organic Complexation on Iron-Bearing Dust Solubility.” *Atmospheric Chemistry and Physics* 13: 4895–4905.
- Pascaud, A., S. Sauvage, P. Coddeville, M. Nicolas, L. Croisé, A. Mezdour, and A. Probst. 2016. “Contrasted Spatial and Long-Term Trends in Precipitation Chemistry and Deposition Fluxes at Rural Stations in France.” *Atmospheric Environment, Acid Rain and its Environmental Effects: Recent Scientific Advances* Papers from the Ninth International Conference on Acid Deposition, 146: 28–43. doi:10.1016/j.atmosenv.2016.05.019.
- Pashynska, Vlada, Reinhilde Vermeylen, Gyorgy Vas, Willy Maenhaut, and Magda Claeys. 2002. “Development of a Gas Chromatographic/ion Trap Mass Spectrometric Method for the Determination of Levoglucosan and Saccharidic Compounds in Atmospheric

- Aerosols. Application to Urban Aerosols.” *Journal of Mass Spectrometry* 37 (12): 1249–1257.
- Paw-Armart, Ittipol, and Kunio Yoshizumi. 2013. “Size Distributions of Atmospheric Aerosol Compositions in Saitama, Japan.” *Open Journal of Air Pollution* 2 (1): 1–6. doi:10.4236/ojap.2013.21001.
- Pérez, Noemí, Jorge Pey, Cristina Reche, Joaquim Cortés, Andrés Alastuey, and Xavier Querol. 2016. “Impact of Harbour Emissions on Ambient PM10 and PM2.5 in Barcelona (Spain): Evidences of Secondary Aerosol Formation within the Urban Area.” *Science of The Total Environment* 571 (November): 237–50. doi:10.1016/j.scitotenv.2016.07.025.
- Pernigotti, Denise, Claudio A. Belis, and Luca Spanò. 2016. “SPECIEUROPE: The European Data Base for PM Source Profiles.” *Atmospheric Pollution Research* 7 (2): 307–14. doi:10.1016/j.apr.2015.10.007.
- Petit, J. -E., O. Favez, A. Albinet, and F. Canonaco. 2017. “A User-Friendly Tool for Comprehensive Evaluation of the Geographical Origins of Atmospheric Pollution: Wind and Trajectory Analyses.” *Environmental Modelling & Software* 88: 183–87. doi:10.1016/j.envsoft.2016.11.022.
- Pietrogrande, M. C., M. Mercuriali, M. G. Perrone, L. Ferrero, G. Sangiorgi, and E. Bolzacchini. 2010. “Distribution of N-Alkanes in the Northern Italy Aerosols: Data Handling of GC-MS Signals for Homologous Series Characterization.” *Environmental Science & Technology* 44 (11): 4232–4240.
- Pincus, Robert, and Marcia B. Baker. 1994. “Effect of Precipitation on the Albedo Susceptibility of Clouds in the Marine Boundary Layer.” *Nature* 372 (6503): 250–252.
- Pio, Casimiro A., Luis M. Castro, Mario A. Cerqueira, Isabel M. Santos, Filipa Belchior, and Maria L. Salgueiro. 1996. “Source Assessment of Particulate Air Pollutants Measured at the Southwest European Coast.” *Atmospheric Environment* 30 (19): 3309–3320.
- Pio, Casimiro, and Célia Alves. 2013. “Atmospheric PM across Europe: Concentration Levels and Variability.” In *Particulate Matter: Environmental Monitoring and Mitigation*, 34–52. Unitec House, 2 Albert Place, London N3 1QB, UK (Future Science Ltd).
- Pio, Casimiro, Mário Cerqueira, Roy M. Harrison, Teresa Nunes, Fátima Mirante, Célia Alves, César Oliveira, Ana Sanchez de la Campa, Begoña Artíñano, and Manuel Matos. 2011. “OC/EC Ratio Observations in Europe: Re-Thinking the Approach for Apportionment between Primary and Secondary Organic Carbon.” *Atmospheric Environment* 45 (34): 6121–32. doi:10.1016/j.atmosenv.2011.08.045.
- Piot, Christine, Jean-Luc Jaffrezo, Julie Cozic, Nicolas Pissot, Imad El Haddad, Nicolas Marchand, and Jean-Luc Besombes. 2012. “Quantification of Levoglucosan and Its Isomers by High Performance Liquid Chromatography-Electrospray Ionization Tandem Mass Spectrometry and Its Application to Atmospheric and Soil Samples.” *Atmospheric Measurement Techniques* 5: 141–148.
- Pla, N. 2016. “Rapport D’activité LCSQA 2015.” <http://www.lcsqa.org/rapport/2016/ineris-lne-mines-douai/rapport-activite-lcsqa-2015>.
- Poirot, Richard L., Paul R. Wishinski, Philip K. Hopke, and Alexander V. Polissar. 2001. “Comparative Application of Multiple Receptor Methods to Identify Aerosol Sources in Northern Vermont.” *Environmental Science & Technology* 35 (23): 4622–4636.
- Pope III, C. Arden, and Douglas W. Dockery. 2006. “Health Effects of Fine Particulate Air Pollution: Lines That Connect.” *Journal of the Air & Waste Management Association* 56 (6): 709–742.
- Putaud, J.-P., R. Van Dingenen, A. Dell’Acqua, F. Raes, E. Matta, S. Decesari, M. C. Facchini, and S. Fuzzi. 2004. “Size-Segregated Aerosol Mass Closure and Chemical

- Composition in Monte Cimone (I) during MINATROC.” *Atmospheric Chemistry and Physics* 4 (4): 889–902.
- Puxbaum, Hans, Alexandre Caseiro, Asunción Sánchez-Ochoa, Anne Kasper-Giebl, Magda Claeys, András Gelencsér, Michel Legrand, Susanne Preunkert, and Casimiro Pio. 2007. “Levoglucosan Levels at Background Sites in Europe for Assessing the Impact of Biomass Combustion on the European Aerosol Background.” *Journal of Geophysical Research: Atmospheres* 112 (D23): D23S05. doi:10.1029/2006JD008114.
- Quan, Chunli, Qinghua Sun, Morton Lippmann, and Lung-Chi Chen. 2010. “Comparative Effects of Inhaled Diesel Exhaust and Ambient Fine Particles on Inflammation, Atherosclerosis, and Vascular Dysfunction.” *Inhalation Toxicology* 22 (9): 738–53. doi:10.3109/08958371003728057.
- “Rapport_essai_caracterisation_PM10_Nogent_version_Finale.pdf.” 2016. Accessed October 29. http://www.atmopicardie.com/publications/fichiers/199/Rapport_essai_caracterisation_PM10_Nogent_version_Finale.pdf.
- Riffault, Véronique, Jovanna Arndt, Hélène Marris, Saliou Mbengue, Ari Setyan, Laurent Y. Alleman, Karine Deboudt, et al. 2015. “Fine and Ultrafine Particles in the Vicinity of Industrial Activities: A Review.” *Critical Reviews in Environmental Science and Technology* 45 (21): 2305–56. doi:10.1080/10643389.2015.1025636.
- Rogge, Wolfgang F., Lynn M. Hildemann, Monica A. Mazurek, Glen R. Cass, and Bernd R. T. Simoneit. 1993. “Sources of Fine Organic Aerosol. 2. Noncatalyst and Catalyst-Equipped Automobiles and Heavy-Duty Diesel Trucks.” *Environmental Science & Technology* 27 (4): 636–51. doi:10.1021/es00041a007.
- . 1996. “Mathematical Modeling of Atmospheric Fine Particle-Associated Primary Organic Compound Concentrations.” *Journal of Geophysical Research D* 101 (D14): 19379–94.
- Rogge, Wolfgang F., Lynn M. Hildemann, Monica A. Mazurek, Glen R. Cass, and Bernd RT Simoneit. 1997. “Sources of Fine Organic Aerosol. 7. Hot Asphalt Roofing Tar Pot Fumes.” *Environmental Science & Technology* 31 (10): 2726–2730.
- . 1998. “Sources of Fine Organic Aerosol. 9. Pine, Oak, and Synthetic Log Combustion in Residential Fireplaces.” *Environmental Science & Technology* 32 (1): 13–22.
- Rouil, Laurence, Cécile Honoré, Bertrand Bessagnet, Laure Malherbe, Frédéric Meleux, Robert Vautard, Matthias Beekmann, et al. 2009. “Prev’air: An Operational Forecasting and Mapping System for Air Quality in Europe.” *Bulletin of the American Meteorological Society* 90 (1): 73–83. doi:10.1175/2008BAMS2390.1.
- Rutter, A. P., D. C. Snyder, E. A. Stone, J. J. Schauer, R. Gonzalez-Abraham, L. T. Molina, C. Márquez, B. Cárdenas, and B. de Foy. 2009. “In Situ Measurements of Speciated Atmospheric Mercury and the Identification of Source Regions in the Mexico City Metropolitan Area.” *Atmos. Chem. Phys.* 9 (1): 207–20. doi:10.5194/acp-9-207-2009.
- Saffari, Arian, Nancy Daher, Constantini Samara, Dimitra Voutsas, Athanasios Kouras, Evangelia Manoli, Olga Karagkiozidou, et al. 2013. “Increased Biomass Burning due to the Economic Crisis in Greece and Its Adverse Impact on Wintertime Air Quality in Thessaloniki.” *Environmental Science & Technology* 47 (23): 13313–13320.
- Salvador, Pedro, Begoña Artíñano, Xavier Querol, and Andres Alastuey. 2008. “A Combined Analysis of Backward Trajectories and Aerosol Chemistry to Characterise Long-Range Transport Episodes of Particulate Matter: The Madrid Air Basin, a Case Study.” *Science of the Total Environment* 390 (2): 495–506.

- Samoli, Evangelia, Roger Peng, Tim Ramsay, Marina Pipikou, Giota Touloumi, Francesca Dominici, Rick Burnett, et al. 2008. "Acute Effects of Ambient Particulate Matter on Mortality in Europe and North America: Results from the APHENA Study." *Environmental Health Perspectives* 116 (11): 1480–86. doi:10.1289/ehp.11345.
- Sang, Xue-Fang, Chuen-Yu Chan, Guenter Engling, Lo-Yin Chan, Xue-Mei Wang, Yi-Nan Zhang, Si Shi, Zhi-Sheng Zhang, Ting Zhang, and Ming Hu. 2011. "Levoglucosan Enhancement in Ambient Aerosol during Springtime Transport Events of Biomass Burning Smoke to Southeast China." *Tellus Series B Chemical and Physical Meteorology B* 63: 129–139.
- Sartelet, Karine N., Florian Couvidat, Christian Seigneur, and Yelva Roustan. 2012. "Impact of Biogenic Emissions on Air Quality over Europe and North America." *Atmospheric Environment* 53: 131–141.
- Schauer, James J., Michael J. Kleeman, Glen R. Cass, and Bernd R. T. Simoneit. 1999. "Measurement of Emissions from Air Pollution Sources. 1. C1 through C29 Organic Compounds from Meat Charbroiling." *Environmental Science & Technology* 33 (10): 1566–77. doi:10.1021/es980076j.
- . 2002. "Measurement of Emissions from Air Pollution Sources. 5. C1–C32 Organic Compounds from Gasoline-Powered Motor Vehicles." *Environmental Science & Technology* 36 (6): 1169–80. doi:10.1021/es0108077.
- Schauer, James J., Michael J. Kleeman, Glen R. Cass, and Bernd RT Simoneit. 2001. "Measurement of Emissions from Air Pollution Sources. 3. C1-C29 Organic Compounds from Fireplace Combustion of Wood." *Environmental Science & Technology* 35 (9): 1716–1728.
- Schauer, James J., Wolfgang F. Rogge, Lynn M. Hildemann, Monica A. Mazurek, Glen R. Cass, and Bernd R. T. Simoneit. 1996. "Source Apportionment of Airborne Particulate Matter Using Organic Compounds as Tracers." *Atmospheric Environment* 30 (22): 3837–55. doi:10.1016/1352-2310(96)00085-4.
- Schmid, Heidrun, Lothar Laskus, Hans Jürgen Abraham, Urs Baltensperger, Vincent Lavanchy, Mirko Bizjak, Peter Burba, et al. 2001. "Results of the 'carbon Conference' International Aerosol Carbon Round Robin Test Stage I." *Atmospheric Environment* 35 (12): 2111–2121.
- Schmidl, Christoph, Heidi Bauer, Astrid Dattler, Regina Hitzenberger, Gerlinde Weissenboeck, Iain L. Marr, and Hans Puxbaum. 2008. "Chemical Characterisation of Particle Emissions from Burning Leaves." *Atmospheric Environment* 42 (40): 9070–79. doi:10.1016/j.atmosenv.2008.09.010.
- Sciare, J., O. d'Argouges, Q. J. Zhang, R. Sarda-Estève, C. Gaimoz, V. Gros, M. Beekmann, and O. Sanchez. 2010. "Comparison between Simulated and Observed Chemical Composition of Fine Aerosols in Paris (France) during Springtime: Contribution of Regional versus Continental Emissions." *Atmos. Chem. Phys.* 10 (24): 11987–4. doi:10.5194/acp-10-11987-2010.
- Sciare, J., K. Oikonomou, O. Favez, E. Liakakou, Z. Markaki, H. Cachier, and N. Mihalopoulos. 2008. "Long-Term Measurements of Carbonaceous Aerosols in the Eastern Mediterranean: Evidence of Long-Range Transport of Biomass Burning." *Atmos. Chem. Phys.* 8 (18): 5551–63. doi:10.5194/acp-8-5551-2008.
- Sciare, Jean, Odile D'Argouges, Roland Sarda-Estève, Cécile Gaimoz, Cristina Dolgorouky, Nicolas Bonnaire, Olivier Favez, Bernard Bonsang, and Valérie Gros. 2011. "Large Contribution of Water-Insoluble Secondary Organic Aerosols in the Region of Paris (France) during Wintertime." *Journal of Geophysical Research: Atmospheres* 116: D22203.

- Sehmel, G. A. 1980. "Particle Resuspension: A Review." *Environment International* 4 (2): 107–27. doi:10.1016/0160-4120(80)90005-7.
- Seibert, P., H. Kromp-Kolb, U. Baltensperger, D. T. Jost, M. Schwikowski, A. Kasper, and H. Puxbaum. 1994. "Trajectory Analysis of Aerosol Measurements at High Alpine Sites." *Transport and Transformation of Pollutants in the Troposphere*, 689–693.
- Seinfeld, John H., and Spyros N. Pandis. 1998. *Atmospheric Chemistry and Physics: From Air Pollution to Climate Change*. University of Michigan: Wiley.
- . 2006. *Atmospheric Chemistry and Physics: From Air Pollution to Climate Change*. 2, illustrated ed. University of Michigan: Wiley.
- Sempère, Richard, and Kimitaka Kawamura. 1994. "Comparative Distributions of Dicarboxylic Acids and Related Polar Compounds in Snow, Rain and Aerosols from Urban Atmosphere." *Atmospheric Environment* 28 (3): 449–459.
- Sempère, Richard, and Kimitaka Kawamura. 1996. "Low Molecular Weight Dicarboxylic Acids and Related Polar Compounds in the Remote Marine Rain Samples Collected from Western Pacific." *Atmospheric Environment* 30 (10): 1609–1619.
- Sexauer Gustin, M., P. S. Weiss-Penzias, and C. Peterson. 2012. "Investigating Sources of Gaseous Oxidized Mercury in Dry Deposition at Three Sites across Florida, USA." *Atmos. Chem. Phys.* 12 (19): 9201–19. doi:10.5194/acp-12-9201-2012.
- Sicard, Pierre, Patrice Coddeville, Stéphane Sauvage, and Jean-Claude Galloo. 2007. "Trends in Chemical Composition of Wet-Only Precipitation at Rural French Monitoring Stations over the 1990–2003 Period." *Water, Air, & Soil Pollution: Focus* 7 (1–3): 49–58.
- Simoneit, Bernd R. T. 1984. "Organic Matter of the troposphere—III. Characterization and Sources of Petroleum and Pyrogenic Residues in Aerosols over the Western United States." *Atmospheric Environment (1967)* 18 (1): 51–67. doi:10.1016/0004-6981(84)90228-2.
- . 1989. "Organic Matter of the Troposphere — V: Application of Molecular Marker Analysis to Biogenic Emissions into the Troposphere for Source Reconciliations." *Journal of Atmospheric Chemistry* 8 (3): 251–75. doi:10.1007/BF00051497.
- Simoneit, Bernd RT, Minoru Kobayashi, Michihiro Mochida, Kimitaka Kawamura, Meehye Lee, Ho-Jin Lim, Barbara J. Turpin, and Yuichi Komazaki. 2004. "Composition and Major Sources of Organic Compounds of Aerosol Particulate Matter Sampled during the ACE-Asia Campaign." *Journal of Geophysical Research. Atmosphere* 109 (D19): D19S10.
- Simoneit, Bernd RT, James J. Schauer, C. G. Nolte, Daniel R. Oros, Vladimir O. Elias, M. P. Fraser, W. F. Rogge, and Glen R. Cass. 1999. "Levoglucosan, a Tracer for Cellulose in Biomass Burning and Atmospheric Particles." *Atmospheric Environment* 33 (2): 173–182.
- Staelens, Jeroen, Dennis Mooibroek, Rebecca Cordell, Tiphaine Delaunay, Pavlos Panteliadis, Ernie Weijers, Christine Matheussen, et al. 2016. "Composition and Source Apportionment of PM10 (JOAQUIN 2015)." *ResearchGate*, January. https://www.researchgate.net/publication/293605872_Composition_and_source_apportionment_of_PM10_JOAQUIN_2015.
- Stein, A. F., R. R. Draxler, G. D. Rolph, B. J. B. Stunder, M. D. Cohen, and F. Ngan. 2015. "NOAA's HYSPLIT Atmospheric Transport and Dispersion Modeling System." *Bulletin of the American Meteorological Society* 96 (12): 2059–77. doi:10.1175/BAMS-D-14-00110.1.
- Stohl, Andreas. 1998. "Computation, Accuracy and Applications of Trajectories—a Review and Bibliography." *Atmospheric Environment* 32 (6): 947–966.

- Stohl, Andreas, Gerhard Wotawa, Petra Seibert, and Helga Kromp-Kolb. 1995. "Interpolation Errors in Wind Fields as a Function of Spatial and Temporal Resolution and Their Impact on Different Types of Kinematic Trajectories." *Journal of Applied Meteorology* 34 (10): 2149–2165.
- Stone, Elizabeth, James Schauer, Tauseef A. Quraishi, and Abid Mahmood. 2010. "Chemical Characterization and Source Apportionment of Fine and Coarse Particulate Matter in Lahore, Pakistan." *Atmospheric Environment* 44 (8): 1062–70. doi:10.1016/j.atmosenv.2009.12.015.
- Stull, Roland B. 1988. *An Introduction to Boundary Layer Meteorology*. Softcover reprint of the original 1st ed. 1988 edition. Dordrecht: Springer.
- Su, Lin, Zibing Yuan, Jimmy C. H. Fung, and Alexis K. H. Lau. 2015. "A Comparison of HYSPLIT Backward Trajectories Generated from Two GDAS Datasets." *Science of The Total Environment* 506–507 (February): 527–37. doi:10.1016/j.scitotenv.2014.11.072.
- Sun, Yele, Guoshun Zhuang, Ying Wang, Lihui Han, Jinghua Guo, Mo Dan, Wenjie Zhang, Zifa Wang, and Zhengping Hao. 2004. "The Air-Borne Particulate Pollution in Beijing—concentration, Composition, Distribution and Sources." *Atmospheric Environment* 38 (35): 5991–6004.
- Sunyer, J. 2001. "Urban Air Pollution and Chronic Obstructive Pulmonary Disease: A Review." *European Respiratory Journal* 17 (5): 1024–1033.
- Taiwo, A. M., D. C. S. Beddows, G. Calzolari, Roy M. Harrison, F. Lucarelli, S. Nava, Z. Shi, G. Valli, and R. Vecchi. 2014. "Receptor Modelling of Airborne Particulate Matter in the Vicinity of a Major Steelworks Site." *The Science of the Total Environment* 490 (August): 488–500. doi:10.1016/j.scitotenv.2014.04.118.
- Tanase, Ion Gh, Dana Elena Popa, Gabriela Elena Udriștioiu, Andrei A. Bunaciu, and Hassan Y. Aboul-Enein. 2015. "Estimation of the Uncertainty of the Measurement Results of Some Trace Levels Elements in Document Paper Samples Using ICP-MS" 5 (15): 11445–57. doi:10.1039/C4RA12645A.
- Terzi, Eleni, George Argyropoulos, Aikaterini Bougatioti, Nikolaos Mihalopoulos, Kostas Nikolaou, and Constantini Samara. 2010. "Chemical Composition and Mass Closure of Ambient PM10 at Urban Sites." *Atmospheric Environment* 44 (18): 2231–39. doi:10.1016/j.atmosenv.2010.02.019.
- THEREFORE, SUBJECT TO CHANGE, MAYNOTBE AS, and A. SAUDI STANDARD UNTIL APPROVED. 2016. "Guide to the Expression of Uncertainty in Measurement." Accessed November 24. <http://chapon.arnaud.free.fr/documents/resources/stat/GUM.pdf>.
- Trochkin, D., Y. Iwasaka, A. Matsuki, M. Yamada, Y.-S. Kim, D. Zhang, G.-Y. Shi, Z. Shen, and G. Li. 2003. "Comparison of the Chemical Composition of Mineral Particles Collected in Dunhuang, China and Those Collected in the Free Troposphere over Japan: Possible Chemical Modification during Long-Range Transport." *Water, Air and Soil Pollution: Focus* 3 (2): 161–72. doi:10.1023/A:1023286306728.
- Turpin, Barbara J., and Ho-Jin Lim. 2001. "Species Contributions to PM2.5 Mass Concentrations: Revisiting Common Assumptions for Estimating Organic Mass." *Aerosol Science and Technology* 35 (1): 602–10. doi:10.1080/02786820152051454.
- Twomey, S. 1974. "Pollution and the Planetary Albedo." *Atmospheric Environment (1967)* 8 (12): 1251–1256.
- Udisti, Roberto, Francesco Rugi, Silvia Becagli, Ezio Bolzacchini, Giulia Calzolari, Massimo Chiari, Daniele Frosini, et al. 2013. "Spatial Distribution of Biogenic Sulphur Compounds in the Arctic Aerosol Collected during the AREX 2011 and 2012 Oceania

- Ship Cruises.” In *EGU General Assembly Conference Abstracts*, 15:10400. <http://adsabs.harvard.edu/abs/2013EGUGA..1510400U>.
- Ulbrich, I. M., M. R. Canagaratna, Q. Zhang, D. R. Worsnop, and J. L. Jimenez. 2009. “Interpretation of Organic Components from Positive Matrix Factorization of Aerosol Mass Spectrometric Data.” *Atmos. Chem. Phys.* 9 (9): 2891–2918. doi:10.5194/acp-9-2891-2009.
- Vardoulakis, Sotiris, and Pavlos Kassomenos. 2008. “Sources and Factors Affecting PM 10 Levels in Two European Cities: Implications for Local Air Quality Management.” *Atmospheric Environment* 42 (17): 3949–3963.
- Vercauteren, Jordy, Christina Matheeußen, Eric Wauters, Edward Roekens, René van Grieken, Agnieszka Krata, Yaroslava Makarovska, Willy Maenhaut, Xuguang Chi, and Benny Geypens. 2011a. “Chemkar PM10: An Extensive Look at the Local Differences in Chemical Composition of PM10 in Flanders, Belgium.” *Atmospheric Environment* 45 (1): 108–116.
- . 2011b. “Chemkar PM10: An Extensive Look at the Local Differences in Chemical Composition of PM10 in Flanders, Belgium.” *Atmospheric Environment* 45 (1): 108–116. doi:10.1016/j.atmosenv.2010.09.040.
- Vestenius, Mika, Sirkka Leppänen, Pia Anttila, Katriina Kyllönen, Juha Hatakka, Heidi Hellén, Antti-Pekka Hyvärinen, and Hannele Hakola. 2011. “Background Concentrations and Source Apportionment of Polycyclic Aromatic Hydrocarbons in South-Eastern Finland.” *Atmospheric Environment* 45 (20): 3391–99. doi:10.1016/j.atmosenv.2011.03.050.
- Viana, M., T. A. J. Kuhlbusch, X. Querol, A. Alastuey, R. M. Harrison, P. K. Hopke, W. Winiwarter, et al. 2008. “Source Apportionment of Particulate Matter in Europe: A Review of Methods and Results.” *Journal of Aerosol Science* 39 (10): 827–849.
- Wählén, Peter. 2003. “COPREM—A Multivariate Receptor Model with a Physical Approach.” *Atmospheric Environment* 37 (35): 4861–67. doi:10.1016/j.atmosenv.2003.08.032.
- Waked, A., O. Favez, L. Y. Alleman, C. Piot, J.-E. Petit, T. Delaunay, E. Verlinden, et al. 2014. “Source Apportionment of PM10 in a North-Western Europe Regional Urban Background Site (Lens, France) Using Positive Matrix Factorization and Including Primary Biogenic Emissions.” *Atmos. Chem. Phys.* 14 (7): 3325–46. doi:10.5194/acp-14-3325-2014.
- Watson, John G. 1984. “Overview of Receptor Model Principles.” *Journal of the Air Pollution Control Association* 34 (6): 619–23. doi:10.1080/00022470.1984.10465780.
- Watson, John G., L.-W. Antony Chen, Judith C. Chow, Prakash Doraiswamy, and Douglas H. Lowenthal. 2008. “Source Apportionment: Findings from the U.S. Supersites Program.” *Journal of the Air & Waste Management Association* 58 (2): 265–88. doi:10.3155/1047-3289.58.2.265.
- Watson, John G, Tan Zhu, Judith C Chow, Johann Engelbrecht, Eric M Fujita, and William E Wilson. 2002. “Receptor Modeling Application Framework for Particle Source Apportionment.” *Chemosphere* 49 (9): 1093–1136. doi:10.1016/S0045-6535(02)00243-6.
- Weijers, Ernie, and Martijn Schaap. 2013. “Anthropogenic and Natural Constituents in PM10 at Urban and Rural Sites in North-Western Europe: Concentrations, Chemical Composition and Sources.” In *Urban Air Quality in Europe*, 239–258. Springer. http://link.springer.com/chapter/10.1007/978-94-007-698-2_207.
- Weiss-Penzias, Peter S., Mae S. Gustin, and Seth N. Lyman. 2011. “Sources of Gaseous Oxidized Mercury and Mercury Dry Deposition at Two Southeastern US Sites.” *Atmospheric Environment* 45 (27): 4569–4579.

- White, W. H., and P. T. Roberts. 1977. "On the Nature and Origins of Visibility-Reducing Aerosols in the Los Angeles Air Basin." *Atmospheric Environment* (1967) 11 (9): 803–12. doi:10.1016/0004-6981(77)90042-7.
- "WHO | Ambient Air Pollution: A Global Assessment of Exposure and Burden of Disease." 2016. WHO. Accessed November 24. <http://www.who.int/phe/publications/air-pollution-global-assessment/en/>.
- Winiwarter, W., H. Bauer, A. Caseiro, and H. Puxbaum. 2009. "Quantifying Emissions of Primary Biological Aerosol Particle Mass in Europe." *Atmospheric Environment, Natural and Biogenic Emissions of Environmentally Relevant Atmospheric Trace Constituents in Europe*, 43 (7): 1403–9. doi:10.1016/j.atmosenv.2008.01.037.
- Xu, X., and U. S. Akhtar. 2010. "Identification of Potential Regional Sources of Atmospheric Total Gaseous Mercury in Windsor, Ontario, Canada Using Hybrid Receptor Modeling." *Atmospheric Chemistry and Physics* 10 (15): 7073–7083.
- Yao, Xiaohong, Chak K. Chan, Ming Fang, Steven Cadle, Tai Chan, Patricia Mulawa, Kebin He, and Boming Ye. 2002. "The Water-Soluble Ionic Composition of PM_{2.5} in Shanghai and Beijing, China." *Atmospheric Environment* 36 (26): 4223–4234.
- Yao, Xiaohong, Ming Fang, and Chak K. Chan. 2002. "Size Distributions and Formation of Dicarboxylic Acids in Atmospheric Particles." *Atmospheric Environment* 36 (13): 2099–2107.
- Yenisoy-Karakaş, Serpil. 2012. "Estimation of Uncertainties of the Method to Determine the Concentrations of Cd, Cu, Fe, Pb, Sn and Zn in Tomato Paste Samples Analysed by High Resolution ICP-MS." *Food Chemistry* 132 (3): 1555–1561.
- Yin, Jianxin, Roy M. Harrison, Qiang Chen, Andrew Rutter, and James J. Schauer. 2010. "Source Apportionment of Fine Particles at Urban Background and Rural Sites in the UK Atmosphere." *Atmospheric Environment* 44 (6): 841–51. doi:10.1016/j.atmosenv.2009.11.026.
- Yttri, K. E., W. Aas, A. Bjerke, J. N. Cape, F. Cavalli, D. Ceburnis, C. Dye, et al. 2007. "Elemental and Organic Carbon in PM₁₀: A One Year Measurement Campaign within the European Monitoring and Evaluation Programme EMEP." *Atmospheric Chemistry and Physics* 7 (22): 5711–5725.
- Yttri, Karl Espen, David Simpson, Jacob Klenø Nøjgaard, Kasper Kristensen, Johan Genberg, Kristina Stenström, Erik Swietlicki, et al. 2011. "Source Apportionment of the Summer Time Carbonaceous Aerosol at Nordic Rural Background Sites." *Atmospheric Chemistry and Physics* 11 (24): 13339–13357.
- Yue, Wei, Matthias Stölzel, Josef Cyrus, Mike Pitz, Joachim Heinrich, Wolfgang G. Kreyling, H. -Erich Wichmann, Annette Peters, Sheng Wang, and Philip K. Hopke. 2008. "Source Apportionment of Ambient Fine Particle Size Distribution Using Positive Matrix Factorization in Erfurt, Germany." *Science of The Total Environment* 398 (1–3): 133–44. doi:10.1016/j.scitotenv.2008.02.049.
- Zhang, Lian, Qunying Wang, Atsushi Sato, Yoshihiko Ninomiya, and Toru Yamashita. 2007. "Interactions among Inherent Minerals during Coal Combustion and Their Impacts on the Emission of PM₁₀. 2. Emission of Submicrometer-Sized Particles." *Energy & Fuels* 21 (2): 766–777.
- Zhang, Ting, Magda Claeys, Hélène Cachier, Shuping Dong, Wan Wang, Willy Maenhaut, and Xiande Liu. 2008. "Identification and Estimation of the Biomass Burning Contribution to Beijing Aerosol Using Levoglucosan as a Molecular Marker." *Atmospheric Environment* 42 (29): 7013–7021.
- Zhang, X., A. Hecobian, M. Zheng, N. H. Frank, and R. J. Weber. 2010. "Biomass Burning Impact on PM_{2.5} over the Southeastern US during 2007: Integrating Chemically

- Speciated FRM Filter Measurements, MODIS Fire Counts and PMF Analysis.” *Atmospheric Chemistry and Physics* 10 (14): 6839–6853.
- Zhang, Xiaolei, Weihong Yang, and Wlodzimierz Blasiak. 2012. “Thermal Decomposition Mechanism of Levoglucosan during Cellulose Pyrolysis.” *Journal of Analytical and Applied Pyrolysis* 96: 110–119.
- Zhao, Weixiang, and Philip K. Hopke. 2006. “Source Identification for Fine Aerosols in Mammoth Cave National Park.” *Atmospheric Research* 80 (4): 309–22. doi:10.1016/j.atmosres.2005.10.002.
- Zhou, Liming, Philip K. Hopke, and Wei Liu. 2004. “Comparison of Two Trajectory Based Models for Locating Particle Sources for Two Rural New York Sites.” *Atmospheric Environment* 38 (13): 1955–1963.
- Zieger, Paul Christoph. 2011. “Effects of Relative Humidity on Aerosol Light Scattering.” doi:10.3929/ethz-a-006668068.

ANNEXES

ANNEX 1: UNCERTAINTIES AND CORRELATIONS

Uncertainties

Uncertainties and detection limits for the site of Lens

Table A1. 1: Uncertainties parameters for the metals for the site of Lens

		Al 27 (cps)	Ca 44 (cps)	Fe 56 (cps)	K 39 (cps)	Mg 24 (cps)	Na 23 (cps)	As 75 (cps)
Precision	u²	7.25 10 ⁻⁴	1.09 10 ⁻³	1.45 10 ⁻³	2.16 10 ⁻³	1.10 10 ⁻²	4.02 10 ⁻²	2.07 10 ⁻³
Accuracy	u²	3.14 10 ⁻²	8.25 10 ⁻²	1.06 10 ⁻²	2.22 10 ⁻²	3.72 10 ⁻²	3.70 10 ⁻²	8.37 10 ⁻³
Volume	u²	2.89 10 ⁻³	2.89 10 ⁻³	2.89 10 ⁻³	2.89 10 ⁻³	2.89 10 ⁻³	2.89 10 ⁻³	2.89 10 ⁻³
Contamination	Blanks	4.18 10 ⁻²	6.50 10 ⁻²	2.41 10 ⁻²	8.01 10 ⁻³	1.52 10 ⁻¹	2.69 10 ⁻²	2.71 10 ⁻⁴
	u²	1.04 10 ⁻²	1.62 10 ⁻²	6.01 10 ⁻³	2.00 10 ⁻³	3.79 10 ⁻²	6.74 10 ⁻³	6.78 10 ⁻⁵
TOTAL	u	2.13 10 ⁻¹	3.20 10 ⁻¹	1.45 10 ⁻¹	1.71 10 ⁻¹	2.98 10 ⁻¹	2.95 10 ⁻¹	1.16 10 ⁻¹
		Ba 137 (cps)	Bi 209 (cps)	Cd 111 (cps)	Ce 140 (cps)	Co 59 (cps)	Cr 52 (cps)	Cs 133 (cps)
Precision	u²	5.66 10 ⁻⁴		2.85 10 ⁻²	1.44 10 ⁻³	1.21 10 ⁻³	9.11 10 ⁻⁴	2.79 10 ⁻³
Accuracy	u²	3.15 10 ⁻²	1.53 10 ⁻²	1.61 10 ⁻²	1.37 10 ⁻²	3.25 10 ⁻²	7.49 10 ⁻²	
Volume	u²	2.89 10 ⁻³	2.89 10 ⁻³	2.89 10 ⁻³	2.89 10 ⁻³	2.89 10 ⁻³	2.89 10 ⁻³	2.89 10 ⁻³
Contamination	Blanks	1.38 10 ⁻⁴	3.28 10 ⁻⁶	6.10 10 ⁻⁶	1.22 10 ⁻⁵	4.40 10 ⁻⁵	1.35 10 ⁻³	3.19 10 ⁻⁶
	u²	3.44 10 ⁻⁵	8.20 10 ⁻⁷	1.53 10 ⁻⁶	3.05 10 ⁻⁶	1.10 10 ⁻⁵	3.39 10 ⁻⁴	7.97 10 ⁻⁷
TOTAL	u	1.87 10 ⁻¹	1.35 10 ⁻¹	2.18 10 ⁻¹	1.34 10 ⁻¹	1.91 10 ⁻¹	2.81 10 ⁻¹	7.54 10 ⁻²

		Cu 63 (cps)	La 139 (cps)	Mn 55 (cps)	Mo 98 (cps)	Ni 60 (cps)	Pb 208 (cps)	Rb 85 (cps)
Precision	u²	6.76 10 ⁻³	3.57 10 ⁻³	1.86 10 ⁻³		3.93 10 ⁻³	1.76 10 ⁻³	
Accuracy	u²	1.91 10 ⁻²	1.32 10 ⁻²	9.47 10 ⁻³	7.05 10 ⁻⁴		1.36 10 ⁻²	3.35 10 ⁻³
Volume	u²	2.89 10 ⁻³	2.89 10 ⁻³	2.89 10 ⁻³	2.89 10 ⁻³	2.89 10 ⁻³	2.89 10 ⁻³	2.89 10 ⁻³
Contamination	Blanks	3.47 10 ⁻⁴	5.25 10 ⁻⁶	2.64 10 ⁻³	4.74 10 ⁻⁴	4.61 10 ⁻⁴	4.28 10 ⁻⁴	4.81 10 ⁻⁵
	u²	8.68 10 ⁻⁵	1.31 10 ⁻⁶	6.61 10 ⁻⁴	1.19 10 ⁻⁴	1.15 10 ⁻⁴	1.07 10 ⁻⁴	1.20 10 ⁻⁵
TOTAL	u	1.70 10 ⁻¹	1.40 10 ⁻¹	1.22 10 ⁻¹	6.09 10 ⁻²	8.32 10 ⁻²	1.36 10 ⁻¹	7.91 10 ⁻²
		Sb 121 (cps)	Sr 88 (cps)	Ti 47 (cps)	Tl 205 (cps)	U 238 (cps)	Zn 64 (cps)	V-1 51 (cps)
Precision	u²	1.41 10 ⁻³		5.20 10 ⁻⁴			1.64 10 ⁻³	1.72 10 ⁻³
Accuracy	u²	8.51 10 ⁻³	2.78 10 ⁻³		1.18 10 ⁻²	3.80 10 ⁻³	1.62 10 ⁻¹	2.22 10 ⁻²
Volume	u²	2.89 10 ⁻³	2.89 10 ⁻³	2.89 10 ⁻³	2.89 10 ⁻³	2.89 10 ⁻³	2.89 10 ⁻³	2.89 10 ⁻³
Contamination	Blanks	1.81 10 ⁻⁴	9.88 10 ⁻⁵	3.58 10 ⁻²	2.68 10 ⁻⁶	2.82 10 ⁻⁶	5.31 10 ⁻³	1.07 10 ⁻⁴
	u²	4.54 10 ⁻⁵	2.47 10 ⁻⁵	8.96 10 ⁻³	6.70 10 ⁻⁷	7.05 10 ⁻⁷	1.33 10 ⁻³	2.67 10 ⁻⁵
TOTAL	u	1.13 10 ⁻¹	7.55 10 ⁻²	1.11 10 ⁻¹	1.21 10 ⁻¹	8.18 10 ⁻²	4.09 10 ⁻¹	1.64 10 ⁻¹

Table A1. 2: Uncertainties parameters for EC/OC, ions and organic species for the site of Lens (expanded relative uncertainty – u% and coefficient of variability)

	EC	OC	Cl⁻	NO₃⁻	SO₄²⁻	Na⁺	NH₄⁺	K⁺	Mg²⁺
u%	0.1	0.15	0.05	0.05	0.05	0.05	0.05	0.1	0.1
CV	x	x	0.58	0.44	0.26	0.94	0.36	0.84	1.26
	MSA	Oxalate	Levoglucozan	Mannosan	Galactosan	Arabitrol	Mannitol	Glucose	Mannose
u%	0.1	0.1	0.15	0.15	0.15	0.15	0.15	0.15	0.15
CV	1.99	0.59	0.57	0.49	0.32	0.59	0.89	0.60	1.38

Table A1. 3: Detection limits of the measured species for the site of Lens (in $\mu\text{g m}^{-3}$)

Detection limits								
EC	OC	Cl⁻	NO₃⁻	SO₄²⁻	Na⁺	NH₄⁺	K⁺	Mg²⁺
2.02 10 ⁻¹	1.16	8.88 10 ⁻³	4.39 10 ⁻¹	7.12 10 ⁻¹	5.96 10 ⁻³	1.25 10 ⁻¹	1.61 10 ⁻²	1.71 10 ⁻³
MSA	Oxalate	Levoglucozan	Mannosan	Galactosan	Arabitol	Mannitol	Glucose	Mannose
3.00 10 ⁻³	2.44 10 ⁻⁴	1.58 10 ⁻²	3.11 10 ⁻⁵	3.04 10 ⁻⁴	1.72 10 ⁻⁴	1.01 10 ⁻⁴	2.55 10 ⁻⁴	1.61 10 ⁻⁴
Al	Fe	Ca	As	Ba	Cd	Ce	Co	Cs
1.92 10 ⁻³	3.50 10 ⁻³	1.81 10 ⁻²	7.35 10 ⁻⁵	2.14 10 ⁻⁴	2.17 10 ⁻⁵	7.73 10 ⁻⁵	1.18 10 ⁻⁵	2.47 10 ⁻⁶
Cu	La	Mn	Mo	Ni	Pb	Rb	Sb	Se
1.68 10 ⁻³	3.15 10 ⁻⁵	1.84 10 ⁻⁴	8.18 10 ⁻⁶	7.88 10 ⁻⁵	7.71 10 ⁻⁴	1.00 10 ⁻⁴	2.74 10 ⁻⁴	1.34 10 ⁻⁴
Sr	Ti	U	Zn					
2.64 10 ⁻⁴	2.59 10 ⁻³	3.07 10 ⁻⁶	6.63 10 ⁻⁴					

Uncertainties and detection limits for the site of Nogent-sur-Oise

Table A1. 4: Uncertainties parameters for the metals for the site of Nogent-sur-Oise

		Al 27 (cps)	Ca 44 (cps)	Fe 56 (cps)	K 39 (cps)	Mg 24 (cps)	Na 23 (cps)	As 75 (cps)
Precision	u²	1.60 10 ⁻³	2.17 10 ⁻³	4.41 10 ⁻³	1.24 10 ⁻²	1.18 10 ⁻²	4.15 10 ⁻²	3.04 10 ⁻²
Accuracy	u²	1.78 10 ⁻²		7.41 10 ⁻²	2.06 10 ⁻²	6.04 10 ⁻²	3.41 10 ⁻²	1.38 10 ⁻²
Volume	u²	2.89 10 ⁻³	2.89 10 ⁻³	2.89 10 ⁻³	2.89 10 ⁻³	2.89 10 ⁻³	2.89 10 ⁻³	2.89 10 ⁻³
Contamination	Blanks	6.53 10 ⁻²	1.56 10 ⁻¹	4.45 10 ⁻²	1.34 10 ⁻²		1.99 10 ⁻²	5.27 10 ⁻⁴
	u²	1.63 10 ⁻²	3.90 10 ⁻²	1.11 10 ⁻²	3.34 10 ⁻³		4.97 10 ⁻³	1.32 10 ⁻⁴
TOTAL	u	1.97 10 ⁻¹	2.10 10 ⁻¹	3.04 10 ⁻¹	1.98 10 ⁻¹	2.74 10 ⁻¹	2.89 10 ⁻¹	2.17 10 ⁻¹
		Ba 137 (cps)	Bi 209 (cps)	Cd 111 (cps)	Ce 140 (cps)	Co 59 (cps)	Cr 52 (cps)	Cs 133 (cps)
Precision	u²	9.61 10 ⁻⁴	1.41 10 ⁻²	7.47 10 ⁻³	3.58 10 ⁻³	1.17 10 ⁻³	3.56 10 ⁻³	2.66 10 ⁻³
Accuracy	u²	1.33 10 ⁻²	1.90 10 ⁻²	1.78 10 ⁻²	1.88 10 ⁻²	1.20 10 ⁻²	1.33 10 ⁻²	2.73 10 ⁻²
Volume	u²	2.89 10 ⁻³	2.89 10 ⁻³	2.89 10 ⁻³	2.89 10 ⁻³	2.89 10 ⁻³	2.89 10 ⁻³	2.89 10 ⁻³
Contamination	Blanks	3.36 10 ⁻⁴	9.24 10 ⁻⁶	1.74 10 ⁻⁵	1.68 10 ⁻⁵	5.68 10 ⁻⁵	1.56 10 ⁻³	1.80 10 ⁻⁶
	u²	8.41 10 ⁻⁵	2.31 10 ⁻⁶	4.35 10 ⁻⁶	4.21 10 ⁻⁶	1.42 10 ⁻⁵	3.90 10 ⁻⁴	4.50 10 ⁻⁷
TOTAL	u	1.31 10 ⁻¹	1.90 10 ⁻¹	1.68 10 ⁻¹	1.59 10 ⁻¹	1.27 10 ⁻¹	1.42 10 ⁻¹	1.81 10 ⁻¹
		Cu 63 (cps)	La 139 (cps)	Mn 55 (cps)	Mo 98 (cps)	Ni 60 (cps)	Pb 208 (cps)	Rb 85 (cps)
Precision	u²	7.61 10 ⁻³	9.85 10 ⁻³	1.62 10 ⁻³	1.18 10 ⁻³	4.17 10 ⁻³	1.51 10 ⁻³	5.53 10 ⁻⁵
Accuracy	u²	1.46 10 ⁻²	1.37 10 ⁻²	1.12 10 ⁻²	2.13 10 ⁻²	1.54 10 ⁻²	1.54 10 ⁻²	1.39 10 ⁻²
Volume	u²	2.89 10 ⁻³	2.89 10 ⁻³	2.89 10 ⁻³	2.89 10 ⁻³	2.89 10 ⁻³	2.89 10 ⁻³	2.89 10 ⁻³
Contamination	Blanks	1.03 10 ⁻³	8.81 10 ⁻⁶	1.28 10 ⁻³	2.79 10 ⁻⁴	6.69 10 ⁻⁴	2.72 10 ⁻⁴	3.55 10 ⁻⁵
	u²	2.57 10 ⁻⁴	2.20 10 ⁻⁶	3.19 10 ⁻⁴	6.99 10 ⁻⁵	1.67 10 ⁻⁴	6.81 10 ⁻⁵	8.89 10 ⁻⁶
TOTAL	u	1.59 10 ⁻¹	1.63 10 ⁻¹	1.27 10 ⁻¹	1.60 10 ⁻¹	1.50 10 ⁻¹	1.41 10 ⁻¹	1.30 10 ⁻¹

		Sb 121 (cps)	Sr 88 (cps)	Ti 47 (cps)	Tl 205 (cps)	U 238 (cps)	Zn 64 (cps)	V¹ 51 (cps)
Precision	u²	2.29 10 ⁻³	2.22 10 ⁻²	4.68 10 ⁻⁴		4.62 10 ⁻³	3.01 10 ⁻³	4.14 10 ⁻³
Accuracy	u²	1.49 10 ⁻²	1.73 10 ⁻²	6.12 10 ⁻²	1.79 10 ⁻²	1.52 10 ⁻²		3.64 10 ⁻²
Volume	u²	2.89 10 ⁻³	2.89 10 ⁻³	2.89 10 ⁻³	2.89 10 ⁻³	2.89 10 ⁻³	2.89 10 ⁻³	2.89 10 ⁻³
Contamination	Blanks	6.51 10 ⁻⁵	1.75 10 ⁻⁴	1.79 10 ⁻²	4.78 10 ⁻⁶	2.20 10 ⁻⁶	9.57 10 ⁻³	1.25 10 ⁻⁴
	u²	1.63 10 ⁻⁵	4.37 10 ⁻⁵	4.47 10 ⁻³	1.19 10 ⁻⁶	5.50 10 ⁻⁷	2.39 10 ⁻³	3.11 10 ⁻⁵
TOTAL	u	1.42 10 ⁻¹	2.06 10 ⁻¹	2.63 10 ⁻¹	1.44 10 ⁻¹	1.51 10 ⁻¹	9.11 10 ⁻²	2.09 10 ⁻¹

Table A1. 5: Uncertainties parameters for EC/OC, ions and organic species for the site of Nogent-sur-Oise (expanded relative uncertainty – u% and coefficient of variability)

	EC	OC	Cl⁻	NO₃⁻	SO₄²⁻	Na⁺	NH₄⁺	K⁺	Mg²⁺
u%	0.10	0.15	0.05	0.05	0.05	0.05	0.10	0.10	0.10
CV	x	x	0.40	2.19	4.26	0.85	0.55	0.84	0.93
	MSA	Oxalate	Levogluconan	Mannosan	Galactosan	Arabitol	Mannitol	Glucose	Mannose
u%	0.10	0.10	0.15	0.15	0.15	0.15	0.15	0.15	0.15
CV	5.08	1.12	1.61	1.77	2.23	1.82	2.81	3.13	1.87

Table A1. 6: Detection limits of the measured species for the site of Nogent-sur-Oise (in µg m⁻³)

Detection limits										
EC	OC	Cl⁻	NO₃⁻	SO₄²⁻	Na⁺	NH₄⁺	K⁺	Mg²⁺		
3.53 10 ⁻¹	1.57E+00	1.22 10 ⁻²	4.00 10 ⁻¹	4.00 10 ⁻¹	2.00 10 ⁻²	1.67 10 ⁻²	2.00 10 ⁻²	1.26 10 ⁻³		
MSA	Oxalate	Levogluconan	Mannosan	Galactosan	Arabitol	Mannitol	Glucose	Mannose	Al	
2.59 10 ⁻⁴	1.66 10 ⁻³	1.53 10 ⁻⁴	2.84 10 ⁻⁵	1.93 10 ⁻⁴	3.87 10 ⁻⁴	2.46 10 ⁻⁴	4.58 10 ⁻⁴	4.08 10 ⁻⁴	2.47 10 ⁻⁵	
Fe	Ca	As	Ba	Cd	Co	Cu	La	Mn	Mo	
1.54 10 ⁻⁵	5.83 10 ⁻²	3.70 10 ⁻⁵	1.59 10 ⁻³	2.00 10 ⁻⁵	2.61 10 ⁻⁵	5.30 10 ⁻³	2.64 10 ⁻⁵	2.03 10 ⁻³	1.21 10 ⁻⁴	
	Ni	Pb	Rb	Sb	Sr	V	Zn			
	4.60 10 ⁻⁴	1.51 10 ⁻³	9.29 10 ⁻⁵	2.88 10 ⁻⁴	2.35 10 ⁻⁴	9.40 10 ⁻⁵	6.98 10 ⁻³			

Uncertainties and detection limits for the site of Revin

Table A1. 7: Uncertainties parameters for the metals for the site of Revin

		Al 27 (cps)	Ca 44 (cps)	Fe 56 (cps)	K 39 (cps)	Mg 24 (cps)	Na 23 (cps)	As 75 (cps)
Precision	u²	1.35 10 ⁻³	2.01 10 ⁻³	4.53 10 ⁻³	1.19 10 ⁻²	1.14 10 ⁻²	4.15 10 ⁻²	3.06 10 ⁻²
Accuracy	u²			9.92 10 ⁻²	9.48 10 ⁻²	1.39 10 ⁻¹	1.31 10 ⁻¹	2.18 10 ⁻²
Volume	u²	2.89 10 ⁻³	2.89 10 ⁻³	2.89 10 ⁻³	2.89 10 ⁻³	2.89 10 ⁻³	2.89 10 ⁻³	2.89 10 ⁻³
Contamination	Blanks	4.11 10 ⁻²	6.65 10 ⁻²	2.67 10 ⁻²	1.49 10 ⁻³	1.25 10 ⁻¹	9.68 10 ⁻³	4.52 10 ⁻⁴
	u²	1.03 10 ⁻²	1.66 10 ⁻²	6.66 10 ⁻³	3.73 10 ⁻⁴	3.11 10 ⁻²	2.42 10 ⁻³	1.13 10 ⁻⁴
TOTAL	u	1.21 10 ⁻¹	1.47 10 ⁻¹	3.37 10 ⁻¹	3.32 10 ⁻¹	4.29 10 ⁻¹	4.21 10 ⁻¹	2.35 10 ⁻¹
		Ba 137 (cps)	Bi 209 (cps)	Cd 111 (cps)	Ce 140 (cps)	Co 59 (cps)	Cr 52 (cps)	Cs 133 (cps)
Precision	u²	2.99 10 ⁻⁴	2.34 10 ⁻³	1.04 10 ⁻²	1.85 10 ⁻³	1.91 10 ⁻³	3.97 10 ⁻³	3.23 10 ⁻³
Accuracy	u²	2.07 10 ⁻²	3.42 10 ⁻²	1.39 10 ⁻²	1.98 10 ⁻²	2.01 10 ⁻²	1.85 10 ⁻²	1.57 10 ⁻²
Volume	u²	2.89 10 ⁻³	2.89 10 ⁻³	2.89 10 ⁻³	2.89 10 ⁻³	2.89 10 ⁻³	2.89 10 ⁻³	2.89 10 ⁻³
Contamination	Blanks	3.74 10 ⁻⁴	5.56 10 ⁻⁶	1.06 10 ⁻⁵	1.62 10 ⁻⁵	5.81 10 ⁻⁵	2.62 10 ⁻³	1.31 10 ⁻⁶
	u²	9.34 10 ⁻⁵	1.39 10 ⁻⁶	2.65 10 ⁻⁶	4.05 10 ⁻⁶	1.45 10 ⁻⁵	6.55 10 ⁻⁴	3.27 10 ⁻⁷
TOTAL	u	1.55 10 ⁻¹	1.99 10 ⁻¹	1.65 10 ⁻¹	1.57 10 ⁻¹	1.58 10 ⁻¹	1.61 10 ⁻¹	1.48 10 ⁻¹
		Cu 63 (cps)	La 139 (cps)	Mn 55 (cps)	Mo 98 (cps)	Ni 60 (cps)	Pb 208 (cps)	Rb 85 (cps)
Precision	u²	1.01 10 ⁻²	8.91 10 ⁻³	1.66 10 ⁻³	1.88 10 ⁻³	7.13 10 ⁻³	1.37 10 ⁻³	1.70 10 ⁻⁴
Accuracy	u²	1.60 10 ⁻²	2.16 10 ⁻²	1.73 10 ⁻²	2.14 10 ⁻²	2.16 10 ⁻²	3.04 10 ⁻²	2.24 10 ⁻²
Volume	u²	2.89 10 ⁻³	2.89 10 ⁻³	2.89 10 ⁻³	2.89 10 ⁻³	2.89 10 ⁻³	2.89 10 ⁻³	2.89 10 ⁻³
Contamination	Blanks	7.45 10 ⁻⁴	5.54 10 ⁻⁶	3.37 10 ⁻³	2.68 10 ⁻⁴	8.69 10 ⁻⁴	1.33 10 ⁻⁴	1.86 10 ⁻⁵
	u²	1.86 10 ⁻⁴	1.38 10 ⁻⁶	8.41 10 ⁻⁴	6.71 10 ⁻⁵	2.17 10 ⁻⁴	3.32 10 ⁻⁵	4.66 10 ⁻⁶
TOTAL	u	1.71 10 ⁻¹	1.83 10 ⁻¹	1.51 10 ⁻¹	1.62 10 ⁻¹	1.78 10 ⁻¹	1.86 10 ⁻¹	1.59 10 ⁻¹

		Sb 121 (cps)	Sr 88 (cps)	Ti 47 (cps)	Tl 205 (cps)	U 238 (cps)	Zn 64 (cps)	V¹ 51 (cps)
Precision	u²	1.52 10 ⁻³	3.45 10 ⁻²	5.53 10 ⁻⁴		1.93 10 ⁻³	2.07 10 ⁻³	3.61 10 ⁻³
Accuracy	u²	1.31 10 ⁻²	1.93 10 ⁻²	4.32 10 ⁻²	2.08 10 ⁻²	4.17 10 ⁻²	4.45 10 ⁻²	8.59 10 ⁻³
Volume	u²	2.89 10 ⁻³	2.89 10 ⁻³	2.89 10 ⁻³	2.89 10 ⁻³	2.89 10 ⁻³	2.89 10 ⁻³	2.89 10 ⁻³
Contamination	Blanks	5.46 10 ⁻⁵	1.05 10 ⁻⁴	2.04 10 ⁻²	3.31 10 ⁻⁶	1.47 10 ⁻⁶	5.24 10 ⁻³	8.39 10 ⁻⁵
	u²	1.37 10 ⁻⁵	2.62 10 ⁻⁵	5.09 10 ⁻³	8.28 10 ⁻⁷	3.67 10 ⁻⁷	1.31 10 ⁻³	2.10 10 ⁻⁵
TOTAL	u	1.32 10 ⁻¹	2.38 10 ⁻¹	2.28 10 ⁻¹	1.54 10 ⁻¹	2.16 10 ⁻¹	2.25 10 ⁻¹	1.23 10 ⁻¹

Table A1. 8: Uncertainties parameters for EC/OC, ions and organic species for the site of Revin (expanded relative uncertainty – u% and coefficient of variability)

	EC	OC	Cl⁻	NO₃⁻	SO₄²⁻	Na⁺	NH₄⁺	K⁺	Mg²⁺
u%	0.10	0.15	0.05	0.05	0.05	0.05	0.05	0.10	0.10
CV	x	x	0.81	1.32	0.35	0.47	1.06	0.93	1.42
	MSA	Oxalate	Levoglucosan	Mannosan	Galactosan	Arabitol	Mannitol	Glucose	Mannose
u%	0.10	0.10	0.15	0.15	0.15	0.15	0.15	0.15	0.15
CV	0.88	0.73	1.00	0.46	0.84	0.53	0.99	0.23	0.06

Table A1. 9: Detection limits of the measured species for the site of Revin (in µg m⁻³)

Detection limits									
EC	OC	Cl⁻	NO₃⁻	SO₄²⁻	Na⁺	NH₄⁺	K⁺	Mg²⁺	
3.25 10 ⁻²	8.93 10 ⁻¹	2.86 10 ⁻⁴	2.12 10 ⁻¹	2.56 10 ⁻¹	1.87 10 ⁻³	2.41 10 ⁻³	3.03 10 ⁻³	9.43 10 ⁻⁴	
MSA	Oxalate	Levoglucosan	Mannosan	Galactosan	Arabitol	Mannitol	Glucose	Mannose	
2.72 10 ⁻⁴	6.59 10 ⁻⁴	2.82 10 ⁻³	1.24 10 ⁻³	1.93 10 ⁻⁴	3.87 10 ⁻⁴	2.46 10 ⁻⁴	4.58 10 ⁻⁴	4.08 10 ⁻⁴	
Al	Fe	Ca	As	Cd	Ce	Co	Cs	Cu	
3.49 10 ⁻²	1.22 10 ⁻³	6.98 10 ⁻³	1.11 10 ⁻⁴	3.15 10 ⁻⁵	5.37 10 ⁻⁵	1.31 10 ⁻⁵	7.29 10 ⁻⁶	1.74 10 ⁻⁴	
La	Mn	Mo	Pb	Rb	Sb	Se	Sr	Ti	Zn
1.59 10 ⁻⁵	9.55 10 ⁻⁴	1.26 10 ⁻⁵	1.14 10 ⁻³	9.95 10 ⁻⁵	1.56 10 ⁻⁵	1.46 10 ⁻⁴	3.12 10 ⁻⁴	1.67 10 ⁻⁴	3.33 10 ⁻³

Uncertainties and detection limits for the site of Rouen

Table A1. 10: Uncertainties parameters for the metals for the site of Rouen

		Al 27 (cps)	Ca 44 (cps)	Fe 56 (cps)	K 39 (cps)	Mg 24 (cps)	Na 23 (cps)	As 75 (cps)
Precision	u²	1.45 10 ⁻³	1.87 10 ⁻³	4.54 10 ⁻³	1.24 10 ⁻²	1.13 10 ⁻²	4.16 10 ⁻²	3.00 10 ⁻²
Accuracy	u²	8.41 10 ⁻²	2.43 10 ⁻²		1.05 10 ⁻¹	1.52 10 ⁻¹	1.29 10 ⁻¹	4.56 10 ⁻³
Volume	u²	2.89 10 ⁻³	2.89 10 ⁻³	2.89 10 ⁻³	2.89 10 ⁻³	2.89 10 ⁻³	2.89 10 ⁻³	2.89 10 ⁻³
Contamination	Blanks	3.29 10 ⁻²	5.80 10 ⁻²	8.94 10 ⁻³	1.33 10 ⁻²	3.22 10 ⁻²	1.08 10 ⁻²	7.76 10 ⁻⁵
	u²	8.21 10 ⁻³	1.45 10 ⁻²	2.24 10 ⁻³	3.33 10 ⁻³	8.06 10 ⁻³	2.71 10 ⁻³	1.94 10 ⁻⁵
TOTAL	u	3.11 10 ⁻¹	2.09 10 ⁻¹	9.83 10 ⁻²	3.51 10 ⁻¹	4.17 10 ⁻¹	4.20 10 ⁻¹	1.94 10 ⁻¹
		Ba 137 (cps)	Bi 209 (cps)	Cd 111 (cps)	Ce 140 (cps)	Co 59 (cps)	Cr 52 (cps)	Cs 133 (cps)
Precision	u²	1.84 10 ⁻⁴	4.71 10 ⁻³	8.70 10 ⁻³	1.23 10 ⁻³	1.27 10 ⁻³	3.32 10 ⁻³	2.68 10 ⁻³
Accuracy	u²	3.35 10 ⁻³	5.90 10 ⁻³	1.26 10 ⁻²	9.67 10 ⁻⁴	1.42 10 ⁻³	3.79 10 ⁻³	3.15 10 ⁻³
Volume	u²	2.89 10 ⁻³	2.89 10 ⁻³	2.89 10 ⁻³	2.89 10 ⁻³	2.89 10 ⁻³	2.89 10 ⁻³	2.89 10 ⁻³
Contamination	Blanks	3.26 10 ⁻⁵	5.49 10 ⁻⁶	1.16 10 ⁻⁵	7.28 10 ⁻⁶	1.08 10 ⁻⁵	5.40 10 ⁻⁴	4.09 10 ⁻⁶
	u²	8.14 10 ⁻⁶	1.37 10 ⁻⁶	2.90 10 ⁻⁶	1.82 10 ⁻⁶	2.70 10 ⁻⁶	1.35 10 ⁻⁴	1.02 10 ⁻⁶
TOTAL	u	8.01 10 ⁻²	1.16 10 ⁻¹	1.56 10 ⁻¹	7.13 10 ⁻²	7.47 10 ⁻²	1.01 10 ⁻¹	9.33 10 ⁻²
		Cu 63 (cps)	La 139 (cps)	Mn 55 (cps)	Mo 98 (cps)	Ni 60 (cps)	Pb 208 (cps)	Rb 85 (cps)
Precision	u²	7.08 10 ⁻³	8.89 10 ⁻³	1.81 10 ⁻³	3.81 10 ⁻³	4.56 10 ⁻³	1.81 10 ⁻³	8.55 10 ⁻⁴
Accuracy	u²	3.52 10 ⁻³	2.01 10 ⁻³	3.11 10 ⁻³	4.36 10 ⁻³	2.91 10 ⁻³	1.70 10 ⁻²	7.09 10 ⁻⁴
Volume	u²	2.89 10 ⁻³	2.89 10 ⁻³	2.89 10 ⁻³	2.89 10 ⁻³	2.89 10 ⁻³	2.89 10 ⁻³	2.89 10 ⁻³
Contamination	Blanks	5.10 10 ⁻⁴	2.85 10 ⁻⁶	3.08 10 ⁻⁴	9.87 10 ⁻⁵	2.39 10 ⁻⁴	4.76 10 ⁻⁵	1.27 10 ⁻⁵
	u²	1.28 10 ⁻⁴	7.13 10 ⁻⁷	7.69 10 ⁻⁵	2.47 10 ⁻⁵	5.98 10 ⁻⁵	1.19 10 ⁻⁵	3.17 10 ⁻⁶
TOTAL	u	1.17 10 ⁻¹	1.17 10 ⁻¹	8.88 10 ⁻²	1.05 10 ⁻¹	1.02 10 ⁻¹	1.47 10 ⁻¹	6.67 10 ⁻²

		Sb 121 (cps)	Sr 88 (cps)	Ti 47 (cps)	Tl 205 (cps)	U 238 (cps)	Zn 64 (cps)	V⁻¹ 51 (cps)
Precision	u²	4.14 10 ⁻³	2.47 10 ⁻⁴	6.18 10 ⁻⁴		7.16 10 ⁻⁴	3.74 10 ⁻³	3.49 10 ⁻³
Accuracy	u²	3.07 10 ⁻³	9.33 10 ⁻⁴	6.86 10 ⁻³	6.45 10 ⁻³	8.64 10 ⁻³		2.46 10 ⁻²
Volume	u²	2.89 10 ⁻³	2.89 10 ⁻³	2.89 10 ⁻³	2.89 10 ⁻³	2.89 10 ⁻³	2.89 10 ⁻³	2.89 10 ⁻³
Contamination	Blanks	9.66 10 ⁻⁶	2.41 10 ⁻⁵	3.91 10 ⁻³	8.02 10 ⁻⁶	2.14 10 ⁻⁶	1.09 10 ⁻³	5.46 10 ⁻⁵
	u²	2.41 10 ⁻⁶	6.02 10 ⁻⁶	9.77 10 ⁻⁴	2.01 10 ⁻⁶	5.36 10 ⁻⁷	2.73 10 ⁻⁴	1.37 10 ⁻⁵
TOTAL	u	1.00 10 ⁻¹	6.38 10 ⁻²	1.07 10 ⁻¹	9.66 10 ⁻²	1.11 10 ⁻¹	8.30 10 ⁻²	1.76 10 ⁻¹

Table A1. 11: Uncertainties parameters for EC/OC, ions and organic species for the site of Rouen (expanded relative uncertainty – u% and coefficient of variability)

	EC	OC	Cl⁻	NO₃⁻	SO₄²⁻	Na⁺	NH₄⁺	K⁺	Mg²⁺
u%	0.10	0.15	0.05	0.05	0.05	0.05	0.05	0.10	0.10
CV	x	x	0.31	0.58	0.72	0.55	0.89	0.43	0.78
	MSA	Oxalate	Levogluconan	Mannosan	Galactosan	Arabitol	Mannitol	Glucose	Mannose
u%	0.10	0.10	0.15	0.15	0.15	0.15	0.15	0.15	0.15
CV	1.53	0.68	1.72	1.66	1.72	1.60	1.87	1.58	1.60

Table A1. 12: Detection limits of the measured species for the site of Rouen (in µg m⁻³)

Detection limits									
EC	OC	Cl⁻	NO₃⁻	SO₄²⁻	Na⁺	NH₄⁺	K⁺	Mg²⁺	
3.98 10 ⁻¹	1.46E+00	1.63 10 ⁻²	3.39 10 ⁻¹	3.18 10 ⁻¹	3.01 10 ⁻²	2.85 10 ⁻²	3.33 10 ⁻²	3.73 10 ⁻³	
MSA	Oxalate	Levogluconan	Mannosan	Galactosan	Arabitol	Mannitol	Glucose	Mannose	
1.62 10 ⁻³	2.44 10 ⁻⁴	3.04 10 ⁻⁴	3.11 10 ⁻⁵	3.04 10 ⁻⁴	1.72 10 ⁻⁴	1.01 10 ⁻⁴	2.55 10 ⁻⁴	1.61 10 ⁻⁴	
Fe	Ca	As	Cd	Ce	Co	Cs	Cu	La	
2.87 10 ⁻³	2.22 10 ⁻²	9.25 10 ⁻⁵	2.20 10 ⁻⁵	9.66 10 ⁻⁵	3.97 10 ⁻⁵	1.28 10 ⁻⁵	5.66 10 ⁻³	2.84 10 ⁻⁵	
Mn	Mo	Ni	Pb	Rb	Sb	Se	Sr	Zn	
1.43 10 ⁻³	1.37 10 ⁻⁵	1.22 10 ⁻⁵	1.61 10 ⁻³	1.29 10 ⁻⁴	4.28 10 ⁻⁴	1.43 10 ⁻⁴	6.06 10 ⁻⁴	4.97 10 ⁻³	

Uncertainties and detection limits for the site of Roubaix

Table A1. 13: Uncertainties parameters for the metals for the site of Roubaix

		Al 27 (cps)	Ca 44 (cps)	Fe 56 (cps)	K 39 (cps)	Mg 24 (cps)	Na 23 (cps)	As 75 (cps)
Precision	u²	1.21 10 ⁻³	1.83 10 ⁻³	4.25 10 ⁻³	1.20 10 ⁻²	1.14 10 ⁻²	4.11 10 ⁻²	3.00 10 ⁻²
Accuracy	u²	5.33 10 ⁻³	4.80 10 ⁻²	1.54 10 ⁻²	4.75 10 ⁻³	1.47 10 ⁻²	8.66 10 ⁻³	5.78 10 ⁻⁴
Volume	u²	2.89 10 ⁻³	2.89 10 ⁻³	2.89 10 ⁻³	2.89 10 ⁻³	2.89 10 ⁻³	2.89 10 ⁻³	2.89 10 ⁻³
Contamination	Blanks	2.70 10 ⁻²	3.61 10 ⁻²	7.76 10 ⁻³	4.87 10 ⁻³	3.39 10 ⁻²	1.44 10 ⁻²	1.96 10 ⁻⁴
	u²	6.75 10 ⁻³	9.03 10 ⁻³	1.94 10 ⁻³	1.22 10 ⁻³	8.47 10 ⁻³	3.59 10 ⁻³	4.89 10 ⁻⁵
TOTAL	u	1.27 10 ⁻¹	2.48 10 ⁻¹	1.56 10 ⁻¹	1.45 10 ⁻¹	1.93 10 ⁻¹	2.37 10 ⁻¹	1.83 10 ⁻¹
		Ba 137 (cps)	Bi 209 (cps)	Cd 111 (cps)	Ce 140 (cps)	Co 59 (cps)	Cr 52 (cps)	Cs 133 (cps)
Precision	u²	3.70 10 ⁻⁴	2.11 10 ⁻²	7.93 10 ⁻³	4.85 10 ⁻³	1.19 10 ⁻²	4.42 10 ⁻³	3.40 10 ⁻³
Accuracy	u²	9.35 10 ⁻³	2.95 10 ⁻³	8.65 10 ⁻³	6.12 10 ⁻³	5.17 10 ⁻³	6.98 10 ⁻³	2.90 10 ⁻³
Volume	u²	2.89 10 ⁻³	2.89 10 ⁻³	2.89 10 ⁻³	2.89 10 ⁻³	2.89 10 ⁻³	2.89 10 ⁻³	2.89 10 ⁻³
Contamination	Blanks	8.48 10 ⁻⁵	1.08 10 ⁻⁵	7.22 10 ⁻⁶	1.60 10 ⁻⁵	9.84 10 ⁻⁶	5.53 10 ⁻⁴	3.53 10 ⁻⁶
	u²	2.12 10 ⁻⁵	2.70 10 ⁻⁶	1.80 10 ⁻⁶	4.00 10 ⁻⁶	2.46 10 ⁻⁶	1.38 10 ⁻⁴	8.83 10 ⁻⁷
TOTAL	u	1.12 10 ⁻¹	1.64 10 ⁻¹	1.40 10 ⁻¹	1.18 10 ⁻¹	1.41 10 ⁻¹	1.20 10 ⁻¹	9.59 10 ⁻²
		Cu 63 (cps)	La 139 (cps)	Mn 55 (cps)	Mo 98 (cps)	Ni 60 (cps)	Pb 208 (cps)	Rb 85 (cps)
Precision	u²	7.92 10 ⁻³	1.32 10 ⁻²	1.70 10 ⁻³	7.80 10 ⁻²	8.09 10 ⁻³	1.57 10 ⁻³	9.45 10 ⁻⁵
Accuracy	u²	7.06 10 ⁻³	1.05 10 ⁻²	1.83 10 ⁻³	5.27 10 ⁻³	1.08 10 ⁻²	3.65 10 ⁻³	2.35 10 ⁻³
Volume	u²	2.89 10 ⁻³	2.89 10 ⁻³	2.89 10 ⁻³	2.89 10 ⁻³	2.89 10 ⁻³	2.89 10 ⁻³	2.89 10 ⁻³
Contamination	Blanks	3.52 10 ⁻⁴	8.08 10 ⁻⁶	5.10 10 ⁻⁴	1.47 10 ⁻⁴	1.41 10 ⁻⁴	4.89 10 ⁻⁵	1.83 10 ⁻⁵
	u²	8.79 10 ⁻⁵	2.02 10 ⁻⁶	1.27 10 ⁻⁴	3.68 10 ⁻⁵	3.52 10 ⁻⁵	1.22 10 ⁻⁵	4.59 10 ⁻⁶
TOTAL	u	1.34 10 ⁻¹	1.63 10 ⁻¹	8.09 10 ⁻²	2.94 10 ⁻¹	1.48 10 ⁻¹	9.01 10 ⁻²	7.30 10 ⁻²

		Sb 121 (cps)	Sr 88 (cps)	Ti 47 (cps)	Tl 205 (cps)	U 238 (cps)	Zn 64 (cps)	V¹ 51 (cps)
Precision	u²	1.36 10 ⁻³	2.43 10 ⁻²	5.29 10 ⁻⁴		5.46 10 ⁻⁴	2.98 10 ⁻³	3.41 10 ⁻³
Accuracy	u²	6.23 10 ⁻³	4.13 10 ⁻³	4.56 10 ⁻²	3.62 10 ⁻³	4.10 10 ⁻³	6.47 10 ⁻²	7.44 10 ⁻³
Volume	u²	2.89 10 ⁻³	2.89 10 ⁻³	2.89 10 ⁻³	2.89 10 ⁻³	2.89 10 ⁻³	2.89 10 ⁻³	2.89 10 ⁻³
Contamination	Blanks	5.22 10 ⁻⁵	6.12 10 ⁻⁵	3.68 10 ⁻³	7.09 10 ⁻⁶	2.57 10 ⁻⁶	4.12 10 ⁻³	3.02 10 ⁻⁵
	u²	1.31 10 ⁻⁵	1.53 10 ⁻⁵	9.19 10 ⁻⁴	1.77 10 ⁻⁶	6.42 10 ⁻⁷	1.03 10 ⁻³	7.55 10 ⁻⁶
TOTAL	u	1.02 10 ⁻¹	1.77 10 ⁻¹	2.24 10 ⁻¹	8.07 10 ⁻²	8.68 10 ⁻²	2.68 10 ⁻¹	1.17 10 ⁻¹

Table A1. 14: Uncertainties parameters for EC/OC, ions and organic species for the site of Roubaix (expanded relative uncertainty – u% and coefficient of variability)

	EC	OC	Cl⁻	NO₃⁻	SO₄²⁻	Na⁺	NH₄⁺	K⁺	Mg²⁺
u%	0.10	0.15	0.05	0.05	0.05	0.05	0.05	0.10	0.10
CV	x	x	0.54	0.76	0.73	0.71	5.17	1.09	0.75
	MSA	Oxalate	Levoglucosan	Mannosan	Galactosan	Arabitol	Mannitol	Glucose	Mannose
u%	0.10	0.10	0.15	0.15	0.15	0.15	0.15	0.15	0.15
CV	2.10	0.61	0.28	0.40	0.49	1.06	0.64	0.40	0.90

Table A1. 15: Detection limits of the measured species for the site of Roubaix (in µg m⁻³)

Detection limits									
EC	OC	Cl⁻	NO₃⁻	SO₄²⁻	Na⁺	NH₄⁺	K⁺	Mg²⁺	
2.77 10 ⁻¹	9.20 10 ⁻¹	2.97 10 ⁻³	3.60 10 ⁻¹	4.26 10 ⁻¹	1.97 10 ⁻²	1.21 10 ⁻²	3.04 10 ⁻²	7.16 10 ⁻³	
MSA	Oxalate	Levoglucosan	Mannosan	Galactosan	Arabitol	Mannitol	Glucose	Mannose	
1.61 10 ⁻³	1.22 10 ⁻⁴	1.36 10 ⁻⁴	4.03 10 ⁻⁵	7.52 10 ⁻⁵	1.89 10 ⁻⁴	6.28 10 ⁻⁵	1.61 10 ⁻⁴	1.76 10 ⁻⁴	
Al	Fe	Ca	As	Ba	Cd	Ce	Co	Cs	
1.75 10 ⁻²	1.14 10 ⁻¹	3.82 10 ⁻²	1.33 10 ⁻⁵	3.79 10 ⁻⁵	2.14 10 ⁻⁵	2.08 10 ⁻⁴	5.73 10 ⁻⁵	3.64 10 ⁻⁶	
Cu	La	Mn	Mo	Ni	Pb	Rb	Sb	Se	
5.85 10 ⁻³	6.01 10 ⁻⁵	2.40 10 ⁻³	2.39 10 ⁻⁴	7.07 10 ⁻⁴	8.76 10 ⁻⁴	1.34 10 ⁻⁴	5.71 10 ⁻⁴	1.96 10 ⁻⁴	
		Sr	Ti	U	Zn				
		4.93 10 ⁻⁴	8.37 10 ⁻⁵	4.70 10 ⁻⁶	3.95 10 ⁻³				

Correlations

Lens

Table A1. 16: Correlation between the measured species in the site of Lens (correlation coefficient – R)

R Pearson	EC	OC	Cl -	NO3 -	SO4 2-	nssSO4	ssSO4	Na +	NH4 +	K +	Mg 2+	Ca 2+	MSA	Oxalate	Levogluconan	Polysac	Alcohols	Monosac	Al	Fe	Ca	As	Ba	Cd	Ce	Co	Cs	Cu	La	Mn	Mo	Ni	Pb	Rb	Sb	Se	Sr	Ti	U	Zn								
EC	1.00																																															
OC	0.33	1.00																																														
Cl -	-0.14	-0.17	1.00																																													
NO3 -	0.26	0.70	-0.13	1.00																																												
SO4 2-	0.12	0.65	-0.15	0.73	1.00																																											
nssSO4	0.13	0.66	-0.21	0.74	1.00	1.00																																										
ssSO4	-0.23	-0.39	0.92	-0.30	-0.30	-0.36	1.00																																									
Na +	-0.23	-0.39	0.92	-0.30	-0.30	-0.36	1.00	1.00																																								
NH4 +	0.23	0.74	-0.18	0.96	0.88	0.88	-0.37	-0.37	1.00																																							
K +	0.32	0.80	0.13	0.68	0.60	0.60	-0.10	-0.10	0.69	1.00																																						
Mg 2+	-0.21	-0.37	0.90	-0.27	-0.28	-0.34	0.99	0.99	-0.35	-0.09	1.00																																					
Ca 2+	0.32	0.37	-0.13	0.42	0.25	0.25	-0.14	-0.14	0.33	0.28	-0.03	1.00																																				
MSA	-0.14	0.00	-0.21	0.01	0.17	0.17	-0.04	-0.04	0.04	-0.09	0.01	0.22	1.00																																			
Oxalate	0.17	0.43	-0.14	0.44	0.32	0.33	-0.22	-0.22	0.42	0.31	-0.18	0.31	-0.09	1.00																																		
Levogluconan	0.45	0.81	0.05	0.52	0.42	0.42	-0.17	-0.17	0.53	0.75	-0.22	0.08	-0.23	0.25	1.00																																	
Polysac	0.24	0.65	0.01	0.54	0.60	0.59	-0.17	-0.17	0.62	0.58	-0.19	0.11	-0.11	0.12	0.68	1.00																																
Alcohols	0.04	0.29	-0.23	-0.06	0.10	0.12	-0.26	-0.26	0.02	0.07	-0.23	0.01	0.22	0.09	0.06	0.12	1.00																															
Monosac	0.05	0.12	-0.22	-0.06	-0.01	0.00	-0.22	-0.22	-0.03	-0.05	-0.19	0.03	0.15	0.14	-0.06	0.11	0.70	1.00																														
Al	0.23	0.25	-0.11	0.30	0.10	0.11	-0.14	-0.14	0.22	0.15	-0.05	0.81	0.01	0.46	0.04	0.04	-0.04	0.11	1.00																													
Fe	0.40	0.47	-0.17	0.47	0.17	0.18	-0.23	-0.23	0.38	0.30	-0.17	0.72	-0.02	0.56	0.30	0.22	0.01	0.14	0.83	1.00																												
Ca	0.21	0.30	-0.07	0.36	0.11	0.11	-0.08	-0.08	0.25	0.17	0.00	0.87	0.05	0.44	0.08	0.06	-0.05	0.07	0.89	0.85	1.00																											
As	0.28	0.69	-0.10	0.69	0.47	0.48	-0.25	-0.25	0.67	0.54	-0.23	0.38	-0.06	0.59	0.53	0.53	0.02	0.09	0.41	0.68	0.49	1.00																										
Ba	0.25	0.36	-0.14	0.41	0.13	0.14	-0.17	-0.17	0.32	0.25	-0.12	0.46	0.02	0.34	0.22	0.19	-0.02	0.09	0.50	0.69	0.57	0.63	1.00																									
Cd	0.44	0.78	-0.12	0.71	0.49	0.50	-0.30	-0.30	0.68	0.66	-0.27	0.46	-0.08	0.54	0.66	0.60	0.04	0.03	0.43	0.74	0.52	0.85	0.58	1.00																								
Ce	0.37	0.38	-0.15	0.33	0.09	0.10	-0.20	-0.20	0.25	0.22	-0.15	0.69	-0.07	0.47	0.24	0.16	-0.03	0.12	0.86	0.88	0.84	0.52	0.54	0.60	1.00																							
Co	0.24	0.35	-0.08	0.37	0.14	0.14	-0.12	-0.12	0.28	0.21	-0.08	0.61	0.03	0.39	0.21	0.16	-0.02	0.06	0.55	0.70	0.77	0.54	0.53	0.58	0.67	1.00																						
Cs	0.16	0.43	-0.11	0.51	0.37	0.38	-0.19	-0.19	0.48	0.41	-0.12	0.51	0.24	0.45	0.20	0.22	0.08	0.09	0.45	0.63	0.49	0.52	0.43	0.63	0.46	0.53	1.00																					
Cu	0.52	0.39	-0.16	0.32	0.12	0.13	-0.24	-0.24	0.26	0.25	-0.18	0.56	-0.03	0.42	0.30	0.22	0.05	0.12	0.69	0.81	0.65	0.57	0.58	0.66	0.73	0.46	0.37	1.00																				
La	0.25	0.31	-0.10	0.36	0.12	0.12	-0.12	-0.12	0.27	0.17	-0.07	0.68	0.02	0.48	0.15	0.10	-0.07	0.08	0.81	0.83	0.85	0.51	0.53	0.53	0.90	0.80	0.52	0.59	1.00																			
Mn	0.35	0.55	-0.17	0.52	0.29	0.30	-0.25	-0.25	0.46	0.43	-0.17	0.75	0.06	0.59	0.32	0.32	0.09	0.16	0.74	0.90	0.80	0.71	0.65	0.80	0.76	0.68	0.70	0.73	0.72	1.00																		
Mo	0.36	0.56	-0.10	0.52	0.34	0.34	-0.23	-0.23	0.48	0.43	-0.17	0.63	-0.01	0.47	0.41	0.38	0.07	0.12	0.73	0.84	0.71	0.61	0.53	0.73	0.75	0.57	0.50	0.77	0.65	0.79	1.00																	
Ni	0.21	0.28	-0.10	0.34	0.15	0.16	-0.12	-0.12	0.27	0.16	-0.06	0.62	0.12	0.41	0.12	0.13	0.02	0.13	0.77	0.78	0.75	0.45	0.55	0.50	0.76	0.71	0.55	0.61	0.78	0.69	0.79	1.00																
Pb	0.43	0.78	-0.10	0.70	0.46	0.47	-0.29	-0.29	0.67	0.66	-0.26	0.49	-0.06	0.53	0.66	0.60	0.06	0.05	0.48	0.78	0.56	0.85	0.59	0.97	0.63	0.62	0.64	0.69	0.57	0.80	0.78	0.55	1.00															
Rb	0.40	0.68	-0.12	0.64	0.39	0.40	-0.25	-0.25	0.58	0.57	-0.20	0.67	0.01	0.59	0.51	0.45	0.03	0.08	0.71	0.89	0.74	0.77	0.61	0.87	0.79	0.66	0.77	0.70	0.74	0.89	0.81	0.69	0.90	1.00														
Sb	0.41	0.64	-0.14	0.57	0.27	0.28	-0.27	-0.27	0.49	0.48	-0.24	0.51	-0.11	0.50	0.52	0.45	0.02	0.10	0.51	0.75	0.56	0.68	0.52	0.79	0.66	0.59	0.49	0.67	0.60	0.71	0.68	0.52	0.84	0.76	1.00													
Se	0.33	0.64	-0.20	0.68	0.44	0.45	-0.32	-0.32	0.64	0.49	-0.26	0.48	0.17	0.53	0.39	0.37	0.12	0.14	0.42	0.70	0.48	0.72	0.53	0.79	0.50	0.54	0.74	0.54	0.50	0.74	0.66	0.52	0.80	0.80	0.65	1.00												
Sr	0.12	0.14	0.15	0.18	0.00	-0.01	0.16	0.16	0.08	0.18	0.25	0.71	0.00	0.35	0.00	-0.01	-0.11	0.04	0.83	0.74	0.83	0.36	0.50	0.39	0.75	0.59	0.45	0.57	0.74	0.68	0.63	0.71	0.43	0.64	0.43	0.36	1.00											
Ti	0.21	0.28	-0.11	0.35	0.15	0.15	-0.13	-0.13	0.27	0.16	-0.04	0.82	0.07	0.47	0.03	0.04	-0.04	0.12	0.95	0.86	0.91	0.50	0.56	0.49	0.85	0.63	0.52	0.66	0.84	0.78	0.71	0.75	0.53	0.75	0.53	0.50	0.82	1.00										
U	0.30	0.44	-0.08	0.41	0.17	0.17	-0.15	-0.15	0.33	0.29	-0.10	0.67	-0.06	0.51	0.26	0.23	-0.01	0.15	0.79	0.86	0.79	0.66	0.58	0.69	0.85	0.73	0.52	0.70	0.80	0.80	0.73	0.73	0.72	0.81	0.74	0.59	0.72	0.82	1.00									
Zn	0.36	0.70	-0.14	0.58	0.43	0.44	-0.32	-0.32	0.57	0.55	-0.27	0.49	-0.04	0.46	0.54	0.54	0.13	0.08	0.43	0.67	0.51	0.72	0.48	0.85	0.53	0.49	0.45																					

Nogent-sur-Oise

Table A1. 17: Correlation between the measured species in the site of Nogent-sur-Oise (correlation coefficient – R)

<i>R Pearson</i>	EC	OC	Cl -	NO3 -	SO4 2-	nssSO4	ssSO4	Na +	NH4 +	K +	Mg 2+	Ca 2+	MSA	Oxalate	Levoglucosan	Polysac	Alcohols	Fe	Ca	As	Ba	Cd	Co	Cu	La	Mn	Mo	Ni	Pb	Rb	Sb	Sr	V	Zn			
EC	1.00																																				
OC	0.77	1.00																																			
Cl -	0.02	0.01	1.00																																		
NO3 -	0.23	0.54	-0.03	1.00																																	
SO4 2-	0.06	0.48	-0.11	0.72	1.00																																
nssSO4	0.07	0.48	-0.17	0.71	1.00	1.00																															
ssSO4	-0.07	-0.04	0.76	0.00	-0.09	-0.17	1.00																														
Na +	-0.07	-0.04	0.76	0.00	-0.09	-0.17	1.00	1.00																													
NH4 +	0.07	0.42	-0.13	0.94	0.83	0.83	-0.08	-0.08	1.00																												
K +	0.67	0.92	0.18	0.48	0.48	0.47	0.09	0.09	0.35	1.00																											
Mg 2+	0.11	0.15	0.86	-0.05	-0.06	-0.11	0.76	0.76	-0.22	0.33	1.00																										
Ca 2+	0.31	0.22	0.07	0.23	0.08	0.07	0.08	0.08	0.13	0.15	0.17	1.00																									
MSA	-0.12	0.02	-0.22	0.09	0.23	0.24	-0.12	-0.12	0.13	-0.01	-0.04	-0.01	1.00																								
Oxalate	0.10	0.39	-0.24	0.38	0.60	0.62	-0.25	-0.25	0.48	0.32	-0.17	0.08	0.21	1.00																							
Levoglucosan	0.71	0.84	0.19	0.46	0.26	0.26	0.05	0.05	0.30	0.80	0.21	0.16	-0.03	0.15	1.00																						
Polysac	0.70	0.88	0.20	0.48	0.31	0.31	0.05	0.05	0.31	0.86	0.24	0.14	-0.02	0.17	0.98	1.00																					
Alcohols	0.23	0.22	-0.31	-0.08	0.08	0.10	-0.32	-0.32	-0.04	0.14	-0.22	0.05	0.23	0.23	0.02	0.06	1.00																				
Fe	0.56	0.63	0.00	0.25	0.29	0.28	0.10	0.10	0.15	0.60	0.18	0.16	0.07	0.27	0.45	0.48	0.19	1.00																			
Ca	0.50	0.52	-0.02	0.24	0.20	0.20	0.03	0.03	0.10	0.45	0.18	0.26	-0.04	0.13	0.29	0.33	0.11	0.52	1.00																		
As	0.16	0.35	-0.18	0.40	0.46	0.46	-0.08	-0.08	0.47	0.28	-0.18	0.05	0.07	0.17	0.23	0.25	0.13	0.18	0.37	1.00																	
Ba	0.52	0.43	-0.11	0.15	0.05	0.06	-0.09	-0.09	0.05	0.35	0.03	0.24	-0.10	-0.01	0.21	0.25	0.16	0.23	0.69	0.52	1.00																
Cd	0.57	0.76	0.00	0.48	0.45	0.44	0.07	0.07	0.39	0.71	0.10	0.18	-0.01	0.31	0.61	0.64	0.13	0.60	0.59	0.56	0.49	1.00															
Co	0.53	0.55	-0.06	0.31	0.29	0.29	0.04	0.04	0.23	0.46	0.09	0.34	0.04	0.22	0.34	0.36	0.13	0.60	0.87	0.49	0.64	0.67	1.00														
Cu	0.69	0.66	0.03	0.34	0.21	0.21	0.02	0.02	0.21	0.59	0.13	0.29	-0.04	0.06	0.53	0.55	0.15	0.54	0.70	0.49	0.74	0.70	0.79	1.00													
La	0.28	0.34	-0.12	0.24	0.26	0.25	0.04	0.04	0.20	0.24	0.03	0.34	0.11	0.25	0.14	0.15	0.15	0.36	0.70	0.43	0.54	0.51	0.81	0.54	1.00												
Mn	0.46	0.58	0.00	0.35	0.36	0.35	0.01	0.01	0.28	0.53	0.10	0.19	-0.01	0.22	0.44	0.45	0.02	0.52	0.62	0.42	0.48	0.62	0.70	0.69	0.50	1.00											
Mo	0.44	0.62	0.05	0.53	0.41	0.40	0.07	0.07	0.47	0.55	0.09	0.27	0.08	0.17	0.58	0.58	0.01	0.36	0.49	0.53	0.53	0.61	0.67	0.76	0.47	0.66	1.00										
Ni	0.38	0.41	-0.01	0.24	0.27	0.27	0.02	0.02	0.18	0.37	0.13	0.21	0.16	0.18	0.27	0.30	0.09	0.53	0.60	0.29	0.33	0.45	0.80	0.56	0.58	0.51	0.49	1.00									
Pb	0.53	0.63	-0.06	0.43	0.34	0.34	-0.01	-0.01	0.37	0.57	-0.03	0.20	-0.06	0.34	0.45	0.46	0.15	0.50	0.55	0.48	0.45	0.87	0.62	0.60	0.49	0.53	0.49	0.36	1.00								
Rb	0.49	0.63	-0.02	0.40	0.35	0.34	0.03	0.03	0.32	0.58	0.07	0.26	-0.07	0.23	0.53	0.55	0.06	0.28	0.69	0.55	0.66	0.70	0.74	0.70	0.72	0.62	0.71	0.41	0.63	1.00							
Sb	0.33	0.34	-0.08	0.32	0.12	0.12	-0.09	-0.09	0.27	0.23	-0.12	0.21	-0.02	0.11	0.35	0.32	0.08	0.23	0.31	0.32	0.35	0.43	0.41	0.56	0.35	0.34	0.47	0.24	0.48	0.42	1.00						
Sr	0.35	0.37	0.10	0.16	0.09	0.08	0.20	0.20	0.03	0.34	0.29	0.33	-0.06	0.09	0.23	0.24	0.02	0.34	0.86	0.31	0.65	0.49	0.76	0.58	0.78	0.50	0.43	0.43	0.46	0.76	0.25	1.00					
V	0.19	0.23	-0.14	0.15	0.25	0.24	0.05	0.05	0.16	0.16	0.02	0.22	0.27	0.19	0.09	0.10	0.18	0.25	0.42	0.34	0.31	0.30	0.66	0.35	0.72	0.33	0.34	0.65	0.24	0.47	0.17	0.48	1.00				
Zn	0.43	0.44	-0.01	0.34	0.25	0.23	0.13	0.13	0.28	0.41	0.05	0.16	-0.05	0.07	0.29	0.32	0.14	0.45	0.46	0.47	0.42	0.52	0.50	0.57	0.32	0.44	0.41	0.33	0.50	0.43	0.29	0.38	0.18	1.00			

Color scale: Green for the highest values (1.0) and red to the minimum value observed.

Revin

Table A1. 18: Correlation between the measured species in the site of Revin (correlation coefficient – R)

R Pearson	EC	OC	Cl -	NO3 -	SO4 2-	nssSO4	ssSO4	Na +	NH4 +	K +	Mg 2+	Ca 2+	MSA	Oxalate	Levoglucosan	Polysac	Alcohols	Monosac	Al	Fe	Ca	As	Cd	Ce	Co	Cs	Cu	La	Mn	Mo	Pb	Rb	Sb	Se	Sr	Ti	Zn					
EC	1.00																																									
OC	0.64	1.00																																								
Cl -	-0.20	-0.33	1.00																																							
NO3 -	0.45	0.42	-0.05	1.00																																						
SO4 2-	0.42	0.58	-0.16	0.70	1.00																																					
nssSO4	0.42	0.58	-0.21	0.70	1.00	1.00																																				
ssSO4	-0.18	-0.22	0.75	-0.10	-0.19	-0.25	1.00																																			
Na +	-0.18	-0.22	0.75	-0.10	-0.19	-0.25	1.00	1.00																																		
NH4 +	0.45	0.53	-0.16	0.91	0.88	0.88	-0.25	-0.25	1.00																																	
K +	0.54	0.56	-0.02	0.61	0.58	0.58	-0.02	-0.02	0.62	1.00																																
Mg 2+	-0.14	-0.27	0.89	-0.07	-0.20	-0.25	0.84	0.84	-0.22	0.00	1.00																															
Ca 2+	0.36	0.33	-0.04	0.23	0.21	0.20	0.11	0.11	0.16	0.33	0.13	1.00																														
MSA	-0.07	0.02	-0.11	-0.08	0.10	0.10	0.09	0.09	-0.05	-0.17	0.07	0.08	1.00																													
Oxalate	0.40	0.39	0.01	0.44	0.48	0.47	0.04	0.04	0.44	0.56	-0.04	0.37	-0.03	1.00																												
Levoglucosan	0.36	0.40	-0.01	0.34	0.24	0.25	-0.13	-0.13	0.39	0.56	-0.10	-0.13	-0.37	0.12	1.00																											
Polysac	0.40	0.38	0.16	0.41	0.37	0.36	0.00	0.00	0.46	0.52	0.01	-0.03	-0.28	0.27	0.80	1.00																										
Alcohols	-0.07	0.21	-0.10	-0.20	-0.01	-0.02	0.10	0.10	-0.18	0.00	-0.09	0.09	0.17	0.13	-0.25	-0.08	1.00																									
Monosac	-0.02	0.24	0.04	-0.05	0.05	0.05	0.10	0.10	-0.03	0.09	-0.01	0.06	0.05	0.16	0.00	0.19	0.76	1.00																								
Al	0.37	0.37	-0.10	0.10	0.17	0.17	-0.04	-0.04	0.08	0.20	0.03	0.87	0.01	0.25	-0.07	0.00	0.03	0.02	1.00																							
Fe	0.58	0.60	-0.12	0.34	0.35	0.35	-0.04	-0.04	0.31	0.36	0.03	0.77	0.03	0.31	0.09	0.15	0.01	0.02	0.87	1.00																						
Ca	0.37	0.35	-0.02	0.11	0.13	0.12	0.14	0.14	0.05	0.21	0.14	0.92	0.03	0.28	-0.09	-0.02	0.10	0.06	0.94	0.86	1.00																					
As	0.45	0.70	-0.23	0.42	0.57	0.58	-0.24	-0.24	0.51	0.44	-0.20	0.22	-0.05	0.29	0.20	0.23	0.15	0.17	0.26	0.45	0.22	1.00																				
Cd	0.44	0.63	-0.15	0.40	0.46	0.46	-0.16	-0.16	0.49	0.47	-0.14	0.05	-0.08	0.22	0.55	0.48	-0.12	0.03	0.15	0.39	0.13	0.50	1.00																			
Ce	0.43	0.44	-0.09	0.12	0.18	0.18	-0.03	-0.03	0.09	0.23	0.04	0.83	0.01	0.25	-0.05	0.00	0.07	0.06	0.93	0.85	0.91	0.29	0.17	1.00																		
Co	0.40	0.37	-0.04	0.13	0.19	0.19	0.01	0.01	0.12	0.24	0.07	0.53	-0.07	0.16	0.06	0.10	0.16	0.15	0.59	0.68	0.63	0.36	0.21	0.66	1.00																	
Cs	0.45	0.60	-0.19	0.35	0.53	0.52	-0.08	-0.08	0.42	0.33	-0.09	0.49	0.09	0.31	0.07	0.16	0.04	0.07	0.51	0.69	0.51	0.56	0.45	0.53	0.52	1.00																
Cu	0.55	0.64	-0.17	0.39	0.40	0.40	-0.09	-0.09	0.40	0.34	-0.04	0.28	0.17	0.22	0.19	0.19	0.02	0.02	0.26	0.58	0.30	0.47	0.60	0.35	0.38	0.51	1.00															
La	0.42	0.43	-0.10	0.12	0.22	0.21	-0.01	-0.01	0.11	0.23	0.05	0.80	0.04	0.28	-0.07	0.04	0.09	0.07	0.89	0.85	0.87	0.34	0.20	0.91	0.67	0.60	0.38	1.00														
Mn	0.57	0.63	-0.15	0.38	0.36	0.36	-0.07	-0.07	0.36	0.35	-0.01	0.58	0.06	0.23	0.15	0.19	-0.05	0.01	0.63	0.87	0.64	0.48	0.46	0.65	0.58	0.76	0.67	0.70	1.00													
Mo	0.39	0.47	-0.13	0.35	0.38	0.38	-0.08	-0.08	0.38	0.22	-0.09	0.15	0.04	0.09	0.17	0.16	-0.04	0.00	0.17	0.52	0.20	0.40	0.44	0.20	0.51	0.64	0.56	0.30	0.66	1.00												
Pb	0.58	0.68	-0.15	0.52	0.54	0.54	-0.16	-0.16	0.58	0.47	-0.10	0.20	-0.03	0.25	0.38	0.37	-0.13	-0.02	0.21	0.54	0.22	0.64	0.62	0.26	0.33	0.65	0.64	0.35	0.71	0.64	1.00											
Rb	0.63	0.76	-0.20	0.40	0.49	0.50	-0.15	-0.15	0.45	0.52	-0.11	0.68	-0.06	0.37	0.30	0.33	-0.03	0.03	0.77	0.88	0.73	0.58	0.52	0.78	0.60	0.82	0.54	0.77	0.83	0.48	0.63	1.00										
Sb	0.44	0.52	0.03	0.37	0.40	0.40	-0.03	-0.03	0.42	0.35	0.05	0.17	-0.02	0.18	0.23	0.24	-0.05	0.03	0.17	0.40	0.18	0.48	0.44	0.21	0.28	0.41	0.52	0.29	0.48	0.45	0.59	0.43	1.00									
Se	0.33	0.47	-0.13	0.31	0.37	0.37	0.02	0.02	0.35	0.23	-0.03	0.08	0.10	0.11	0.19	0.18	0.04	0.06	0.09	0.36	0.14	0.48	0.46	0.14	0.38	0.57	0.53	0.30	0.53	0.68	0.62	0.42	0.48	1.00								
Sr	0.26	0.22	0.12	0.04	0.10	0.08	0.20	0.20	-0.01	0.17	0.28	0.87	0.03	0.22	-0.11	-0.02	0.01	0.02	0.92	0.77	0.93	0.14	0.06	0.86	0.55	0.45	0.19	0.83	0.54	0.08	0.13	0.67	0.13	0.07	1.00							
Ti	0.40	0.49	-0.16	0.15	0.28	0.28	-0.05	-0.05	0.16	0.19	-0.02	0.81	0.10	0.27	-0.13	-0.03	0.11	0.09	0.93	0.86	0.87	0.39	0.21	0.90	0.59	0.61	0.38	0.88	0.69	0.26	0.32	0.80	0.24	0.19	0.83	1.00						
Zn	0.50	0.48	-0.05	0.30	0.20	0.20	-0.08	-0.08	0.27	0.32	-0.02	0.14	-0.04	0.06	0.37	0.33	-0.14	-0.08	0.17	0.45	0.21	0.35	0.44	0.23	0.30	0.40	0.46	0.26	0.63	0.55	0.66	0.46	0.37	0.46	0.13	0.20	1.00					

Color scale: Green for the highest values (1.0) and red to the minimum value observed.

Rouen

Table A1. 19: Correlation between the measured species in the site of Rouen (correlation coefficient – R)

R Pearson	EC	OC	Cl -	NO3 -	SO4 2-	nssSO4	ssSO4	Na +	NH4 +	K +	Mg 2+	Ca 2+	MSA	Oxalate	Levogluconan	Polysac	Alcohols	Monosac	Fe	Ca	As	Cd	Ce	Co	Cs	Cu	La	Mn	Mo	Ni	Pb	Rb	Sb	Se	Sr	Zn				
EC	1.00																																							
OC	0.79	1.00																																						
Cl -	0.04	-0.08	1.00																																					
NO3 -	0.39	0.68	0.09	1.00																																				
SO4 2-	0.15	0.52	-0.01	0.76	1.00																																			
nssSO4	-0.05	0.49	-0.25	0.75	1.00	1.00																																		
ssSO4	-0.11	-0.31	0.93	-0.12	-0.23	-0.28	1.00																																	
Na +	-0.11	-0.31	0.93	-0.12	-0.23	-0.28	1.00	1.00																																
NH4 +	0.00	0.57	-0.14	0.96	0.86	0.86	-0.20	-0.20	1.00																															
K +	0.57	0.86	0.04	0.56	0.44	0.43	0.03	0.03	0.52	1.00																														
Mg 2+	-0.14	-0.34	0.91	-0.15	-0.22	-0.27	0.97	0.97	-0.22	-0.02	1.00																													
Ca 2+	0.22	0.52	-0.11	0.58	0.53	0.53	-0.12	-0.12	0.52	0.43	-0.08	1.00																												
MSA	-0.08	-0.06	-0.21	-0.07	0.17	0.18	-0.07	-0.07	-0.05	-0.16	-0.04	0.02	1.00																											
Oxalate	0.45	0.69	0.01	0.74	0.70	0.75	-0.34	-0.34	0.71	0.42	-0.31	0.60	0.13	1.00																										
Levogluconan	0.57	0.61	0.12	0.49	0.26	0.13	-0.03	-0.03	0.25	0.40	-0.08	0.07	-0.23	0.37	1.00																									
Polysac	0.40	0.50	0.01	0.38	0.19	0.13	-0.08	-0.08	0.24	0.38	-0.13	0.06	-0.29	0.20	0.92	1.00																								
Alcohols	0.08	0.03	-0.23	-0.20	-0.01	0.03	-0.21	-0.21	-0.12	0.04	-0.18	-0.03	0.10	0.06	-0.15	-0.16	1.00																							
Monosac	0.34	0.26	-0.08	0.02	0.03	0.00	-0.10	-0.10	-0.09	0.16	-0.08	-0.04	-0.10	0.18	0.24	0.17	0.71	1.00																						
Fe	0.65	0.64	-0.11	0.32	0.24	0.17	-0.20	-0.20	0.19	0.49	-0.20	0.58	0.03	0.41	0.20	0.15	0.14	0.13	1.00																					
Ca	0.23	0.45	-0.10	0.43	0.41	0.44	-0.10	-0.10	0.44	0.42	-0.05	0.95	0.01	0.43	0.07	0.06	-0.03	-0.02	0.64	1.00																				
As	0.25	0.55	-0.24	0.52	0.53	0.58	-0.29	-0.29	0.62	0.54	-0.26	0.59	-0.02	0.54	0.08	0.08	0.17	0.09	0.58	0.62	1.00																			
Cd	0.39	0.60	-0.06	0.50	0.44	0.42	-0.11	-0.11	0.46	0.53	-0.14	0.38	0.01	0.48	0.28	0.24	0.16	0.17	0.44	0.38	0.48	1.00																		
Ce	0.55	0.66	-0.19	0.39	0.33	0.31	-0.26	-0.26	0.32	0.50	-0.22	0.72	0.00	0.49	0.22	0.16	0.12	0.19	0.74	0.79	0.66	0.43	1.00																	
Co	0.31	0.53	-0.23	0.43	0.47	0.51	-0.26	-0.26	0.49	0.49	-0.24	0.72	0.09	0.46	0.14	0.14	0.10	0.05	0.70	0.74	0.69	0.47	0.69	1.00																
Cs	0.10	0.43	-0.26	0.39	0.54	0.58	-0.29	-0.29	0.48	0.37	-0.27	0.48	0.42	0.48	0.05	0.01	0.07	0.04	0.37	0.50	0.55	0.39	0.49	0.62	1.00															
Cu	0.84	0.66	-0.07	0.29	0.14	0.05	-0.15	-0.15	0.06	0.42	-0.17	0.36	-0.02	0.40	0.36	0.26	0.17	0.27	0.82	0.42	0.43	0.44	0.66	0.51	0.23	1.00														
La	0.30	0.44	-0.13	0.16	0.25	0.27	-0.15	-0.15	0.21	0.41	-0.13	0.39	0.05	0.21	0.18	0.26	0.16	0.18	0.46	0.45	0.39	0.28	0.58	0.47	0.34	0.43	1.00													
Mn	0.43	0.49	-0.12	0.32	0.23	0.20	-0.17	-0.17	0.28	0.36	-0.15	0.47	0.03	0.39	0.13	0.08	0.13	0.13	0.71	0.53	0.57	0.37	0.61	0.68	0.42	0.60	0.34	1.00												
Mo	0.34	0.35	-0.10	0.15	0.08	0.07	-0.13	-0.13	0.12	0.31	-0.14	0.41	0.01	0.18	-0.01	-0.02	0.13	-0.01	0.74	0.44	0.41	0.25	0.40	0.54	0.18	0.46	0.20	0.52	1.00											
Ni	0.31	0.41	-0.18	0.23	0.32	0.33	-0.16	-0.16	0.24	0.33	-0.14	0.32	0.27	0.32	0.10	0.09	0.22	0.17	0.47	0.37	0.44	0.35	0.49	0.70	0.54	0.42	0.53	0.41	0.27	1.00										
Pb	0.54	0.84	-0.15	0.69	0.59	0.59	-0.28	-0.28	0.69	0.76	-0.29	0.55	-0.01	0.63	0.41	0.37	0.02	0.17	0.57	0.53	0.70	0.64	0.66	0.62	0.58	0.55	0.42	0.59	0.32	0.40	1.00									
Rb	0.62	0.91	-0.13	0.69	0.59	0.58	-0.30	-0.30	0.61	0.79	-0.31	0.67	0.04	0.69	0.48	0.39	-0.03	0.16	0.65	0.64	0.64	0.61	0.76	0.67	0.69	0.58	0.46	0.54	0.34	0.48	0.85	1.00								
Sb	0.73	0.61	-0.10	0.29	0.17	0.11	-0.21	-0.21	0.11	0.36	-0.23	0.31	-0.01	0.42	0.30	0.21	0.20	0.27	0.67	0.35	0.39	0.39	0.59	0.45	0.24	0.88	0.42	0.52	0.41	0.38	0.56	0.52	1.00							
Se	0.09	0.45	-0.28	0.42	0.59	0.65	-0.30	-0.30	0.58	0.45	-0.28	0.46	0.33	0.49	-0.03	-0.05	0.21	0.06	0.37	0.44	0.64	0.48	0.47	0.55	0.74	0.21	0.30	0.40	0.27	0.42	0.64	0.58	0.25	1.00						
Sr	0.31	0.34	0.15	0.33	0.27	0.23	0.23	0.23	0.16	0.25	0.30	0.58	0.19	0.36	0.16	0.03	-0.10	0.04	0.34	0.58	0.27	0.25	0.55	0.35	0.33	0.32	0.29	0.31	0.15	0.23	0.34	0.46	0.28	0.23	1.00					
Zn	0.57	0.80	-0.14	0.59	0.49	0.48	-0.29	-0.29	0.52	0.66	-0.31	0.51	-0.04	0.59	0.38	0.31	0.01	0.16	0.55	0.51	0.60	0.59	0.63	0.53	0.48	0.54	0.35	0.49	0.31	0.32	0.86	0.79	0.54	0.60	0.35	1.00				

Color scale: Green for the highest values (1.0) and red to the minimum value observed.

Roubaix

Table A1. 20: Correlation between the measured species in the site of Roubaix (correlation coefficient – R)

R Pearson	EC	OC	Cl -	NO3 -	SO4 2-	nssSO4	ssSO4	Na +	NH4 +	K +	Mg 2+	Ca 2+	MSA	Oxalate	Levoglucosan	Polysac	Alcohols	Monosac	Al	Fe	Ca	As	Ba	Cd	Ce	Co	Cs	Cu	La	Mn	Mo	Ni	Pb	Rb	Sb	Se	Sr	Ti	U	Zn											
EC	1.00																																																		
OC	0.27	1.00																																																	
Cl -	0.06	-0.08	1.00																																																
NO3 -	0.02	0.56	-0.13	1.00																																															
SO4 2-	-0.02	0.35	-0.11	0.78	1.00																																														
nssSO4	-0.02	0.36	-0.16	0.78	1.00	1.00																																													
ssSO4	-0.05	-0.24	0.92	-0.25	-0.22	-0.27	1.00																																												
Na +	-0.05	-0.24	0.92	-0.25	-0.22	-0.27	1.00	1.00																																											
NH4 +	-0.01	0.49	-0.13	0.95	0.88	0.89	-0.28	-0.28	1.00																																										
K +	0.03	0.26	0.24	0.23	0.34	0.33	0.11	0.11	0.23	1.00																																									
Mg 2+	-0.06	-0.17	0.90	-0.22	-0.20	-0.25	0.97	0.97	-0.26	0.24	1.00																																								
Ca 2+	0.15	0.53	-0.07	0.39	0.24	0.25	-0.13	-0.13	0.27	0.27	0.01	1.00																																							
MSA	-0.18	-0.13	-0.25	0.01	0.15	0.15	-0.05	-0.05	-0.01	-0.12	-0.03	0.05	1.00																																						
Oxalate	-0.09	0.46	-0.22	0.66	0.61	0.61	-0.27	-0.27	0.66	0.10	-0.20	0.40	0.18	1.00																																					
Levoglucosan	0.34	0.59	0.20	0.24	0.12	0.12	0.01	0.01	0.24	0.22	0.00	0.09	-0.41	0.05	1.00																																				
Polysac	0.33	0.59	0.20	0.31	0.21	0.20	0.02	0.02	0.30	0.26	0.02	0.12	-0.36	0.18	0.93	1.00																																			
Alcohols	0.09	0.13	-0.21	-0.08	0.07	0.08	-0.22	-0.22	-0.04	-0.05	-0.21	0.07	0.12	0.08	-0.08	-0.13	1.00																																		
Monosac	0.16	0.22	-0.07	-0.05	-0.12	-0.11	-0.12	-0.12	-0.07	0.01	-0.08	0.04	-0.15	-0.16	0.25	0.17	0.48	1.00																																	
Al	0.14	0.37	-0.13	0.30	0.12	0.13	-0.17	-0.17	0.20	0.00	-0.08	0.68	-0.09	0.31	0.00	0.04	0.07	0.09	1.00																																
Fe	0.53	0.66	-0.10	0.34	0.11	0.12	-0.19	-0.19	0.22	0.02	-0.09	0.64	-0.07	0.24	0.26	0.28	0.12	0.21	0.71	1.00																															
Ca	0.25	0.47	-0.09	0.29	0.12	0.12	-0.14	-0.14	0.17	0.14	-0.02	0.91	-0.06	0.30	0.04	0.07	0.07	0.10	0.82	0.75	1.00																														
As	0.12	0.73	-0.04	0.66	0.53	0.53	-0.20	-0.20	0.62	0.40	-0.11	0.47	-0.10	0.42	0.40	0.44	0.02	0.08	0.34	0.49	0.40	1.00																													
Ba	0.46	0.65	-0.11	0.27	0.10	0.10	-0.17	-0.17	0.16	0.08	-0.06	0.66	0.04	0.22	0.24	0.24	0.09	0.17	0.53	0.89	0.65	0.48	1.00																												
Cd	0.14	0.51	0.07	0.29	0.20	0.20	-0.05	-0.05	0.25	0.41	0.02	0.30	-0.17	0.18	0.33	0.36	-0.01	0.12	0.12	0.31	0.25	0.52	0.31	1.00																											
Ce	0.38	0.69	-0.18	0.28	0.08	0.10	-0.24	-0.24	0.17	0.04	-0.13	0.76	0.01	0.29	0.21	0.20	0.14	0.22	0.71	0.83	0.77	0.46	0.84	0.31	1.00																										
Co	0.31	0.45	-0.10	0.46	0.50	0.50	-0.15	-0.15	0.41	0.13	-0.11	0.56	0.22	0.37	0.08	0.12	0.25	0.04	0.40	0.55	0.49	0.51	0.59	0.25	0.55	1.00																									
Cs	-0.06	0.37	-0.12	0.48	0.44	0.44	-0.17	-0.17	0.42	0.32	-0.06	0.42	0.27	0.32	-0.04	0.03	0.08	0.02	0.21	0.31	0.32	0.50	0.29	0.27	0.32	0.44	1.00																								
Cu	0.56	0.66	-0.07	0.24	0.07	0.08	-0.15	-0.15	0.14	0.06	-0.07	0.56	0.04	0.16	0.30	0.29	0.11	0.23	0.38	0.84	0.54	0.43	0.92	0.37	0.78	0.54	0.25	1.00																							
La	0.12	0.56	-0.23	0.42	0.26	0.27	-0.24	-0.24	0.31	0.06	-0.13	0.78	0.22	0.40	0.01	0.03	0.09	0.10	0.67	0.67	0.75	0.48	0.69	0.24	0.84	0.63	0.53	0.59	1.00																						
Mn	0.28	0.66	-0.10	0.41	0.32	0.32	-0.19	-0.19	0.31	0.48	-0.04	0.77	0.08	0.29	0.21	0.23	0.09	0.11	0.49	0.69	0.68	0.63	0.78	0.42	0.76	0.63	0.56	0.72	0.74	1.00																					
Mo	0.25	0.66	-0.15	0.47	0.31	0.32	-0.24	-0.24	0.38	0.13	-0.15	0.61	0.15	0.34	0.17	0.18	0.16	0.14	0.40	0.67	0.53	0.59	0.71	0.28	0.71	0.69	0.55	0.70	0.68	0.79	1.00																				
Ni	0.07	0.28	-0.11	0.29	0.29	0.30	-0.13	-0.13	0.24	0.14	-0.06	0.36	0.27	0.24	-0.06	-0.04	0.22	0.02	0.21	0.34	0.28	0.32	0.40	0.15	0.34	0.73	0.40	0.36	0.51	0.49	0.60	1.00																			
Pb	0.30	0.67	0.04	0.46	0.37	0.37	-0.11	-0.11	0.41	0.55	0.00	0.45	-0.14	0.26	0.41	0.43	-0.01	0.11	0.25	0.49	0.39	0.73	0.49	0.76	0.49	0.45	0.52	0.52	0.42	0.70	0.57	0.27	1.00																		
Rb	0.06	0.39	0.10	0.31	0.37	0.36	-0.02	-0.02	0.28	0.92	0.15	0.46	-0.02	0.15	0.18	0.21	-0.01	0.05	0.18	0.22	0.34	0.53	0.28	0.44	0.29	0.32	0.58	0.24	0.34	0.70	0.38	0.28	0.68	1.00																	
Sb	0.41	0.53	-0.17	0.25	0.10	0.11	-0.23	-0.23	0.16	0.06	-0.17	0.42	0.05	0.17	0.17	0.19	0.07	0.15	0.24	0.59	0.40	0.34	0.64	0.32	0.56	0.43	0.20	0.78	0.42	0.54	0.52	0.26	0.42	0.20	1.00																
Se	0.01	0.61	-0.27	0.58	0.42	0.43	-0.33	-0.33	0.50	0.10	-0.24	0.47	0.19	0.39	0.15	0.15	0.27	0.23	0.40	0.55	0.43	0.66	0.51	0.27	0.55	0.55	0.63	0.49	0.64	0.63	0.72	0.41	0.50	0.34	0.43	1.00															
Sr	0.10	0.40	0.13	0.21	0.11	0.10	0.12	0.12	0.09	0.31	0.26	0.86	0.08	0.23	0.04	0.07	-0.03	0.00	0.65	0.57	0.81	0.37	0.64	0.25	0.74	0.50	0.40	0.51	0.75	0.76	0.56	0.35	0.41	0.51	0.31	0.38	1.00														
Ti	0.10	0.40	0.13	0.21	0.11	0.10	0.13	0.13	0.09	0.30	0.27	0.86	0.08	0.23	0.03	0.06	-0.03	0.00	0.65	0.57	0.81	0.37	0.64	0.25	0.73	0.50	0.40	0.51	0.75	0.75	0.55	0.34	0.41	0.50	0.31	0.38	1.00	1.00													
U	0.13	0.60	-0.22	0.45	0.28	0.29	-0.27	-0.27	0.34	0.05	-0.17	0.86	0.08	0.42	0.11	0.13	0.16	0.15	0.65	0.64	0.79	0.53	0.66	0.24	0.83	0.61	0.48	0.55	0.87	0.74	0.75	0.39	0.43	0.31	0.40	0.63	0.78	0.78	1.00												

ANNEX 2: PMF SOLUTIONS

Q_{true}/Q_{exp} value for PMF solutions

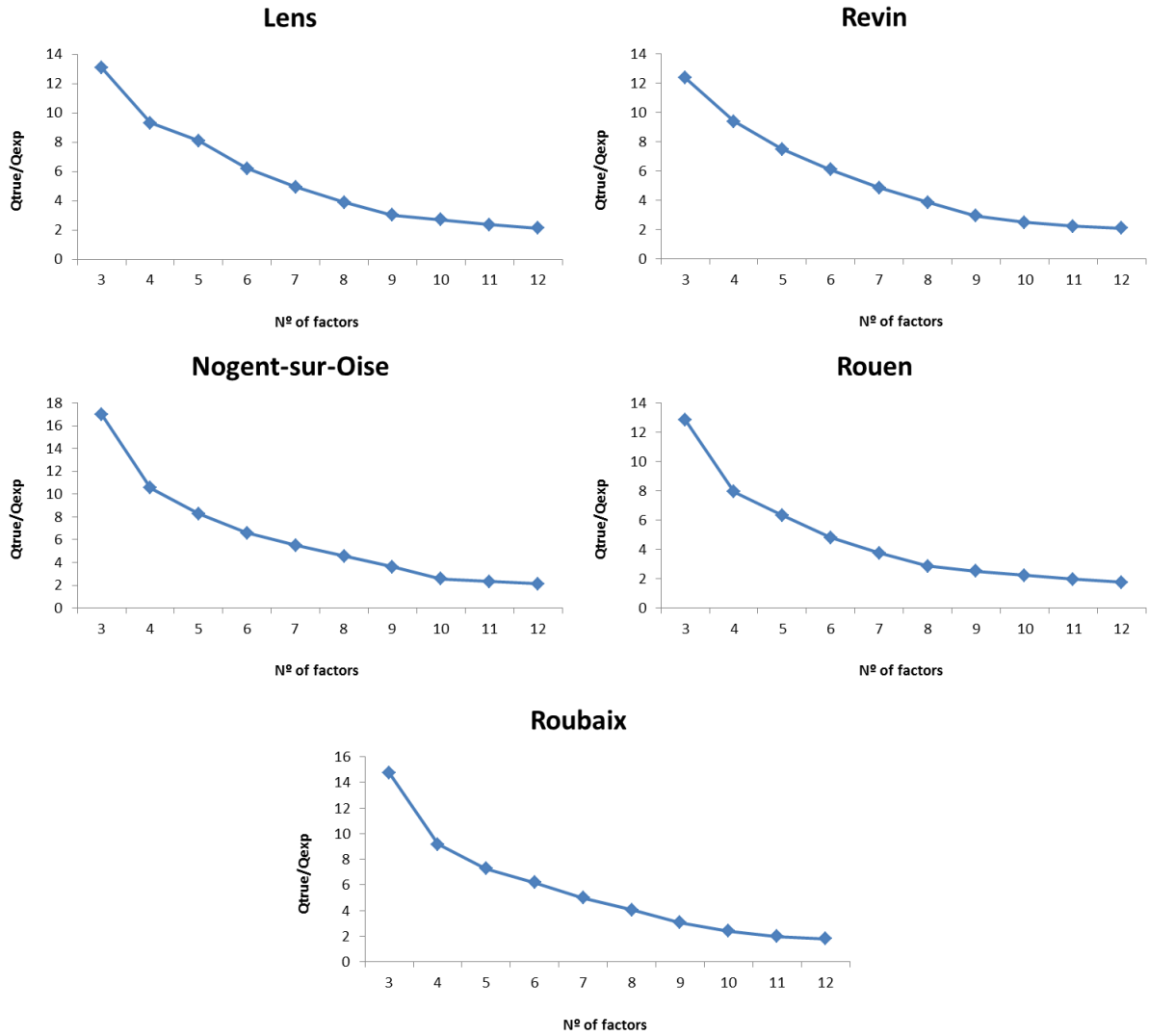


Figure A2. 1: Q_{true}/Q_{exp} values for different number of factors on the 5 sampling sites

IM and IS values for PMF solutions

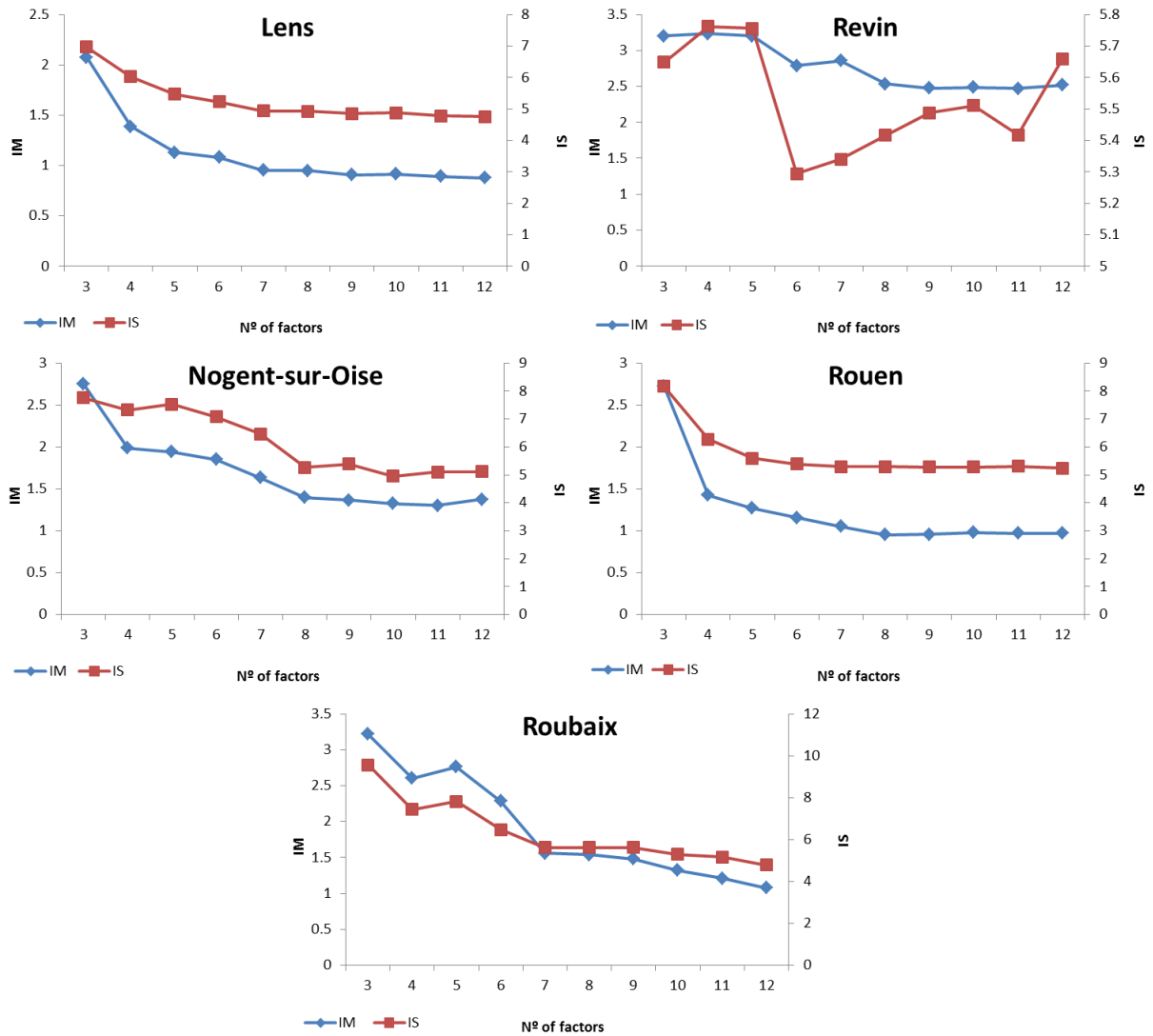


Figure A2. 2: IM and IS values for different number of factors on the 5 sampling sites

Bootstrap

Lens

Table A2. 1: Bootstrap results for the PMF solution in Lens

Biomass burning	Marine biogenic	Oxalate rich	Land biogenic	Aged marine	Traffic	Nitrate rich	Fresh marine	Sulfate rich	Unmapped
100	0	0	0	0	0	0	0	0	0
0	99	0	0	1	0	0	0	0	0
0	0	100	0	0	0	0	0	0	0
0	0	0	100	0	0	0	0	0	0
0	0	0	0	100	0	0	0	0	0
0	0	0	0	0	100	0	0	0	0
0	0	0	0	0	0	100	0	0	0
0	0	0	0	0	0	0	100	0	0
0	0	0	0	0	0	0	0	100	0

Nogent-sur-Oise

Table A2. 2: Bootstrap results for the PMF solution in Nogent-sur-Oise

Sulfate rich	Marine biogenic	Aged marine	Nitrate rich	Fresh marine	Land biogenic	Biomass burning	Oxalate rich	Traffic	Unmapped
97	0	1	0	0	0	0	0	0	0
0	90	0	1	0	0	2	1	1	3
0	0	96	0	0	0	1	0	0	1
0	0	0	98	0	0	0	0	0	0
0	0	0	0	98	0	0	0	0	0
0	0	0	0	0	98	0	0	0	0
0	0	0	0	0	0	98	0	0	0
0	0	0	0	0	0	0	98	0	0
0	0	0	0	0	0	0	0	94	4

Revin

Table A2. 3: Bootstrap results for the PMF solution in Revin

Fresh marine	Aged marine	Sulfate rich	Land biogenic	Marine biogenic	Oxalate rich	Nitrate rich	Crustal	Traffic	Biomass burning	Unmapped
100	0	0	0	0	0	0	0	0	0	0
0	100	0	0	0	0	0	0	0	0	0
0	0	100	0	0	0	0	0	0	0	0
0	0	0	99	0	0	0	0	0	0	1
0	1	0	0	98	0	0	0	0	1	0
0	0	0	0	0	100	0	0	0	0	0
0	0	0	0	0	0	100	0	0	0	0
0	1	0	0	0	0	0	85	7	7	0
0	0	0	0	0	0	0	0	97	3	0
0	0	0	0	0	0	0	0	0	100	0

Rouen

Table A2. 4: Bootstrap results for the PMF solution in Rouen

Fresh marine	Biomass burning	Oxalate rich	Traffic	Sulfate rich	Land biogenic	Nitrate rich	Marine biogenic	Unmapped
100	0	0	0	0	0	0	0	0
0	99	0	0	0	0	0	0	1
0	0	99	1	0	0	0	0	0
0	0	1	99	0	0	0	0	0
1	0	0	2	97	0	0	0	0
0	0	0	0	0	100	0	0	0
0	0	0	0	0	0	100	0	0
2	0	0	5	0	0	0	93	0

Roubaix

Table A2. 5: Bootstrap results for the PMF solution in Roubaix

Biomass burning	Sulfate rich	Oxalate rich	Marine biogenic	Crustal	Aged marine	Fresh marine	Nitrate rich	Traffic	Land biogenic	Unmapped
100	0	0	0	0	0	0	0	0	0	0
0	98	0	0	0	0	0	0	0	0	2
0	0	100	0	0	0	0	0	0	0	0
0	0	0	99	0	0	0	0	0	0	1
0	0	0	0	99	0	0	0	0	0	1
0	0	0	0	0	100	0	0	0	0	0
0	0	0	0	0	0	100	0	0	0	0
0	0	0	0	0	0	0	100	0	0	0
0	0	0	0	0	0	0	0	100	0	0
0	0	0	0	0	0	0	0	0	100	0

PMF solution in Lens

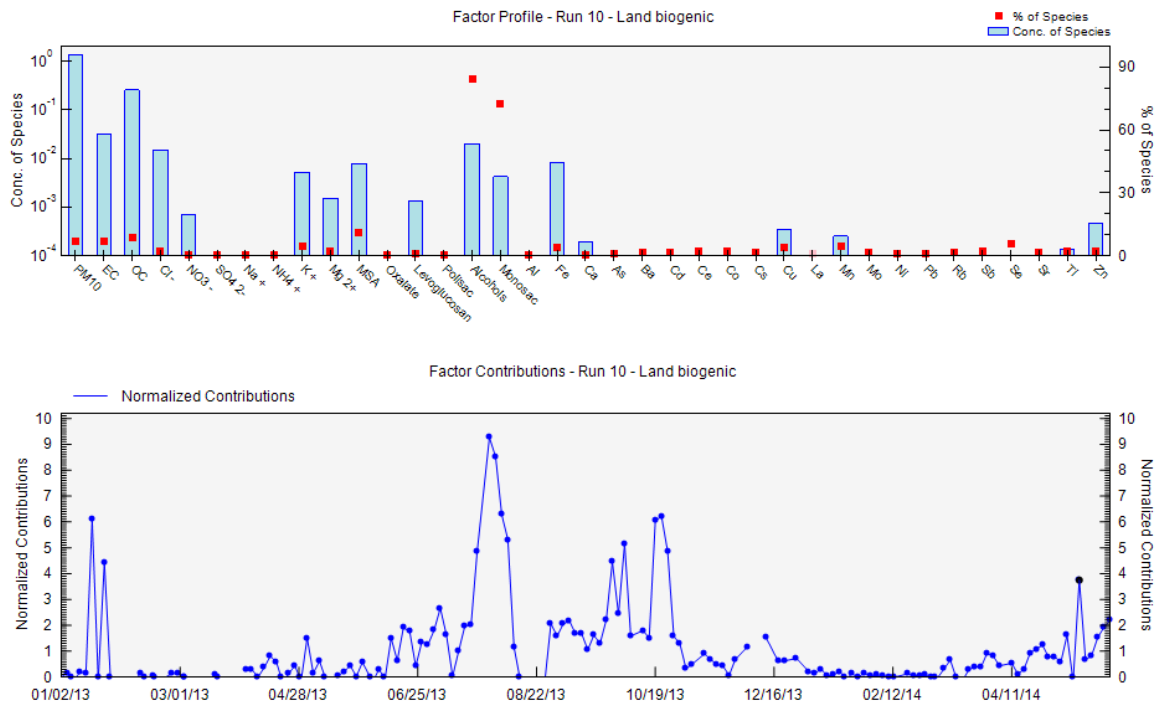


Figure A2. 3: Chemical profile (top) and time variability (bottom) of the land biogenic factor in Lens

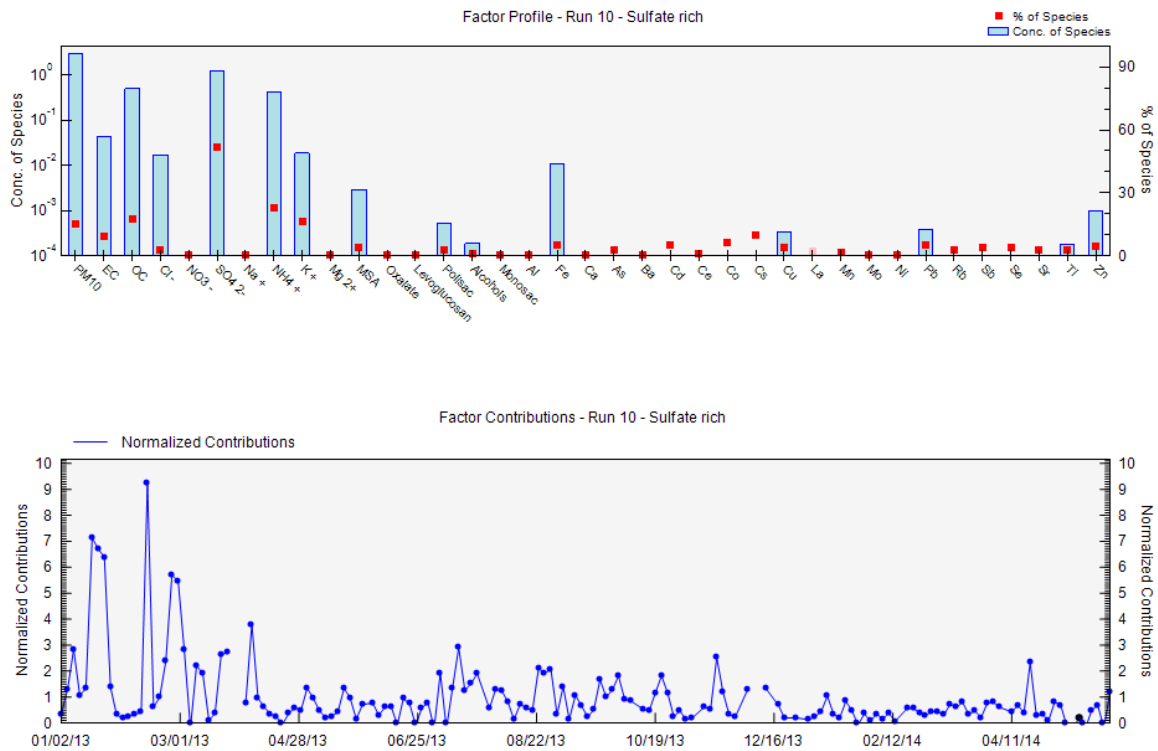


Figure A2. 4: Chemical profile (top) and time variability (bottom) of the sulfate rich factor in Lens

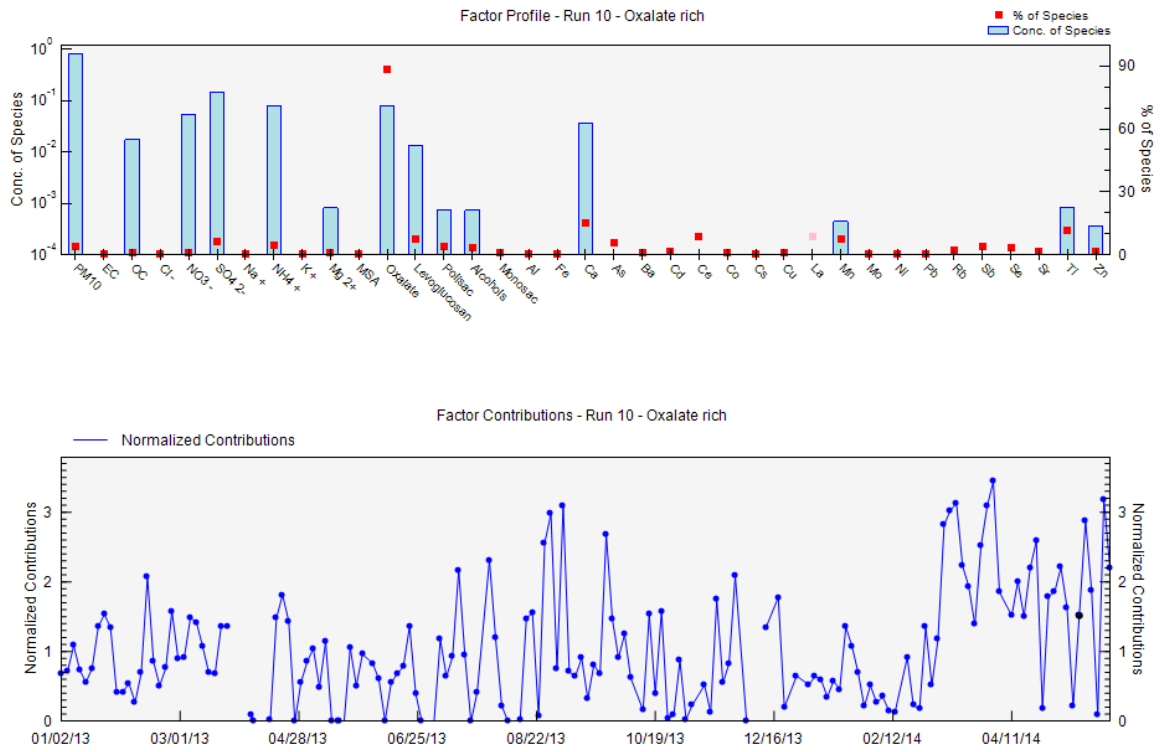


Figure A2. 5: Chemical profile (top) and time variability (bottom) of the oxalate rich factor in Lens

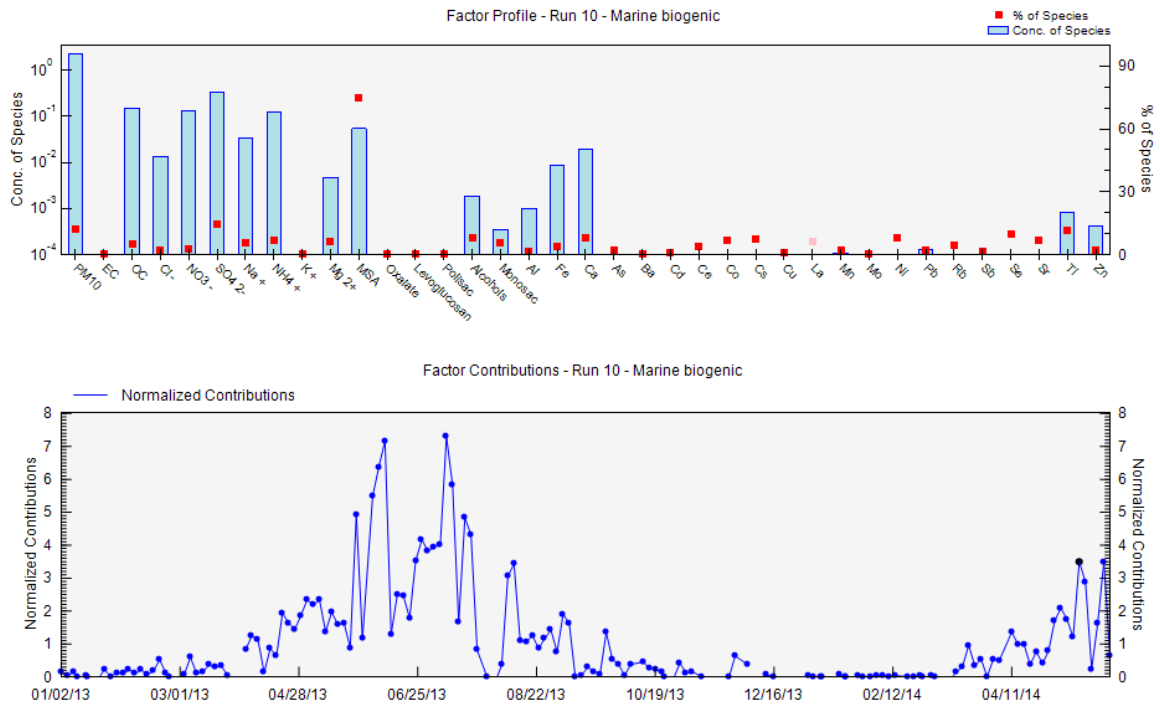


Figure A2. 6: Chemical profile (top) and time variability (bottom) of the marine biogenic factor in Lens

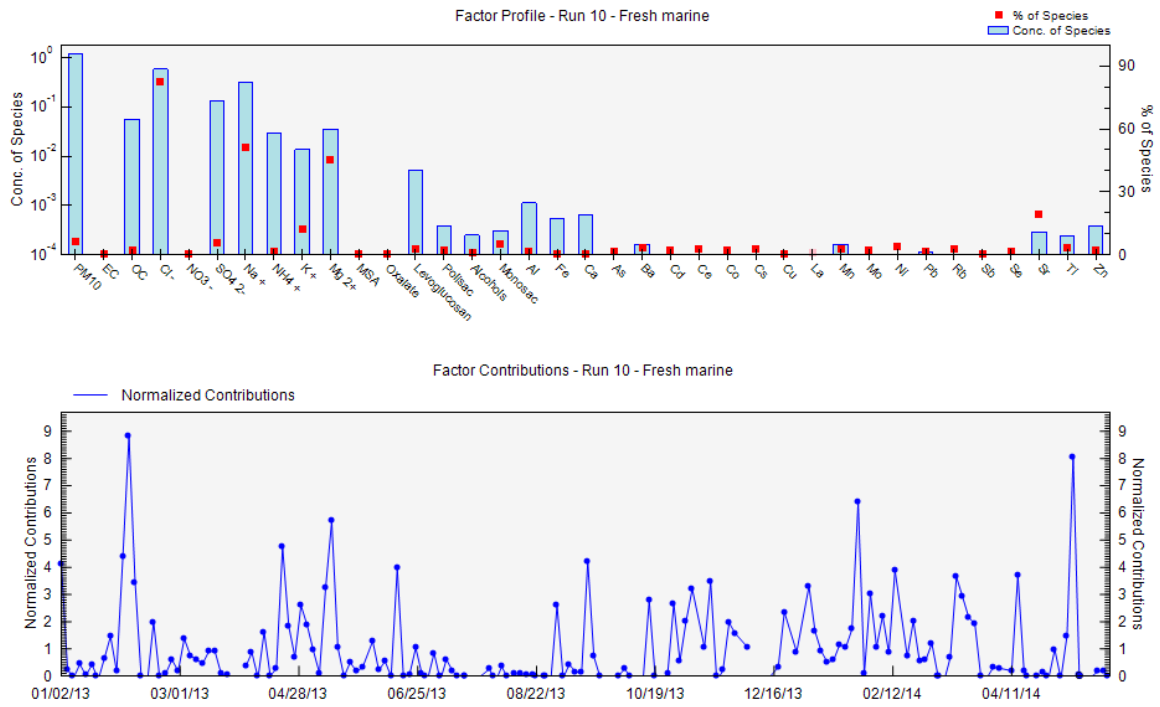


Figure A2. 7: Chemical profile (top) and time variability (bottom) of the fresh marine factor in Lens

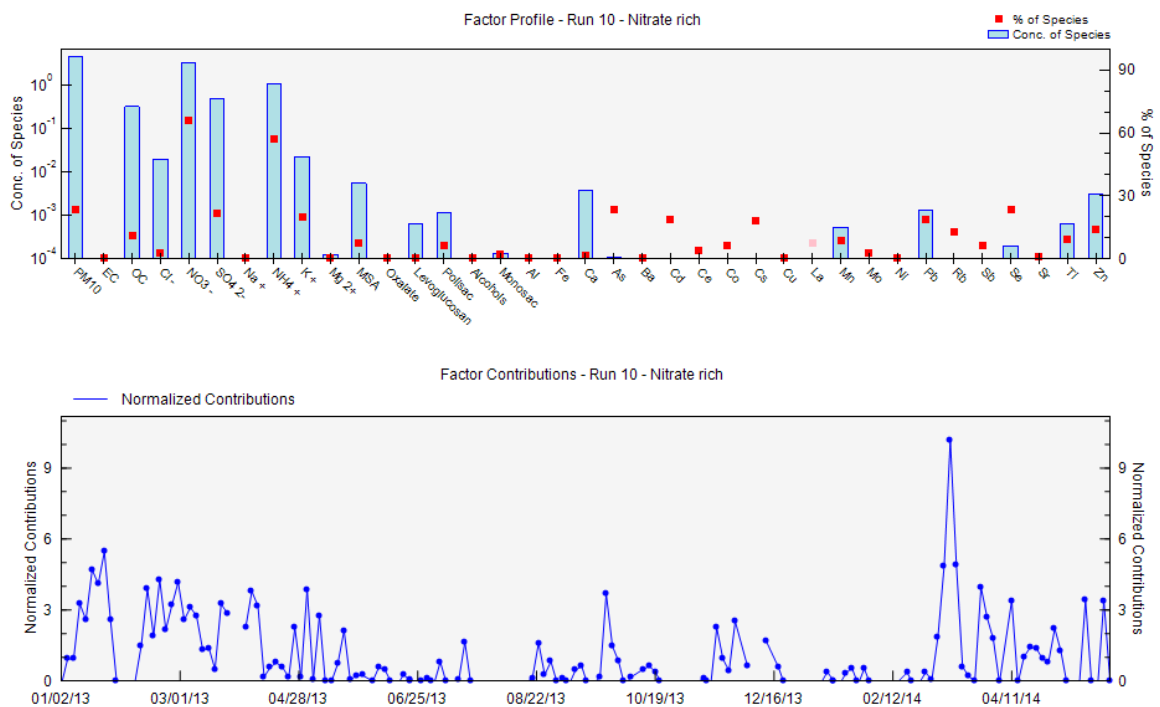


Figure A2. 8: Chemical profile (top) and time variability (bottom) of the land nitrate rich in Lens

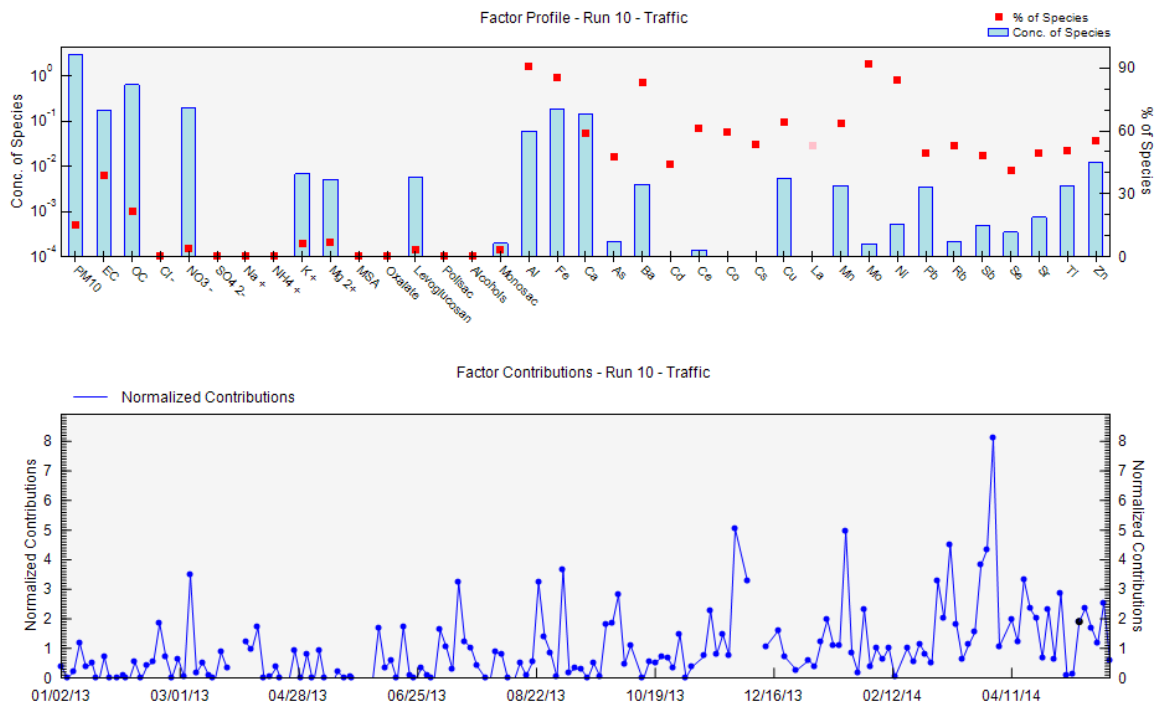


Figure A2. 9: Chemical profile (top) and time variability (bottom) of the land traffic in Lens

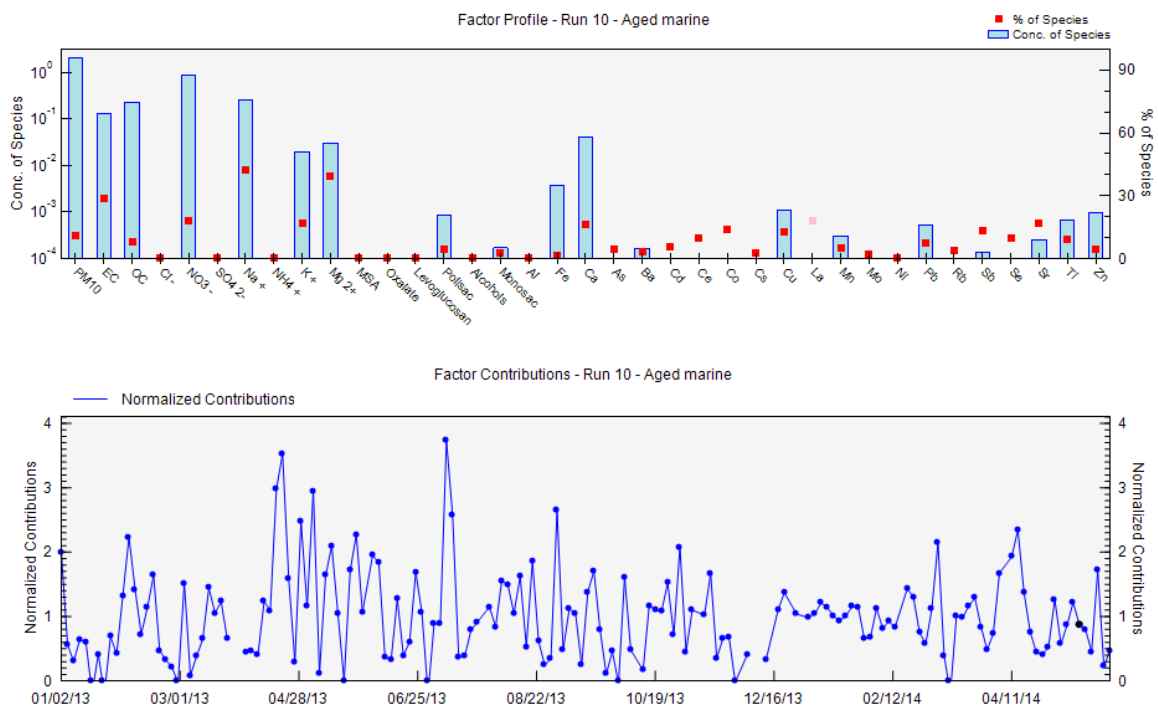


Figure A2.10: Chemical profile (top) and time variability (bottom) of the aged marine factor in Lens

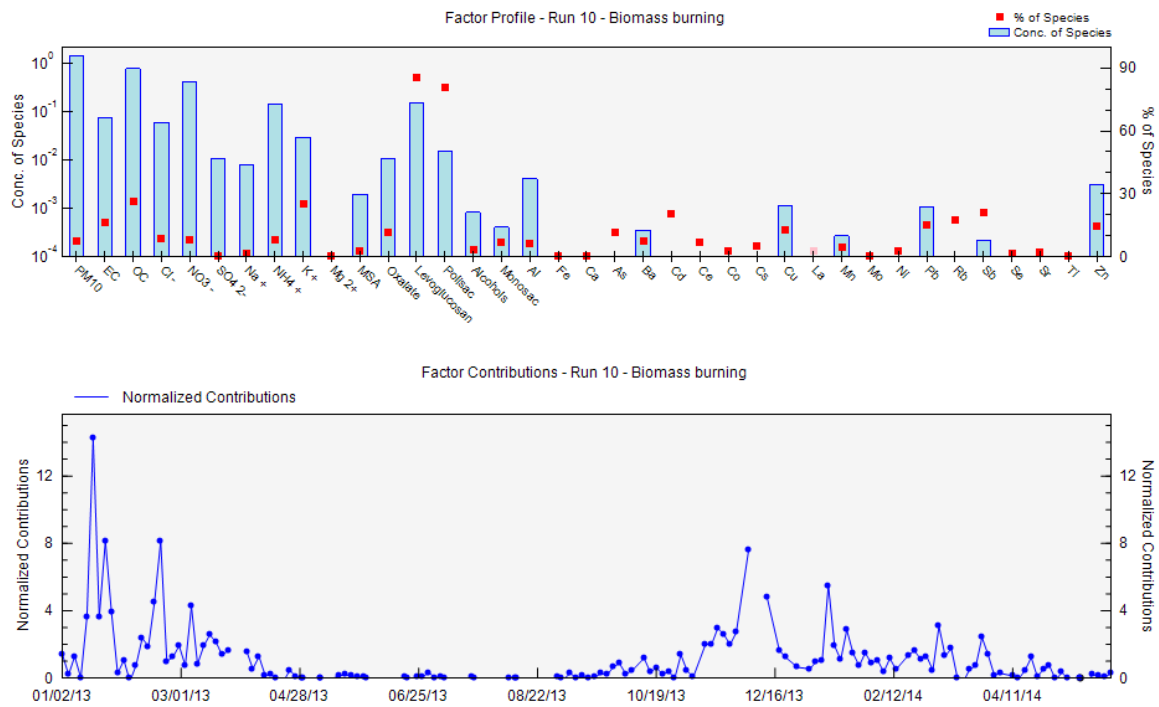


Figure A2. 11: Chemical profile (top) and time variability (bottom) of the biomass burning factor in Lens

PMF solution Nogent-sur-Oise

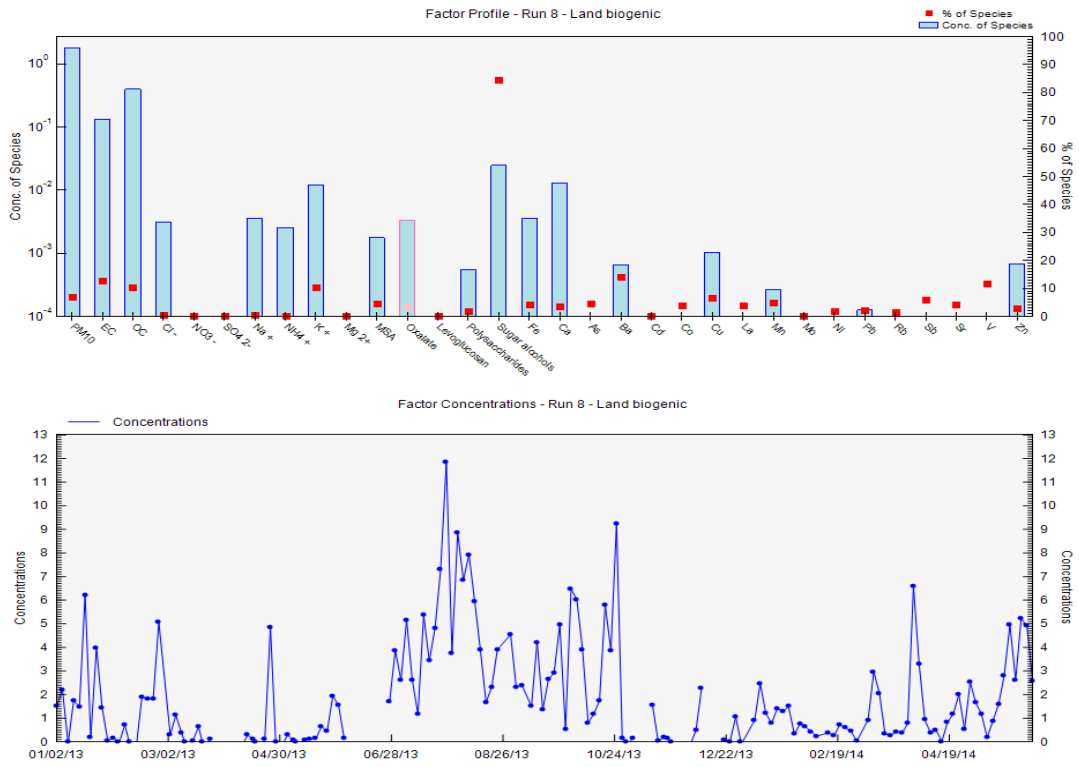


Figure A2. 12: Chemical profile (top) and time variability (bottom) of the land biogenic factor in Nogent-sur-Oise

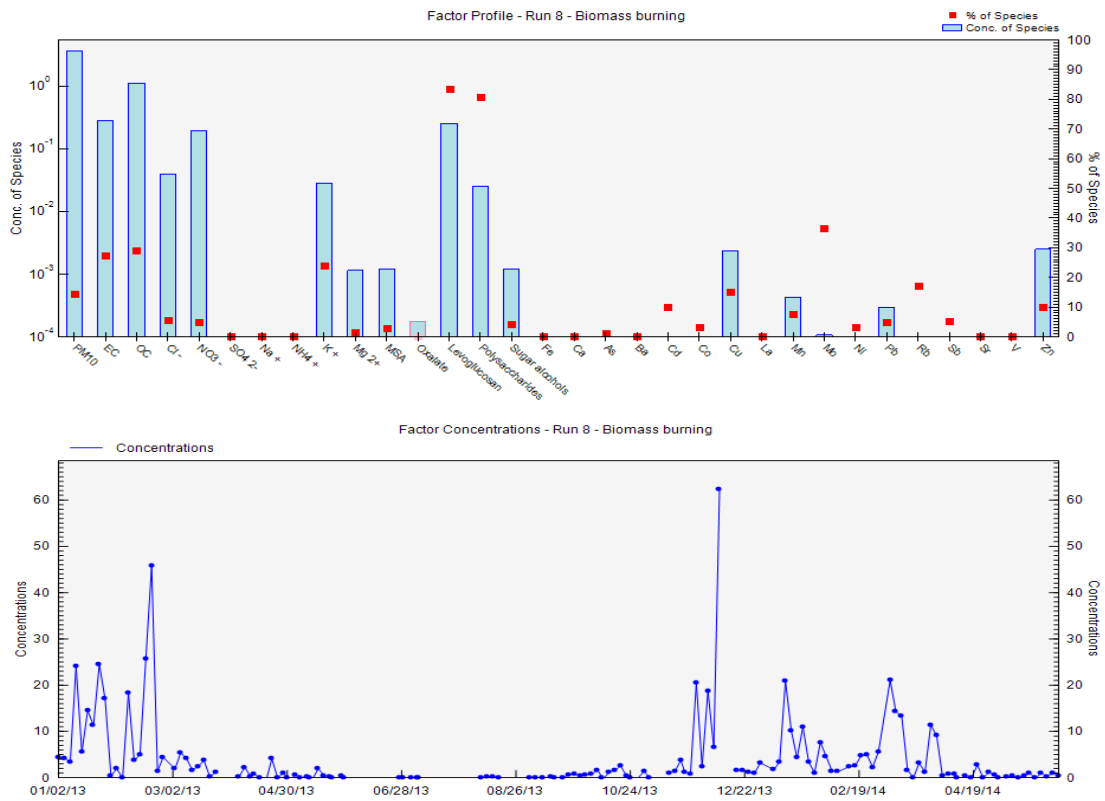


Figure A2. 13: Chemical profile (top) and time variability (bottom) of the biomass burning factor in Nogent-sur-Oise

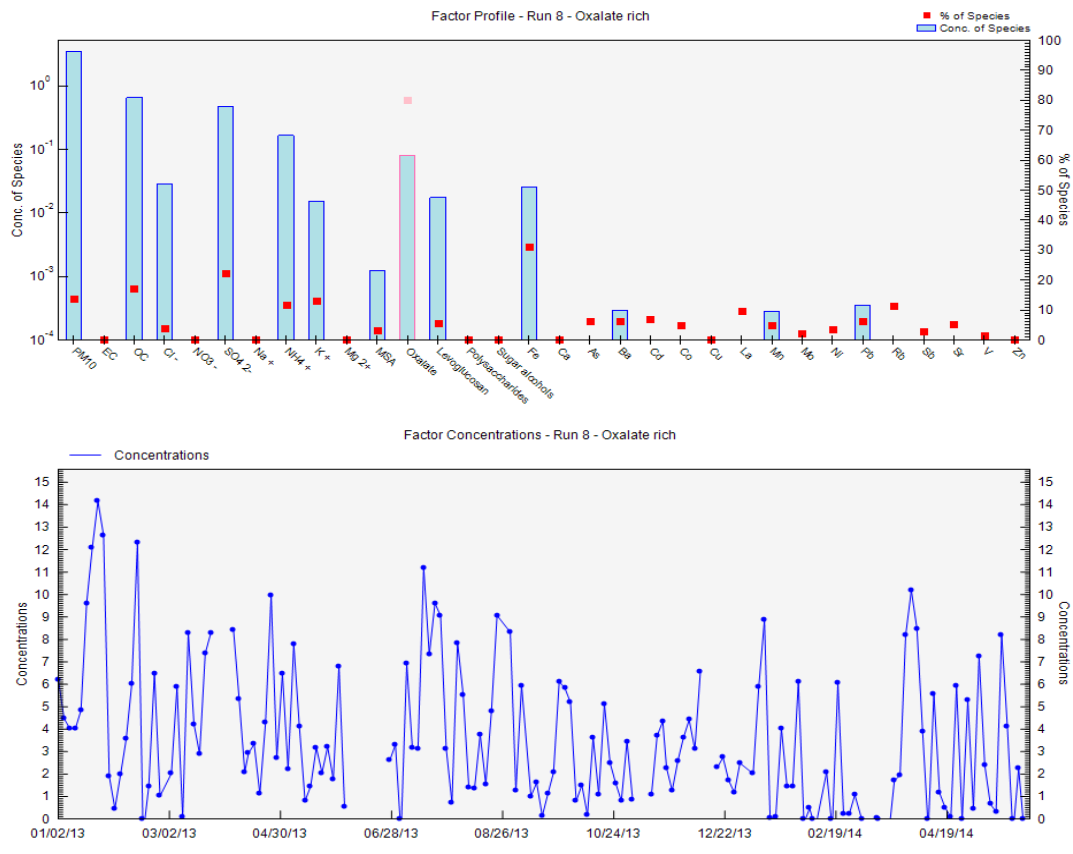


Figure A2.14: Chemical profile (top) and time variability (bottom) of the oxalate rich factor in Nogent-sur-Oise

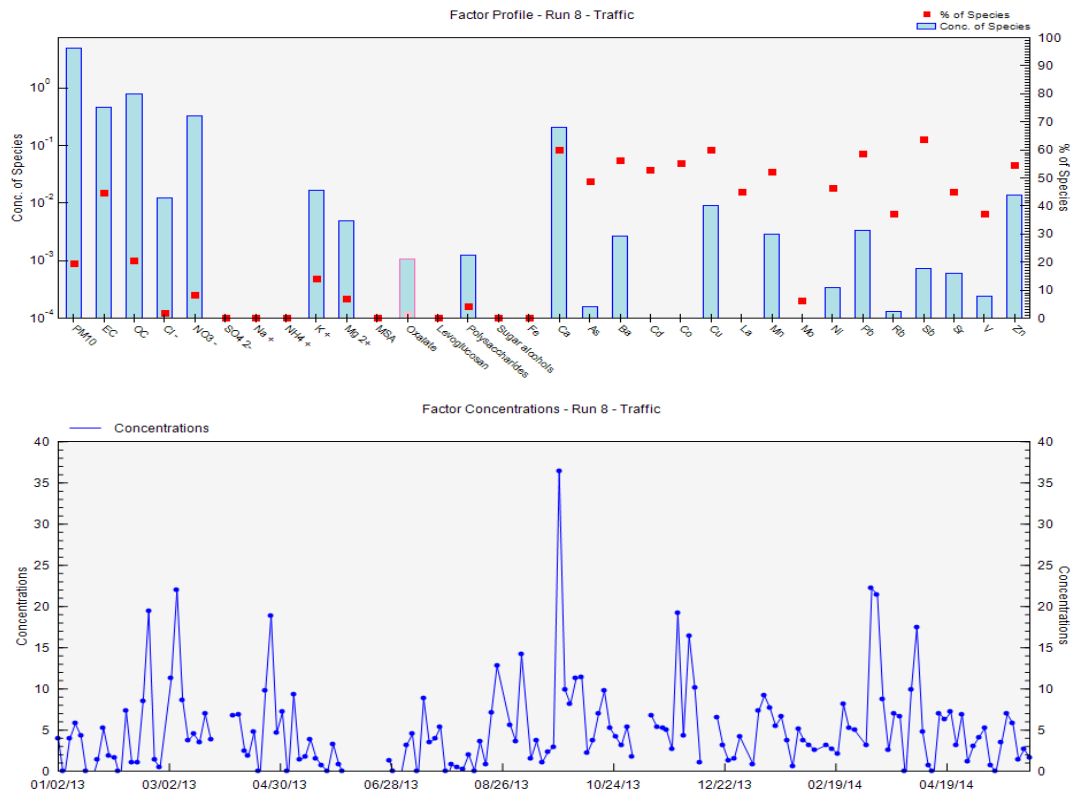


Figure A2.15: Chemical profile (top) and time variability (bottom) of the traffic factor in Nogent-sur-Oise

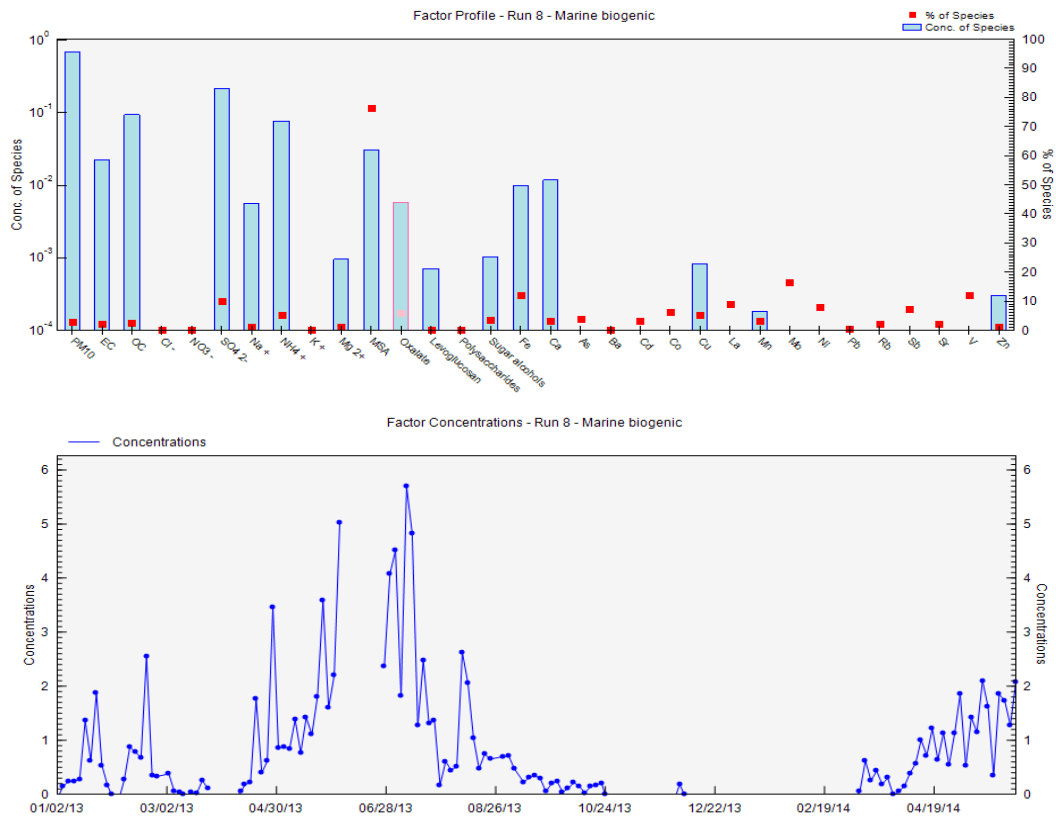


Figure A2.16: Chemical profile (top) and time variability (bottom) of the marine biogenic factor in Nogent-sur-Oise

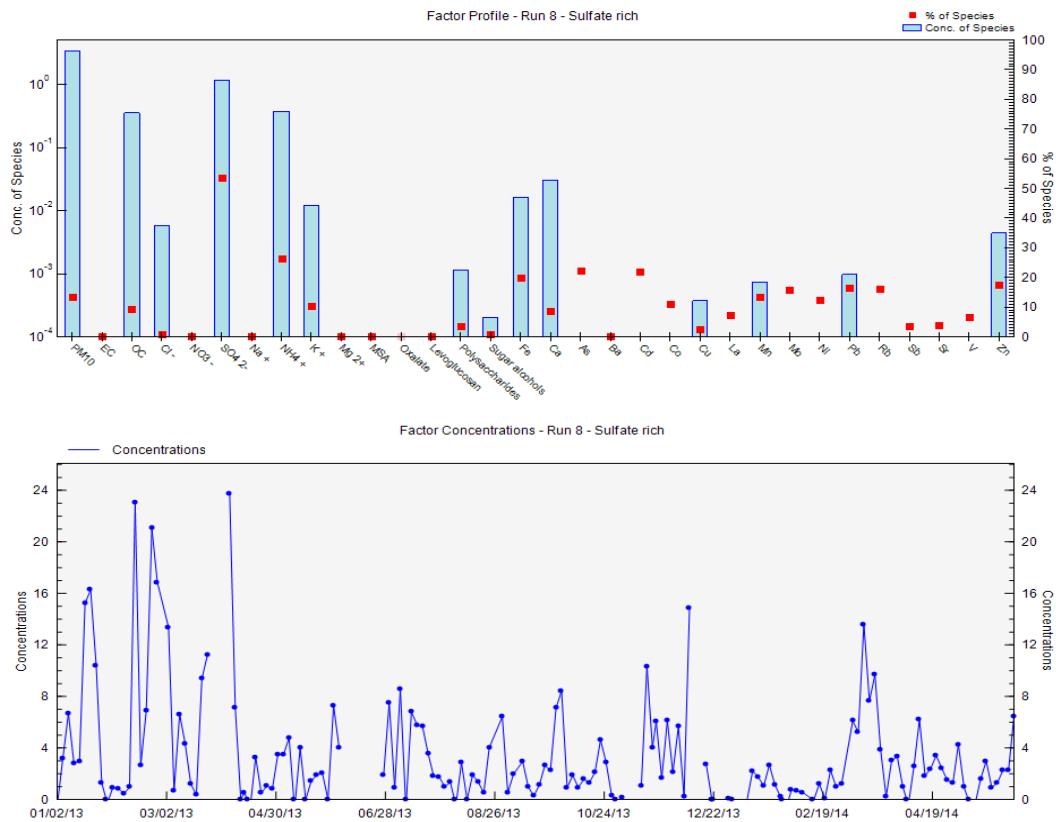


Figure A2.17: Chemical profile (top) and time variability (bottom) of the sulfate rich factor in Nogent-sur-Oise

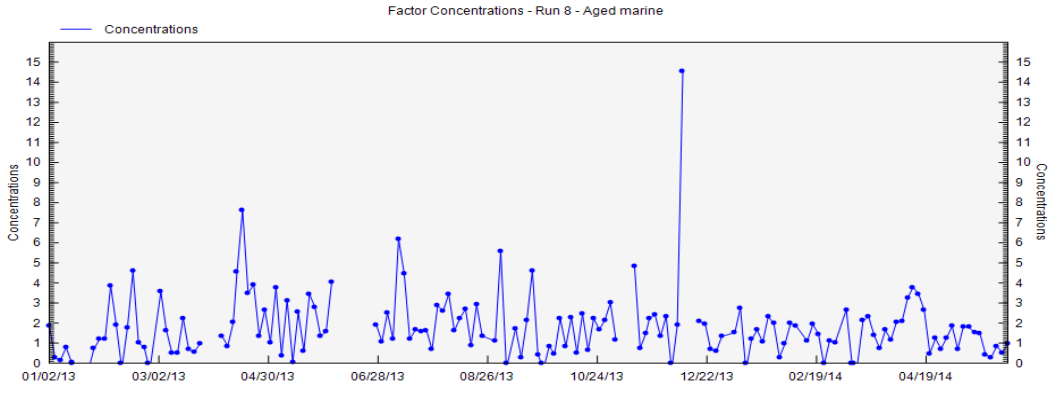
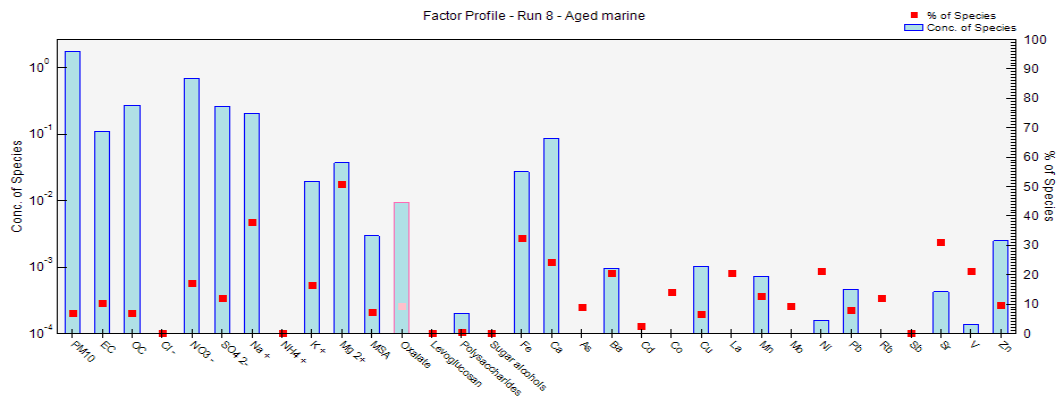


Figure A2. 18: Chemical profile (top) and time variability (bottom) of the aged marine factor in Nogent-sur-Oise

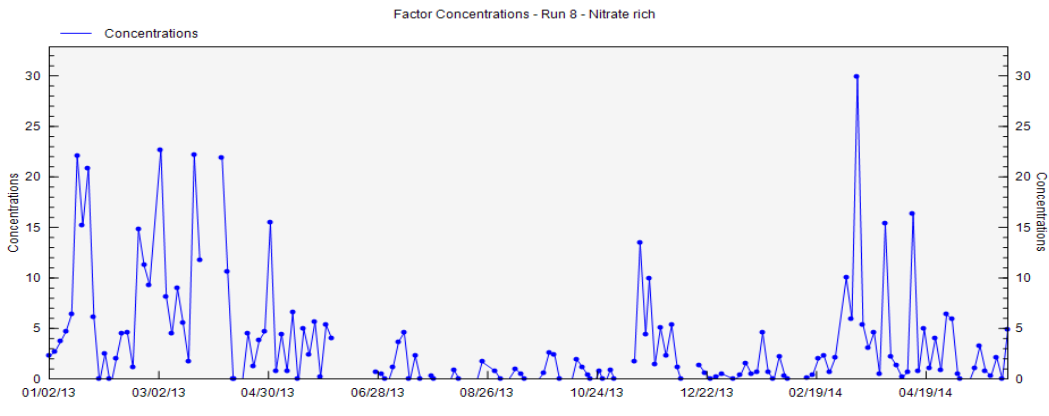
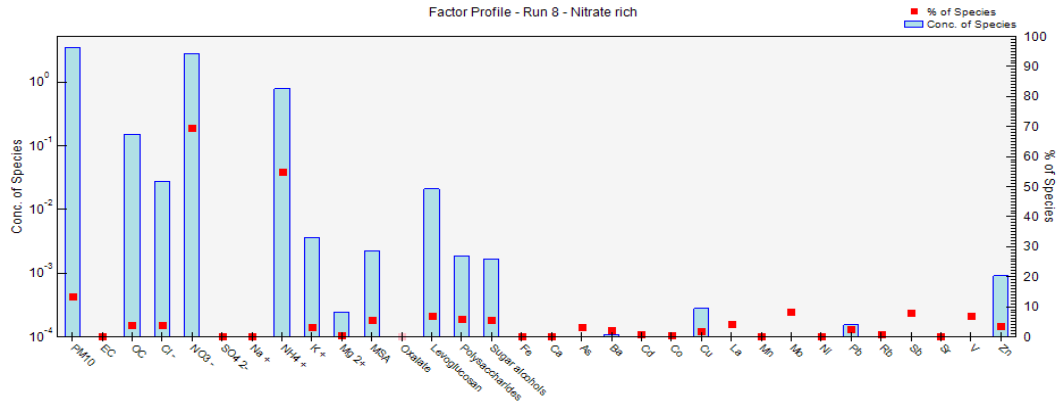


Figure A2. 19: Chemical profile (top) and time variability (bottom) of the nitrate rich factor in Nogent-sur-Oise

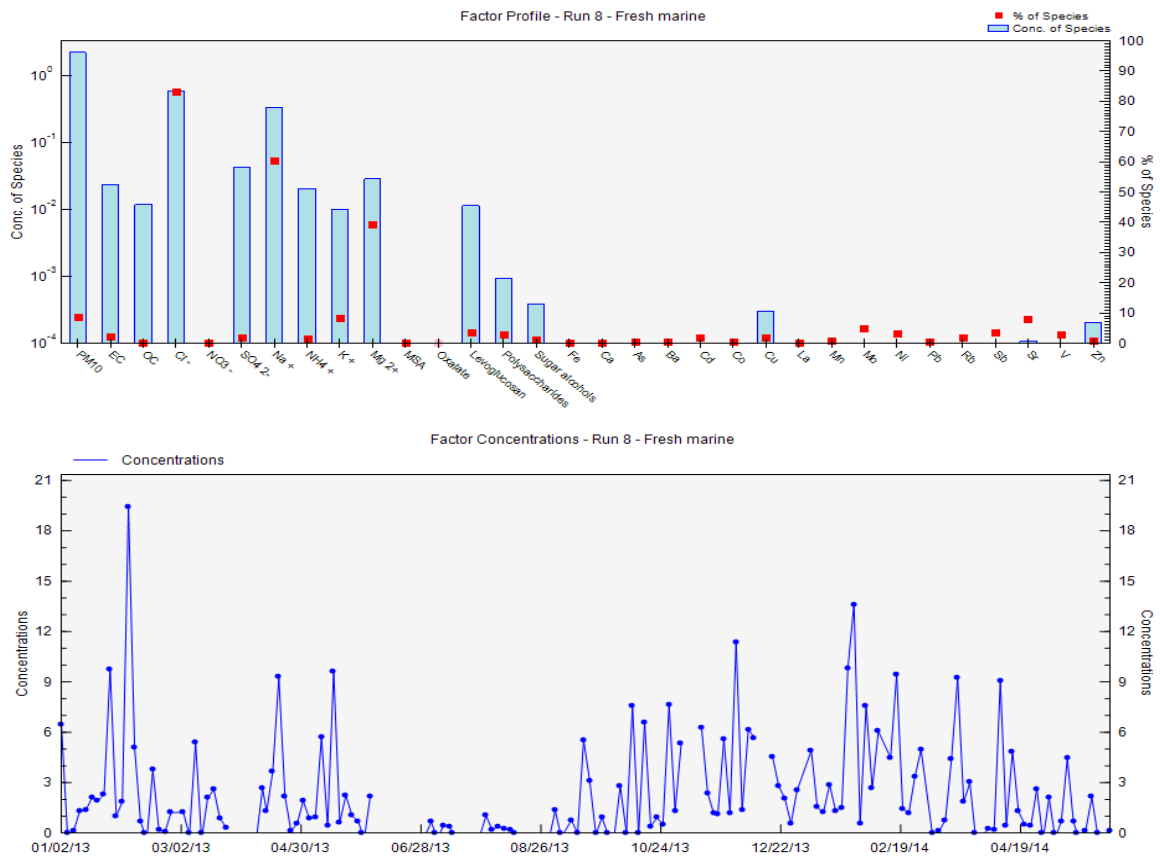


Figure A2. 20: Chemical profile (top) and time variability (bottom) of the fresh marine factor in Nogent-sur-Oise

PMF solution Revin

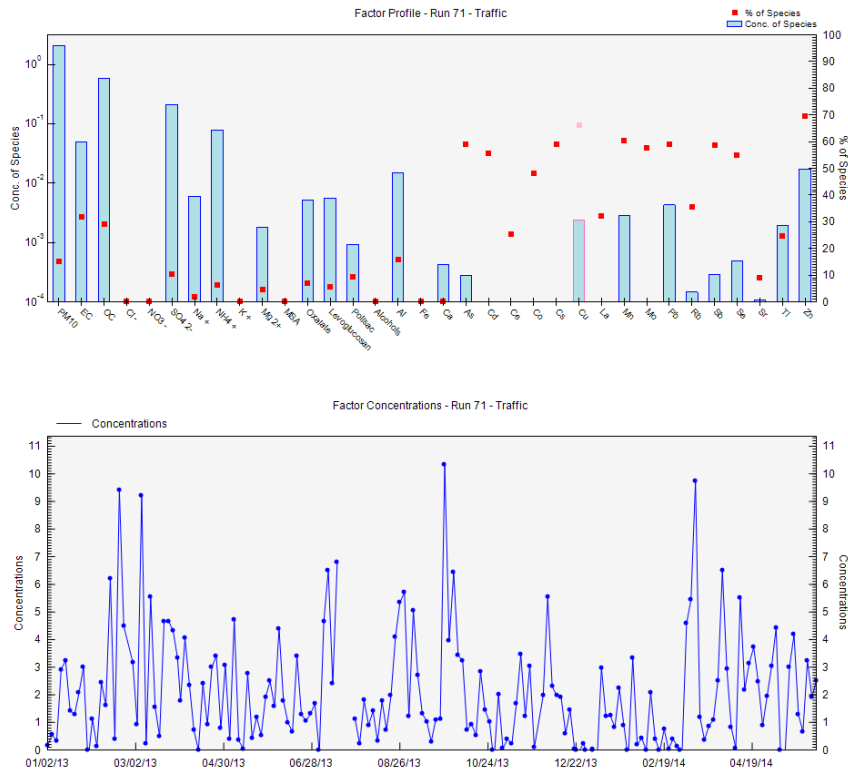


Figure A2. 21: Chemical profile (top) and time variability (bottom) of the traffic factor in Revin

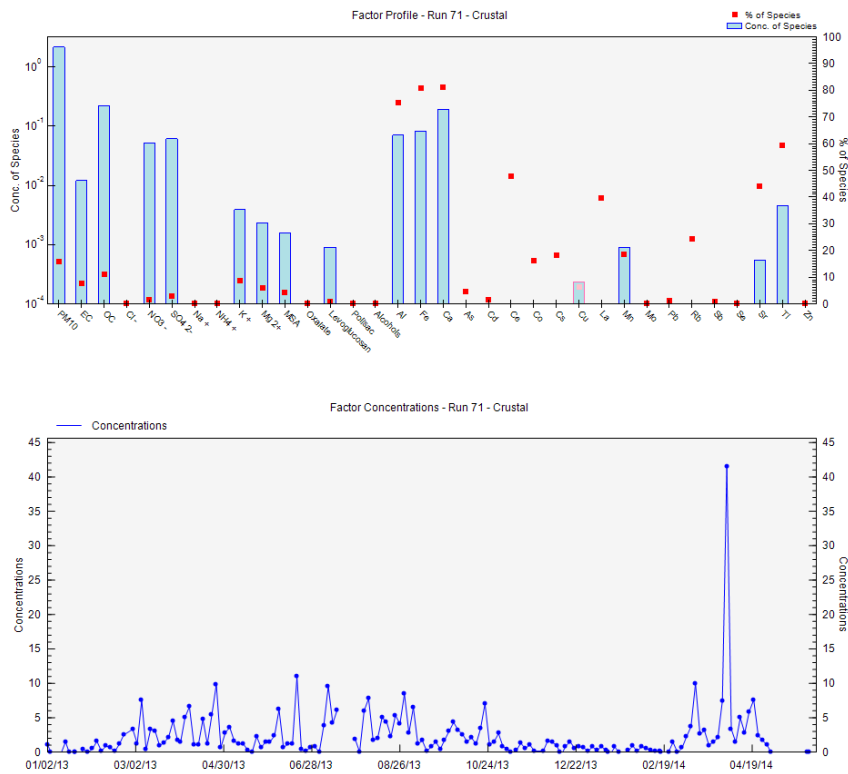


Figure A2. 22: Chemical profile (top) and time variability (bottom) of the crustal factor in Revin

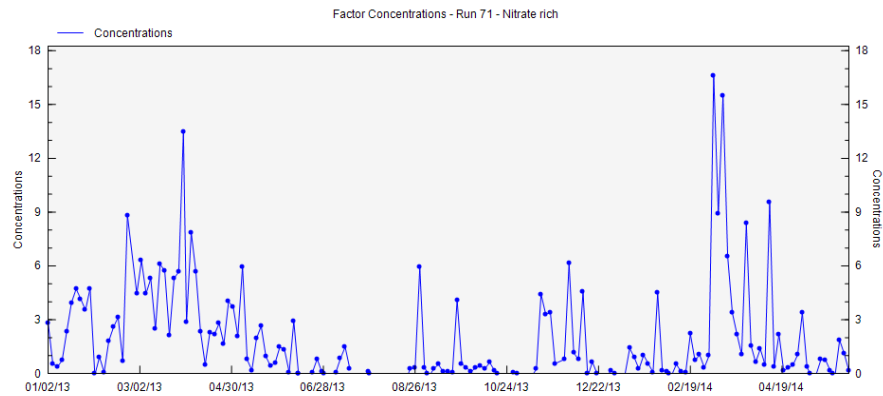
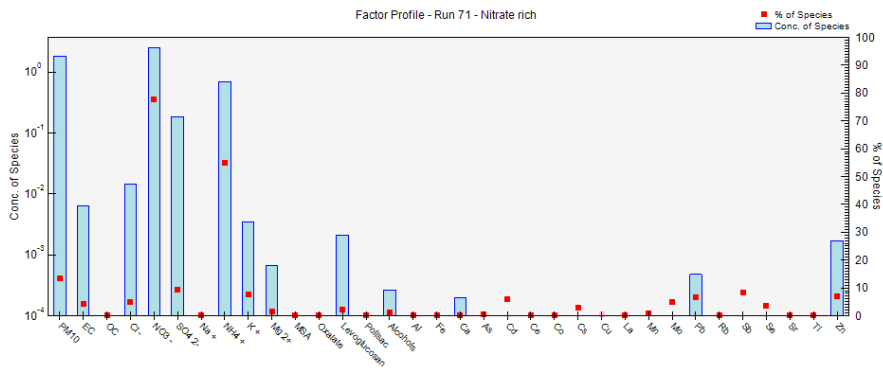


Figure A2. 23: Chemical profile (top) and time variability (bottom) of the nitrate rich factor in Revin

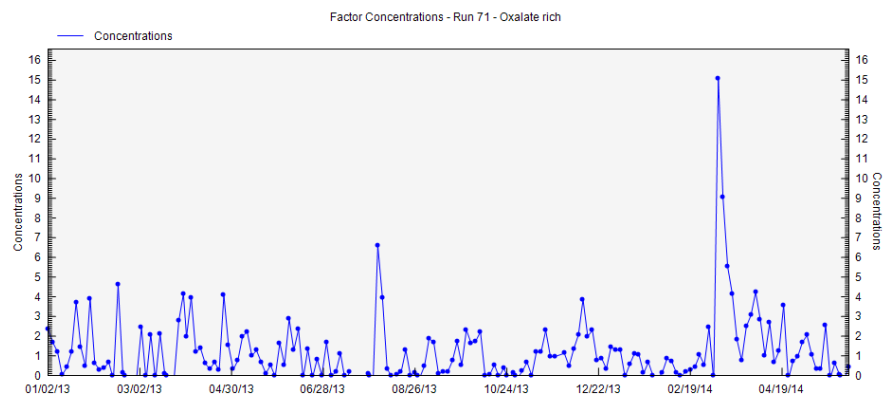
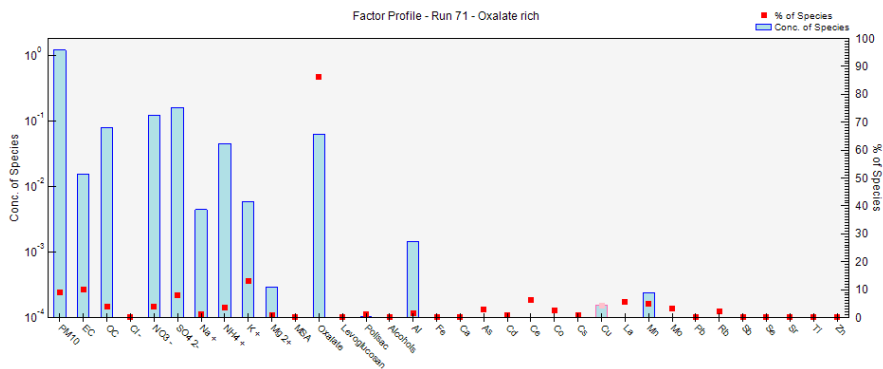


Figure A2. 24: Chemical profile (top) and time variability (bottom) of the oxalate rich factor in Revin

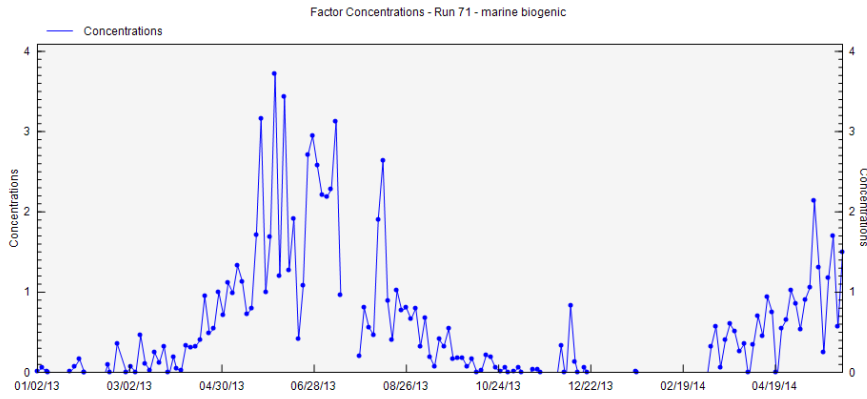
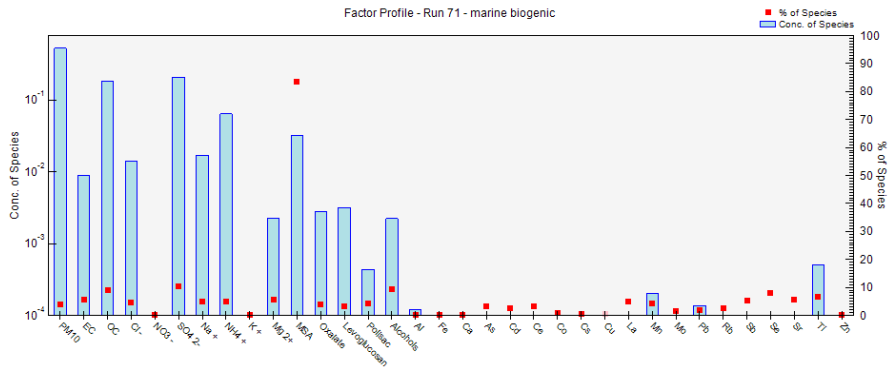


Figure A2. 25: Chemical profile (top) and time variability (bottom) of the marine biogenic factor in Revin

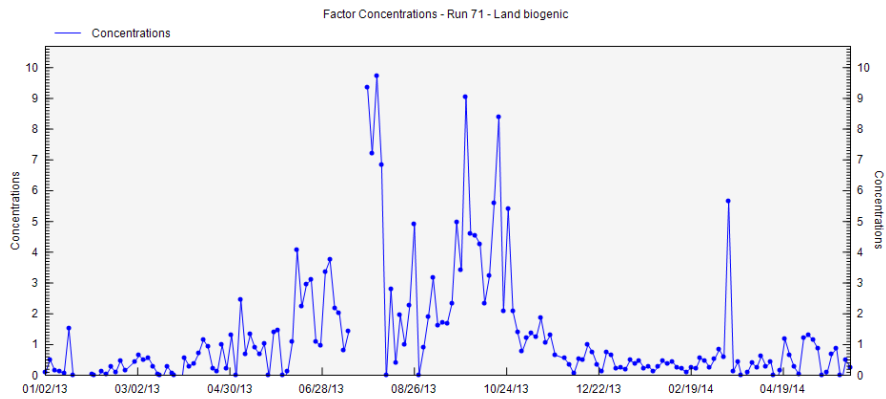
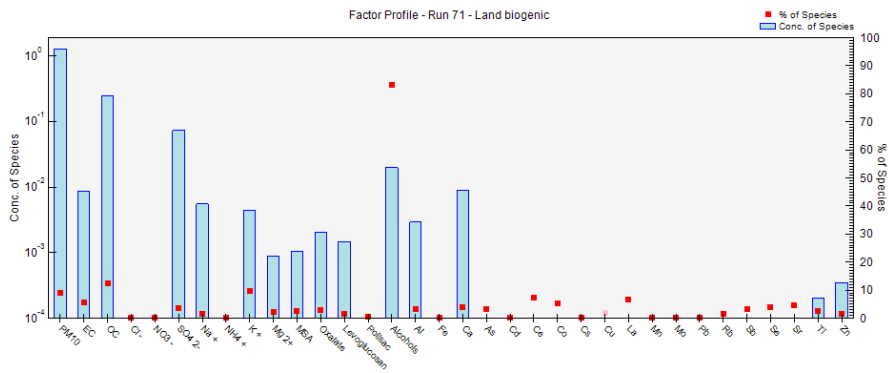


Figure A2. 26: Chemical profile (top) and time variability (bottom) of the land biogenic factor in Revin

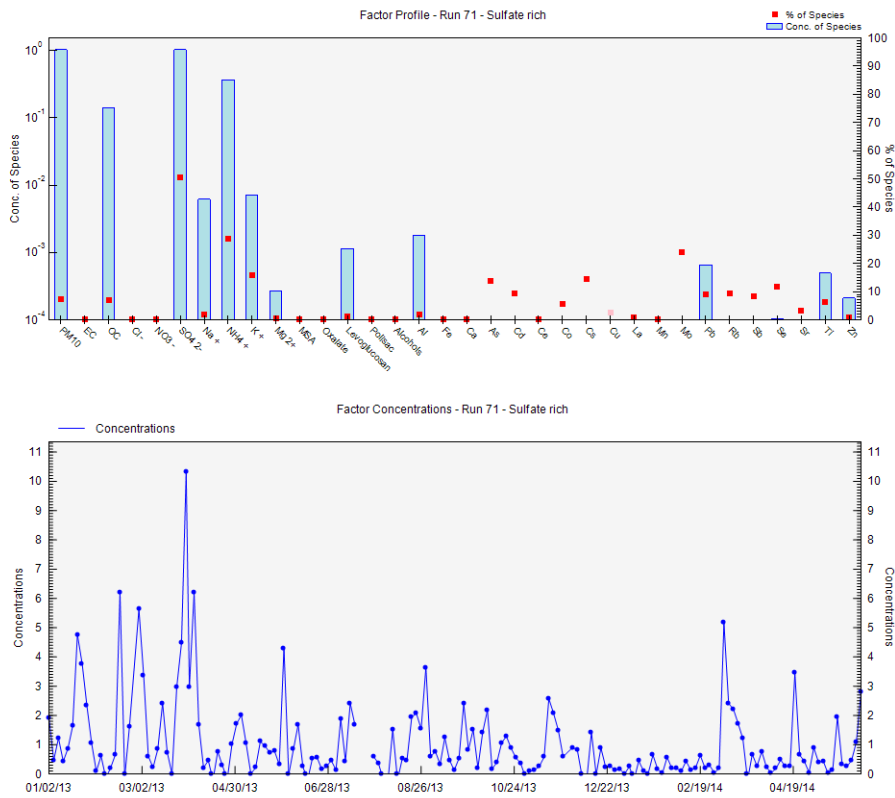


Figure A2. 27: Chemical profile (top) and time variability (bottom) of the sulfate rich factor in Revin

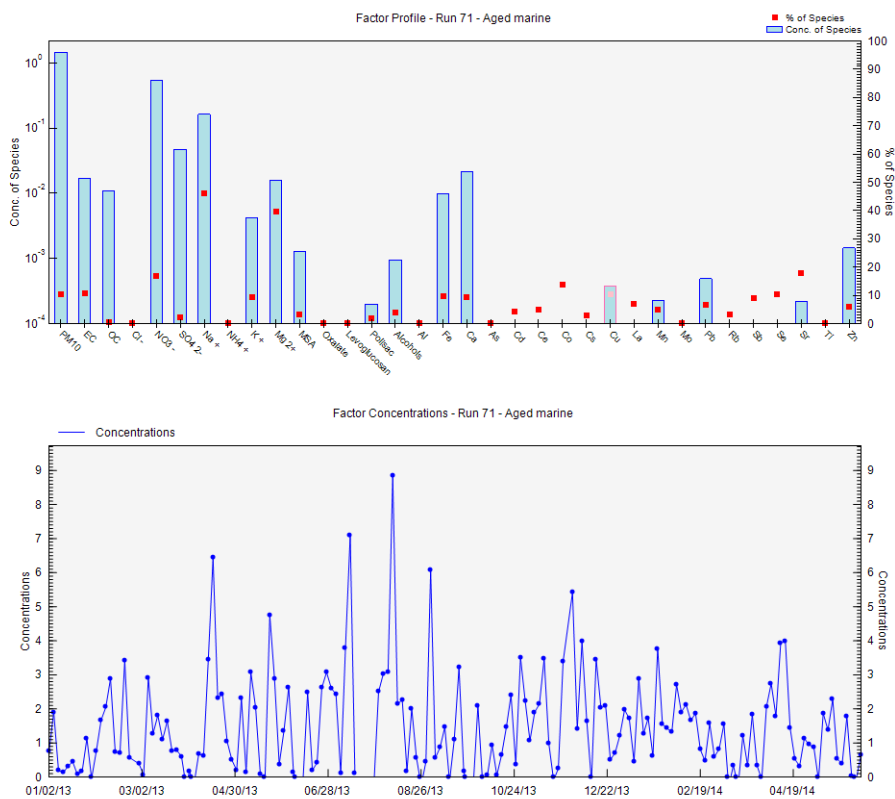


Figure A2. 28: Chemical profile (top) and time variability (bottom) of the aged marine factor in Revin

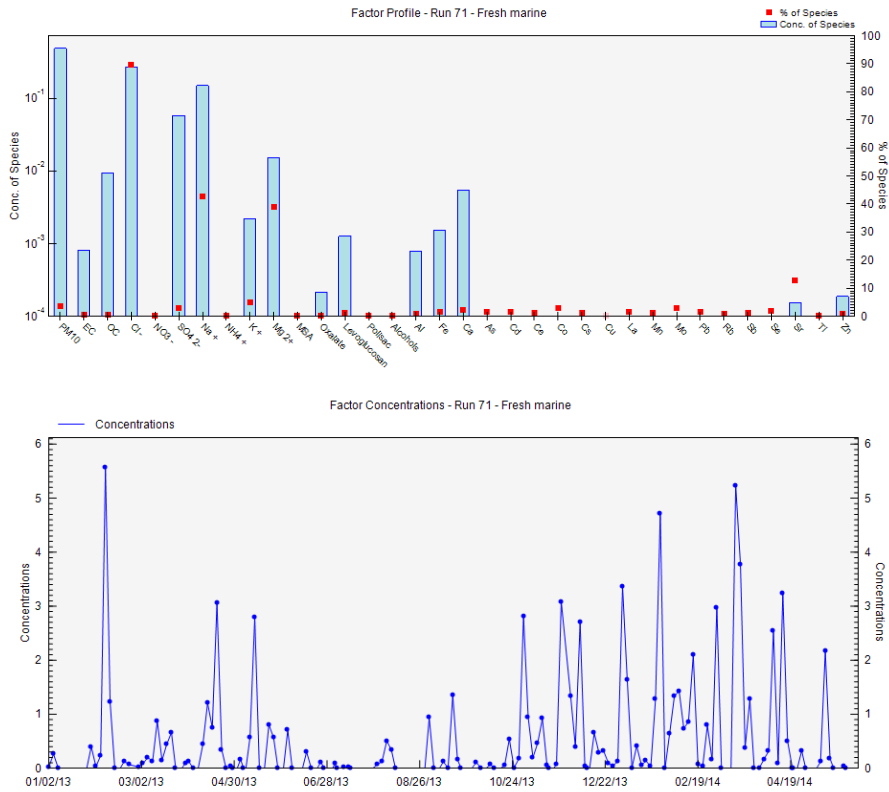


Figure A2. 29: Chemical profile (top) and time variability (bottom) of the fresh marine factor in Revin

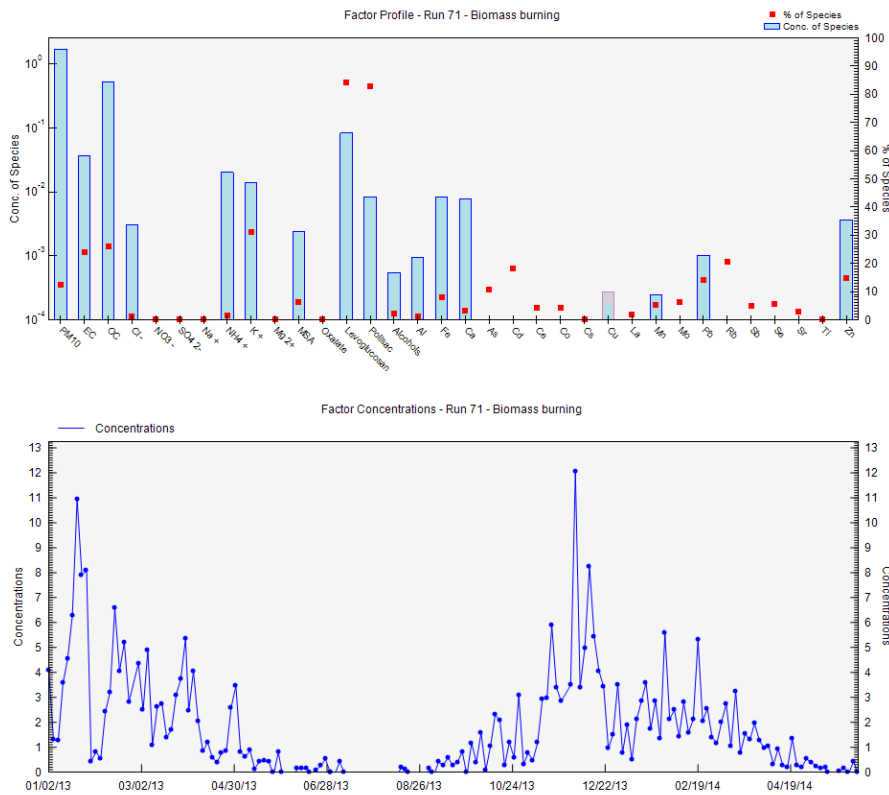


Figure A2. 30: Chemical profile (top) and time variability (bottom) of the biomass burning factor in Revin

PMF solution Rouen

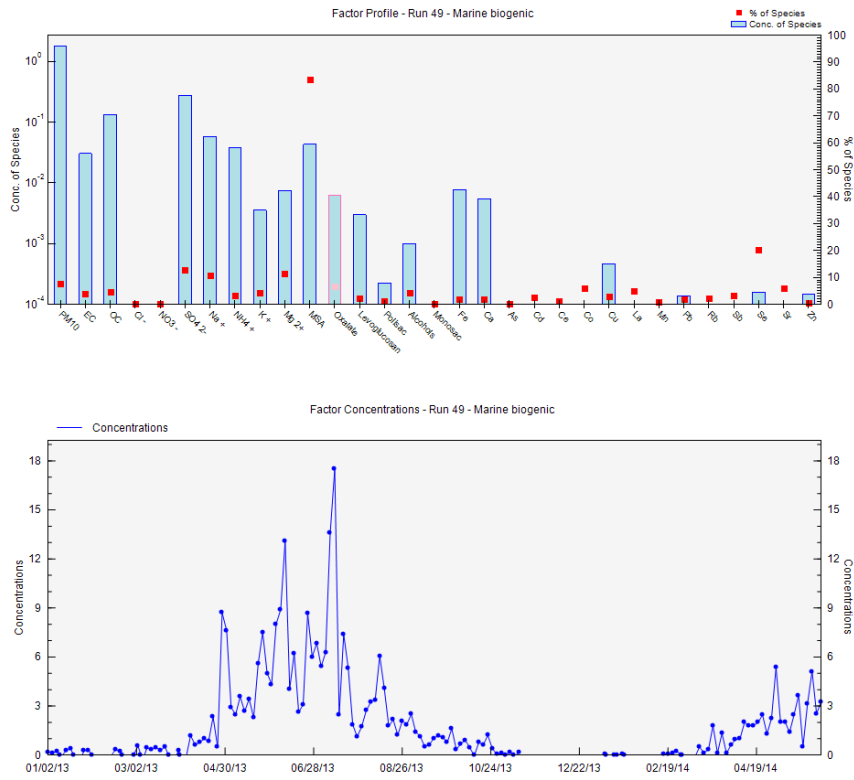


Figure A2. 31: Chemical profile (top) and time variability (bottom) of the marine biogenic factor in Rouen

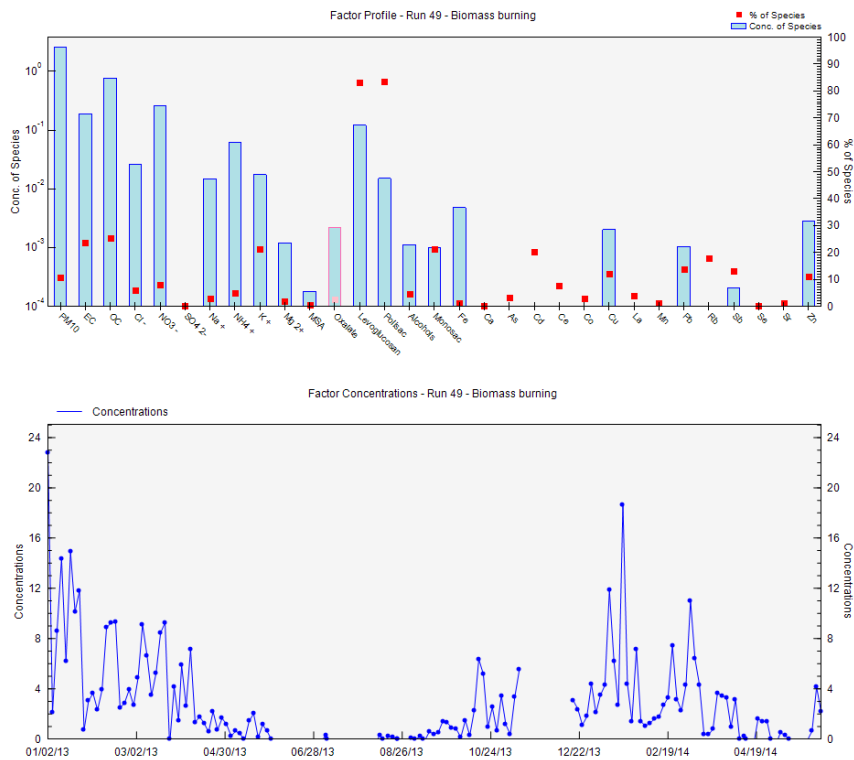


Figure A2. 32: Chemical profile (top) and time variability (bottom) of the biomass burning factor in Rouen

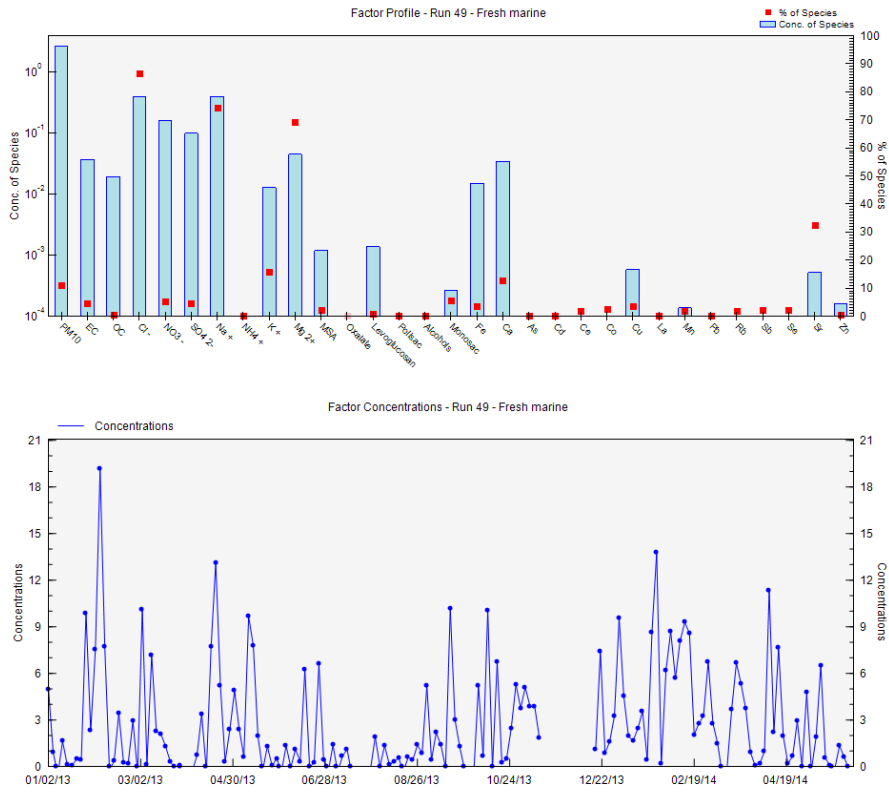


Figure A2.33: Chemical profile (top) and time variability (bottom) of the fresh marine factor in Rouen

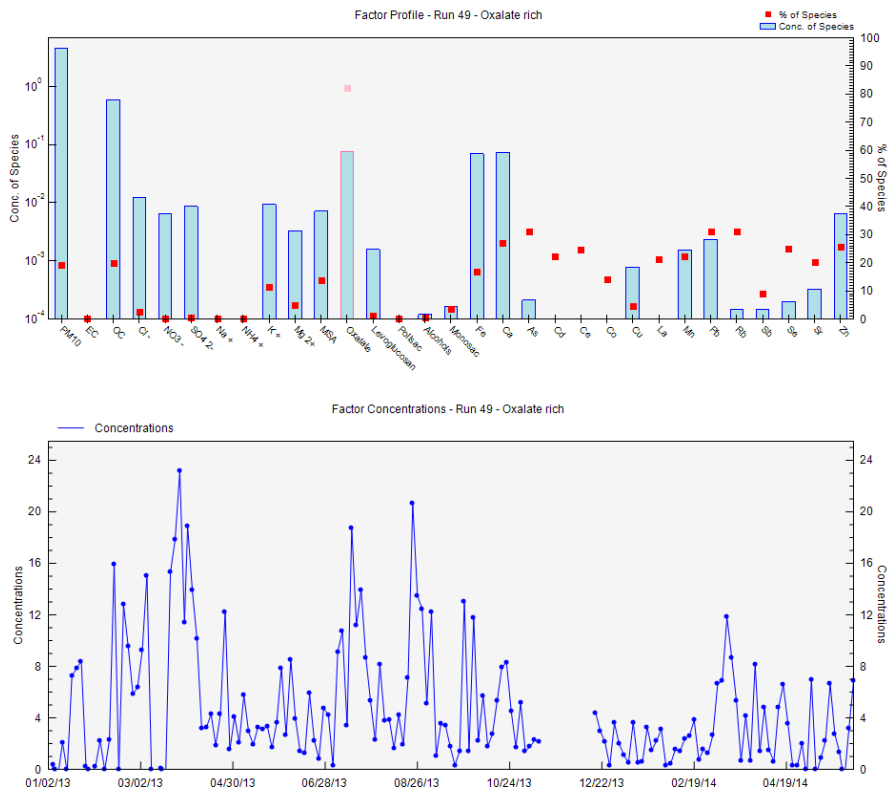


Figure A2.34: Chemical profile (top) and time variability (bottom) of the oxalate rich factor in Rouen

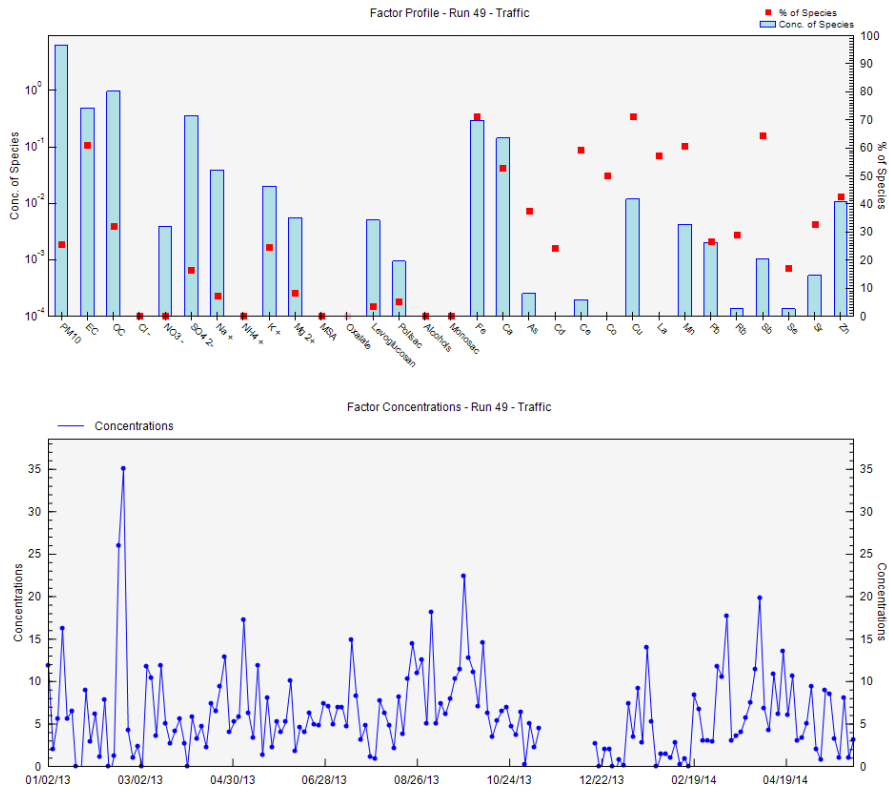


Figure A2. 35: Chemical profile (top) and time variability (bottom) of the traffic factor in Rouen

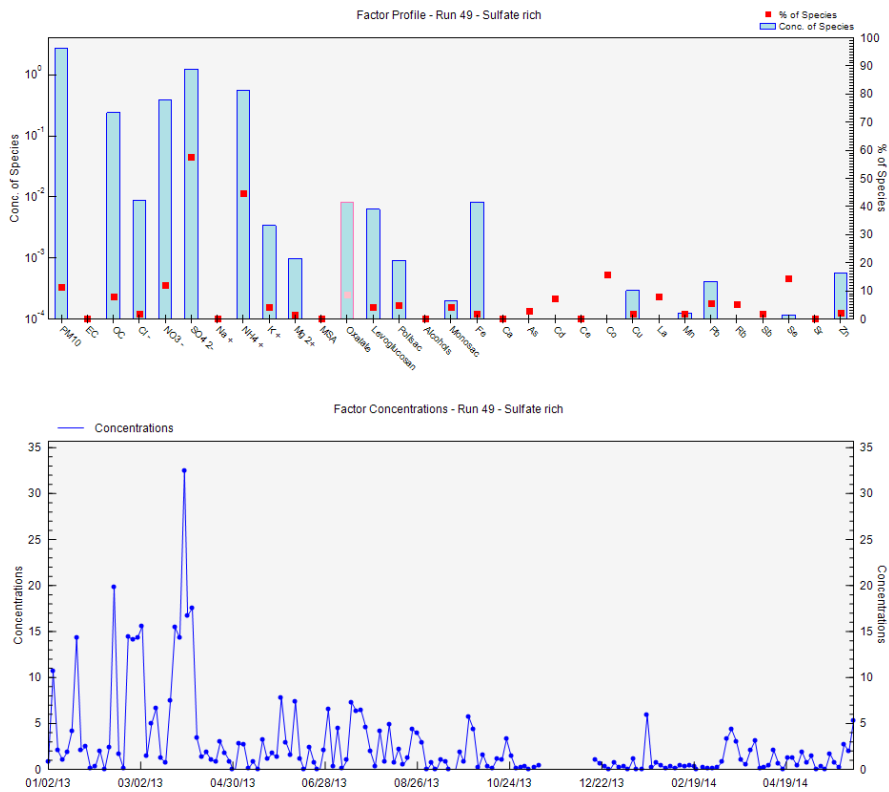


Figure A2. 36: Chemical profile (top) and time variability (bottom) of the sulfate rich factor in Rouen

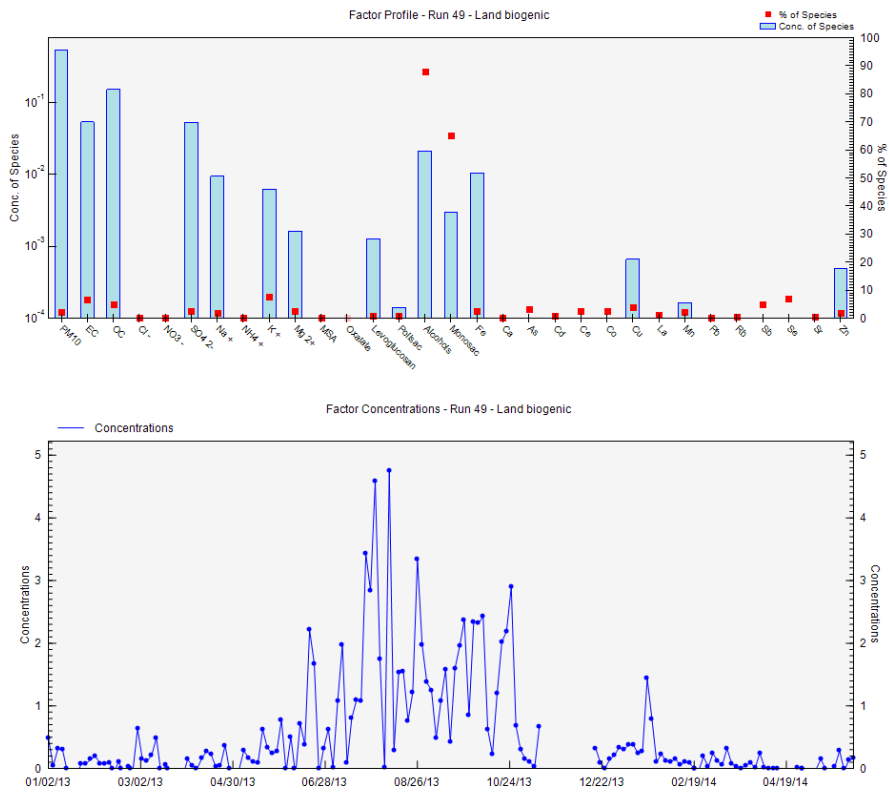


Figure A2. 37: Chemical profile (top) and time variability (bottom) of the land biogenic factor in Rouen

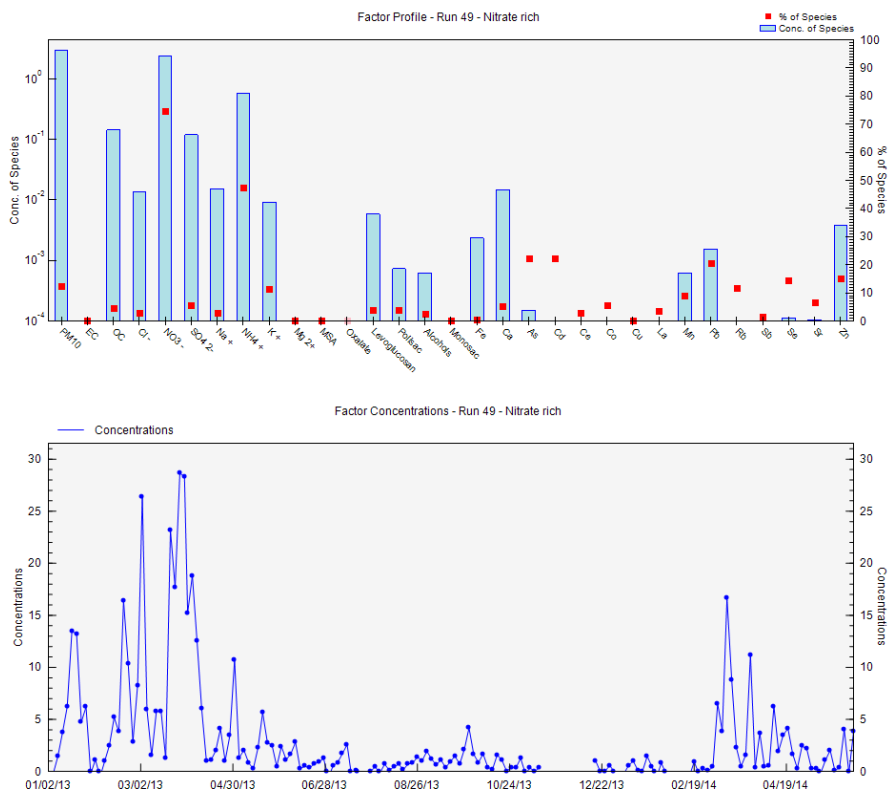


Figure A2. 38: Chemical profile (top) and time variability (bottom) of the nitrate rich factor in Rouen

PMF solution Roubaix

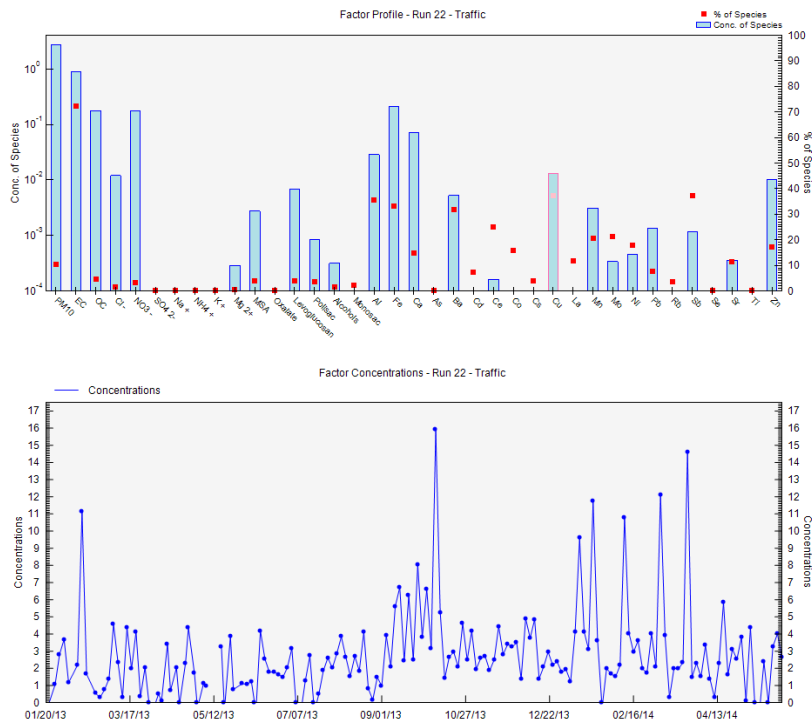


Figure A2. 39: Chemical profile (top) and time variability (bottom) of the traffic factor in Roubaix

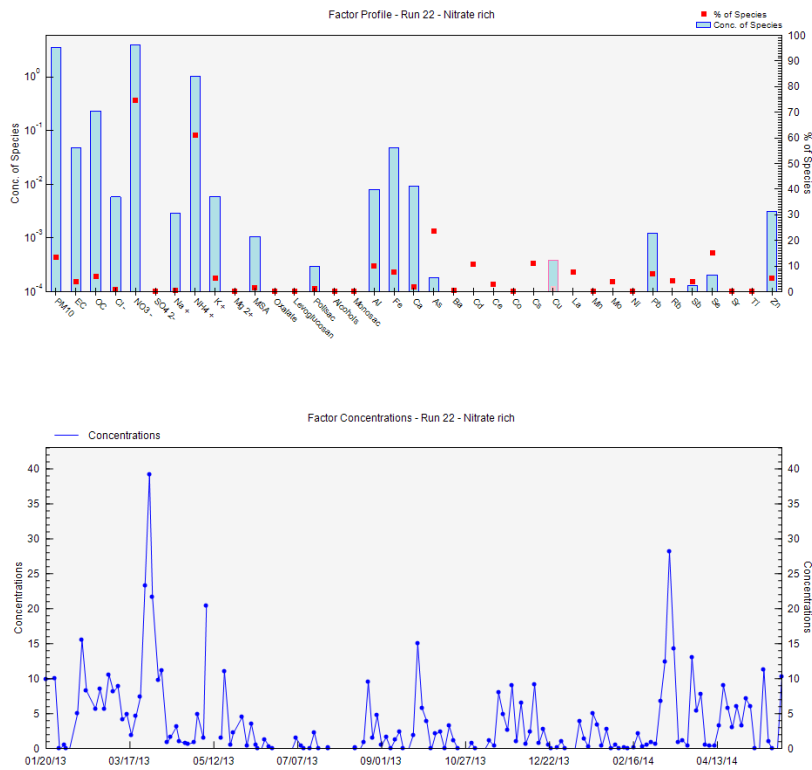


Figure A2. 40: Chemical profile (top) and time variability (bottom) of the nitrate rich factor in Roubaix

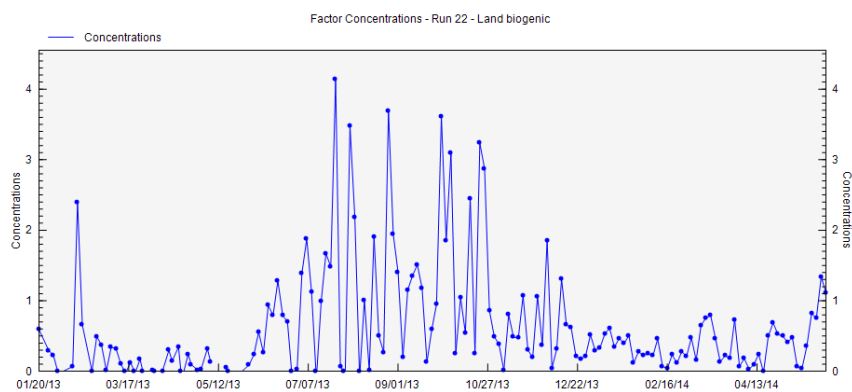
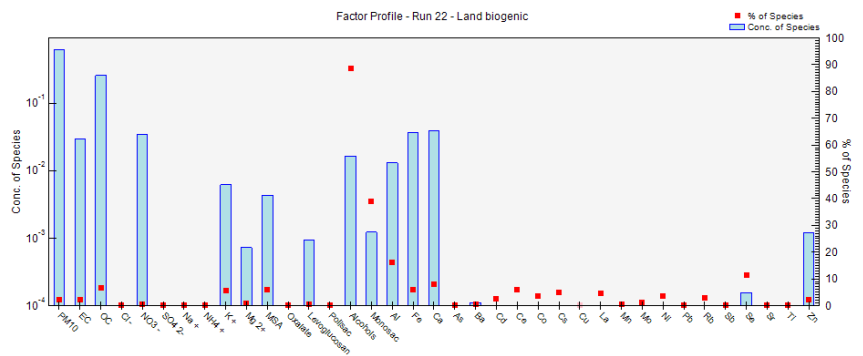


Figure A2. 41: Chemical profile (top) and time variability (bottom) of the land biogenic factor in Roubaix

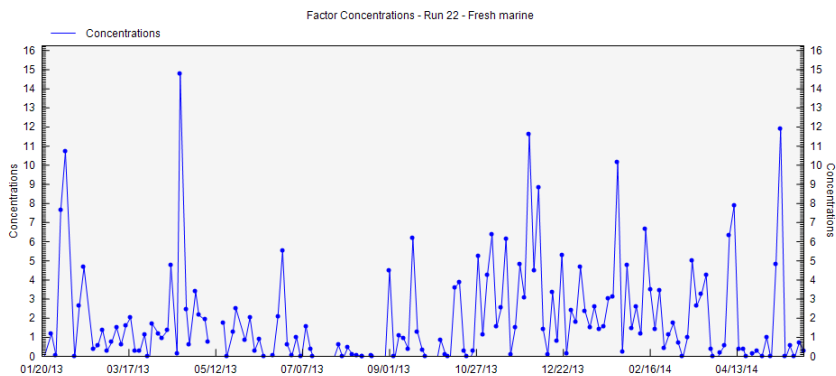
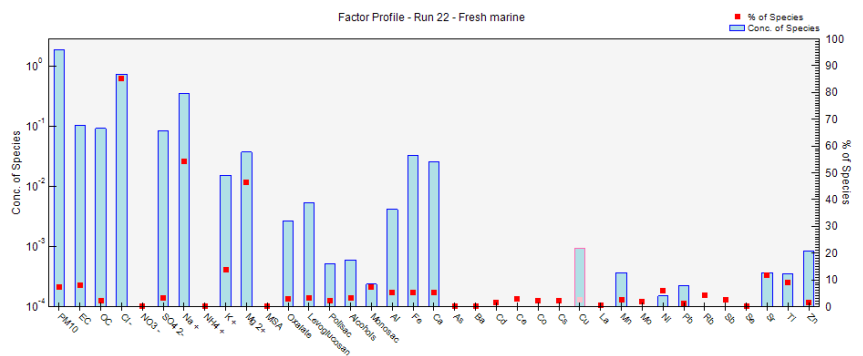


Figure A2. 42: Chemical profile (top) and time variability (bottom) of the fresh marine factor in Roubaix

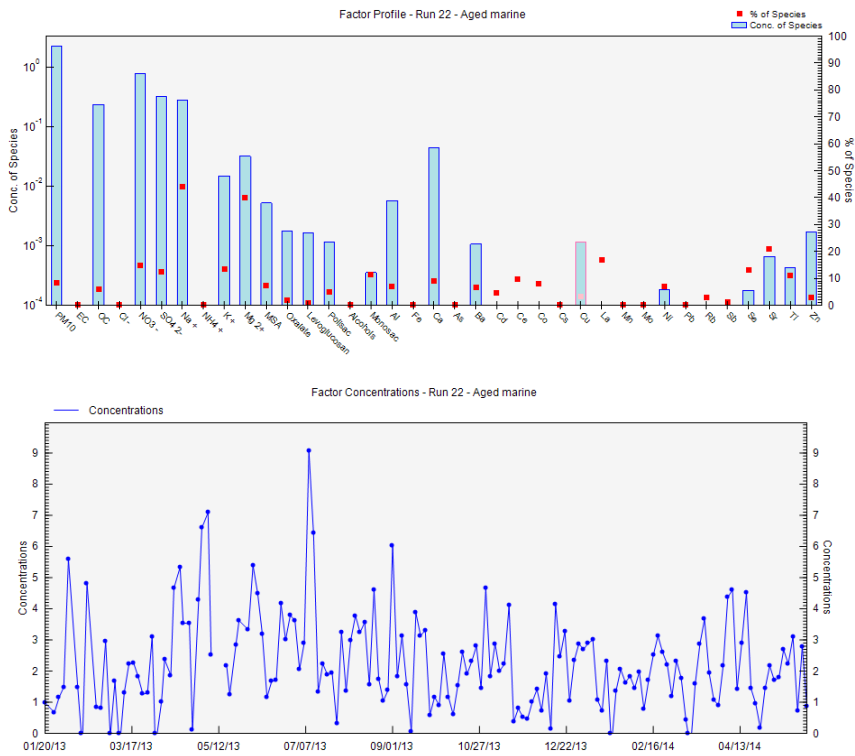


Figure A2.43: Chemical profile (top) and time variability (bottom) of the aged marine factor in Roubaix

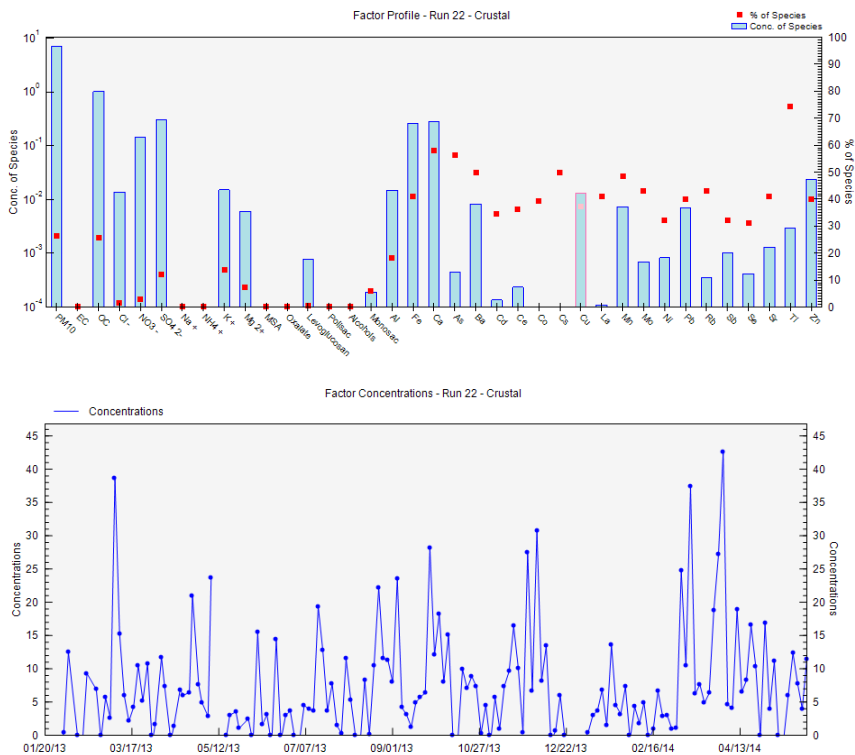


Figure A2.44: Chemical profile (top) and time variability (bottom) of the crustal factor in Roubaix

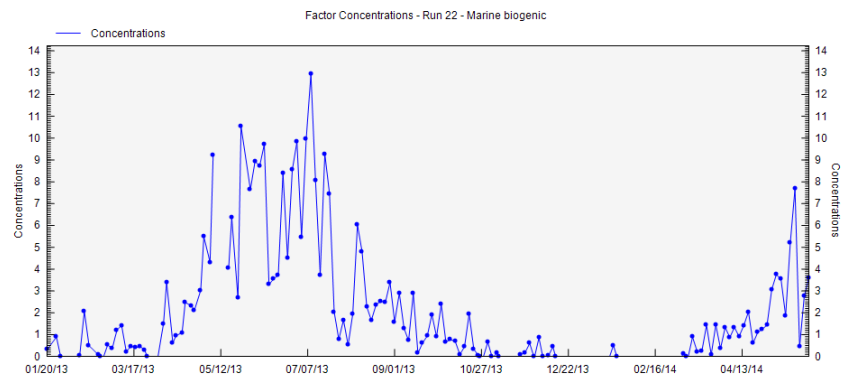
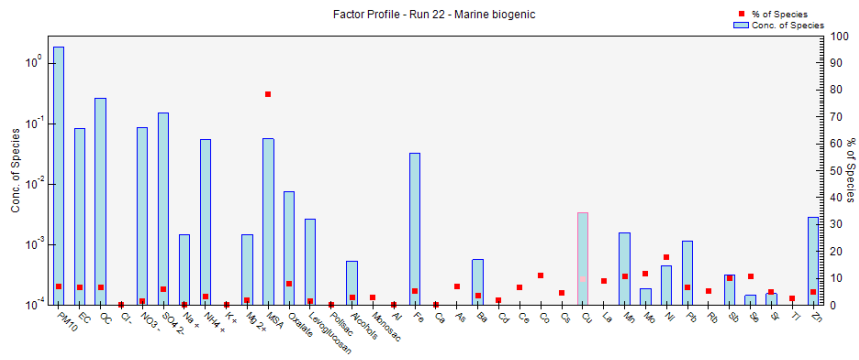


Figure A2. 45: Chemical profile (top) and time variability (bottom) of the marine biogenic factor in Roubaix

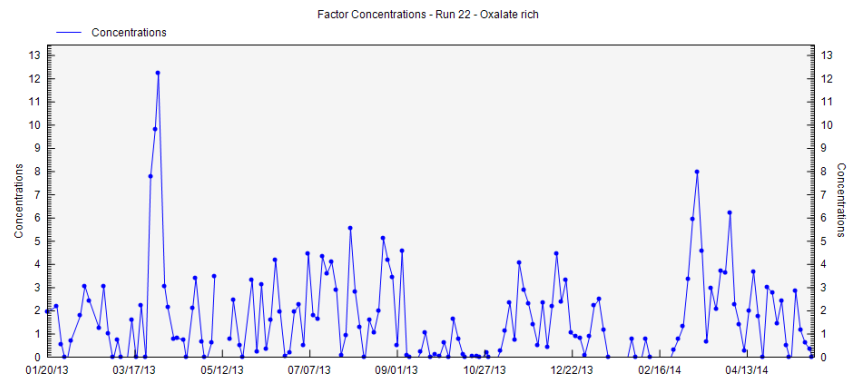
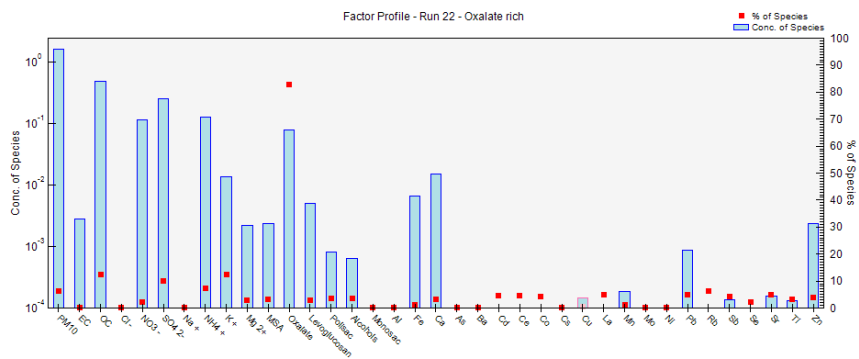


Figure A2. 46: Chemical profile (top) and time variability (bottom) of the oxalate rich factor in Roubaix

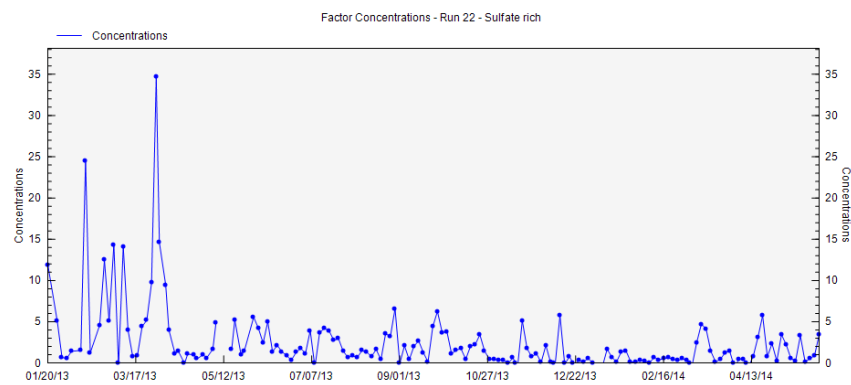
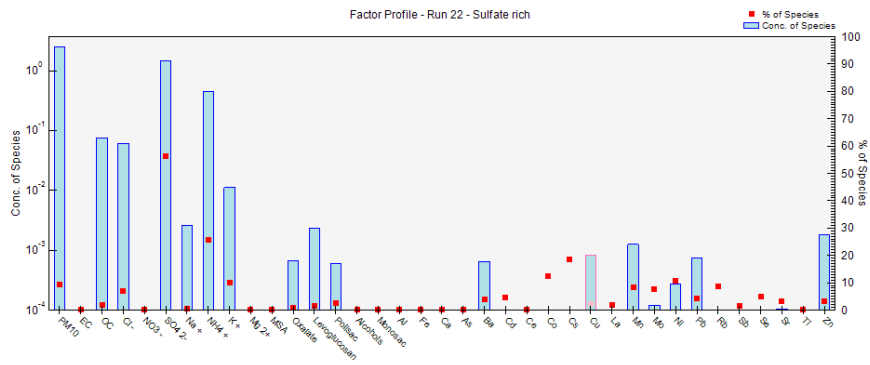


Figure A2. 47: Chemical profile (top) and time variability (bottom) of the sulfate rich factor in Roubaix

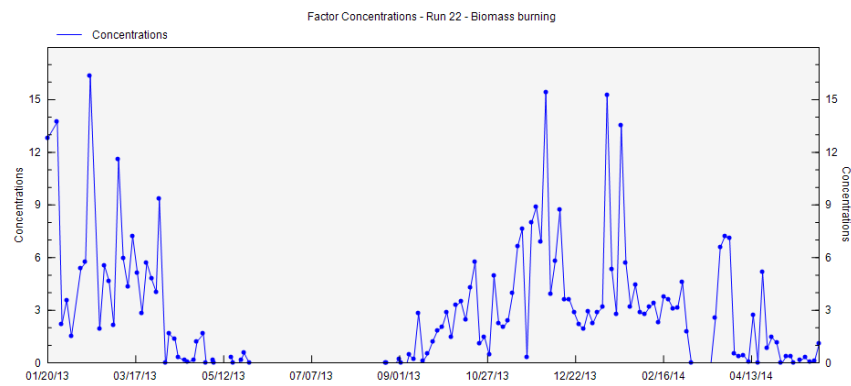
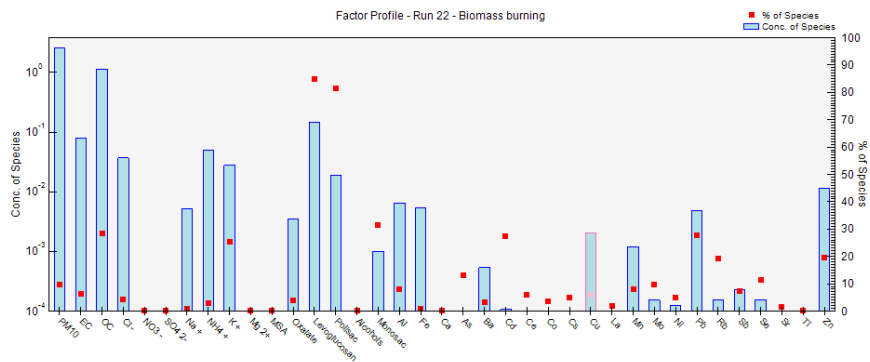


Figure A2. 48: Chemical profile (top) and time variability (bottom) of the biomass burning factor in Roubaix

Correlation between ionic compounds and factor contributions

Lens (urban site)

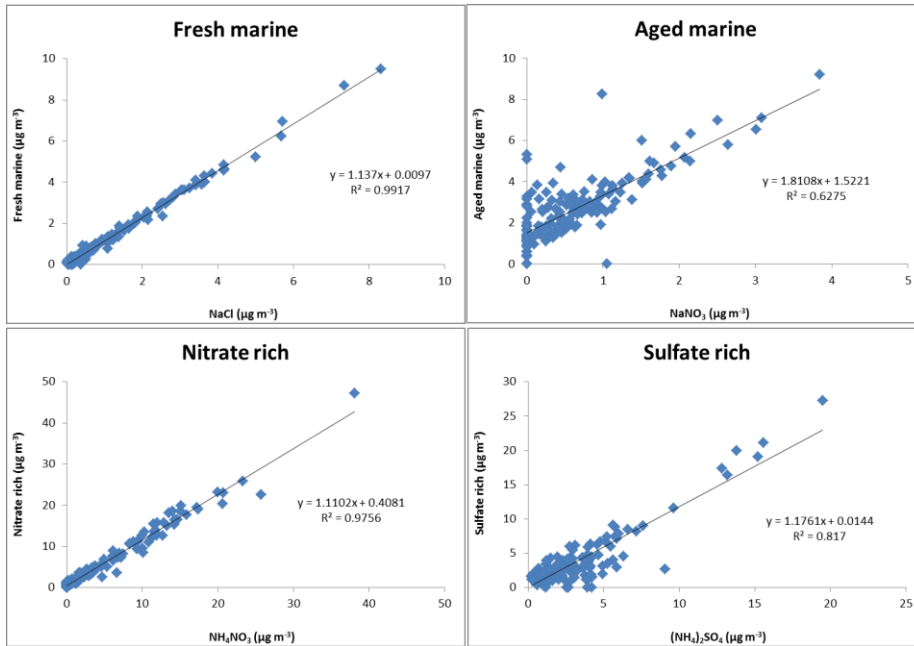


Figure A2. 49: Correlations between factor contributions and the main ions for the sampling site of Lens

Nogent-sur-Oise (urban site)

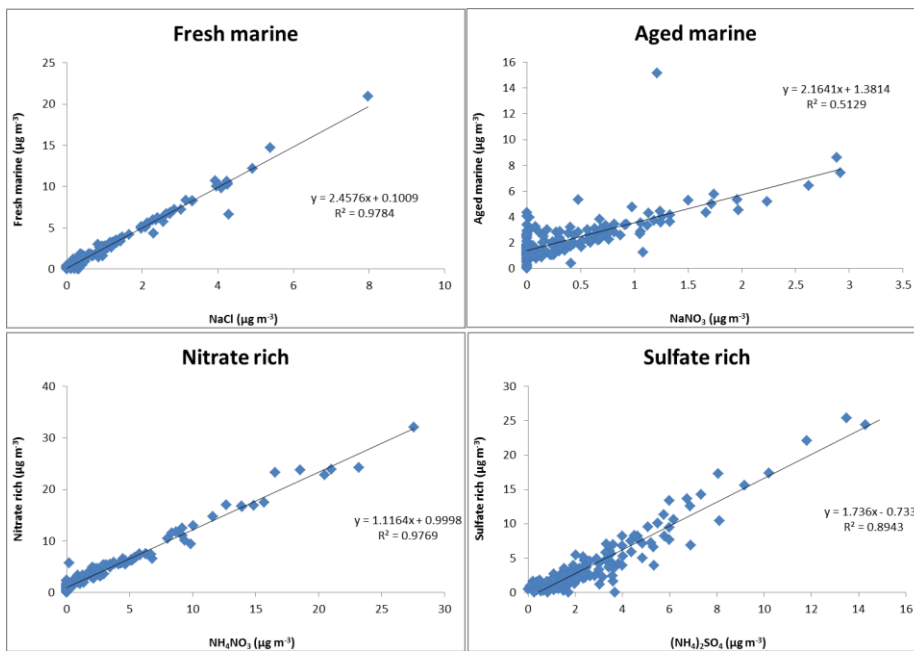


Figure A2. 50: Correlations between factor contributions and the main ions for the sampling site of Nogent-sur-Oise

Revin (remote site)

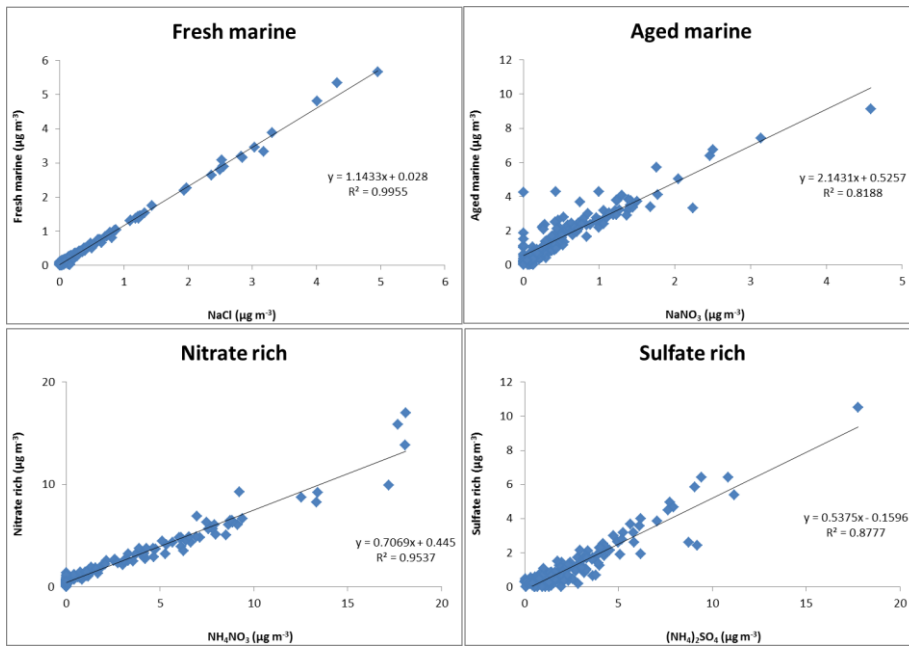


Figure A2. 51: Correlations between factor contributions and the main ions for the sampling site of Revin

Rouen (urban site)

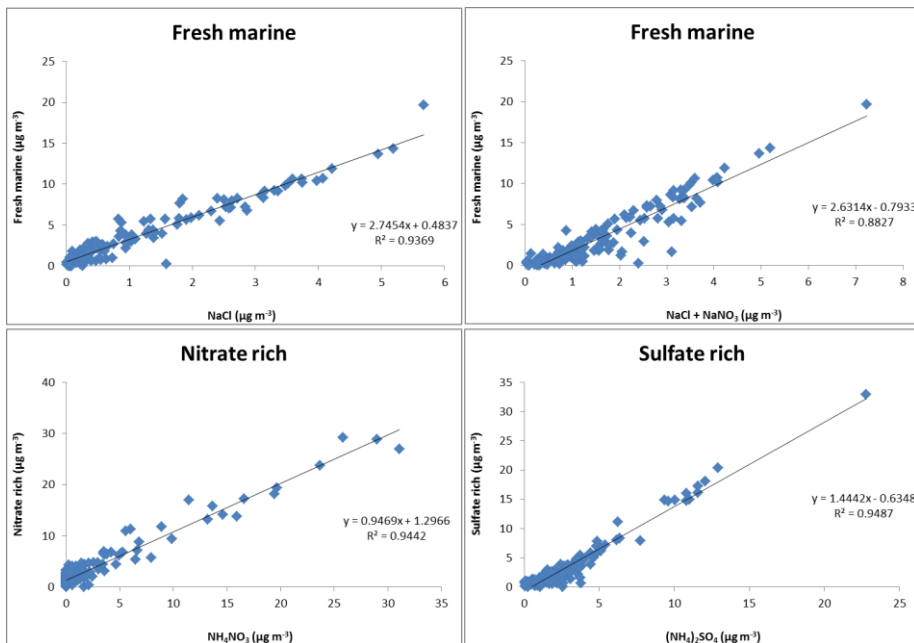


Figure A2. 52: Correlations between factor contributions and the main ions for the sampling site of Rouen

Roubaix (traffic site)

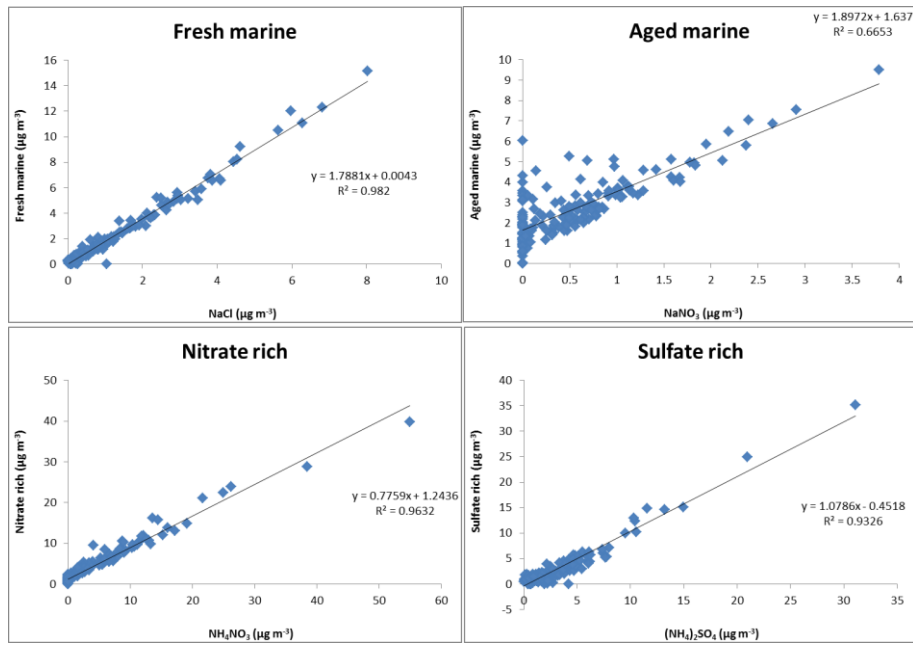


Figure A2. 53: Correlations between factor contributions and the main ions for the sampling site of Roubaix

ANNEX 3: CONCENTRATION FIELDS

Trajectory cluster analysis:

Each line represents the mean trajectory of a cluster, numbered from 1 to 5. A different color is given to each line for better visualization. The percentage of the total number of trajectories assigned to each cluster is indicated.

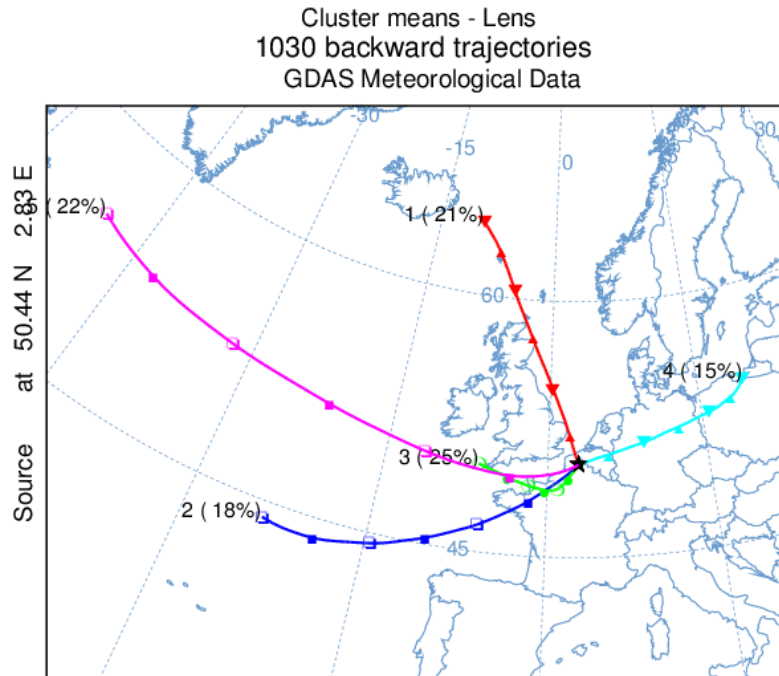


Figure A3. 1: Cluster analysis on the backtrajectories arriving to the site of Lens (Number of endpoints skipped: 3)

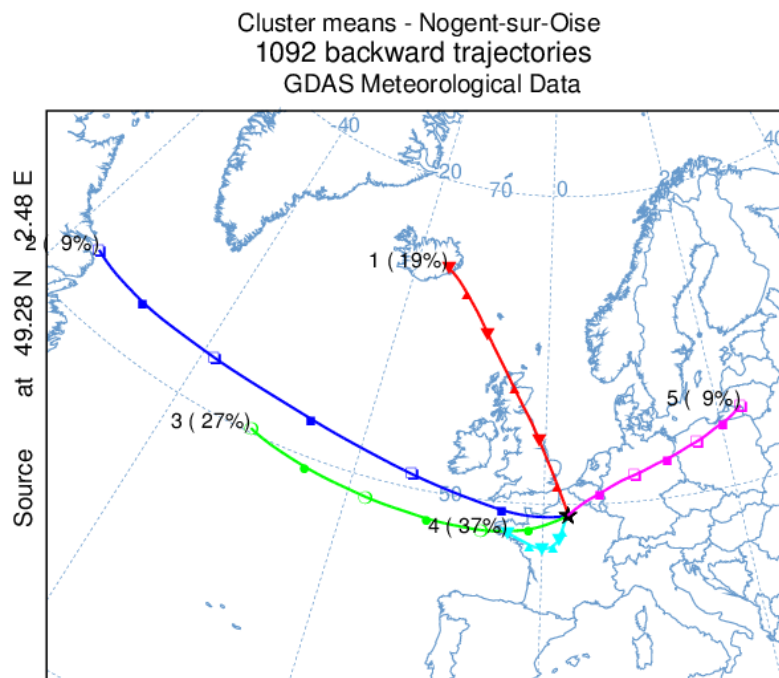


Figure A3. 2: Cluster analysis on the backtrajectories arriving to the site of Nogent-sur-Oise (Number of endpoints skipped: 3)

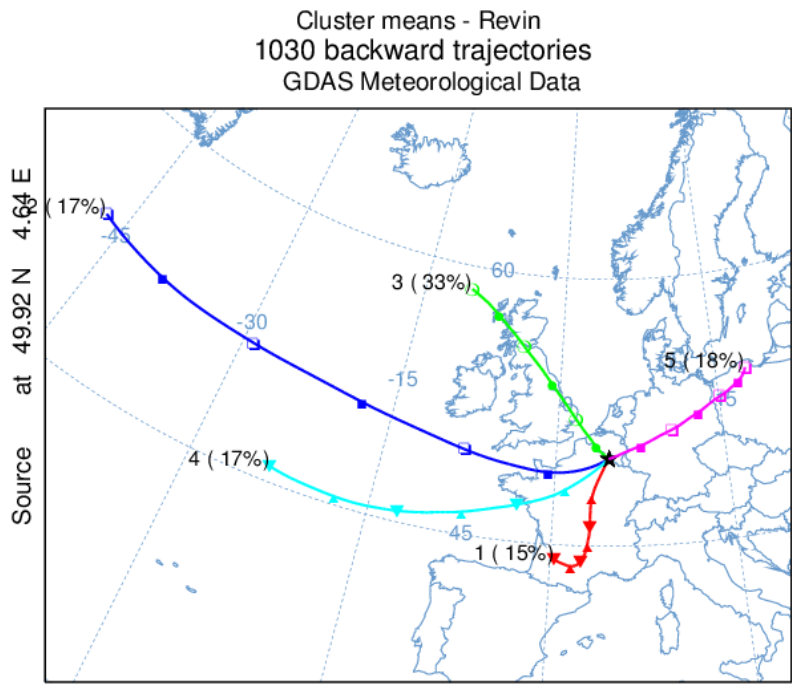


Figure A3. 3: Cluster analysis on the backtrajectories arriving to the site of Revin (Number of endpoints skipped: 3)

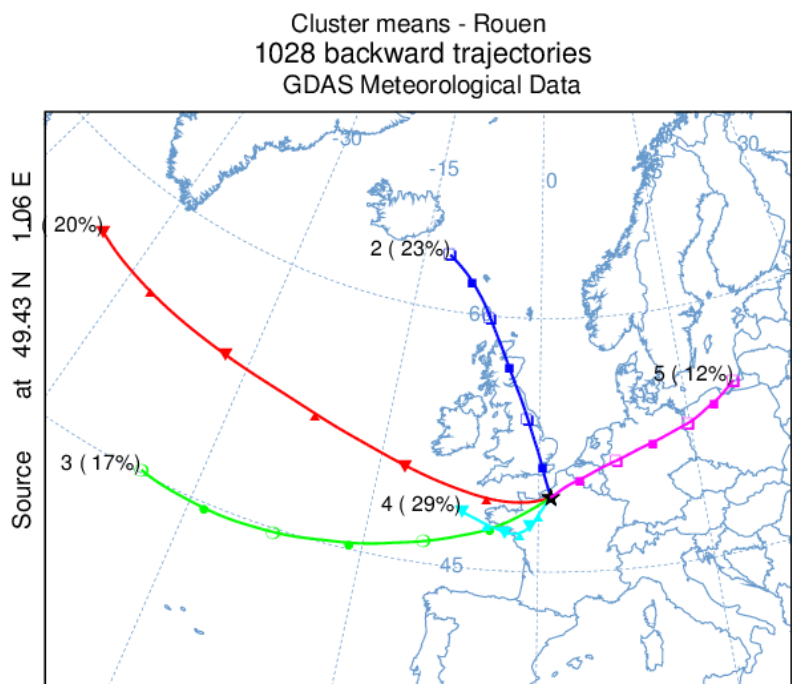


Figure A3. 4: Cluster analysis on the backtrajectories arriving to the site of Rouen (Number of endpoints skipped: 3)

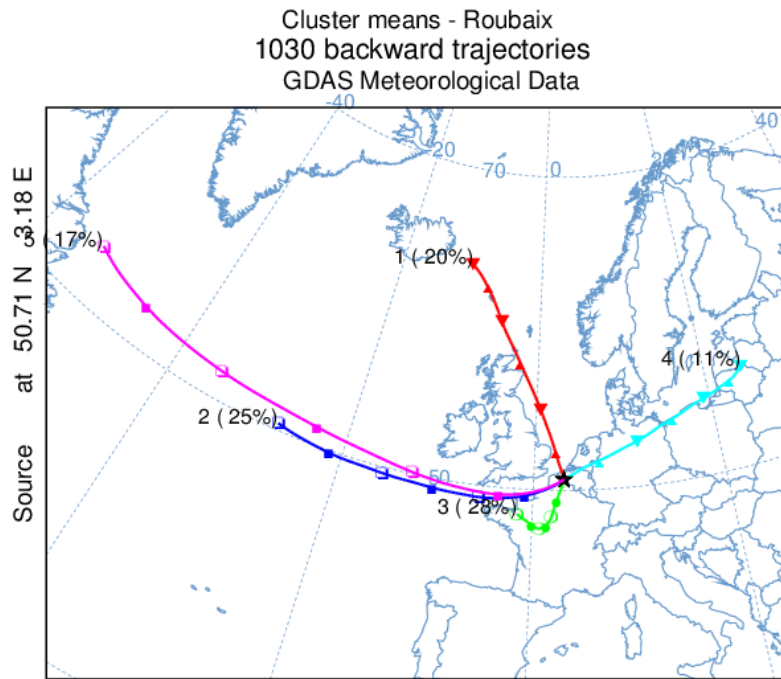


Figure A3. 5: Cluster analysis on the backtrajectories arriving to the site of Roubaix (Number of endpoints skipped: 3)

Comparison between trajectory density with and without trajectory cut-offs

Lens

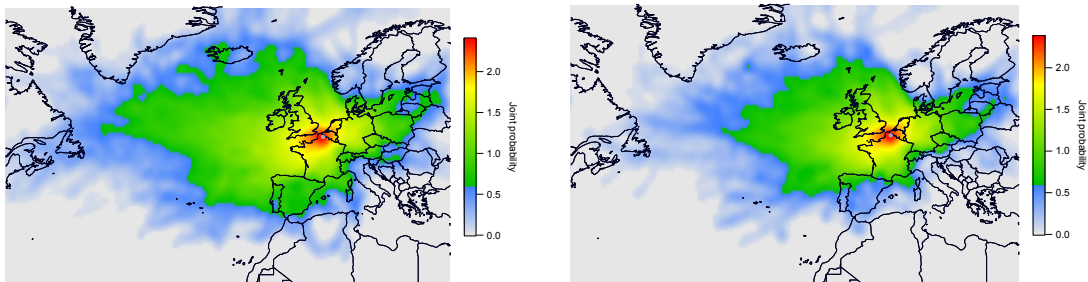


Figure A3. 6: Trajectory density without (left) and with (right) altitude and rainfall cutoffs for the site of Lens

Nogent-sur-Oise

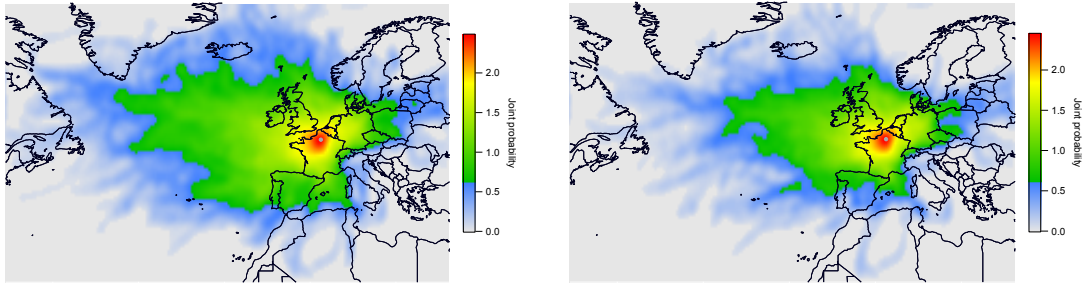


Figure A3. 7: Trajectory density without (left) and with (right) altitude and rainfall cutoffs for the site of Nogent-sur-Oise

Revin

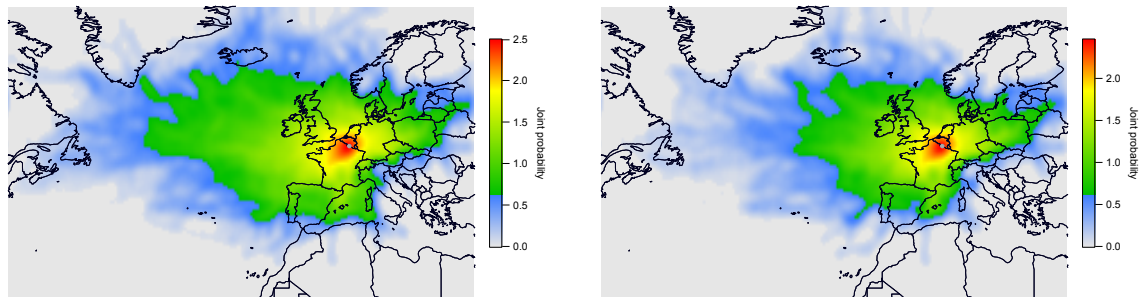


Figure A3. 8: Trajectory density without (left) and with (right) altitude and rainfall cutoffs for the site of Revin

Rouen

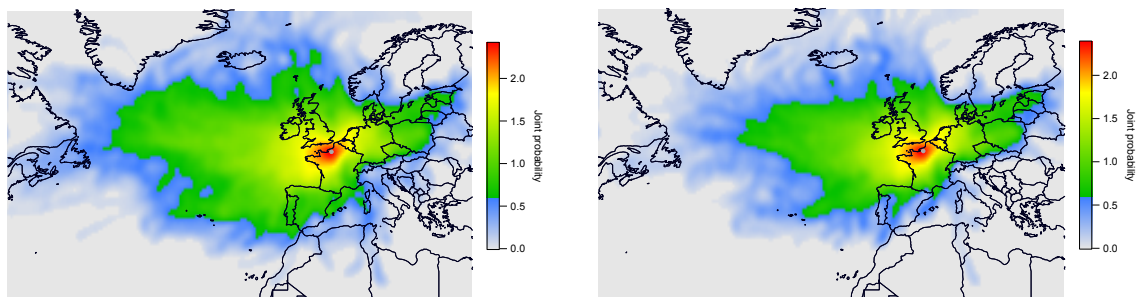


Figure A3. 9: Trajectory density without (left) and with (right) altitude and rainfall cutoffs for the site of Rouen

Roubaix

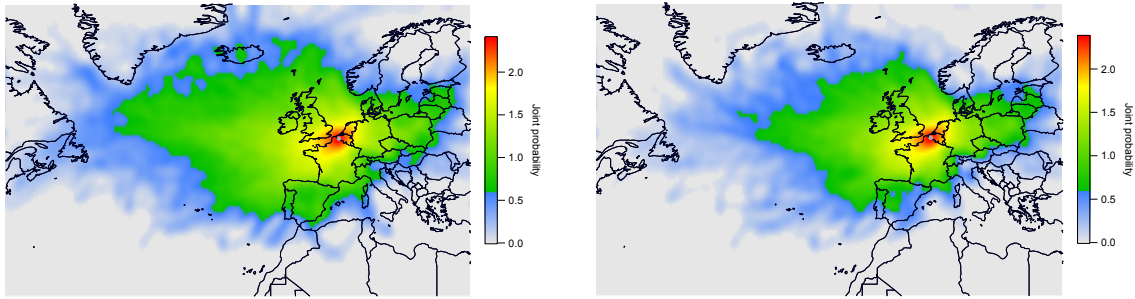


Figure A3. 10: Trajectory density without (left) and with (right) altitude and rainfall cutoffs for the site of Roubaix

Fresh marine aerosols

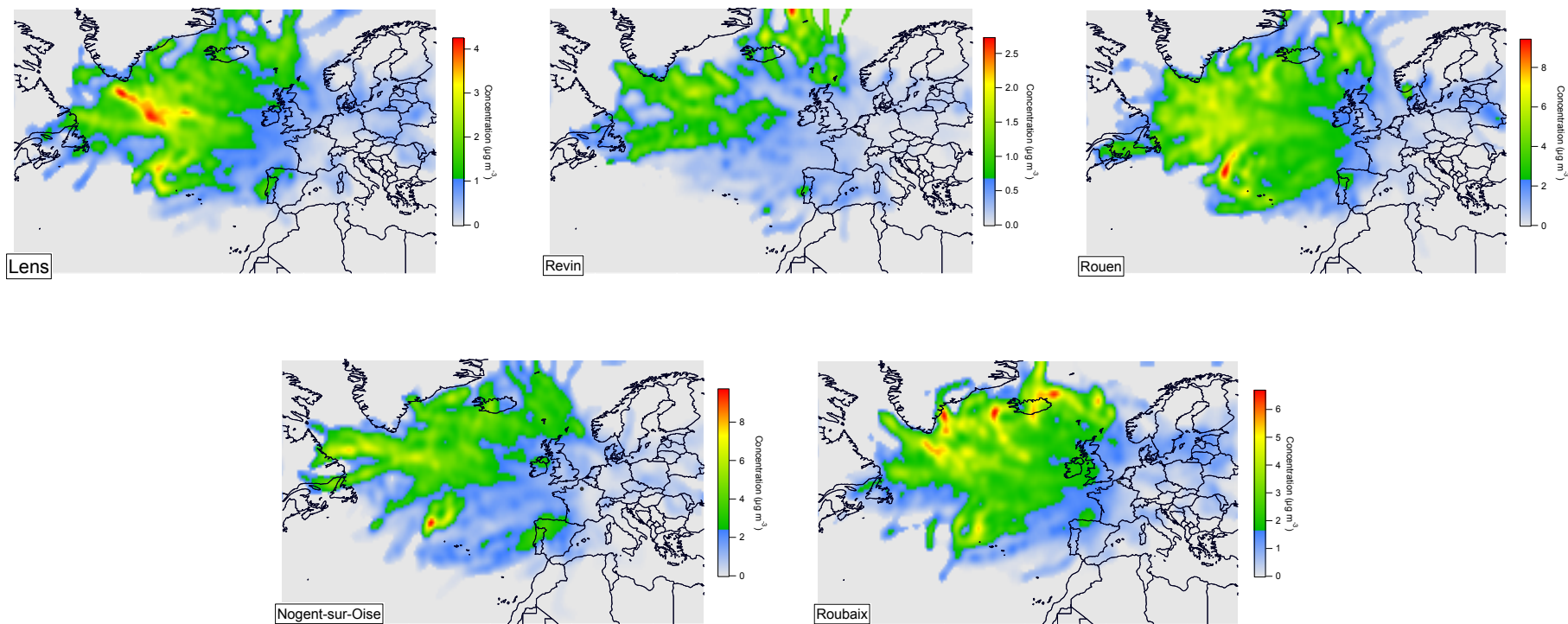


Figure A3. 11: Concentration field maps for fresh marine aerosols on the 5 sites

Aged marine aerosols

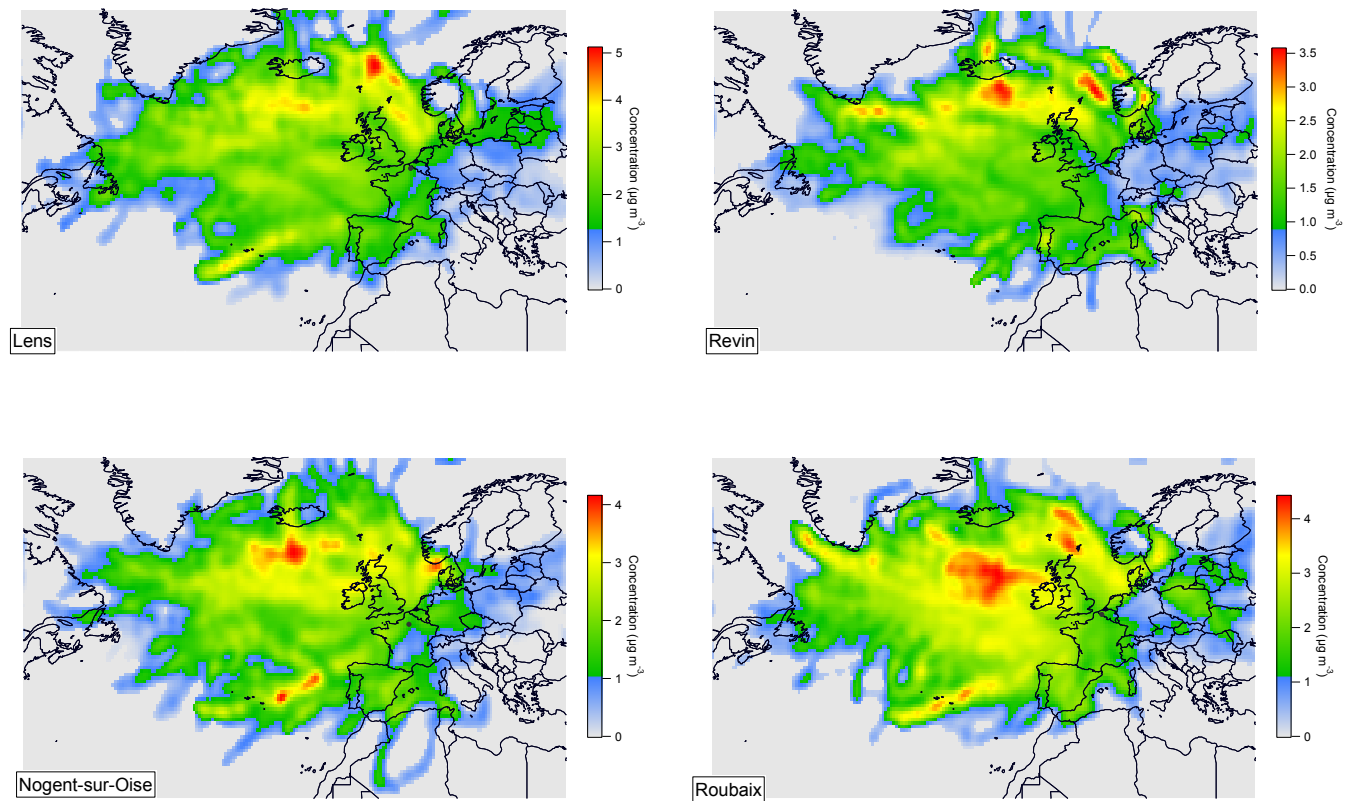


Figure A3. 12: Concentration field maps for aged marine aerosols on the 5 sites

Marine biogenic aerosols

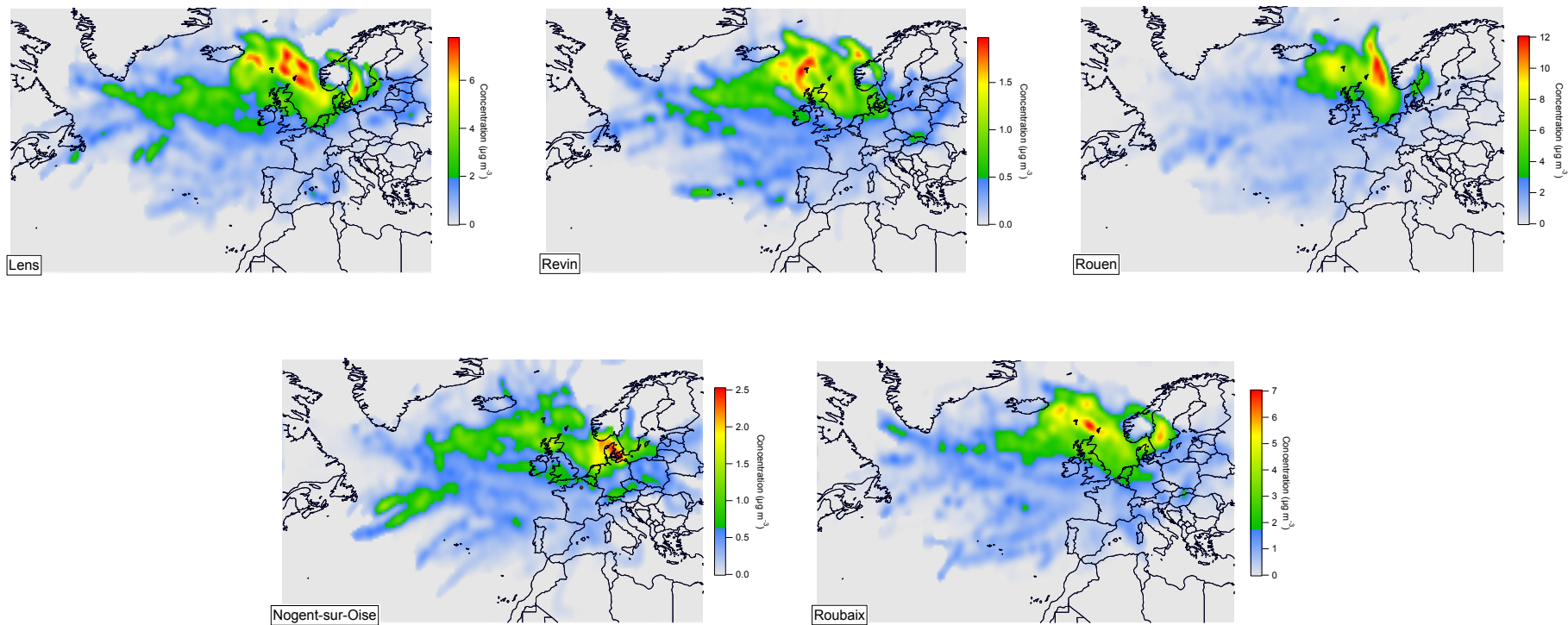


Figure A3. 13: Concentration field maps for marine biogenic aerosols on the 5 sites

Nitrate rich aerosols

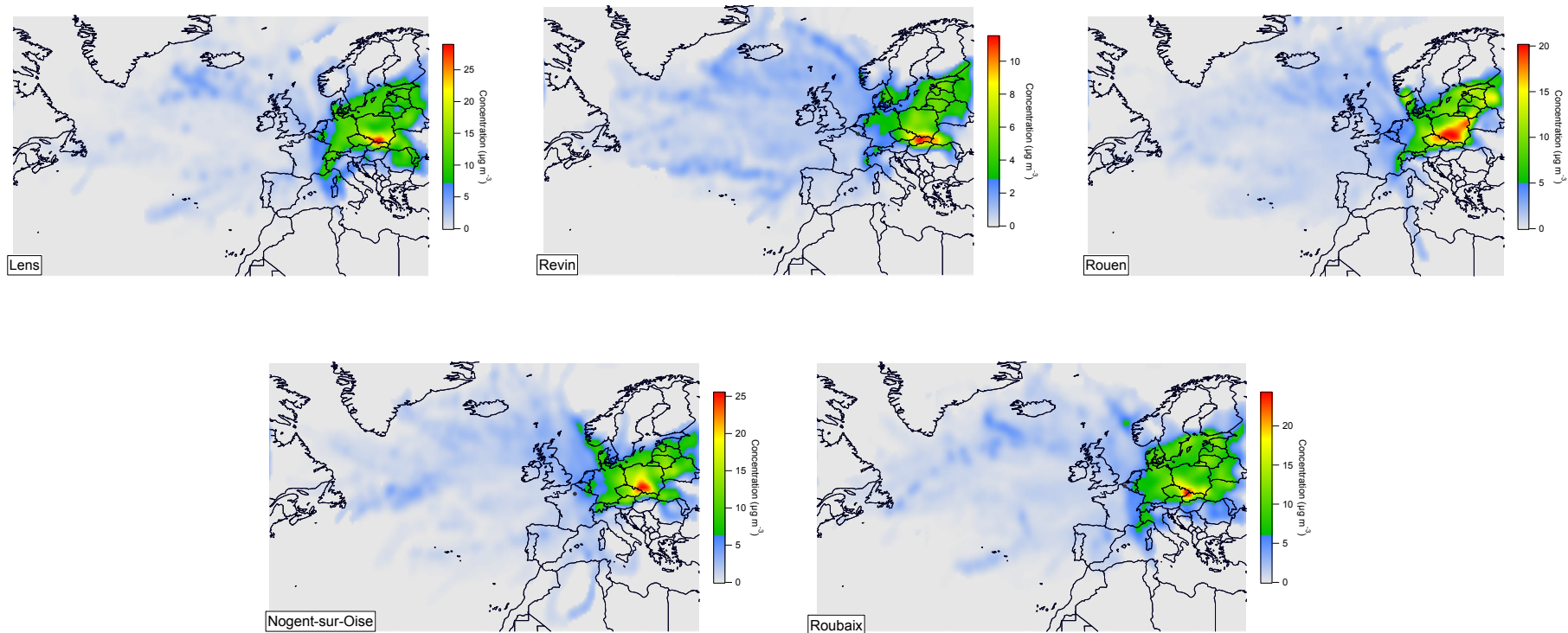


Figure A3. 14: Concentration field maps for nitrate rich aerosols on the 5 sites

Sulfate rich aerosols

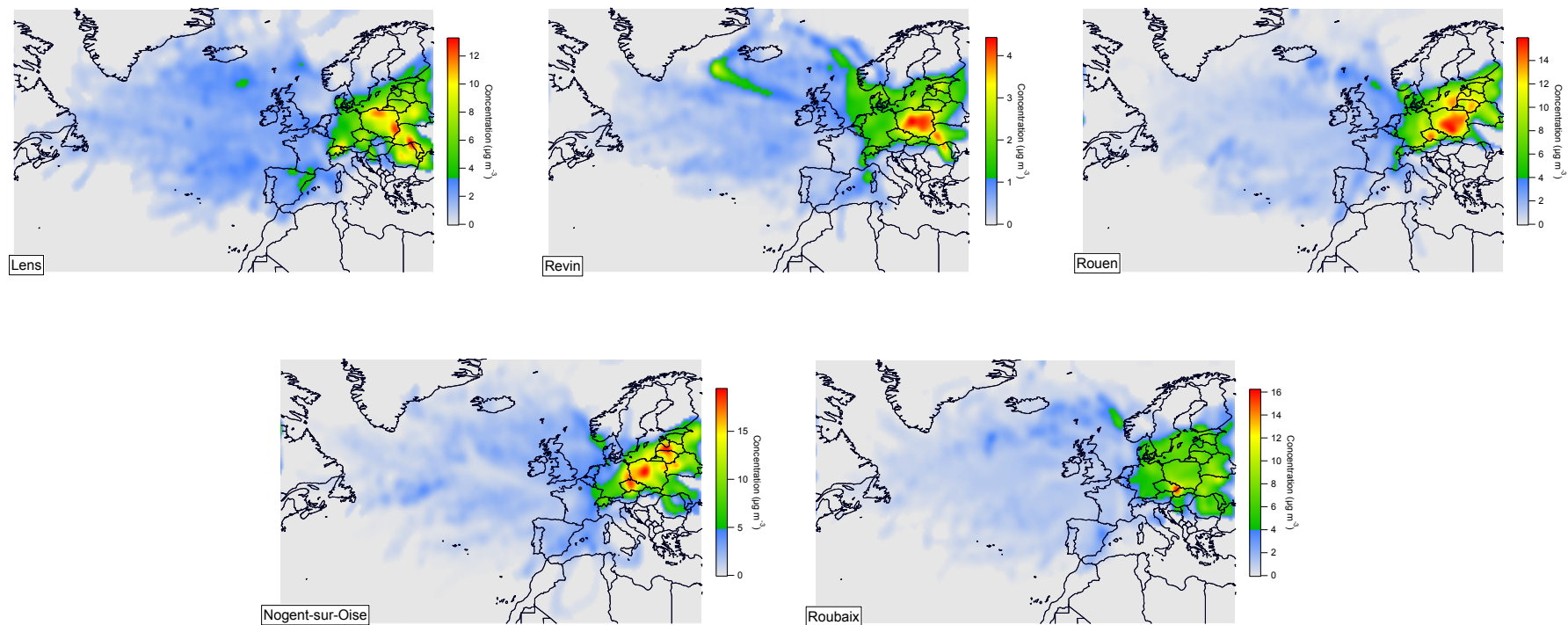


Figure A3. 15: Concentration field maps for sulfate rich aerosols on the 5 sites

Oxalate rich aerosols

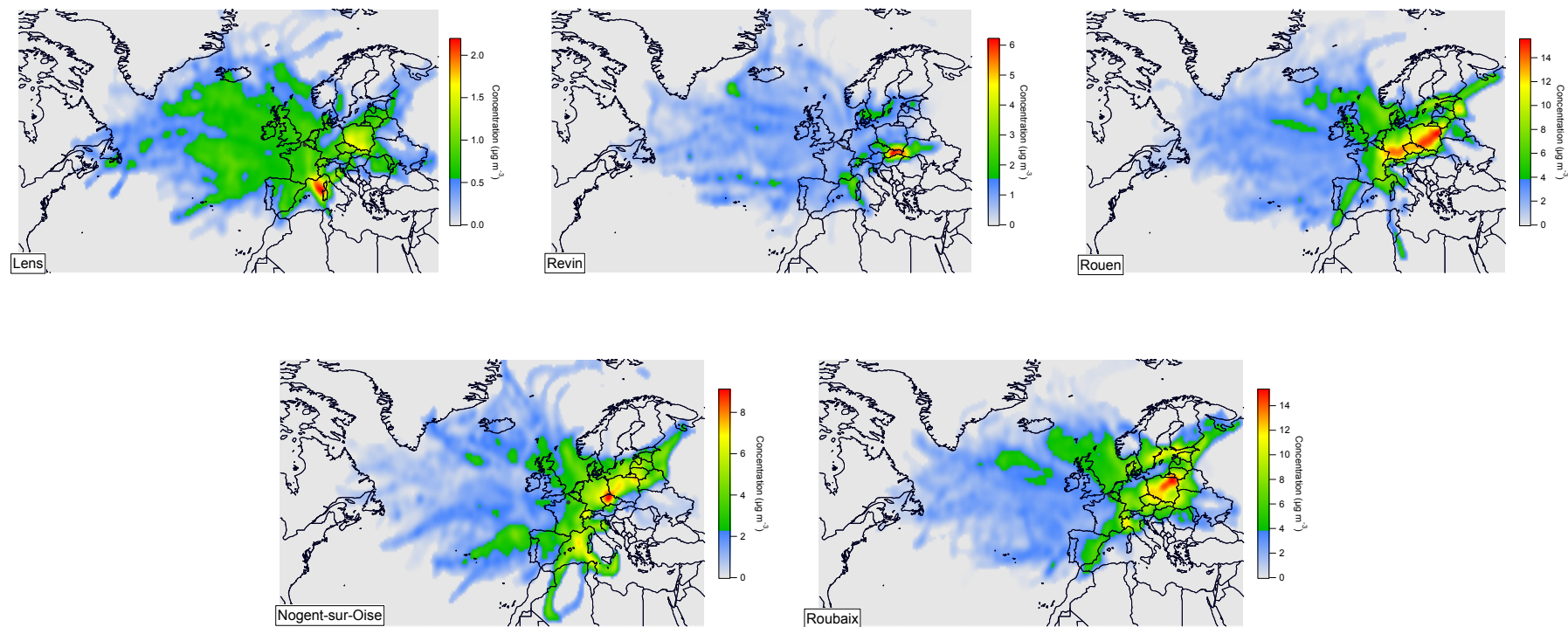


Figure A3. 16: Concentration field maps for oxalate rich aerosols on the 5 sites